Heterómeros de receptores de dopamina. Nuevos mecanismos para la regulación de la transmisión dopaminérgica

Estefanía Moreno Guillén

Tesis Doctoral

Barcelona, 2012

HETERÓMEROS DE RECEPTORES DE DOPAMINA. NUEVOS MECANISMOS PARA LA REGULACIÓN DE LA TRANSMISIÓN DOPAMINÉRGICA

Estefanía Moreno Guillén

HETERÓMEROS DE RECEPTORES DE DOPAMINA. NUEVOS MECANISMOS PARA LA REGULACIÓN DE LA TRANSMISIÓN DOPAMINÉRGICA

Tesis Doctoral

Estefanía Moreno Guillén

Portada: Imagen de Nicolas P. Rougier (2005)

UNIVERSIDAD DE BARCELONA
FACULTAD DE BIOLOGÍA
DEPARTAMENTO DE BIOQUÍMICA Y BIOLOGÍA MOLECULAR

HETERÓMEROS DE RECEPTORES DE DOPAMINA. NUEVOS MECANISMOS PARA LA REGULACIÓN DE LA TRANSMISIÓN DOPAMINÉRGICA

Memoria presentada por la Licenciada en Biología

ESTEFANÍA MORENO GUILLÉN

para optar al grado de Doctor por la Universidad de Barcelona

Esta tesis se ha inscrito dentro del programa de doctorado de Fisiología del Departamento de Fisiología de la Universidad de Barcelona, bienio 2007-2009.

El trabajo experimental y la redacción de la presente memoria han sido realizados en el Departamento de Bioquímica y Biología Molecular de la Facultad de Biología (Universidad de Barcelona) por Estefanía Moreno Guillén bajo la dirección del Dr. Rafael Franco Fernández y la Dra. Carme Lluís Biset

Barcelona, Febrero de 2012

Dr. Rafael Franco Fernández Dra. Carme Lluís Biset

Estefanía Moreno Guillén

A mis padres, Francisco y Ángeles,
sin ellos no habría podido llegar hasta aquí,
a ellos les debo quien soy,
Gracias.

Siempre he pensado que mi tesis tendría algo que la haría especial y diferente a las demás, pero eso no se encuentra en ella, sino en todas y cada una de las personas que a su manera me han ayudado a poder llegar hasta aquí. Ahora, después de varios años de duro trabajo ha llegado el momento de defender esta tesis doctoral, y al hacerlo no quiero olvidarme de ellas, gracias.

La primera persona por la que quiero empezar es la hermana Dolores, por acogerme, cuidarme, animarme a superar mis retos y mis miedos, ayudarme a ser mejor persona y sobre todo por contagiarme su amor por la ciencia y por la vida en general. La vida se puede ver desde muchos puntos de vista, gracias por mostrármelos todos.

I com a grup de laboratori he d'agrair a totes aquelles persones que han format part d'ell i que en formen, perquè sense elles tampoc podria haver-ho aconseguit. Empezando por mis jefes, agradecer a Rafa la ayuda que me ha prestado en todo momento que lo he necesitado, sus consejos y la confianza ciega que siempre ha depositado en mí. Eres una persona muy auténtica, gracias. Enric i Pepi gràcies per estar sempre que us he necessitat, no m`heu fallat mai. Enric ets admirable i és un plaer poder formar part d'aquest grup amb tu, i Pepi, una persona molt treballadora i eficaç, en poques paraules, ets imprescindible per a mi i per aquest grup. Antoni, ets una persona encantadora i molt intel·ligent, amb tu he aprés molt. Has de saber que encara et queda molt per ensenyar-me. Vicent, gràcies a tu vaig conèixer aquest grup i ara ja no vull marxar d'ell, ets un dels millors científics que coneixeré i una persona genial. M'encanta aprendre coses amb tu, gràcies per prestar-me la teva ajuda sempre que l'he necessitat, per confiar tant en mi i per entendre'm. Al Peter, contigo he aprendido una manera diferente de entender la ciencia, y de ver las cosas que de verdad son importantes, gracias por preocuparte siempre por mí. Me habéis dado otra oportunidad de seguir haciendo lo que más me gusta, sabes que no te decepcionaré y que siempre podrás contar conmigo. Al Sergi, no he tingut el plaer de tenir-te al meu costat cada dia, però per a mi sempre has estat com un cap més, al que admiro moltíssim. Al Jordi, gràcies per acollir-me tant bé en el teu grup, per fer-me sentir tant a gust treballant amb vosaltres, i per haver-me permès aprendre tantes coses noves. I per últim, a la Carme, només puc dir-te que per a mi ets molt més que un cap, sempre has estat en tot moment que t'he necessitat, m'has aconsellat, m'has ensenyat a entendre la ciència, sempre amb els teus per què, els teus fantàstics raonaments i les teves explicacions. Ets una persona molt especial per a mi, en gran part és culpa teva que m'agradi tant el que faig, que tingui aquesta curiositat científica i haver pogut aconseguir tot això. Has dipositat molta confiança en mi, i jo a canvi només et puc prometre que intentaré no decebre't mai. T'admiro molt. Carme, de tot cor, moltes gràcies.

I com a companys de grup, vull recordar algunes de les persones amb les que he compartit més temps i més vivències, i que s'han convertit en persones molt importants per a mi, però sense

oblidar-me de les que no menciono, perquè sempre portaré el seu record amb mi. A la Milena, te echo mucho de menos, dejaste un vacío en el grupo y en mi, que aún nadie ha sabido llenar, mereces ser feliz. A la Jana, una de les persones més autèntiques que he conegut. A la Gemma, només puc dir de tu que ets increïble, que t'admiro molt, i que al teu costat cada dia he aprés quelcom nou, és un plaer poder treballar cada dia amb tu. Moltes gràcies per tot. Marc, ets encantador i vals molt, és un luxe poder ésser la teva companya de laboratori i la teva amiga. Victor i Isaac formeu un tàndem genial, arribareu lluny. Victor, seràs un gran científic. I Isaac, de persones com tu n'hi han molt poques, quina sort haver-te conegut. Sergio, muchas gracias por todo, sin ti los momentos duros aún lo habrían sido más, gracias por enseñarme que las apariencias engañan, y que las cosas no siempre son blancas o negras. Lucía, admiro tu manera diferente de ver la vida y la pasión con la que sientes las cosas, no cambies nunca. Dani, gracias por entenderme, ayudarme y hacerme reír en los días que nada sale como a uno le gustaría. Jordi, gràcies per ser-hi, sentir-te riure m'alegra el dia. És fantàstic poder ésser la teva companya. Al Jorge, siempre se puede contar contigo, eres una gran persona. Jasmina, siempre dispuesta a ayudarme, gracias. Al David, gran científic i millor persona, gràcies.

Y por último a mi auténtica familia, a los que pase lo que pase siempre puedes contar con ellos y sabes que no te fallarán nunca. A mi yayi Ángela, te quiero mucho, ojalá sea sólo la mitad de fuerte de lo que tú eres. Al meu tiet Josep, no canviïs mai, he aprés a entendre't i t'estimo molt. A mi padres Paco y Ángeles, las dos personas más importantes de mi vida, ellos me han dado tolo lo que soy y permitido llegar hasta aquí, siempre me han apoyado, aconsejado, cuidado, querido…siempre anteponiendo vuestra felicidad a la mía, gracias. Por mi padre sólo puedo sentir admiración, siempre habrás llegado más lejos de donde lo haremos el Jordi y yo. A mi madre, amiga y confidente, sabes que lo eres todo para mí y que sin ti… Me has enseñado a que uno puede conseguir todo lo que se propone, siempre y cuando tú estés a su lado. No olvides nunca que eres la persona que nos hace cada día ser mejores y nos mantiene unidos. A mi hermano Jordi, junto a él he vivido los mejores momentos de mi vida y el peor hasta el momento. Admiro tu fortaleza, tus ganas de vivir y ser feliz, llegarás muy lejos. Ves el mundo con unos ojos diferentes a los de los demás, gracias por dejarme ver por ellos. Chor, siempre juntos!

A Eric, sé que siempre podré contar contigo y tú conmigo. Siempre serás una persona especial y muy importante en mi vida, gracias. A mi familia y amigos de Jatiel, y a mi familia de Arenas de San Juan, gracias por ayudarme a hacerme ver, durante todo este tiempo, que existe algo más que el laboratorio y la tesis. Gracias por estar a mi lado.

Gràcies a la Marcel·la, el Joan, l'Anna, la Mònica, el Nica, el David gran, el David petit i la Maria, la meva petita família, us estimo molt.

I per últim, a una persona molt especial, l'Eduard. Tant de bo t'hagués conegut abans. M'has ensenyat que la vida no és sempre fàcil i que la gent no sempre té el que es mereix, però l'esperança és l'últim que es perd i les coses es tenen que seguir intentant, perquè només així s'aconsegueixen. M'has fet ser millor persona, i m'has ensenyat a ser feliç, sempre que tu ho siguis. Gràcies per ensenyar-me a sentir que la meva vida només té sentit si tu formes part d'ella.

Vigila tus pensamientos, porque se convierten en palabras.
Vigila tus palabras, porque se convierten en actos.
Vigila tus actos, porque se convierten en hábitos.
Vigila tus hábitos, porque se convierten en carácter.
Vigila tu carácter, porque se convierte en tu destino.

Mahatma Gandhi

ÍNDICE DE CONTENIDOS

ÍNDICE DE CONTENIDOS **Pág**

ABREVIATURAS

6-OHDA	6-hidroxidopamina
AA-NAT	*Arylalkylamine N-acetyltransferase*
AC	Adenilato ciclasa
AD	Enfermedad de Alzheimer
ADA	Adenosina desaminasa
ADHD	*Attention-Deficit/Hyperactivity Disorder*
ADN	Ácido desoxirribonucleico
ADO	Adenosina
ADP	Adenosina difosfato
AMP	Adenosina monofosfato
AMPc	Adenosina monofosfato cíclico
A_nR	Receptor de adenosina
Arg	Arginina
ARNi	Ácido ribonucleico de interferencia
ARNm	Ácido ribonucleico mensajero
ATP	Adenosina trifosfato
BH_2	Dihidrobiopterina
BH_4	Tetrahidrobiopterina
BiFC	*Bimolecular fluorescence complementation*
B_{max}	Unión máxima
BRET	*Bioluminescence Resonance Energy Transfer*
CaCC	*Ca^{2+} dependent chloride channel*
CaM	Calmodulina
CaMK	*Ca^{2+}/Calmodulin Dependent Protein Kinase*
CB_nR	Receptor de cannabinoides
CK1/2	*Casein kinase 1/2*
COMT	Catecol-O-metiltransferasa
CREB	*cAMP Response Element-Binding protein*
DAG	Diacilglicerol
DARPP-32	*Dopamine and cyclic adenosine 3'-5'-monophosphate Regulated Phospho Protein, 32 KDa*
DAT	Transportador de dopamina
DC	DOPA descarboxilasa
D_C	Índice de cooperatividad
D_nR	Receptor de dopamina
DOPA	Dihidroxifenilalanina
DsRed	Proteína fluorescente roja
EC	Bucle extracelular
EPN	Núcleo entopeduncular
ERK	*Extracelular Regulated Kinase*
FRET	*Fluorescence or Förster Resonance EnergyTtransfer*
GABA	Ácido γ-aminobutírico
$GABA_BR$	Receptores de ácido γ-aminobutírico
GAIP	*G Alpha Interacting Protein*
GDP	Guanosina difosfato
GFP	Proteína fluorescente verde
GIPC	*GAIP interacting protein, C terminus*
GIRK	*G-protein-regulated inwardly rectifying K^+ (GIRK) channels*
GMPc	Guanosina monofosfato cíclico
G_n	Subunidad de la proteína G
GP	Globus pallidus
GPCR	Receptores acoplados a proteína G

Grb2	*Growth factor receptor-bound 2*
GRK	*G protein-coupled receptor kinases*
GTP	Guanosina trifosfato
GTPasa	Guanosina trifosfatasa
$5HT_n$	Receptor de serotonina
IC	Bucle intracelular
IP_3	Inositol 1,4,5-trifosfato
JNK	*c-Jun amino-terminal kinase*
kDa	KiloDalton
K_D	Constante de afinidad
K_{DH}	Constante de disociación de alta afinidad
K_{DL}	Constante de disociación de baja afinidad
KO	*Knockout*
L	Ligando
l	Longitud de onda
L-DOPA	Levodopa
LTP	Potenciación a largo plazo
MAO	Monoaminooxidasa
MAPK	*Mitogen Activated Protein Kinase*
MEK	*Mitogen-Induced Extracellular Kinase*
mGluR	Receptor metabotrópico de glutamato
MPTP	*N-Methyl-4-phenyl-1,2,3,6-tetrahydropyridine*
NAT	Serotonina-N-Acetiltransferasa
NCK	*Non-catalytic region of tyrosine kinase adaptor protein*
NHE	Intercambiador de Na^+/H^+
NKE	Intercambiador de Na^+/K^+
NMDA	N-metil-D-aspartato
NRTK	*Nonreceptor tyrosine kinases*
PACAP	Polipéptido activador de la adenilato ciclasa pituitaria
PD	Enfermedad de Parkinson
PDK-1	*Phosphoinosotide-Dependent Protein-Kinase 1*
PDZ	*Post-synaptic-Density-95/Discs-large/ZO1*
PI3K	*Phosphatidylinositol 3-Kinase*
PIP2	*Phosphatidylinositol Bisphosphate*
PIP3	*Phosphatidylinositol Trisphosphate*
PKA	Proteína kinasa A
PKB	Proteína kinasa B
PKC	Proteína kinasa C
PLA	Fosfolipasa A
PLA_2	Fosfolipasa A_2
PLC	Fosfolipasa C
PP	Proteína fosfatasa
PP-1	Proteína fosfatasa-1
PTH	Hormona paratiroidea
R	Receptor inactivo
R*	Receptor activo (con actividad constitutiva)
RAMH	R-α-metilhistamina
RE	Retículo endoplasmático
RET	*Resonance Energy Transfer*
Rluc	*Renilla luciferase*
RTK	*Receptor tyrosine kinase*
RT-PCR	*Retro-transcriptase polymerase chain reaction*
Ser_n	Serina
Shc	*Src homology and collagen*

SIDA	Síndrome de inmuno deficiencia adquirida
SNC	Sistema Nervioso Central
SNc	Sustancia nigra pars compacta
SNr	Sustancia nigra pars reticulata
SRET	*Sequential Resonance Energy Transfer*
$SSTR_n$	Receptor de somatostatina
STN	Núcleo subtalámico
TH	Tirosina hidroxilasa
THC	Tetrahidrocannabinol
Thr_n	Treonina
TM	Núcleo tuberomamilar
TMn	Segmento transmembrana
TPH	Triptófano Hidroxilasa
VDCC	Canal de calcio dependiente de voltaje
VIP	Péptido intestinal vasoactivo
VTA	Área tegmental ventral
YFP	Proteína fluorescente amarilla

INTRODUCCIÓN

1. INTRODUCCIÓN

1.1 RECEPTORES ACOPLADOS A PROTEÍNA G

La comunicación entre células individuales es un requisito para el buen mantenimiento de la homeostasis dentro de un organismo. Para ello, las células tienen la habilidad de liberar moléculas al medio extracelular y de procesar gran cantidad de información procedente de moléculas extracelulares. Muchas de estas moléculas no entran dentro de la célula y para ejercer su función interactúan con un receptor de la superficie celular. De entre los diferentes receptores que se pueden hallar en la membrana destacan los receptores acoplados a proteína G, GPCR (*G-protein coupled receptors*). Esta familia constituye el mayor y más versátil grupo de receptores de superficie celular implicados en la transducción de señales (Gudermann *et al.* 1997). Los GPCR están codificados por una gran familia de genes; en el caso del genoma humano, más del 1% codifica para más de 1000 proteínas de las que más del 90% se expresan en el Sistema Nervioso Central (SNC) (George *et al.* 2002). Los GPCR son activados por una gran variedad de ligandos, tanto endógenos como exógenos, entre los que se incluyen hormonas, péptidos, aminoácidos, aminas biogénicas, lípidos, nucleótidos, iones, moléculas de olor y fotones de luz, transduciendo la señal a través de un gran número de efectores como las adenilato ciclasas, las fosfolipasas o los canales iónicos entre otros. Llevan a cabo multitud de funciones en el SNC y en la periferia, jugando un papel clave en la fisiología celular y controlando procesos biológicos como la proliferación, la supervivencia celular, el metabolismo, la secreción, la diferenciación, las respuestas inflamatorias e inmunes o la neurotransmisión, de ahí que su disfunción de lugar a diversas enfermedades (Gether 2000; Marinissen and Gutkind 2001) (Figura 1).

La expresión de los GPCR en el sistema nervioso central muestra patrones diferenciales en las distintas regiones del cerebro, lo que sugiere que la combinación de distintos receptores es clave en la regulación de diferentes procesos neurofisiológicos.

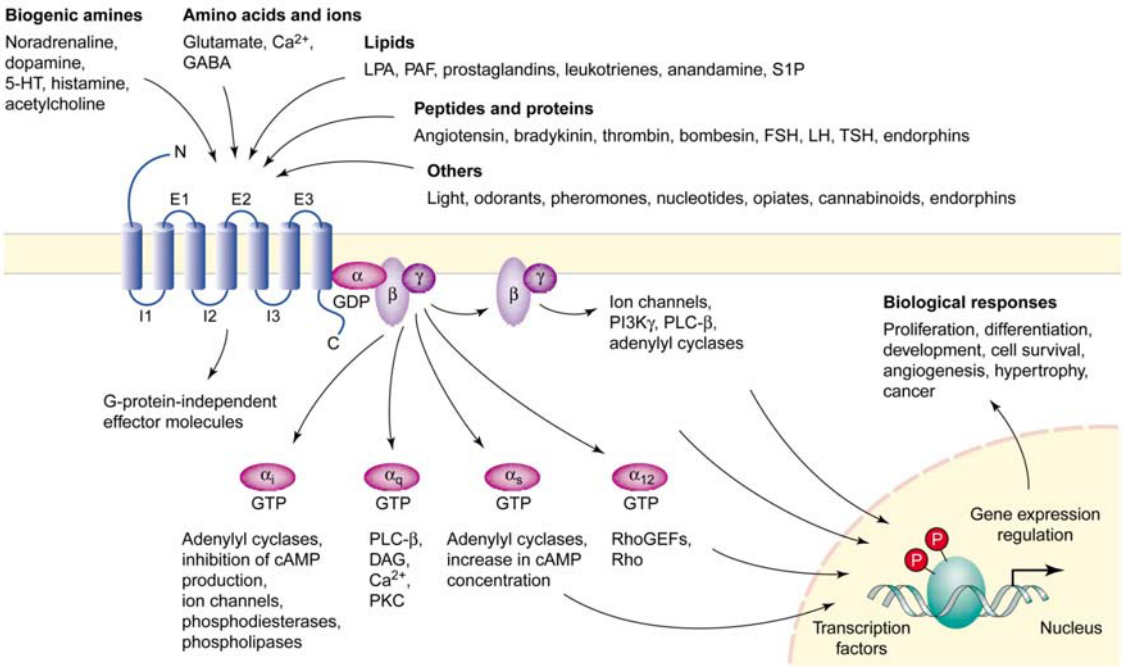

Figura 1. Estructura general de un receptor acoplado a proteína G mostrando los ligandos endógenos y mecanismos de señalización celular responsables de las diversas funciones biológicas (Extraído de Marinissen and Gutkind 2001).

Numerosas enfermedades y desórdenes están asociadas a mutaciones y polimorfismos de estos receptores (Spiegel 1996; Rana *et al.* 2001), por lo que son diana de un número creciente de agentes terapéuticos (Arrang 1994; Flower 1999; Bouvier 2001; Howard *et al.* 2001; Marinissen and Gutkind 2001; Binaei *et al.* 2003; Schmedtje *et al.* 2003).

1.1.1 ESTRUCTURA Y CLASIFICACIÓN DE LOS GPCR

Para que una proteína sea clasificada como receptor acoplado a proteína G debe cumplir dos requisitos principales. El primero consiste en estar constituido por una sola cadena proteica capaz de cruzar siete veces la membrana plasmática. Para ello, debe presentar una estructura con siete secuencias de 25-35 residuos aminoacídicos consecutivos, que muestren un relativamente alto grado de hidrofobicidad, dispuestos en una estructura de hélices α que atraviesan la membrana plasmática. Estas hélices están conectadas por tres bucles intracelulares y tres bucles extracelulares, quedando el dominio amino terminal orientado hacia el medio extracelular y el carboxilo terminal hacia el intracelular, formando así una unidad de reconocimiento y conexión que permite que un ligando extracelular ejerza su efecto específico dentro de la célula (Figura 2b). El segundo requisito es que este receptor tenga la capacidad de interactuar con una proteína G, por lo que reciben el nombre de receptores acoplados a proteína G.

Como otras proteínas de membrana, los receptores acoplados a proteína G están parcialmente inmersos en la bicapa lipídica, en un ambiente no polar, formando una estructura compacta de hélices transmembrana. La correcta orientación e integración de la cadena polipeptídica es guiada por un complejo aparato de translocación que reside en el retículo endoplasmático (RE). Se pueden distinguir dos estados de plegamiento diferentes que se producen tras la translocación inicial del receptor a través del extremo amino terminal dentro del lumen del RE. En el primer plegamiento las hélices hidrofóbicas α se disponen a través de la bicapa lipídica y el plegamiento de la proteína está dirigido principalmente por los efectos hidrofóbicos. Para minimizar la superficie polar expuesta dentro del ambiente lipídico, los dominios transmembrana adoptan una estructura secundaria dejando los aminoácidos hidrofóbicos enfrentados a la bicapa lipídica y los aminoácidos más hidrofílicos orientados hacia la hendidura generada por el empaquetamiento de los dominios transmembrana. Finalmente, en el segundo plegamiento se forma una estructura terciaria por interacciones específicas hélice-hélice, permitiendo un fuerte empaquetamiento, con estructura tipo anillo de los dominios transmembrana para formar un receptor funcional (Scarselli *et al.* 2000). Dos residuos de cisteína del bucle extracelular 1 y 2 (EC1-2), que están conservados en muchos GPCR forman un puente disulfuro que es probablemente, importante en el empaquetamiento y la estabilización de un número restrictivo de conformaciones de los 7 dominios transmembrana.

La primera estructura cristalina de un GPCR fue descrita en el año 2000, cuando se estudió con una alta resolución la estructura cristalina del receptor de rodopsina bovino (Palczewski *et al.* 2000). Se confirmó la existencia de una estructura altamente organizada en la región extracelular, incluyendo puentes disulfuro conservados que conforman la base para que las siete hélices transmembrana se dispongan formando el núcleo del receptor. Este núcleo en la mayoría de los GPCR participa en la unión del ligando (Figura 2a). Más recientemente, se ha obtenido la estructura cristalina del receptor de opsina acoplado a la proteína G, lo que ha permitido una mejor interpretación de los cambios estructurales asociados a la transducción de señal (Park *et al.* 2008; Scheerer *et al.* 2008). Desde entonces, se han cristalizado otros GPCR (Jaakola *et al.* 2008; Weis and Kobilka 2008; Rosenbaum *et al.* 2009; Jaakola and Ijzerman 2010) incluyendo el receptor de dopamina D_3 humano (Chien *et al.* 2010) y el receptor β_2-adrenérgico (Cherezov *et al.* 2007; Rasmussen *et al.* 2011) y se han propuesto mecanismos para su activación (Weis and Kobilka 2008; Maurice *et al.* 2010).

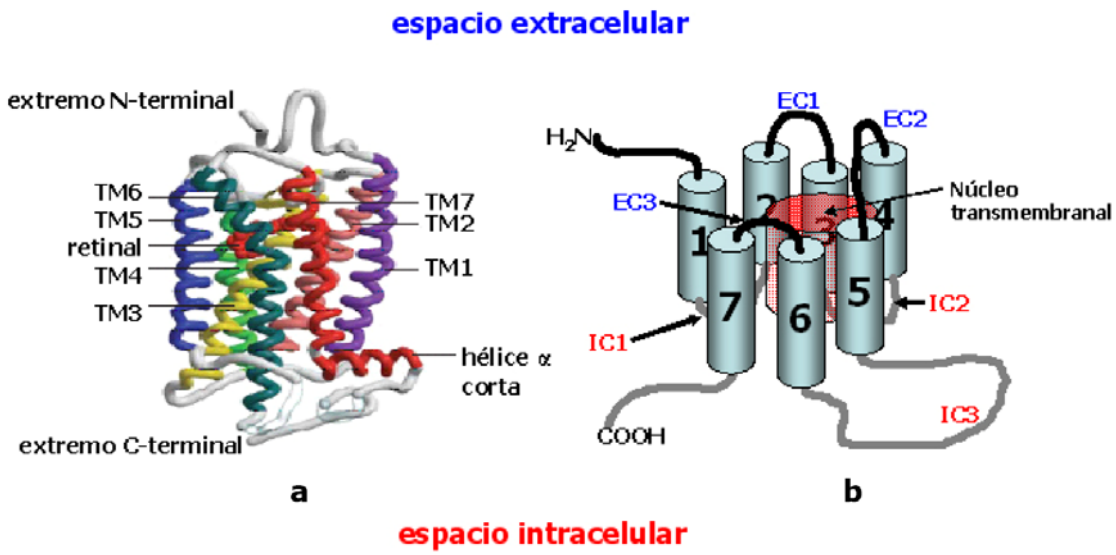

Figura 2. a) Estructura cristalina de la rodopsina y b) esquema de la estructura típica de un GPCR (Extraído de Palczewski *et al*. 2000).

Las regiones amino y carboxilo terminales permiten también regular la funcionalidad del receptor. La región amino terminal puede estar glicosilada y la región carboxilo terminal está expuesta a la interacción con otras moléculas de señalización, como cinasas y proteínas β-arrestinas, responsables de procesos de sensibilización, desensibilización e internalización (Lefkowitz 1998). Además, la región carboxilo terminal y los bucles intracelulares dos y tres son críticos para la transducción de la señal hacia el interior de la célula, ya que son los dominios de unión a la proteína G y, en la mayoría de los casos, los responsables de iniciar la señalización intracelular.

Los receptores acoplados a proteína G en general no comparten una gran homología en su secuencia aminoacídica (Probst *et al.* 1992; Kolakowski 1994), la única característica estructural común a todos los GPCR es la presencia de las siete hélices α que atraviesan la membrana y que están conectadas por bucles intracelulares y extracelulares alternados. Además de las variaciones de secuencia, estos receptores difieren en el tamaño y la función de los dominios amino terminal, carboxilo terminal y los seis bucles intracelular y extracelular alternados, otorgando cada uno de estos dominios propiedades específicas al receptor. Pese a que todos los GPCR comparten una estructura común, las distintas familias no tienen secuencias homólogas, indicando que, probablemente, no están relacionados filogenéticamente y que la similitud en su estructura transmembrana sólo se debe a los requerimientos funcionales comunes. No obstante, dentro de la superfamilia de los GPCR se han encontrado ciertas homologías (Attwood and Findlay 1994); así, estos receptores se han clasificado en diferentes familias según diferentes sistemas. Uno de los más conocidos es el sistema Kolakowski (Kolakowski 1994), en el que se clasifican los GPCR en 6 familias (A-F) según su estructura y

características genéticas. Hay tres familias mayoritarias, la familia A incluye aquellos receptores relacionados con el receptor de rodopsina y el receptor β_2-adrenérgico, la familia B contiene a los receptores relacionados con el receptor de glucagón, y la familia C incluye a los receptores metabotrópicos de glutamato y a los de ácido γ-aminobutírico (GABA). (Figura 3). Los receptores de feromonas de levadura constituyen dos subfamilias menores no relacionadas, la familia D (receptores STE2) y la familia E (receptores STE3). Por último, en el *Dictyostelium discoideum*, cuatro diferentes receptores de AMPc conforman una familia menor, pero única, la familia F.

En la figura 3 se ilustran las 3 familias mayoritarias.

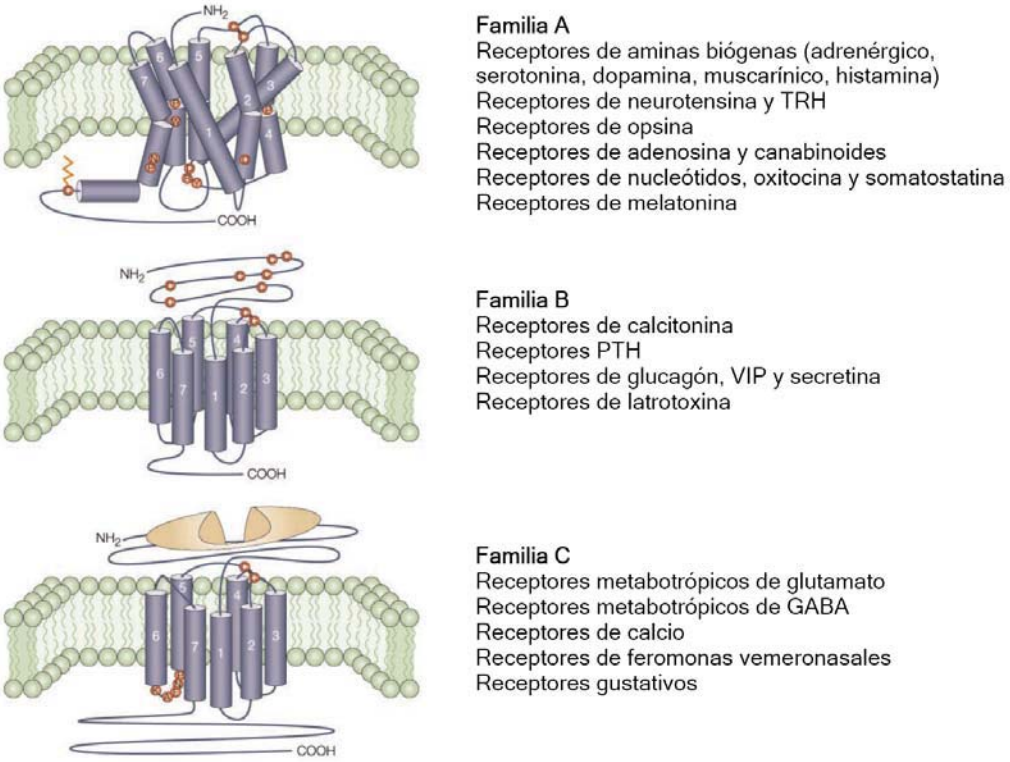

Figura 3. Representación esquemática de las tres principales familias de receptores acoplados a proteína G. Los residuos altamente conservados se indican en círculos rojos (Extraído de George, *et al*. 2002).

La familia A, también llamada *rodopsin-like* contiene el 90% de todos los GPCR, siendo la más grande y la más estudiada, e incluye a receptores para odorantes y una gran variedad de hormonas glicoproteicas y neurotransmisores. La homología entre este tipo de receptores es baja y limitada a un número de residuos altamente conservados. El alto grado de conservación entre estos residuos sugiere que todos ellos tienen un papel esencial en la integridad estructural y funcional de los receptores. El único residuo conservado en toda la familia A corresponde a la arginina del motivo Asp-Arg-Tyr (DRY) en el lado citoplasmático del tercer tercer segmento transmembrana (Probst *et al.* 1992) y podría estar involucrado en la

activación de la proteína G (Fraser *et al.* 1988). Además, los receptores de esta familia se caracterizan por tener un puente disulfuro que conecta el primer y el segundo bucle extracelular. Muchos receptores de esta familia tienen una cisteína palmitoilada en la cola carboxilo terminal que sirve de anclaje a la membrana plasmática (Figura 3 zigzag naranja). El estudio de la estructura cristalográfica de la rodopsina (Palczewski *et al.* 2000) indica que los dominios transmembrana están distorsionados y enroscados debido a la presencia del aminoácido prolina que distorsiona los dominios helicoidales transmembrana. En esta familia, el ligando se une en una cavidad formada por los dominios transmembrana, aunque para alguna subfamilia en los que los receptores son activados por pequeños péptidos, el reconocimiento se produce a nivel de los bucles extracelulares y del dominio amino terminal (George *et al.* 2002; Jacoby *et al.* 2006).

La familia B incluye aproximadamente 50 receptores diferentes para una variedad de hormonas peptídicas y neuropéptidos, como el péptido intestinal vasoactivo (VIP), la calcitonina, la hormona paratiroidea (PTH) y el glucagón. La principal característica de esta familia es un extremo amino terminal relativamente largo (aproximadamente 100 residuos), que contiene diversas cisteínas que forman una red de puentes disulfuro (Ulrich *et al.* 1998). Así, los ligandos peptídicos son reconocidos por el extenso dominio amino terminal de estos receptores (George *et al.* 2002; Jacoby *et al.* 2006). Son de morfología similar a la familia A, pero no parecen palmitoilarse y los residuos y motivos conservados son diferentes. Excepto por el puente disulfuro que conecta el primer y segundo bucle extracelular, esta familia no tiene ningún elemento en común con la familia A y el motivo DRY no existe. Se sabe poco de la orientación de los dominios transmembrana, pero teniendo en cuenta la divergencia de las secuencias aminoacídicas, probablemente son diferentes de los de la familia A.

La familia C, que contiene al receptor metabotrópico de glutamato, los receptores sensibles a calcio y al receptor de ácido γ-aminobutirico (GABA), se caracteriza por un largo extremo carboxilo y amino terminal (500-600 aminoácidos). La estructura del lugar de unión del ligando (representada en la figura 3 en amarillo) se ha deducido mediante estudios de cristalografía del extremo amino terminal del receptor metabotrópico de glutamato solubilizado y unido a glutamato (He *et al.* 2002). Se ha visto que forma un dímero unido por puente disulfuro (Pin *et al.* 2003) y que actúa como una planta carnívora, ya que puede abrirse y cerrarse en el proceso de unión de ligando (He *et al.* 2002). Excepto por las dos cisteínas conservadas en los bucles extracelulares 1 y 2 que forman un putativo puente disulfuro, esta familia no tiene ninguna característica común con las familias A y B. Una característica única de estos receptores es un tercer bucle intracelular corto y altamente conservado. Al igual que la familia B, no se conoce la orientación de los dominios transmembrana. (George *et al.* 2002; Jacoby *et al.* 2006).

Aunque la clasificación A-F está ampliamente aceptada, se ha realizado un estudio filogenético de toda la superfamilia de GPCR en el genoma de mamífero (comprendiendo alrededor del 2% de los genes en el genoma humano) que ha dado lugar a una nueva clasificación más precisa (Fredriksson *et al.* 2003). El análisis muestra que hay cinco familias principales para los GPCR humanos: *Glutamate, Rhodopsin, Adhesion, Frizzled/Tasted2 y Secretin* (la clasificación GRAFS, basada en sus iniciales) y que dentro de cada familia los receptores comparten un origen evolutivo común. Las familias *Rhodopsin* (A), *Secretin* (B), *Glutamate* (C) se corresponden con la clasificación A-F, mientras que las otras dos familias, *Adhesion y Frizzled,* no están incluidas en este sistema. En esta clasificación, la familia *Rhodopsin* sigue siendo la mayor, y se ha dividido en cuatro grupos principales con trece ramas distintas. Los autores de este nuevo sistema de clasificación defienden la teoría de que los receptores acoplados a proteína G surgieron a partir de un único predecesor común, que evolucionó a través de duplicaciones génicas, desde la mayor simplicidad en cuanto a sus orígenes a la enorme complejidad que muestra esta superfamilia de receptores en la actualidad. La enorme diversidad que alcanza esta superfamilia de proteínas de membrana da a entender el gran papel que juegan en la fisiología de cualquier organismo.

1.1.2 VÍAS DE SEÑALIZACIÓN

Cuando el receptor es activado por el ligando se inicia una serie de eventos intracelulares que modulan la función celular. Estos eventos pueden ser independientes o dependientes de la proteína G a la que se encuentre acoplado el receptor y dependen de la maquinaria molecular con la que cuente la célula. Las proteínas G están presentes en todos los organismos eucariotas y tienen un papel esencial en la transducción de señales, ya que asocian al receptor con las proteínas efectoras localizadas en el interior celular.

Las proteínas G son proteínas heterotriméricas, constituidas por las subunidades α (39-46 kDa), β (37 kDa) y γ (8 kDa). Clásicamente, la unidad básica de transducción de la señal está formada por el receptor, por la proteína heterotrimérica G y por un efector. Cuando el receptor es activado por un ligando, se inducen cambios conformacionales que se transmiten desde el receptor a la proteína G que hacen que la subunidad α libere GDP permitiendo la unión de GTP. Esta acción desestabiliza el trímero permitiendo un cambio conformacional entre la subunidad α y las subunidades βγ distanciándolas (Marinissen and Gutkind 2001; Maurice *et al.* 2010). La subunidad Gα posee un lugar de unión con alta afinidad por nucleótidos de guanina (GTP o GDP), así como actividad GTPasa (Hepler and Gilman 1992). El cambio de conformación inducido por la unión del ligando al receptor repercute en la afinidad de la subunidad Gα por los

nucleótidos de guanina, haciéndola más afín por GTP (Bourne *et al.* 1991; Maurice *et al.* 2010; Rasmussen *et al.* 2011). Tanto la subunidad Gα como el complejo Gβγ son moléculas señalizadoras que, actuando con diferentes moléculas efectoras, pueden activar o inhibir una gran variedad de segundos mensajeros. Las 16 proteínas Gα de mamíferos se agrupan en cuatro grandes familias según su estructura primaria y la cascada de señalización que activan (Milligan 2006; Milligan and Kostenis 2006). Los miembros de la familia estimuladora $G\alpha_s$ se acoplan a la adenilato ciclasa y causan un incremento en los niveles de AMPc intracelular. Los miembros de la familia $G\alpha_{i/o}$ inhiben la adenilato ciclasa además de actuar sobre otros eventos de señalización. Los miembros de la familia $G\alpha_{q/11}$ activan la fosfolipasa Cβ (PLCβ), provocando la hidrólisis intramembrana de fosfatidilinositol-4,5-bifosfato (PIP_2) a inositol-1,4,5-trifosfato (IP_3) y diacilglicerol (DAG), lo que desencadena la liberación de iones calcio desde las reservas intracelulares y el aumento de la actividad de la PKC. Finalmente, los miembros de la familia $G\alpha_{12/13}$ regulan las proteínas Rho. Los dímeros Gβγ son combinaciones de cinco isoformas de la subunidad Gβ y catorce isoformas de la subunidad Gγ (Milligan and Kostenis 2006), y cada isoforma individual puede asociarse con un conjunto de efectores y reguladores. Los dímeros Gβγ señalizan a través de un gran número de efectores, incluyendo canales iónicos, fosfolipasas, fosfoinositol cinasas, y la vía ras/raf/ERK. Algunos ejemplos de efectores incluyen el canal rectificador del influjo de potasio regulado por la proteína G (GIRK1-4), el canal de calcio dependiente de voltaje (VDCC), las fosfolipasas A_2 (PLA_2) y PLCβ y el intercambiador de Na^+/H^+ (NHE) (Jacoby *et al.* 2006). Dos ejemplos típicos de cascadas de señalización iniciadas por receptores acoplados a proteína G son las que conducen a la formación de IP_3/DAG y AMPc como segundos mensajeros y se ilustran en la Figura 4.

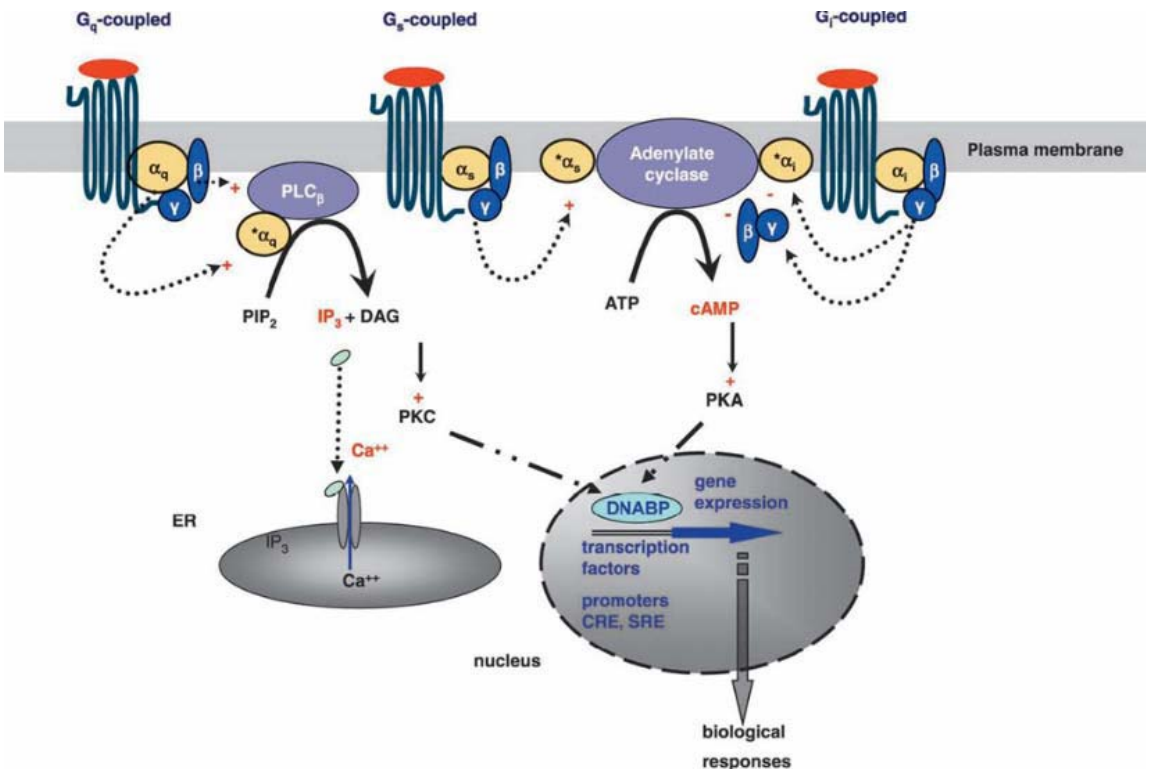

Figura 4. Vías de señalización clásicas inducidas por receptores acoplados a proteína G. Al ser estimulado por el agonista el receptor activa a su vez a la proteína G correspondiente ($G_{\alpha q}$, $G_{\alpha s}$ o $G_{\alpha i}$) (Extraído de Jacoby, *et al*. 2006).

Muchas de las respuestas mediadas por estos receptores no consisten únicamente en la estimulación de segundos mensajeros convencionales, si no que son el resultado de la integración de diferentes redes de señalización, entre las que se incluyen la vía de las MAPKs y las JNKs. Se ha descrito la activación por proteína G de sistemas efectores que clásicamente se creían únicamente activados por receptores de factores de crecimiento con actividad tirosina cinasa (RTK). Un ejemplo característico es la activación de las rutas de señalización de las MAPKs (*Mitogen Activated Protein Kinases*), entre las que se encuentran las ERKs (*Extracelular Regulated Kinases*) y p38 (Crespo *et al.* 1995; Yamauchi *et al.* 1997; Schulte and Fredholm 2003; Rozengurt 2007). En la activación de la vía de las MAPKs por GPCR se creía que el mecanismo involucraba proteínas G sensibles a la toxina de la *Bordetella pertussis* ($G\alpha_{i/o}$) y que dependía fundamentalmente del complejo Gβγ y de tirosina cinasas no identificadas (van Corven *et al.* 1993; Faure *et al.* 1994; Koch *et al.* 1994). Posteriormente, un buen número de investigaciones orientadas a este tópico han permitido deducir que en ausencia de ligandos para los RTKs, la activación de receptores acoplados a proteínas Gαq inducía la fosforilación de la proteína Shc y la formación del complejo Shc-Grb2 (Cazaubon *et al.* 1994; Chen *et al.* 1996; Sadoshima and Izumo 1996). Puesto que ambas proteínas adaptadoras están involucradas en la activación de la vía Ras-Raf-MEK-ERK a través de su unión a las fosfotirosinas de un RTK

activado, se sugirió que el RTK había sido activado sin necesidad de interactuar con su ligando. Por lo tanto, en ausencia de ligandos para los RTKs, la activación de receptores acoplados a proteína G puede inducir la estimulación de un RTK generando señales mitogénicas. Este fenómeno se denominó transactivación y puede ser mediado por varios mecanismos, incluyendo la activación de RTK a través de tirosina cinasas citoplasmáticas (NRTK), la formación de complejos entre GPCR y RTK, y la liberación de ligandos de RTK (Marinissen and Gutkind 2001). Una vez transactivado, el RTK inicia una cascada de señalización idéntica a la generada por su propio ligando, es decir, la activación de las MAPK es a través de la vía Ras/Raf/MEK/ERK (Figura 5). El proceso es iniciado con las subunidades Gβγ dando lugar a que se reclute Sos hacia la membrana. Ello activa el intercambio de GDP por GTP en la proteína Ras, siendo esta proteína el intermediario que conecta la cascada de señalización generada por la activación o transactivación de un RTK con la fosforilación de ERK (Marinissen and Gutkind 2001). Ras es una GTPasa pequeña, que es regulada por proteínas liberadoras de nucleótidos de guanina (GNRPs) y por proteínas estimuladoras de la actividad de GTPasa (GAPs). Las GNRPs activan a Ras al favorecer el intercambio de GDP por GTP, mientras que las GAPs finalizan la señalización al aumentar la actividad de GTPasa intrínseca a Ras que hidroliza el GTP unido a GDP (Matozaki *et al.* 2000). Tanto las GNRPs como las GAPs son proteínas que se activan por unión a fosfotirosinas presentes en los RTKs activados. Cabe destacar que también existen otras vías independientes del fenómeno de transactivación que pueden inducir la activación de Ras. Como por ejemplo, vías dependientes de la concentración de calcio intracelular inducidas por receptores acoplados a Gαq (Figura 5).

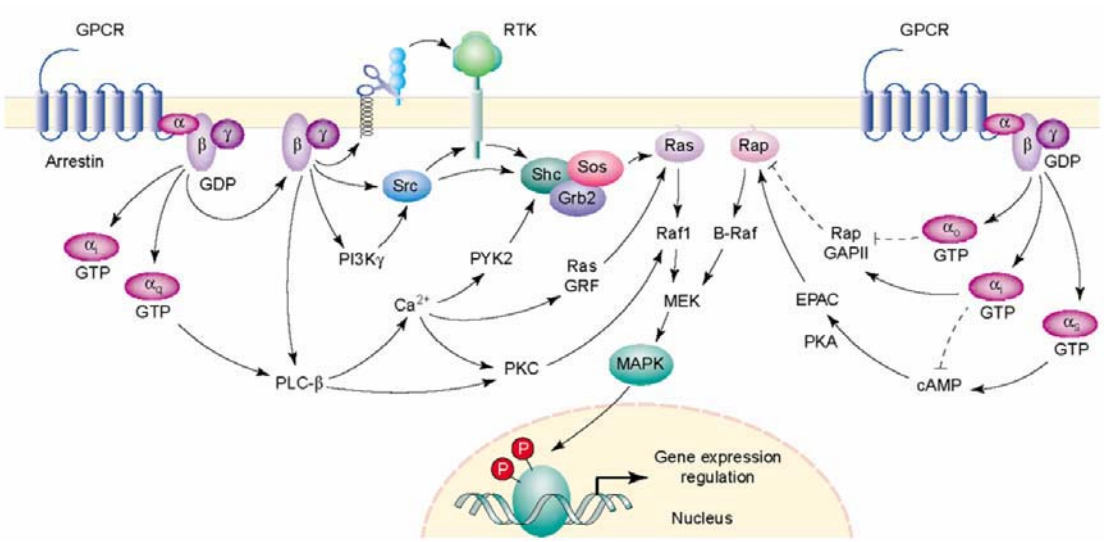

Figura 5. Representación de algunas de las vías que enlazan los GPCR con la vía de las MAPK (Extraído de Marinissen and Gutkind 2001).

Una vez Ras está activada, inicia la cascada de ERK al unirse y activar a Raf, una serina/treonina cinasa que a su vez fosforila y activa a la cinasa de ERK/MAPK (denominada MEK), enzima que fosforila residuos de serina/treonina y de tirosina. La activación de ERK requiere de su fosforilación en un residuo de treonina y en uno de tirosina, separados por un solo aminoácido. Esta función sólo puede ser realizada por una enzima altamente especializada, por lo que se considera a MEK una enzima limitante en la activación de ERK que hace altamente específico este proceso. La activación de MEK también puede lograrse a través de B-Raf, cinasa que es activada por Rap, que a su vez es activada por la proteína cinasa A (PKA) dependiente de AMPc y por lo tanto bajo el control de receptores acoplados a Gαs (Figura 5). Finalmente, la ERK fosforilada fosforila a proteínas diana en el citoplasma celular, activando por lo tanto una respuesta. Según la magnitud de la activación de ERK, ésta pasa del citoplasma al núcleo y regula, por fosforilación, a otras cinasas y factores de transcripción (Pelech and Sanghera 1992; Davis 1995; Treisman 1996).

Un aspecto muy importante es que los GPCR pueden actuar no sólo a través de la proteína heterotrimérica G, sino que también actúan por vías de señalización independientes de proteínas G y de RTK y que, probablemente, implican la unión directa de Src y/o β-arrestina al receptor (Daaka *et al.* 1998; Lefkowitz 1998; Luttrell *et al.* 1999; Brzostowski and Kimmel 2001; Luttrell and Lefkowitz 2002). Un ejemplo paradigmático es la señalización mediada por la fosforilación del receptor por GRK (G protein-coupled Receptor Kinases), la unión de β–arrestinas y el subsiguiente secuestro del GPCR de la superficie celular (Krupnick and Benovic 1998), que no sólo es importante para la finalización de la señal mediada por proteína G, sino que también juega un papel importante en el inicio de la señal mediada por β–arrestinas (Luttrell *et al.* 1999). Las β–arrestinas desempeñan un papel en la señalización celular que va más allá del simple desacoplamiento entre el receptor y la proteína G. El hecho que las β–arrestinas puedan interaccionar directamente con tirosina cinasas de la familia de las Src y con componentes de la cascada de MAPK (Perry and Lefkowitz 2002), sugiere que las β–arrestinas pueden funcionar como adaptadores o scaffolds reclutando proteínas involucradas en la señalización de un determinado receptor (Figura 6). De esta manera, se ha demostrado la capacidad de diferentes receptores acoplados a proteína G de reclutar componentes de las cascadas de las JNK o las ERK, incluyendo las cinasas más relevantes de la cascada, como pueden ser JNK3, Raf-1, MEK1 o ERK1/2. Estos complejos pueden permanecer unidos incluso durante la internalización del receptor, presentando diferentes localizaciones subcelulares, presumiblemente en los endosomas hacia donde el receptor es conducido en su proceso de internalización y por lo tanto, aproximando las cinasas a sus posibles sustratos citosólicos (DeFea *et al.* 2000a; DeFea *et al.* 2000b; Pierce *et al.* 2001).

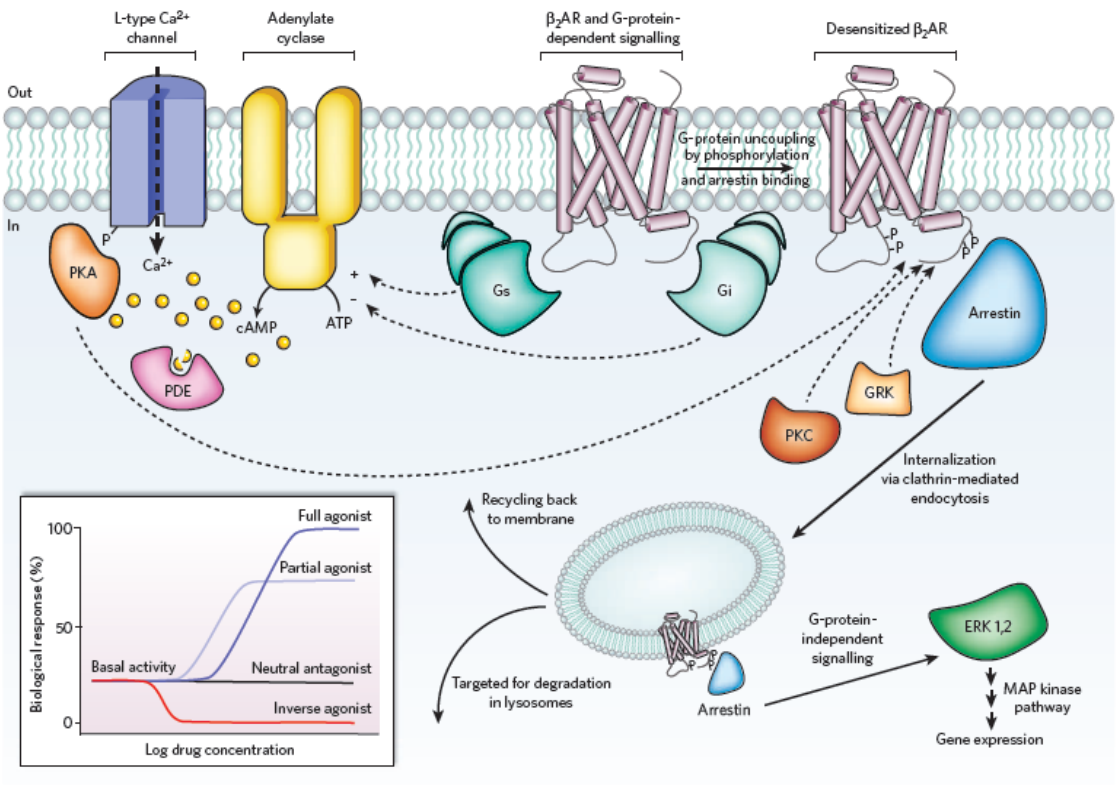

Figura 6. Transducción de señal en los receptores acoplados a proteína G. (Extraído de Rosenbaum *et al.* 2009).

1.1.3. REGULACIÓN DE LA ACTIVIDAD DE LOS GPCR POR DESENSIBILIZACIÓN

Cuando un agonista interacciona con un GPCR, normalmente comporta una rápida atenuación de la respuesta del receptor. Este proceso se denomina desensibilización y es consecuencia de una combinación de diferentes mecanismos (Golan *et al.* 2009; Moser *et al.* 2010). Estos mecanismos incluyen el desacoplamiento del receptor de las proteínas G como consecuencia de su fosforilación (Hausdorff *et al.* 1989; Lohse *et al.* 1990; Ferguson 2001; Golan *et al.* 2009), la internalización del receptor de la superficie celular a compartimentos intracelulares (Hermans *et al.* 1997; Trejo *et al.* 1998; Ferguson 2001), la disminución del número total de receptores debido a la disminución del RNA mensajero (ARNm) y de la síntesis proteica, así como la degradación de los receptores preexistentes (Jockers *et al.* 1999; Pak *et al.* 1999; Tsao *et al.* 2001; Prossnitz 2004). El tiempo en el que transcurren estos procesos puede variar de segundos, como ocurre con la fosforilación, a minutos en el caso de las endocitosis y horas para los casos de regulación de la expresión de los receptores. La desensibilización del receptor puede ser completa, como ocurre en sistemas olfatorios y visuales o atenuada, disminuyendo la potencia del agonista y su respuesta máxima, como ocurre con el receptor β_2 adrenérgico (Krupnick and Benovic 1998; Sakmar 1998). Sin embargo, el grado de

desensibilización del receptor depende de un gran número de factores que van desde la estructura del receptor al tipo de célula.

La forma más rápida por la cual un GPCR se desacopla de la proteína G es a través de modificaciones covalentes en el receptor como consecuencia de su fosforilación por cinasas intracelulares. Tanto las proteínas cinasas dependientes de segundo mensajero (cAMP-*dependent protein kinase* (PKA) y *protein kinase* C (PKC)) como las GRKs (G-protein coupled receptor kinases) fosforilan en residuos de serina y treonina del tercer bucle intracelular y del extremo carboxilo terminal del receptor (Lefkowitz *et al.* 1993; Krupnick and Benovic 1998; Ferguson 2001). Estas proteínas cinasas dependientes de segundo mensajero no sólo fosforilan GPCR activados por agonista, sino que también fosforilan indiscriminadamente receptores que no han sido expuestos a agonista (Hausdorff *et al.* 1989). Por el contrario, los miembros de la familia GRK fosforilan selectivamente receptores activados por agonista (Lohse *et al.* 1990; Ferguson 2001; Premont and Gainetdinov 2007), de forma que promueven la unión de cofactores citosólicos proteicos como las β-arrestinas, que desacoplan estericamente el receptor de la proteína G.

La internalización de los GPCR es un fenómeno común observado tras la estimulación por agonista, pero no está claro cual es su relación con la desensibilización y resensibilización del receptor. Mientras hay alguna evidencia que apunta a que este fenómeno es parte del proceso de desensibilización, otras sugieren que la internalización es una de las formas principales por la cual el receptor es resensibilizado. De hecho, el tráfico de receptores desacoplados a compartimentos endosomales permite la desfosforilación y el reciclaje del receptor a la superficie celular (Krueger *et al.* 1997; Ferguson 2001; Boulay and Rabiet 2005). Además parte de los receptores internalizados pueden degradarse tras la exposición prolongada al agonista, lo que implica que el receptor sea marcado para entrar en la vía de degradación (Bohm *et al.* 1997). El mecanismo de internalización de GPCR mejor caracterizado es a través de clatrina (Kelly *et al.* 2008). Una vez el receptor es fosforilado por GRK, las β-arrestinas actúan como moléculas reguladoras que interactúan con componentes de la vía endocítica mediada por vesículas de clatrina. En respuesta a la activación de los GPCR, las proteínas β-arrestinas citosólicas translocan hacia la membrana plasmática uniéndose a los receptores a la vez que se inicia el proceso de endocitosis mediado por clatrina (Ritter and Hall 2009) (Figura 7).

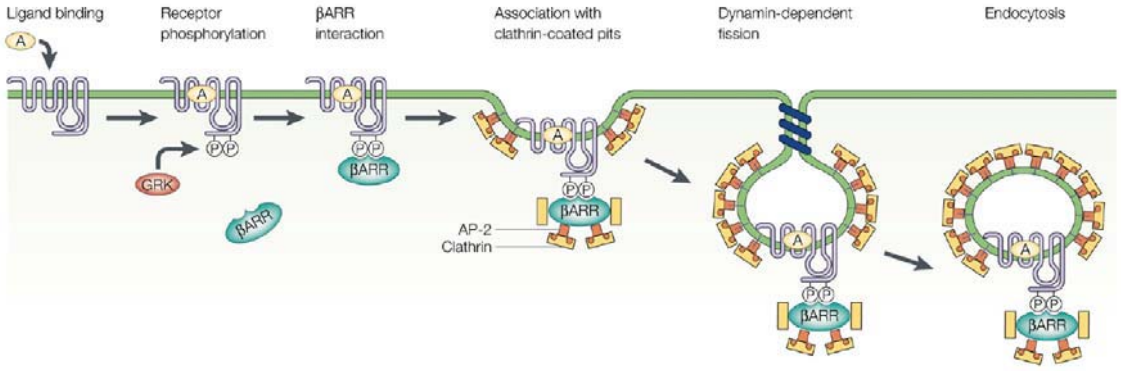

Figura 7. Ejemplo de un modelo propuesto para la desensibilización, internalización y downregulation de los GPCR (Extraído de Pierce and Lefkowitz 2001).

No obstante, no todos los GPCR necesariamente se internalizan por un mecanismo dependiente de β-arrestina y clatrina. Existen evidencias experimentales que sugieren que los GPCR pueden internalizarse por vías endocíticas alternativas. Algunos GPCR se han encontrado en estructuras de membrana ricas en colesterol denominadas caveolas (Chun *et al.* 1994; Huang *et al.* 1997; Burgueño *et al.* 2003). Estos dominios también son dominios de señalización donde los GPCR pueden localizarse e interaccionar específicamente con proteínas de señalización (Ostrom and Insel 2004). Además, las caveolas tienen un papel clave en la desensibilización y tráfico de los receptores ya que el uso de agentes bioquímicos que disrumpen estas estructuras son efectivos en la inhibición de la endocitosis de ciertos GPCR (Gines *et al.* 2001; Escriche *et al.* 2003; Kong *et al.* 2007; Wu *et al.* 2008). Por otra parte, ciertos receptores son susceptibles de usar una tercera vía endocítica alternativa. Aunque no se han identificado ni las proteínas de cubierta, ni las proteínas adaptadoras para la generación de estas vesículas (Claing *et al.* 2000).

Una vez internalizados, los receptores son marcados para entrar en vías de reciclaje o de degradación. Algunos GPCR, entre los que se incluye el receptor β_2-adrenérgico, pueden ser reciclados a la membrana plasmática, como receptores totalmente competentes después de unos minutos de haber sido internalizados (Pippig *et al.* 1995). Otros receptores, como el receptor de vasopresina tipo 2, es retenido dentro de la célula durante un cierto periodo de tiempo antes de ser reciclado a la membrana celular (Innamorati *et al.* 2001), mientras que algunos, como los receptores de δ-opiodes o de trombina son mayoritariamente degradados (Tsao and von Zastrow 2000). Sin embargo, para la mayoría de GPCR una parte es reciclada y otra parte es degradada, como ocurre con los receptores de adenosina (Escriche *et al.* 2003).

1.1.4 ACTIVIDAD CONSTITUTIVA Y LIGANDOS DE LOS GPCR

La activación de un receptor acoplado a proteína G se explica como un cambio de conformación que sufre el receptor una vez une el ligando agonista, pasando de un estado inactivo a uno activo, existiendo un equilibrio entre ambos estados. La actividad constitutiva que presentan estos receptores representa una isomerización del receptor al estado activo en ausencia de ligando (Seifert and Wenzel-Seifert 2002). Como consecuencia de este cambio en el equilibrio conformacional del receptor, se produce el intercambio GDP-GTP en las proteínas G acopladas al receptor, aumentando la actividad basal de dicha proteína G y de los subsiguientes sistemas efectores. Este fenómeno fue descrito por primera vez para el receptor δ-opiodes (Costa and Herz 1989).

De esta manera, en ausencia de ligandos, existen conformaciones del receptor en estado activo o en estado inactivo que están en equilibrio y este equilibrio puede desplazarse a un lado o a otro en función de la unión de distintos ligandos al receptor (Seifert and Wenzel-Seifert 2002). La actividad constitutiva es inhibida por la acción de los compuestos conocidos como agonistas inversos, que actúan sobre el receptor de manera que estabilizan el estado inactivo y por lo tanto, minimizan el intercambio GDP-GTP. Los agonistas inversos pueden ser parciales o totales y se diferencian en su capacidad de estabilizar al receptor en su estado inactivo en un menor o mayor grado respectivamente, reduciendo la actividad basal o constitutiva del receptor. Los agonistas inversos son compuestos que actúan de forma opuesta a los agonistas, los cuales estabilizan el receptor en la forma activa y por lo tanto, inducen su señalización. La más favorable para la señalización del receptor es aquella conformación estabilizada por un agonista total; seguidas por los agonistas parciales, que serían compuestos con una menor eficiencia para estabilizar el receptor en la conformación más activa y por lo tanto, promueven un menor intercambio GDP-GTP. Otro tipo de ligandos son los antagonistas neutros o simplemente, antagonistas que no alteran el equilibrio entre las conformaciones activa e inactiva, pero tienen la capacidad de bloquear el efecto de los agonistas y de los agonistas inversos. El tipo de ligandos y los efectos producidos se esquematizan en la figura 8.

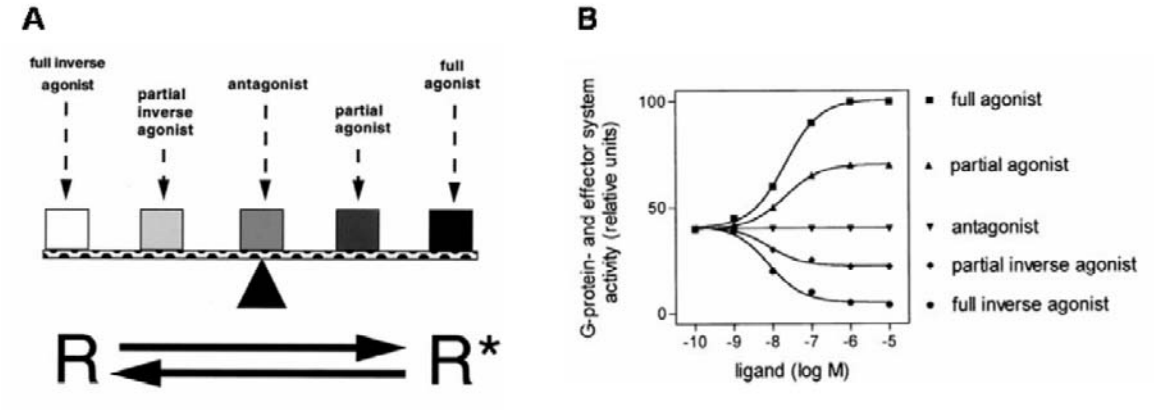

Figura 8. Activación de los receptores acoplados a proteína G según el modelo de dos estados. A) Modelo de dos estados que asume la isomerización del receptor de un estado inactivo R a uno activo R*. B) Acción de los diferentes tipos de ligandos sobre la actividad constitutiva del receptor (Extraído y modificado de Seifert and Wenzel-Seifert 2002).

Los ligandos también pueden ser clasificados en función del lugar de unión al receptor. La mayoría de ligandos de los GPCR que actúan como agonistas, antagonistas o agonistas inversos, se unen al mismo dominio del receptor reconocido por los agonistas endógenos, es decir, el lugar de unión ortostérico (Neubig *et al.* 2003). En cambio, muchos GPCR poseen sitios alostéricos topográficamente distintos. Esto ha llevado a la identificación de ligandos que actúan como moduladores alostéricos, que pueden regular indirectamente la actividad de los ligandos ortostéricos y/o mediar directamente efectos agonista/agonista inverso (Christopoulos 2002; Gilchrist 2007; May *et al.* 2007; Bridges and Lindsley 2008).

Tanto los ligandos alostéricos como los ortostéricos de los GPCR han despertado gran interés farmacológico. Los GPCR representan la familia de proteínas de mayor impacto social, terapéutico y económico (Fredholm *et al.* 2007; Lefkowitz 2007). Hoy en día, más del 50% de los fármacos, con unas ventas anuales en el mundo que superan los 50 billones de dólares, regulan la función de los GPCR, y un 30% de estos fármacos está directamente dirigidos a los GPCR (Liebmann 2004; Jacoby *et al.* 2006; Lundstrom 2006). Los GPCR están involucrados en una amplia diversidad de enfermedades como son; alergias, disfunción cardiovascular, depresión, obesidad, cáncer, dolor, diabetes, y una variedad de trastornos del sistema nervioso central.

1.2 OLIGOMERIZACIÓN DE GPCR

Las características estructurales y la localización subcelular de los GPCR permite a estos receptores interaccionar con una gran variedad de proteínas, tanto en el lado intracelular como extracelular de la membrana plasmática, así como, exhibir interacciones proteína-proteína con otros receptores o canales iónicos a nivel de membrana plasmática (Franco *et al.* 2003). Estas interacciones determinan las propiedades del receptor, como la compartimentación celular o la selección de señal y pueden promover el ensamblaje en complejos que integran una función. Entre las proteínas que pueden interaccionar con los GPCR se incluyen los propios miembros de la misma familia.

Los GPCR tienen una topología que permite su interacción con una amplia variedad de proteínas para ejercer unas determinadas funciones (Figura 9).

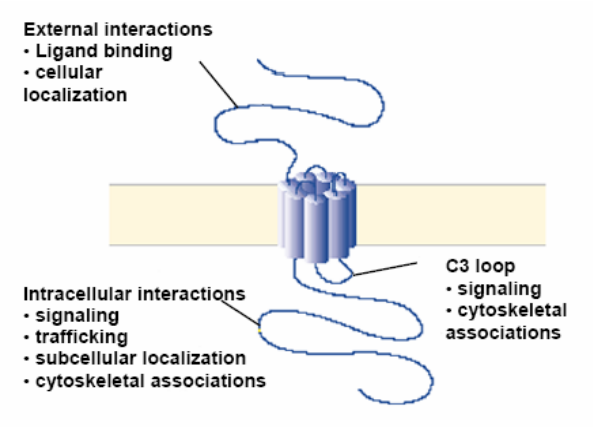

Figura 9. Representación esquemática de un GPCR con las regiones identificadas implicadas en la interacción con otras proteínas y su función genérica.

Las proteínas que interactúan con los GPCR están involucradas principalmente, en la organización de estructuras supramoleculares en las cuales se incluye todo tipo de receptores, proteínas implicadas en la transducción de señal e incluso proteínas citoesqueléticas (Franco *et al.* 2003).

En el espacio extracelular, donde tiene lugar la unión a ligando, las regiones de los GPCR implicadas en la interacción con proteínas son, en la mayoría de casos, secuencias presentes en el extremo amino terminal, ya que los bucles extracelulares son muy cortos. Existen crecientes evidencias de que las interacciones receptor-proteína extracelulares pueden jugar un papel importante en la farmacología de los GPCR. Un ejemplo, es el caso de la enzima adenosina desaminasa (ADA), proteína multifuncional localizada en el citoplasma pero también en la superficie celular anclada a diferentes proteínas como los receptores de adenosina A_1 y A_{2B} (Saura *et al.* 1996; Herrera *et al.* 2001; Gracia *et al.* 2008). Estas interacciones parecen ser esenciales para que estos receptores muestren el estado de alta afinidad por su ligando.

En la cara intracelular, tanto el extremo carboxilo terminal como el tercer bucle intracelular (IC3) pueden presentar un tamaño considerable en los GPCR, por lo que son estas regiones las más probables para interaccionar con proteínas implicadas en la señalización, en la localización subcelular y en el tráfico de estos receptores. La naturaleza de estas interacciones puede ser transitoria, por ejemplo para señalizar, o mucho más estables. Un ejemplo de proteína citosólica que interactúa con GPCR sería la calmodulina (CaM), un pequeño péptido con capacidad para unirse a distintos dominios citoplasmáticos de diferentes GPCR, entre los que se encuentra el extremo carboxilo terminal del receptor A_{2A} de adenosina o el tercer bucle intracelular del receptor D_2 de dopamina, desarrollando una señal dependiente de calcio (Bofill-Cardona *et al.* 2000; Woods 2004; Navarro *et al.* 2009). Respecto a las interacciones receptor-proteína intracelulares, además de las clásicas implicadas en la transducción de señal, se han descrito un gran número de interacciones que son la base de la formación de complejos macromoleculares responsables de la localización de estos receptores en determinados dominios celulares. Las proteínas andamio o *scaffolding proteins* o *scaffolds,* actualmente, son consideradas como organizadoras de complejos multiproteicos en diversos compartimentos celulares como por ejemplo, las densidades post-sinápticas neuronales y son las responsables de mantener estos receptores en esta localización (Hering and Sheng 2001; Huber 2001).

A nivel de la membrana plasmática, desde mediados de los años 90, diversos estudios han demostrado la oligomerización de numerosos GPCR (George *et al.* 2002). Estos receptores, clásicamente, se han considerado como unidades funcionales independientes, por lo que el descubrimiento de la oligomerización revolucionó la forma de afrontar el estudio de su funcionalidad. Hoy en día, se acepta que la oligomerización es un hecho común en la biología de estos receptores y que pueden formar homodímeros, heterodímeros y/u oligómeros de orden superior (Bouvier 2001; Devi 2001; Agnati *et al.* 2003; Franco *et al.* 2003; Prinster *et al.* 2005; Pin *et al.* 2007; Carriba *et al.* 2008; Ferré *et al.* 2009; Ferré *et al.* 2010). Los olígomeros presentan características funcionales diferentes a las de los receptores que los constituyen; así, la oligomerización confiere nuevas propiedades a los GPCR, lo que establece un posible mecanismo para generar nuevas funciones en estos receptores. Por tanto, este fenómeno ha dado lugar a un nuevo nivel de complejidad que gobierna la señalización y regulación de estas proteínas.

1.2.1 INTERACCIÓN ENTRE RECEPTORES ACOPLADOS A PROTEINA G

A mediados de los años 70, ciertas evidencias farmacológicas indirectas llevaron a pensar a los investigadores en la posibilidad de que los receptores acoplados a proteína G pudieran actuar como dímeros. Las complejas curvas de unión, tanto de agonistas como de antagonistas de estos receptores, se interpretaron como evidencias de una cooperatividad que se podía explicar mediante interacciones entre monómeros en complejos diméricos o multiméricos (Limbird *et al.* 1975). Pero, no fue hasta la década de los 90 que se reabrió la cuestión a raíz de los estudios de complementación y de coinmunoprecipitación de Maggio y colaboradores (Maggio *et al.* 1993), que sugirieron la formación de heterodímeros entre GPCR. Estos autores utilizaron quimeras de los receptores α_2-adrenérgicos y M_3 muscarínicos compuestas de los cinco primeros dominios transmembrana de uno de los receptores y de los dos últimos dominios del otro receptor, y viceversa. Cuando cada quimera se expresaba independientemente, no se podía observar ni unión ni señalización tras la exposición a ligando, pero cuando ambas eran co-transfectadas se recuperaba la unión y la señalización tanto para ligandos adrenérgicos como muscarínicos.

Otros experimentos de tipo bioquímico apoyaban también la idea de la oligomerización de los receptores acoplados a proteína G. Utilizando una estrategia de coinmunoprecipitación usando los receptores β_2-adrenérgicos marcados con diferentes epítopos se obtuvo una evidencia bioquímica directa de la formación de homodímeros (Hebert *et al.* 1996). Cuando los receptores β_2-adrenérgicos marcados con los epítopos Myc y HA se co-expresaban y se inmunoprecipitaban con un anticuerpo contra el epítopo Myc, se detectaba inmunoreactividad para el epítopo HA en los inmunoprecipitados, lo que fue considerado como una evidencia de una interacción intermolecular entre los dos tipos de receptores diferencialmente marcados. Mediante aproximaciones similares de coinmunoprecipitación se ha demostrado la dimerización de receptores tales como los $GABA_B$ (White *et al.* 1998), los mGlu5 (Romano *et al.* 1996) o los δ-opiodes (Jordan and Devi 1999), entre otros.

Durante la última década, diversos descubrimientos han puesto de manifiesto que las asociaciones proteína-proteína pueden ser entre dos monómeros para formar un dímero o entre múltiples monómeros para formar oligómeros (Bouvier 2001; Devi 2001; Rios *et al.* 2001; Agnati *et al.* 2003; Franco *et al.* 2003; Terrillon and Bouvier 2004; Agnati *et al.* 2005; Prinster *et al.* 2005; Milligan 2006; Ferré *et al.* 2009) y se ha podido detectar la expresión de oligómeros de receptores in vivo (Vassart 2010). La dimerización no está limitada sólo a la formación de homodímeros (homómeros), sino que también pueden interaccionar con otros miembros

cercanos o alejados de la familia de GPCR para formar heterodímeros (hetero-olígomeros). La homodimerización está definida como la asociación física entre proteínas idénticas, mientras que la heteromerización es la asociación entre proteínas distintas. Esta asociación puede ser entre dos monómeros para formar dímeros o entre múltiples monómeros para formar olígomeros (Ferré *et al.* 2009; Rozenfeld and Devi 2011).Ya que las técnicas disponibles hasta la fecha no permiten distinguir entre dímeros u olígomeros, el término dímero es a menudo usado entendiendo que es la forma más simple de una unidad funcional oligomérica.

Se ha demostrado la formación de dímeros para una gran variedad de receptores. En las tablas 1 y 2 se describen algunos ejemplos de homodímeros y heterodímeros.

Tabla 1. Ejemplos de homodímeros

Familia 1	
Adenosina A_1	Serotonina 5-HT_{1B}
Adenosina A_{2A}	Serotonina 5-HT_{1D}
Angiotensina II AT_2	Somatostatina $SSTR_{1A}$
Bradiquinina B_2	Somatostatina $SSTR_{1B}$
Dopamina D_1	Somatostatina $SSTR_{1C}$
Dopamina D_2	Somatostatina $SSTR_{2A}$
Dopamina D_3	Tirotropina
Histamina H_2	Vasopresina V_2
Histamina H_4	β-adrenérgico
Hormona Luteinizante	
Melatonina MT_1	**Familia 2**
Melatonina MT_2	Hormona liberadora de gonadotropina
Muscarinico M_2	
Muscarinico M_3	Repta IgG
Opiode σ	
Opiode k	**Familia 3**
Opiode μ	$GABA_BR_1$
Citoquina CCR2	$GABA_BR_2$
Citoquina CCR5	Metabotropico de glutamato $mGlu_1$
Citoquina CXCR4	Metabotropico de glutamato $mGlu_5$
	Sensor de Ca^{2+}

Tabla 2. Ejemplos de heterodímeros

Adenosina A_1-Dopamina D_1
Adenosina A_1-$mGlu_1$
Adenosina A_1-Purinérgico $P2Y_1$
Adenosina A_{2A}-Dopamina D_2
Adenosina A_{2A}-$mGlu_5$
Angiotensina AT_1-AT_2
Angiotensina AT_1-Bradiquinina B_2
Dopamina D_2-Dopamina D_3
$GABA_BR_1$-$GABA_BR_2$
Melatonina MT_1- MT_2
Muscarinico M_2-M_3
Opiode σ-β-adrenérgico
Opiode σ-K
Opiode σ-μ
Opiode k-β-adrenérgico
Citoquina CCR2-CCR5
Serotonina 5-HT_{1B}-5-HT_{1D}
Somatostatina $SSTR_{1A}$-$SSTR_{2C}$
Somatostatina $SSTR_{1B}$-Dopamina D_2
Somatostatina $SSTR_{1B}$-$SSTR_{2A}$
TIR1-TIR3
TIR2-TIR3

El ensamblaje de olígomeros proteicos permitiría expandir la diversidad con un número limitado de elementos modulares, esto es más la regla que la excepción dentro de la Biología. Hasta hace poco, se creía únicamente que el conjunto de interacciones intramoleculares podían caracterizar las conformaciones activas e inactivas tras la unión del ligando. Actualmente, ya hay evidencias de que además de las interacciones específicas intramoleculares, las interacciones intermoleculares entre más de un receptor en la formación de homo- y hetero-olígomeros también son importantes para definir los estados de activación de un receptor. Por tanto, se ha propuesto que las interacciones intermoleculares participan en la actividad de los GPCR (Brady and Limbird 2002). Las interacciones entre GPCR son cruciales para entender el variado cross-talk que se observa, sobre todo entre receptores de neurotransmisores (Casadó *et al.* 2007; Casadó *et al.* 2009a; Casadó *et al.* 2009b). La oligomerización de receptores neuronales permite formular hipótesis sobre el alto grado de diversidad y plasticidad que es característico de una estructura altamente organizada y compleja como es el cerebro. El número creciente de publicaciones en este campo ha hecho necesario establecer nuevas definiciones y dotar de nomenclatura a los homómeros y heterómeros de GPCR, como recientemente han publicado Ferré y colaboradores (Ferré *et al.* 2009).

1.2.2 ESTRUCTURA CUATERNARIA DE LOS DÍMEROS DE GPCR

Para explicar el fenómeno de la dimerización de los receptores acoplados a proteína G se pueden considerar dos posibilidades: que estas interacciones sean directas, implicando contacto entre ambos receptores, o bien que sean indirectas, cuando son necesarias otras proteínas que hagan de puente, como pueden ser las proteínas del citoesqueleto. Las interacciones directas entre miembros de la familia de GPCR no precisan de otras proteínas. En el caso de las interacciones indirectas entre GPCR hace falta la mediación de terceras proteínas. Los dominios intracelulares de los GPCR se unen a un gran número de proteínas citosólicas, algunas de las cuales, por sus características intrínsecas, han sido propuestas como posibles candidatas a participar en la dimerización de los receptores con los que interaccionan. Muchas de estas proteínas son proteínas andamio o *scaffolding proteins*, que, como se ha mencionado anteriormente, proporcionan una estructura compleja en la cual diversos receptores pueden interaccionar entre ellos y con otras proteínas involucradas en la transducción de señal, controlando la velocidad y la especificidad de dicha señalización (Ciruela *et al.* 2005).

Se cree que en la mayoría de las interacciones directas los olígomeros se pre-forman en el retículo endoplasmático (RE), por lo que no son modulables por ligando, entendiendo la modulación como la formación o destrucción del oligómero. La oligomerización, y especialmente la producida por interacciones directas, puede conferir nuevas características a los receptores implicados ya que los cambios conformacionales sobre uno de los receptores se transmiten directamente al otro receptor, lo que constituye un nivel más de regulación de las funciones del receptor. La gran complejidad estructural que existe en esta superfamilia no permite pensar en un único mecanismo de interacción directa (Bouvier 2001). Así pues, las interacciones directas pueden tener lugar mediante enlaces covalentes (puentes disulfuro) y/o no covalentes (fuerzas hidrofóbicas y/o electroestáticas) entre los dominios transmembrana y/o los dominios intracelulares de los receptores (Figura 10).

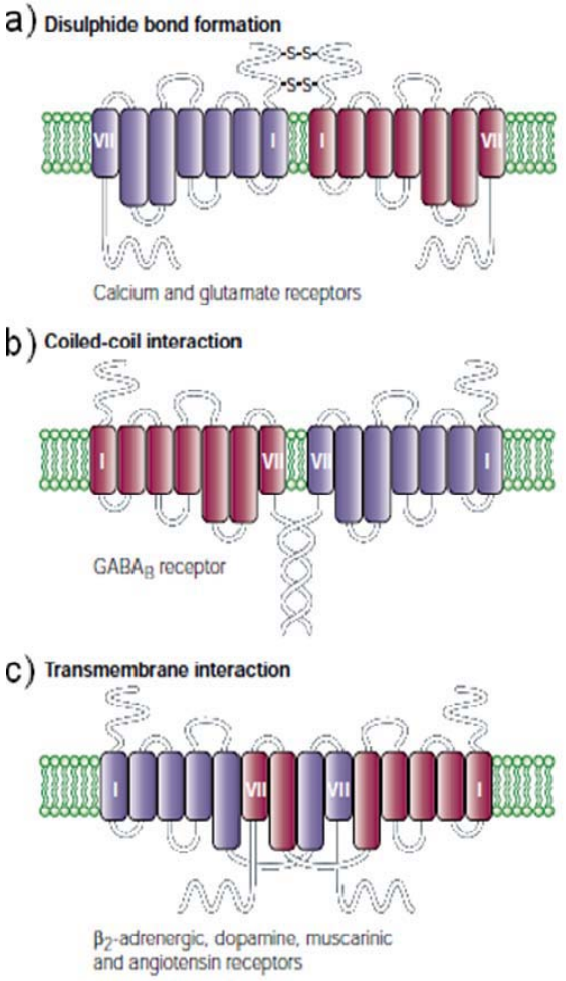

Figura 10. Mecanismos de oligomerización directa entre GPCR (Extraído de Bouvier 2001).

Se han encontrado distintas interacciones intermoleculares involucradas en varios homómeros y heterómeros de GPCR. En la familia C de receptores acoplados a proteína G el gran dominio amino terminal extracelular contiene varios residuos de cisteína que pueden contribuir a la dimerización mediante puentes disulfuro (Romano *et al.* 1996; Robbins *et al.* 1999; Romano *et al.* 2001). Este es el caso de los receptores sensibles a calcio; así; se ha demostrado que la eliminación de este dominio previene la dimerización del receptor metabotrópico de glutamato mGlu$_1$R. También se ha observado que la existencia de puentes disulfuro entre los extremos amino terminal, además de otras interacciones no covalentes, juegan un papel clave en la dimerización de los receptores de glutamato mGlu5 (Romano *et al.* 1996). Por otro lado, una mutación puntual de un residuo clave de cisteína de estos receptores indica que este residuo participa en la dimerización pero que no es el único responsable (Ray and Hauschild 2000; Tsuji *et al.* 2000). También se ha demostrado la necesidad de puentes disulfuro en la oligomerización de algunos receptores de la familia A. Así, se ha descrito la disociación del homodímero mediante agentes reductores para los receptores κ- y δ-opiodes o

los receptores D_1 de dopamina, entre otros (Cvejic and Devi 1997; Jordan and Devi 1999; Lee *et al.* 2000).

En la heterodimerización de las dos isoformas de los receptores $GABA_B$ ($GABA_{B1}$ Y $GABA_{B2}$) se ha descrito una interacción directa entre dominios *coiled-coil* localizados en los extremos carboxilo terminal de los mismos (White *et al.* 1998). Sin embargo, estudios de mutagénesis han revelado que si bien el dominio *coiled-coil* es importante para la funcionalidad del receptor, no es el único responsable de la formación del heterodímero, ya que la deleción de este dominio no consigue eliminar la formación del mismo (Margeta-Mitrovic *et al.* 2000). Otro ejemplo, donde el dominio carboxilo terminal del receptor ha sido descrito como fundamental para la homodimerización del receptor, lo constituye el receptor δ-opiode, ya que al delecionarse los últimos 15 aminoácidos del receptor se pierde la capacidad de formar dímeros (Cvejic and Devi 1997).

Finalmente, la dimerización directa entre receptores acoplados a proteína G puede estar mediada por interacciones iónicas o hidrofóbicas entre los dominios extracelulares, o intracelulares del receptor. Se ha demostrado la existencia de interacciones ionicas entre péptidos presentes en los dominios intracelulares que contienen respectivamente dos o más cargas positivas adyacentes (por ejemplo, RR, KK o RKR) y dos o más cargas negativas (por ejemplo, DD o EE) o residuos aminoacídicos fosforilados (Woods and Huestis 2001; Woods *et al.* 2002). Un ejemplo de estas interacciones sería la participación de residuos cargados y/o fosforilados en la heteromerización de los receptores A_{2A} de adenosina y D_2 de dopamina (Ciruela *et al.* 2004).

La idea de que las interacciones hidrofóbicas podrían tener un papel relevante en la formación de los dímeros se propuso por primera vez para el receptor β_2-adrenérgico. Mediante el uso de péptidos sintéticos y mutagénesis dirigida se propuso que residuos concretos de glicina y de leucina situados en el sexto dominio transmembrana del receptor estaban involucrados en su dimerización (Hebert *et al.* 1996). Las interacciones entre dominios transmembrana han sido implicadas en la homodimerización de receptores de dopamina (Ng *et al.* 1996). Mediante estudios computacionales Gouldson y colaboradores (Gouldson *et al.* 2000) propusieron dos modelos tridimensionales alternativos que explicarían la dimerización de los receptores acoplados a proteína G. En ambos modelos se propuso que los dominios transmembrana cinco y seis (TM5-6) estarían involucrados en el contacto o interfase de dimerización entre receptores, así como también tiene un papel importante el tercer bucle intracelular (IC3). El primer modelo se conoce como *domain swapping model*, o modelo del intercambio de dominio y considera que cada unidad funcional en el dímero está compuesta por los cinco primeros dominios transmembrana de un receptor y los dos últimos dominios del otro. Se ha demostrado, por

ejemplo en el caso del receptor D_2 de dopamina, que la coexpresión de dos polipéptidos, uno conteniendo los cinco primeros dominios transmembrana y el otro expresando los últimos dos dominios del receptor, resulta en la recuperación del receptor funcional, lo que confirma que al menos dos dominios independientes que están insertados en la bicapa lipídica como unidades separadas, se ensamblan para formar una proteína transmembrana funcional (Scarselli *et al.* 2000). Este modelo racionaliza la complementación funcional observada por Maggio y colaboradores con las quimeras de los receptores α_2-adrenérgico y M_3 muscarínico (Maggio *et al.* 1993) que se han comentado anteriormente. El segundo modelo es el de contacto y considera que el dímero se formaría por empaquetamiento lateral de monómeros individuales, donde los dominios cinco y seis de cada monómero formarían la interfase de interacción. Éste sería el caso para el receptor V_2 de vasopresina (Schulz *et al.* 2000). Ambos modelos se esquematizan en la figura 11.

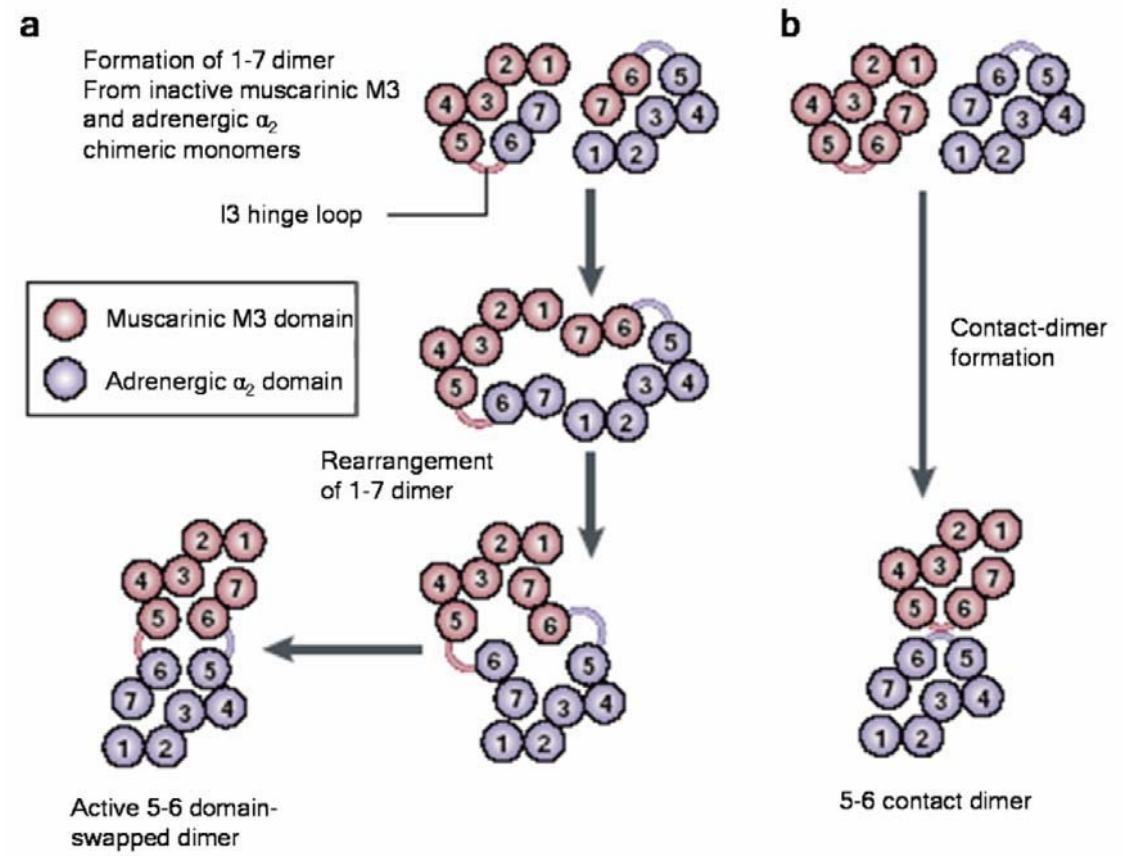

Figura 11. Modelos tridimensionales de la dimerización de GPCR. a) Domain swapping model o modelo de intercambio de dominio. (b) Contact model o modelo de contacto (Extraído de Bouvier 2001).

La cristalización de algunos GPCR ha permitido establecer modelos de interacción entre diferentes dominios de transmembrana para dímeros de diversos receptores como los beta-adrenérgicos (Fung *et al.* 2009) o los dopaminérgicos (Han *et al.* 2009).

1.2.3 TÉCNICAS PARA EL ESTUDIO DE LA OLIGOMERIZACIÓN DE GPCR

Las técnicas utilizadas para el estudio de la formación de olígomeros de GPCR son de índole muy variada, como técnicas farmacológicas, utilización de quimeras, aproximaciones bioquímicas y técnicas de biofísica. A menudo, la demostración de la oligomerización de GPCR requiere la utilización de algunas o incluso todas ellas.

Los estudios farmacológicos pueden constituir la primera evidencia de la existencia de homodímeros entre GPCR como resultado del análisis de la unión de radioligandos a los receptores, en aquellos casos en los que se detecte tanto cooperatividad positiva como negativa. El fenómeno de la cooperatividad no puede ser explicado considerando la existencia de distintos estados de activación de los receptores monoméricos en equilibrio, y requiere la formulación de un modelo que considera la forma dimérica del receptor y explica la cooperatividad de manera natural por analogía a los enzimas (Limbird *et al.* 1975; Mattera *et al.* 1985; Hirschberg and Schimerlik 1994; Wreggett and Wells 1995; Franco *et al.* 1996; Franco *et al.* 2003; Franco *et al.* 2005a; Casadó *et al.* 2007) . Una evidencia de la existencia de hetero-olígomeros, la constituyen los cambios cinéticos en la unión de radioligandos a un receptor provocados por la unión de ligandos no radioactivos al otro receptor del heterómero, utilizando preparados de membrana de células o de tejido que expresen los dos receptores. En preparaciones de membrana aisladas no existe ninguna maquinaria celular que pueda producir un *cross-talk* indirecto (por ejemplo, un *cross-talk* a nivel de segundos mensajeros) y la explicación más sencilla de la existencia de una modulación a nivel de unión de radioligandos es la existencia de una interacción molecular entre ambos receptores. En estos casos la unión de un ligando a un receptor induce cambios conformacionales en el otro receptor que modulan su capacidad de unir ligandos. Estos cambios conformacionales sólo se pueden producir si ambas proteínas interaccionan molecularmente directa o indirectamente (Franco *et al.* 2007; Franco *et al.* 2008a). En muchos casos esta clase de interacción se ha encontrado en tejido nativo, hecho que puede ser interpretado como un indicador de la existencia de receptores heteroméricos in-vivo (Gonzalez-Maeso *et al.* 2008; Marcellino *et al.* 2008).

Respecto a la utilización de receptores quimera y mutantes, un estudio pionero que demostraba que los GPCR pueden funcionar como dímeros fue el elegante estudio llevado a cabo por Maggio y colaboradores (Maggio *et al.* 1993), usando quimeras de los receptores α_2-adrenérgico/M_3 muscarínico compuestas por los 5 primeros dominios transmembrana de uno de los receptores y los dos últimos dominios transmembrana del otro, que ya se ha mencionado anteriormente. En esta línea se ha observado que diversos receptores mutantes actúan de dominantes negativos cuando son expresados con el receptor en la forma nativa (*wild type*)

(Benkirane *et al.* 1997; Bai *et al.* 1998; Zhu and Wess 1998). En estos casos, la dimerización entre el receptor *wild type* y el receptor inactivo es la única explicación de este fenómeno. Utilizando el receptor de la hormona luteinizante como modelo, (Rivero-Müller *et al.* 2010) han demostrado que un ratón transgénico que no expresa el receptor nativo pero expresa una forma mutante del receptor que une agonista pero no es funcional puede recuperar completamente la funcionalidad del receptor de la hormona luteinizante por complementación intermolecular (transactivación) si el ratón coexpresa un mutante que es funcional pero que no puede unir ligando, demostrando la expresión de dímeros in vivo.

En los últimos años, una de las técnicas bioquímicas más comúnmente usadas para el estudio de la dimerización de GPCR ha sido la coinmunoprecipitación de receptores marcados con epítopos diferentes. El primer estudio que se llevo a cabo utilizando esta técnica fue realizado por Hebert y colaboradores (Hebert *et al.* 1996) en el cual demostraban la existencia de interacciones específicas entre los receptores β_2-adrenérgicos. Desde entonces, estrategias similares han sido usadas para documentar la homodimerización de receptores D_2 de dopamina (Ng *et al.* 1996), receptores metabotrópicos de glutamato tipo 5 ($mGlu_5R$) (Romano *et al.* 1996), receptores δ-opiodes (Cvejic and Devi 1997) y serotonina $5\text{-}HT_{2C}$ (Herrick-Davis *et al.* 2004) entre otros. Más recientemente, se han efectuado estudios de coinmunoprecipitación para demostrar la heterodimerización de receptores del mismo neurotransmisor, como los subtipos $GABA_BR_1$ y $GABA_BR_2$ (Jones *et al.* 1998; Kaupmann *et al.* 1998; White *et al.* 1998) o como los δ-opiodes y κ-opiodes (Jordan and Devi 1999), e incluso entre receptores menos relacionados como los receptores de adenosina A_1 y D_1 de dopamina (Gines *et al.* 2000), los receptores A_{2A} de adenosina y metabotrópico $mGlu_5$ (Ferré *et al.* 2002), los receptores de cannabinoides CB_1 y de dopamina D_2 (Kearn *et al.* 2005), los receptores de angiotensina AT_1 y bradikinina B_2 (AbdAlla *et al.* 2000), o los de δ-opiodes y β_2- adrenérgico (Jordan *et al.* 2001).

Aunque se utilizan comúnmente para estudiar las interacciones proteína-proteína, las coinmunoprecipitaciones y análisis por western-blot requieren la solubilización del receptor de la membrana mediante detergentes, lo que no permite descartar que los dímeros observados puedan ser artefactuales por una solubilización incompleta, debida a la naturaleza hidrofóbica de estas proteínas. A pesar de todos los controles usados para descartar esta posibilidad, la aceptación generalizada de la dimerización de GPCR dependía de una demostración directa de que estos complejos existen en células en cultivo. Esto fue posible con el desarrollo y la utilización de métodos biofísicos basados en la transferencia de energía por resonancia (RET: *resonance energy transfer*).

En 1948 Theodor Förster formuló la teoría de transferencia de energía por resonancia (Förster 1948) que más tarde fue aplicada al estudio de interacciones entre GPCR. Esta aproximación biofísica está basada en la transferencia no radioactiva de energía de excitación entre dos dipolos electromagnéticos, es decir, desde un cromóforo en estado excitado (dador energético) a una molécula cercana que absorbe (aceptor). En el caso de la transferencia de energía de resonancia fluorescente (FRET; *Fluorescence or Förster Resonance Energy Transfer*), tanto el dador como el aceptor son moléculas fluorescentes, mientras que en la transferencia de energía de resonancia bioluminiscente (BRET; *Bioluminescence Resonance Energy Transfer*) el dador es biolumiscente y el aceptor fluorescente (Bouvier *et al.* 2007; Gandía *et al.* 2008; Ciruela *et al.* 2010; Ferré *et al.* 2010; De 2011; Schaferling and Nagl 2011). Para que este fenómeno tenga lugar es necesario que se cumplan dos requisitos. El primero, consiste en que el espectro de emisión del dador y el espectro de excitación del aceptor se solapen, de forma que el dador no emite completamente la energía que debiera, si no que transfiere parte de su energía de emisión de forma directa al fluoróforo aceptor, el cual emite como si hubiera sido excitado directamente. El segundo requisito para que tenga lugar el fenómeno de transferencia de energía es que tanto el dador como el aceptor han de estar muy próximos en el espacio (<100 Å o 10 nm). Así, a diferencia de la coinmunoprecipitación, las técnicas de transferencia de energía ofrecen una aproximación única que permite detectar la dimerización de proteínas en células vivas, sin perturbar el entorno donde este fenómeno ocurre.

La dependencia crítica de la distancia entre dador y aceptor para la transferencia de energía, donde la eficiencia de la transferencia disminuye con la sexta potencia de la distancia, hace que los sistemas de BRET/FRET sean los elegidos para monitorizar las interacciones proteína-proteína en cultivos celulares. Hay que destacar que entre 10 y 100 Å se encuentran la mayor parte de complejos multiproteicos biológicos de una célula (Stryer 1978; Sheng and Hoogenraad 2007).

Para la técnica de FRET se utilizan las diferentes variantes de la proteína fluorescente verde (GFP: *Green Fluorescence Protein*) obtenidas por mutación. Estas mutaciones confieren diferentes propiedades espectrales, de forma que utilizando dos formas diferentes de mutantes, con las características espectrales adecuadas, fusionadas a las proteínas en estudio, permite determinar si estas están lo suficientemente cercanas como para transferirse energía (Pfleger and Eidne 2005; Ferré *et al.* 2010; Schaferling and Nagl 2011). La pareja más ampliamente utilizada para los experimentos de FRET son las variantes GFP^2 y YFP (*Yellow Fluorescence Protein*). Esta última variante de la GFP ha sido optimizada para ser usada como pareja de FRET con la GFP^2. La GFP^2 se excita a 400 nm y emite a 510 nm, mientras que la YFP se excita a 485 nm y emite a 530 nm. En la técnica de FRET, como se esquematiza en la Figura 12, cuando un haz de

luz excita la proteína GFP^2 fusionada a un receptor, esta emite fluorescencia a 510 nm y si esta proteína de fusión está cercana a la proteína de fusión receptor-YFP en el espacio, tendrá lugar una transferencia de energía entre la GFP^2 y la YFP, y la YFP emitirá fluorescencia con un pico a 530 nm (Pfleger and Eidne 2005; Gandía *et al.* 2008). Ambas emisiones (la del dador y la del aceptor) se recogen en dos canales diferentes. En ambos canales de detección hay una contribución de ambas fluorescencias por que hay un cierto solapamiento de los espectros, de forma que para cuantificar la señal de FRET se han de separar los dos espectros de emisión (Zimmermann *et al.* 2002).

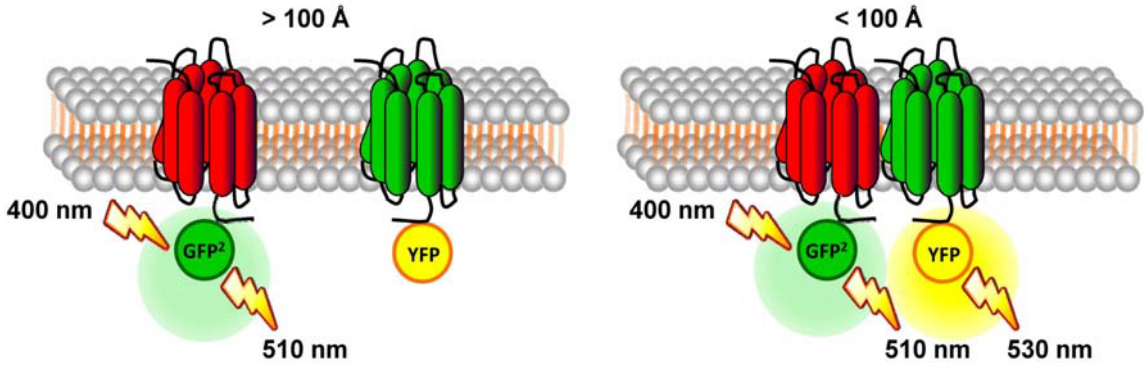

Figura 12. Representación esquemática del fenómeno de FRET.

Similar al FRET y con los mismos requerimientos, cabe considerar la técnica de transferencia de energía por resonancia bioluminiscente, BRET. En esta técnica, la bioluminiscencia es el resultado de la degradación catalítica de cierto sustrato por la enzima *Renilla luciferasa* (*Rluc*) en presencia de oxígeno, generando luz. Esta luz es transferida a una variante de la proteína GFP, la cual a su vez emite fluorescencia a una longitud de onda característica si ambas proteínas están lo suficientemente cerca, indicando la dimerización de las proteínas fusionadas a *Rluc* y a GFP (Pfleger and Eidne 2005; Bouvier *et al.* 2007; Gandía *et al.* 2008; Ciruela *et al.* 2010; Ferré *et al.* 2010; De 2011).

Hasta la fecha se han descrito dos variantes principales de esta técnica, el BRET^1 y el BRET^2. En ambos casos el principio es el mismo, pero difiere el sustrato que utiliza la *Rluc* y la proteína aceptora. En el BRET^1 el sustrato que se usa es la coelenterazine H, que al ser metabolizado por la *Rluc* genera luz con un pico de emisión a 480 nm; emisión que permite excitar a la proteína YFP, que emitirá a 530 nm. En el BRET^2 el sustrato es DeepBlueC que al ser oxidado por la *Rluc* emite una luz a 400 nm de forma que puede excitar a la proteína GFP^2; en este caso la longitud de onda a la que emite esta variante de la GFP es 510 nm (Figura 13).

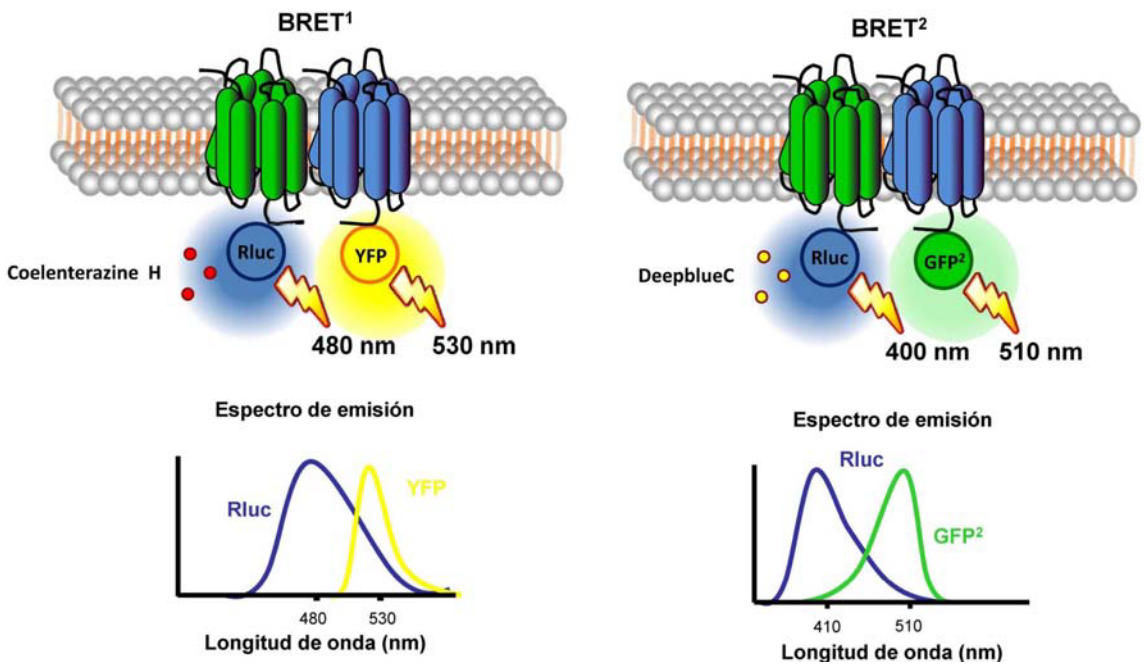

Figura 13. Representación esquemática de los fenómenos de BRET[1] y BRET[2] con sus correspondientes espectros de emisión.

Las ventajas de este fenómeno han sido utilizadas por los investigadores para el estudio de la dimerización de GPCR. Se generan proteínas de fusión que unen en el extremo carboxilo terminal de un receptor la proteína fluorescente GFP o una de sus variantes y en el otro receptor la proteína luminiscente *Rluc* y se determina BRET en células que co-expresan ambas proteínas de fusión. Mediante estas técnicas de transferencia de energía se ha demostrado la existencia de homodímeros de los receptor β_2-adrenérgico (Angers *et al.* 2000), δ-opiodes (McVey *et al.* 2001) y A_{2A} de adenosina (Canals *et al.* 2004) entre otros. También se ha realizado una aproximación similar para el estudio de heterómeros de receptores acoplados a proteína G, como por ejemplo entre los receptores de somatostatina $SSTR_{2A}$ y $SSTR_{1B}$ (Rocheville *et al.* 2000b), los receptores $SSTR_{1B}$ de somatostatina y los D_2 de dopamina (Rocheville *et al.* 2000a), los receptores A_{2A} de adenosina y D_2 de dopamina (Canals *et al.* 2003), los receptores A_1 y A_{2A} de adenosina (Ciruela *et al.* 2006), los receptores A_{2A} de adenosina y CB_1 de cannabinoide (Carriba *et al.* 2007), los receptores D_1 o D_2 de dopamina y H_3 de histamina (Ferrada *et al.* 2008) o los receptores D_1 y D_3 de dopamina (Marcellino *et al.* 2008) entre otros.

En los últimos años se han desarrollado multitud de variaciones de estas técnicas entre las que cabe destacar; la técnica de SRET (*squential resonance energy transfer*) basada en la combinación secuencial de las técnicas de BRET y FRET (Carriba *et al.* 2008), el *photobleaching* FRET o el *time-resolved* FRET (Pfleger and Eidne 2005), con la que se ha demostrado recientemente un crosstalk conformacional entre el receptor α_2-adrenérgico y μ-

opioide (Vilardaga *et al.* 2008), y la técnica de BRET con complementación bimolecular (Navarro *et al.* 2008) que permiten la detección de heterómeros de más de dos receptores.

El descubrimiento de técnicas como BiFC (*Bimolecular fluorescence complementation*) ha aportado una nueva forma muy eficaz para detectar interacciones proteína-proteína en células vivas. Esta técnica utiliza receptores fusionados a la mitad N-terminal o a la mitad C-terminal no fluorescentes de la proteína YFP (nYFP y cYFP). Cuando la proteína YFP se reconstituye a partir de la interacción directa entre las proteínas de fusión, se genera una señal fluorescente (Hu *et al.* 2002) (Figura 14). Esta señal sólo se genera si las proteínas de fusión están muy próximas en el espacio (menos de 6 nm). Más adelante, en la misma línea de investigación, se han desarrollado técnicas que utilizan dos fragmentos de la proteína *Rluc*. Cuando las proteínas fusionadas a estos fragmentos interaccionan, se reconstituye la proteína *Rluc* enzimáticamente activa (Paulmurugan and Gambhir 2003). Finalmente, muy recientemente, se ha desarrollado la técnica de multicolor BiFC (mcBiFC) que utiliza diferentes fragmentos de diferentes proteínas facilitando la investigación de redes de complejos de proteínas (Gehl *et al.* 2009).

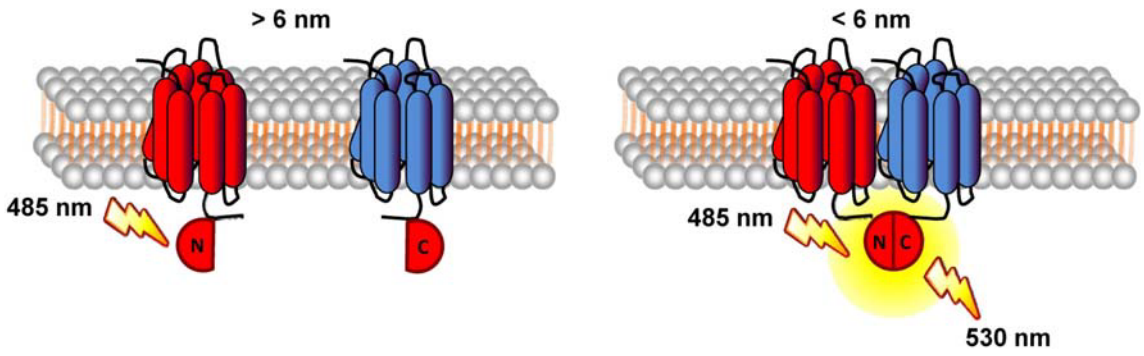

Figura 14. **Representación esquemática de la *Bimolecular fluorescence complementation* (BiFC).**

Las técnicas de transferencia de energía ponen de manifiesto que dos proteínas tienen la capacidad de interaccionar molecularmente en cultivos celulares, y esta es evidentemente, la primera condición que se debe cumplir para que las proteínas en estudio estén formando heterómeros in vivo. Sin embargo, una señal positiva en células transfectadas con proteínas de fusión no significa necesariamente que en un tejido que exprese endógenamente estas proteínas, éstas formen heterómeros. Para detectar heterómeros en tejidos nativos deben utilizarse otro tipo de estrategias.

Existen técnicas directas para detectar oligómeros de GPCR en tejidos nativos. Una de ellas utiliza la microscopía de fuerza atómica. Palczewski y colaboradores (Fotiadis *et al.* 2003) usando microscopia de fuerza atómica demostraron, por primera vez, oligómeros de rodopsina en la retina con un determinado patrón de distribución (Figura 15). Esta técnica es factible

cuando la concentración de receptores en el tejido es muy elevada como ocurre con la rodopsina en la retina, pero es de difícil aplicación para la mayoría de receptores del sistema nervioso central cuya expresión es moderada.

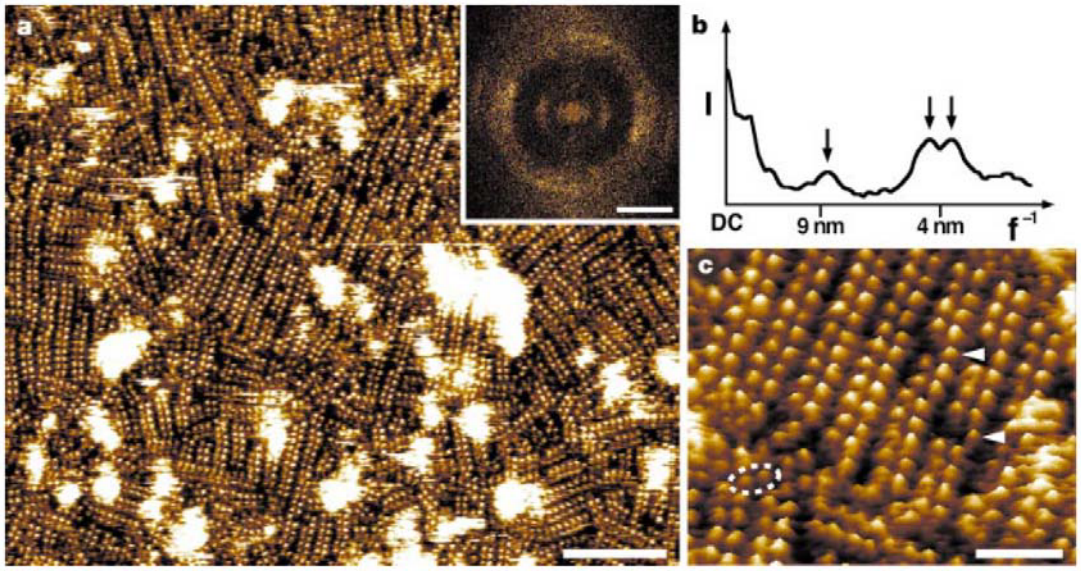

Figura 15. Organización y topografía de la distribución dimérica de la rodopsina en la cara citoplasmática de los discos de la retina (Extraído de Fotiadis *et al.* 2003).

La técnica de *In Situ Proximity Ligation Assay* (PLA) es una técnica directa muy útil si se dispone de anticuerpos específicos para los receptores que heteromerizan (Gustafsdottir *et al.* 2005; Soderberg *et al.* 2006; Thymiakou *et al.* 2007; Soderberg *et al.* 2008; Yu *et al.* 2008; Massinen *et al.* 2009; Miyazono *et al.* 2009; Baan *et al.* 2010; Vuoriluoto *et al.* 2010; Weibrecht *et al.* 2010; Hervouet *et al.* 2011; Renfrow *et al.* 2011). Esta tecnología amplía las capacidades de los inmunoensayos tradicionales al incluir la detección directa de proteínas, interacciones entre proteínas y modificaciones de estas interacciones con alta sensibilidad y especificidad. El principio de la técnica se basa en la utilización de dos anticuerpos primarios que reconocen el antígeno o antígenos de interés, unidos a una cadena de ADN. Cada sonda PLA consta de un anticuerpo unido a una única cadena de ADN sintética, para un anticuerpo una cadena (+) y para el otro una cadena (-). Cuando el anticuerpo se une al antígeno, si los antígenos interaccionan, la proximidad de las sondas permite la ligación del ADN en el lugar exacto donde estas sondas se juntan por proximidad. La distancia que permite la hibridación y la ligación del ADN es pequeña (< 40 nm) y por lo tanto, sólo las proteínas que interactúan pueden permitir la ligación. Después de la unión de los dos oligonucleótidos por el proceso de ligación, el ADN ligado es amplificado en presencia de oligonucleótidos marcados con sondas fluorescentes. La amplificación es específica ya que depende del principio de hibridación ADN-ADN y también ofrece una alta sensibilidad. El ADN amplificado se puede detectar como pequeños puntos

fluorescentes visible con un microscopio de fluorescencia. Como la fluorescencia puede ser cuantificada, la señal PLA proporciona no sólo la información espacial exacta (la localización de los eventos de interacción), sino también una manera objetiva de cuantificar estos eventos (Gustafsdottir *et al.* 2005; Soderberg *et al.* 2008).

La técnica es igualmente aplicable utilizando un anticuerpo específico no marcado y anticuerpos secundarios unidos a ADN (Figura 16).

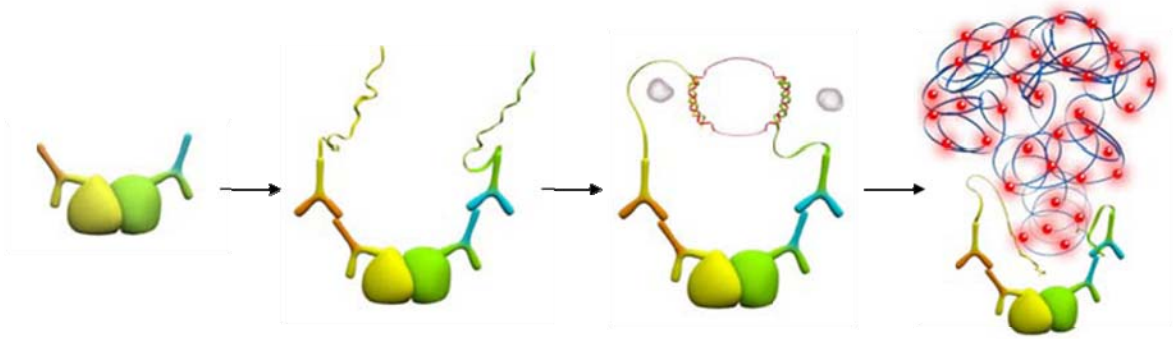

Figura 16. Representación esquemática de In Situ Proximity Ligation Assay (PLA) (Extraído de Olink Bioscence).

La utilización de ligandos para heterómeros constituye otra técnica directa para su detección. Se pueden seguir varias estrategias dependiendo de las propiedades del heterodímero (Rozenfeld *et al.* 2006). Uno de los enfoques consiste en el diseño y síntesis de ligandos bivalentes que interaccionen con los dos receptores del dímero. Estos ligandos pueden tener mayor afinidad y selectividad si se compara con los ligandos clásicos de los receptores. Esta estrategia se ha utilizado para determinar la presencia de heterómeros de receptores de adenosina A_{2A} y de dopamina D_2 en el estriado de cerebro de cordero (Soriano *et al.* 2009). Otra aproximación es el desarrollo de ligandos selectivos de un determinado heterodímero. Estos ligandos interaccionan con el centro de unión únicamente cuando forma parte del heterodímero (Waldhoer *et al.* 2005).

Existen técnicas indirectas para detectar oligómeros en tejidos nativos. Una manera bastante eficaz de detectar oligómeros en tejidos nativos es determinar alguna característica específica de los heterómeros en células donde se haya demostrado la heteromerización y utilizar esta propiedad como huella dactilar para detectar el heterómero en tejidos nativos. La determinación de cross-talk entre cascadas de señalización intracelular, el antagonismo cruzado en el que un antagonista específico de un receptor inhibe la señalización mediada por un agonista del otro receptor, o bien, el estudio de cambios en la unión de ligandos en uno de los receptores en presencia de un ligando para el otro receptor en preparaciones de membranas obtenidas de tejidos, pueden constituir una huella dactilar si se ha demostrado previamente que

es una característica del heterómero. Estas estrategias se han utilizado para detectar heterómeros entre receptores de dopamina D_1 y histamina H_3 o entre receptores de dopamina D_1 y receptores sigma-1 en el tejido estriatal de cerebro entre otros (véase resultados).

1.2.4. PAPEL FUNCIONAL DE LA DIMERIZACIÓN

La disponibilidad de un gran número de técnicas para el estudio de la oligomerización de GPCR ha facilitado enormemente la investigación del papel funcional de estos receptores. La formación de homómeros y heterómeros tiene un papel importante en la regulación de la funcionalidad del receptor a diferentes niveles, desde la modulación de la expresión del receptor en la superficie celular hasta el hecho de conferir nuevas propiedades farmacológicas a los receptores expresados en el oligómero (Ferré *et al.* 2009). Esto ha proporcionado una nueva perspectiva para considerar cual es la unidad de señalización de los GPCR, además de una nueva vía para el diseño de drogas que actúen a través de estos receptores.

Aunque en muchos casos la relevancia fisiológica no se conoce completamente, diversos estudios llevados a cabo en sistemas de expresión heterólogos han sugerido distintos papeles funcionales para la oligomerización de GPCR (Figura 17). Por ejemplo, la oligomerización puede estar implicada en la ontogénesis de GPCR, es decir, en el control de calidad del plegamiento y de la destinación a la membrana de receptores sintetizados de novo (Figura 17.1). Asimismo, en algunos casos, se ha observado una regulación de la formación/separación de oligómeros presentes en la membrana plasmática mediada por ligando (Figura 17.2). También, se ha constatado que la oligomerización confiere diversidad farmacológica, ya que la unión de un ligando a un receptor del dímero puede influir en la unión de otro ligando al segundo receptor dentro del dímero (Ferré *et al.* 2007; Franco *et al.* 2008b) (Figura 17.3). La oligomerización también puede modificar las propiedades de señalización de un determinado ligando afectando la selectividad de interacción entre el receptor correspondiente y su proteína G, resultando en una potenciación, atenuación o acoplamiento con otra proteína G (Figura 17.4). Finalmente, también se ha visto que la oligomerización puede alterar el patrón endocítico para un determinado receptor (Terrillon and Bouvier 2004) (Figura 17.5).

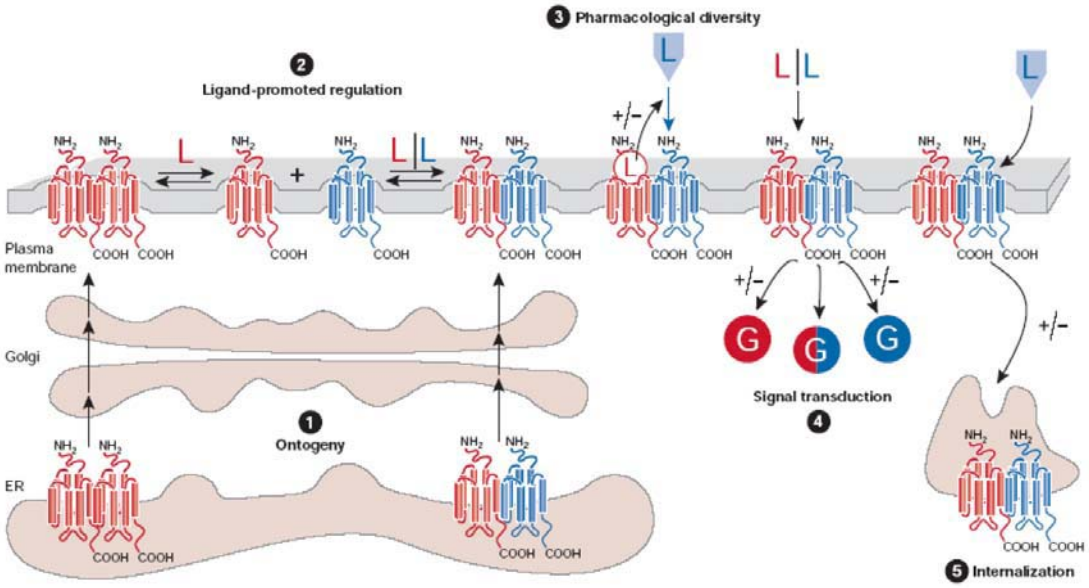

Figura 17. Posibles papeles funcionales de la oligomerización de GPCR. ER, retículo endoplasmático, L, ligando (Extraído de Terrillon and Bouvier 2004).

Un ejemplo claro del papel de la heteromerización en la modulación de la expresión del receptor en la superficie celular lo constituían los receptores metabotrópicos $GABA_B$, donde la heteromerización de los receptores $GABA_{B1}$ y $GABA_{B2}$ es necesaria para el correcto plegamiento del receptor y su transporte a la membrana plasmática, además de para su señalización (Jones *et al.* 1998; Kaupmann *et al.* 1998; White *et al.* 1998). En estudios posteriores se ha demostrado que $GABA_{B2}$ sirve como una chaperona esencial para el apropiado plegamiento y transporte a la superficie celular de $GABA_{B1}$ (Margeta-Mitrovic *et al.* 2000) (Figura 18).

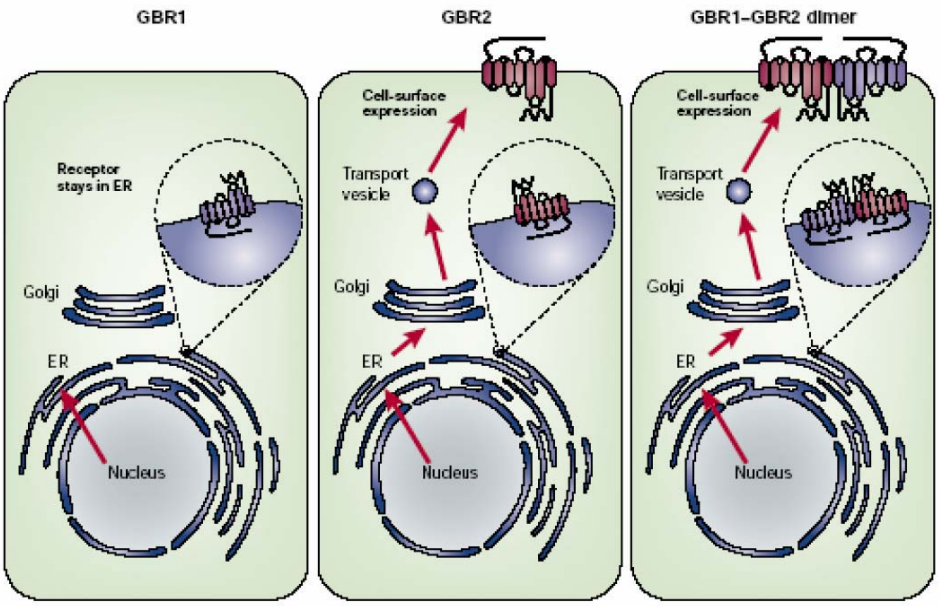

Figura 18. Heteromerización de los receptores $GABA_{B1}$/$GABA_{B2}$ (Extraído de Bouvier 2001).

El papel de la oligomerización como un evento temprano en la maduración y transporte del receptor se ha demostrado claramente para heterómeros de receptores de vasopresina y citocinas. Se ha observado que la expresión de formas truncadas de los receptores de vasopresina V_2 y citocina CCR5 provoca la retención intracelular de los homodímeros correspondientes, causando diabetes nefrogénica insípida en el primer caso y una lenta aparición de los efectos del SIDA, en el segundo (Benkirane *et al.* 1997; Zhu and Wess 1998).

En este mismo sentido cabe mencionar que los receptores que forman heterómeros pueden tener diferentes características de internalización, es decir, la oligomerización también puede modular las propiedades de tráfico de GPCR mediadas por agonista. Este es el caso de los heterodímeros de los receptores de somatostatina $SSTR_1$ y $SSTR_5$, en el cual la internalización del heterodímero ocurre a pesar de la resistencia a la internalización que presenta el monómero $SSTR_1$ (Rocheville *et al.* 2000b). En el mismo sentido se ha descrito que los receptores A_1 y A_{2A} de adenosina de astrocitos se internalizan conjuntamente al ser estimulado el heterómero por agonistas de cualquiera de los dos receptores (Cristóvão-Ferreira *et al.* 2011).

El estado dimérico de los GPCR puede representar la unidad funcional básica del receptor, que se acopla a la proteína heterotrimérica G y exhibe características farmacológicas que difieren de la de los monómeros que los constituyen (Bulenger *et al.* 2005). Los estudios de unión de ligando han dado algunas pistas de la relevancia fisiológica de la formación de oligómeros de GPCR, ya que la formación de estos complejos puede resultar en la generación de sitios de unión con nuevas propiedades para la unión de ligando. La formación de homodímeros de GPCR puede conferir cooperatividad a la unión de ligandos ya que se ha visto que la unión de un ligando específico sobre uno de los protómeros del homómero puede incrementar o disminuir la afinidad del ligando para el otro protómero (Franco *et al.* 2006). En un escenario donde se asumía que los GPCR actuaban como monómeros, esta cooperatividad era difícil de explicar. Una posible explicación era que el receptor podía estar en dos estados conformacionales diferentes con diferentes afinidades por los agonistas: un estado de alta afinidad en el cual el receptor estaba acoplado a proteína G y otro de baja afinidad en el que no estaba acoplado. En cambio, la existencia de oligómeros permite un nuevo modelo en el cual la interacción receptor-receptor es la base de la cooperatividad entre receptores. Un ejemplo de ello lo constituye, la modulación del heterodímero formado por los receptores de somatostatina $SSTR_5$ y de dopamina D_2 (Rocheville *et al.* 2000a) en el cual se observa cooperatividad positiva, y la cooperatividad negativa en el homodímero de receptores de glutamato $mGluR_1$ (Suzuki *et al.* 2004) o de receptores A_1 de adenosina o D_1 de dopamina (Franco *et al.* 2005b; Casadó *et al.* 2009b). Considerando todos estos aspectos, se han formulado modelos que tienen en cuenta la formación de homodímeros (Franco *et al.* 2005a; Franco *et al.* 2006) y

recientemente se han desarrollado las ecuaciones para ajustar los datos de unión de ligandos a partir de uno de estos modelos, el two-state dimer receptor model (Casadó *et al.* 2007; Casadó *et al.* 2009a).

La formación de heterómeros entre dos receptores distintos implica que se pueda establecer una interacción alostérica entre ellos, de manera que la unión de un ligando a uno de los receptores en el heterómero modifique la afinidad del otro ligando por el otro receptor en el heterómero. El primer heterómero descrito con distintas propiedades respecto de los receptores constituyentes fue el heterodímero formado por los receptores κ- y δ-opioides (Jordan and Devi 1999). Este heterodímero no presenta alta afinidad por la unión de ligandos selectivos de los receptores κ- y δ-opioide, en cambio si presenta alta afinidad por ligandos selectivos parciales. De la misma manera, los heterodímeros de receptores μ-δ-opioide también presentan propiedades funcionales propias, ya que el tratamiento con un antagonista específico de uno de los receptores del dímero provoca un incremento tanto en la potencia como en la eficiencia de la señalización del otro receptor del dímero, mientras que el tratamiento conjunto con agonistas de ambos receptores da lugar a una potenciación sinérgica de la señal mediada por el heterómero (Gomes *et al.* 2000).

Un caso interesante y complejo es el de los receptores de dopamina y adenosina, entre los que se ha descrito un crosstalk negativo. Los agonistas del receptor A_1 inducen la desaparición del estado de alta afinidad en preparaciones de membrana que contienen el receptor de dopamina D_1 (Gines *et al.* 2000) y la estimulación del receptor de adenosina A_{2A} reduce la afinidad de agonistas por el receptor de dopamina D_2 (Ferré *et al.* 1991). Otro caso de especial interés es el heterodímero formado por los receptores A_1 y A_{2A} de adenosina, en el que la estimulación del receptor A_{2A} disminuye enormemente la afinidad del receptor A_1 por su agonista e inhibe la señalización (Ciruela *et al.* 2006). Teniendo en cuenta que la afinidad por la adenosina del receptor A_1 es más grande que la que muestra el receptor A_{2A} en este heterómero A_1/A_{2A}, cuando la concentración de adenosina es pequeña, el neuromodulador se une al receptor A_1 inhibiendo la liberación de glutamato en el estriado. Cuando la concentración de adenosina es elevada, por ejemplo en casos de hipoxia, la adenosina se une también al receptor A_{2A} provocando en el heterómero la inhibición farmacológica y funcional del receptor A_1. En estas condiciones la adenosina estimula la liberación de glutamato en el estriado (Ciruela *et al.* 2006) (Figura 19). El heterómero A_1/A_{2A} actúa como un interruptor mediante el cual, según sea la concentración de adenosina en el medio, se produce la inhibición o la estimulación de la liberación de glutamato en el estriado (Ciruela *et al.* 2006). Por otro lado, algunos antagonistas del receptor de adenosina A_{2A} muestran una mayor selectividad para el heterómero de receptores de adenosina A_1-A_{2A} que para el heterómero adenosina A_{2A}-dopamina D_2 (Orru *et al.*

2011).

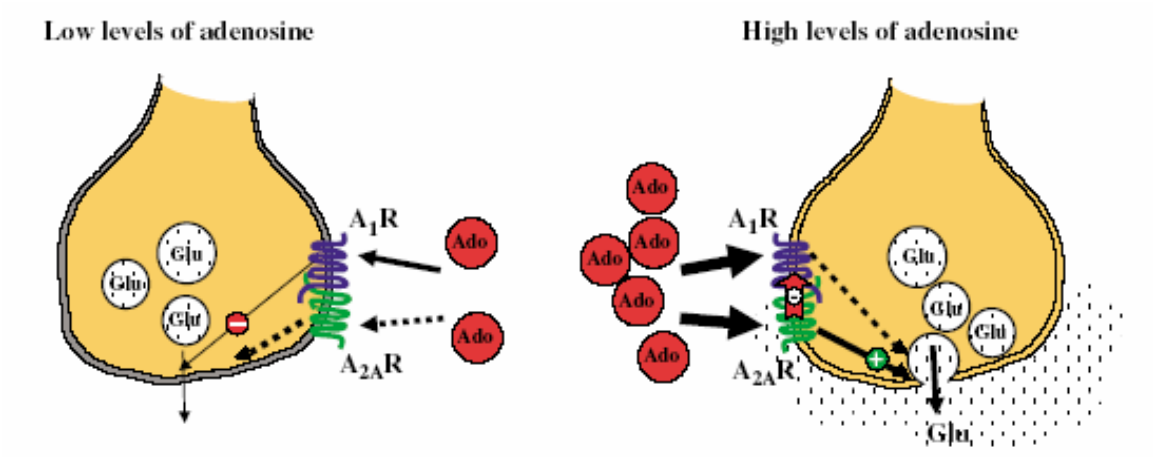

Figura 19. El heterómero A_1/A_{2A} media la regulación de la liberación de glutamato por la adenosina (Extraído de Franco *et al.* 2008a).

La homomerización y la heteromerización pueden afectar diferencialmente la señal inducida por diversos agonistas. Una de las primeras evidencias de que los dímeros forman una unidad compleja de señalización proviene de estudios que demuestran que la disrupción del homodímero del receptor β_2-adrenérgico con un péptido derivado del sexto dominio transmembrana, implicado en la dimerización, inhibe la producción de AMPc inducida por el agonista (Hebert *et al.* 1996). Estos resultados indican que el dímero es la especie activa del receptor, aunque tampoco se puede descartar la posibilidad de que el péptido esté modificando interacciones intramoleculares dentro del monómero que provocan la falta de funcionalidad, siendo la pérdida de la unidad dimérica más bien una consecuencia y no una causa de la no señalización por parte del receptor. En el mismo sentido, (AbdAlla *et al.* 2000) describe que la heterodimerización entre los receptores de angiotensina AT_1 y B_2 de bradiquinina, mejora la señalización de AT_1, mientras que inhibe la del receptor B_2, mostrando que la heteromerización entre receptores diferentes puede ser un nuevo modelo para la modulación de la respuesta de GPCR por sus respectivos ligandos. En 2004, se demostró que los receptores de dopamina D_1 y D_2 forman heterómeros en células transfectadas (Lee *et al.* 2004). Los receptores D_1 están acoplados a proteína G_s mientras que los D_2 están acoplados a la proteína G_i. Pero cuando los receptores D_1-D_2 forman el heterómero, se acoplan a una proteína G diferente, $G_{q/11}$. De hecho, cuando la dopamina activa a los receptores D_1 y D_2 en el heterómero, no da lugar a la señalización vía PKA y AMPc sino que moviliza calcio y activa la calmodulin cinasa (Rashid *et al.* 2007). También se ha descrito que los receptores A_{2A} y CB_1 heterodimerizan, y que es necesaria la activación del receptor A_{2A} para que el receptor CB_1 inhiba la producción de AMPc en el heterómero (Carriba *et al.* 2007).

Actualmente, para los GPCR y proteínas G asociadas, se postula que una simple proteína G interactúa con un receptor en un dímero (Baneres and Parello 2003; Filipek *et al.* 2004; Fotiadis *et al.* 2004). Para el receptor de glutamato, se ha demostrado que sólo una subunidad del receptor por cada dímero puede alcanzar un estado activo completo al mismo tiempo (Goudet *et al.* 2005; Hlavackova *et al.* 2005), lo que ha llevado a proponer que la proteína G es la responsable de este funcionamiento asimétrico de un dímero. Damian *et al.* (2006) publicó la primera demostración experimental de este modelo considerando el dímero del receptor de leucotrieno BLT1 (Damian *et al.* 2006).

1.2.5 "TWO-STATE DIMER RECEPTOR MODEL", EL "MODELO DE RECEPTORES DIMÉRICOS"

Cuando se ha tratado de analizar la unión de ligandos, tradicionalmente, los GPCR han sido considerados especies monoméricas. Por este motivo, hasta ahora, se han desarrollado una serie de modelos que consideran al receptor monomérico como la unidad básica. Cuando el ajuste de datos experimentales de unión de ligando genera diagramas de Scatchard lineales los datos se ajustan a un modelo de un centro de unión que permite calcular la K_D (constante de afinidad) del único estado de afinidad del receptor. Sin embargo, la unión de agonistas a receptores de siete dominios transmembrana a menudo genera diagramas de Scatchard no lineales y, en estos casos, los resultados se ajustan tradicionalmente, al modelo de "dos centros independientes" considerando la existencia de dos estados independientes del receptor (estados no interconvertibles): un estado de alta afinidad (o acoplado a proteína G) y un estado de baja afinidad (o desacoplado a proteína G). El ajuste de los datos a este modelo permite el cálculo de dos K_D: una para el estado de alta afinidad (K_{DH}) y otra para el estado de baja afinidad (K_{DL}). Sin embargo, se ha observado que el agonista induce cambios en la proporción de los llamados estados de "alta" y "baja" afinidad, lo cual indica que estos dos estados no pueden existir separadamente, sino que están interconectados (Wong *et al.* 1986) y esta aparente interconversión entre estados es independiente de la proteína G (Casadó *et al.* 1991). Además, trabajando con receptores de adenosina A_1, se demostró que un agonista total puede provocar un cambio aparente en la proporción de receptores en estado de alta y baja afinidad (Casadó *et al.* 1991). Si el agonista es capaz de variar la proporción de los estados de alta y baja afinidad, estas dos formas deben estar en equilibrio y, consecuentemente, el modelo de dos centros independientes no puede representar adecuadamente el comportamiento de los receptores si los estados de afinidad están en equilibrio.

Dado que actualmente se conoce que los GPCR forman dímeros, las isotermas de unión bifásicas (representaciones de Scatchard no lineales) y las curvas de competición bifásicas pueden interpretarse de una manera más directa y evidente ya que pueden explicarse como un fenómeno de cooperatividad. La cooperatividad positiva o negativa puede explicarse de manera natural asumiendo que la unión de la primera molécula de ligando a uno de los monómeros del dímero modifica los parámetros de unión de la segunda molécula de ligando al otro monómero del dímero, como ocurre en el caso de las enzimas. Recientemente, se han desarrollado modelos que consideran al dímero como la unidad básica (Durroux 2005; Franco *et al.* 2005a; Albizu *et al.* 2006; Franco *et al.* 2006). El grupo de investigación en el que se ha desarrollado esta Tesis ha formulado el *"Two-State Dimer Receptor Model"* ("modelo de receptores diméricos"), que considera el homodímero como la unidad básica (Franco *et al.* 2005a; Franco *et al.* 2006) (Figura 20).

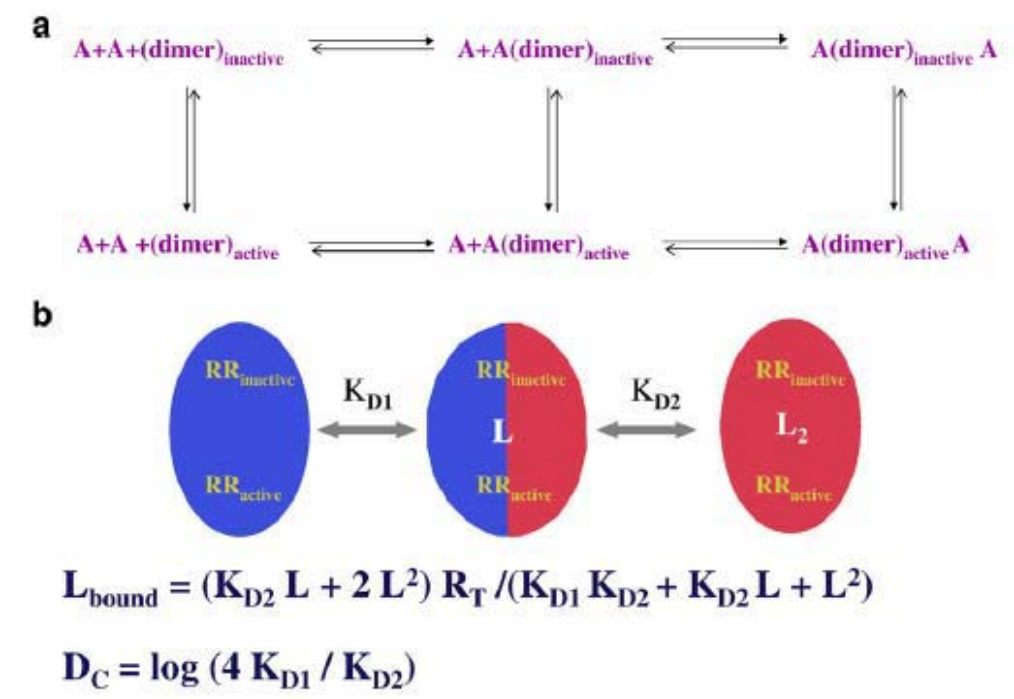

Figura 20. Esquema y ecuaciones del "modelo de receptores dimérico" *("Two-State Dimer Receptor Model").* El dímero puede ser inactivo o activo y puede estar vacío u ocupado por una o dos moléculas de ligando. a) Modelo macroscópico b) Modelo simplificado que incluye las constantes de disociación macroscópicas en el equilibrio, (K_{D1} y K_{D2}) que definen la unión de la primera y segunda molécula de ligando al dímero. Se muestran las ecuaciones para el ajuste de los valores de unión del radioligando (L) a los receptores que forman el dímero y para calcular el índice de cooperatividad del dímero (D_C). Ver (Franco *et al.* 2005a; Franco *et al.* 2006; Casadó *et al.* 2007) para más detalles (Extraído de Franco *et al.* 2008b).

Este modelo considera que el cambio conformacional inducido por un ligando desde uno de los componentes del dímero es transmitido al otro componente del dímero a través de un fenómeno de cooperatividad y permite calcular un parámetro que mide el grado de cooperatividad (Dc). Este modelo es una extensión del modelo de "dos estados de activación de

un receptor", pero considera que las estructuras diméricas son capaces de unir una molécula en el centro ortostérico de cada monómero. Asumiendo la isomerización del receptor entre las especies inactiva (RR) y activa (RR*), el modelo es capaz de explicar el comportamiento de los receptores de siete dominios transmembrana para los cuales muchas veces la representación de Scatchard no es lineal (Franco *et al.* 2005a; Franco *et al.* 2006).

Nuestro grupo de investigación ha profundizado en el desarrollo del "modelo de receptores diméricos" y ha formulado ecuaciones para unión de radioligandos que tienen en cuenta las constantes macroscópicas y que permiten ajustar los datos de experimentos de saturación y de experimentos de competición. Estas ecuaciones permiten el cálculo de las constantes de disociación macroscópicas correspondientes a la unión de la primera molécula de ligando al dímero no ocupado (K_{D1}) y a la unión de la segunda molécula de ligando al dímero semiocupado (K_{D2}). A su vez, las ecuaciones permiten el cálculo del índice de cooperatividad (Dc) que mide el grado de cooperatividad que se produce entre la primera entrada de ligando al receptor vacío y la segunda entrada de ligando al receptor en el dímero semiocupado; es decir, es un parámetro que detecta los cambios estructurales que ocurren en una molécula de receptor en el dímero cuando el ligando se une al otro receptor en el dímero (Casadó *et al.* 2007; Casadó *et al.* 2009a; Casadó *et al.* 2009b).

La posibilidad de calcular las constantes de disociación de la unión de la primera molécula de ligando (K_{D1}) y la segunda molécula de ligando (K_{D2}) al homodímero y el índice de cooperatividad (D_C) permite una cuantificación sencilla de los efectos de los reguladores alostéricos. Estos reguladores alostéricos son moléculas naturales o sintéticas que interaccionan con un centro alostérico del receptor y alteran la unión del ligando al centro ortostérico y por consiguiente regulan la activación del receptor. En el "modelo de receptores diméricos", *"two-state dimer receptor model"*, la proteína G heterotrimérica se considera un modulador alostérico del dímero ya que se une a un centro de unión no ortostérico y puede modificar las características de unión de los centros ortostéricos en el dímero (Hepler and Gilman 1992). El "modelo de receptores diméricos" considera que un modulador alostérico puede ser cualquier molécula que se una a un centro no ortostérico, u otra proteína que interacciona con el receptor y afecta sus características de unión. Puede afectar tanto a las constantes de disociación como al índice de cooperatividad.

1.3 RECEPTORES DE DOPAMINA

1.3.1 LA DOPAMINA COMO NEUROTRANSMISOR

La dopamina es la principal catecolamina que actúa como neurotransmisor en el sistema nervioso central (representa el 80% del contenido total de catecolaminas del cerebro) y controla una gran variedad de funciones como la modulación de la actividad sensorial, la actividad motora, la actividad endocrina, el aprendizaje, la memoria, la emotividad, la afectividad y la motivación. La dopamina también ejerce múltiples funciones en el sistema periférico como modulador de la liberación de catecolaminas, de la secreción hormonal, del tono vascular, de la función renal y de la motilidad gastrointestinal (Cooper *et al.* 1996; Missale *et al.* 1998). Como otros neurotransmisores, la dopamina no es capaz de cruzar la barrera hematoencefálica, pero sí sus precursores fenilalanina y tirosina. La síntesis de dopamina ocurre en el citosol de las terminales nerviosas dopaminérgicas tal como se indica en la Figura 21 (Elsworth and Roth 1997). La liberación de dopamina en la hendidura sináptica tiene lugar mediante un mecanismo clásico de liberación de neurotransmisores: la entrada de calcio a través de canales de calcio dependientes de voltaje promueve la fusión de vesículas llenas de dopamina con la membrana presináptica, formándose un poro y dando lugar a la exocitosis de la dopamina, que por difusión cruza el espacio de la hendidura sináptica hasta unirse a sus receptores localizados pre- y postsinápticamente. Después de la unión, ocurre un cambio conformacional en el receptor que induce una compleja cadena de eventos intracelulares, y el resultado final de la liberación de dopamina es la activación o inhibición de la neurona postsináptica.

La señal dopaminérgica finaliza por eliminación de la dopamina del espacio intersináptico, lo que implica mecanismos de recaptación específicos en el terminal presináptico donde puede ser almacenada o metabolizada (Elsworth and Roth 1997). Aunque existen enzimas extraneuronales que catabolizan la dopamina liberada, la finalización del efecto se debe principalmente, a la recaptación del neurotransmisor por los propios terminales nerviosos que la liberaron mediante transportadores específicos (DAT*: Dopamine Transporters*) que juegan un papel importante en la función, inactivación y reciclaje de la dopamina liberada (Adell and Artigas 2004; Sotnikova *et al.* 2006).

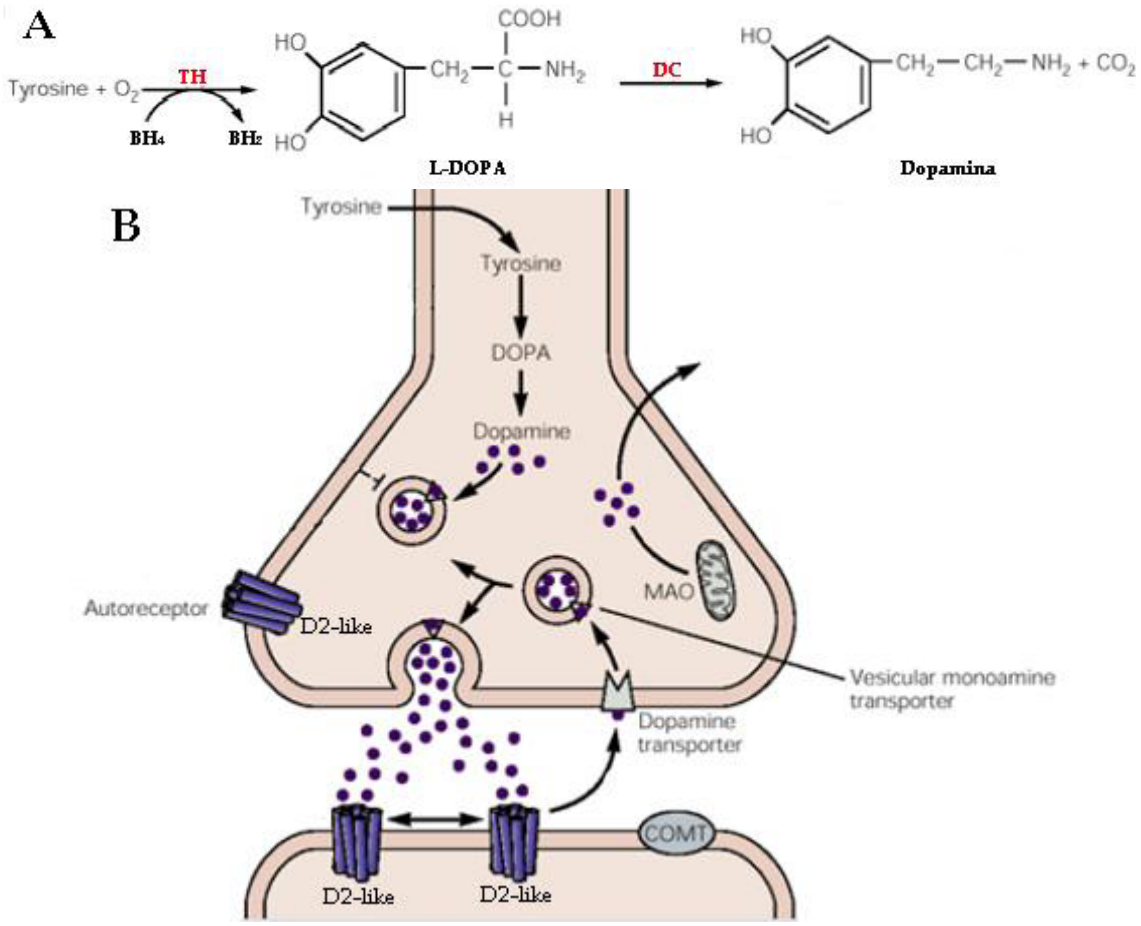

Figura 21. Síntesis de la dopamina (modificado de Kandel *et al.* 2000). A) La tirosina hidroxilasa emplea oxígeno molecular, tirosina y tetrahidrobiopterina (cofactor) para sintetizar L-DOPA, la cual será descarboxilada por la DOPA descarboxilasa dando lugar a dopamina y CO_2. B) Una vez sintetizada, la dopamina es almacenada en vesículas sinápticas hasta su posterior liberación al espacio sináptico. En él, puede interactuar con sus receptores específicos, ser recaptada y degradada.

Los receptores dopaminérgicos localizados presinapticamente son principalmente, autoreceptores y constituyen uno de los mecanismos responsables de la regulación de la transmisión dopaminérgica (Langer 1997; Koeltzow *et al.* 1998). Cuando la dopamina es liberada al espacio sináptico, la estimulación de los autorreceptores presentes en las terminales nerviosas induce una inhibición de la liberación continuada de dopamina. Todos los autorreceptores dopaminérgicos pertenecen a la subfamilia D_2-like (Langer 1997; Mercuri *et al.* 1997; Vallone *et al.* 2000). Se han desarrollado numerosos agonistas y antagonistas específicos de los receptores de dopamina lo que ha dado la oportunidad de modular la transmisión dopaminérgica incrementando o bloqueando la acción de este neurotransmisor con fines terapéuticos (Sokoloff *et al.* 2006; Rankin *et al.* 2010; Rondou *et al.* 2010). El sistema dopaminérgico ha sido de gran interés por la relación entre la desregulación de este sistema y algunas patologías tales como el Parkinson, la esquizofrenia, el síndrome de Tourette, la hiperprolactinémia y la adicción a drogas (Missale *et al.* 1998; Segawa 2003; Santini *et al.*

2008; Dalley and Everitt 2009; Zack and Poulos 2009). De hecho, la degeneración de la vía nigroestriatal produce la enfermedad de Parkinson en humanos, caracterizada por una fuerte reducción de la liberación de dopamina (Mercuri *et al.* 1997; Shimohama *et al.* 2003).

1.3.2 ESTRUCTURA, CLASIFICACIÓN Y FUNCIÓN DE LOS RECEPTORES DE DOPAMINA

En 1978, en base a evidencias farmacológicas y bioquímicas, los receptores de dopamina se clasificaron en dos grupos: receptores activadores de la adenilato ciclasa (AC) y receptores inhibidores de la AC (Spano *et al.* 1978). Sin embargo, posteriormente, usando técnicas de clonaje, se han aislado 5 receptores distintos para la dopamina (Gingrich and Caron 1993). Estos receptores se han clasificado en dos subfamilias en función de sus propiedades bioquímicas y farmacológicas: los receptores D_1-*like*, que comprenden los receptores D_1 y D_5 y los receptores D_2-*like* que incluye a los receptores D_2, D_3 y D_4. La subfamilia D_1-*like*, producen incrementos de AMPc intracelular a través de proteínas $G_{s/olf}$ que estimulan la AC y se localizan principalmente en los terminales postsinápticos (Civelli *et al.* 1993; Missale *et al.* 1998; Nieoullon and Amalric 2002; Neve *et al.* 2004). Los receptores D_2-*like*, en cambio, inhiben la AC por acoplamiento a proteínas $G_{i/o,}$ además de activar canales de K^+ y disminuir la entrada de Ca^{2+} a través de canales dependientes de voltaje (Missale *et al.* 1998; Nicola *et al.* 2000; Neve *et al.* 2004; Gershon *et al.* 2007). Los receptores D_2-*like* pueden localizarse en terminales presinápticos y postsinápticos (Dal Toso *et al.* 1989; De Mei *et al.* 2009).

La organización genómica de los receptores de dopamina sugiere que provienen de dos familias génicas que difieren principalmente por la presencia o no de intrones en su secuencia codificadora. Los receptores D_1-*like* no contienen intrones, característica que comparten con la mayoria de GPCR (Dohlman *et al.* 1987; Gingrich and Caron 1993); en cambio, análogamente al gen de rodopsina, los genes que codifican para los receptores D_2-*like* están interrumpidos por intrones lo que permite la generación de variantes de estos receptores (Ogawa 1995; Vallone *et al.* 2000). El gen del receptor D_2 esta compuesto por 8 exones, 7 de los cuales se transcriben. En el sexto exón tienen lugar un splicing alternativo, el cual codifica para 29 aminoácidos adicionales en el tercer bucle intracelular (IC3), generando las dos isoformas que se encuentran tanto en rata como humano (Giros *et al.* 1989; Monsma *et al.* 1989; Usiello *et al.* 2000; De Mei *et al.* 2009; Beaulieu and Gainetdinov 2011). El primer cDNA de los receptores de dopamina aislado fue el del receptor D_2 (Bunzow *et al.* 1988) que se clonó a partir de una librería de cDNAs de pituitaria de rata. La región codificadora de esta proteína se encuentra en el cromosoma 11q23. El cDNA aislado por Bunzow y colaboradores contenía una secuencia de

1245 nucleótidos que codificaban para una proteína de 415 residuos, que posteriormente se llamo $D_{2S}R$ (receptor de dopamina D_2 short), con un perfil farmacológico típico de los receptores D_2-like. Más tarde, varios grupos clonaron una variante por splice de este receptor, el $D_{2L}R$ (receptor de dopamina D_2 long) de diferentes especies (rata, ratón, bovino, humano) y tejidos (cerebro, pituitaria, retina), que contenía 444 aminoácidos (Figura 22).

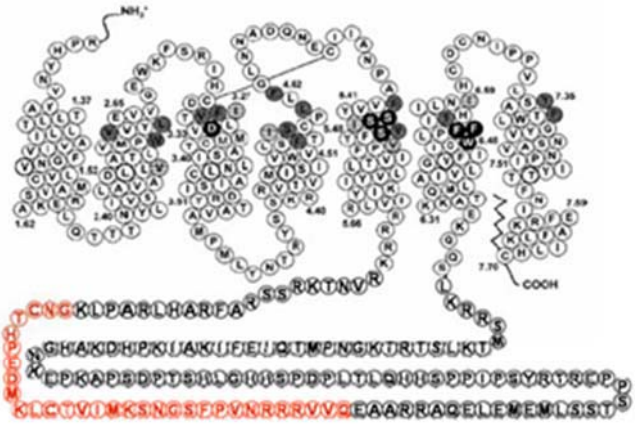

Figura 22. Estructura prototipo del receptor de dopamina D_2. El receptor D_2 short no contiene los aminoácidos indicados en rojo.

Los receptores D_2 tienen un extremo carboxilo terminal corto y un IC3 largo, el cual parece estar implicado en el acoplamiento a la proteína G (Malek *et al.* 1993; Lachowicz and Sibley 1997; Filteau *et al.* 1999; Ilani *et al.* 2002), además de permitirle interaccionar con otras proteínas, como el receptor de adenosina A_{2A} (Canals *et al.* 2003).

Los dos subgrupos, D_1-*like* y D_2-*like*, presentan, además, diferencias estructurales como se muestra en la Figura 23: los receptores D_1-*like* tienen un dominio carboxilo terminal unas siete veces más largo que los D_2-*like*, mientras que estos últimos tienen el tercer bucle intracelular (IC3) mucho más largo, característica común en muchos receptores acoplados a la proteína G_i (Missale *et al.* 1998) (Gingrich and Caron 1993).

D_1R-*like* **D_2R-*like***

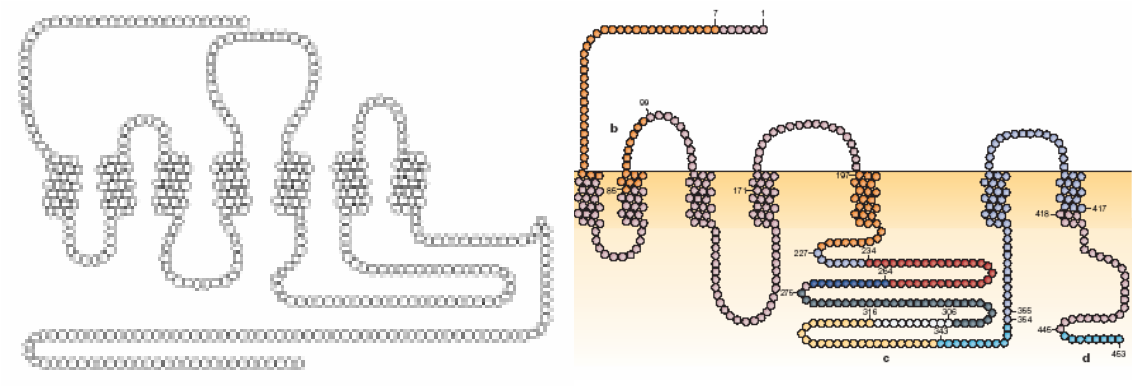

Figura 23. Representación esquemática de las dos subfamilias de receptores de dopamina.

Existe una alta homología de secuencia entre los dos miembros de la familia de receptores D_1-*like*, del orden del 80%. En cambio, entre los miembros de la subfamilia D_2-*like* la homología es de un 75% entre los receptores D_2 y D_3 y de un 53% entre los receptores D_2 y D_4. Por el contrario, la homología entre los receptores D_1-*like* y D_2-*like* es solo del 42-46%. La región con homología más elevada se encuentra en los dominios transmembrana y en aquellos residuos que son clave para la unión de catecolaminas. El extremo carboxilo terminal, en ambas familias, contiene lugares de fosforilación y palmitoilación que se cree juegan un papel importante en la desensibilización del receptor y en la formación de un cuarto bucle intracelular, respectivamente. Por el contrario, los receptores de dopamina presentan diferencias en las modificaciones post-traduccionales, como diferentes lugares consenso de N-glicosilación.

El gen correspondiente al receptor D_4 de dopamina se clonó por primera vez en 1991 por Van Tol y colaboradores; está localizado en el extremo distal del brazo corto del cromosoma 11 en la posición 11p15.5 y próximo al oncogen Harvey-RAS y al gen de la tirosina hidrolasa (Oak *et al.* 2000). El gen del receptor D_4 contiene cuatro exones y un número de polimorfismos variable en la secuencia de codificación; el polimorfismo más extendido es el que se encuentra en el tercer exón, cuya región codifica para el tercer loop citoplasmático. Este polimorfismo consiste en un número variable de repeticiones en tándem (VNTR), es decir, unas secuencias de 48bp que codifican para diferentes polipéptidos formados por 16 aminoácidos. Éstos pueden formar combinaciones distintas que pueden presentar de 2 a 11 repeticiones dando así el subnombre al receptor de $D_{4.2}$ a $D_{4.11}$ y proporcionando un tamaño variable a cada polimorfismo (Figura 24).

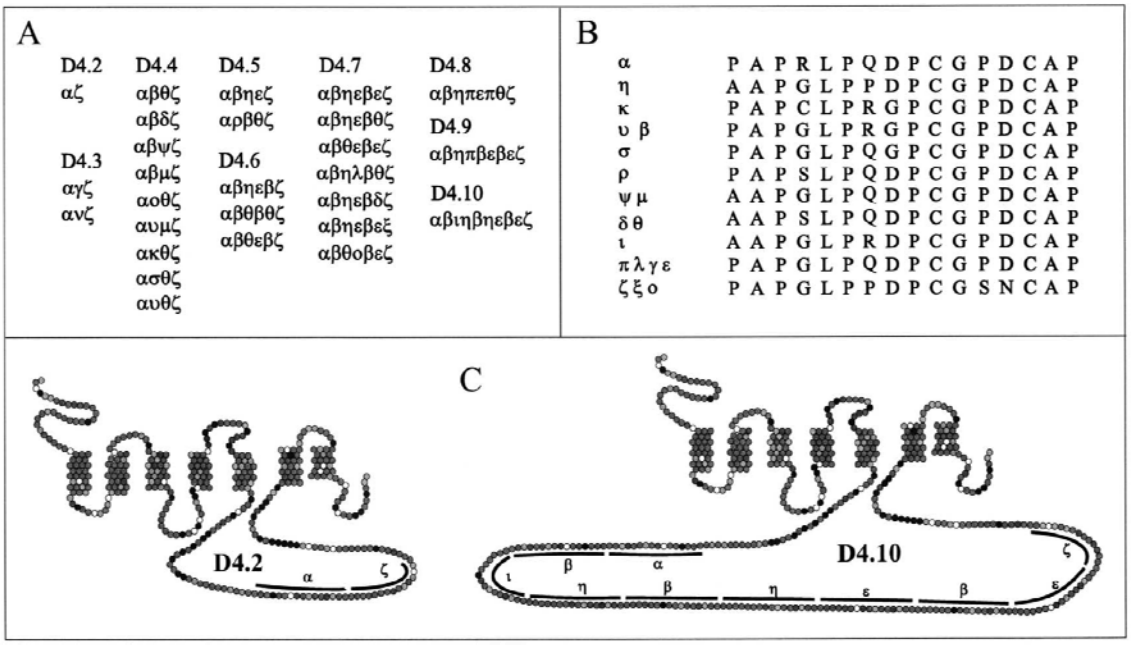

Figura 24. Representación de las diferentes VNTR presentes en el tercer loop intracelular de los receptores D_4 de dopamina. a) Representación de los diferentes haplotipos presentes en la población humana y las combinaciones de secuencias de 48bp que los forman. b) Los péptidos formados por 16 aminoácidos correspondientes a los diferentes haplotipos. c) representación esquemática del largo loop intracelular como consecuencia de las diferentes VNTR (Extraído de Oak *et al*. 2000).

La frecuencia de la presencia de los diferentes polimorfismos varía de forma considerable en función de la población y la etnia (Swanson *et al.* 2001), a pesar de ello, estudios genéticos de población sobre la diversidad alélica demostraron que los polimorfismos $D_{4.2}$, $D_{4.4}$ y $D_{4.7}$ son los más prevalentes, presentándose así en el 90% de la población. Como se muestra en la Figura 25 dentro de los polimorfismos más abundantes, el $D_{4.4}$ ocurre con más frecuencia, en aproximadamente el 64 % de la población, seguido del $D_{4.7}$ en aproximadamente el 21 % y $D_{4.2}$ en aproximadamente el 8 % (Ding *et al.* 2002; Floet *et al.* 2010).

Dado que el receptor D_4 pertenece a la subfamilia de receptores *D_2-like*, presenta homología con los otros miembros de esta subfamilia, especialmente en los siete dominios de transmembrana que son altamente conservados. Muestra una serie de modificaciones post-transcripcionales como N-glicosilaciones en la cola amino terminal extracelular, y la presencia de regiones de fosforilación de proteína cinasa A (PKA), proteína cinasa C (PKC) y casein cinasa II (Asghari *et al.* 1995; Jovanovic *et al.* 1999; Neve *et al.* 2004; Rondou *et al.* 2010).

El tercer loop citoplasmático del receptor D_4 es característicamente largo si se compara con cualquier otro miembro de su subfamilia *D_2-like*. Posee regiones ricas en prolina además de

la región hipervariable VNTR anteriormente descrita y contiene una secuencia SH3 que le permite interaccionar con proteínas como Src, Grb2 y Nck (Oldenhof *et al.* 1998; Oak *et al.* 2001; Rondou *et al.* 2010). Aunque se conocen las diferentes regiones de unión a proteínas de señalización intracelular todavía se desconocen sus funciones y el porqué de la existencia de los diferentes polimorfismos.

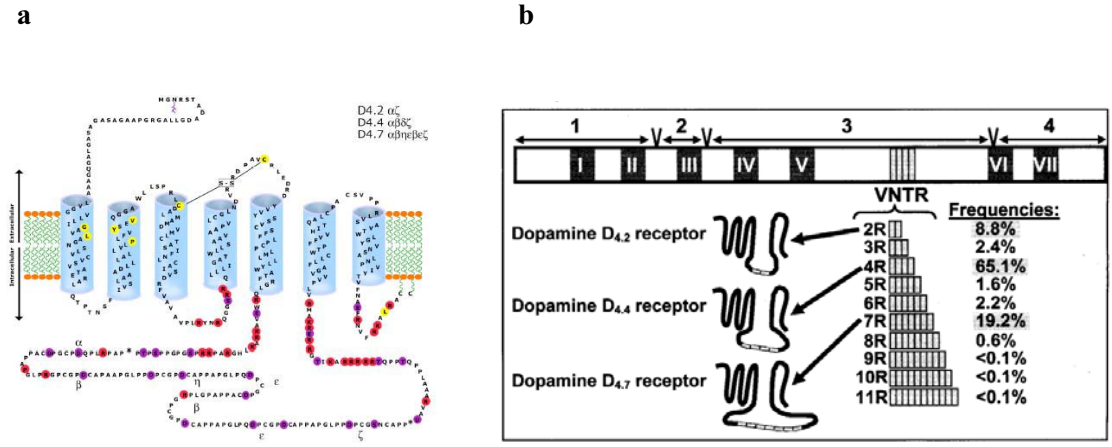

Figura 25. Representación esquemática de la estructura del receptor D_4 de dopamina y la frecuencia de los diferentes polimorfismos (Extraído y modificado de Ding *et al.* 2002).

Para el estudio de las propiedades farmacológicas de los receptores de dopamina se dispone de ligandos que fácilmente discriminan entre las dos subfamilias D_1-*like* y D_2-*like*, aunque es mucho más difícil encontrar ligandos selectivos para los miembros de cada subfamilia. Los receptores D_1-*like* muestran alta afinidad por benzazepinas (agonistas) y baja afinidad por butiroferonas y benzamidas sustituidas (antagonistas). Se ha detectado una diferencia remarcable entre los receptores D_1-*like*, y es la afinidad que presentan sus miembros por la dopamina, el receptor D_5 tiene una afinidad 10 veces superior a la que muestra el receptor D_1 (Missale *et al.* 1998). Las propiedades farmacológicas de los receptores D_2-*like* difieren más que las que muestran los D_1-*like*. Así, las afinidades por muchos agonistas y antagonistas varían entre uno y dos órdenes de magnitud entre subtipos, incluyendo la dopamina por la que el receptor D_3 tiene una afinidad unas 20 veces más alta que el receptor D_2. Cada uno de estos receptores, sin embargo, tiene el sello característico de unión de ligando de los receptores D_2, es decir, alta afinidad por butirofenonas, como las espiperonas y haloperidol, y baja afinidad por benzazepinas, como el SKF 38393. El receptor D_4 se caracteriza por ser el más diferenciado, presentando baja afinidad por la mayoría de antagonistas dopaminérgicos, por ejemplo, el raclopride y exhibiendo una relativamente alta afinidad por el neuroléptico atípico clozapina (Missale *et al.* 1998).

La diferencia de afinidad que presentan los receptores de dopamina por su ligando endógeno puede permitir la activación de unos receptores o de otros en función de la cantidad de dopamina liberada (Tabla 3). Teniendo en cuenta los diferentes mecanismos de transducción de señal de cada subtipo de receptor, esto genera una gran variedad de respuestas a una misma sustancia, dependiendo del tipo de proteína G a la que se acople el receptor y las moléculas efectoras que modulan (Tabla 3). Esta diversidad dentro de los receptores de dopamina es un reflejo de la diversidad funcional que ejerce este neurotransmisor, sobre todo si se considera la expresión diferencial de estos receptores dentro del SNC.

La expresión de los distintos subtipos de receptores de dopamina en el cerebro ha sido determinada mediante la combinación de técnicas de unión de radioligandos y de hibridación in situ. Así se ha demostrado que el receptor D_1 es el más abundante y su distribución es la más amplia de todos los receptores dopaminérgicos (Dearry *et al.* 1990; Barishpolets *et al.* 2009; Beaulieu and Gainetdinov 2011). Estudios de RT-PCR y proteómica han demostrado la expresión del receptor D_1 en el estriado (dorsal y ventral), núcleo accumbens, tubérculo olfactorio y en menor medida en el sistema límbico, hipotálamo y tálamo, localizándose de manera postsináptica preferencialmente en las neuronas estriatales GABAérgicas que coexpresan sustancia P (Gerfen *et al.* 1990). El receptor D_5 se expresa con mucha menor intensidad que el subtipo D_1 y su localización parece restringirse al hipocampo y a los núcleos lateral mamilar y parafascicular del tálamo (Jaber *et al.* 1996). Los receptores D_5 de dopamina se expresan en niveles bajos en la mayoría de regiones del cerebro, entre las que se incluyen neuronas piramidales de la corteza prefrontal, la corteza premotora, la corteza cingulada, la substancia nigra, el hipotálamo y el giro dentado. Niveles de expresión muy bajos han sido detectados en neuronas espinosas medianas del núcleo caudado y del núcleo accumbens (Missale *et al.* 1998; Gerfen 2000; Sokoloff *et al.* 2006; Rankin *et al.* 2010; Beaulieu and Gainetdinov 2011). El receptor D_5, junto con el receptor D_4, muestran un patrón de expresión limitado en regiones primarias motoras del cerebro, y consecuentemente tienen una importancia limitada en el control del movimiento (Missale *et al.* 1998; Sibley 1999; Rondou *et al.* 2010; Beaulieu and Gainetdinov 2011). En el SNC, la expresión del ARNm del receptor D_5 se ha demostrado en el hipocampo, el tálamo, el neoestriado, el hipotálamo y la corteza cerebral en sus regiones frontal y temporal. Adicionalmente a los receptores funcionales, se han descrito dos pseudogenes para el subtipo D_5 que codifican formas truncadas del receptor no funcionales (Grandy *et al.* 1991; Missale *et al.* 1998; Beaulieu and Gainetdinov 2011).

En cuanto a los receptores D_2-*like*, el receptor D_2 se expresa principalmente en núcleo accumbens, tubérculo olfactorio e hipocampo, tanto pre-sináptica como postsinápticamente y su expresión es elevada en las neuronas GABAérgicas estriatopalidales. Este receptor actúa como

autoreceptor en las terminales dopaminérgicas, donde regula la síntesis y liberación de dopamina (Mercuri *et al.* 1997). El receptor D_3 se localiza específicamente en las regiones límbicas del núcleo accumbens con una localización post-sináptica en neuronas que expresan sustancia P y neurotensina. Por último, el receptor D_4 se expresa en interneuronas GABAérgicas tanto piramidales como no-piramidales de la corteza pre-frontal e hipocampo, en el bulbo olfatorio, la amígdala, el mesencéfalo (Missale *et al.* 1998), en la glándula pineal (Klein, et al., 2009) y en menor medida en el núcleo accumbens y estriado (Almeida and Mengod 2010; Gasca-Martinez *et al.* 2010). El receptor D_4 se expresa mayoritariamente en córtex prefrontal, hipocampo, amígdala, hipotálamo (Missale *et al.* 1998) y en las neuronas piramidales glutamatérgicas y no piramidales del córtex cerebral y en las terminaciones de sus proyecciones estriatales (Tarazi *et al.* 1998; Svingos *et al.* 2000; Lauzon and Laviolette 2010), en las que se incluyen el núcleo talámico, globus pallidus y sustancia nigra pars reticulata, donde también se encuentran las interneuronas gabaérgicas. Estudios de northern-blot, hibridación *in situ*, inmunohistoquímica y RT-PCR han demostrado que el receptor D_4 presenta una gran diversidad de expresión en diferentes tejidos como la glándula pineal, linfocitos o retina (Burgueño *et al.* 2007; Beaulieu and Gainetdinov 2011).

Familia	**D_1R- like**		**D_2R- like**		
Subtipo	D_1R	D_5R	D_2R	D_3R	D_4R
Proteína G	$G_{s/olf}$	$G_{s/olf}$	$G_{i/o}$	$G_{i/o}$	$G_{i/o}$
Mecanismo de transducción de señal	+ AC + PLC	+ AC	- AC + PLC - canales Ca^{2+} + canales K^+	- AC + PLC - canales Ca^{2+} + canales K^+	- AC + PLC
Moléculas efectoras	↑ AMPc ↑ PKA ↑ IP3	↑ AMPc	↓ AMPc ↑ IP_3 ↓ Ca^{2+} ↑ K^+	↓ AMPc ↑ IP_3 ↓ Ca^{2+} ↑ K^+ ↑ NKE*	↓ AMPc ↑ ác. araquid. ↑ NKE*
Afinidad por la dopamina K_D en nM	2340	261	2,8-474	4-27	28-450
Agonista	SKF-38393	NPA	Quinpirole	Bromocriptina	(-)Apomorfina
Antagonista	SCH-23390	SCH-23390	Raclopride	UH 232	Clozapina

*NKE: Na+ /K+ exchange: intercambiador Na+/K+.

Tabla 3. Resumen de las principales características de los receptores de dopamina.

En distintas situaciones patológicas se ha observado la existencia de diferencias cuantitativas en cuanto a la expresión de los receptores de dopamina o bien en su señalización. Por ejemplo, los receptores D_1 se ven incrementados en la esquizofrenia y su señalización varia en la enfermedad de Parkinson. Por otro lado, la densidad de los receptores D_2 post-sinápticos

incrementa en la esquizofrenia y también en los enfermos de Parkinson no tratados con L-DOPA (Matsukawa *et al.* 2007; Reeves *et al.* 2009).

El receptor D_1 media su respuesta fisiológica por acoplamiento a la proteína G estimuladora, específicamente este receptor se acopla a proteína $G\alpha_s$ y $G\alpha_{olf}$, las cuales provocan una activación secuencial de la adenilato ciclasa, proteína cinasa dependiente de AMPc (PKA) y fosforila DARPP-32 (*Dopamine and cyclic adenosine 3', 5'- monophosphate Regulated Phospho Protein,* 32 kDa), que a su vez inhibe a la proteína fosfatasa-1 (PP-1) previniendo la defosforilación de varias fosfoproteínas (Greengard *et al.* 1999; Neve *et al.* 2004). El incremento en la fosforilación de factores de transcripción, que resulta del efecto combinado de la activación de la PKA y la inhibición de PP-1, regula la actividad de varios receptores, enzimas, canales iónicos y factores de transcripción (Greengard *et al.* 1999). La estimulación de los receptores D_1 también afecta la actividad de canales de calcio, tanto en las neuronas estriatales de rata como en las células GH_4C_1, transfectadas con el receptor D_1, produciendo incrementos en el flujo de calcio vía los canales de calcio tipo L. En ambos casos, los efectos son mimetizados por análogos de AMPc y bloqueados por inhibidores de la PKA, sugiriendo que este efecto puede ser el resultado de una fosforilación de los canales de calcio vía PKA (Liu *et al.* 1992b; Surmeier *et al.* 1995). Por otra parte, también se ha descrito que los receptores D_1 regulan otros canales iónicos, como los canales de potasio y de sodio (Neve *et al.* 2004).

Si bien la señalización vía incrementos de AMPc es la más aceptada para los receptores D_1, existen ciertas controversias. Los receptores D_1 estriatales parecen estar acoplados a proteínas $G\alpha_i$ cuando se reconstituyen en vesículas de fosfolípidos (Sidhu *et al.* 1991). Además, la inmunoprecipitación con anticuerpos específicos contra distintos subtipos de proteína G ponen de manifiesto que el receptor D_1 coinmunoprecipita con $G\alpha_o$ (Kimura *et al.* 1995) y con $G\alpha_q$ para mediar la formación de inositol fosfato en estriado de rata (Wang, et al., 1995), además se ha descrito que los receptores D_1 en células Ltk- estimulan la producción de fosfatidilinositoles (Liu *et al.* 1992b). Esta acción de los receptores de dopamina es controvertida, ya que si bien agonistas del receptor D_1 causan incrementos en el metabolismo de los fosfoinositoles de varias regiones del cerebro, lo hacen a concentraciones muy altas (Undie and Friedman 1990), lo que pone en entredicho la relevancia fisiológica de esta respuesta. Por otro lado, algunos autores han demostrado en células COS-7 que estos receptores no pueden estimular el recambio de fosfoinositoles (Tiberi *et al.* 1991; Sugamori *et al.* 1994; Demchyshyn *et al.* 1995). Además se ha descrito que ni D_1 ni D_5 afectan los niveles de calcio intracelular en células CHO (*chinese hamster ovary*) (Pedersen *et al.* 1994), pero D_1 promueve la movilización de calcio intracelular mediante la activación de PLC en oocitos de Xenopus (Mahan *et al.* 1990; Neve *et al.* 2004). El conjunto de estos resultados sugiere que la señalización generada tras la

activación de los receptores D_1 depende de la célula en la que se produzca, es decir, que en este caso y probablemente en muchos otros, la señalización depende del conjunto de proteínas G y otros componentes propios de cada célula (Missale *et al.* 1998).

El receptor D_1 también se ha relacionado con la activación de la vía de las MAPK. Se ha descrito que la unión de un agonista a este receptor induce la activación de ERK1/2, p38 y JNK en células de neuroblastoma humano a través de un mecanismo dependiente de PKA, en el caso de p38 y JNK, y parcialmente independiente de PKA o AMPc en el caso de ERK1/2 (Neve *et al.* 2004). Incluso se ha mostrado por coinmunoprecipitación que ERK1/2 fosforilada es capaz de formar un complejo estable con el receptor D_1 y β-arrestina (Zhen *et al.* 1998; Chen *et al.* 2004). También se ha descrito que la activación de ERK1/2 en el estriado de ratones, después de una administración aguda de cocaína, es bloqueada por un antagonista de D_1, lo que sugiere que este receptor controla la actividad estriatal inducida por cocaína a través de una vía dependiente de ERK1/2 (Valjent *et al.* 2000). Asimismo, la activación de c-fos por el receptor D_1 después de una administración crónica con cocaína depende de la activación de ERK1/2 (Zhang *et al.* 2004; Acquas *et al.* 2007). Además se ha publicado que el bloqueo del receptor D_1 previene también la activación de ERK1/2 inducida por tetrahidrocannabinol (THC) en neuronas estriatales (Valjent *et al.* 2001). Estos antecedentes apuntan a una posible vía intracelular común a diferentes drogas de abuso que activan ERK1/2 en poblaciones de neuronas estriatales que expresan el receptor D_1 y en las que este receptor actuaría como mediador (Valjent *et al.* 2001; Valjent *et al.* 2004). Por otro lado, se ha descrito que la estimulación por agonistas del receptor D_1 en la vía directa del estriado dorsal en ratas, induce genes tempranos como c-fos independientemente de la activación de ERK1/2, a diferencia de lo que ocurre en estriado ventral que normalmente usa la vía de las MAPK. Sin embargo, después de la degeneración de la vía dopaminérgica nigroestriatal el tratamiento con agonistas de este receptor resulta en la activación de ERK1/2, indicando que la activación de esta cinasa está regulada por distintos mecanismos en el estriado dorsal y en el ventral, y que después de la depleción de dopamina en estriado hay un cambio en el mecanismo por el cual la activación de ERK1/2 es mediada por el receptor D_1 (Gerfen *et al.* 2002).

De manera similar al subtipo D_1, la activación de los receptores D_5 conduce a la formación de AMPc y a la activación de la proteína PKA por estimulación de una o más isoformas de la adenilato ciclasa, proceso mediado por proteínas $G\alpha_{s/olf}$. Como se ha mencionado anteriormente, existen evidencias que indican que, además de los efectos en la señalización dependiente de AMPc, los receptores de dopamina pueden también acoplarse a la proteína $G\alpha_q$ para regular la PLC. En el año 1989, Felder y colaboradores (Felder *et al.* 1989) describieron que el agonista SKF 82526 del receptor D_1 podía estimular la actividad de la PLC

independientemente de AMPc en membranas de túbulos renales. Es importante destacar que este tipo de activación de los receptores D_1-*like* ha sido observada en ratones D_1 *knockout (Friedman et al. 1997)* pero no en ratones carentes en el receptor D_5 (Sahu *et al.* 2009). Además, se ha descrito que la expresión de receptores D_1 en células HEK293 no afectó a la señalización de calcio intracelular, mientras que la expresión del receptor D_5 en la misma línea celular indujo una movilización substancial después de estimularlas (So *et al.* 2009; Beaulieu and Gainetdinov 2011). Aunque con estas observaciones no es posible descartar completamente la contribución del receptor D_1 en la señalización a través de $G\alpha_q$, sugieren que el receptor D_5 es el regulador principal en este tipo de señalización *in vivo* o que el receptor D_1 tiene que interaccionar con otras proteínas para poder acoplarse a $G\alpha_q$ (Beaulieu and Gainetdinov 2011).

Se ha descrito que los receptores de dopamina pueden formar interacciones directas con receptores ionotrópicos y receptores GABAérgicos. En el caso del receptor D_5 se ha descrito que su extremo carboxi terminal interacciona con el segundo *loop* intracelular de la subunidad 2 del receptor GABA-A en el hipocampo de rata (Liu *et al.* 2000; Beaulieu and Gainetdinov 2011). Es importante destacar que esta interacción con el receptor GABA-A parece ser específica del receptor D_5, ya que no ocurre con el receptor D_1. Las consecuencias funcionales de las interacciones con estos receptores son diversas, en el caso de la interacción del receptor D_5 con el receptor GABA-A, es la reducción de la transmisión eléctrica en la célula (Liu *et al.* 2000; Beaulieu and Gainetdinov 2011).

El receptor D_2 de dopamina ha sido ampliamente estudiado, demostrándose su participación en numerosas e importantes funciones fisiológicas como el control de la actividad motora.

Ambas isoformas del receptor D_2, D_{2L} y D_{2S}, tienen la misma capacidad de unir ligando pero difieren tanto en la expresión como en la capacidad de acoplarse a la proteína G. La isoforma larga se expresa unas 10 veces más que la corta y tiene una capacidad de acoplarse a la proteína G_i mucho menor, lo que da lugar a una diversidad de señal. De hecho existen evidencias que indican que los receptores D_{2L} y el D_{2S} se acoplan a distintas proteínas G, G_i y G_o respectivamente, debido principalmente a sus diferencias estructurales (Senogles *et al.* 1987; Ohara *et al.* 1988; De Keyser *et al.* 1989; Beaulieu and Gainetdinov 2011). La inactivación genética tanto de la AC_5, la principal isoforma de la AC en el estriado (Mons *et al.* 1995; Lee *et al.* 2002), como de la PKA provoca un daño importante en la función de estos receptores, como la pérdida de los efectos bioquímicos y del comportamiento de los antagonistas de los receptores D_2 (Adams *et al.* 1997; Lee *et al.* 2002). La inhibición sobre la AC provocada por la activación de los receptores D_2 se ha observado en varias células y parece ser dependiente del

acoplamiento del receptor a la proteína $G_{i/o}$ (Ghahremani *et al.* 1999; Banihashemi and Albert 2002).

Además de inhibir la AC, la activación de los receptores D_2 da lugar a cambios en la actividad de canales de Ca^{2+} (Taraskevich and Douglas 1978; Hernandez-Lopez *et al.* 2000) y de K^+ (Castelletti *et al.* 1989; Missale *et al.* 1998) provocando una hiperpolarización celular. Los agonistas del receptor activan a la fosfolipasa C (PLC) e incrementan la concentración de Ca^{2+} intracelular (Beaudry *et al.* 1986; Enjalbert *et al.* 1986; Martemyanov and Arshavsky 2009; Beaulieu and Gainetdinov 2011) dependiente de IP_3 y la activación de la calcineurina, una serina-treonina fosfatasa dependiente de Ca^{2+} (PP-2A) (Hernandez-Lopez *et al.* 2000). Esta vía parece implicar a las subunidades $G_{\beta\gamma}$ de la proteína G_o. La calcineurina no solo reduce las corrientes de Ca^{2+} a través de los canales de Ca^{2+} dependientes de voltaje tipo L (L-type VDCC: L-type Voltage Dependent Ca^{2+} Channel) (Ghahremani *et al.* 1999; Hernandez-Lopez *et al.* 2000; Banihashemi and Albert 2002), sino que además, la calcineurina parece ser la principal fosfatasa implicada en la desfosforilación de DARPP-32. Por lo tanto, la activación del receptor D_2 de dopamina produce la desfosforilación de DARPP-32 debida tanto a la inhibición de la actividad de la AC como a la calcineurina dependiente de Ca^{2+} e independiente de AC (Nishi *et al.* 1997).

La estimulación de los receptores D_2 activa también la vía de las MAPKs y la fosforilación de CREB (*cAMP Response Element-Binding protein*) en cortes cerebrales (Yan *et al.* 1999), en cultivos estriatales primarios (Brami-Cherrier *et al.* 2002) y en diferentes líneas celulares (Faure *et al.* 1994; Oak *et al.* 2001; Banihashemi and Albert 2002; Kim *et al.* 2006). Tanto la PKC como DARPP-32 y la calmodulina cinasa, junto con los incrementos en los niveles de Ca^{2+}, parecen ser importantes en la activación de estas vías (Yan *et al.* 1999; Lee *et al.* 2004; Sahu and August 2009). La activación de la vía de las MAPKs, en las interneuronas estriatales, se cree que juega un papel importante en la regulación de la expresión génica inducida por dopamina y la adaptación neuronal a largo plazo en el estriado. La activación de la vía de las MAPKs puede estar implicada en la sensibilización locomotora en respuesta a la estimulación del receptor D_2 en ratas lesionadas unilateralmente con 6-hidroxidopamina (Santini, et al., 2007; Cai, et al., 2000). A pesar de los resultados comentados anteriormente, existen datos contradictorios, los agonistas del receptor D_2 se ha descrito que inhiben específicamente la activación de la vía de las MAPK en neuronas de proyección estriatopalidales activadas por estimulación aferente corticoestriatal (Gerfen *et al.* 2002; Chen *et al.* 2009; Yoon *et al.* 2011). Para la activación de la vía de las MAPKs es necesario la formación de un complejo entre la calmodulina y el VDCC tipo L, que juega un papel importante en la conversión de la información de la membrana (activación neuronal) hacia el núcleo (plasticidad neuronal) (Dolmetsch *et al.* 2001). En las neuronas de proyección estriatopalidales el receptor

D_2 media la inhibición de los VDCC tipo L, lo que parece ser el principal mecanismo implicado en la inhibición de la activación de las MAPKs.

Una de las diferencias más significativas entre las dos isoformas del receptor D_2 es la respuesta diferencial que presentan ambas isoformas a la exposición prolongada a agonistas. En algunas células se ha visto que ambas isoformas experimentan una internalización tras exposición a agonista, proceso que implica a GRKs y β-arrestinas (Ito *et al.* 1999; Kim *et al.* 2001). Sin embargo, el grado de internalización del receptor D_{2S} es mayor que el del D_{2L} (Ito *et al.* 1999) de acuerdo con el hecho de que ambas isoformas pueden ser fosforiladas diferencialmente por GRKs y β-arrestina (Liu *et al.* 1992a; Senogles 1994; Guiramand *et al.* 1995). La resistencia a la internalización inducida por ligando del receptor D_{2L} se hace muy patente en algunas células en las que el receptor D_{2L} se expresa más en la membrana en respuesta al pretratamiento con agonistas (Filtz *et al.* 1993; Zhang *et al.* 1994; Starr *et al.* 1995; Ng *et al.* 1997), lo que es debido a la translocación a la membrana de los receptores intracelulares ya existentes y a la síntesis de novo de receptores (Ng *et al.* 1997; Thibault *et al.* 2011). Se ha descrito que este incremento de expresión puede ser la causa de la resistencia que presentan los receptores D_{2L} a la desensibilización (Filtz *et al.* 1993; Zhang *et al.* 1994; Starr *et al.* 1995; Ng *et al.* 1997; Hillion *et al.* 2002).

Debido a la tardía clonación del receptor D_4 y a la limitación en la disponibilidad de agonistas selectivos y/o antagonistas, la farmacología y los estudios de señalización intracelular del receptor D_4 son todavía muy reducidos. A pesar de ello ya se había descrito que en células mesencefálicas MN9D de rata y en otras líneas celulares éste receptor se acopla mayoritariamente a proteína G_i (Chio *et al.* 1994; Watts *et al.* 1999; Kazmi *et al.* 2000) pero también puede acoplarse a $G\alpha_A$, $G\alpha_B$ y G_{ilr2r3} dependiendo del tejido en el que se encuentra (O'Hara *et al.* 1996). Es el primer receptor no-opsina capaz de unirse a la proteína mutante G_{t2} resistente a la toxina pertusis (Yamaguchi *et al.* 1997). La activación de GIRK1 en oocitos de *Xenopus* mediada por D_4 sugiere también que éstos están implicados en la apertura de canales de K^+ por vía $G_{\beta\gamma}$ (Werner *et al.* 1996; Pillai *et al.* 1998).

Recientemente, tras la síntesis de nuevos ligandos para el receptor D_4 como los agonistas parciales RO 10-5824 (K_D 5,2nM), PD 168077 (K_D 8,7nM) o CP-226,269 (K_D 6nM) y antagonistas como SCH 66712 (K_D 6,6nM), L-741,742 (K_D 3,5nM) o IPMPP (K_D 0,39nM), se ha empezado a entender y definir la vías de señalización mediante las cuales el receptor es capaz de abrir canales iónicos, fosforilar segundos mensajeros o activar factores de transcripción (Pillai *et al.* 1998; Clifford and Waddington 2000; Powell *et al.* 2003; Newman-Tancredi *et al.* 2007).

Una de las características más interesantes del receptor D_4 de dopamina humano es que ha sido relacionado con el trastorno de hiperactividad y déficit de atención (ADHD: *Attention-Deficit Hyperactivity Disorder*). El ADHD es un desorden del desarrollo caracterizado por un patrón persistente de inatención e hiperactividad, así como falta de memoria y elevada impulsividad, agitación y distracción**.** Este desorden afecta del 1 al 10% de la población infantil mundial, dependiendo del método de evaluación (American Academy of Pediatrics 2001) con una prevalencia de 2 a 6 niños por cada niña; entre los cuales, el 60% de los casos persiste en adultos (Scahill and Schwab-Stone 2000). Dicho trastorno se clasifica clínicamente en tres subtipos en función de sus características psicomotrices (Carte *et al.* 1996; Adler and Chua 2002; Mediavilla-Garcia 2003; Faraone *et al.* 2005; Antshel *et al.* 2011), subtipo de hiperactividad-impulsividad, subtipo de déficit de atención y subtipo combinado.

Diversos estudios clasifican las causas de ADHD en niños con edad escolar en dos subgrupos, factores socioambientales y factores genético-moleculares. Factores socioambientales como complicaciones en el nacimiento, exposición prenatal a alcohol y/o tabaco, conflictos familiares y pobreza, entre otros, son causantes de un trastorno de hiperactividad y falta de atención que no tiene una base molecular, pero son igualmente perjudiciales y dificultan la capacidad del individuo para concentrarse e integrarse socialmente (Burgueño *et al.* 2007). Por otro lado, los factores genéticos tienen un carácter hereditario ya que están relacionados con la presencia del polimorfismo de un gen o el mal funcionamiento de una proteína, lo que implica un patrón de ADHD debido a una anomalía en el funcionamiento de la comunicación neuronal. En este tipo de casos, se observa, entre otras alteraciones, una disminución de un 8,1% en el metabolismo de la glucosa en el cerebro, así como una disminución de la actividad en córtex prefrontal, ganglio basal y cerebelo.

Desde hace ya varios años, se ha relacionado el receptor D_4 de dopamina, concretamente el polimorfismo $D_{4.7}$, y el transportador de dopamina DAT, como responsables en parte de ADHD, pero a pesar de ello, hoy en día se desconocen las bases moleculares mediante las cuales estas proteínas pueden causar dichas anomalías. Estudios de meta-análisis realizados con individuos ADHD e individuos control (sanos) han descrito una relación estadística significativa entre la presencia del polimorfismo $D_{4.7}$ y el trastorno ADHD (Roman *et al.* 2001; Holmes *et al.* 2002; Grady *et al.* 2003; Faraone *et al.* 2005). Estos estudios definen un *odds ratio* (OR) de 1.9 (OR superior a 1.0 implica un incremento de riesgo significativo) de asociación entre $D_{4.7}$ – ADHD con un 95% de intervalo de confianza (Faraone and Doyle 2001; Faraone *et al.* 2005).

El receptor de dopamina $D_{4.7}$ presente en los niños con ADHD presenta una mayor expresión en ciertas áreas del cerebro como estriado y córtex prefrontal, y a su vez, estas áreas presentan una morfología variable comparadas con un individuo sano (Eisenberg *et al.* 2000; Yang *et al.* 2008) . Filbey y colaboradores, han descrito que el cortex prefrontal y el estriado de individuos con ADHD presentaban una activación menor respecto a individuos control tras la administración de diferentes fármacos dirigidos al receptor D_4 de dopamina, se desconocen las causas de estas diferencias en la actividad cerebral de estos individuos (Filbey *et al.* 2008). A pesar de no existir diferencias significativas respecto al perfil farmacológico de los diferentes polimorfismos de D_4, la activación de $D_{4.7}$ presenta una menor inhibición de la adenilato ciclasa y, por lo tanto, una mayor concentración de AMP cíclico intracelular comparada con los otros polimorfismos (Oak *et al.* 2000; Wang *et al.* 2004; Burgueño *et al.* 2007).

El transportador de dopamina DAT, que tiene la función de recaptar la dopamina liberada en el espacio sináptico, tiene una mayor actividad en niños que padecen este trastorno, con lo que la concentración de dopamina presente en la comunicación sináptica es menor y, por consiguiente, también lo es la activación de los receptores dopaminérgicos presentes en la sinapsis (Ciruela *et al.* 2005; Madras *et al.* 2005). Una de las teorías más aceptadas es la presencia de 10 repeticiones en tándem (480-bp) presentes en el extremo a 3' del gen que codifica para el transportador DAT, que da lugar a un ARNm cuya conformación le proporciona una gran estabilidad y resistencia frente a la actividad de las RNAsas celulares. De este modo, se produce una gran densidad presináptica de transportadores DAT, dando lugar a una disminución de la concentración de dopamina en el espacio sináptico (Curran *et al.* 2001; Madras *et al.* 2005; Thapar *et al.* 2005).

1.3.3 LOS GANGLIOS BASALES Y CIRCUITOS DOPAMINÉRGICOS EN EL SISTEMA NERVIOSO CENTRAL

A pesar de que las neuronas que utilizan la dopamina como neurotransmisor en el cerebro son muy pocas, este sistema de neurotransmisión juega un papel esencial en la regulación del movimiento, la conducta y liberación de hormonas (Dale 2000). Los circuitos dopaminérgicos del SNC se pueden dividir en: nigroestriado, mesolímbico-mesocortical y tuberohipofisario (Figura 26). Las alteraciones de estas tres vías de transmisión se han asociado con diversas enfermedades. Así, la enfermedad de Parkinson se ha asociado con alteraciones en la vía nigroestriada, la esquizofrenia con alteraciones en la vía mesolímbica-mesocortical y una gran variedad de alteraciones hormonales con anomalías en la vía tuberoinfundibular (Dale 2000).

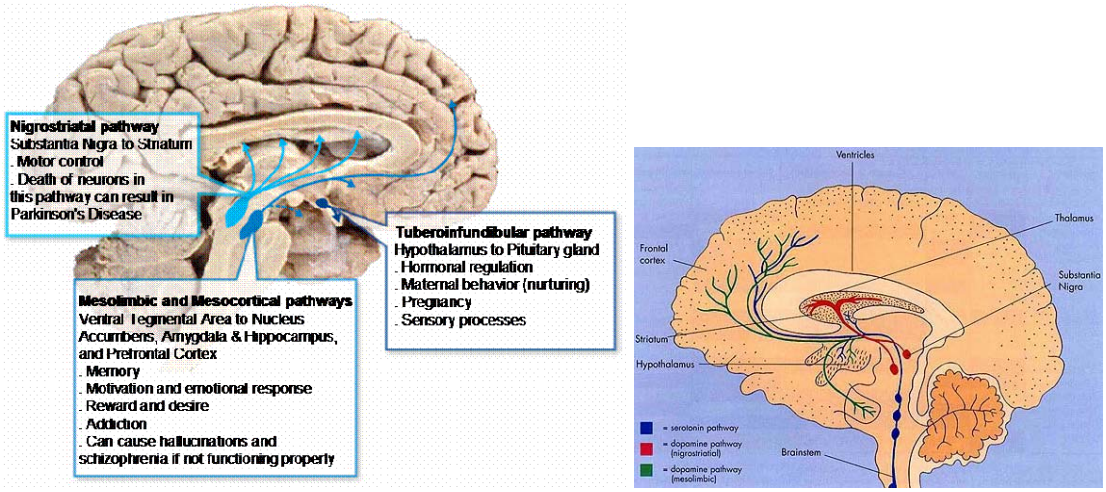

Figura 26. Representación de los circuitos dopaminérgicos (Extraído de Salazar *et al*. 2006).

El sistema nigroestriado se origina en la sustancia nigra, que es un núcleo de neuronas localizado en el mesencéfalo. La sustancia nigra se puede dividir en dos partes: la compacta, formada por neuronas dopaminérgicas, y la reticulata, formada principalmente por neuronas GABAérgicas. Las neuronas dopaminérgicas con origen en la sustancia nigra constituyen el principal tracto dopaminérgico en el cerebro, y proyectan axones que proporcionan una densa inervación al núcleo caudado y al putamen del estriado; aproximadamente un 80% de toda la dopamina que se encuentra en el cerebro se halla en el estriado. Este sistema es el implicado en la regulación motora y la ejecución de tareas, permitiendo que el movimiento se realice de forma armoniosa y obedezca a las órdenes voluntarias del individuo de acuerdo con patrones motores bien establecidos (Flórez and Pazos 2003). Un ejemplo es lo que ocurre en los pacientes con Parkinson en los que se produce una pérdida de neuronas dopaminérgicas de la vía nigroestriada, dando lugar a claras anomalías motoras. La inervación dopaminérgica hacia regiones límbicas y corticales también está alterada, aunque en menor medida y, al parecer, la enfermedad no se manifiesta hasta que la pérdida neuronal en el estriado representa el 80% (Elsworth and Roth 1997).

El sistema mesolímbico-mesocortical tiene su origen en el área tegmental ventral, también localizada en el mesencéfalo. Dicho núcleo contiene células dopaminérgicas que envían proyecciones a la corteza frontal y el lóbulo límbico, conformando los circuitos mesocortical y mesolímbico respectivamente. El sistema mesolímbico se distribuye por el sistema límbico con excepción del hipocampo; principalmente se proyecta hacia el núcleo accumbens, tubérculo olfatorio, núcleo central de la amígdala, septum lateral y núcleo intersticial de la estría terminal (Flórez and Pazos 2003). El sistema mesocortical se proyecta desde la sustancia nigra y el área tegmental ventral hacia las cortezas motoras, promotoras y suplementarias y a las cortezas parietal, temporal y cingular posterior, es decir, hasta las principales áreas sensorimotoras y de

asociación. Ambos sistemas contribuyen a mantener la atención, la ideación, la evaluación correcta de la realidad, la motivación y el control del pensamiento (Flórez and Pazos 2003), es decir, están implicados en todos aquellos procesos en los que la motivación forma parte esencial de la conducta, ya sea fisiológica para atender necesidades elementales del individuo, o patológica, creada por hiperestimulación del sistema, que es lo que ocurre en procesos de adicción a sustancias de abuso. Los mecanismos implicados en estos últimos procesos se denominan sistemas de premio o recompensa, ya que son circuitos que al activarse producen un efecto placentero (Wise 1996). La mayoría de sustancias que provocan adicción, interaccionan directa o indirectamente con proteínas presentes en las neuronas dopaminérgicas a nivel de la vía mesolímbica-mesocortical, provocando un incremento de la liberación de dopamina por la neurona presináptica hacia el espacio extracelular. La continua administración de estas sustancias produce una activación continua de la liberación de dopamina, consiguiéndose sensaciones positivas, perdiéndose la sensibilidad a estímulos habituales. Cuando se interrumpe administración aparecen sensaciones desagradables, depresión o falta de motivación (Noble, et al., 1994) (Figura 27).

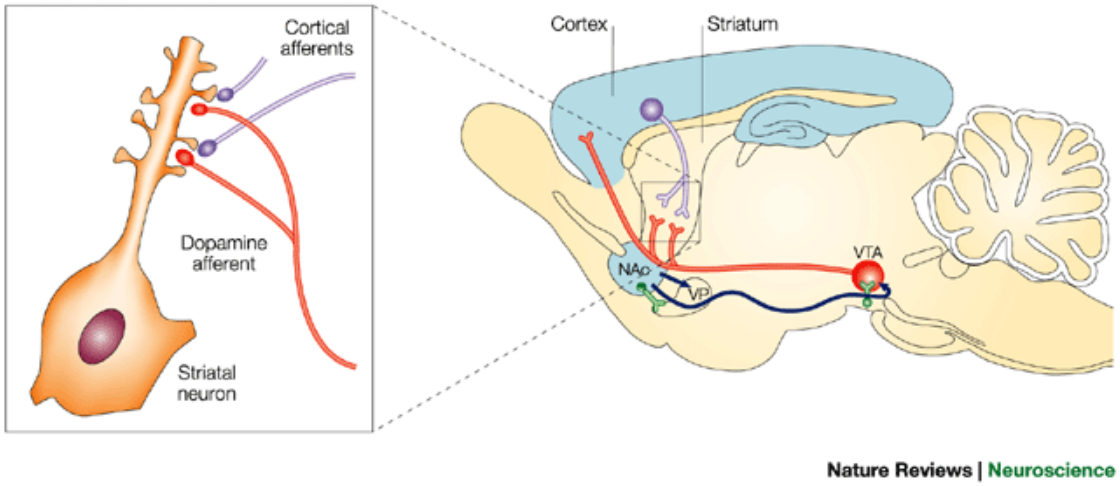

Figura 27. El circuito mesolímbico (cerebro de roedor), (Extraído de Hyman 2007).

El sistema mesolímbico-mesocortical parece jugar un papel importante en el desarrollo de la esquizofrenia. Las conexiones con el núcleo accumbens tienen una especial relevancia, ya que la falta de regulación de las vías dopaminérgicas mesolímbicas provocarían una descoordinación en el núcleo accumbens que, a su vez, sobre-estimularía ciertas regiones implicadas en el procesamiento de la información de los sentidos, contribuyendo a los síntomas positivos de la esquizofrenia (alucinaciones, delirios, pensamientos incoherentes,..). Por otro lado, dado que las vías dopaminérgicas mesocorticales juegan un papel fundamental en el buen funcionamiento cognitivo de la corteza prefrontal, alteraciones en este sistema estarían

relacionadas con los síntomas negativos de la esquizofrenia (aislamiento social, retraimiento social, falta de iniciativa) (Pani 2002; Abi-Dargham 2004).

En las situaciones patológicas que se acaban de comentar se han observado diferencias cuantitativas en cuanto a la expresión de los receptores de dopamina o bien en su señalización. Por ejemplo, los receptores D_1 se ven incrementados en la esquizofrenia y su señalización varia en la enfermedad de Parkinson. La densidad de los receptores D_2 localizados post-sinápticamente incrementa en la esquizofrenia y también en los enfermos de Parkinson no tratados con L-DOPA (profármaco que, a diferencia de la dopamina, puede traspasar la barrera hematoencefálica, y es un precursor biológico de la dopamina) (Missale *et al.* 1998; Vallone *et al.* 2000; Carlsson *et al.* 2001; Fuentes *et al.* 2010; Beaulieu and Gainetdinov 2011). Es por ello que el estudio de los receptores de dopamina es altamente importante, tanto para poder entender una gran cantidad de anomalías funcionales tales como Parkinson, Alzheimer, esquizofrenia e hiperactividad, como para crear nuevas dianas terapéuticas para dichas anomalías (Missale *et al.* 1998; Segawa 2003; Sokoloff *et al.* 2006; Santini *et al.* 2008; Dalley and Everitt 2009; Zack and Poulos 2009; Rankin *et al.* 2010; Rondou *et al.* 2010).

Por último, el sistema tuberohipofisario se origina en el hipotálamo y se proyecta hacia la hipófisis. Las neuronas del sistema tuberohipofisario desempeñan un papel importante en la regulación de la liberación de las hormonas pituitarias, como por ejemplo la prolactina, en la que la dopamina juega un papel inhibitorio en la liberación de esta hormona (Dale 2000).

Los ganglios basales están constituidos por cinco núcleos principales en roedores: el estriado, la sustancia nigra, el globus pallidus, el núcleo subtalámico y el núcleo entopeduncular. El estriado es la principal estructura de entrada de los ganglios basales y está funcionalmente subdividido en estriado dorsal y ventral (Figura 28).

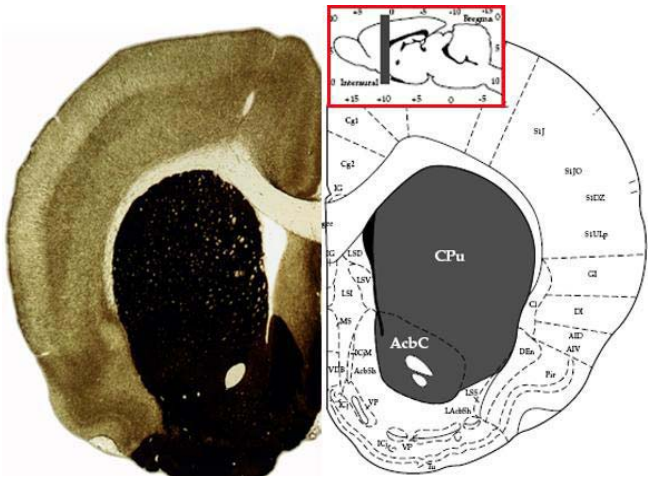

Figura 28. Localización del estriado dorsal y ventral en el cerebro de rata. Bregma 2.16mm (Extraído de Paxinos and Watson 2005)**.** CPu: caudado-putamen; AcbC: nucleus accumbens core.

El estriado dorsal (núcleo caudado y putamen) está implicado en la ejecución y aprendizaje de actos motores complejos. El estriado ventral (núcleo accumbens) forma parte de los circuitos cerebrales implicados en la conversión de la motivación en acción. En el estriado más del 90% de las neuronas son GABAérgicas de proyección o *mediumsize spiny neurons* y reciben dos vías de entrada que convergen en sus espinas dendríticas: por un lado las neuronas dopaminérgicas del mesencéfalo, localizadas en la sustancia nigra pars compacta y el área ventral tegmental y por otro lado las neuronas glutamatérgicas procedentes de áreas corticales, límbicas y talámicas (hipocampo y amígdala) (Gerfen 2004) (Figura 29).

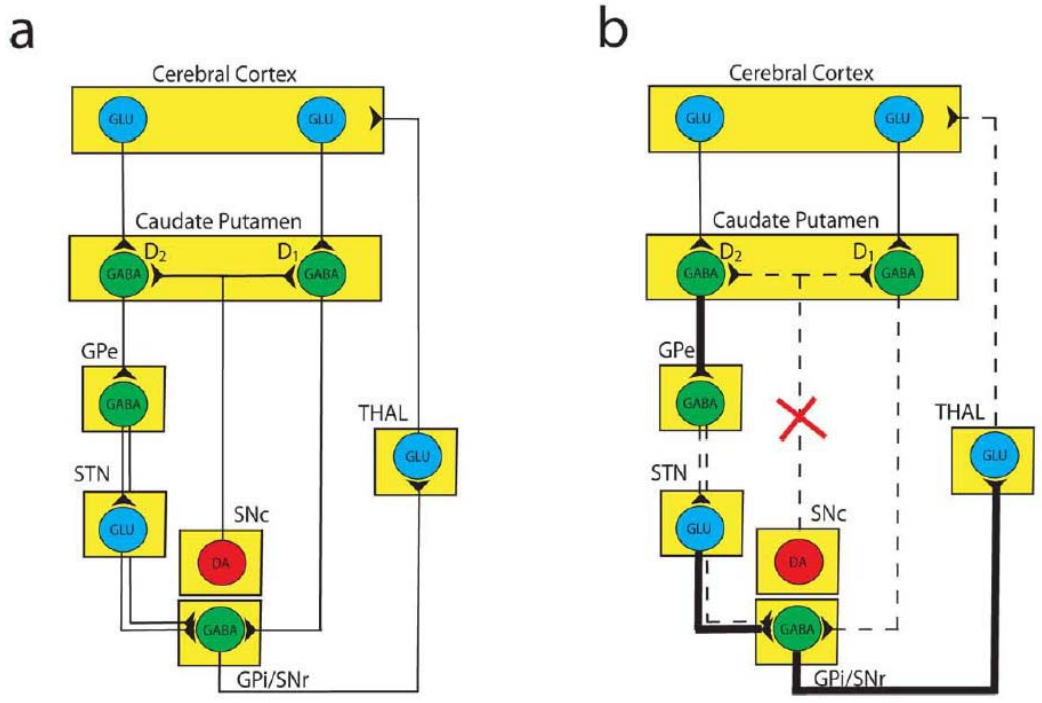

Figura 29. Funcionamiento de los ganglios basales en rata. Existen dos vías de salida del estriado: la vía directa, que conecta el estriado al núcleo entopeduncular/sustancia nigra pars reticulata (EPN/SNr) y la vía indirecta, que conecta el estriado con el globus pallidus (GP) – el núcleo subtalámico (STN) - sustancia nigra pars reticulata/núcleo entopeduncular (EPN/SNr). a) estado "normal" y b) Degeneración de la sustancia nigra pars compacta en la enfermedad de Parkinson que hace disminuir la liberación de dopamina en el estriado, (Cedido por el Dr. Sergi Ferré).

Hay dos subtipos de neuronas GABAérgicas eferentes en el estriado, que proyectan al tálamo a través de dos vías: las neuronas estriatopalidales (vía indirecta) y las neuronas estriatonigroentopedunculares (vía directa). Los dos tipos de neuronas GABAérgicas estriatales se pueden distinguir neuroanatómicamente. Las neuronas estriatopalidales contienen el péptido encefalina, receptores de dopamina (predominantemente del subtipo D_2) y receptores A_1 y A_{2A} de adenosina, entre otros. Las neuronas estriatonigroentopedunculares contienen dinorfina, sustancia P, receptores de dopamina (predominantemente del subtipo D_1) (Alexander and

Crutcher 1990) y receptores A_1 de adenosina, pero no receptores A_{2A} (Ferré *et al.* 2007; Schiffmann *et al.* 2007). La estimulación de la vía directa produce activación motora, mientras que la de la vía indirecta produce inactivación motora. La vía directa tiende a activar los movimientos voluntarios, y la vía indirecta a inhibir la aparición de componentes involuntarios en el movimiento. Un adecuado equilibrio entre las dos produce los movimientos normales. La dopamina provoca la activación de la actividad motora por activación de los receptores D_1 de las neuronas estriatonigroentopedunculares, mientras que deprimen la actividad de las neuronas estriatopalidales actuando sobre los receptores D_2 produciendo también, indirectamente, una activación motora (Alexander and Crutcher 1990). La dopamina por tanto, estimula el movimiento a través de las dos vías, porque estimula la vía estimuladora e inhibe a la vía inhibidora (Figura 29a).

La enfermedad de Parkinson está producida por la degeneración progresiva de las neuronas dopaminérgicas nigroestriatales que proyectan de la sustancia nigra al caudado-putamen. Esto da lugar a una disminución de la liberación de dopamina en el estriado, lo que provoca una hipoactividad de las neuronas GABAérgicas estriatonigroentopedunculares (vía directa) y una hiperactividad de las neuronas GABAérgicas estriatopalidales (vía indirecta) debido a la liberación de los efectos inhibitorios de la dopamina endógena (Obeso *et al.* 2008), con el consiguiente descontrol de la actividad de los ganglios basales (Figura 29b). Los síntomas clínicos más relevantes incluyen bradiquinesia (lentitud en los movimientos), rigidez, temblor en reposo y alteraciones en el equilibrio. El tratamiento paliativo de esta enfermedad es suministrar un precursor de dopamina, la L-DOPA, que aunque efectivo en los primeros estadios de la enfermedad, acaba por perder la efectividad y provoca la aparición de complicaciones motoras como la disquinesia (movimientos anormales e involuntarios) (Nutt 1990). Actualmente, existen avances importantes en el desarrollo de nuevos fármacos dopaminérgicos y no dopaminérgicos para la enfermedad de Parkinson, así como para las complicaciones motoras de las terapias en uso (Schapira *et al.* 2006).

1.4 EFECTOS DE LA COCAÍNA MEDIADOS POR LOS RECEPTORES DE DOPAMINA D_1 Y D_2

La cocaína es un extracto purificado de la planta de coca, *Erythroxylum coca*, procedente originariamente de América del sur (Figura 30). Las hojas de coca han formado parte de las culturas Inca, Ayamara y Quechua durante siglos. Para conseguir los efectos estimulantes, de euforia y eliminación del apetito, las hojas de coca eran masticadas. Originariamente, la coca era administrada, exclusivamente, en forma de hoja hasta que en 1860,

Albert Neiman aisló un extracto de la hoja de coca, la cocaína. Su utilización se extendió rápidamente por todo el mundo y hoy en día su posesión, cultivo y distribución son ilegales, exceptuando requisitos médicos o normas gubernamentales; sin embargo, su uso está ampliamente extendido. Actualmente, la adicción a cocaína es un problema social y resulta complicado encontrar un buen tratamiento debido al alto grado de recaída que presenta el consumo de esta sustancia.

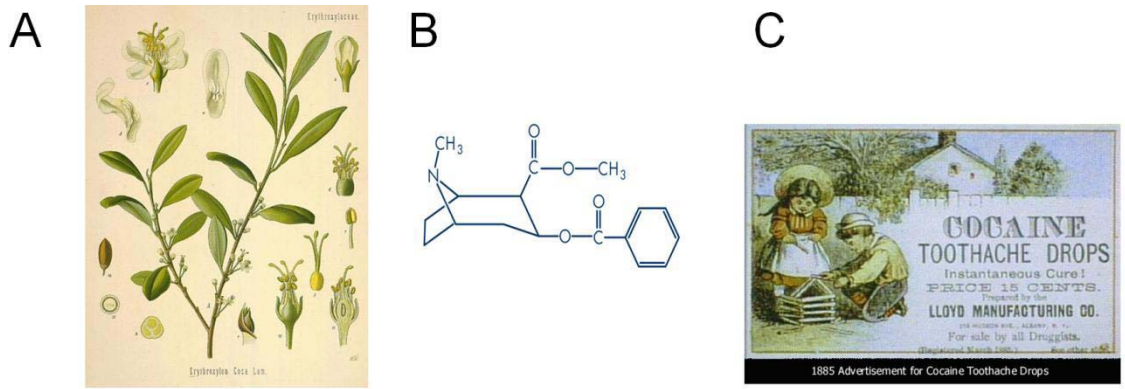

Figura 30. Cocaína. A) La planta *Erytroxylon coca* contiene cocaína en sus hojas B) Estructura molecular del [1R-(exo,exo)]-3-(benzoyloxy)-8-methyl-8-azabicyclo[3.2.1]octane-2-carboxylic acid methyl ester, también conocida como cocaína. C) Anuncio de unas gotas para el dolor de muelas, que contenían cocaína (1885).

Se conoce desde antiguo que la cocaína actúa inhibiendo la recaptación de monoaminas como la dopamina (Moore and Gudelsky 1977; Heikkila *et al.* 1979; Ritz *et al.* 1987), norepinefrina (Moore and Gudelsky 1977) y serotonina (Ross and Renyi 1967). Sin embargo, aunque la cocaína actúa con el mismo grado de efecto en los tres transportadores, la mayoría de los efectos en el comportamiento (De Wit and Wise 1977; Colpaert *et al.* 1978; Miczek and Yoshimura 1982) y la actividad motora (Giros *et al.* 1996) de esta sustancia se atribuyen al bloqueo de la recaptación de dopamina por inhibición del transportador de dopamina (DAT) presináptico. Una vez administrada, la cocaína muestra una acción rápida aumentando los niveles de dopamina en el espacio sináptico, lo que causa una sobreestimulación de las vías dopaminérgicas (Figura 31). Los picos de dopamina pueden aparecer a los cinco minutos y no recuperarse los niveles basales hasta los treinta minutos (Bradberry 2000). Además, la vida media de la cocaína en rata es corta, puede oscilar entre quince minutos y una hora dependiendo de la vía de administración utilizada (Nayak *et al.* 1976) y se cree que una administración repetitiva podría prolongar los altos niveles de dopamina en el espacio sináptico y la vida media de esta sustancia (Volkow *et al.* 1999). Se considera que la hidrólisis del éster de cocaína es la principal ruta de su catatabolismo.

Analizando los efectos de la cocaína desde una perspectiva morfológica, Roberts y colaboradores describieron una inhibición en los efectos de recompensa de la cocaína en ratas con el núcleo acumbens lesionado (Roberts *et al.* 1977). Posteriormente, en estudios de ratas adictas a la cocaína, se escogió el córtex prefrontal como región implicada en la autoadministración de microinyecciones de cocaína (Goeders and Smith 1983). Por otro lado las vías nigroestriatales controlan gran variedad de funciones motoras, además de contener la concentración más elevada de neuronas dopaminérgicas. Estos datos convierten al córtex prefrontal y las vías nigroestriatales en las regiones más importantes en la integración de los efectos de la cocaína, aunque no son las únicas (Bardo 1998). El consumo de cocaína aumenta los niveles de dopamina en el estriado, principalmente en la parte ventral, y más concretamente en el núcleo acumbens, el cual ha sido descrito como parte anatómica preferencial en mecanismos de recompensa (Koob, 2006; Di Chiara and Bassareo, 2007). La cocaína hace uso del sistema dopaminérgico para generar parte de sus efectos celulares y de comportamiento (De Mei, et al., 2009). En ratas, la *shell* del núcleo acumbens es requerida para la adquisición inicial de la conducta de autoadministración de cocaína mientras que es el *core* el que se encarga de la adquisición de la conducta de búsqueda condicionada a estímulos asociados a dicha droga (Ito *et al.* 2004). Del mismo modo, una vez que los estímulos de recompensa asociados a cocaína están consolidados, es el estriado dorsal el que juega un papel central (Everitt and Robbins 2005). Es decir, se hipotetiza que se pasa progresivamente de una búsqueda motivada por una recompensa (conducta dependiente del núcleo acumbens) a hábitos estímulo-respuesta que dependen del estriado dorsal.

A pesar de la gran relevancia del sistema dopaminérgico en los trastornos adictivos, éste no es el único sistema de neurotransmisión implicado. Por ejemplo, hay evidencias de que el sistema histaminérgico podría jugar un papel inhibidor sobre diversos efectos provocados por las drogas de abuso (Ito *et al.* 1997). La cocaína interfiere con la actividad de las neuronas histaminérgicas de los núcleos tuberomamilares (Nath and Gupta 2001) y la histamina reduce la hiperactividad producida por cocaína (Ito *et al.* 1997). Esto indica que las neuronas histaminérgicas están implicadas en el control inhibidor de la recompensa.

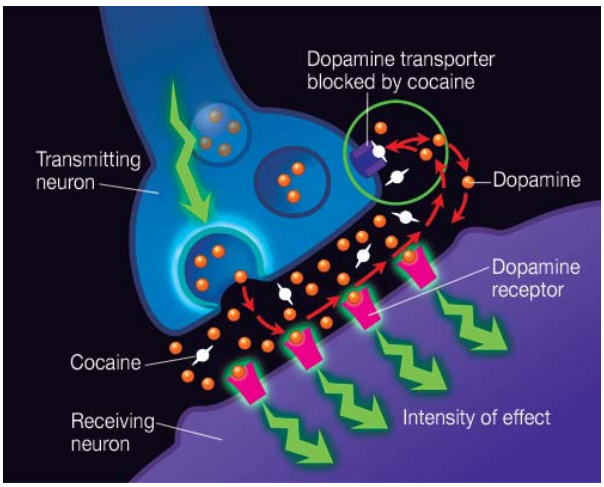

Figura 31. Efecto del bloqueo de los transportadores de dopamina (DAT) por la cocaína. (Extraído del artículo Stimulant Addiction del Nacional Institute on Drug Abuse (NIDA)).

Un hipotético mecanismo de los cambios de comportamiento consecuentes a la administración crónica de cocaína es una alteración de la plasticidad sináptica del cerebro. Hasta el momento, han sido descritos diferentes cambios en la estructura de las dendritas (Robinson and Kolb 1999; Robinson *et al.* 2001). Estos cambios podrían ser debidos a alteraciones en la expresión de las proteínas de los neurofilamentos, las proteínas del citoesqueleto y/o las *"gap junctions"*, todas ellas muy importantes para la estabilidad y la buena integración de los receptores en la sinapsis neuronal.

1.4.1 PROTEÍNAS DE UNIÓN DE LA COCAÍNA

La cocaína ejerce sus funciones por interacción con proteínas específicas. Como hemos comentado anteriormente, la proteína más reconocida que puede unir cocaína es el transportador de dopamina DAT. Se ha estudiado a nivel molecular la interacción de la cocaína con DAT. Mediante el modelaje molecular de DAT basado en la estructura cristalina de Aquifex aeolicus LeuT(Aa), un transportador de leucina homólogo en bacterias (Ravna *et al.* 2009), se ha postulado que la unión de la cocaína a DAT ocurre en un dominio de unión análogo al lugar de unión de la leucina en el transportador LeuT(Aa).

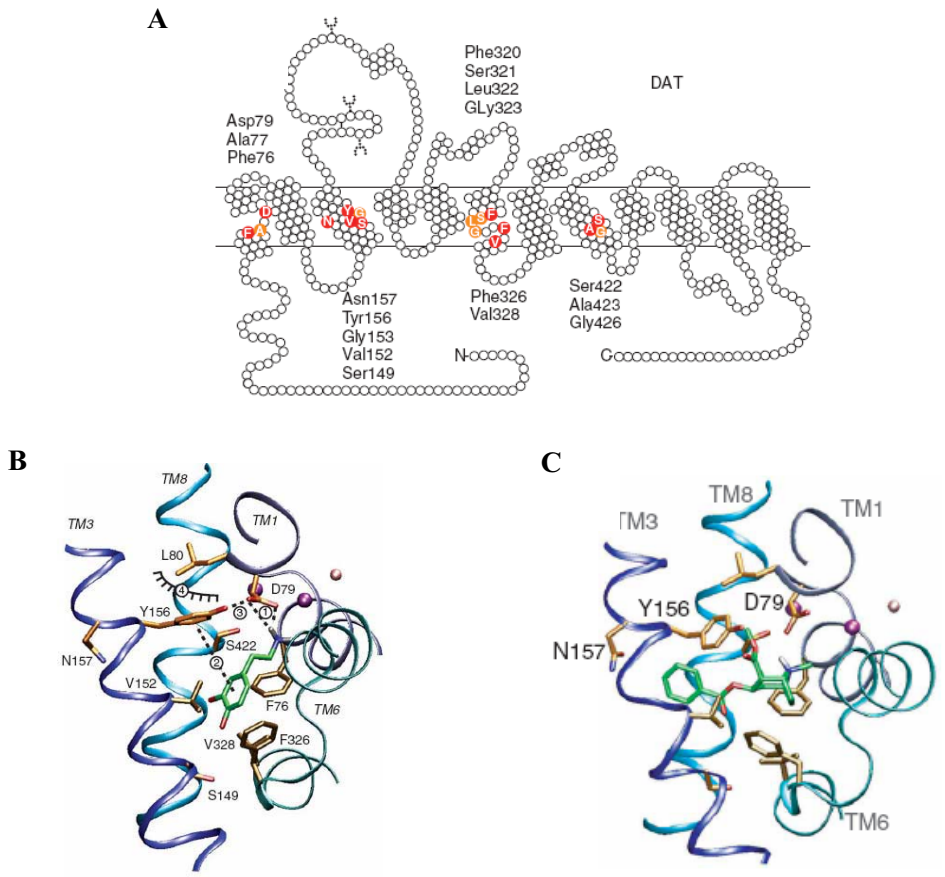

Figura 32. Esquema de la interacción de la cocaína y la dopamina con DAT. A) Representación del transportador de dopamina, DAT. Los círculos pintados corresponden a los lugares donde coincide la interacción de DAT con la dopamina y la cocaína. B) Esquema de la interacción de DAT con la dopamina. C) Esquema de la interacción de DAT con la cocaína. (Extraído de Bertolino *et al*. 2009).

En el centro de interacción de la cocaína con DAT intervienen las hélices transmembrana 1, 3, 6 y 8 del transportador. Este centro de unión se superpone con el sitio de unión de la dopamina y las anfetaminas, pero es claramente diferente del lugar de unión de distintos antidepresivos (Beuming *et al.* 2008). Este hecho explica el bloqueo de la unión de la dopamina a DAT inducido por la cocaína (Figura 32) y, consecuentemente, el incremento en los niveles de dopamina en el espacio extracelular.

Mediante estudios in vitro (Bertolino *et al.* 2009) e in vivo (Meiergerd *et al.* 1993; Dickinson *et al.* 1999; Mortensen and Amara 2003), se ha podido demostrar que existe una relación directa entre DAT y el receptor D_2 de dopamina ya que ambos se regulan de forma recíproca a nivel presináptico. Bertolino y colaboradores han demostrado que se produce una interacción molecular entre DAT y los receptores D_2 (Bertolino *et al.* 2009). Esta interacción puede ser fundamental para entender como la señalización de la dopamina se ve claramente

regulada, a nivel presináptico, por DAT y por el receptor de dopamina D_2 en el estriado y en el córtex prefrontal.

Además de DAT, la cocaína puede interaccionar con otras proteínas. Hoy en día es un hecho aceptado que la cocaína interacciona con los receptores sigma a concentraciones fisiológicas (Cobos *et al.* 2008). Esta familia de proteínas está formada por los receptores sigma-1 y sigma-2. La cocaína es la droga de abuso más estudiada con referencia a su interacción con los receptores sigma-1 (Hayashi and Su 2005). Una de las razones es que la cocaína posee una afinidad moderada por sigma-1 en ensayos de unión de radioligando (Sharkey *et al.* 1988; Matsumoto *et al.* 2003). Matsumoto y colaboradores describieron que los antagonistas del receptor sigma inhiben de forma significativa las convulsiones y letalidad inducidas por dosis tóxicas de cocaína (Matsumoto *et al.* 2002; Matsumoto *et al.* 2004). La toxicidad de la cocaína se ve potenciada con los agonistas del receptor sigma-1 (Matsumoto *et al.* 2002; Matsumoto *et al.* 2004). Este descubrimiento indica que las acciones de la cocaína, al menos en parte, pueden ser mediadas por su unión al receptor sigma-1. La estructura del receptor sigma-2 aún no se conoce. Por otro lado, la estructura de sigma-1 es muy distinta de cualquier otra proteína conocida de mamíferos. Muestra un 66% de homología con una esterol isomerasa fúngica, careciendo sin embargo de su actividad enzimática (Su and Hayashi 2003). Se caracteriza por poseer tres regiones altamente hidrofóbicas que formarían dos segmentos trasmembrana con los extremos amino y carboxilo terminales intracelulares (Figura 33).

Figura 33. Esquema de la estructura del receptor sigma-1. (Extraído de Steve Beyer's blog 2009).

El receptor sigma-1 es una chaperona que modula las señales dependientes de calcio y se localiza principalmente en el retículo endoplasmático de la célula, aunque también se encuentra en la membrana plasmática, nuclear y mitocondrial (Alonso *et al.* 2000). Se encuentra ampliamente distribuido por todo el SNC y la periferia. En 1976 fue clasificado como receptor opioide (Martin *et al.* 1976); sin embargo, la acción de los ligandos de sigma-1 no era bloqueada por los antagonistas opioides, naloxona y naltrexona, y fue considerado como

receptor huérfano no opioide. El receptor sigma interacciona con diferentes sustancias, además de la cocaína, entre las que destacan el haloperidol o los esteroides como la progesterona (Hayashi and Su 2003).

Muy recientemente se ha encontrado un alucinógeno endógeno que interacciona con el receptor sigma-1, el DMT (*N,N* dimethyltryptamine). Esta sustancia actuaría como agonista endógeno del receptor inhibiendo los canales de Na^+ dependientes de voltaje en los miocitos (Guitart *et al.* 2004; Fontanilla *et al.* 2009). El receptor sigma-1 también está implicado en la modulación de la liberación de calcio, la modulación de la contracción cardiaca y la inhibición de los canales de K^+ dependientes de voltaje (Monassier and Bousquet 2002). En 2001 Hayashi describió la interacción del receptor sigma-1 con los receptores IP_3 en el retículo endoplasmático (Hayashi and Su 2001). Más adelante, se demostró que la activación del receptor sigma-1 mediante sus agonistas (PRE-084 o carbetapentane) fosforila la subunidad NR1 del receptor NMDA vía PKC y PKA aumentando su expresión y reforzando la inducción de dolor a través del receptor NMDA. Esta señal se veía reducida por el tratamiento con el antagonista específico del receptor sigma-1 (Kim *et al.* 2008). Hasta el momento no se ha encontrado ninguna interacción de estos receptores con ningún GPCR, aunque existen numerosas evidencias de la amplificación de señales de GPCR mediante los receptores sigma-1. Actualmente, son considerados como receptores auxiliares o amplificadores de otras señales.

El receptor sigma-1 se encuentra estrechamente relacionado con la acción de la cocaína en diferentes aspectos, como son la hiperlocomoción (Menkel *et al.* 1991), la sensibilización (Ujike *et al.* 1996), el mecanismo de recompensa (Romieu *et al.* 2000; Romieu *et al.* 2002), las convulsiones y la letalidad (Matsumoto *et al.* 2001a), aunque se desconoce el mecanismo de acción de todos ellos. Estudios recientes han descrito que una reducción del receptor sigma-1 en cerebro, mediante oligonucleótidos anti-sense, disminuye las acciones convulsivas y locomotoras estimulantes de la cocaína (Matsumoto *et al.* 2001b; Matsumoto *et al.* 2002). Por otro lado, antagonistas sintéticos del receptor sigma-1 reducen las acciones de la cocaína en modelos animales (Matsumoto *et al.* 2003). A pesar de que recientemente han aparecido estudios que también involucran el receptor sigma-2 con las acciones de la cocaína (Matsumoto *et al.* 2007), su papel aún no está definido debido a la falta de ligandos completamente selectivos para este subtipo. Para añadir complejidad, el receptor sigma-2 aún no ha sido clonado.

1.4.2 IMPLICACIÓN DE LOS RECEPTORES DE DOPAMINA D_1 Y D_2 EN LOS EFECTOS DE LA COCAÍNA

A pesar de que se ha visto que la administración crónica de cocaína induce cambios en la expresión génica de muchos receptores como el receptor metabotrópico 5 de glutamato (mGluR5) (Ghasemzadeh *et al.* 1999) o el receptor μ-opioide (Yuferov *et al.* 1999), estudios en humanos postmortem no indicaron ningún cambio en el ARNm de los receptores de dopamina D_1 o D_2 en individuos adictos a la cocaína con referencia a los controles (Little *et al.* 1993). Estos resultados han sido controvertidos ya que se ha demostrado una disminución de la expresión de los receptores D_2 y D_3 de dopamina en individuos adictos a la cocaína en comparación con individuos sanos mediante la técnica PET (*positrón emisión tomography*) (Martinez *et al.* 2009). La variación de la expresión de receptores de dopamina inducida por cocaína puede variar mucho según la especie y la región del cerebro, ya que en ratas, después de cuatro semanas de autoadministración de cocaína, se observó un incremento del ARNm del receptor D_1 en el cerebro anterior y un incremento del ARNm de los receptores D_1 y D_2 en el sistema límbico (Laurier *et al.* 1994).

A parte de la modificación o no de la expresión de los receptores, la cocaína induce un incremento de la liberación de dopamina y una sobreestimulación de las vías dopaminérgicas (Anderson and Pierce 2005; De Mei *et al.* 2009). Mediante la potenciación de la transmisión dopaminérgica en el estriado, la cocaína induce los efectos de recompensa así como la aparición de nuevos estímulos (Volkow and Swanson 2003; Zink *et al.* 2003). Los receptores D_2 están involucrados en la mediación de estos efectos. Los agonistas del receptor D_2 reducen la autoadministración de cocaína, mientras los antagonistas incrementan este comportamiento. Estos resultados sugieren que el receptor D_2 actúe por un mecanismo feed-back para disminuir la autoadministración de cocaína (Corrigall and Coen 1991; Caine *et al.* 1999).

Los antagonistas glutamatérgicos y dopaminérgicos reducen la activación de la transcripción génica inducida por la cocaína (Konradi 1998; Valjent *et al.* 2005). La activación de los receptores de dopamina D_1 es un requerimiento imprescindible para la respuesta celular y conductual inducida por la cocaína tal como se demuestra en estudios realizados con ratones *KO* para el receptor D_1 (Xu *et al.* 1994). Estudios recientes utilizando ratones transgénicos, donde las células que expresan los receptores D_1 y D_2 se encuentran marcadas mediante proteínas fluorescentes, han confirmado estos datos, mostrando que la respuesta celular aguda inducida por la cocaína involucra principalmente las neuronas que expresan los receptores D_1 de dopamina (Bertran-Gonzalez *et al.* 2008). En este escenario cabría esperar que una inhibición de la expresión génica del receptor D_{2S} amplificaría los efectos de la cocaína in vivo, debido a la

inhibición ejercida por el receptor D_{2S} de la liberación de dopamina. Sin embargo, no es esto lo que se observa. El efecto de la cocaína en ratones *KO* para receptores D_2 ha sido estudiado tanto en tratamientos agudos, crónicos como en autoadministración de cocaína, con el resultado que los ratones *KO* para D_2 tienen alteradas las respuestas a cocaína. Así, la estimulación de la actividad motora inducida por cocaína en los ratones *KO* para receptores D_2 no incrementa de forma dosis-dependiente (Chausmer *et al.* 2002; Welter *et al.* 2007). De forma sorprendente, la administración de cocaína en los ratones *KO* para D_2 no induce la expresión de c-fos (Centonze *et al.* 2002). Esto conduce a hipotetizar que en ausencia del receptor D_2, aparece un circuito inhibitorio, normalmente controlado por los receptores D_2, provocando la supresión de la inducción de c-fos. En este contexto, el GABA y la acetilcolina pueden aumentar de forma considerable debido a la pérdida del control de su liberación por el receptor D_2 y jugar un papel en el bloqueo de la inducción de c-fos (Centonze *et al.* 2002). De forma alternativa, la pérdida de los receptores D_2 afecta la formación de complejos macromoleculares entre los receptores D_2 y otras proteínas que normalmente controlan la respuesta celular y conductual de la cocaína (Liu *et al.* 2006).

Los efectos de recompensa de la cocaína en los ratones *KO* para receptores D_2 se ven atenuados (Welter *et al.* 2007). Sin embargo, estudios de autoadministración de cocaína en ratones *KO* para el receptor D_2 demostraron que los ratones *KO* se autoadministraban más cocaína que los ratones WT (Caine *et al.* 2002). No puede excluirse la contribución de otros neuromoduladores (como por ejemplo la noradrenalina o la serotonina) y se requiere un análisis más profundo para esclarecer este fenómeno. Este punto es importante debido a la existencia de numerosos estudios que muestran una pérdida de los efectos de recompensa de diferentes drogas de abuso en ratones *KO* para receptores D_2. (Risinger *et al.* 2000; Elmer *et al.* 2005).

Por otro lado, los ratones *KO* para D_{2L}, que por lo tanto siguen expresando los autoreceptores D_{2S}, mantienen la respuesta locomotora y de recompensa a la cocaína parecida a los animales WT (Usiello *et al.* 2000; Wang *et al.* 2000; Rouge-Pont *et al.* 2002). Así, parece ser que el receptor D_{2S} es el principal implicado en la respuesta celular y conductual de las drogas de abuso. Esto sugiere que los efectos presinápticos de los receptores D_2 no involucran únicamente la liberación de dopamina, sino también de GABA, glutamato y acetilcolina en respuesta a las drogas de abuso. Así, existe una diferente implicación de las isoformas D_{2S} y D_{2L} en la señalización dopaminérgica inducida por drogas de abuso. La ausencia de la señalización del receptor D_{2L} no altera los efectos motores y de recompensa inducidos por la cocaína. Contrariamente, la señalización del receptor D_{2S} parece ser un requisito imprescindible para los efectos motores y de recompensa de la cocaína y otras drogas de abuso. De todos modos, se requieren más estudios para poder decidir que componente presináptico se encuentra

involucrado en estas respuestas y si se encuentra en las neuronas dopaminérgicas o en las neuronas postsinápticas.

No se han observado cambios significativos en los niveles de expresión del receptor D_2 en el estriado dorsal en animales con diez días de alto consumo de cocaína (Marcellino *et al.* 2007). Éste es un descubrimiento importante que indica que cambios en la expresión de los receptores D_2 en esta zona del cerebro no están involucrados en la adaptación de la respuesta a los efectos de recompensa de la cocaína en este modelo. Recientemente, cambios bifásicos en los receptores D_2 en el core del núcleo accumbens han sido observados después de una retirada de pocos días de acceso a cocaína intravenosa (Ben-Shahar *et al.* 2007). Parece ser, que la dosis y la exposición a la cocaína son las responsables de estas diferencias. La autoadministración crónica de cocaína en monos rhesus por periodos de varios meses provoca una disminución de la densidad del receptor D_2 en el estriado detectada por autoradiografía (Moore *et al.* 1998; Nader *et al.* 2002). Mediante estudios de imágenes se ha podido detectar una disminución en la cantidad de receptores D_2 en humanos adictos a la cocaína comparado con los sujetos controles (Volkow *et al.* 1993; Martinez *et al.* 2004). De forma similar, mediante la técnica de PET se ha observado una reducción en los receptores D_2 en primates con autoadministración crónica de cocaína y un año de abstinencia (Morgan *et al.* 2002a; Morgan *et al.* 2002b; Nader *et al.* 2006). Una persistente disminución de los receptores D_2 en el estriado puede involucrar la internalización de los receptores D_2 después de una autoadministración crónica de cocaína.

1.5 INTERACCIÓN FUNCIONAL ENTRE LOS RECEPTORES DE GALANINA Y DOPAMINA

1.5.1 LA GALANINA COMO NEUROTRANSMISOR

La galanina es un neurotransmisor peptídico, ampliamente distribuido en el SNC, que activa receptores acoplados a proteína G. Para la mayor parte de las especies, la galanina es un neuropéptido de 29 aminoácidos con un dominio carboxilo terminal amida, excepto la galanina humana que contine una serina terminal adicional y no muestra amidación (Evans and Shine 1991; Lang *et al.* 2007). Éste péptido fue inicialmente aislado del intestino del cerdo (Tatemoto *et al.* 1983; Lang *et al.* 2007) pero más tarde se encontró en muchas otras especies, como en el cerebro de los mamíferos. Todos las espécies, excepto el atún (Kakuyama *et al.* 1997; Branchek *et al.* 1998), comparten un dominio amino terminal muy conservado (residuos 1-14) responsable de la interacción del péptido con sus receptores (Kask *et al.* 1995; Lundkvist *et al.* 1995; Branchek *et al.* 1998) y una región carboxilo terminal variable. El péptido precursor de la

galanina (preprogalanina) está codificado por un único gen organizado en 6 pequeños exones que abarca unas 6 kb de ADN genómico, dependiendo de la especie (Kofler *et al.* 1996; Lang *et al.* 2007) (Figura 34). La galanina es proteolíticamente procesada en un pro-péptido de 123 (cerdo, humano) o 124 (ratón) aminoácidos junto con un péptido de 59 o 60 aminoácidos conocido como *galanin message associated peptide* (GMAP) (Rokaeus and Brownstein 1986; Vrontakis *et al.* 1987; Kaplan *et al.* 1988; Evans and Shine 1991; Lang *et al.* 2007). La galanina ha demostrado tener una amplia distribución en el sistema nervioso central (Tabla 4) y periférico de muchas especies de mamíferos y una gran diversidad de efectos biológicos.

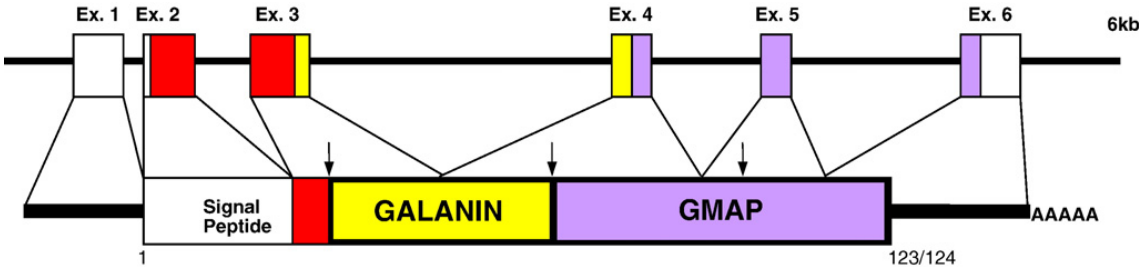

Figura 34. Organización del gen de la preprogalanina (modificado de Kofler *et al.* 1996). El primer exón codifica la región 5', región no traducida del ARNm de la preprogalanina. El exón 2 empieza con el codón inicio de la traducción del péptido señal y termina antes del sitio proteolítico, precediendo el péptido de galanina maduro. Los primeros trece aminoácidos de la galanina están codificados por el exón 3; los restantes 16 aminoácidos y el GMAP están codificados por los exones 4 y 5. La porción restante de GMAP y el sitio de poliadenilación están localizados en el exón 6. Las flechas indican las zonas de corte de las endopeptidasas.

La galanina está ampliamente distribuida en tejidos como el cerebro, la médula espinal y el intestino (Kask *et al.* 1995; Kask *et al.* 1997), y puede regular numerosas acciones fisiológicas como; la alimentación, la liberación de insulina, la lactancia, el reflejo espinal, la contractibilidad y secreción intestinal, el crecimiento, el aprendizaje, la liberación neuroendocrina, la regeneración nerviosa, la memoria, la depresión (Bartfai *et al.* 1993; Bedecs *et al.* 1995; Kask *et al.* 1995; Kask *et al.* 1997; Lang *et al.* 2007), la regulación del ciclo del sueño/vigilia (Sherin *et al.* 1998; Steininger *et al.* 2001), la regulación de la energía y homeostasis osmótica (Crawley 1999; Landry *et al.* 2000; Gundlach 2002), la reproducción (Rossmanith *et al.* 1996; Gundlach 2002), la nocicepción (Liu and Hokfelt 2002), la cognición (McDonald *et al.* 1998; Kinney *et al.* 2002; Lang *et al.* 2007), y tiene múltiples efectos en los comportamientos relacionados con el estrés y la adicción (Holmes and Picciotto 2006; Picciotto *et al.* 2009). Los efectos de la galanina están mediados por la interacción del péptido con sus receptores.

Brain area	State	Effect	Route of galanin administration	Mechanism	Subregion	References
Striatum		↓ DA release	Bath application to striatal slice	Gi	NAc	Tsuda et al. (1998)
Striatum		↑ DA release	Intra-PVN	Gi	PVN⊕NAc	Rada et al. (1998)
Striatum		↑ DOPA accumulation	Intra-VTA, ICV		VTA, NAc and DS	Ericson and Ahlenius (1999)
Striatum		↓ Glutamate release	Bath application to striatal slice	ATP-sensitive K^+ channels		Ellis and Davies (1994)
Striatum		~ GABA release	Bath application to striatal slice			Ellis and Davies (1994)
Striatum		↓ACh	Intra-striatal			Antoniou et al. (1997)
Striatum		↓ACh	Intra-PVN		PVN⊕NAc	Rada et al. (1998)
Striatum	Anesthetized	↑ACh	Intra-striatal			Antoniou et al. (1997)
Olfactory tubercles		↑ DOPA accumulation	ICV			Ericson and Ahlenius (1999)
LC		↓ Spontaneous firing, ↓ membrane potential	Bath applied to slice	GalR1 activation of GIRK channels		Pieribone et al., 1995; Seutin et al., 1989; Ma et al., 2001
LC		↑ NE induced outward current	Bath applied to slice			Xu et al. (2001)
VTA		↓ DA neuron activity	Endogenous, from LC			Grenhoff et al. (1993)
Hippocampus	Stressed	↑ NE release ↑ 5-HT release	Transgenic overexpression		Ventral	Kehr et al. (2001)
DR		↓ Membrane potential	Bath applied to slice	GalR3 component		Swanson et al. (2005)
DR		↓ Membrane potential	Bath applied to slice	Non-ATP-sensitive K^+ channel activation		Xu et al. (1998b)
DR		↓$GABA_A$-mediated IPSPs	Bath applied to raphe slice	Presynaptic GalR1, postsynaptic GalR2/3		Sharkey et al. (2007)
DR		↑5-HT_{1A} response	Bath applied to raphe slice			Xu et al. (1998b)
Hypothalamus		↓ Membrane potential	Bath applied to hypothalamic slice	Outward K^+ current	Magnocellular neurons	Papes and Bourque (1997)
Hypothalamus		↓ Presynaptic glutamate release	Bath applied to hypothalamic slice	$GABA_B$ is required	Arcuate and supraoptic nuclei	Kinney et al., 1998; Kozoriz et al., 2006; Tyszkiewicz et al., 2008
Hypothalamus		↓ Membrane potential	Bath applied to hypothalamic slice	Outward K^+ current	Arcuate nucleus	Dong et al., 2006; Poulain et al., 2003
Hypothalamus	Dehydrated	↓ Input resistance	Bath applied to hypothalamic slice		PVN	Kozoriz et al. (2006)

Legend: DA=dopamine; PVN=paraventricular nucleus; NAc=nucleus accumbens; DS=dorsal striatum; ACh=acetylcholine; LC=locus coeruleus; NE=norepinephrine; DR=dorsal raphe.

Tabla 4. Efectos de la galanina en la neurotransmisión (Extraído y modificado de Picciotto *et al.* 2009).

1.5.2 ESTRUCTURA, CLASIFICACIÓN Y FUNCIÓN DE LOS RECEPTORES DE GALANINA

La galanina es capaz de regular numerosos procesos fisiológicos y patológicos por su interacción con los tres subtipos de receptores de galanina: (Gal_1, Gal_2, Gal_3). Los receptores de galanina están involucrados en diversas alteraciones patológicas como la enfermedad del Alzheimer, desórdenes del estado de ánimo, ansiedad o adicción al consumo de alcohol entre otras (Mitsukawa *et al.* 2008) (Tabla 5). Por tanto, en la actualidad se considera a los receptores de galanina posibles dianas terapéuticas para diferentes enfermedades y a sus agonistas y antagonistas posibles agentes terapéuticos (Mitsukawa *et al.* 2008) (Tabla 6).

Various physiological and pathological effects	Involved receptor subtype(s)
Feeding	GalR1 in the hypothalamus
Learning and memory	GalR1 and GalR2 in the hippocampus
Seizure	GalR1 and GalR2 in the hippocampus
Pain	GalR1 and GalR2 in the spinal cord and the DRG
Anxiety and mood disorders	GalR1, GalR2 and GalR3 in the DRN, the hypothalamus, the locus coeruleus, the amygdala and BNST
Tumor	GalR1 and GalR2

Tabla 5. Implicación de los subtipos de receptores de galanina en diferentes funciones fisiológicas y patológicas (Extraído de Mitsukawa *et al*. 2008).

Galanin receptor ligands		Various indicated therapeutic aspects
GalR1	Agonist	Analgesic, anticonvulsant, anxiolytic
	Antagonist	Antidepressant, cognitive enhancement, regulation of feeding
GalR2	Agonist	Analgesic, anticonvulsant, antidepressant, anxiolytic, neuroprotection/neuroregeneration
GalR3	Antagonist	Antidepressant, anxiolytic, block alcohol intake in addiction

Tabla 6. Ligandos de los receptores de galanina como posibles dianas terapéuticas (Extraído de Mitsukawa *et a*l. 2008).

Hasta la fecha, se han identificado, por clonación molecular y caracterización farmacológica, tres receptores de galanina, Gal_1, Gal_2 y Gal_3, que pertenecen a la familia de GPCR (Branchek *et al.* 2000; Lang *et al.* 2007). Los receptores de un subtipo determinado están altamente conservados entre especies; dentro de una especie, los subtipos de receptores diferentes muestran bajas similitudes se secuencia (Howard *et al.* 1997; Iismaa *et al.* 1998; Kolakowski *et al.* 1998; Branchek *et al.* 2000; Lang *et al.* 2007). El receptor Gal_1 fue el primer receptor de galanina clonado en 1994 a partir de células de melanoma humano de Bowes (Habert-Ortoli *et al.* 1994; Branchek *et al.* 1998), mientras que los receptores Gal_2 y Gal_3 fueron clonados a partir de hipotálamo de rata en 1997 (Howard *et al.* 1997; Smith *et al.* 1997; Wang *et al.* 1997b). Ya que los tres receptores de galanina muestran distintos pero superpuestos patrones de expresión en el SNC y en la periferia (Tabla 7), se han desarrollado una variedad de ligandos para poder investigar los roles específicos de cada receptor en la mediación de los efectos fisiológicos de la galanina (Mitsukawa *et al.* 2008).

	CNS								Pancreas	Solid tumors
	BNST	Amygdala	Hippo-campus	Hypo-thalamus	DRN	Locus coeruleus	Spinal cord	DRG		
Galanin	+++	+++	+	+++	+	+++	++	++	+	++
GalR1	+++	+++	++	+++	++	+++	++	+++	+++	+++
GalR2	++	++	++	++	++	++	++	+++	++	++
GalR3	+/0	+/0	+/0	+	+/0	+/0	+/0	+/0	NA	NA
References	[13, 47, 48, 58, 70, 79, 84–99]								[57, 87, 100–106]	[73, 78–81, 107–111]

BNST, bed nucleus of the stria terminalis; DRG, dorsal root ganglia; DRN, dorsal raphe nucleus; GalR, galanin receptor; NA, not applicable.

Tabla 7. Distribución de la galanina y de los subtipos de receptores de galanina en diferentes tejidos (Extraído de Mitsukawa *et al.* 2008).

El cDNA para el receptor Gal_1 humano codifica una proteína de 349 aminoácidos con significativa homología con el receptor de la rodopsina (Probst *et al.* 1992). El gen para el receptor Gal_1 humano está localizado en el cromosoma 18q23 (Nicholl *et al.* 1995). El receptor Gal_1 homólogo de rata fue clonado de la línea celular de rata RIN14b (Parker *et al.* 1995; Gustafson *et al.* 1996) y, por homología, del cerebro de rata (Burgevin *et al.* 1995). El cDNA de este receptor de galanina codifica una proteína de 346 aminoácidos con una homología de un 92 % respecto el receptor Gal_1 humano (Figura 35). Los receptores Gal_1 humanos y de rata comparten los mismos sitios consenso para la glicosilación en los dominios extracelulares. Los sitios consenso para la fosforilación por proteínas cinasas también se conservan entre el receptor Gal_1 de rata y humano, con la excepción de que el receptor de Gal_1 humano contiene dos sitios adicionales en el dominio carboxilo terminal. Recientemente, también se ha descrito un homólogo de ratón del receptor Gal_1 (Jacoby *et al.* 1997; Wang *et al.* 1997c) con una homología del 91% con el receptor Gal_1 humano y un 94% con el receptor Gal_1 de rata (Branchek *et al.* 1998).

El ARNm que codifica para el receptor Gal_1 de rata tiene aproximadamente unas 9.5 kb con una distribución limitada en diversos tejidos de rata, como se determinó por análisis de Northern blot (Parker *et al.* 1995). El receptor Gal_1 fue detectado fácilmente por Northern blot en células pancreáticas, así como en el cerebro y la médula espinal, pero no en otros tejidos (Parker *et al.* 1995). Dentro del sistema nervioso, la distribución del ARNm del receptor Gal_1 de rata determinado por hibridación in situ está en concordancia con la unión de la ^{125}I-galanina y la expresión del péptido galanina; los niveles más altos se observaron en el hipotálamo (núcleo supraóptico), amígdala, hipocampo ventral, tálamo, tallo encefálico (médula oblonga, locus ceruleus y núcleo lateral parabraquial) y la médula espinal (cuerno dorsal) (Burgevin *et al.* 1995; Parker *et al.* 1995; Gustafson *et al.* 1996). Así, la distribución del receptor Gal_1 se superpone con la unión de la ^{125}I-galanina en el SNC (Melander *et al.* 1988). El ARNm del receptor Gal_1 no fue detectado en la pituitaria anterior de rata (Parker *et al.* 1995; Fathi *et al.*

1997) lo que sugiere que los efectos dependientes de la galanina en esta región pueden ser debidos a otro subtipo de receptor en rata (Branchek *et al.* 1998).

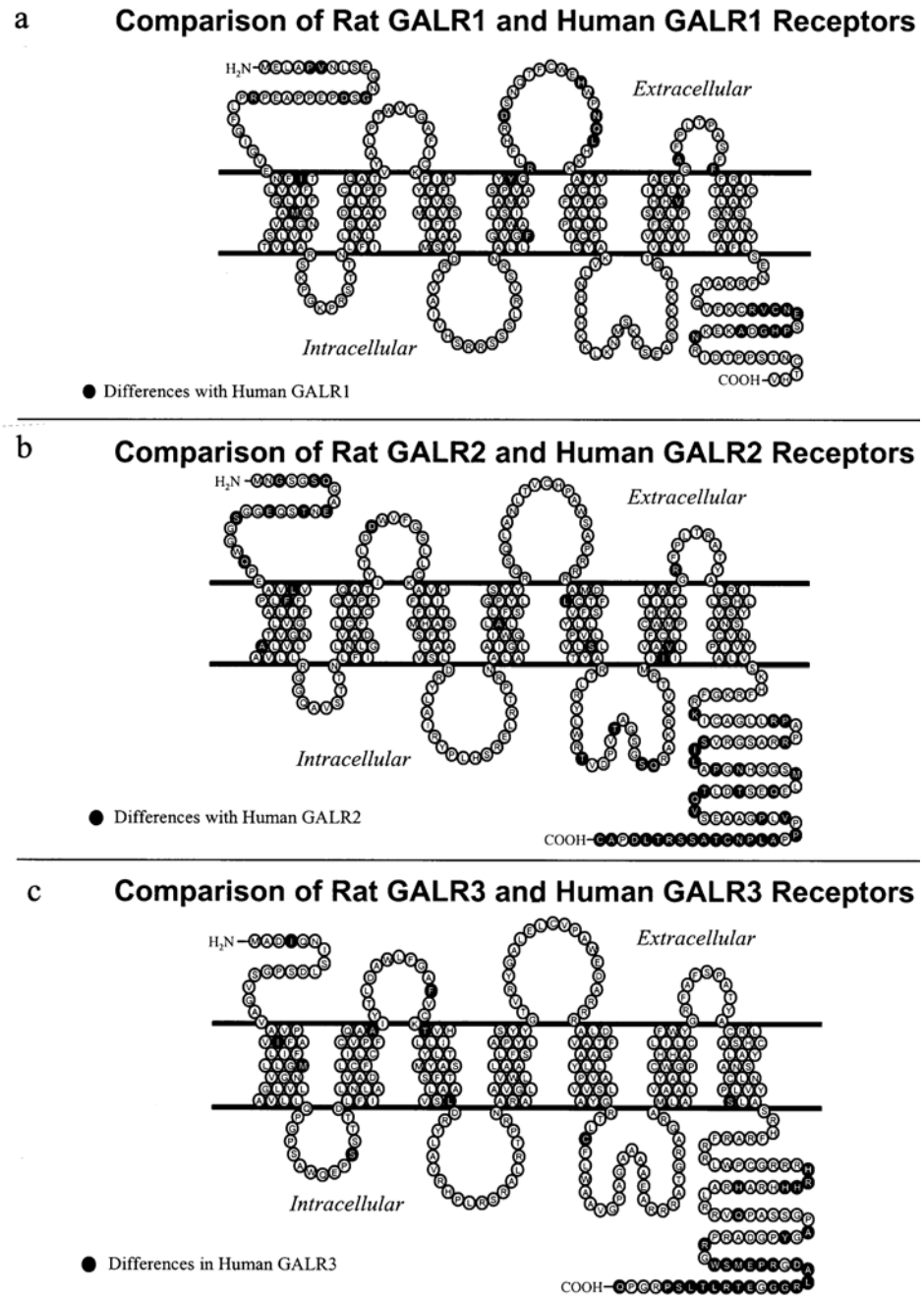

Figura 35. Secuencia de aminoácidos para los receptores Gal_1, Gal_2 y Gal_3 de rata. Los residuos negros son diferentes respecto los receptores humanos. (a) Comparación de los receptores Gal_1 de rata y Gal_1 humano. (b) Comparación de los receptores Gal_2 de rata y Gal_2 humano. (c) Comparación de los receptores Gal_3 de rata y Gal_3 humano. (Extraído de Branchek *et al.* 1998).

El receptor de galanina, Gal_2, muestra un bajo nivel de homología aminoacídica, un 38 %, con respecto el receptor Gal_1 de rata y humano (Howard *et al.* 1997; Smith *et al.* 1997; Wang *et al.* 1997a; Branchek *et al.* 1998). El cDNA del receptor Gal_2 de rata codifica para una

proteína de 372 aminoácidos con 7 dominios transmembrana (Figura 35), 3 lugares consenso para glicosilación en dominios extracelulares (1 compartido con el receptor Gal_1), y lugares de fosforilación distintos a los del receptor Gal_1 en las regiones intracelulares. El ARNm que codifica para el receptor Gal_2 de rata tiene aproximadamente unas 1.8 kb, se detectó por Northern Blot y contiene un intrón que puede sufrir splicing incompleto (Howard *et al.* 1997; Smith *et al.* 1997). En comparación con el receptor Gal_1 de rata, el ARNm que codifica para el receptor Gal_2 de rata se encuentra más ampliamente distribuido; el transcrito del receptor Gal_2 está presente en el cerebro (con niveles elevados en hipotálamo, hipocampo, amígdala y corteza piriforme (Fathi *et al.* 1997) y tejidos periféricos como en vasos deferentes, próstata, útero, ovario, estómago, intestino grueso, raíz dorsal ganglionar y células pancreáticas (Howard *et al.* 1997; Smith *et al.* 1997; Sten Shi *et al.* 1997; Wang *et al.* 1997a). Además, el ARNm del receptor Gal_2 se encuentra en la glándula pituitaria anterior de rata, no así el receptor Gal_1, (Fathi *et al.* 1997) hecho que sugiere que el receptor Gal_2 puede mediar los efectos de la galanina sobre la secreción hormonal a nivel de pituitaria (Branchek *et al.* 1998).

Se ha descrito la clonación del cDNA que codifica para el receptor Gal_2 humano (Bloomquist *et al.* 1998; Borowsky *et al.* 1998). El receptor Gal_2 humano comparte tan solo un 85% de homología aminoacídica con el receptor Gal_2 de rata y contiene 387 aminoácidos, siendo 15 aminoácidos más largo en el extremo carboxilo terminal que su homólogo en rata (Figura 35). Además, los receptores Gal_2 en humano y en rata están menos conservados que los receptores Gal_1 (Branchek *et al.* 1998).

El tercer subtipo de receptor de galanina en rata, Gal_3, ha sido clonado por dos grupos diferentes (Wang *et al.* 1997b; Smith *et al.* 1998). Wang y colaboradores clonaron un fragmento por homología al receptor Gal_1 a partir de cDNA de hígado de rata. La secuencia completa del clon fue posteriormente aislada a partir de hipotálamo de rata. El receptor aislado por Smith y colaboradores fue obtenido por una combinación de técnicas de expresión de clones y homología de una librería de cDNA a partir de hipotálamo de rata (Smith *et al.* 1998). Las dos secuencias descritas divergen en cuatro posiciones; el motivo de esta divergencia permanece por determinar. El cDNA del receptor Gal_3 de rata descrito por Smith y colaboradores codifica para una proteína de 370 aminoácidos, compartiendo una homología aminoacídica del 35% con el receptor Gal_1 de rata y del 52% con el receptor Gal_2 de rata, el receptor más relacionado. La similitud con la secuencia del receptor Gal_2 es más elevada entre los dominios transmembrana II y IV, en los que la homología aminoacídica oscila entre el 70% i el 90%. Aunque, Wang y colaboradores no hacen referencia a un intrón en la secuencia del receptor Gal_3 de rata, (Wang *et al.* 1997b) un intrón contenido en la secuencia humana del *GenBank* indica una relación intrón/exón conservada para los receptores Gal_3 y Gal_2. La secuencia del receptor Gal_3 contiene

un lugar simple para glicosilación y múltiples lugares de fosforilación de proteínas cinasa en lugares intracelulares (Branchek *et al.* 1998).

Por Northern Blot, Wang y colaboradores detectaron el ARNm del receptor Gal_3 como un transcrito de aproximadamente 3,8 kb (con un peso molecular dependiente del tejido) en corazón, bazo y testículo pero no en cerebro (Wang *et al.* 1997b); el aislamiento del receptor Gal_3 de una librería de cDNA a partir de hipotálamo de rata, sin embargo, indica que se encuentra en SNC de rata de forma poco abundante. Usando el método más sensible de RPA (Recombinase Polymerase Amplification), Smith y colaboradores detectaron transcritos del receptor Gal_3 en regiones del SNC de rata, con elevados niveles en hipotálamo, bajos niveles en bulbo olfatorio, corteza cerebral, medula oblonga, caudado putamen, cerebelo y médula espinal, y niveles no significativos en hipocampo y sustancia negra. Por el mismo método, el ARNm del receptor Gal_3 fue detectado en tejidos periféricos con elevados niveles en pituitaria, bajos niveles en hígado, riñón, estómago, testículo, corteza adrenal, pulmón, médula adrenal, bazo y páncreas, y niveles no significativos en corazón, útero, vaso deferente, plexo coroideo y raíz dorsal ganglionar (Branchek *et al.* 1998; Smith *et al.* 1998).

Las vías de señalización de cada subtipo de receptor de galanina han sido descritas (Figura 36), aunque pueden darse alteraciones teniendo en cuenta las diferentes células o su particular tipo de proteínas G (Lang *et al.* 2007).

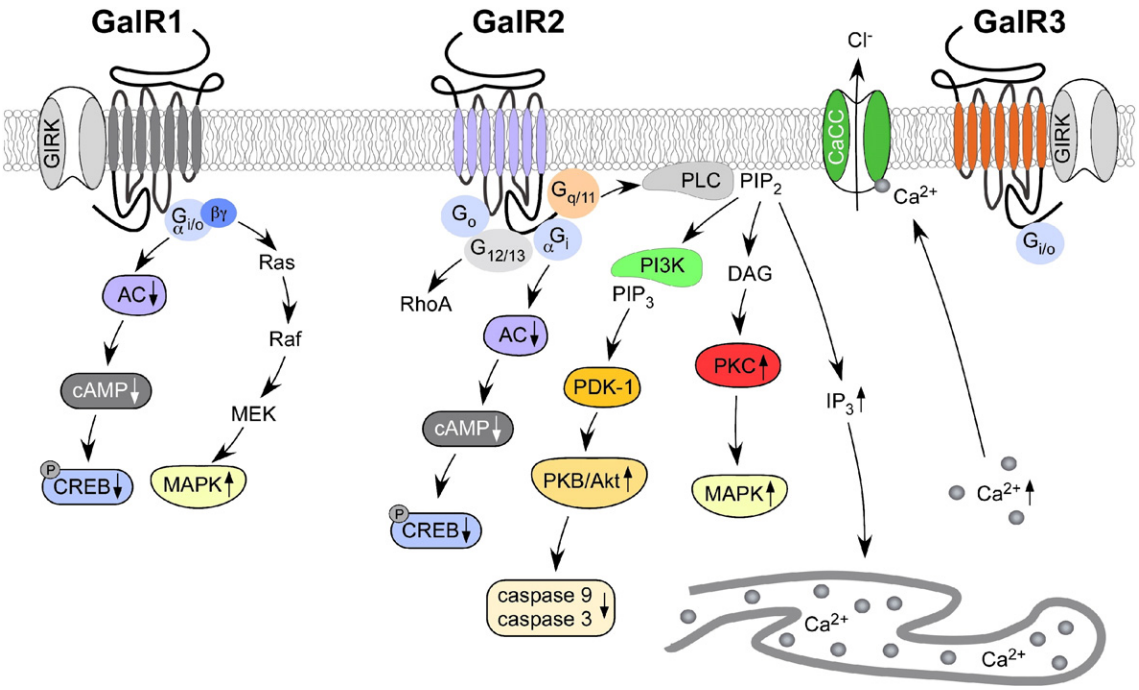

Figura 36. Vías de señalización de los diferentes subtipos de receptores de galanina. (Extraído de Lang *et al.* 2007).

La estimulación del receptor Gal_1, de rata o humano, expresados en líneas celulares inhibe la producción de AMPc dependiente de forskolina de manera sensible a la toxina pertusis (PTX) (Habert-Ortoli *et al.* 1994; Parker *et al.* 1995; Smith *et al.* 1997; Fitzgerald *et al.* 1998; Wang *et al.* 1998b). Además, la activación del receptor Gal_1 abre canales de K^+ tipo GIRK (G-protein-regulated inwardly rectifying K^+) (Smith *et al.* 1998) y estimulan la actividad MAPK de forma independiente de PKC (Wang *et al.* 1998b). Estos resultados indican que el receptor se acopla a proteína G tipo G_i (Kanazawa *et al.* 2007). La activación del receptor Gal_1 expresado en células de carcinoma escamoso induce una marcada y significativa activación de ERK1/2, en este caso vía subunidades $G\alpha_i$, lo que conlleva la inducción de las proteínas $p27^{Kip1}$ y $p57^{Kip2}$ implicadas en el control del ciclo celular y a la supresión de la ciclina D1 (Kanazawa *et al.* 2007). La unión de galanina al receptor Gal_1 produce la internalización del receptor en células CHO transfectadas (Wang *et al.* 1998a), hecho que puede ser un mecanismo de regulación endógeno de la cascada de señalización en células nativas (Lang *et al.* 2007).

La señalización vía el receptor Gal_2 implica múltiples clases de proteínas G y estimula múltiples vías intracelulares. La vía más común descrita implica la activación de la fosfolipasa c (PLC), la cual provoca un aumento de la hidrólisis del inositol fosfato, mediando la liberación de Ca^{2+} desde sus reservorios intracelulares hasta el citoplasma y abriendo canales de cloro dependientes de Ca^{2+} (Fathi *et al.* 1997; Smith *et al.* 1997; Borowsky *et al.* 1998; Pang *et al.* 1998; Wang *et al.* 1998a). Estos efectos intracelulares mediados por el receptor Gal_2 no son sensibles a PTX, demostrando que el receptor Gal_2 puede actuar también a través de proteínas G, tipo $G_{q/11}$. La señalización del receptor Gal_2 vía proteína G tipo G_i es controvertida. El receptor Gal_2 de rata transfectado en células CHO (Smith *et al.* 1997), en células COS-7 (Pang *et al.* 1998) y en células HEK-293 (Fathi *et al.* 1997) no produce alteraciones en la acumulación de AMPc dependiente de forskolina, previa estimulación con galanina. Sin embargo, según otros autores sí que se observa una inhibición dependiente de galanina, de la producción de AMPc dependiente de forskolina en células CHO transfectadas con el receptor Gal_2 de rata (Wang *et al.* 1997a) y células HEK-293 transfectadas con el receptor Gal_2 humano (Fathi *et al.* 1998). De forma parecida al receptor Gal_1, esta inhibición es sensible a la PTX (Wang *et al.* 1997a; Fathi *et al.* 1998). Además, la activación tanto de Gal_1 como de Gal_2 inhibe la proteína CREB (cyclic AMP-responsive element-binding) (Badie-Mahdavi *et al.* 2005; Lang *et al.* 2007).

También hay evidencias derivadas de estudios in vivo e in vitro que muestran que el receptor Gal_2 acoplado a proteína G_o, activa MAPK de manera dependiente de PKC i sensible a PTX (Wang *et al.* 1997a; Hawes *et al.* 2006; Hobson *et al.* 2006; Elliott-Hunt *et al.* 2007). Se ha propuesto otra vía de señalización para el receptor Gal_2 a partir del acoplamiento funcional al subtipo $G_{12/13}$ de proteína G, y la consiguiente activación de RhoA en células cancerígenas de

intestino delgado (Wittau *et al.* 2000). El aumento de la supervivencia neuronal mediado por la galanina implica la señalización vía Akt, llevando a la supresión de la actividad caspasa-3 y caspasa-9 (Ding *et al.* 2006; Hobson *et al.* 2006; Elliott-Hunt *et al.* 2007; Lang *et al.* 2007).

Las propiedades de señalización del receptor Gal_3 son menos conocidas. El receptor Gal_3 parece estar acoplado a la proteína $G_{i/o}$ para estimular la activación de una corriente de K^+ sensible a la PTX cuando se coexpresa con GIRK1 y GIRK4 en oocitos de *Xenopus* (Smith *et al.* 1998). La implicación de la proteína G_i en la señalización por el receptor Gal_3 se basa en estudios con el receptor Gal_3 humano transfectado en melanóforos de Xenopus (Kolakowski *et al.* 1998; Lang *et al.* 2007).

1.5.3 INTERACCIÓN FUNCIONAL ENTRE RECEPTORES DE GALANINA Y DOPAMINA EN LA MODULACIÓN DE LA TRANSMISIÓN COLINÉRGICA

El neuropéptido galanina está ampliamente distribuido en el SNC (Melander *et al.* 1986a; Melander *et al.* 1986b; Hökfelt *et al.* 1998; Ögren *et al.* 1998), donde está correlacionado con la noradrenalina, serotonina, histamina y la acetilcolina (ACh) (Hökfelt *et al.* 1998). Se ha dedicado una atención especial a la presencia de galanina en la población de neuronas colinérgicas del núcleo septal y en la banda diagonal del área de Broca, las cuales se proyectan hacia el hipocampo (Melander *et al.* 1985), debido a su posible relevancia en procesos de aprendizaje, memoria y en la enfermedad de Alzheimer (Ögren *et al.* 1998; Mitsukawa *et al.* 2008). Los receptores Gal_1 y Gal_2 son los subtipos de receptores de galanina predominantes en el cerebro (Branchek *et al.* 2000). La falta de ligandos selectivos y anticuerpos fiables (Hawes and Picciotto 2004) ha dificultado la identificación de la distribución de los receptores Gal_1 y Gal_2 en el sistema septohipocampal. El ARNm del receptor Gal_1 presenta una elevada expresión a nivel del área septal, mientras que la expresión del ARNm de Gal_2 es moderada y se encuentra confinada a unas pocas neuronas dispersas (Parker *et al.* 1995; O'Donnell *et al.* 1999). Se ha descrito que los centros de unión de ^{125}I-galanina en el hipocampo ventral se ven reducidos de forma significativa después de una lesión en la proyección septohipocampal, que comporta la eliminación de múltiples señales colinérgicas hacia el hipocampo ventral (Fisone *et al.* 1987). De esta afirmación se desprenden evidencias claras de la existencia de una población significativa de receptores de galanina a nivel presináptico en el hipocampo, localizados en las terminales nerviosas colinérgicas, aunque el subtipo de receptor de galanina implicado aún es materia de debate (Miller *et al.* 1997). Respecto a los receptores de galanina postsinápticos, el receptor Gal_1 se expresa de forma preferente en el hipocampo

ventral, CA1 y subículo, mientras que el receptor Gal_2 se expresa en el giro dentado tanto del hipocampo ventral como del dorsal (O'Donnell *et al.* 1999).

Estudios in vivo en roedores a los que se les ha administrado galanina de manera sistémica sugieren que ésta inhibe la neurotransmisión colinérgica en el hipocampo ventral (Fisone *et al.* 1987; Ögren *et al.* 1998; Laplante *et al.* 2004a). Es más, la administración sistémica de galanina conlleva deficiencias cognitivas en diversas tareas (Crawley 1996; Ögren *et al.* 1998). No obstante, estudios postmortem a partir de cerebros de pacientes con la enfermedad de Alzheimer sugieren que la galanina puede reducir la estimulación de la neurotransmisión colinérgica, de manera que podría atenuar los síntomas derivados del desarrollo de esta enfermedad (Counts *et al.* 2008; Ögren *et al.* 2010).

Además de la galanina, la dopamina también tiene un papel modulador en la vía colinérgica septohipocampal. Se ha demostrado que la dopamina facilita la liberación de acetilcolina en el hipocampo mediante la activación de receptores D_1-like, los cuales es conocido que se localizan en las terminales colinérgicas del hipocampo (Hersi *et al.* 1995). De los dos subtipos de receptores D_1-like, D_1 y D_5, el receptor D_5 es el predominante en el hipocampo (Ciliax *et al.* 2000) y es el que con más probabilidad está involucrado en la modulación de la liberación de acetilcolina hipocampal (Hersi *et al.* 2000; Laplante *et al.* 2004b). Todos estos antecedentes, demuestran que tanto la galanina como la dopamina modulan la liberación de acetilcolina en el hipocampo, y por lo tanto sugieren la existencia de una relación entre los receptores D_1 o D_5 y los receptores Gal_1 en la modulación de la liberación de acetilcolina en el hipocampo.

1.6 INTERACCIÓN FUNCIONAL ENTRE RECEPTORES DE DOPAMINA Y H_3 DE HISTAMINA

1.6.1 LA HISTAMINA COMO NEUROTRANSMISOR Y VÍAS HISTAMINÉRGICAS

La histamina es una monoamina sintetizada en el cerebro de casi todas las especies animales, específicamente por neuronas localizadas en el núcleo tuberomamilar (TM) del hipotálamo posterior (Passani *et al.* 2000). Estas neuronas se proyectan difusamente hacia la mayoría de las áreas cerebrales, incluyendo la corteza cerebral (Figura 37), y han sido implicadas en diversas funciones en los mamíferos, tales como sueño/vigilia, secreción hormonal, control cardiovascular, secreción de ácidos gástricos y alergia e inflamación (Haas and Panula 2003).

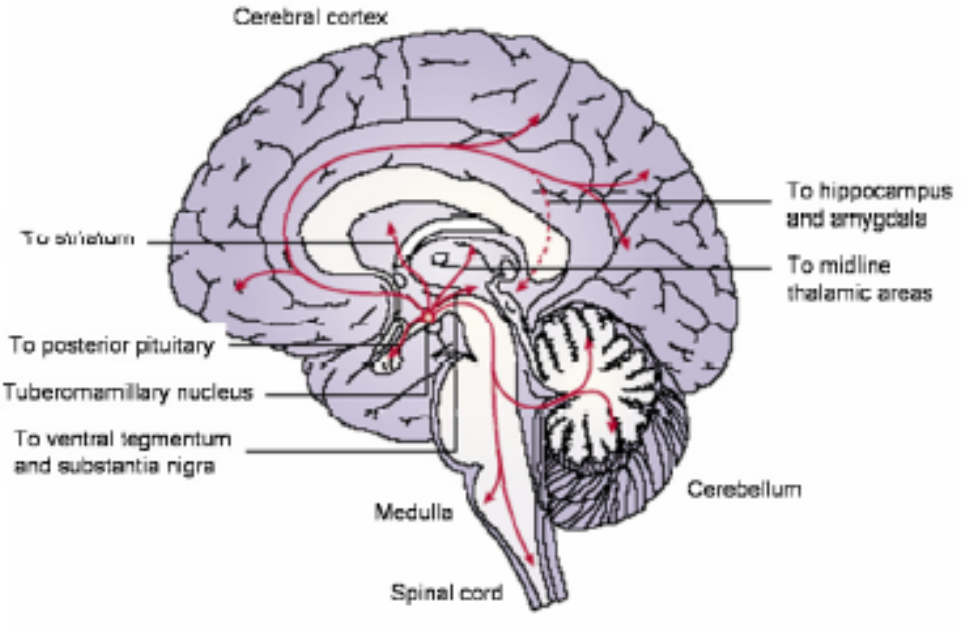

Figura 37. Origen y proyecciones del sistema histaminérgico en el cerebro humano (Haas and Panula 2003).

La histamina no cruza fácilmente la barrera hematoencefálica, y su síntesis en el cerebro ocurre a partir de L-histidina, aminoácido que es transportado dentro de las neuronas por el transportador de L-aminoácidos. Una vez allí, la histidina es casi exclusivamente descarboxilada por la enzima histidina descarboxilasa para sintetizar la histamina, que se incluye en vesículas para ser liberada (Passani *et al.* 2000; Brown *et al.* 2001). Una vez liberada en el espacio sináptico, la histamina es metilada por la enzima histamina-metiltransferasa a un metabolito inactivo que luego es degradado, constituyendo esta metilación el principal mecanismo de inactivación en ausencia de un sistema de recaptación de alta afinidad para la histamina (Brown *et al.* 2001) (Figura 38). El recambio neuronal de histamina es muy alto, y su vida media, que es normalmente de 30 minutos, puede cambiar rápidamente dependiendo de la actividad neuronal, por ejemplo, en situaciones de estrés la velocidad de recambio de histamina puede verse incrementada (Haas and Panula 2003).

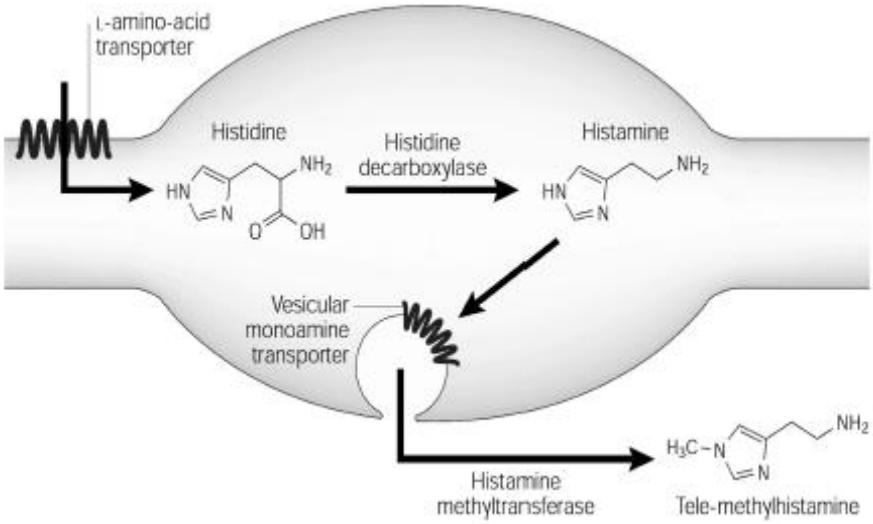

Figura 38. Estructura química y metabolismo de la histamina (2-(3H-imidazol-4-yl)-ethylamine), (Extraído de Haas *et al.* 2008).

Las áreas a donde se dirigen las proyecciones histaminérgicas son ligeramente diferentes entre distintas especies, pero cubren esencialmente todas las áreas del SNC (Fernandez-Novoa and Cacabelos 2001; Gu 2002). En todos los mamíferos se ha detectado moderada o densa inervación histaminérgica en la corteza cerebral, la amígdala, la sustancia nigra y el estriado, y en el hipocampo y el tálamo la densidad de estas proyecciones es variable, además la retina y espina cordal también reciben fibras histaminérgicas desde el núcleo TM (Brown *et al.* 2001; Haas and Panula 2003). Las proyecciones aferentes a las neuronas TM son amplias y provienen desde diferentes áreas, incluyendo grupos celulares GABAérgicos, serotonérgicos y dopaminérgicas (Brown *et al.* 2001).

En muchas especies, una proporción importante de la histamina total del cerebro se encuentra en células no neuronales como las células mastocito, desde donde la histamina puede ser liberada. Aunque la función de estas células mastocito cerebrales no es bien conocida, se ha sugerido su participación en el control cerebrovascular, en la regulación neuroinmune, en la actividad neurotrófica y/o neurotóxica y en reacciones neuroinflamatorias (Fernandez-Novoa and Cacabelos 2001). Como ocurre en otras neuronas aminérgicas, las neuronas TM están bajo el control por retroalimentación negativa mediada por un autorreceptor (el receptor H_3 de histamina), que participa no solo en la inhibición de la liberación de histamina, sino también en la liberación de otros neurotransmisores, como serotonina, noradrenalina y dopamina, donde el receptor H_3 actua como heteroreceptor (Passani *et al.* 2000).

A diferencia de lo que ocurre con otros sistemas aminérgicos, se ha observado que tanto la histamina como sus metabolitos incrementan en el fluido espinal con la edad. Por otro lado, la histamina involucrada en funciones superiores del SNC disminuye con la edad y aumenta en regiones neuroendocrinas y neurovegetativas, lo que sugiere que en aquellas vías en las que la histamina tiene un papel como neurotransmisor ésta disminuye con la edad, mientras que aumenta en otras zonas que dependen de las células mastocito. Esto podría indicar que la histamina cerebral tiene diferentes funciones dependiendo de si su origen es neuronal o no neuronal (Fernandez-Novoa and Cacabelos 2001). En la enfermedad de Alzheimer (AD) muchos grupos subcorticales de proyecciones neuronales, incluyendo las neuronas histaminérgicas, manifiestan una prominente degeneración (Haas and Panula 2003). Se ha descrito que los niveles de histamina y/o la actividad de la histidina descarboxilasa disminuyen en áreas del cerebro que se ven afectadas en AD y el síndrome de Down (Schneider *et al.* 1997; Panula *et al.* 1998). Sin embargo, también se ha publicado que en pacientes con AD hay un importante incremento en los niveles de histamina del cerebro, así como también en el suero de estos pacientes (Fernandez-Novoa and Cacabelos 2001). Parece claro que el sistema histaminérgico está involucrado en estados patológicos relacionados con neurodegeneración, como AD, y que la disfunción de este sistema debe contribuir como un evento secundario en la etiopatogénesis de esta enfermedad, particularmente, en mecanismos asociados con reacciones inflamatorias en zonas cercanas a las placas seniles que conducen a una acelerada muerte neuronal.

En la enfermedad de Parkinson (PD), las neuronas TM parecen morfológicamente normales y la actividad de la histidina descarboxilasa también, pero, los niveles de histamina en el cerebro de estos pacientes están selectivamente incrementados en el putamen, sustancia nigra y globus pallidus externo (Nakamura *et al.* 1996; Rinne *et al.* 2002; Haas and Panula 2003). Además, se ha observado que las fibras histaminérgicas cambian su morfología e incrementan su densidad en la sustancia nigra de cerebros de pacientes con PD, posiblemente porque alrededor de las terminales nerviosas que contienen histamina las neuronas nigrales degeneran (Anichtchik *et al.* 2000b; Haas and Panula 2003).

En pacientes con esquizofrenia también se han observado evidencias que implican al sistema histaminérgico. Las proyecciones histaminérgicas inervan áreas cerebrales involucradas en la patofisiología de esta enfermedad, aunque también en este caso los estudios han dado lugar a resultados controvertidos. Por un lado, se ha observado en pacientes esquizofrénicos que el principal metabolito de la histamina está incrementado en el fluido espinal, así como también la actividad histaminérgica. En otros estudios, se ha visto una disminución significativa de histamina en sangre y suero de estos pacientes, lo que podría estar relacionado con el papel que

juega la histamina en el control vascular del cerebro en personas sanas y en pacientes esquizofrénicos con alteraciones hemodinámicas (Fernandez-Novoa and Cacabelos 2001). Estos datos sugieren que en la esquizofrenia hay una disfunción en el sistema histaminérgico central y periférico, que, junto con alteraciones en la homeostasis vascular del cerebro, pueden participar en la patogénesis de la enfermedad, ya que la histamina estaría implicada en las alteraciones observadas en las funciones vasculares cerebrales de pacientes con esquizofrenia (Ito 2004).

Estos ejemplos muestran que la histamina está involucrada en la regulación de complejas conductas que están controladas por varios sistemas diferentes de neurotransmisores, como dopamina, GABA y glutamato. Aunque los mecanismos en detalle no se conocen, hay evidencia que indica que los receptores H_3 cooperan con los receptores D_2 en la regulación de la expresión génica estriatal (Pillot *et al.* 2002), e interacciones entre ambos pueden ser relevantes tanto en la regulación cognitiva como la motora.

1.6.2 ESTRUCTURA Y CLASIFICACIÓN DE LOS RECEPTORES DE HISTAMINA

Mediante métodos de farmacología tradicional, se han identificado cuatro receptores de histamina, el H_1, el H_2 y el H_3, que se expresan en el cerebro en compartimentos celulares específicos, y el H_4, descubierto más recientemente que se detecta principalmente en la periferia, por ejemplo en leucocitos y médula ósea (Tabla 8) (Leurs *et al.* 1995; Nguyen *et al.* 2001).

Properties	H_1R	H_2R	H_3R	H_4R
G protein isoforms	$G_{q/11}$	$G\alpha_s$	$G_{i/o}$	$G_{i/o}$
Constitutive activity	+	+	++	?
Signal transduction	PLC IP_3, DAG Ca^{2+}, PKC AMPK, $NF_{-K}B$	AC cAMP, PKA CREB	AC ↓ cAMP ↓ MAPK Akt/GSK3	AC ↓ cAMP ↓ MAPK
Effector pathways	TRPC IK_{leak} ↓	I_h(HCN2) I_{AHP} ↓	I_{Ca} ↓	Cytoskeleton
Cellular function	Postsynaptic excitability and plasticity	Postsynaptic excitability and plasticity	Presynaptic transmitter release and plasticity	?
Systemic function	Behavioral state and reinforcement (novelty, arousal) Working memory Feeding rhythms Energy metabolism Endocrine control	Learning and memory (consolidation)	Numerous CNS functions, cognition, emotion, learning, and memory Blood-brain barrier control	Chemotaxis
Pathophysiology	Disorders of sleep, mood, memory, eating, and addiction Pain and neuroinflammation	Schizophrenia Pain and neuroinflammation	Disorders of sleep, mood, memory, eating, and addiction Pain and neuroinflammation	?

Tabla 8. Señalización y funciones de los receptores de histamina (modificado de Haas *et al.* 2008).

El receptor H_1 tiene 486-491 aminoácidos y está codificado por un gen que no tiene intrones. Se distribuye ampliamente en el organismo, incluyendo el SNC, donde media acciones excitatorias. En cerebro humano se encuentra alta densidad de este receptor en neocorteza, hipocampo, núcleo accumbens, tálamo e hipotálamo posterior, mientras que en cerebelo y ganglios basales su densidad es más baja (Hill *et al.* 1997). Las antihistaminas clásicas actúan vía antagonistas del receptor H_1, y su efecto sedativo es bien conocido. A nivel celular, se acopla a proteína $G\alpha_{q/11}$ que activa la PLC, lo que lleva a la formación de dos segundos mensajeros, DAG e IP_3 (Togias 2003), el primero activa la PKC y el segundo moviliza calcio intracelular desde los reservorios internos activando varios procesos dependientes de calcio, entre ellos, la formación de óxido nítrico y GMPc (Hill *et al.* 1997; Smit *et al.* 1999; Haas and Panula 2003).

El receptor H_2 fue identificado durante el estudio del mecanismo de acción de la histamina en la secreción de ácidos estomacales, en el cual tiene un importante papel como regulador. Este receptor también tiene una amplia distribución en el organismo, incluyendo el SNC, donde usualmente media acciones excitatorias. En el cerebro humano, el receptor H_2 se encuentra en ganglios basales, hipocampo, amígdala y corteza, detectándose en menor densidad

en hipotálamo y cerebelo (Hill *et al.* 1997). Como el receptor H_1, el gen que codifica para este receptor no tiene intrones y su proteína contiene 358-359 residuos (Haas and Panula 2003). El receptor H_2 está acoplado a proteína $G\alpha_s$, por tanto activa la AC incrementando los niveles de AMPc, y activa la PKA activando factores de transcripción como CREB (Del Valle and Gantz 1997; Haas and Panula 2003).

El receptor H_3, que se acopla a proteína $G\alpha_{i/o}$, se localiza predominantemente en el sistema nervioso central. Es un autorreceptor presináptico con significativa actividad constitutiva, que controla la liberación y síntesis de histamina endógena (Morisset *et al.* 2000), así como de otros neurotransmisores tales como glutamato, acetilcolina, noradrenalina y dopamina, entre otros, en diversas áreas, como la sustancia nigra, amígdala, corteza cerebral y estriado (Brown and Haas 1999; Molina-Hernandez *et al.* 2000; Molina-Hernandez *et al.* 2001; Haas and Panula 2003). Este receptor no sólo se localiza presinápticamente, también se encuentra a nivel postsináptico en neuronas eferentes GABAérgicas del estriado (Pillot *et al.* 2002).

En 1999 se logró clonar el receptor H_3, que tiene una homología en secuencia aminoacídica de un 22% y 20% con el receptor H_1 y H_2, respectivamente (Lovenberg *et al.* 1999). Al analizar la secuencia aminoacídica de este receptor, que consta de 445 aminoácidos, se han identificado sitios para N-glicosilación así como sitios consenso de fosforilación mediada por PKA en el tercer bucle intracelular y PKC en varios residuos del primer, segundo y tercer bucle intracelular. Para el receptor H_3 se han detectado varios polimorfismos en su secuencia aminoacídica, en el residuo 19 se puede observar glutamato o aspartato, en la posición 280 alanina o valina, y en la posición 197 cisteína o fenilalanina (Hancock *et al.* 2003). El gen humano posee varios intrones, a diferencia de la mayoría de los receptores asociados a proteína G, y cuatro exones (Figura 39) que pueden dar lugar a diferentes variantes por *splicing alternativo*, de las cuales algunas son funcionales.

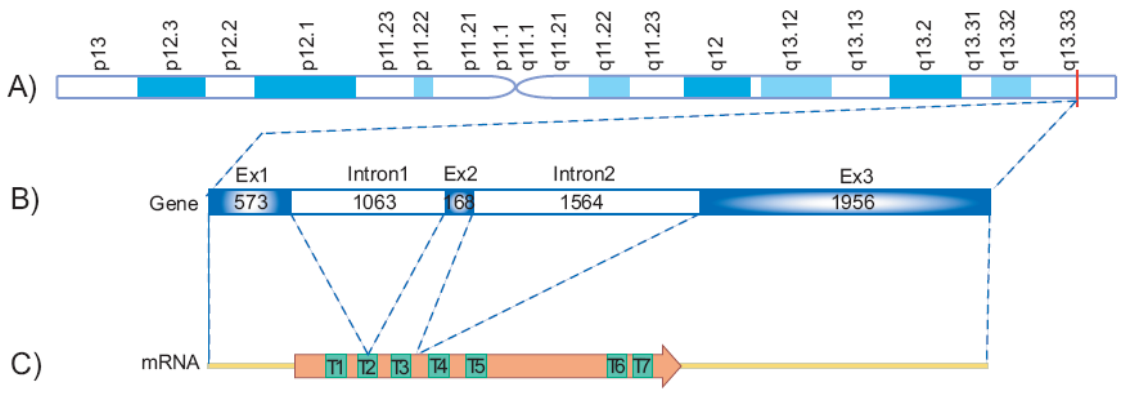

Figura 39. Organización genómica del receptor H_3 de histamina humano. A) Representación esquemática del cromosoma humano 20 y la localización del gen del receptor H_3 de histamina humano en la región q13.33. B) Representación esquemática del gen del receptor H_3 de histamina humano y sus exones (cajas azules) y intrones (cajas blancas). C) Representación esquemática del ARNm del receptor H_3 de histamina, donde se muestra la región no traducida (en amarillo), las regiones codificantes (naranja), y los dominios transmembrana (verde), (Extraído de Bongers *et al*. 2007a).

Al menos existen 20 isoformas del receptor H_3 humano y también muchas de ellas han sido identificadas en rata, cobaya y ratón (Nakamura *et al.* 2000; Tardivel-Lacombe *et al.* 2000; Cogé *et al.* 2001; Drutel *et al.* 2001; Morisset *et al.* 2001; Tardivel-Lacombe *et al.* 2001; Wellendorph *et al.* 2002; Wiedemann *et al.* 2002; Rouleau *et al.* 2004; Ding *et al.* 2005) (Tabla 9).

H_3R(aa)	A 7-42	B 85-98	197	226	234	263	C (variable area) 274	305	315	341	353	393	417	D	Functional	First Reference
453														+8	B/F	[28]
445															B/F	[10]
431		-14													NB	[22]
415					-30										ND	[22]
413							-32								ND	[23]
409	-36														B	[27]
395	-36	-14													ND	[27]
379	-36				-30										ND	[27]
373									-80					+8	F	[24]
365									-80						B/F	[22]
351		-14							-80						ND	[25]
340									-80			-25			ND	[26]
329a						-116									B	[22]
329b	-36								-80						ND	[27]
326						-119									ND	[22]
309										-144				+8	ND	[24]
301										-144					NF	[24]
293	-36					-116									ND	[27]
290	-36					-119									ND	[27]
200	spliced at aa 170 + 30 new aa														NF	[24]
Location	N-Term	TM2	TM5				IL3					TM6	TM7	C-Term		

Tabla 9. Isoformas del receptor H_3 de histamina humano. Las isoformas del receptor H_3 están indicadas por su número de aminoácidos. También se indican las regiones del splicing alternativo y su localización en la proteina. Se indican características de las isoformas, como si son capaces de unir radioligando (B), si son funcionales (F), si no son funcionales (NF) o funcionalidad no determinada (ND) (Extraído y modificado de Leurs *et al.* 2005).

En rata se han descrito tres isoformas funcionales del receptor H_3 denominadas rH_{3A}, rH_{3B} y rH_{3C} y una no funcional truncada denominada rH_{3T} que posee sólo un dominio transmembrana (Drutel *et al.* 2001). La isoforma H_{3A} corresponde a la proteína completa de 445 aminoácidos y tiene un 93% de identidad con el receptor humano, que en su mayoría corresponde a los dominios transmembrana. Existen entre ambos receptores ciertas diferencias en el perfil farmacológico que podrían ser consecuencia de las diferencias entre especie (Lovenberg *et al.* 2000). Las isoformas de rata, al igual que ocurre en humano, son generadas por *splicing alternativo*, y es en el tercer bucle intracelular donde rH_{3B} y rH_{3C} pierden 32 y 48 aminoácidos, respectivamente, comparadas con rH_{3A}. Por otro lado, también existen diferencias de expresión de estas isoformas en varias regiones cerebrales. Esta distribución heterogénea sugiere que la regulación histaminérgica es específica de las isoformas del receptor H_3 y podría ser importante para explicar diferencias entre diversas áreas del cerebro (Drutel *et al.* 2001). Recientemente, se han identificado tres nuevas isoformas del receptor H_3 de rata designadas rH_{3D}, rH_{3E} y rH_{3F} que se diferencian de las previamente publicadas en que resultan de un splicing alternativo adicional, que genera la pérdida del séptimo dominio transmembrana y que contienen un carboxilo terminal alternativo (Bakker *et al.* 2006). Estas nuevas isoformas también se expresan abundantemente y de forma heterogénea en el cerebro; sin embargo, parecen estar localizadas intracelularmente y tienen la capacidad de interferir en la expresión en la superficie celular de las isoformas del receptor H_3, rH_{3A}, rH_{3B} y rH_{3C}, y por tanto, de reducir la señalización mediada por ellas, actuando como isoformas dominante-negativas (Bakker *et al.* 2006).

La función de las diferentes isoformas del receptor H_3 en humano no ha sido completamente identificada, aunque se ha descrito que existen variantes funcionales y no funcionales, siendo estas últimas formas truncadas del receptor H_3 (Cogé *et al.* 2001). Por otra parte, se ha observado que las isoformas funcionales del receptor H_3 tienen características farmacológicas particulares y es probable que las deleciones descritas en el tercer bucle intracelular influyan también en la eficiencia del acoplamiento de estos receptores a proteína G, y que, similarmente a lo observado con las isoformas funcionales de rata, la señalización de las isoformas sea diferente (Drutel *et al.* 2001; Bakker 2004; Bakker *et al.* 2006).

Los receptores H_3 pueden expresarse como dímeros a nivel de la membrana celular. La primera evidencia de dimerización del receptor H_3 proviene de la identificación, en cerebro de rata y ratón, de dos especies inmunoreactivas en condiciones reductoras, lo que es consistente con la presencia de dímeros de las isoformas del receptor H_3 (Shenton *et al.* 2005). El mismo fenómeno se observa al expresar el receptor recombinante H_3 humano en una línea celular (Shenton *et al.* 2005). Con posterioridad, se ha demostrado mediante *time-resolved*-FRET, que

el receptor $rH_{3A,}$ en cerebro de rata o expresado en células, forma dímeros o complejos oligoméricos de orden superior (Bakker *et al.* 2006). Por otro lado, la heterodimerización de isoformas funcionales del receptor H_3 con una forma no funcional que carece de los dominios de retención en RE que son necesarios para la expresión en la superficie celular, podría explicar la retención observada de este receptor en RE (Bakker *et al.* 2006; Bongers *et al.* 2007a).

La localización del receptor H_3 ha sido descrita con bastante detalle en rata, donde se ha observado, mediante hibridación *in situ,* una expresión importante de ARNm en corteza cerebral, núcleo talámico, hipocampo, ganglios basales (estriado y tubérculo olfatorio), sustancia nigra, amígdala e hipotálamo; además, la localización homogénea de este receptor en caudado putamen y núcleo accumbens sugiere que muchos de los receptores H_3 estriatales están presentes en la vía motora directa e indirecta (Pillot *et al.* 2002). No todos los receptores H_3 cerebrales son autorreceptores, los receptores H_3 postsinápticos están localizados en las dendritas y espinas neuronales de muchas poblaciones neuronales, sin embargo, el papel fisiológico de estos últimos no está bien definido (Pillot *et al.* 2002; Arrang *et al.* 2007).

La inhibición del receptor H_3 con un antagonista específico incrementa la actividad motora (Chiavegatto *et al.* 1998), indicando que la estimulación del receptor H_3 induce una disminución en la locomoción que probablemente se debe a la reducción de la actividad del sistema dopaminérgico estriatal. En ratones *knockout* para el receptor H_3 se observó una clara disminución de los niveles de histamina en la corteza, que podría ser consecuencia de la eliminación del efecto estimulador del receptor H_3 en la síntesis de histamina, y una reducción en la locomoción, además de una ligera disminución en la actividad dopaminérgica (Toyota *et al.* 2002). Estos datos sugieren el importante papel que tiene este receptor en la regulación de la actividad motora. La modulación que el receptor H_3 ejerce en la actividad motora se pone también de manifiesto en trabajos que relacionan este receptor con PD. Aunque se ha descrito que no hay diferencias en la densidad de este receptor en estriado de pacientes con PD (Goodchild *et al.* 1999), en otros estudios se ha detectado un aumento en la densidad del receptor en sustancia nigra, y un incremento en la expresión de ARNm en estriado de pacientes con Parkinson (Anichtchik *et al.* 2001). Por otro lado, en modelos animales de la enfermedad se ha observado un incremento de la expresión del receptor H_3. Por ejemplo, en ratas tratadas con 6-hidroxidopamina (6-OHDA) se ha observado un incremento de los sitios de unión y en la expresión de ARNm del receptor H_3 en estriado y sustancia nigra (Ryu *et al.* 1994b; Anichtchik *et al.* 2000a), lo que sugiere que el sistema histaminérgico está involucrado en el proceso patológico después del tratamiento con 6-OHDA a través del receptor H_3. También se ha publicado que en monos marmoset lesionados con MTPT, modelo de PD, la coadministración de un agonista del receptor H_3 con L-DOPA, mitiga de forma significativa las disquinesias que a

largo plazo produce la L-DOPA sin alterar las acciones antiparkinsonianas de esta droga. No obstante, el tratamiento con el agonista como monoterapia fue asociado a una exacerbación de los síntomas parkinsonianos. Todo ello sugiere que los receptores H_3 están involucrados de manera compleja en los mecanismos neuronales subyacentes a PD (Gomez-Ramirez *et al.* 2006).

La actividad constitutiva, actividad espontánea en ausencia de agonistas, del receptor H_3 de rata y humano se reconoció por primera vez en sistemas celulares en los que se observó un cambio en la señalización de las células que expresaban el receptor comparadas con las células *wild-type*. Así, las líneas celulares que expresaban este receptor tenían aumentada la liberación de ácido araquidónico y la unión de [^{35}S]GTPγ[S] y reducida la acumulación de AMPc (Arrang *et al.* 2007). Se ha descrito que el receptor recombinante H_3 de rata exhibe una alta actividad constitutiva a diferentes densidades de expresión, incluso fue posible demostrar en membranas cerebrales de ratón este tipo de actividad del receptor H_3, lo que proporciona por primera vez evidencia de actividad constitutiva *in vivo* de un receptor nativo (Morisset *et al.* 2000). La señalización constitutiva puede ser inhibida por un agonista inverso, que es capaz de estabilizar el receptor en una conformación inactiva, lo que disminuye el acoplamiento espontáneo del receptor a la proteína G y por lo tanto, suprime la actividad constitutiva (Leurs *et al.* 2005; Arrang *et al.* 2007). La mayoría de los compuestos originalmente clasificados como antagonistas del receptor H_3 son en realidad agonistas inversos. El uso de antagonistas y agonistas inversos ha sido crucial para el estudio de la actividad constitutiva del receptor H_3 tanto in *vitro como in vivo*, ya que este fenómeno sólo puede ser establecido una vez que la putativa activación selectiva por un agonista endógeno ha sido excluida, y esto no se consigue con agonistas inversos, sino con antagonistas neutros (Arrang *et al.* 2007).

Utilizando el agonista (R)-α-[^{3}H]metilhistamina (RAMH) se ha determinado la unión del radioligando a membranas de cerebro de rata mediante ensayos de saturación y competición. Se observó que el receptor H_3 tiene aparentemente una cinética monoexponencial. Sin embargo, en estudios de asociación y disociación se observó que este receptor tiene una cinética biexponencial de unión, es decir, dos estados de afinidad, pero que por causa de las condiciones experimentales y porque las constantes de afinidad son muy cercanas, ambos estados son indistinguibles en el equilibrio en un amplio rango de concentraciones de ligando que saturan entre el 10% y el 90% de receptores (West *et al.* 1990). Estas diferencias cinéticas no se han podido explicar con los modelos de unión de radioligandos tradicionales y se han atribuido a la existencia de múltiples subtipos del receptor H_3 que farmacológicamente no se pueden distinguir (West *et al.* 1990). Recientemente, se ha descrito que en experimentos de saturación con células que expresan el receptor H_3 de rata o humano, un agonista inverso radiomarcado es

capaz de marcar una población mayor de receptores comparado con agonistas radiomarcados, lo que se interpretó como que este compuesto se une a receptores en estado activo e inactivo, a diferencia de los agonistas que sólo se unen al receptor H_3 en estado activo (Witte *et al.* 2006).

Dado que los agonistas inversos del receptor H_3 aumentan la actividad de las neuronas histaminérgicas, el interés terapéutico en estos ligandos está basado en gran medida en el papel de estas neuronas en obesidad, vigilia y función cognitiva (Arrang *et al.* 2007). Se ha observado que antagonistas/agonistas inversos no imidazólicos del receptor H_3 tienen un efecto antiobesidad en modelos animales, así como también una amplia eficacia en pruebas de conducta de desórdenes cognitivos, que incluyen el déficit de atención por hiperactividad (ADHD), AD y esquizofrenia (Leurs *et al.* 2005; Hancock 2006). Se ha observado en varios modelos animales que antagonistas/agonistas inversos imidazólicos y no imidazólicos del receptor H_3 son capaces de aumentar la vigilia, lo que podría ser útil en el tratamiento de desórdenes del sueño como la narcolepsia, así como también mejorar la función cognitiva, cuyo déficit es una parte integral de enfermedades como AD, ADHD y esquizofrenia. Por lo tanto, el receptor H_3 parece una diana muy interesante para mejorar la atención y mitigar las disfunciones cognitivas (Leurs *et al.* 2005). Por otro lado, los agonistas del receptor H_3 también han sido considerados para uso terapéutico para el tratamiento del insomnio, por su capacidad de inducir el sueño, en la prevención y tratamiento de arritmias isquémicas miocardiales, por su implicación en la modulación de la liberación de noradrenalina cardiaca mediante los receptores H_3 presentes en las terminales nerviosas simpatéticas, así como también en inflamación, asma y migraña, ya que se ha descrito que agonistas de este receptor inhiben procesos inflamatorios en varios tejidos, incluyendo pulmones y dura mater (Leurs *et al.* 2005). Últimamente se ha realizado un gran esfuerzo en crear ligandos que eliminan el anillo imidazólico, característico del agonista natural del receptor H_3, la histamina, ya que se ha descrito que sería el responsable de la interacción de estas drogas con enzimas de la familia del citocromo P450, actuando como inhibidores de la metabolización de drogas por estas enzimas (Hancock 2006).

La señalización celular mediada por el receptor H_3 se estableció con claridad cuando el grupo de Lovenberg demostró en 1999 la inhibición de la activación de la adenilato ciclasa inducida por agonistas del receptor H_3 en células transfectadas con este receptor. Posteriormente, experimentos utilizando toxina pertúsica y ensayos de unión de $[^{35}S]GTP\gamma[S]$ inducida por agonistas del receptor H_3 en cerebro de rata (Bongers *et al.* 2007a), confirmaron la interacción del receptor H_3 con proteínas $G\alpha_i$ o $G\alpha_o$ (Figura 40).

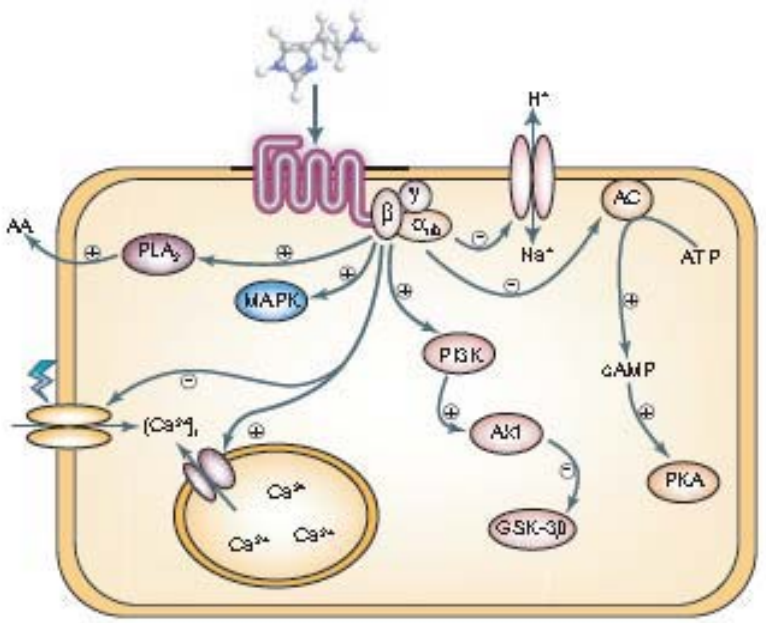

Figura 40. Representación esquemática de la transducción de señal mediada por el receptor H_3. El receptor H_3 modula varias vías de señalización, incluyendo la inhibición de la AC, activación de MAPK, activación de PLA_2, movilización de calcio intracelular, activación del eje Akt/GSK-3β e inhibición del intercambiador de Na^+/K^+ (Extraído de Bongers *et al*. 2007a).

La activación del receptor H_3 inhibe la síntesis de histamina por un proceso que implica la inhibición de PKA mediada por descensos de AMPc (Morisset *et al.* 2000; Gomez-Ramirez *et al.* 2002). La activación del receptor H_3 expresado en una variedad de líneas celulares como células CHO (Morisset *et al.* 2000; Cogé *et al.* 2001), C6 (Bongers *et al.* 2007b), HEK (Uveges *et al.* 2002; Wulff *et al.* 2002), SK-N-MC (Wieland *et al.* 2001), SH-SY5Y (Seyedi *et al.* 2005) o presente en cortes estriatales de rata (Sanchez-Lemus and Arias-Montano 2004), produce la inhibición de la AC causando una disminución del AMPc intracelular y la consecuente reducción de la actividad de la PKA (Bongers *et al.* 2007a). En cultivos neuronales de corteza de rata, el antagonista del receptor H_3 clobenpropit proteje contra la necrosis inducida por NMDA. Esta protección se revierte en presencia del agonista del receptor H_3, RAMH, lo que sugiere que este receptor tiene un papel potenciador en la necrosis inducida por NMDA (Dai *et al.* 2007). El clobenpropit produce la liberación de GABA, fenómeno que no ocurre en presencia de inhibidores de la AC y PKA. Ello indica que el receptor H_3 tiene un importante papel como modulador negativo de la neurotransmisión GABAérgica actuando a través de la vía AC-PKA, y que su acción inhibidora probablemente explica el que los antagonistas del receptor H_3 disminuyan la neurotoxicidad inducida por NMDA (Dai *et al.* 2007).

Se ha descrito que los agonistas del receptor H_3 pueden activar la vía de señalización de MAPK en diversas líneas celulares. Así, utilizando células COS, Drutel y colaboradores (2001)

transfectaron diversas isoformas del receptor H_3 de rata, en las que variaba el tamaño del tercer bucle intracelular, y se determinó que la isoforma *wild type* era la más efectiva en la estimulación de la activación de la vía ERK1/2 y, a su vez, era la menos efectiva en la inhibición de la producción de AMPc inducida por forskolina. En células CHO transfectadas con el receptor H_3 se ha observado que hay un incremento en la actividad de MAPK con agonistas de este receptor, pero que no muestra actividad constitutiva para esta vía de señalización (Gbahou *et al.* 2003). Recientemente se ha demostrado que la estimulación del receptor H_3 activa ERK2 en células hipocampales CA3 in vitro y mejora la consolidación de la memoria (Giovannini *et al.* 2003). Sin embargo, este receptor no parece estar directamente acoplado a la vía de las ERK1/2 en neuronas piramidales, lo que podría sugerir que su activación promueve la liberación de un neurotransmisor no definido que activaría la cascada de las ERK1/2 en las células piramidales CA3, por lo que el papel del receptor H_3 en la señalización vía MAPK in vivo está controvertido. Por otro lado, utilizando terminales nerviosas simpatéticas cardiacas y en corazón completo *ex vivo*, se ha demostrado la implicación del receptor H_3 en la atenuación de la liberación de norepinefrina por la activación de la cascada de la MAPK (Levi *et al.* 2007).

In vivo la activación del receptor H_3 reduce el influjo de calcio, particularmente en las terminales nerviosas noradrenérgicas de miocardio y en el SNC. Se ha demostrado en células y sinaptosomas cardiacos que el aumento de la liberación de norepinefrina en situación de isquemia miocardial puede ser reducida al agregar un agonista del receptor H_3 y este efecto es consecuencia directa de la reducción de la concentración del calcio intracelular (Levi and Smith 2000; Silver *et al.* 2002; Hancock *et al.* 2003). Paralelamente, en neuronas tuberomamilares disociadas, se observó que la activación del receptor H_3 suprime significativamente la corriente de los canales VDCC tipo-N y tipo-P (Takeshita *et al.* 1998). Recientemente, se ha mostrado que la activación del receptor H_3 reduce la concentración de calcio intracelular al inhibir el influjo de calcio a través de los canales tipo-N y tipo-L, como consecuencia de la disminución de la actividad de la PKA que sería responsable de la activación por fosforilación de los canales de calcio activados por voltaje (Seyedi *et al.* 2005). Por último, se ha descrito que la activación del receptor H_3 en un sistema heterólogo incrementa la corriente en canales rectificadores de la entrada de potasio acoplados a proteína G (GIRK), representando este canal un nuevo sistema efector del receptor H_3 (Sahlholm *et al.* 2007).

El intercambiador de Na^+/H^+ es un sistema esencial para la restauración del pH fisiológico intracelular, eliminando un protón intracelular e introduciendo un ión sodio, y previniendo así la acidificación durante la isquemia. Sin embargo, el paulatino incremento de sodio intraneuronal fuerza el intercambio de sodio y cloruro dependiente del transportador de

norepinefrina, lo que lleva a un incremento de la liberación de este neurotransmisor. La estimulación del receptor H_3 disminuye marcadamente la actividad neuronal del intercambiador, y este efecto podría ser también uno de los factores que relacionan a este receptor con la modulación negativa de la liberación de norepinefrina en situación de isquemia miocardial (Silver *et al.* 2001), sin embargo, el mecanismo por el cual el receptor H_3 inhibe la actividad del intercambiador todavía es desconocido.

Por otro lado, la activación de la fosfolipasa A_2 mediada por el receptor H_3 conduce a la liberación de ácido araquidónico, y la actividad de esta enzima está bajo el control de la elevada actividad constitutiva de este receptor (Morisset *et al.* 2000; Bongers *et al.* 2007a). La PLA_2 también libera otros metabolitos que son sustrato para la síntesis de mediadores lipídicos potentes, como el factor activador de plaquetas, eicosanoides y el 4-hidroxinonenal, este último es un metabolito muy citotóxico asociado con el tipo apoptótico de muerte neuronal y que aumenta de manera importante en enfermedades neurológicas como isquemia, AD y PD (Bongers *et al.* 2007a).

Finalmente, también se ha descrito que el eje Akt/GSK-3β es activado por el receptor H_3 en una línea celular de neuroblastoma, en cultivo primario de neuronas corticales y en cortes de estriado de rata. Este proceso ocurre a través de la estimulación de PI3 cinasa por la subunidad Gβγ de la proteína $G_{i/o}$. En el SNC el eje Akt/GSK-3β tiene un importante papel en la función cerebral y ha sido implicado en migración neuronal y protección contra apoptosis neuronal, así la estimulación de esta vía por el receptor H_3 podría ser un mecanismo por el cual este receptor ejerce un efecto neuroprotector (Bongers *et al.* 2007a; Bongers *et al.* 2007c).

El receptor H_4 ha sido recientemente identificado de forma independiente por varios grupos mediante análisis y comparación de secuencias con el receptor H_3, y al igual que este último, el receptor H_4 también estaría acoplado a proteína $G\alpha_{i/o}$ (Nakamura *et al.* 2000; Oda *et al.* 2000; Liu *et al.* 2001; Nguyen *et al.* 2001; Zhu *et al.* 2001). Se localiza preferentemente en los tejidos periféricos al sistema nervioso central, como por ejemplo leucocitos y médula ósea, y su función biológica no es completamente conocida, aunque se ha postulado que modula numerosas funciones en el sistema inmune (de Esch *et al.* 2005; Tanaka and Ichikawa 2006; Zhang *et al.* 2007).

1.6.3 INTERRELACIÓN ENTRE RECEPTORES DE DOPAMINA Y H_3 DE HISTAMINA

Se ha publicado que en ratas lesionadas con 6-hidroxidopamina, un modelo de la enfermedad de Parkinson, se observan cambios en la inervación histaminérgica, la densidad de los receptores y la expresión de ARNm del receptor H_3. El aumento del número y la actividad de estos receptores en la sustancia nigra y el estriado de estas ratas lesionadas, sugiere que este receptor está bajo la influencia dopaminérgica (Anichtchik *et al.* 2000a). Más recientemente, se ha descrito que el sistema histaminérgico puede estar involucrado en las disquinesias inducidas por los agonistas del receptor D_1, aunque el mecanismo de acción no ha sido establecido (Nowak *et al.* 2006).

Se ha descrito que el receptor de dopamina D_1 se localiza en las neuronas GABAérgicas de estriado y sustancia nigra pars reticulata (SNr), en las que codistribuye con el receptor de histamina H_3 (Ryu *et al.* 1994a). En cortes de estriado y SNr de rata, la activación del receptor H_3 inhibe marcada y selectivamente la liberación de GABA, dependiente de la estimulación del receptor D_1 (Garcia *et al.* 1997; Arias-Montano *et al.* 2001), por lo que existe una interacción funcional entre estos receptores a nivel postsináptico. Recientemente se ha descrito que la activación del receptor H_3 inhibe la acumulación de AMPc mediada por el receptor D_1, efecto que es bloqueado por la acción de un antagonista del receptor H_3 en cortes de estriado de rata (Sanchez-Lemus and Arias-Montano 2004). Esto sugiere una codistribución y una interacción antagónica de los receptores D_1 y H_3 en las neuronas GABAérgicas de la vía directa. Sin embargo, los ratones knock-out del receptor H_3 muestran una respuesta comportamental disminuida cuando se administra metanfetamina, que produce la liberación de dopamina. Este resultado parece reflejar un efecto sinérgico entre el receptor H_3 y la respuesta motora a dopamina que se pierde en el knock-out. El efecto puede, no obstante, ser consecuencia secundaria de otros fenotipos del knock-out que muestra muy baja actividad motora y una marcada disminución de temperatura corporal en la fase de actividad nocturna (Toyota *et al.* 2002).

La mayoría de las neuronas que expresan encefalina y, por lo tanto el receptor de dopamina D_2, expresan ARNm para el receptor H_3 (Pillot *et al.* 2002) lo que demuestra que existe una codistribución de los receptores D_2 y H_3 en las neuronas GABAérgicas de la vía indirecta. Además, se ha descrito que el bloqueo del receptor H_3 produce una profunda supresión de la expresión de c-fos inducida por haloperidol en la parte dorsolateral del estriado, un área implicada en el desarrollo de síntomas motores extrapiramidales, que son consecuencia

del tratamiento crónico con haloperidol. Al mismo tiempo, antagonistas del receptor H_3 suprimen los efectos del haloperidol en otras zonas del estriado (Hussain *et al.* 2002). Recientemente se ha publicado que en estriado de rata los efectos de agonistas para los receptores D_2 y H_3 son aditivos, que ligandos para el receptor D_2 no modifican el efecto del ligando del receptor H_3, y viceversa (Humbert-Claude *et al.* 2007). Estos datos parecen indicar que estos receptores no interactúan a través de su acoplamiento a proteína G; sin embargo, se ha observado una hiperactividad de las neuronas histaminérgicas y dopaminérgicas en la esquizofrenia, y la activación aditiva de los receptores H_3 y D_2 sugiere que ambos receptores cooperan para generar algunos síntomas esquizofrénicos (Humbert-Claude *et al.* 2007).

Ultimamente, en nuestro grupo de investigación se ha demostrado la existencia de heterómeros entre los receptores H_3 de histamina y D_2 de dopamina en células vivas y en estriado de cerebro y la existencia de interacciones antagónicas funcionales entre los receptores H_3 de histamina y D_1 y D_2 de dopamina (Ferrada *et al.* 2008). Así, los agonistas del receptor H_3 producen un claro cambio hacia la derecha en la curva de competición del antagonista del receptor D_2 [^{3}H]YM-09151-2 versus el agonista del receptor D_2-*like* quinpirole. El análisis de las curvas de competición, en presencia y ausencia del agonista del receptor H_3 RAMH, indican que este efecto se debe a la disminución en unas 50 veces del valor de la constante de afinidad (K_D) correspondiente al estado de alta afinidad y de unas 4 veces el valor correspondiente al estado baja afinidad. La evaluación de la actividad locomotora inducida por agonistas del receptor de dopamina en ratones reserpinizados es un modelo *in vivo* muy útil para el estudio de la función de los receptores D_1 y D_2 postsinápticos estriatales, sin la influencia de la dopamina endógena. En ratones reserpinizados, el agonista selectivo del receptor H_3 imetit inhibe, mientras que el antagonista del receptor H_3 tioperamida potencia la activación locomotora inducida por el agonista del receptor D_1 SKF 38393 y el agonista del receptor D_2 quinpirole, siendo este efecto máximo cuando ambos receptores se coactivan (Ferrada *et al.* 2008).

La interacción intramembrana receptor-receptor implica un *cross-talk* que no involucra ninguna vía de señalización, pero si una modificación alostérica de un receptor secundaria a la estimulación de un receptor adyacente (Agnati *et al.* 2003; Franco *et al.* 2003; Ferré *et al.* 2007). Una interacción intramembrana receptor-receptor constituye una característica bioquímica común de un heterómero de receptores (Ferré *et al.* 2007). Como se ha comentado anteriormente, la existencia de una interacción intramembrana receptor-receptor en la unión de radioligandos refleja una modificación alostérica de un receptor consecuencia de la estimulación de un receptor vecino (Agnati *et al.* 2003; Franco *et al.* 2003; Ferré *et al.* 2007). De acuerdo con esto, se ha demostrado la capacidad de heteromerización de los receptores H_3-D_2 en células vivas utilizando la técnica de BRET. El conjunto de estos resultados sugiere que la potente

interacción antagónica intramembrana entre heterómeros de los receptores H_3-D_2 probablemente juega un papel modulador clave de la función de la neurona GABAérgica encefalinérgica (Ferrada *et al.* 2008).

También se ha puesto de manifiesto que en ratones reserpinizados, el agonista selectivo del receptor H_3 imetit inhibe, mientras que el antagonista del receptor H_3 tioperamida potencia la activación locomotora inducida por el agonista del receptor de dopamina D_1 SKF 38393 (Ferrada *et al.* 2008). Estos resultados concuerdan con los descritos por Arias-Montaño y colaboradores (2001), analizando la liberación del neurotransmisor GABA en cortes estriatales, indicando la existencia de interacciones antagónicas entre los receptores H_3-D_1. A diferencia de los receptores H_3, el receptor D_1 se acopla a proteína $G_{s/olf}$ y su principal vía de señalización es la estimulación de la cascada de la adenilato ciclasa-PKA (Neve *et al.* 2004). Los efectos opuestos de los receptores H_3 y D_1 sobre la adenilato ciclasa predicen la existencia de interacciones antagónicas entre ambos receptores en la neurona GABAérgica dinorfinérgica a nivel de señalización. De hecho, Sánchez-Lemus y Arias-Montaño (2004) han demostrado recientemente que la activación del receptor H_3 inhibe eficientemente la activación de la adenilato ciclasa mediada por el receptor D_1 en cortes estriatales de rata, pero no encontraron evidencia para la existencia de una interacción intramembrana directa entre los receptores H_3-D_1 (Sanchez-Lemus and Arias-Montano 2004). Por lo tanto, una interacción antagónica entre los receptores H_3-D_1 a nivel de segundos mensajeros, con su consecuente modulación de la función dinorfinérgica GABAérgica, se creyó que debería ser la responsable de la interacción antagónica entre los receptores H_3-D_1 observada en ratones reserpinizados.

En la enfermedad de Parkinson (PD) una degeneración preferencial del sistema dopaminérgico nigroestriatal produce la depleción de dopamina con la consecuente deficiencia del funcionamiento de los circuitos de los ganglios basales y la consiguiente hipoquinesia. De hecho, los ratones reserpinizados son usados como modelo para evaluar la posible actividad antiparkinsoniana de una droga. El antagonista del receptor H_3 tioperamida no produce activación locomotora en ratones reserpinizados, pero, como se ha comentado anteriormente, potencia la activación locomotora inducida por el agonista de D_1 SKF 38393 o por el agonista de D_2 quinpirole. Lo que es destacable es que se observa una gran activación locomotora cuando la tioperamida es coadministrada con SKF 38393 y quinpirole. Aunque estos resultados sugieren que los antagonistas del receptor H_3 podrían ser usados como un adyuvante para los agonistas de receptores de dopamina en PD, debe tenerse en cuenta que la tioperamida no fue capaz de potenciar los efectos mediados por L-DOPA en otro modelo de PD, las ratas lesionadas unilateralmente con 6-hidroxidopamina (Huotari *et al.* 2000). Estos resultados negativos pueden estar relacionados con las neuroadaptaciones que se desarrollan en una

situación de denervación crónica de dopamina. Por ejemplo, el aumento de los receptores H_3 observado después de la denervación estriatal de dopamina (Ryu *et al.* 1994a; Ryu *et al.* 1996; Anichtchik *et al.* 2000a) puede estar acompañada por una reducción en las interacciones entre los receptores H_3-D_1 y H_3-D_2. No obstante, no se puede descartar un posible papel antiparkinsoniano de las drogas que actúan como antagonistas del receptor H_3, así como tampoco el papel que podrían tener estas drogas en otros desórdenes que involucran a los circuitos cortico-estriatales-tálamo-corticales (enfermedad de Huntington, síndrome de Tourette, desorden obsesivo compulsivo, esquizofrenia y abuso de drogas) y que podrían beneficiarse de una aproximación terapéutica basada en las interacciones antagónicas descritas entre los receptores H_3-D_1 y H_3-D_2.

Todos estos antecedentes, algunos de ellos incluso contradictorios, suponen una relación estrecha entre los receptores de histamina H_3 y los receptores de dopamina D_1 y D_2; sin embargo, todavía no está claro como ocurre este fenómeno ni a que niveles, y tampoco las posibles consecuencias funcionales en la regulación de procesos neuronales.

1.7 INTERACCIÓN FUNCIONAL ENTRE LOS RECEPTORES DE DOPAMINA Y LOS RECEPTORES ADRENÉRGICOS α_{1B} Y β_1

1.7.1 LA ADRENALINA COMO NEUROTRANSMISOR Y VÍAS NORADRENÉRGICAS

En 1913 se aisló por primera vez la adrenalina y se probaron sus efectos sobre la vasodilatación y la vasoconstricción, pero no fue hasta la década de 1950 que se estableció la función neurotransmisora de las catecolaminas (noradrenalina y adrenalina) en el encéfalo. Fue en 1988 cuando se definió que las neuronas noradrenérgicas de la periferia son neuronas simpáticas postganglionares, cuyos cuerpos celulares se encuentran en los ganglios simpáticos (Weiner *et al.* 1967; Fillenz 1990; Marshall *et al.* 1991). Estas neuronas generalmente poseen largos axones que terminan en una serie de varicosidades dispersas a lo largo de la red terminal ramificada. Estas variosidades contienen numerosas vesículas sinápticas que constituyen el lugar de síntesis y liberación de la adrenalina y noradrenalina, junto a otros mediadores tales como el ATP y el neuropéptido Y.

El precursor metabólico de la adrenalina y noradrenalina es la L-tirosina, un aminoácido aromático presente en el plasma y los fluidos intersticiales, que es captado por las neuronas adrenérgicas. La tirosina hidroxilasa, una enzima citosólica que cataliza la conversión de

tirosina a dihidroxifenilalanina, se encuentra sólo en las células que contienen catecolaminas (Figura 41). Es una enzima bastante selectiva, ya que a diferencia de otras enzimas implicadas en el metabolismo de las catecolaminas, no acepta derivados indólicos como sustratos y, por tanto, no interviene en el metabolismo de la 5-hidroxitriptamina. Este primer paso de hidroxilación es el principal punto de control para la síntesis de noradrenalina. La tirosina hidroxilasa es inhibida por el producto final de la vía biosintética, la adrenalina; lo que proporciona un mecanismo de regulación de la velocidad de síntesis (Fuller and Wong 1977; Sneader 2001; Wurtman 2002; Kanagy 2005). El siguiente paso, la conversión de DOPA en dopamina, está catalizado por la dopa descarboxilasa, una enzima citosólica que no se limita a las células que sintetizan catecolaminas. Es una enzima relativamente inespecífica y cataliza la descarboxilación de otros aminoácidos L-aromáticos, como L-histidina y L-triptófano, que son los precursores en la síntesis de histamina, y 5-hidroxitriptamina, respectivamente. La actividad de la dopa descarboxilasa no limita la velocidad de síntesis de adrenalina, con lo que, a pesar de que existen varios fármacos que actúan sobre esta enzima, no es un medio eficaz de regulación de la síntesis de noradrenalina y adrenalina (Axelrod 1972; Axelrod and Weinshilboum 1972; Elsworth and Roth 1997; Kanagy 2005; Daubner *et al.* 2011).

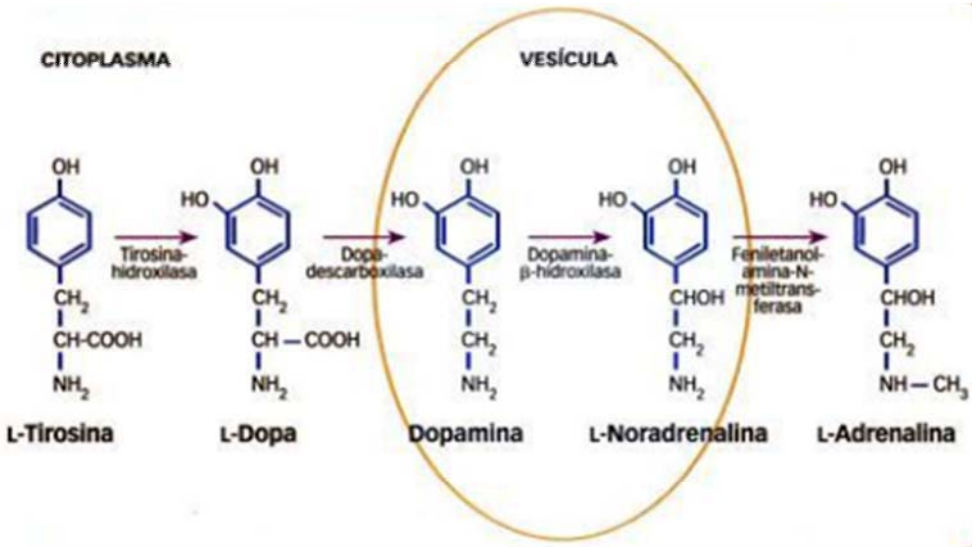

Figura 41. Esquema de la vía de biosíntesis de la noradrenalina y adrenalina.

La dopamina-β-hidroxilasa también es una enzima relativamente inespecífica, pero se encuentra restringida a las células que sintetizan catecolaminas y se localiza en las vesículas sinápticas, con lo que una pequeña cantidad se libera en las terminaciones nerviosas adrenérgicas. Muchos fármacos que inhiben la dopamina-β-hidroxilasa, como los quelantes de cobre y disulfiram, pueden causar depleción parcial de los depósitos de noradrenalina y una interferencia en la trasmisión simpática (Liu and Edwards 1997; Daubner *et al.* 2011). La feniletanolamina N-metiltransferasa cataliza la N-metilación de noradrenalina a adrenalina. La

principal localización de este enzima es la médula suprarrenal, pero también se encuentra en ciertas zonas del encéfalo donde la adrenalina puede funcionar como neurotransmisor.

La mayor parte de noradrenalina y adrenalina de las terminaciones nerviosas se encuentra en las vesículas y sólo una pequeña parte está libre en el citoplasma en circunstancias normales. La concentración en las vesículas es muy elevada (0,3-1mol/l) y se conserva por un mecanismo de transporte similar al del transportador de aminas responsable de la recaptación de noradrenalina en la terminación nerviosa. En estas vesículas, y junto a la noradrenalina, hay otros constituyentes como ATP y cromogranina A que se liberan en el momento de la sinapsis y tienen funciones diversas tal como la producción del potencial sináptico excitador rápido (Lundberg 1996; Esler *et al.* 2003; Sugita 2008).

Los procesos ligados a la llegada de un impulso nervioso a una terminación nerviosa noradrenérgica que conllevan a la liberación de noradrenalina son básicamente los mismos que los de otras sinapsis de transmisión química. La despolarización de la membrana de la terminación nerviosa abre sus canales de calcio y la entrada resultante induce la fusión y descarga de las vesículas sinápticas. Se produce un mecanismo de efecto inhibidor inducido por la adrenalina liberada al espacio sináptico denominado retroalimentación autoinhibidora y mediado por receptores α_2-adrenérgicos presentes en la membrana de la neurona presináptica (Starke *et al.* 1989; Kanagy 2005).

Los cuerpos celulares de las neuronas noradrenérgicas se agrupan en pequeños núcleos situados en la protuberancia y el bulbo raquídeo, desde donde envían axones con extensas ramificaciones hasta otras muchas partes del encéfalo y la médula espinal (Figura 42). El núcleo más importante es el *locus coeruleus* (LC), localizado en la sustancia gris de la protuberancia. Aunque en el ser humano sólo contiene unas 10.000 neuronas noradrenérgicas, los axones acaban en muchos millones de terminaciones nerviosas noradrenérgicas distribuidas por toda la corteza, el hipocampo, el Área Tegmental Ventral y el cerebelo (Aston-Jones 2005; Aston-Jones and Cohen 2005; Mandela and Ordway 2006; Meitzen *et al.* 2011). Estas terminaciones nerviosas no establecen contactos sinápticos separados, sino que parecen liberar el transmisor de una manera difusa. El *locus coeruleus* es el origen de la mayor parte de la noradrenalina liberada en el encéfalo. En general, las neuronas del LC permanecen silentes durante el sueño y su actividad aumenta con la activación conductual. Los estímulos amenazantes excitan a estas neuronas con mucha mayor eficacia que los estímulos familiares y, debido a ello, se cree que la depresión se debe, en parte, a una diferencia funcional de noradrenalina en determinadas regiones encefálicas (Delgado and Moreno 2000; Garland *et al.* 2002).

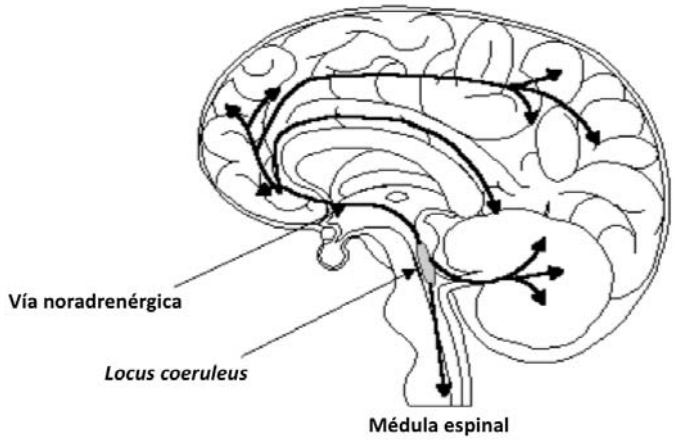

Figura 42. Vías noradrenérgicas en el SNC que parten del locus coeruleus (Extraído y modificado de Brain Vascular Disorder, Canada).

En las proximidades del *locus coeruleus,* en la protuberancia y el bulbo raquídeo existen otras neuronas noradrenérgicas cuyos axones inervan el hipotálamo y el hipocampo, entre otras partes, además de proyectarse hacia el cerebelo y la médula espinal (Fung *et al.* 1994; Sasa and Yoshimura 1994; Sara 2009; Gargaglioni *et al.* 2010). Existe también otro grupo más pequeño de neuronas adrenérgicas cuyos cuerpos celulares se encuentran en una situación más ventral del tronco del encéfalo. Sus fibras se dirigen sobre todo a la protuberancia, el bulbo y el hipotálamo, y liberan adrenalina en lugar de noradrenalina. Los conocimientos sobre estas últimas neuronas son muy escasos, pero se cree que son importantes para el control cardiovascular (Ma and Huang 2002; Keys and Koch 2004).

1.7.2 CLASIFICACIÓN, ESTRUCTURA Y FARMACOLOGÍA DE LOS RECEPTORES ADRENÉRGICOS

En la primera clasificación de los receptores adrenérgicos, realizada por Ahlquist y colaboradores, se definió que el orden de la potencia de diversas catecolaminas, como adrenalina, noradrenalina e isoprenalina, tenía dos patrones diferentes dependiendo de la respuesta que se determinara. Así, se postuló por primera vez la existencia de dos tipos de receptores, definidos como α y β, en función de la potencia del agonista. Los α tenían más afinidad por la noradrenalina y la adrenalina que por la isoprenalina (una catecolamina sintética) y los β mostraban más afinidad por la isoprenalina que por la noradrenalina.

Experimentos posteriores con antagonistas especificos para receptores α y β adrenérgicos

hipotetizaron la existencia de subdivisiones adicionales dentro de estas subfamilias (Rang *et al.* 2008). Esta hipótesis se confirmó al analizar la farmacología de los receptores y permitió determinar la existencia de dos subfamilias dentro de los receptores α adrenérgicos (α_1 y α_2) y tres subfamilias dentro de los receptores β adrenérgicos (β_1, β_2 y β_3) (Tabla 10). Todos los receptores adrenérgicos son receptores acoplados a proteína G típicos y su clonación ha revelado que cada uno de los receptores α_1 y α_2 comprende tres subclases adicionales que se expresan en diferentes localizaciones (Bylund *et al.* 1994; Liggett 2003; Sugita 2008).

Cada una de estas clases de receptor se asocia a un sistema de segundo mensajero específico. Por ejemplo, los receptores α_1 adrenérgicos están acoplados a la fosfolipasa C y ejercen sus efectos principalmente mediante la liberación de calcio intracelular. Los receptores α_2 adrenérgicos están acoplados a G_i, con lo que su activación hace disminuir los niveles de AMPc intracelular e inhibe canales de calcio. Y por último, los tres subtipos de receptores β actúan estimulando la adenilato ciclasa y activando canales de calcio (Tabla 10).

Receptores Adrenérgicos					
Familia	**α - adrenérgicos**		**β - adrenérgicos**		
Subtipo	**α_1**	**α_2**	**β_1**	**β_2**	**β_3**
Moléculas efectoras	↑Ca^{+2} ↑cAMP ↑Diacilglicerol	↓Ca^{+2} ↓cAMP ↑K^+	↑Ca^{+2} ↑cAMP	↓Liberación histamina en SNC ↑cAMP ↑Liberación adrenalina en SNC	↑Ca^{+2} ↑cAMP
Ligandos	Alta afinidad por noradrenalina	Alta afinidad por noradrenalina	Alta afinidad por isoprenalina	Alta afinidad por isoprenalina	Alta afinidad por isoprenalina
Efectos			↑Frecuencia cardíaca		↑Termogenia en músculo esquelético

Tabla 10. Esquema de la clasificación de los receptores adrenérgicos y sus funciones principales.

Los receptores adrenérgicos, como otros GPCR, poseen un dominio amino terminal extracelular y un dominio carboxilo terminal intracelular y diferentes bucles intracelulares y extracelulares producidos por los *loops* que conectan unas hélices con otras (Figura 43). Los bucles intracelulares permiten a los receptores adrenérgicos interaccionar con proteínas de la cascada de señalización tales como β-arrestina y dinamina (Small *et al.* 2006; Volovyk *et al.* 2006; Tan *et al.* 2009; Cotecchia 2010), mientras que los bucles extracelulares forman un 'bolsillo' estructural que permite la unión del ligando al receptor. A pesar de que la homología en la secuencia aminoacídica entre la familia α y β es baja, no hay diferencias significativas en la estructura y tamaño entre ambas familias. Cabe destacar, que dentro de las distintas subfamilias se encuentran secuencias muy homólogas, indicando que probablemente están relacionadas filogenéticamente y que la similitud de su estructura transmembrana no se deba

únicamente a requerimientos funcionales comunes, sinó a un antecesor funcional común (Garland and Biaggioni 2001; Rang *et al.* 2008).

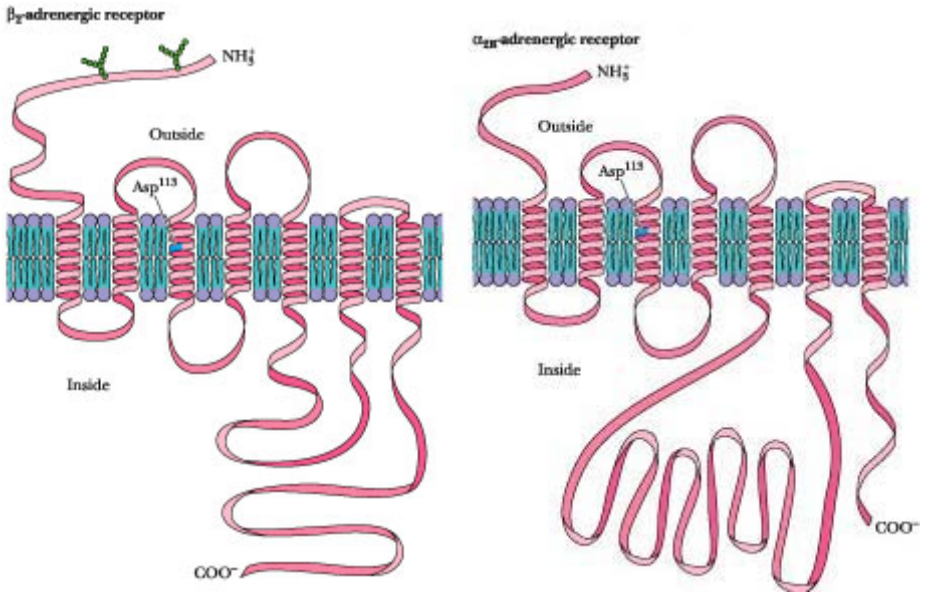

Figura 43. Estructura de un receptor adrenérgico. (a) Modelo de distribución de siete hélices de transmembrana de un receptor β_2-adrenérgico y α_{2B}-adrenergico (Garrett and Grisham 1999).

A pesar de que en el organismo, los ligandos endógenos principales son la adrenalina y noradrenalina (con diferente afinidad para cada receptor adrenérgico), actualmente existe una gran variedad de agonistas y antagonistas selectivos y específicos para cada familia y cada miembro de las subfamilias que se utilizan como fármacos para diferentes patologías. Estos fármacos, dirigidos directa o indirectamente a los receptores adrenérgicos, se clasifican en cinco subclases dependiendo de su funcionalidad; simpaticomiméticos, antagonistas, inhibidores de síntesis, inhibidores de liberación y alteradores de la recaptación (Pfeffer and Stevenson 1996; de Boer *et al.* 1999; Rang *et al.* 2008; Kobilka 2011).

El receptor α_1 adrenérgico es el primer miembro de la subfamilia de α-receptores. Existen tres subtipos de receptores denominados α_{1A}, α_{1B} y α_{1D} que se diferencian entre ellos por sus propiedades farmacológicas y localización en el organismo. En general, los receptores α_1 adrenérgicos se acoplan a proteína G_q, cuya activación inducida por el intercambio de GDP por GTP produce la activación de la PLC y la consiguiente fosforilación de la PKC. Esta fosfolipasa hidroliza al PIP_2 dando lugar a IP_3 y a DAG. Estos metabolitos secundarios permiten la apertura de los canales de calcio de los retículos endoplasmático y sarcoplasmático aumentando así los niveles de calcio intracelular, con la activación de una cascada de fosforilación que conlleva la inducción de varios factores de transcripción (Schmitz *et al.* 1981; Maronde and Stehle 2007;

Cotecchia 2010; Johnson and Liggett 2011) (Figura 44).

El receptor β_1 adrenérgico es el primer miembro de la subfamilia de β- receptores, y actualmente no se han descrito submiembros dentro de esta subfamilia. Se acopla a proteína G_S, con lo que su activación produce un aumento de AMPc catalizado por la adenilato ciclasa. Este incremento de AMPc intracelular induce la activación de CREB mediante fosforilación y la inhibición de la degradación del enzima AA-NAT (Maronde and Stehle 2007; Grimm and Brown 2010; Schiattarella *et al.* 2010), enzima responsable de la síntesis de melatonina (Figura 44).

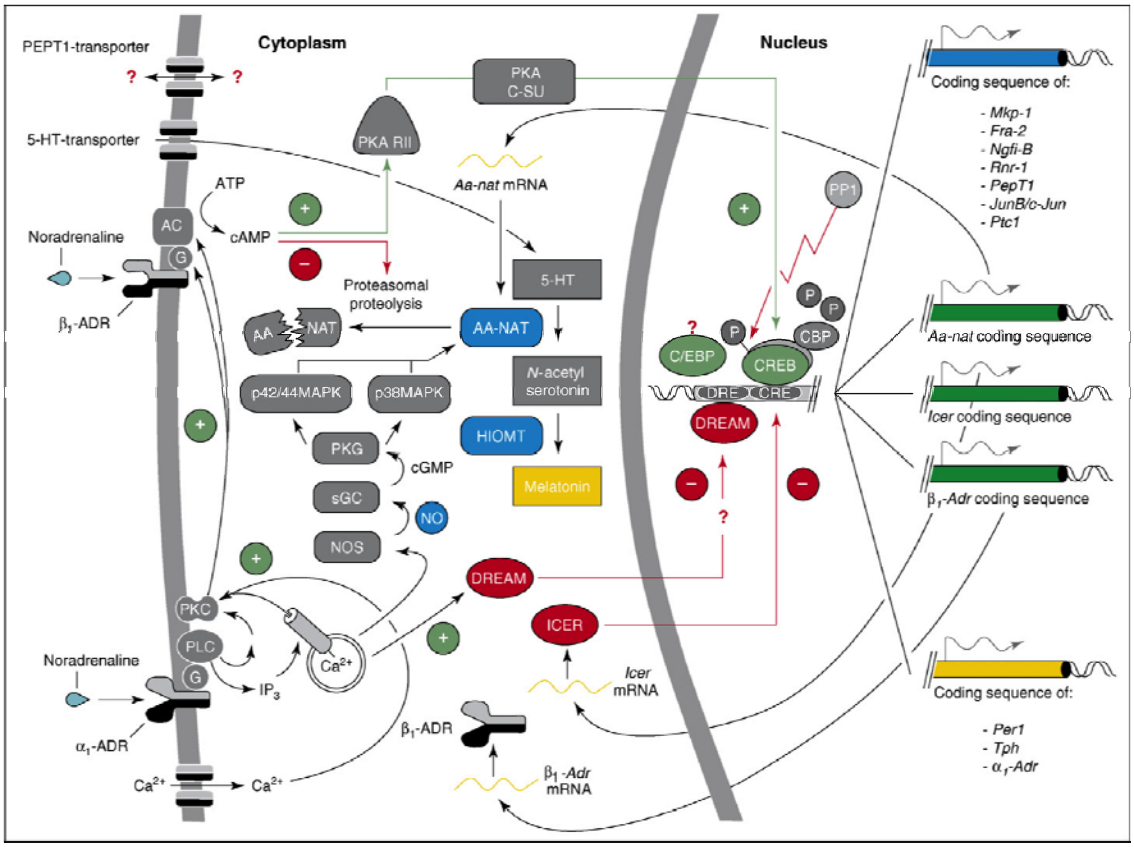

Figura 44. Cascada de activación intracelular inducida por la unión de noradrenalina a los receptores α_{1B} y β_1 adrenérgicos en la glándula pineal (Extraído de Maronde and Stehle 2007).

La acción fisiológica inducida por la activación de estos receptores depende directamente de su localización en el organismo. El receptor α_1 adrenérgico se localiza principalmente en la musculatura lisa, cuya activación produce la vasoconstricción de los vasos sanguíneos (Stiles *et al.* 1983a; Elliott *et al.* 1997); y el receptor β_1 adrenérgico se localiza principalmente en glándulas salivales, cardiomiocitos y córtex cerebral, cuya activación produce la secreción de amilasa y un aumento de la frecuencia cardíaca (Stiles *et al.* 1983b; Moore *et al.*

1999; Ranade *et al.* 2002; Grimm and Brown 2010). Cabe destacar que la presencia de receptores adrenérgicos en el sistema nervioso central (SNC) es minoritaria en comparación con otros tejidos, ya que el número de neuronas noradrenérgicas en el encéfalo es reducido y estos receptores ejercen una gran variedad de funciones en diferentes tejidos del organismo.

Entre los ligandos más utilizados para los receptores α_1 se encuentra la fenilefrina (K_D = 4,7 nM) que actúa como agonista selectivo de la familia α_1 con mayor afinidad por α_{1A} y α_{1B}, (Minneman *et al.* 1994; Morton *et al.* 2007) y REC 15/2615 (K_D = 0,3 nM) que actúa como antagonista selectivo de la familia α_1 con mayor afinidad por α_{1B} (Morton *et al.* 2007). Y para los receptores β_1 adrenérgicos se utiliza principalmente el isoproterenol, que actúa como agonista de receptores β adrenérgicos sin ser selectivo para β_1 (Schmitt and Stork 2000; Akimoto *et al.* 2002) y CGP 20712 (K_D = 0,3 nM) que actúa como antagonista selectivo para receptores β_1 adrenérgicos con mil veces más afinidad por β_1 que por β_2 (Hieble *et al.* 1995).

1.7.3 INTERRELACIÓN ENTRE LOS RECEPTORES DE DOPAMINA D_4 Y LOS RECEPTORES ADRENÉRGICOS α_{1B} y β_1 EN LA GLÁNDULA PINEAL

La glándula pineal, también llamada cuerpo pineal o epífisis, es una pequeña glándula endocrina de secreción interna presente en el sistema nervioso central de los vertebrados. Esta glándula recibe inervaciones simpáticas procedentes del ganglio cervical superior e inervaciones parasimpáticas procedentes de la esfenopalatina y el ganglio ótico. Algunas de estas innervaciones penetran en la glándula, pero la mayor parte de ellas la irrigan de forma superficial permitiendo la entrada del metabolito por difusión. A su vez, neuronas procedentes del núcleo supraquiasmático (Maronde and Stehle 2007), el ganglio cervical superior y del ganglio trigerminal inervan a la glándula pineal, liberando de forma superficial neuropeptina, PACAP (polipéptido activador de la adenilato ciclasa pituitaria), dopamina y noradrenalina, que penetran en ella por difusión pasiva (Axelrod 1970; Tapp and Huxley 1972). Desde hace ya varias décadas, se conoce que en la glándula pineal se expresan los receptores α_{1B} y β_1 adrenérgicos, a los cuales, se une la noradrenalina liberada permitiendo así la activación o inhibición de muchas funciones celulares como la regulación de la síntesis de melatonina y su liberación.

En los mamíferos superiores existe una inervación entre el nervio ocular y la glándula pineal, lo que demuestra una relación directa de las funciones de esta glándula con los ciclos de luz y oscuridad y, por consiguiente, una relación directa con la regulación del ritmo circadiano. Se ha demostrado que la síntesis y liberación de melatonina en la glándula pineal esta bajo el

control de los receptores adrenérgicos (Figura 45) (Borjigin and Deng 2000; Abbas *et al.* 2010; Mitchell and Weinshenker 2010; Rios *et al.* 2010; Hardeland *et al.* 2011). La noradrenalina liberada en la glándula pineal activa receptores β-adrenérgicos que inducen un incremento de los niveles de AMPc, responsable de la activación de los enzimas triptófano hidroxilasa (TPH) y serotonina-N-acetiltransferasa (NAT) induciendo la activación de la síntesis de melatonina. A su vez, la noradrenalina activa receptores α-adrenérgicos que inducen la liberación de serotonina y melatonina mediante difusión vesicular probablemente mediada por incrementos en la concentración de Ca^{2+} intracelular.

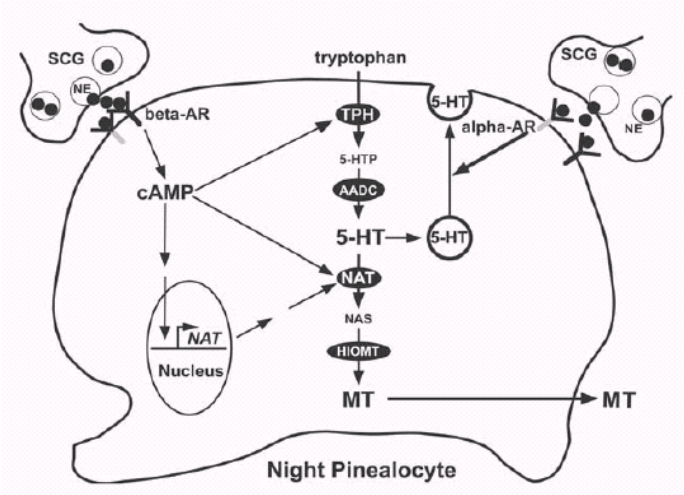

Figura 45. Localización de la glándula pineal en el SNC de humanos y roedores, (Extraído de Borjigin and Deng 2000).

A pesar de que la expresión de los receptores adrenérgicos no está en función del ritmo circadiano, se conoce que durante el periodo de oscuridad se produce un aumento significativo de la producción de melatonina durante las primeras horas del sueño, mientras que durante el periodo de luz, esta producción está altamente inhibida (Borjigin *et al.* 1999; Sun *et al.* 2002).

Ha sido recientemente cuando se ha descrito por primera vez que en la glándula pineal se expresa también el receptor D_4 de dopamina y que presenta un patrón de expresión característico regulado por el ritmo circadiano (Figura 46), siendo éste el único receptor dopaminérgicos presente en la glándula pineal de rata (Bailey *et al.* 2009; Kim *et al.* 2010).

a **b**

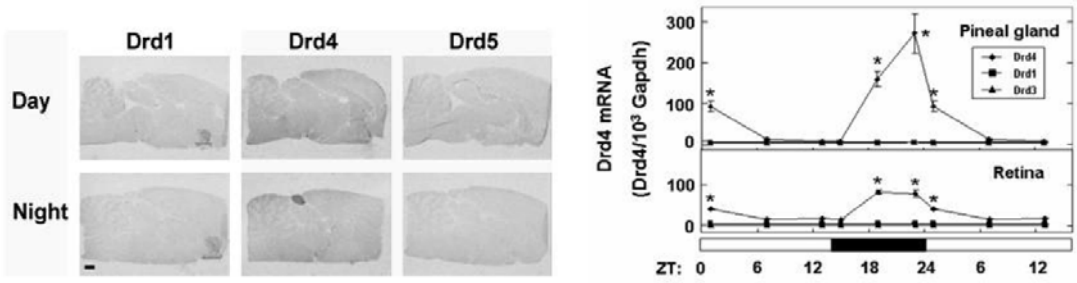

Figura 46. Variación del ARNm de D_4 en la glándula pineal en periodos de luz/oscuridad. a) Hibridación in situ del ARNm del receptor de D_4 de dopamina en la glándula pineal de rata durante el día (luz) o la noche (oscuridad). b) qRT-PCR del ARNm de D_4 de glándulas pineales de ratas extraidas a diferentes horas del día y la noche para determinar el aumento de expresión en periodos de oscuridad, (Extraído de Kim *et al.* 2010).

Mediante técnicas de hibridación *in situ* se observó que la expresión del ARNm de D_4 era prácticamente nula durante el periodo de luz, en cambio, la expresión de este receptor aumentaba drásticamente durante el periodo de oscuridad (Figura 46a). Mediante experimentos de qRT-PCR con glándulas pineales de ratas extraídas a diferentes horas del día y la noche, se demostró que el ARNm del receptor D_4 de dopamina aumentaba hasta 300 veces su expresión en el periodo de oscuridad (Figura 46b) (Kim *et al.* 2010), lo que indica que este receptor juega un papel importante en la glándula pineal en los periodos de oscuridad y, por lo tanto, posiblemente tiene relación con la regulación del ritmo circadiano.

Se ha descrito la existencia de receptores D_1 y D_2 de dopamina en la glándula pineal de pollo y buey (Simonneaux *et al.* 1990; Zawilska *et al.* 2004; Santanavanich *et al.* 2005). Se ha demostrado que la glándula pineal está inervada por terminaciones nerviosas que liberan dopamina. Esta catecolamina se une a los receptores D_1 y D_2 de dopamina presentes en la glándula pineal produciendo una activación y una inhibición de la síntesis de melatonina, respectivamente. Zawilska y colaboradores demostraron que el tratamiento de glándulas pineales con el agonista SKF 38393 (agonista selectivo del receptor D_1) producía la activación del enzima AA-NAT, cuya función es la síntesis directa de melatonina (Zawilska *et al.* 2004). Un año después, otro estudio demostró que el tratamiento de glándulas pineales con el mismo agonista SKF 38393 producía un aumento del AMPc intracelular que inducía la fosforilación de la proteína CREB, responsable de la activación del enzima AA-NAT. A su vez, se demostró que el tratamiento de las glándulas pineales con quinpirole (agonista selectivo del receptor D2-*like*) producía una disminución del AMPc intracelular, disminuyendo la fosforilación de la proteína CREB y la consecuente inhibición del enzima AA-NAT (Santanavanich *et al.* 2005). Estos trabajos demostraron que existe algún tipo de interacción (por ejemplo: *cross-talk* intracelular a

nivel de segundos mensajeros) entre receptores de dopamina y adrenérgicos que permite una fina regulación de la síntesis de melatonina y un mantenimiento de los ritmos circadianos en la glándula pineal, pero se desconoce si existe alguna interacción molecular entre receptores de adrenalina y dopamina de esta procedencia.

OBJETIVOS

2. OBJETIVOS

El objetivo de esta Tesis ha sido el estudio de receptores acoplados a proteína G (GPCRs) focalizando el trabajo en algunos de los receptores que desempeñan un papel relevante en el funcionamiento del sistema nervioso central. A este respecto, los receptores de dopamina de la familia D_1 y D_2, han sido nuestro principal objeto de estudio. Clásicamente se ha considerado que los GPCRs, incluyendo los receptores de dopamina, actúan como unidades individuales para producir su señalización intracelular, pero en la actualidad ya es un hecho aceptado que, a nivel de la membrana plasmática, estos receptores interaccionan unos con otros para formar heterómeros. Los heterómeros se definen como complejos macromoleculares compuestos al menos por dos receptores funcionales distintos y que presentan propiedades bioquímicas que son diferentes a las de los receptores individuales que los constituyen. Por tanto, los heterómeros de GPCRs son nuevas entidades funcionales que hay que tener en cuenta para entender la transmisión neuronal y como nuevas dianas para el desarrollo de fármacos. Con estos conceptos en mente, el *Objetivo General de esta Tesis ha sido investigar la formación y función de heterómeros entre receptores de dopamina y otros receptores que puedan estar implicados en la regulación de la transmisión dopaminérgica, como receptores de galanina, histamina, adrenérgicos o receptores sigma-1.*

Basándonos en que tanto la galanina como la dopamina modulan la liberación de acetilcolina en el hipocampo, el primer objetivo de esta Tesis ha sido:

Objetivo 1.- Investigar si los receptores de dopamina de la familia D_1 (receptores D_1 y D_5) pueden formar heterómeros con los receptores de galanina Gal_1 y Gal_2 y estudiar la función de estos heterómeros en la liberación de acetilcolina en el hipocampo.

En el estriado, los receptores de dopamina D_1 se localizan en las neuronas GABAérgicas dinorfinérgicas donde también se localizan receptores de histamina H_3. Este hecho permite formular la hipótesis de que estos receptores de histamina modulen la transmisión dopaminérgica mediante la formación de heterómeros y que esto pueda explicar algunos de los resultados contradictorios sobre las interacciones funcionales entre receptores H_3 y receptores de dopamina. Teniendo en cuenta todo ello, el segundo objetivo de esta Tesis ha sido:

Objetivo 2.- Investigar si los receptores de dopamina D_1 pueden formar heterómeros con los receptores de histamina H_3 y estudiar las implicaciones funcionales de estos heterómeros en cultivos celulares y en el estriado.

Las vías dopaminérgicas y especialmente la señalización mediada por los receptores D_1 y D_2 de dopamina, están profundamente implicadas en la adicción a cocaína. Una gran parte de los efectos mediados por la cocaína se atribuyen a una sobre-estimulación de la señalización de los receptores de dopamina debida al incremento de dopamina ocasionado por la inhibición por cocaína del transportador de dopamina (DAT). Sin embargo, la cocaína, además de interaccionar con DAT, puede unirse a otras proteínas como los receptores sigma-1. En este contexto, es interesante conocer si los receptores sigma 1 pueden modular la funcionalidad de los receptores de dopamina D_1 y D_2 mediante un proceso de heteromerización. Por ello, el tercer objetivo de esta Tesis ha sido:

Objetivo 3.- Estudiar si los receptores D_1 y D_2 de dopamina pueden formar heterómeros con los receptores sigma-1 e investigar el efecto que ejerce la cocaína, mediado por estos heterómeros, en la transmisión dopaminérgica.

El receptor de dopamina D_4 pertenece a la familia de receptores de dopamina D_2 y, en humanos, es el único que presenta formas polimórficas, las más comunes $D_{4.4}$, $D_{4.2}$ y $D_{4.7}$. Existe una clara relación entre la forma polimorfica $D_{4.7}$ del receptor D_4 humano con el trastorno de hiperactividad y déficit de atención. No existen muchas diferencias funcionales entre las formas polimórficas por lo que no se conoce cuales son las repercusiones bioquímicas de expresar una u otra forma. Nuestra hipótesis de trabajo es que podían existir diferencias en la capacidad de formar heterómeros con otros receptores de dopamina como el D_2 y que estos heterómeros podrían modular la liberación de glutamato en el estriado, lo que podría ser relevante en el trastorno de hiperactividad y déficit de atención. Por ello, el cuarto objetivo de esta Tesis ha sido:

Objetivo 4.- Determinar si los receptores D_2 y D_4 de dopamina pueden formar heterómeros en células vivas y en el tejido estriatal y estudiar su papel en la liberación de glutamato en el estriado.

Otra particularidad del receptor de dopamina D_4 es que es el único receptor dopaminérgico en la glándula pineal de rata sin que se conozca cual es su función a pesar de que se expresa de manera circadiana. Dado que la glándula pineal está bajo el control de los receptores α_{1B} y β_1 adrenérgicos, cuya activación está altamente relacionada con la regulación del ritmo circadiano y la síntesis y liberación de serotonina y melatonina, una posibilidad es que los receptores de dopamina D_4 puedan modular la función de los receptores adrenérgicos de la glándula pineal mediante un proceso de heteromerización. Para estudiar esta posibilidad se ha propuesto el último objetivo de esta Tesis:

Objetivo 5.- Determinar si los receptores D_4 de dopamina pueden formar heterómeros con los receptores α_{1B} y β_1 adrenérgicos e investigar su presencia y función en la glándula pineal de rata.

RESULTADOS

3. RESULTADOS

Los resultados de la presente Tesis están incluidos en los siguientes manuscritos:

3.1 **Estefanía Moreno***, Sandra H. Vaz*, Ning-Sheng Cai, Carla Ferrada, César Quiroz, Sandeep Kumar Barodia, Nadine Kabbani, Enric I. Canela, Peter J. McCormick, Carme Lluís, Rafael Franco, Ribeiro JA, Ana M. Sebastião, Sergi Ferré. **Dopamine–Galanin Receptor Heteromers Modulate Cholinergic Neurotransmission in the Rat Ventral Hippocampus.**

Manuscrito publicado en *Journal of Neuroscience, 2011,* ***31(20)****: 7412-7423.*

3.2 Carla Ferrada, **Estefanía Moreno**, Vicent Casadó, Gerold Bongers, Antoni Cortés, Josefa Mallol, Enric I. Canela, Rob Leurs, Sergi Ferré, Carme Lluís, Rafael Franco. **Marked changes in signal transduction upon heteromerization of dopamine D_1 and histamine H_3 receptors.**

Manuscrito publicado en *British Journal of Pharmacology, 2009,* ***157(1)****: 64-75.*

3.3 **Estefanía Moreno**, Hanne Hoffmann, Marta Gonzalez-Sepúlveda, Gemma Navarro, Vicent Casadó, Antoni Cortés, Josefa Mallol, Michel Vignes, Peter J. McCormick, Enric I. Canela, Carme Lluís, Rosario Moratalla, Sergi Ferré, Jordi Ortiz, Rafael Franco. **Dopamine D_1-histamine H_3 Receptor Heteromers Provide a Selective Link to MAPK Signaling in GABAergic Neurons of the Direct Striatal Pathway.**

Manuscrito publicado en *Journal of Biological Chemistry, 2011,* ***286(7)****: 5846-5854.*

3.4 Gemma Navarro, **Estefanía Moreno**, Marisol Aymerich, Daniel Marcellino, Peter J. McCormick, Josefa Mallol, Antoni Cortés, Vicent Casadó, Enric I. Canela, Jordi Ortiz, Kjell Fuxe, Carme Lluís, Sergi Ferré, Rafael Franco. **Direct involvement of σ-1 receptors in the dopamine D_1 receptor-mediated effects of cocaine.**

Manuscrito publicado en *Proceedings of the National Academy of Sciences of USA,*

2010, ***107(43)****:18676-81.*

3.5 Gemma Navarro, **Estefanía Moreno**, Jordi Bonaventura, Marc Brugarolas, Daniel Farré, Josefa Mallol, Antoni Cortés, Vicent Casadó, Carme Lluís, Sergi Ferre, Rafael Franco, Enric Canela, Peter J. McCormick. **Cocaine inhibits D_2 receptor signalling via sigma-1-dopamine D_2 receptor heteromers.**

Manuscrito enviado para su publicación a *Proceedings of the National Academy of Sciences of USA.*

3.6 Sergio González, Claudia Rangel-Barajas, Marcela Peper, Ramiro Lorenzo, **Estefanía Moreno**, Francisco Ciruela, Janusz Borycz, Jordi Ortiz, Carme Lluís, Rafael Franco, Peter J. McCormick, Nora D. Volkow, Marcelo Rubinstein, Benjamin Floran, Sergi Ferré. **Dopamine D_4 receptor, but not the ADHD-associated $D_{4.7}$ variant, forms functional heteromers with the dopamine D_{2S} receptor in the brain**.

Manuscrito publicado en *Molecular Psychiatry, 2011, 1-13: 1359-4184/11.*

3.7 Sergio González; David Moreno-Delgado; **Estefanía Moreno**; Kamil Perez-Capote; Josefa Mallol; Antoni Cortés; Vicent Casadó; Carme Lluís; Jordi Ortiz; Sergi Ferre; Enric Canela; Peter J. McCormick. **Circadian-related heteromerization of adrenergic and dopamine D_4 receptors modulates melatonin synthesis and release in the pineal gland.**

Manuscrito enviado para su publicación a *Plos Biology.*

3.1 Heterómeros de receptores de dopamina-galanina modulan la neurotransmisión colinérgica en el hipocampo ventral de rata

Estefanía Moreno[1,2*], Sandra H. Vaz[3,4*], Ning-Sheng Cai[5], Carla Ferrada[1,2], César Quiroz[5], Sandeep Kumar Barodia[5], Nadine Kabbani[6], Enric I. Canela[1,2], Peter J. McCormick[1,2], Carme Lluis[1,2], Rafael Franco[1,2,7], Joaquim A. Ribeiro[3,4], Ana M. Sebastião[3,4**], and Sergi Ferré[5**]

[*]Coautores del manuscrito,
[**]Codirectores del manuscrito

[1]Centro de Investigación Biomédica en Red sobre Enfermedades Neurodegenerativas y [2]Facultad de Biología, Departamento de Bioquímica y Biología Molecular, Universidad de Barcelona, 08028 Barcelona, España.
[3]Faculty of Medicine, Institute of Pharmacology and Neurosciences, and
[4]Unit of Neuroscience, Institute of Molecular Medicine, University of Lisbon, 1649-028 Lisbon, Portugal,
[5]Intramural Research Program, National Institute on Drug Abuse, Department of Health and Human Services, National Institutes of Health, Baltimore, Maryland 21224,
[6]Department of Molecular Neuroscience, Krasnow Institute for Advanced Study, Fairfax, Virginia 22030.
[7]Centro de Investigación Médica Aplicada, Universidad de Navarra, 31008 Pamplona, España.

Manuscrito publicado en Journal of Neuroscience, (2011 May), ***31(20):*** *7412-7423.*

En estudios previos se ha descrito que la dopamina y la galanina modulan la transmisión colinérgica en el hipocampo, sin embargo no se conocen los mecanismos involucrados en la modulación. Utilizando técnicas de transferencia de energía de resonancia en células de mamífero transfectadas hemos demostrado la heteromerización entre receptores D_1-like de dopamina (D_1 y D_5) y receptores Gal_1 de galanina, pero no con receptores Gal_2 de galanina. En los heterómeros de receptores D_1–Gal_1 y D_5–Gal_1, la activación de los receptores de dopamina potenció y el bloqueo contrarrestó la activación de la vía de las MAP cinasas (MAPK) a través de la estimulación de los receptores Gal_1, mientras que, la activación o bloqueo del receptor Gal_1 no modificó la activación de la vía MAPK mediada por los receptores D_1-like. La capacidad del antagonista de los receptores D_1-like para bloquear la activación de la vía MAPK inducida por la galanina (antagonismo cruzado) fue utilizado como "huella bioquímica" de los heterómeros $D_{1/5}$-Gal_1, permitiendo su identificación en el hipocampo ventral de rata. El papel funcional de los heterómeros $D_{1/5}$-Gal_1 se demostró en sinaptosomas procedentes del hipocampo ventral de rata, donde la galanina facilita la liberación de acetilcolina, pero únicamente a través de la coestimulación de los receptores $D_{1/5}$. Experimentos de electrofisiología en slices de hipocampo ventral de rata, mostraron que la interacción entre estos receptores modula la transmisión sináptica en el hipocampo. Así, un agonista de los receptores $D_{1/5}$ que se mostró inefectivo al ser administrado por sí solo, convirtió un efecto inhibidor de la galanina en un efecto estimulador, interacción que requiere la neurotransmisión colinérgica. Globalmente, nuestros resultados sugieren que los heterómeros de los receptores $D_{1/5}$-Gal_1 actúan como procesadores que integran señales de dos neurotransmisores distintos, la dopamina y la galanina, para modular la neurotransmisión colinérgica en el hipocampo.

Behavioral/Systems/Cognitive

Dopamine–Galanin Receptor Heteromers Modulate Cholinergic Neurotransmission in the Rat Ventral Hippocampus

Estefanía Moreno,[1,2]* Sandra H. Vaz,[3,4]* Ning-Sheng Cai,[5] Carla Ferrada,[1,2] César Quiroz,[5] Sandeep Kumar Barodia,[5] Nadine Kabbani,[6] Enric I. Canela,[1,2] Peter J. McCormick,[1,2] Carme Lluis,[1,2] Rafael Franco,[1,2,7] Joaquim A. Ribeiro,[3,4] Ana M. Sebastião,[3,4] and Sergi Ferré[5]****

[1]Centro de Investigación Biomédica en Red sobre Enfermedades Neurodegenerativas and [2]Faculty of Biology, Department of Biochemistry and Molecular Biology, University of Barcelona, 08028 Barcelona, Spain, [3]Faculty of Medicine, Institute of Pharmacology and Neurosciences, and [4]Unit of Neuroscience, Institute of Molecular Medicine, University of Lisbon, 1649-028 Lisbon, Portugal, [5]Intramural Research Program, National Institute on Drug Abuse, Department of Health and Human Services, National Institutes of Health, Baltimore, Maryland 21224, [6]Department of Molecular Neuroscience, Krasnow Institute for Advanced Study, Fairfax, Virginia 22030, and [7]Centro de Investigación Médica Aplicada, Universidad de Navarra, 31008 Pamplona, Spain

Previous studies have shown that dopamine and galanin modulate cholinergic transmission in the hippocampus, but little is known about the mechanisms involved and their possible interactions. By using resonance energy transfer techniques in transfected mammalian cells, we demonstrated the existence of heteromers between the dopamine D_1-like receptors (D_1 and D_5) and galanin Gal_1, but not Gal_2 receptors. Within the D_1–Gal_1 and D_5–Gal_1 receptor heteromers, dopamine receptor activation potentiated and dopamine receptor blockade counteracted MAPK activation induced by stimulation of Gal_1 receptors, whereas Gal_1 receptor activation or blockade did not modify D_1-like receptor-mediated MAPK activation. Ability of a D_1-like receptor antagonist to block galanin-induced MAPK activation (cross-antagonism) was used as a "biochemical fingerprint" of D_1-like–Gal_1 receptor heteromers, allowing their identification in the rat ventral hippocampus. The functional role of D_1-like–Gal receptor heteromers was demonstrated in synaptosomes from rat ventral hippocampus, where galanin facilitated acetylcholine release, but only with costimulation of D_1-like receptors. Electrophysiological experiments in rat ventral hippocampal slices showed that these receptor interactions modulate hippocampal synaptic transmission. Thus, a D_1-like receptor agonist that was ineffective when administered alone turned an inhibitory effect of galanin into an excitatory effect, an interaction that required cholinergic neurotransmission. Altogether, our results strongly suggest that D_1-like–Gal_1 receptor heteromers act as processors that integrate signals of two different neurotransmitters, dopamine and galanin, to modulate hippocampal cholinergic neurotransmission.

Introduction

The neuropeptide galanin is widely distributed in the CNS (Melander et al., 1986a,b; Hökfelt et al., 1998; Ögren et al., 1998), where it is coreleased with noradrenaline, serotonin, histamine, and acetylcholine (ACh) (Hökfelt et al., 1998). Particular attention has been given to the presence of galanin in a population of cholinergic neurons in the septal nucleus and diagonal band of Broca, which project to the hippocampal formation (Melander et al., 1985), because of its possible relevance for learning, memory, and Alzheimer's disease (Ögren et al., 1998; Mitsukawa et al., 2008). Gal_1 and Gal_2 receptors are the predominant galanin receptor subtypes in the brain and, together with the less populated subtype Gal_3, they belong to the G-protein-coupled receptor (GPCR) family (Branchek et al., 2000). The lack of selective ligands and reliable antibodies (Hawes and Picciotto, 2005) has made it difficult to identify the distribution of Gal_1 and Gal_2 receptors in the septohippocampal system. Gal_1 mRNA is highly expressed in the septal area, where Gal_2 mRNA expression is moderate and confined to a few scattered neurons (Parker et al., 1995; O'Donnell et al., 1999). ^{125}I-galanin binding sites in the ventral hippocampus are significantly reduced after lesions of the septohippocampal projection, which eliminates most cholinergic input to the ventral hippocampus (Fisone et al., 1987). This provided clear evidence for the existence of a significant population of presynaptic hippocampal galanin receptors localized in cho-

Received Jan. 12, 2011; revised March 31, 2011; accepted April 5, 2011.

Author contributions: N.K., E.I.C., P.J.M., C.L., R.F., J.A.R., A.M.S., and S.F. designed research; E.M., S.H.V., N.-S.C., C.F., and S.B. performed research; E.M., S.H.V., N.-S.C., C.Q., S.B., C.L., A.M.S., and S.F. analyzed data; P.J.M., C.L., J.A.R., A.M.S., and S.F. wrote the paper.

This work was supported by the Spanish Ministerio de Ciencia y Tecnología (Grants SAF2008-03229-E, SAF2009-07276 and SAF2010-18472), the intramural funds of the National Institute on Drug Abuse, EU (Cost B-30 concerted action), and Fundação para a Ciência e Tecnologia (FCT, Portugal). S.H.V. is in receipt of a FCT PhD fellowship (SFRHBD/27989/2006). P.J.M. is a Ramon y Cajal Investigator. We acknowledge the technical help obtained from Jasmina Jiménez (Molecular Neurobiology laboratory, Barcelona University, Barcelona).

*E.M. and S.H.V. contributed equally to this work.

**A.M.S. and S.F. contributed equally to this work.

The authors declare no competing financial interests.

Correspondence should be addressed to Sergi Ferré, National Institute on Drug Abuse, Intramural Research Program, Department of Health and Human Services, NIH, 251 Bayview Boulevard, Baltimore MD 21224. E-mail: sferre@intra.nida.nih.gov.

DOI:10.1523/JNEUROSCI.0191-11.2011

 0270-6474/11/317412-12$15.00/0

linergic nerve terminals, although the galanin receptor subtype involved is still a matter of debate (Miller et al., 1997). With postsynaptic galanin receptors, Gal_1 is preferentially expressed in the ventral hippocampus, CA1, and subiculum, whereas Gal_2 is expressed in the dentate gyrus of both ventral and dorsal hippocampus (O'Donnell et al., 1999).

In vivo studies in rodents with central administration of galanin have suggested that galanin inhibits cholinergic neurotransmission in the ventral hippocampus (Fisone et al., 1987; Ögren et al., 1998; Laplante et al., 2004a). Furthermore, central administration of galanin leads to cognitive deficits in a variety of tasks (Crawley, 1996; Ögren et al., 1998). However, recent postmortem studies on brains from Alzheimer's disease patients suggest that galanin may instead stimulate cholinergic neurotransmission, which could attenuate the development of Alzheimer's symptoms (Counts et al., 2008; Ögren et al., 2010).

In addition to galanin, dopamine also plays a key modulatory role in the septohippocampal cholinergic pathway. Initial studies showed that dopamine facilitates hippocampal ACh release by acting on D_1-like receptors that are thought to be located in hippocampal cholinergic terminals (Hersi et al., 1995). Of the two D_1-like receptor subtypes, D_1 and D_5, D_5 is the predominant subtype in the hippocampus (Ciliax et al., 2000) and the one most probably involved in the modulation of hippocampal ACh release (Hersi et al., 2000; Laplante et al., 2004b). In the present study, we demonstrate that dopamine and galanin work in concert to modulate cholinergic neurotransmission in the ventral hippocampus and that this modulation can occur via heteromers between D_1 or D_5 receptors and Gal_1 receptors.

Materials and Methods

Animals. Male Wistar rats (4–7 weeks old) from Harlan Interfauna Iberica were housed in a temperature- (21 ± 1°C) and humidity-controlled (55 ± 10%) room with a 12 h light/dark cycle with food and water *ad libitum*. Animal procedures were conducted according to standard ethical guidelines (European Communities Council Directive 86/609/EEC) and approved by the local (Portuguese or Spanish) ethical committees. Rats were anesthetized with isoflurane before decapitation.

Cell culture. Human embryonic kidney 293T (HEK-293T) cells were grown in DMEM supplemented with 2 mM L-glutamine, 100 $\mu g \cdot ml^{-1}$ sodium pyruvate, 100 units/ml penicillin/streptomycin, and 5% (v/v) heat-inactivated fetal bovine serum (FBS) (all supplements were from Invitrogen). Chinese hamster ovary (CHO) cells were cultured in MEM α medium without nucleosides supplemented with 100 units/ml of penicillin/streptomycin and 10% (v/v) heat-inactivated FBS. HEK-293T and CHO cells were maintained at 37°C in a humidified atmosphere of 5% CO_2 and were passaged when they were 80–90% confluent, i.e., approximately twice a week.

Fusion proteins and expression vectors. The cDNAs for D_1, D_5, Gal_1,Gal_2, cannabinoid CB_1, and serotonin $5HT_{2B}$ receptors cloned into pcDNA3.1 were amplified without their stop codons using sense and antisense primers harboring unique *Eco*RI and *Bam*HI sites to clone D_1, D_5, and $5HT_{2B}$ receptors and *Eco*RV and *Kpn*I sites to clone Gal_2 receptors in the *Renilla luciferase* (Rluc) vector, or *Eco*RI and *Bam*HI to clone D_1, D_5, and CB_1 receptors and *Eco*RI and *Kpn*I to clone the Gal_1 receptor in the enhanced yellow fluorescent protein (EYFP) vector. The amplified fragments were subcloned to be in-frame into restriction sites of pcDNA3.1-Rluc (*Renilla* luciferase; Clontech) or pEYFP-N1 (Clontech) vectors resulting in the plasmids D_1-Rluc, D_1-YFP, D_5-Rluc, D_5-YFP, Gal_1-YFP, and Gal_2-Rluc. Expression of constructs was tested by confocal microscopy, and the receptor functionality by ERK1/2 phosphorylation (see Results). The cDNA encoding the C terminus of the rat D_1 or D_5 receptors (D_1CT and D_5CT, respectively) were amplified from Rat Brain QUICK-Clone cDNA (Clontech) by PCR using the following primers: D1-CT1012F (CAG AAG GCG TTC TCA ACC) and D1-CT1321R (AGT GGA ATG CTG TCC ACT) or D_5-CT1051F (CCC ATC ATC TAT GCC TTT AAT GCA GAC TTC) and D_5-CT1425R (AGC AGT TTT ATC GAA ACA ATT GGG GGT GAG). The cDNA encoding D_1CT or D_5CT were subcloned into the *Bam*HI/*Eco*RI sites of pGEX-4T-1 (GE Healthcare). A GST fusion protein containing the C terminus of the rat D_1 or D_5 receptors (GST-D_1CT and GST-D_5CT, respectively) were generated corresponding to amino acid residues 227–335 of the rat D_1 receptor and amino acid residues 358–475 of the rat D_5 receptor, respectively. Bacterial BL21 (DE3) cells with pGEX-4T-1/Drd5CT plasmid were grown overnight in imMedia medium (Invitrogen) using ampicillin selection. Protein production was induced with 0.5 mM isopropyl-β-D-thiogalactopyranoside (Sigma) at 20°C for 18 h. Bacteria were harvested by centrifugation at 7,500 × *g* for 15 min at 4°C, and the pellet was suspended in cold PBS buffer with 1 mM PMSF and a protease inhibitor mixture (Roche). Cells were lysed by sonication, and the lysate was incubated for 1 h with 1% Triton X-100 and centrifuged at 18,000 × *g* for 10 min at 4°C. The supernatant was collected for purification of GST fusion protein. Purification of fusion proteins was performed using the Glutathione Sepharose 4B bead matrix (GE Healthcare) as described by the manufacturer.

Transient transfection and protein determination. HEK-293T or CHO cells growing in 35-mm-diameter wells of six-well plates were transiently transfected with the corresponding fusion protein cDNA by the ramified polyethylenimine (PEI; Sigma) method. Cells were incubated (4 h) with the corresponding cDNA together with ramified PEI (5 ml/mg cDNA of 10 mM PEI) and 150 mM NaCl in a serum-starved medium. After 4 h, the medium was changed to a fresh complete culture medium. Forty-eight hours after transfection, cells were washed twice in quick succession in HBSS [containing the following (in mM): 137 NaCl, 5 KCl, 0.34 $Na_2HPO_4 \times 12\ H_2O$, 0.44 KH_2PO_4, 1.26 $CaCl_2 \times 2\ H_2O$, 0.4 $MgSO_4 \times 7\ H_2O$, 0.5 $MgCl_2$, 10 HEPES, pH 7.4], supplemented with 0.1% glucose (w/v), detached by gently pipetting, and resuspended in the same buffer. To control the cell number, sample protein concentration was determined using a Bradford assay kit (Bio-Rad) using bovine serum albumin (BSA) dilutions as standards. HEK-293T cell suspension (20 μg of protein) was distributed into 96-well microplates; black plates with a transparent bottom (Porvair) were used for fluorescence determinations, whereas white opaque plates (Sigma) were used for bioluminescence resonance energy transfer (BRET) experiments.

BRET assays. HEK-293T cells were transiently cotransfected with the indicated amounts of plasmid cDNAs corresponding to the indicated fusion proteins (see corresponding figure legends). To quantify fluorescence proteins, cells (20 μg protein) were distributed in 96-well microplates (black plates with a transparent bottom) and fluorescence was read in a Fluo Star Optima fluorimeter (BMG Lab Technologies) equipped with a high-energy xenon flash lamp, using a 10 nm bandwidth excitation filter at 400 nm reading. Receptor-fluorescence expression was determined as fluorescence of the sample minus the fluorescence of cells expressing receptor-Rluc alone. For BRET measurements, the equivalent of 20 μg of cell suspension was distributed in 96-well microplates (Corning 3600, white plates; Sigma) and 5 μM coelenterazine H (Invitrogen) was added. After 1 min of adding coelenterazine H, readings were collected using a Mithras LB 940 (Berthold), which allows the integration of the signals detected in the short-wavelength filter at 485 nm (440–500 nm) and the long-wavelength filter at 530 nm (510–590 nm). To quantify receptor-Rluc expression, luminescence readings were performed after 10 min of adding 5 μM coelenterazine H. Cells expressing BRET donors alone were used to determine background. The net BRET is defined as [(long-wavelength emission)/(short-wavelength emission)] − *Cf*, where *Cf* corresponds to [(long-wavelength emission)/(short-wavelength emission)] for the Rluc construct expressed alone in the same experiment. Curves were fitted using a nonlinear regression equation and assuming a single phase (GraphPad Prism software). BRET is expressed as mili BRET units (mBU: 1000 × net BRET).

Immunocytochemistry. After 48 h of transfection, HEK-292T cells were fixed in 4% paraformaldehyde for 15 min and washed with PBS containing 20 mM glycine (buffer A) to quench the aldehyde groups. Cells were permeabilized with buffer A containing 0.05% Triton X-100 for 5 min and then were treated with PBS containing 1% bovine serum albumin. After 1 h at room temperature, protein-Rluc was labeled with the primary

mouse monoclonal anti-Rluc antibody (1/100; Millipore Bioscience Research Reagents) for 1 h, washed, and stained with the secondary antibody Cy3 Donkey anti-mouse (1/200; Jackson ImmunoResearch). Protein-YFP was detected by its fluorescence properties. The slides were rinsed several times and mounted with a medium suitable for immunofluorescence (30% Mowiol; Calbiochem). The samples were observed in a Leica SP2 confocal microscope (Leica Microsystems).

Pull-down assay. HEK-293T cells were collected after 48 h of transfection with 25 μg Gal_1-YFP, Gal_2-YFP, or pEYFP-N1 plasmid (control) and extracted in cell extraction buffer (10 mM Tris, pH 7.4, 100 mM NaCl, 1 mM EDTA, 1 mM EGTA, 1 mM NaF, 20 mM $Na_4P_2O_7$, 2 mM Na_3VO_4, 1% Triton X-100, 10% glycerol, 0.1% SDS, 0.5% deoxycholate) with 1 mM PMSF and a protease inhibitor mixture (Roche) for 30 min on ice. The cell extracts were centrifuged at 16,000 × *g* for 10 min at 4°C, and the supernatant was used for pull-down experiments. Pull-down experiments were performed by incubating cell extracts (135 relative fluorescence units per 800 μl) with 50 μg GST-D_1CT, GST-D_5CT, or GST for 2 h with constant rotation at 4°C. Then, 30 μl Glutathione Sepharose 4B beads were added, and incubation was prolonged for 1 h. The beads were then washed four times with cold wash buffer (TBS, 0.1% Triton X-100, and protease inhibitor mixture). Subsequently, 50 μl of elution buffer (10 mM reduced glutathione in 50 mM Tris-HCl, pH 8.0) was added to each sample and kept for 10 min at room temperature. Fluorescence in the eluted solution was measured with SpectraMax M5 microplate readers (Molecular Devices) using 514 nm wavelength excitation and 596 nm wavelength emission filters. Differences in relative fluorescence units among the different groups were statistically analyzed with repeated-measures ANOVA with Bonferroni's correction.

ERK phosphorylation assay. Transfected CHO cells were cultured in serum-free medium for 16 h before the addition of any agent. For assays in hippocampal slices, rat brains were rapidly removed and placed in ice-cold oxygenated (95% O_2/5% CO_2) Krebs-HCO_3^- buffer [containing (in mM) 124 NaCl, 4 KCl, 1.25 NaH_2PO_4, 1.5 $MgCl_2$, 1.5 $CaCl_2$, 10 glucose, and 26 $NaHCO_3$, pH 7.4]. The brains were sliced perpendicularly to the long axis of the hippocampus at 4°C. Slices (400 μm thick) were kept at 4°C in Krebs-HCO_3^- buffer during the dissection. Each hippocampal slice was transferred into an incubation tube containing 1 ml of ice-cold Krebs-HCO_3^- buffer [containing (in mM) 124 NaCl, 4 KCl, 1.25 NaH_2PO_4, 1.5 $MgCl_2$, 1.5 $CaCl_2$, 10 glucose, and 26 $NaHCO_3$]. The temperature was raised to 23°C, and after 30 min the medium was replaced by 2 ml of fresh Krebs-HCO_3^- buffer (23°C) with similar composition. The slices were incubated under constant oxygenation (95% O_2/5% CO_2) at 30°C for 4–5 h in an Eppendorf-5 Prime Thermomixer. The medium was replaced by 200 μl of fresh Krebs-HCO_3^- buffer and incubated for 30 min before the addition of any agent. Cells or slices were treated or not with the indicated ligand for the indicated time and were rinsed with ice-cold PBS and lysed by the addition of 500 μl of ice-cold lysis buffer (50 mM Tris-HCl, pH 7.4, 50 mM NaF, 150 mM NaCl, 45 mM β-glycerophosphate, 1% Triton X-100, 20 μM phenyl-arsine oxide, 0.4 mM $NaVO_4$, and protease inhibitor mixture). The cellular debris was removed by centrifugation at 13,000 × *g* for 5 min at 4°C, and the protein was quantified by the bicinchoninic acid method using bovine serum albumin dilutions as standard. To determine the level of ERK1/2 phosphorylation, equivalent amounts of protein (10 μg) were separated by electrophoresis on a denaturing 7.5% SDS-polyacrylamide gel and transferred onto PVDF-fluorescence membranes. Odyssey blocking buffer (LI-COR Biosciences) was then added, and the membrane was rocked for 90 min. The membranes were then probed with a mixture of a mouse anti-phospho-ERK1/2 antibody (1:2500; Sigma) and rabbit anti-ERK1/2 antibody that recognizes both phosphorylated and nonphosphorylated ERK1/2 (1:40,000; Sigma) for 2–3 h. Bands were visualized by the addition of a mixture of IRDye 800 (anti-mouse) antibody (1:10,000; Sigma) and IRDye 680 (anti-rabbit) antibody (1:10,000; Sigma) for 1 h and scanned by the Odyssey infrared scanner (LI-COR Biosciences). Bands densities were quantified using the scanner software exported to Excel (Microsoft). The level of phosphorylated ERK1/2 isoforms was normalized for differences in loading using the total ERK protein band intensities. Statistical differences between the different groups were analyzed by one-way ANOVA with Bonferroni's correction.

[^{3}H]Ach release from hippocampal synaptosomes. The synaptosomal fraction was prepared according to routine (Vaz et al., 2008). Briefly, after decapitation under halothane anesthesia, each brain was rapidly removed into ice-cold continuously oxygenated (95% O_2/5% CO_2) artificial CSF (aCSF) containing the following (in mM): 124 NaCl, 3 KCl, 1.2 NaH_2PO_4, 25 $NaHCO_3$, 2 $CaCl_2$, 1 $MgSO_4$, and 10 glucose, pH 7.40. The whole hippocampus was dissected out free of the subiculum or enthorinal cortex areas and the ventral part, i.e., the portion lying in the temporal part of the brain, was isolated from the dorsal one (the portion lying just behind the septum) by a cut made perpendicularly to the long hippocampal axis. The ventral hippocampi were homogenized in an ice-cold isosmotic sucrose solution (0.32 M, containing 1 mM EDTA, 1 mg/ml bovine serum albumin, and 10 mM HEPES, pH 7.4) and centrifuged at 3,000 × *g* for 10 min; the supernatant was centrifuged again at 14,000 × *g* for 12 min. The whole procedure was conducted at 4°C. The pellet was resuspended in 45% Percoll in Krebs–Henseleit–Ringer solution containing (in mM) 140 NaCl, 1 EDTA, 10 HEPES, 5 KCl, and 5 glucose, and was centrifuged 14,000 × *g* for 2 min. The synaptosomal fraction corresponds to the top buoyant layer and was collected from the tube. Percoll was removed by two washes with a KHR solution; synaptosomes were then kept on ice and used within 3 h. The synaptosomes were loaded for 20 min at 37°C, with [methyl-^{3}H] choline chloride (10 μCi/ml, 122 nM). Hemicholinium-3 (10 μM) was present in all solutions up the end of the experiments to prevent choline uptake. Synaptosomes were then layered over Whatman GF/C filters and superfused (flow rate, 0.8 ml/min; chamber volume, 90 μl) with gassed aCSF. After a 30 min washout period, the effluent was collected (release period) in 2 min fractions for 36 min. The synaptosomes were stimulated during 2 min with 20 mM K^+ (isomolar substitution of Na^+ with K^+ in the perfusion buffer) at the 5th and 23rd minutes after starting sample collection (S1 and S2, respectively). The tested drugs were added to the superfusion medium at the 17th minute, therefore before S2, and remained in the bath up to the end of the experiments. When we evaluated the changes of galanin effect by the D_1-like receptor agonist SKF 38393, this was applied at the beginning of the washout period, and therefore it was present during S1 and S2 in both test and control chambers, whereas galanin was added before S2 in the test chambers. A "mirror" experiment was also performed to evaluate changes of the effect of SFK 38393 effect by galanin; in this case the neuropeptide was applied at the beginning of the washout period, being therefore present during S1 and S2 in both test and control chambers, whereas SKF 38393 was added before S2 in the test chambers. At the end of each experiment, aliquots (500 μl) of each sample as well as the filters from each superfusion chamber were analyzed by liquid scintillation counting. The fractional release was expressed in terms of the percentage of total radioactivity present in the preparation at the beginning of the collection of each sample. The amount of radioactivity released by each pulse of K^+ (S1 and S2) was calculated by integration of the area of the peak after subtraction of the estimated basal tritium release. In each experiment, two synaptosome-loaded chambers were used as control chambers, the others being used as test chambers. In the test chambers, the test drug was added to the perfusion solution before S2, and the S2/S1 ratios in control and test conditions were calculated. The effect of the drug on the K^+-evoked tritium release was expressed as percentage of change of the S2/S1 ratios in test conditions compared to the S2/S1 ratios in control conditions in the same experiments (i.e., with the same pool of synaptosomes). When present during S1 and S2, neither galanin nor SKF 38393 significantly ($p > 0.05$, Student's *t* test) altered the S2/S1 ratio as compared with the S2/S1 ratio obtained in the absence of these drugs. The values presented are the mean ± SEM of *n* experiments. For comparisons, statistical significance was assessed with Student's *t* test using GraphPad Software (Prism, version 4.02 for Windows).

Field EPSP recordings from hippocampal slices. After decapitation under halothane anesthesia, the hippocampus was dissected out of the brain on ice-cold continuously oxygenated (95% O_2/5% CO_2) aCSF as described above. Ventral and dorsal hippocampal slices (400 μm thick, cut perpendicularly to the long axis of the hippocampus) were allowed to recover functionally and energetically for at least 1 h in a resting chamber filled with continuously oxygenated (95% O_2/5% CO_2) aCSF at room temperature (22–25°C). After recovering, slices were transferred to a recording

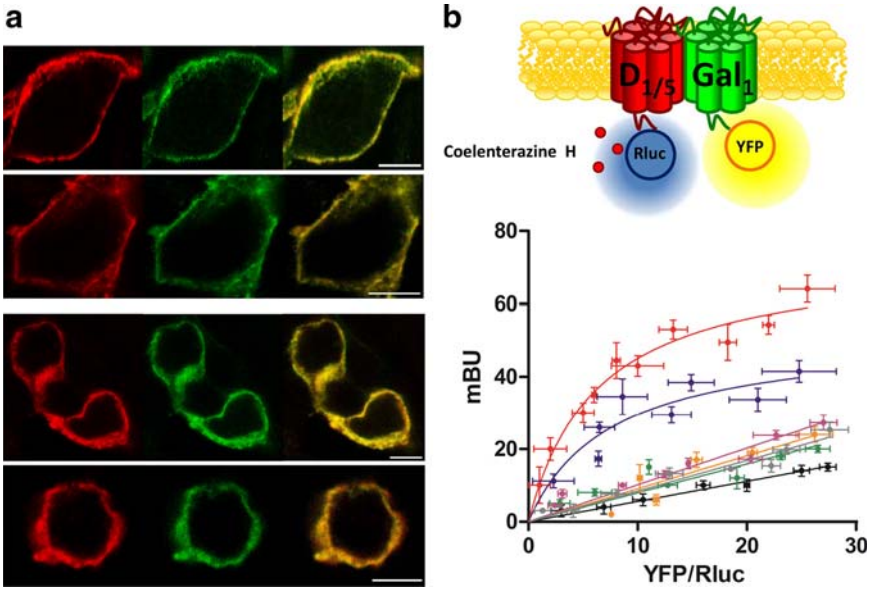

Figure 1. D_1–Gal_1 and D_5–Gal_1 receptor heteromers in living cells. ***a***, Confocal microscopy images of cells expressing (top to bottom) D_5-Rluc (0.6 μg plasmid) and Gal_1-YFP (1 μg plasmid), Gal_2-Rluc (0.5 μg plasmid) and D_5-YFP receptors (1 μg plasmid), D_1-Rluc (0.5 μg plasmid) and Gal_1-YFP (1 μg plasmid), and Gal_2-Rluc (0.5 μg plasmid) and D_1-YFP (1.3 μg plasmid) receptors. Proteins were identified by fluorescence or by immunocytochemistry. D_5-Rluc, D_1-Rluc, or Gal_2-Rluc receptor immunoreactivity is shown in red; Gal_1-YFP, D_5-YFP, or D_1-YFP receptor fluorescence in shown in green; and colocalization is shown in yellow. Scale bars, 5 μm. ***b***, BRET experiments were performed with cells coexpressing D_5-Rluc (400 ng plasmid; red) or D_1-Rluc (300 ng plasmid; blue) and Gal_1-YFP receptors (0.4 to 7 μg plasmid), Gal_2-Rluc (300 ng plasmid) and D_5-YFP receptors (0.5 to 5 μg plasmid; green) or D_1-YFP receptors (0.5 to 4 μg plasmid; purple), or, as negative controls, D_5-Rluc (600 ng plasmid; gray) or D_1-Rluc (500 ng plasmid; orange) and CB_1-YFP receptors (0.5 to 7 μg plasmid) or $5HT_{2B}$-Rluc (1 μg plasmid) and Gal_1-YFP receptors (0.5 to 5 μg plasmid) (black). Both fluorescence and luminescence of each sample were measured before every experiment to confirm similar donor expressions (about 150,000 luminescent units) while monitoring the increase acceptor expression (10,000–70,000 fluorescent units). The relative amount of BRET is given as the ratio between the fluorescence of the acceptor minus the fluorescence detected in cells expressing only the donor and the luciferase activity of the donor. BRET data are expressed as the mean ± SD of 4–16 different experiments grouped as a function of the amount of BRET acceptor. At the top, a scheme corresponding to a BRET assay is shown.

chamber (1 ml plus 5 ml dead volume) for submerged slices, and were continuously superfused (3 ml/min) at 32°C with oxygenated aCSF; the drugs were added to this superfusion solution. To minimize peptide lost resulting from binding to the perfusion system, all of the system was superfused with 0.1 mg/ml BSA before starting any experiment. Field EPSPs (fEPSPs) were recorded according to routine (Diógenes at al., 2004) through an extracellular microelectrode (4 M NaCl, 2–6 MΩ resistance) placed in the stratum radiatum of the CA1 area. Stimulation (rectangular 0.1 ms pulses, once every 15 s) was delivered through a concentric electrode placed on the Schaffer collateral–commissural fibbers in the stratum radiatum near the CA3–CA1 border. The intensity of stimulus (80–200 μA) was initially adjusted to obtain a large fEPSP slope with a minimum population spike contamination. Recordings were obtained with an Axoclamp 2B amplifier and digitized (Molecular Devices). Individual responses were monitored, and averages of eight consecutive responses were continuously stored on a personal computer with the LTP program (Anderson and Collingridge, 2001). Data are expressed as the mean ± SEM from *n* number of slices. To allow comparisons between different experiments, slope values were normalized, taking as 100% of the averaged of the five values obtained immediately before applying the test compound. The significance of differences between the mean values obtained in test and control conditions was evaluated by Student's *t* test. For multiple comparisons, the one-way ANOVA followed by the Bonferroni correction was used.

Drugs. Galanin was from Bachem. (*R*)-(+)-7-chloro-8-hydroxy-3-methyl-1-phenyl-2,3,4,5-te trahydro-1*H*-3-benzazepine hydrochloride (SCH 23390), (±)-6-chloro-2,3,4,5-tetrahydro-1-phenyl-1*H*-3-benzazepine hydrobromide (SKF 81297), (±)-1-phenyl-2,3,4,5-tetrahydro-(1*H*)-3-benzazepine-7,8-diol hydrobromide (SKF 38393), and galanin (1–13)-Pro-Pro-(Ala-Leu-)$_2$Ala amide (M40) were from Tocris Cookson. BSA and atropine were from Sigma. Galanin was supplied as a powder that was resuspended in TBS buffer (50 mM Tris-base, 150 mM NaCl, pH 7.60) in a 0.5 mM concentration stock solution. SCH 23390 (10 mM), SKF 38393 (10 mM), and atropine (50 mM) stock solutions were prepared in water. Aliquots of these stock solutions were kept frozen at −20°C until use.

Results

D_1 and D_5 receptors form heteromers with Gal_1 receptors but not with Gal_2 receptors

We first looked for a molecular interaction between dopamine D_1-like and Gal_1 receptors using an *in vitro* energy transfer assay. First, receptors were cloned as fusion proteins competent for energy transfer experiments. To ensure the fusion proteins trafficked to the correct location in the cell, we performed immunofluorescence experiments in transfected HEK cells. All fusion proteins were found to properly express and localize at the plasma membrane (Fig. 1*a*). Fusion of Rluc or YFP did not modify receptor function, as determined by ERK1/2 phosphorylation assays (data not shown). Next, we examined whether D_1 or D_5 and Gal_1 receptors form heteromers using the BRET technique. The BRET technique allows real-time detection of two proteins in close proximity in living cells. BRET measurements were performed in transiently cotransfected HEK cells using a constant amount of cDNA, corresponding to D_1-Rluc or D_5-Rluc receptors, and increasing amounts of cDNA, corresponding to Gal_1-YFP receptors. A positive and saturable BRET signal was obtained in cells coexpressing D_1-Rluc and Gal_1-YFP receptors, with a $BRET_{max}$ value of 47 ± 4 mBU and a $BRET_{50}$ value of 7 ± 2, or in cells coexpressing D_5-Rluc and Gal_1-YFP receptors, with a $BRET_{max}$ value of 71 ± 3 mBU and a $BRET_{50}$ value of 6 ± 1 (Fig. 1*b*), indicating that both D_1 and D_5 receptors formed heteromers with Gal_1 receptors. As negative controls we first used cells cotransfected with a constant amount of cDNA corresponding to $5HT_{2B}$-Rluc and increasing amounts of cDNA corresponding to Gal_1-YFP receptors. Second, we also used cells cotransfected with a constant amount of cDNA corresponding to D_1-Rluc or D_5-Rluc and increasing amounts of cDNA corresponding to CB_1-YFP receptors. Only a small and linear BRET was detected (Fig. 1*b*), indicating that the saturable BRET between D_1 or D_5 and Gal_1 represented a true complex.

Since D_1-like and Gal_1 receptors can form heteromers, we sought to determine whether D_1-likeand Gal_2 receptors could also form heteromers. Using confocal microscopy, we confirmed expression, proper trafficking of receptors, and colocalization between D_1-YFP and Gal_2-Rluc receptors and between D_5-YFP and Gal_2-Rluc receptors (Fig. 1*a*). When we performed BRET experiments, however, we obtained a linear nonspecific BRET signal in cells expressing a constant amount of Gal_2-Rluc and increasing amounts of D_1-YFP or D_5-YFP receptors (Fig. 1*c*), suggesting that the two pairs of receptors are not able to form heteromers. Therefore, the results indicate that D_1-like receptors

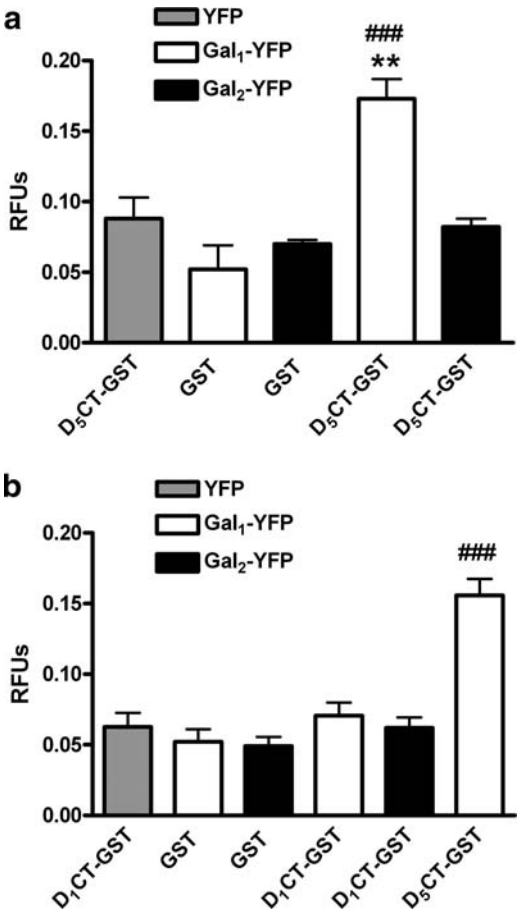

Figure 2. Role of the C-terminal domains of D_1 and D_5 receptors in heteromerization with Gal_1 receptor. ***a***, ***b***, Extracts from cells transfected with either Gal_1-YFP or Gal_2-YFP receptors or just with YFP (see Materials and Methods) were incubated with GST-D_5CT or with just GST (***a***) or GST-D_1CT, GST-D_5CT, or with just GST (***b***). The results of pull-down experiments (see Materials and Methods) were analyzed by measuring fluorescence. Results are expressed as the mean ± SEM (3 independent experiments with 3 replicates) of relative fluorescence units (RFUs); $^{**}p < 0.01$ (significantly different compared to the pull down of YFP with GST-D_5CT); $^{###}p < 0.001$ (significantly different compared to the pull down of Gal1-YFP with GST; repeated-measures ANOVA with Bonferroni's correction).

show a preference for forming receptor heteromers with Gal_1 receptors.

D_1 and D_5 receptors compete for the same molecular determinants of Gal_1 receptors

Previous studies have shown that the C termini of D_1 and D_5 receptors are selectively involved in the formation of heteromers with the ligand-gated ion channels of NMDA and $GABA_A$ receptors (Liu et al., 2000; Lee et al., 2002). We, therefore, reasoned that these same regions might interact with Gal_1 receptors. We constructed plasmids expressing the C-terminal part of the D_1 and D_5 receptors fused to GST protein (GST-D_1CT and GST-D_5CT, respectively). We produced this protein in *Escherichia coli* and then added it to lysates from HEK-293T cells transfected with either Gal_1-YFP or Gal_2-YFP receptors. Using Sepharose beads coated with glutathione, we precipitated GST-D_5CT. With analysis of fluorescence, we found that the GST-D_5CT fusion protein, but not GST alone, pulled down Gal_1-YFP receptors, but not Gal_2-YFP receptors, as demonstrated by a significant increase in fluorescence in the samples from cells expressing Gal_1-YFP, compared with samples from cells expressing YFP alone (Fig. 2*a*).

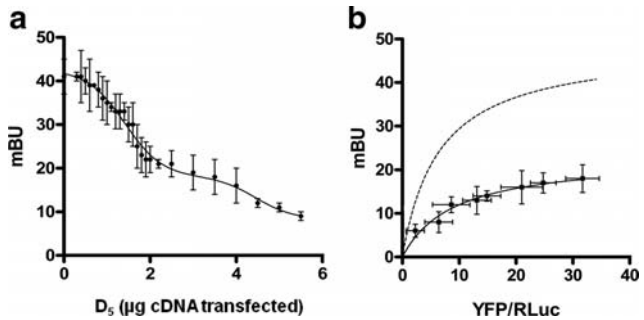

Figure 3. D_1 and D_5 receptors compete for binding to Gal_1 receptors. ***a***, ***b***, BRET experiments were performed with cells coexpressing D_1-Rluc (300 ng plasmid) and Gal_1-YFP receptors (4 μg plasmid) and increasing amounts of D_5 receptors (0 to 5.5 μg plasmid) (***a***) or D_1-Rluc (300 ng plasmid), Gal_1-YFP (0.3 to 5 μg plasmid), and D_5 receptors (1.5 μg plasmid) (***b***). In ***a***, no significant variation in luminescence caused by D_1-Rluc receptors (about 150,000 luminescent units) or fluorescence caused by Gal_1-YFP receptors (about 10,000–70,000 fluorescent units) was observed by increasing D_5 receptor expression. In ***b***, similar luminescence attributable to D_1-Rluc or fluorescence attributable to Gal_1-YFP receptors was obtained in the absence or presence of D_5 receptors. The relative amount of BRET is given as the ratio between the fluorescence of the acceptor minus the fluorescence detected in cells expressing only the donor and the luciferase activity of the donor. BRET data are expressed as the mean ± SD of 4–16 different experiments grouped as a function of the amount of BRET acceptor. The dashed curve represents BRET saturation curve obtained with the D_1-Rluc receptor and increasing amounts of cDNA for the Gal_1-YFP receptor in the absence of D_5 receptors shown in Figure 1.

When we tried the same experiments with GST-D_1CT, we were unable to pull down Gal_1-YFP or Gal_2-YFP (Fig. 2*b*). In view of the very similar results obtained in BRET experiments with the selective heteromerization of both D_1 and D_5 receptors with Gal_1 but not Gal_2 receptors, these results suggest that additional regions outside of the C terminus play a role in forming heteromers and that there are differences between D_1 and D_5 receptors in the regions involved in heteromerization with Gal_1 receptors. BRET competition experiments were then performed to determine whether Gal_1 receptors use the same molecular determinants to heteromerize with D1 and D5 receptors. BRET was measured in cells coexpressing D_1-Rluc and Gal_1-YFP receptors (to give approximately $BRET_{max}$ values) with increasing amounts of D_5 receptors. The BRET signal decreased to very low values in the presence of increasing amounts of D_5 receptors, with a complex dose–response competition curve (Fig. 3*a*). Because the D_1–Gal_1 heteromer is disrupted by adding D_5 receptor, D_1 and D_5 receptors must share a similar interaction surface on the Gal_1 protein. To further support this hypothesis, a BRET saturation curve was performed in cells transfected with a constant amount of cDNA for the D_1-Rluc receptor, with increasing amounts of cDNA for the Gal_1-YFP receptor and with a constant amount of cDNA for D_5 receptors. Under these conditions, there was a very significant decrease in $BRET_{max}$ values (23 ± 1 vs. 47 ± 4 mBU; $p < 0.001$), but not $BRET_{50}$ values (9 ± 2 vs. 7 ± 2), compared to the BRET saturation curve in the absence of D_5 receptors (Fig. 3*b*), strongly suggesting that D_1 and D_5 receptors compete for the same region of Gal_1 receptors.

Functional characteristics of D_1–Gal_1 and D_5–Gal_1 receptor heteromers

To investigate whether D_1-like receptors can modify Gal_1 receptor function, and vice versa, we measured changes in ERK1/2 phosphorylation in the presence or absence of D_1-like and Gal_1 receptor agonists and/or antagonists. First, the D_1-like receptor agonist SKF 81297 (50 nM) time-dependently induced ERK1/2 phosphorylation in cells expressing D_1 or D_5 receptors, whereas

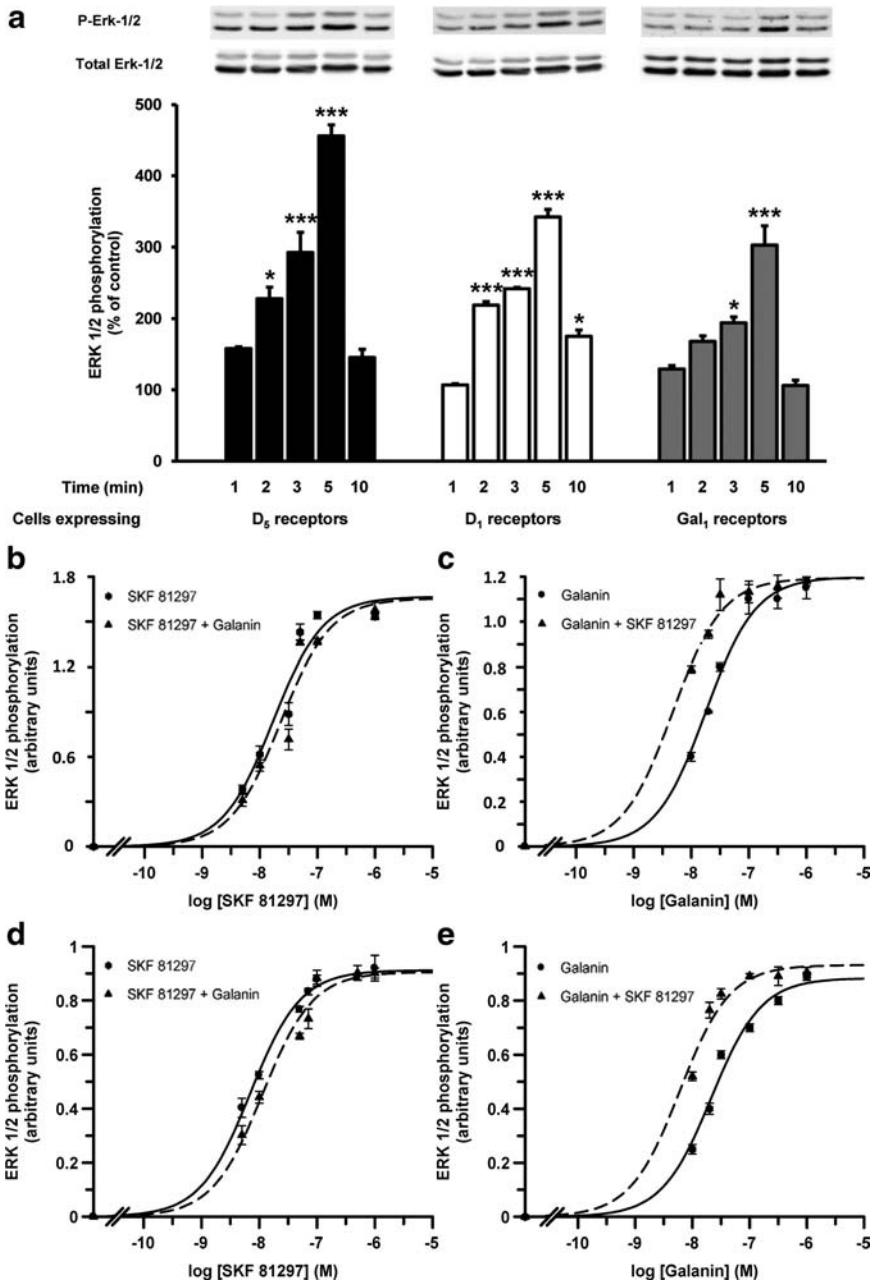

Figure 4. Cross talk between D_1-like receptors and Gal_1 receptors on ERK1/2 phosphorylation in transfected cells. ***a***, Cells transfected with the cDNA corresponding to D_5 (1.5 μg, black), D_1 (1.2 μg, white), or Gal_1 (2 μg, gray) receptors were stimulated for the indicated times with 50 nM (black) or 70 nM (white) of the D_1-like receptor agonist SKF 81297 or with 100 nM galanin (gray). ERK1/2 phosphorylation was determined as indicated in Materials and Methods. The immunoreactive bands from three to five experiments were quantified and the values represent the mean ± SEM of the percentage of phosphorylation relative to the basal levels found in untreated cells; $^*p < 0.05$; $^{***}p < 0.001$ (significantly different compared to the results obtained after 1 min of agonist exposure; one-way ANOVA with Bonferroni's correction). ***b–e***, Cells cotransfected with the cDNA corresponding to D_5 (1.3 μg) and Gal_1 (1.8 μg) receptors (***b***, ***c***) or D_1 (1 μg) and Gal_1 (1.8 μg) receptors (***d***, ***e***) were treated for 5 min with the indicated concentrations of the D_1-like receptor agonist SKF 81297 in the absence (circles) or in the presence (triangles) of 100 nM galanin (***b***, ***d***) or with the indicated concentrations of galanin in absence (circles) or presence (triangles) of 50 nM (***c***) or 70 nM SKF 81297 (***d***). The immunoreactive bands from four independent experiments were quantified and the values represent the mean ± SEM of phosphorylation (arbitrary units) minus the basal levels found in SKF 81297- (***b***, ***d***) or galanin-untreated (***c***, ***e***) cells.

galanin (100 nM) time-dependently induced ERK1/2 phosphorylation in cells expressing Gal_1 receptors (Fig. 4*a*). In cells expressing both D_5 and Gal_1 receptors (Fig. 4*b*,*c*) or D_1 and Gal_1 (Fig. 4*d*,*e*) receptors, SKF 81297-induced dose–response curves were not significantly modified by the presence of galanin (100 nM) (Fig. 4*b*,*d*). EC_{50} values in cells expressing both D_5 and Gal_1 receptors were 17 ± 2 nM and 23 ± 3 nM in the absence and presence of galanin, respectively (nonpaired *t* test, not significant; $n = 5$ in both groups). In cells expressing both D_1 and Gal_1 receptors, EC_{50} values were 7 ± 1 nM and 11 ± 1 nM in the absence and presence of galanin, respectively (nonpaired *t* test, not significant; $n = 5$ in both groups). On the other hand, galanin-induced dose–response curves were significantly shifted to the left in the presence of SKF 81297 (50 nM) (Fig. 4*c*,*e*). EC_{50} values were 17.1 ± 0.7 nM in the absence of SKF 81297 and 4.8 ± 0.6 nM in the presence of SKF 81297 in cells expressing both D_5 and Gal_1 receptors (nonpaired *t* test, $p < 0.001$; $n = 4$ in both groups). EC_{50} values in cells expressing both D_1 and Gal_1 receptors were 21 ± 2 nM in the absence of SKF 81297 and 6 ± 1 nM in the presence of SKF 81297 (nonpaired *t* test, $p < 0.001$; $n = 4$ in both groups). These results demonstrate that D_1-like receptor agonist activation facilitates Gal_1 receptor-mediated MAPK signaling, whereas the reverse is not true, since no significant functional effects were observed in the SKF 81297-induced dose–response curves with galanin. Importantly, in cells expressing both D_1 and Gal_2 receptors or D_5 and Gal_2 receptors, galanin-induced dose–response curves were not significantly modified by the presence of SKF 81297 (Fig. 5), suggesting that the enhancement of Gal_1 receptor-mediated MAPK signaling by D_1-like receptor agonist activation is a biochemical property of D_1–Gal_1 and D_5–Gal_1 receptor heteromers.

Next, we examined the effect of heteromer formation on antagonist-modulation of agonist-induced ERK1/2 phosphorylation. The D_1-like receptor antagonist SCH 23390 (10 μM) was able to block ERK1/2 phosphorylation caused by SKF 81297 in cells expressing D_1 or D_5 receptors, whereas the putative nonselective galanin receptor antagonist M40 (10 μM) blocked galanin-induced ERK1/2 phosphorylation in cells expressing Gal_1 receptors (Fig. 6*a*). It is important to mention that M40, as well as other galanin-like peptides, has been shown to act as full agonists in some cell lines, although they are clearly antagonists *in vivo* (Lang et al., 2007). In our hands, M40 behaved as a galanin receptor antagonist, as evidenced by the complete reversion of galanin-induced signaling. In addition, we established that in cells expressing only D_1 or D_5 receptors, signaling induced by the D_1-like receptor agonist SKF 81297 was not modified by the presence of M40, and in cells expressing only Gal_1, signaling induced by galanin was not altered by addition of SCH 23390 (Fig. 6*a*). In cells coexpressing both D_5 and Gal_1 receptors

(Fig. 6*b*) or both D_1 and Gal_1 receptors (Fig. 6*c*), D_1-like receptor-mediated ERK1/2 phosphorylation could be blocked by SCH 23390 but not by M40. However, galanin-induced ERK1/2 phosphorylation was counteracted by both M40 and SCH 23390 (Fig. 6*b*,*c*). This is a clear example of unidirectional cross-antagonism in a receptor heteromer (Carriba et al., 2007; Ferrada et al., 2009; Navarro et al., 2010). Since, by definition, an antagonist is not able to induce intracellular signaling, the more straightforward way to explain the effect of D_1-like receptor antagonist on Gal_1 receptor activation is through a direct protein-protein interaction between both receptors.

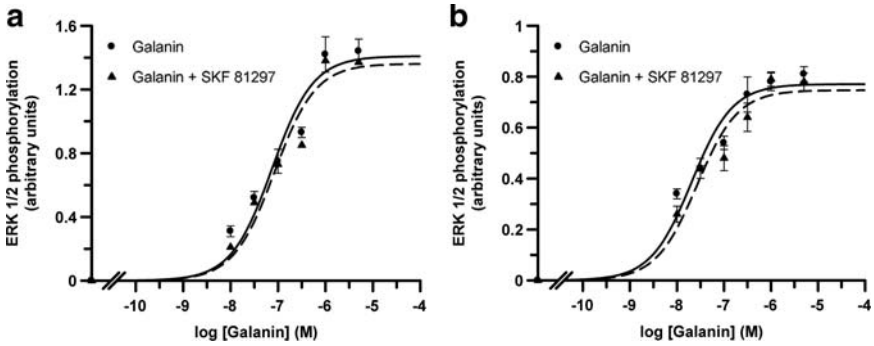

Figure 5. Lack of cross talk between D_1-like receptors and Gal_2 receptors on ERK1/2 phosphorylation in transfected cells. ***a***, ***b***, Cells were cotransfected with the cDNA corresponding to D_5 (1.5 μg) and Gal_2 (2 μg) receptors (***a***) or to D_1 (1 μg) and Gal_2 (2 μg) receptors (***b***). Cells were treated for 5 min with the indicated concentrations of galanin in the absence (circles) or in the presence (triangles) of 50 nM (***a***) or 70 nM (***b***) of SKF 81297. The immunoreactive bands from four independent experiments were quantified and the values represent the mean ± SEM of phosphorylation (arbitrary units) minus the basal levels found in untreated cells.

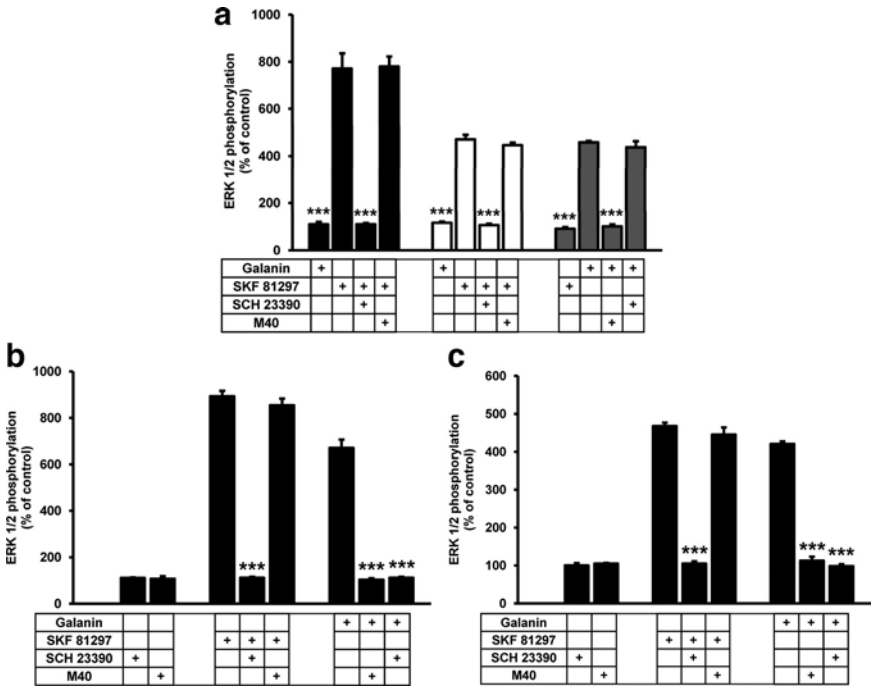

Figure 6. D_1-like receptor antagonist-mediated blockade of galanin-induced ERK1/2 phosphorylation in cells expressing D_1-like and Gal_1 receptors. ***a***, Cells were transfected with the cDNA corresponding to D_5 (1.5 μg, black), D_1 (1.2 μg, white) or Gal_1 receptors (2 μg, gray) and were stimulated with the D_1-like receptor agonist SKF 81297 (70 nM) or with galanin (100 nM) in the presence or absence of the D_1-like receptor antagonist SCH 23390 (10 μM) or the Gal_1 receptor antagonist M40 (10 μM); ***$p < 0.001$ [significantly different compared to the effect of SKF 81297 alone (black and white columns) or to the effect of galanin alone (gray columns); one-way ANOVA with Bonferroni's correction]. ***b***, ***c***, Cells cotransfected with the cDNA corresponding to D_5 (1.3 μg) and Gal_1 receptors (1.8 μg) (***b***) or to D_1 (1 μg) and Gal_1 (1.8 μg) receptors (***c***) were treated with SCH 23390 (10 μM), M40 (10 μM), SKF 81297 (70 nM), or galanin (100 nM) alone or in combination; ***$p < 0.001$ [significantly different compared to the effect of SKF 81297 alone (in cells treated with SKF 81297) or to the effect of galanin alone (in cells treated with galanin); one-way ANOVA with Bonferroni's correction]. In all cases, cells were treated for 5 min with the indicated concentrations of agonists and 20 min before the addition of agonists with the indicated concentrations of antagonists. The inmunoreactive bands from four to five experiments were quantified, and the values represent the mean ± SEM of the percentage of phosphorylation relative to the basal levels found in untreated cells (100%).

D_1-like–Gal_1 receptor heteromers are expressed in the rat ventral hippocampus

In view of the cross-antagonism clearly observed in the transfected cells, we decided to use a similar approach to seek biochemical evidence ("biochemical fingerprint") for the existence of D_1-like–Gal_1 receptor heteromers in the brain (Ferré et al., 2009). Therefore, to test whether D_1–Gal_1 or D_5–Gal_1 receptor heteromers exist in the brain, we isolated rat ventral and dorsal hippocampal slices and compared the ability of the D_1-like receptor antagonist SCH 23390 to block the effect of galanin on ERK1/2 phosphorylation. Slices were incubated with galanin in the absence or in the presence of either SCH 23390 or the galanin receptor antagonist M40. In the ventral hippocampus, the results reproduced the cross-antagonism found in transfected cells (Fig. 7). ERK1/2 phosphorylation induced by galanin (300 nM) was not blocked only by M40 (10 μM), but also by SCH23390 (10 μM). In contrast, in dorsal hippocampus slices, SCH23390 (10 μM) failed to antagonize the effect of galanin (Fig. 7). These results provide strong evidence for the existence of D_1-like–Gal_1 receptor heteromers in the ventral hippocampus.

The role of D_1-like and Gal_1 receptor coactivation on K^+-induced [^{3}H]ACh release in synaptosomes from rat ventral hippocampus

Having established that D_1-like–Gal_1 receptor heteromers occur in the ventral hippocampus, we looked for their functional role by first analyzing the effect of a D_1-like agonist and galanin on K^+-induced [^{3}H]ACh release in isolated synaptosomes from rat ventral hippocampus. The D_1-like receptor agonists SKF 81297 and SKF 38393 have a similar affinity for D_1 and D_5 receptors. The major difference between the two agonists is a significantly higher selectivity for D_1 versus dopamine D_2 receptors and D_1 versus serotonin 5-HT_{2A} receptors of SKF 38393 compared to SKF 81297 (Seeman and Van Tol, 1994; Neumeyer et al., 2003). Since selectivity was a major concern when dealing with hippocampal tissue, we decided to shift to SKF 38393 as the D_1-like receptor agonist in the studies of ACh release in synaptosomes and the electrophysiological studies in slices. Neither galanin, at low nanomolar concentrations (30–100 nM) in the range used by Wang et al. (1999) in rat cortical slices and cortical syn-

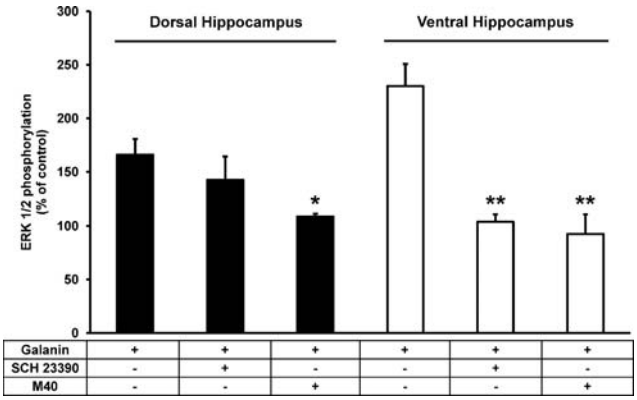

Figure 7. D_1-like receptor antagonist-mediated blockade of galanin-induced ERK1/2 phosphorylation in rat hippocampal slices. Slices from dorsal (black) or ventral (white) hippocampus were treated for 10 min with medium, SCH 23390 (10 μM), or M40 (10 μM) before the addition of galanin (300 nM) and an additional incubation period of 10 min. The inmunoreactive bands from four slices from two different animals were quantified and the values represent the mean ± SEM of the percentage of phosphorylation relative to the basal levels found in untreated slices (100%). *$p < 0.05$; **$p < 0.01$ (significantly different compared to the effect of galanin alone; one-way ANOVA with Bonferroni's correction).

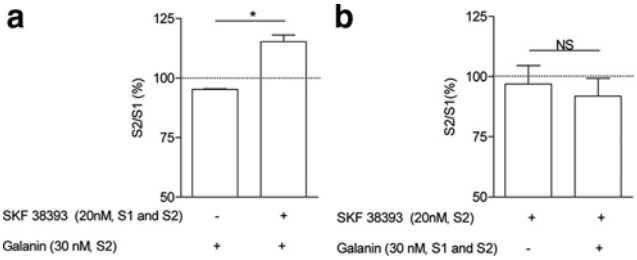

Figure 8. Effect of a D_1-like receptor agonist and galanin on K^+-induced [^{3}H]ACh release from ventral hippocampal synaptosomes. ***a***, Dopamine receptors were activated (right column) by preincubation with the agonist SKF 38393 before addition of galanin. ***b***, Galanin receptors were activated (right column) by preincubation with galanin before addition of SKF 38393. Ordinates represent the S2/S1 ratios as percentage of the control value in the same experiments (see Materials and Methods). Drug conditions during S1 and S2 are indicated below each bar. In the ordinates, 100% represents the S2/S1 ratio in the absence of the test drug, i.e., in the absence of galanin (***a***) or in the absence of SKF 38393 (***b***), using the same synaptosomal batch. An S2/S1 ratio close to 100% represents, therefore, absence of effect of the test drug (galanin in ***a*** or SKF 38393 in ***b***). Values are mean ± SEM (n = 3–6). In ***a***, 100% corresponds to 0.76 ± 0.046, and in ***b*** it corresponds to 0.70 ± 0.029. The presence of SKF 38393 (***a***) or of galanin (***b***) during S1 and S2 did not significantly affect S2/S1 ratios compared with those obtained in the absence of any drug. *$p < 0.05$; NS, $p > 0.05$ (Student's t test).

aptosomal preparations, nor the D_1-like receptor agonist SKF 38393 (20–100 nM) significantly ($p > 0.05$; n = 3–6) affected K^+-induced ACh release, as assessed by modifications of the S2/S1 ratio after addition of the agonists before S2. However, prior addition of SKF 38393 (20 nM; added before S1 and being present during S1 and S2) triggered an excitatory effect ($p < 0.05$; n = 6) of galanin (30 nM; only added before S2) on evoked ACh release (Fig. 8*a*). On the other hand, no significant functional effects where observed with the reverse protocol, since adding galanin (30 nM) before S1 did not influence the absence of effect of SKF 38393 (20 nM, only added before S2) (Fig. 8*b*). These results nicely correlate with the functional results obtained in cells expressing D_1 or D_5 and Gal_1 receptors, showing the selective enhancement of Gal_1 but not Gal_2 receptor-mediated MAPK signaling by a D_1-like receptor agonist. Therefore, the results strongly suggest that D_1–Gal_1 or D_5–Gal_1 receptor heteromers are present in ventral hippocampal cholinergic terminals where they modulate ACh release.

The role of D_1-like and Gal_1 receptor coactivation on rat ventral hippocampus synaptic transmission

To identify whether D_1-like–Gal_1 receptor interactions affect excitatory synaptic transmission in the hippocampus, we evaluated the effect of galanin on EPSPs in hippocampal slices (Fig. 9*a*) in the absence or presence of the dopaminergic receptor agonist SKF 38393. As illustrated in Figure 9, *b* and *e*, when galanin (30 nM) was applied alone to ventral hippocampal slices, there was a statistically significant ($p < 0.05$; n = 9) inhibition (21 ± 2.6%) of the slope of fEPSP. On the other hand, SKF 38393 (20 nM) was virtually devoid of effect (n = 7) on the slope of fEPSP (Fig. 9*c*,*e*). However, in the presence of SKF 38393, the effect of galanin was reversed and it produced a significant increase of 15.4 ± 2.4% ($p < 0.05$; n = 8) in the slope of fEPSPs (Fig. 9*d*,*f*). These results indicate a synergistic effect when both D_1-like and Gal_1 receptors are costimulated by agonists and match those results obtained in synaptosomal preparations when measuring ACh release and those results obtained in transfected cells and in ventral hippocampal slices while measuring EPK phosphorylation. Moreover, blockade of D_1-like receptors with SCH 23390 (1 μM; added 30 min before SKF 38393) completely counteracted the effect of SKF 38393 (Fig. 9*d*,*f*). Indeed, in the presence of SCH 23390 (1 μM) and SKF 38393 (20 nM), galanin (30 nM) decreased ($p < 0.05$; n = 6) the slope of fEPSPs by 21.2 ± 3.4% (Fig. 9*d*), an effect similar to that observed when galanin was applied to the slices alone (Fig. 9*b*,*f*).

Based on our results on the modulation of ACh release from isolated nerve terminals (see Fig. 8) and previous evidence that dopamine and galanin receptors regulate septohippocampal cholinergic neurotransmission, we hypothesized that the cross talk between galanin and dopamine receptors involved in the modulation of hippocampal excitatory transmission resulted from modulation of cholinergic neurotransmission. To test this hypothesis, we used the muscarinic cholinergic receptor antagonist atropine (5 μM), which by itself did not significantly modify fEPSP when applied to ventral hippocampal slices (Fig. 10*b*). The application of SKF 38393 (20 nM) after previous application (at least 30 min before) of atropine also did not significantly affect synaptic transmission (Fig. 10*b*). However, when galanin was added, a significant inhibition ($p < 0.05$; n = 6) of the slope of fEPSP was observed (Fig. 10*a*,*b*). This inhibition (21 ± 5%) was similar to the inhibition obtained when galanin was applied in the absence of any drug (18 ± 0.9%) (Fig. 8*a*,*d*), demonstrating a cholinergic-independent depressant effect of galanin, but a cholinergic-dependent facilitatory action of galanin that requires D_1-like receptor activation. These results suggest that D_1-like–Gal_1 receptor heteromers localized in cholinergic terminals influence excitatory synaptic transmission in the ventral hippocampus. Finally, we performed fEPSP measurements using slices of dorsal hippocampus. Application of galanin (30 nM) to dorsal hippocampal slices had no significant effect on fEPSP slope (Fig. 11*a*). Application of SKF 38393 (20 nM) was also devoid of any effect on fEPSP slope (Fig. 11*b*). Furthermore, previous addition of SKF 38393 (20 nM; 30 min before) did not trigger any effect of galanin on fEPSPs (Fig. 11*c*,*d*). These results agree with the selective existence of D_1-like–Gal_1 receptor interactions in the ventral versus the dorsal hippocampus, as indicated by the ERK1/2 phosphorylation experiments in hippocampal slices.

Discussion

By using a multidisciplinary approach, we provide several important mechanistic and functional insights into the role of galanin and dopamine on regulation of ACh release in the hippocampus. We show, for the first time, that dopamine D_1-like receptors form heteromers with Gal_1 but not Gal_2 receptors in transfected cells and in rat ventral hippocampus. Within the D_1–Gal_1 and D_5–Gal_1 receptor heteromers, dopamine receptor activation and blockade potentiate and counteract, respectively, MAPK activation induced by stimulation of Gal_1 receptors, whereas Gal_1 receptor ligands do not modify D_1-like receptor-mediated MAPK activation. We also demonstrate that dopamine and galanin work in concert to modulate cholinergic neurotransmission in the ventral hippocampus and that this modulation could occur via heteromers between D_1 or D_5 receptors and Gal_1 receptors.

Using an *in vitro* cell culture system, we demonstrated by BRET the ability of both D_1 and D_5 receptors to form heteromers with Gal_1 but not Gal_2 receptors. This is not surprising if we consider that these two galanin receptors have relatively low amino acid similarity (Branchek et al., 2000). Although both D_1 and D_5 receptors were able to compete for their heteromerization with the Gal_1 receptor, only the C terminus of the D_5 receptor pulled down the whole Gal_1 receptor from membrane preparations of transfected cells. On the one hand, these results suggest that additional regions outside of the C terminus play a role in forming heteromers and that there are differences between D_5 and D_1 receptors in the regions involved in heteromerization with Gal_1 receptors. On the other hand, our results strongly suggest that D_1 and D_5 receptors compete for the same region of Gal_1 receptors.

One of the main challenges in the study of membrane protein complexes is their identification in native tissues. Solubility issues and unreliable antibodies make coimmunoprecipitation experiments difficult to interpret, and current spectroscopic approaches, with few exceptions, lack the resolution for an *in situ* approach at the single-molecule level. These limitations thus require indirect approaches to validate the presence of such membrane complexes, such as the determination of a biochemical property of the receptor heteromer, which can be used as a "biochemical fingerprint" (Ferré et al., 2009). The cross-antagonism in which a D_1-like receptor antagonist is able to block the effect of a Gal_1 receptor agonist is very difficult to explain by a mechanism not involving receptor heteromerization, taking into account that an antagonist does not induce intracellular signaling. This cross-antagonism was therefore used as a "biochemical fingerprint" of the D_1-like–Gal_1 receptor heteromer. Using these criteria and measuring MAPK activation as an endpoint, we were able to identify D_1-like–Gal_1 receptor heteromers in the ventral, but not the dorsal, hippocampus.

Although the existence of Gal_1 receptors on septohippocampal cholinergic neurons has been questioned previously (Miller et al., 1997), our observations of the same qualitative cross talk in signaling in synaptosomal preparations as in cells expressing D_1-like and Gal_1 receptors strongly suggests that functional Gal_1 receptors are present in cholinergic terminals of the ventral hippocampus. As mentioned above, in transfected cells, D_1-like receptor stimulation potentiates

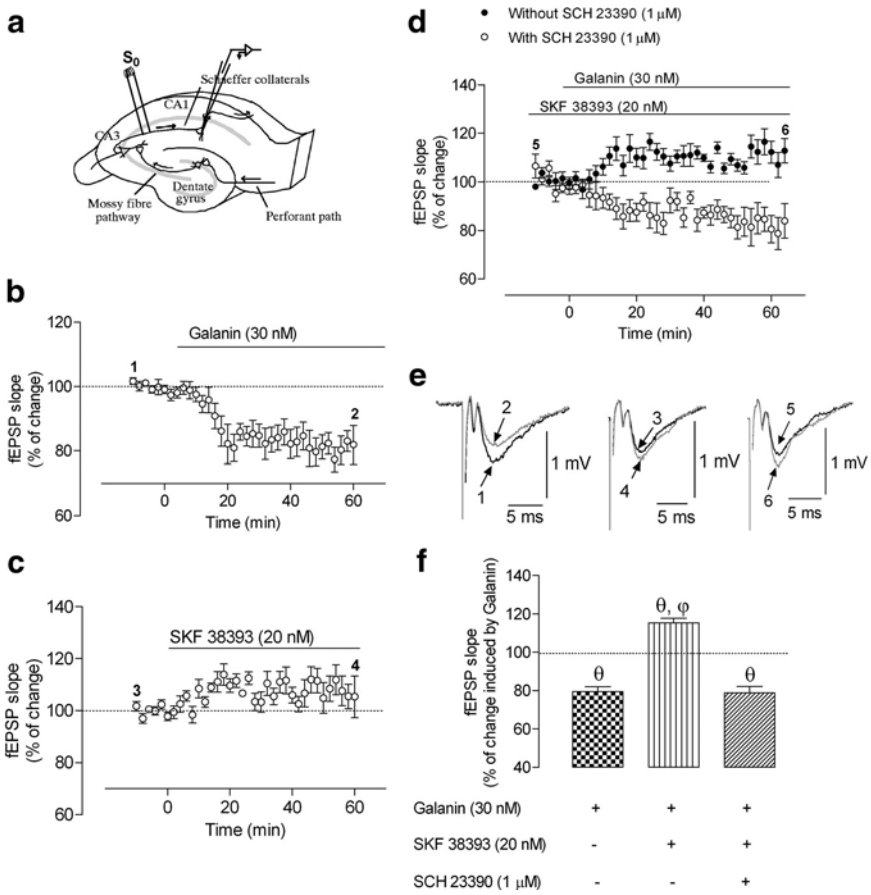

Figure 9. Effect of coactivation of D_1-like and galanin receptors on galanin-mediated modulation of synaptic transmission in the ventral hippocampus. ***a***, Schematic representation of a transverse hippocampal slice with the electrode configuration used to record fEPSPs in the CA1 apical dendritic layer (stratum radiatum) evoked by electric stimulation (S_0) of the Schaffer fibers. ***b***, Averaged time courses of changes in fEPSP slope induced by application of 30 nM galanin alone. ***c***, Averaged time course of changes in fEPSP slope induced by application of 20 nM SKF 38393 alone. ***d***, Averaged time courses of the effect of galanin (30 nM) in the presence of the D_1-like receptor agonist SKF 38393 (20 nM; ●) or in the presence of both SKF 38393 (10 nM) and the D_1-like receptor antagonist SCH23390 (1 μM; ○). SKF 38393 was applied at least 30 min before galanin application, and SCH 23390 was applied 30 min before SKF 38393 application. ***e***, Recordings obtained from representative experiments, where each trace is the average of eight consecutive responses obtained in absence (1) and presence (2) of galanin (30 nM; left), in absence (3) and presence (4) of SKF 38393 (20 nM; middle), and in absence (5) and presence (6) of galanin (30 nM) when the slice was incubated with SKF 38393 (20 nM; right) are shown D_1-like; each trace is composed of the stimulus artifact followed by the presynaptic volley and the fEPSP. Superimposed recordings were obtained from the same slice at the time points indicated in ***b–d***. Note the inhibitory effect of galanin in ***b*** (absence of SKF 38393) and facilitatory effect in ***d*** (presence of SKF 38393). ***f***, Comparison between the averaged effects of galanin on hippocampal synaptic transmission in presence of SKF 38393 and in the presence of both SKF 38393 and SCH 23390. The ordinates show the percent change of fEPSP slope induced by galanin (30 nM) 50–60 min after its application to hippocampal slices not treated or treated with SKF 38393 and treated with both SKF 38393 and SCH 23390, as indicated below each bar. θ, $p < 0.05$ (one-way ANOVA with Bonferroni's correction) as compared with absence of galanin in the same slices; φ, $p < 0.05$ (one-way ANOVA with the Bonferroni's correction) as compared with galanin alone. All values are mean ± SEM [100%, averaged fEPSP slopes at times −10 to 0: ***d***, −0.69 ± 0.073 mV/ms, $n = 8$ (●); −0.66 ± 0.103 mV/ms, $n = 6$ (○); ***b***, −0.69 ± 0.023 mV/ms, $n = 9$; ***c***, −0.64 ± 0.041 mV/ms, $n = 7$].

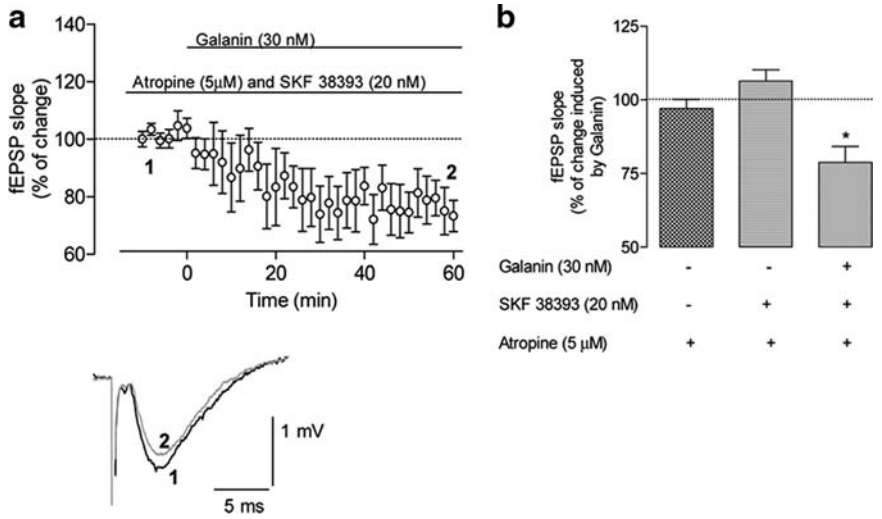

Figure 10. Effect of muscarinic receptor blockade on the dopamine-dependent galanin-mediated modulation of synaptic transmission in the ventral hippocampus. ***a***, Top, Averaged time courses of the effect of galanin (30 nM) in the presence of both the D_1-like receptor agonist SKF 38393 (20 nM) and the muscarinic acetylcholine receptor antagonist atropine (5 μM). SKF 38393 was applied at least 60 min before galanin, and atropine was applied 30 min before SKF 38393. Bottom, Traces obtained with a representative experiment; each trace is the average of eight consecutive responses obtained immediately before (1) and during (2) galanin application, and is composed of the stimulus artifact followed by the presynaptic volley and the fEPSP. ***b***, Comparison between the averaged effects of galanin (30 nM for 50–60 min) in the absence of drugs and in the presence of both SKF 38393 and atropine. The averaged effects of atropine and both atropine and SKF 38393 are also shown; $\theta, p < 0.05$ (Student's *t* test) compared with absence of galanin in the same slices; $\varphi, p < 0.05$ (Student's *t* test) compared with both atropine and SKF 38393 present in the same slices. All values are shown as the mean ± SEM (100%, averaged fEPSP slopes at times −10–0: ***a***, −0.60 ± 0.037 mV/ms; $n = 6$).

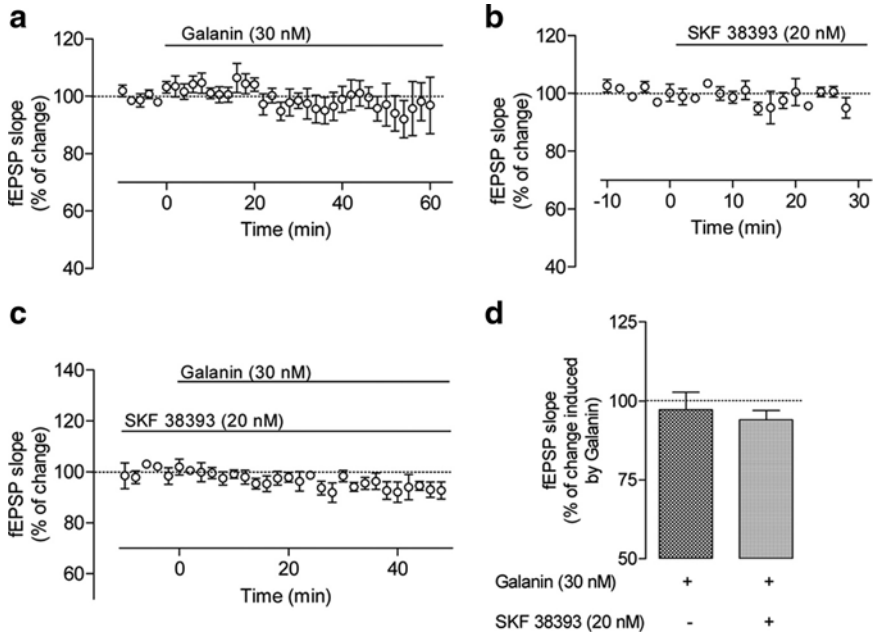

Figure 11. Lack of effect of galanin on synaptic transmission in the dorsal hippocampus. ***a***, ***b***, Averaged time course of changes in fEPSP slope induced by application of 30 nM galanin (***a***) or 20 mM SKF 38393 (***b***). ***c***, Averaged time courses of the effect of galanin (30 nM) in the presence of the D_1-like receptor agonist SKF 38393 (20 nM). SKF 38393 was applied at least 30 min before galanin; ordinates show the percent change of fEPSP slope induced by galanin (30 nM) 50–60 min after its application to hippocampal slices not treated and treated with SKF 38393, as indicated below each bar. All values are shown as the mean ± SEM (100%, averaged fEPSP slopes at times −10–0: ***a***, −0.55 ± 0.070 mV/ms, $n = 5$; ***b***, −0.58 ± 0.048 mV/ms, $n = 3$; ***c***, −0.55 ± 0.064 mV/ms, $n = 3$). ***d***, Comparison between the averaged effects of galanin in the presence and absence of SKF 38393.

the effects of Gal_1 but not Gal_2 receptor activation, but Gal_1 receptor stimulation does not modify D_1-like receptor-mediated signaling. In hippocampal synaptosomal preparations at nanomolar concentrations, neither galanin nor a D_1-like receptor agonist produced any modification of K^+-induced ACh release. Nevertheless, previous activation of D_1-like receptors triggered a facilitatory effect of galanin. Also as in transfected cells, galanin did not modify the lack of effect of a D_1-like receptor agonist. Since D_5 predominates over D_1 receptors in the hippocampus (Ciliax et al., 2000), and D_5 receptors have been shown previously to be involved in the modulation of hippocampal ACh release (Hersi et al., 2000; Laplante et al., 2004b), D_5 is probably the main D_1-like receptor subtype forming heteromers with Gal_1 receptors in cholinergic terminals of the ventral hippocampus.

In previous studies, galanin generally showed an inhibitory effect on hippocampal cholinergic neurotransmission (Fisone et al., 1987; Ögren et al., 1998; Laplante et al., 2004a). However, most of these studies were performed with *in vivo* microdialysis techniques using much higher (micromolar) concentrations of galanin than in the present experiments (Ögren et al., 1998; Laplante et al., 2004a) and with artificially increased extracellular concentrations of ACh because of the addition of acetylcholinesterase inhibitors in the perfusion medium. The use of acetylcholinesterase inhibitors in the dialysis medium has raised concerns about the possibility of not only quantitative but also qualitative artifactual results (DeBoer and Abercrombie, 1996; Acquas and Fibiger, 1998). At the level of the Shaffer–CA1 glutamatergic synapses of the ventral hippocampus, a low (nanomolar) concentration of galanin was inhibitory providing that dopamine receptors were not activated. This result is in accordance with the expression of Gal_1 receptors in the CA1 area of the ventral hippocampus (O'Donnell et al., 1999). In fact, we found galanin to be completely ineffective in the dorsal hippocampus. This cholinergic-independent depressant effect of galanin could be related to its ability to decrease neuronal hippocampal glutamatergic neurotransmission (Zini et al., 1993; Mazarati et al., 2000). Also, galanin has been reported to inhibit LTP in the Shaffer–CA1 glutamatergic synapses (Sakurai et al., 1996). The D_1-like receptor agonist, which was ineffective when administered alone, turned an inhibitory effect of galanin into an excitatory effect, and this interaction depended on cholinergic neurotransmission, since it was completely blocked by a muscarinic ACh receptor antagonist. From our results from ventral hippocampal synaptosomal preparations and slices, a model of the role of galanin in the Shaffer–CA1 synapses of the ventral hippocampus can be proposed: an isolated increase in the activity of the septohippocampal cholinergic input produces a modest release of ACh and galanin. This

modest release of galanin would, nevertheless, be sufficient to inhibit the excitability of glutamatergic synapses by acting on presynaptic or postsynaptic galanin receptors. However, with a concomitant increase in the activity of the ventral tegmental area (VTA)–hippocampal dopaminergic input, coactivation of D_1-like and galanin receptors localized in cholinergic terminals induces a strong release of ACh, which overcomes the inhibitory role of galanin and leads to increased excitability of the glutamatergic synapses.

The interactions reported here occur in the ventral but not in the dorsal hippocampus. These two hippocampal areas have differential efferent connections with the rest of the brain, such that the dorsal hippocampus is primarily connected with the neocortex, whereas the ventral hippocampus is connected to subcortical structures, such as the hypothalamus and the amygdala (Naber and Witter, 1998). Since both the amygdala and the hypothalamus control the activity of the hypothalamus–pituitary–adrenal axis, it is therefore not a surprise that a major function of the ventral hippocampus is the processing of information related to emotion-related behaviors, as increasing evidence now indicates (Segal et al., 2010). Interestingly, injection of acetylcholine into the ventral, but not the dorsal, hippocampus, reduces anxiety (Degroot and Treit, 2004). One can therefore speculate that the cholinergic-dependent facilitatory action of galanin on excitatory Schaffer–CA1 synapses (a last relay of the excitatory output of the hippocampus) may influence the control of anxiety and emotional memory.

Altogether, our results strongly suggest that D_1-like–Gal_1 receptor heteromers that are localized in cholinergic nerve terminals play an important role in the modulation of cholinergic neurotransmission in the ventral hippocampus. Receptor heteromers are becoming the focus of extensive research in the field of GPCRs, and we are just starting to understand the mechanisms involved in heteromerization and its functional meaning (Bulenger et al., 2005; Ferré et al., 2007; Dalrymple et al., 2008; Milligan, 2009; Rozenfeld and Devi, 2010). The present study provides a clear example of a receptor heteromer acting as a processor that integrates signals of different neurotransmitters and modulates cell signaling and neuronal function (Ferré et al., 2007). Since receptor heteromers are increasingly being considered as pharmacological targets (George et al., 2002; Ferré et al., 2010), D_1–Gal_1 and D_5–Gal_1 receptor heteromers could be considered targets for drugs useful in Alzheimer's disease, in view of the involvement of the septohippocampal cholinergic system in this disease (Ögren et al., 1998; Mitsukawa et al., 2008). Importantly, D_1, D_5, and Gal_1 receptors are also colocalized in brain areas other than the hippocampus, such as the mesencephalic dopaminergic nuclei substantia nigra and the VTA (Schilström et al., 2006; Picciotto, 2008). If D_1-like–Gal_1 receptor heteromers are also present in the mesencephalic dopaminergic cells, they could be targets for the treatment of dopamine-related neuropsychiatric disorders, including drug addiction. Finally, the ability of galanin receptors to heteromerize with other GPCRs in other regions of the CNS could explain pharmacological findings that have so far been difficult to explain, such as the well-known biphasic dose-dependent effect of galanin on nociception (Xu et al., 2008).

References

Acquas E, Fibiger HC (1998) Dopaminergic regulation of striatal acetylcholine release: the critical role of acetylcholinesterase inhibition. J Neurochem 70:1088–1093.

Anderson WW, Collingridge GL (2001) The LTP Program: a data acquisition program for on-line analysis of long-term potentiation and other synaptic events. J Neurosci Methods 108:71–83.

Branchek TA, Smith KE, Gerald C, Walker MW (2000) Galanin receptor subtypes. Trends Pharmacol Sci 21:109–117.

Bulenger S, Marullo S, Bouvier M (2005) Emerging role of homo- and heterodimerization in G-protein-coupled receptor biosynthesis and maturation. Trends Pharmacol Sci 26:131–137.

Carriba P, Ortiz O, Patkar K, Justinova Z, Stroik J, Themann A, Müller C, Woods AS, Hope BT, Ciruela F, Casadó V, Canela EI, Lluis C, Goldberg SR, Moratalla R, Franco R, Ferré S (2007) Striatal adenosine A2A and cannabinoid CB1 receptors form functional heteromeric complexes that mediate the motor effects of cannabinoids. Neuropsychopharmacology 32:2249–2259.

Ciliax BJ, Nash N, Heilman C, Sunahara R, Hartney A, Tiberi M, Rye DB, Caron MG, Niznik HB, Levey AI (2000) Dopamine D(5) receptor immunolocalization in rat and monkey brain. Synapse 37:125–145.

Counts SE, Perez SE, Mufson EJ (2008) Galanin in Alzheimer's disease: neuroinhibitory or neuroprotective? Cell Mol Life Sci 65:1842–1853.

Crawley JN (1996) Minireview. Galanin-acetylcholine interactions: relevance to memory and Alzheimer's disease. Life Sci 58:2185–2199.

Dalrymple MB, Pfleger KD, Eidne KA (2008) G protein-coupled receptor dimers: functional consequences, disease states and drug targets. Pharmacol Ther 118:359–371.

DeBoer P, Abercrombie ED (1996) Physiological release of striatal acetylcholine *in vivo*: modulation by D1 and D2 dopamine receptor subtypes. J Pharmacol Exp Ther 277:775–783.

Degroot A, Treit D (2004) Anxiety is functionally segregated within the septo-hippocampal system. Brain Res 1001:60–71.

Diógenes MJ, Fernandes CC, Sebastião AM, Ribeiro JA (2004) Activation of adenosine A2A receptor facilitates brain-derived neurotrophic factor modulation of synaptic transmission in hippocampal slices. J Neurosci 24:2905–2913.

Ferrada C, Moreno E, Casadó V, Bongers G, Cortés A, Mallol J, Canela EI, Leurs R, Ferré S, Lluís C, Franco R (2009) Marked changes in signal transduction upon heteromerization of dopamine D1 and histamine H3 receptors. Br J Pharmacol 157:64–75.

Ferré S, Ciruela F, Woods AS, Lluis C, Franco R (2007) Functional relevance of neurotransmitter receptor heteromers in the central nervous system. Trends Neurosci 30:440–446.

Ferré S, Baler R, Bouvier M, Caron MG, Devi LA, Durroux T, Fuxe K, George SR, Javitch JA, Lohse MJ, Mackie K, Milligan G, Pfleger KD, Pin JP, Volkow ND, Waldhoer M, Woods AS, Franco R (2009) Building a new conceptual framework for receptor heteromers. Nat Chem Biol 5:131–134.

Ferré S, Navarro G, Casadó V, Cortés A, Mallol J, Canela EI, Lluís C, Franco R (2010) G protein-coupled receptor heteromers as new targets for drug development. Prog Mol Biol Transl Sci 91:41–52.

Fisone G, Wu CF, Consolo S, Nordström O, Brynne N, Bartfai T, Melander T, Hökfelt T (1987) Galanin inhibits acetylcholine release in the ventral hippocampus of the rat: histochemical, autoradiographic, in vivo, and in vitro studies. Proc Natl Acad Sci U S A 84:7339–7343.

George SR, O'Dowd BF, Lee SP (2002) G-protein-coupled receptor oligomerization and its potential for drug discovery. Nat Rev Drug Discov 1:808–820.

Hawes JJ, Picciotto MR (2005) Characterization of GalR1, GalR2, and GalR3 immunoreactivity in catecholaminergic nuclei of the mouse brain. J Comp Neurol 2004 479:410–423. Erratum in: J Comp Neurol 2005 490:98–100.

Hersi AI, Richard JW, Gaudreau P, Quirion R (1995) Local modulation of hippocampal acetylcholine release by dopamine D_1 receptors: a combined receptor autoradiography and *in vivo* dialysis study. J Neurosci 15:7150–7157.

Hersi AI, Kitaichi K, Srivastava LK, Gaudreau P, Quirion R (2000) Dopamine D-5 receptor modulates hippocampal acetylcholine release. Mol Brain Res 76:336–340.

Hökfelt T, Xu ZQ, Shi TJ, Holmberg K, Zhang X (1998) Galanin in ascending systems. Focus on coexistence with 5-hydroxytryptamine and noradrenaline. Ann N Y Acad Sci 863:252–263.

Lang R, Gundlach AL, Kofler B (2007) The galanin peptide family: receptor pharmacology, pleiotropic biological actions, and implications in health and disease. Pharmacol Ther 115:177–207.

Laplante F, Crawley JN, Quirion R (2004a) Selective reduction in ventral hippocampal acetylcholine release in awake galanin-treated rats and galanin-overexpressing transgenic mice. Regul Pept 122:91–98.

Laplante F, Sibley DR, Quirion R (2004b) Reduction in acetylcholine release in the hippocampus of dopamine D5 receptor-deficient mice. Neuropsychopharmacology 29:1620–1627.

Lee FJ, Xue S, Pei L, Vukusic B, Chéry N, Wang Y, Wang YT, Niznik HB, Yu XM, Liu F (2002) Dual regulation of NMDA receptor functions by direct protein-protein interactions with the dopamine D1 receptor. Cell 111:219–230.

Liu F, Wan Q, Pristupa ZB, Yu XM, Wang YT, Niznik HB (2000) Direct protein-protein coupling enables cross-talk between dopamine D5 and gamma-aminobutyric acid A receptors. Nature 403:274–280.

Mazarati AM, Hohmann JG, Bacon A, Liu H, Sankar R, Steiner RA, Wynick D, Wasterlain CG (2000) Modulation of hippocampal excitability and seizures by galanin. J Neurosci 20:6276–6281.

Melander T, Staines WA, Hökfelt T, Rökaeus A, Eckenstein F, Salvaterra PM, Wainer BH (1985) Galanin-like immunoreactivity in cholinergic neurons of the septum-basal forebrain complex projecting to the hippocampus of the rat. Brain Res 360:130–138.

Melander T, Hökfelt T, Rökaeus A, Cuello AC, Oertel WH, Verhofstad A, Goldstein M (1986a) Coexistence of galanin-like immunoreactivity with catecholamines, 5-hydroxytryptamine, GABA and neuropeptides in the rat CNS. J Neurosci 6:3640–3654.

Melander T, Staines WA, Rökaeus A (1986b) Galanin-like immunoreactivity in hippocampal afferents in the rat, with special reference to cholinergic and noradrenergic inputs. Neuroscience 19:223–240.

Miller MA, Kolb PE, Raskind MA (1997) GALR1 galanin receptor mRNA is coexpressed by galanin neurons but not cholinergic neurons in the rat basal forebrain. Brain Res Mol Brain Res 52:121–129.

Milligan G (2009) G protein-coupled receptor hetero-dimerization: contribution to pharmacology and function. Br J Pharmacol 158:5–14.

Mitsukawa K, Lu X, Bartfai T (2008) Galanin, galanin receptors and drug targets. Cell Mol Life Sci 65:1796–1805.

Naber PA, Witter MP (1998) Subicular efferents are organized mostly as parallel projections: a double-labeling, retrograde-tracing study in the rat. J Comp Neurol 393:284–297.

Navarro G, Moreno E, Aymerich M, Marcellino D, McCormick PJ, Mallol J, Cortés A, Casadó V, Canela EI, Ortiz J, Fuxe K, Lluís C, Ferré S, Franco R (2010) Direct involvement of σ1 receptors in the dopamine D1 receptor-mediated effects of cocaine. Proc Natl Acad Sci U S A 107:18676–18681.

Neumeyer JL, Kula NS, Bergman J, Baldessarini RJ (2003) Receptor affinities of dopamine D1 receptor-selective novel phenylbenzazepines. Eur J Pharmacol 474:137–140.

O'Donnell D, Ahmad S, Wahlestedt C, Walker P (1999) Expression of the novel galanin receptor subtype GALR2 in the adult rat CNS: distinct distribution from GALR1. J Comp Neurol 409:469–481.

Ögren SO, Schött PA, Kehr J, Yoshitake T, Misane I, Mannström P, Sandin J (1998) Ann N Y Acad Sci 863:342–363.

Ögren SO, Kuteeva E, Elvander-Tottie E, Hökfelt T (2010) Neuropeptides in learning and memory processes with focus on galanin. Eur J Pharmacol 626:9–17.

Parker EM, Izzarelli DG, Nowak HP, Mahle CD, Iben LG, Wang J, Goldstein ME (1995) Cloning and characterization of the rat GALR1 galanin receptor from Rin14B insulinoma cells. Mol Brain Res 34:179–189.

Picciotto MR (2008) Galanin and addiction. Cell Mol Life Sci 65:1872–1879.

Rozenfeld R, Devi LA (2010) Exploring a role for heteromerization in GPCR signalling specificity. Biochem J 433:11–18.

Sakurai E, Maeda T, Kaneko S, Akaike A, Satoh M (1996) Galanin inhibits long-term potentiation at Schaffer collateral-CA1 synapses in guinea-pig hippocampal slices. Neurosci Lett 212:21–24.

Schilström B, Yaka R, Argilli E, Suvarna N, Schumann J, Chen BT, Carman M, Singh V, Mailliard WS, Ron D, Bonci A (2006) Cocaine enhances NMDA receptor-mediated currents in ventral tegmental area cells via dopamine D5 receptor-dependent redistribution of NMDA receptors. J Neurosci 26:8549–8558.

Seeman P, Van Tol HH (1994) Dopamine receptor pharmacology. Trends Pharmacol Sci 15:264–270.

Segal M, Richter-Levin G, Maggio N (2010) Stress-induced dynamic routing of hippocampal connectivity: A hypothesis. Hippocampus 20:1332–1338.

Vaz SH, Cristóvão-Ferreira S, Ribeiro JA, Sebastião AM (2008) Brain-derived neurotrophic factor inhibits GABA uptake by the rat hippocampal nerve terminals. Brain Res 1219:19–25.

Wang HY, Wild KD, Shank RP, Lee DHS (1999) Galanin inhibits acetylcholine release from rat cerebral cortex via pertussis toxin-sensitive Gi protein. Neuropeptides 33:197–205.

Xu XJ, Hökfelt T, Wiesenfeld-Hallin Z (2008) Galanin and spinal pain mechanisms: where do we stand in 2008? Cell Mol Life Sci 65:1813–1819.

Zini S, Roisin MP, Langel U, Bartfai T, Ben-Ari Y (1993) Galanin reduces release of endogenous excitatory amino acids in the rat hippocampus. Eur J Pharmacol 245:1–7.

3.2 La heteromerización entre los receptores D_1 de dopamina y H_3 de histamina produce cambios significativos en la transducción de la señal

Carla Ferrada[1], Estefanía Moreno[1], Vicent Casadó[1], Gerold Bongers[2], Antoni Cortés[1], Josefa Mallol[1], Enric I Canela[1], Rob Leurs[2], Sergi Ferré[3], Carme Lluís[1] and Rafael Franco[1,4]

[1]Unidad de Neurobiología Molecular, IDIBAPS, CIBERNED, Departamento de Bioquímica y Biología Molecular, Facultad de Biología, Universidad de Barcelona, Barcelona, España,
[2]VU Drug Discovery Center, Division of Medicinal Chemistry, Leiden/Amsterdam Center for Drug Research, Faculty of Science, Vrije University, Amsterdam, The Netherlands,
[3]National Institute on DrugAbuse, I.R.P., N.I.H., D.H.H.S., Baltimore, MD, USA, and
[4]Centro de Investigación Médica Aplicada, Navarra University,Pamplona, España.

Manuscrito publicado en British Journal of Pharmacology (2009 May); ***157 (1)****: 64-75.*

Antecedentes y objetivos: Las interacciones funcionales entre receptores acoplados a proteína G como receptores D_1 de dopamina y H_3 de histamina en el cerebro han sido descritas previamente pero se desconoce si son debidas a una interacción molecular entre estos receptores. En este trabajo investigamos la existencia de heterómeros de receptores D_1-H_3 y sus características bioquímicas.
Enfoque experimental: La heteromerización de los receptores D_1-H_3 se estudió en células transfectadas mediante las técnicas de transferencia de energía de resonancia bioluminiscente (BRET) y unión de radioligandos. Además, se estudió de manera comparativa la señalización a través de la vía de las MAP cinasas (MAPK) y de la adenilato ciclasa en células cotransfectadas y en células que expresaban únicamente el receptor D_1 o el receptor H_3.
Resultados: Mediante experimentos de transferencia de energía de resonancia bioluminiscente (BRET) y ensayos de unión de radioligandos se puso de manifiesto que los receptores D_1 y H_3 pueden heteromerizar. Por un lado, la activación de los receptores H_3 de histamina no transducen la señal a través de la vía MAPK a menos que estos receptores se coexpresen con los receptores D_1 de dopamina. Por otro lado, los receptores D_1 de dopamina, que se acoplan a proteína G_s y que inducen incrementos de AMPc, no se acoplan a la proteína G_s, sino que se acoplan a la proteína G_i en células cotransfectadas. Finalmente, la señalización a través de cada uno de los receptores en el heterómero puede ser bloqueada, no solo por su antagonista selectivo, sino que también puede ser bloqueada por el antagonista del otro receptor en el heterómero.
Conclusiones e implicaciones: Estos resultados indican que los heterómeros de los receptores D_1-H_3 constituyen un mecanismo único para dirigir la señalización dopaminérgica e histaminérgica a través de la vía MAPK de forma independiente de la proteína G_s y de forma dependiente de la proteína G_i. La unión de un antagonista de uno de los receptores en el heterómero D_1-H_3 puede inducir cambios conformacionales que se transmiten a la otra unidad del heterómero, bloqueando la señal originada en el heterómero. Este hallazgo pone de manifiesto nuevos potenciales terapéuticos para los antagonistas de receptores acoplados a proteína G.

British Journal of Pharmacology (2009), 157, 64–75

0007-1188/09
www.brjpharmacol.org

RESEARCH PAPER

Marked changes in signal transduction upon heteromerization of dopamine D_1 and histamine H_3 receptors

Carla Ferrada[1], Estefanía Moreno[1], Vicent Casadó[1], Gerold Bongers[2], Antoni Cortés[1], Josefa Mallol[1], Enric I Canela[1], Rob Leurs[2], Sergi Ferré[3], Carme Lluís[1] and Rafael Franco[1,4]

[1]*Molecular Neurobiology Unit, IDIBAPS, CIBERNED, Department of Biochemistry and Molecular Biology, School of Biology, University of Barcelona, Barcelona, Spain,* [2]*VU Drug Discovery Center, Division of Medicinal Chemistry, Leiden/Amsterdam Center for Drug Research, Faculty of Science, Vrije University, Amsterdam, The Netherlands,* [3]*National Institute on Drug Abuse, I.R.P., N.I.H., D.H.H.S., Baltimore, MD, USA, and* [4]*Centro de Investigación Médica Aplicada, Navarra University, Pamplona, Spain*

Background and purpose: Functional interactions between the G protein-coupled dopamine D_1 and histamine H_3 receptors have been described in the brain. In the present study we investigated the existence of D_1–H_3 receptor heteromers and their biochemical characteristics.
Experimental approach: D_1–H_3 receptor heteromerization was studied in mammalian transfected cells with Bioluminescence Resonance Energy Transfer and binding assays. Furthermore, signalling through mitogen-activated protein kinase (MAPK) and adenylyl cyclase pathways was studied in co-transfected cells and compared with cells transfected with either D_1 or H_3 receptors.
Key results: Bioluminescence Resonance Energy Transfer and binding assays confirmed that D_1 and H_3 receptors can heteromerize. Activation of histamine H_3 receptors did not lead to signalling towards the MAPK pathway unless dopamine D_1 receptors were co-expressed. Also, dopamine D_1 receptors, usually coupled to G_s proteins and leading to increases in cAMP, did not couple to G_s but to G_i in co-transfected cells. Furthermore, signalling via each receptor was blocked not only by a selective antagonist but also by an antagonist of the partner receptor.
Conclusions and implications: D_1–H_3 receptor heteromers constitute unique devices that can direct dopaminergic and histaminergic signalling towards the MAPK pathway in a G_s-independent and G_i-dependent manner. An antagonist of one of the receptor units in the D_1–H_3 receptor heteromer can induce conformational changes in the other receptor unit and block specific signals originating in the heteromer. This gives rise to unsuspected therapeutic potentials for G protein-coupled receptor antagonists.
British Journal of Pharmacology (2009) **157**, 64–75; doi:10.1111/j.1476-5381.2009.00152.x

Keywords: dopaminergic transmission; histaminergic transmission; receptor heteromers; signal transduction; dopamine D_1 receptor; histamine H_3 receptor; MAPK pathway; bioluminescent resonance energy transfer

Abbreviations: [^{3}H]RAMH, [^{3}H]R-α-methyl histamine; BRET, Bioluminescence Resonance Energy Transfer; CTX, cholera toxin; EYFP, enhanced yellow variant of green fluorescent protein; GPCR, G protein-coupled receptor; PEI, polyethylenimine; PTX, *Pertussis* toxin; RAMH, R-α-methyl histamine; *RLuc*, *Renilla* luciferase

Introduction

Although with some initial resistance from the scientific community, the existence of neurotransmitter receptor heteromers is becoming accepted. Neurotransmitter receptors cannot only be considered as single functional units, but as forming part of multimolecular aggregates localized in the plane of the plasma membrane, which can contain other interacting proteins, including receptors for the same or other neurotransmitters (Agnati *et al.*, 2003; 2005; Franco *et al.*, 2003; Bockaert *et al.*, 2004). The functional significance of receptor heteromers is however just beginning to be understood. It is becoming clear that heteromerization of neurotransmitter receptors leads to functional entities that possess different biochemical characteristics with respect to

Correspondence: Rafael Franco, Centro de Investigación Médica Aplicada, Navarra University, Avenida Pio XII 55, Pamplona 31008, Spain. E-mail: rfranco@unav.es
Received 25 November 2008; accepted 5 January 2009

the individual components of the heteromer. Thus, the quantitative or qualitative aspects of the signalling generated by stimulation of either receptor unit in the heteromer are different from those obtained during co-activation (Ferré *et al*., 2007; 2009; Franco *et al*., 2007; Rashid *et al*., 2007).

The striatum is the main input structure of the basal ganglia, which are subcortical structures involved in the processing of information related with the performance and learning of complex motor acts. GABAergic striatal efferent neurons constitute more than 95% of the striatal neuronal population (Gerfen, 2004). There are two subtypes of GABAergic striatal efferent neurons: GABAergic dynorphinergic neurons, which express the peptide dynorphin and dopamine D_1 receptors, and GABAergic enkephalinergic neurons, which express the peptide enkephalin and dopamine D_2 receptors (Gerfen, 2004). Histamine is an important neuromodulator of striatal function, and the striatum contains one of the highest densities of histamine H_3 receptors in the brain (Pollard *et al*., 1993; Anichtchik *et al*., 2001; Brown *et al*., 2001). Both D_1 receptors and H_3 receptors are co-expressed in striatal GABAergic dynorphinergic neurons (Ryu *et al*., 1994; Pillot *et al*., 2002), where they have been reported to establish functional interactions (Arias-Montano *et al*., 2001; Sanchez-Lemus and Arias-Montano, 2004). In the present study we show that heteromerization of dopamine D_1 receptors and histamine H_3 receptors, produces dramatic changes in G protein coupling and signalling in human cell lines. Furthermore, both D_1 receptor and H_3 receptor antagonists could block the heteromer-mediated signalling, a fact that highlights new possibilities for G protein-coupled receptor (GPCR) pharmacology.

Methods

Expression vectors

A plasmid encoding the cDNA of the human H_3 receptor was provided by Johnson & Johnson Pharmaceutical Research & Development, L.L.C. (San Diego, CA, USA). The H_3 receptor cDNA without its stop codon was amplified by using sense and antisense primers harbouring a unique EcoRI site. The fragment was then subcloned to be in-frame with enhanced yellow variant of green fluorescent protein (EYFP) into the EcoRI site of pEYFP-N1 (Clontech, Heidelberg, Germany) to provide the plasmid H_3 receptor–YFP, which expresses EYFP on the C-terminal ends of the receptor. The human cDNAs for cannabinoid CB_1 receptors, $5HT_{2B}$ receptors or D_1 receptors cloned in pcDNA3.1 were amplified without their stop codons using sense and antisense primers harbouring unique BamHI and EcoRI to clone D_1 receptors and CB_1 receptors in EYFP vector or to clone $5HT_{2B}$ receptors or D_1 receptors in a *Renilla luciferase*-expressing vector (pcDNA3.1-*RLuc*). A pcDEF3 plasmid encoding the human cDNA of the H_4 receptor fused to EYFP was also used as negative control. The cDNA for the human D_1 receptor was also subcloned into BamHI and ApaI restriction sites of the pcDNA3.1/Hygro (Invitrogen, Grand Island, NY, USA) for the cell line stably expressing D_1 receptors and H_3 receptors. All constructs were verified by nucleotide sequencing. Nomenclature for receptors conforms to the BJP's Guide to Receptors and Channels (Alexander *et al*., 2008)

Cell culture and transfection

Human embryonic kidney (HEK)-293 cells were cultured in Dulbecco's modified Eagle's medium supplemented with 10% fetal bovine serum (FBS), 100 units·mL^{-1} penicillin, 100 μg·mL^{-1} streptomycin, 2 mmol·L^{-1} L-glutamine and 100 μg·mL^{-1} sodium pyruvate (all from Invitrogen), at 37°C in a humidified atmosphere of 5% CO_2 For Bioluminescence Resonance Energy Transfer (BRET) experiments cells were seeded in 35 mm diameter wells of 6-well plates, and transient transfection with the corresponding fusion protein cDNAs was performed the following day by using the calcium phosphate precipitation method (Jordan *et al*., 1996). Cells were harvested for 48 h after transfection and used for BRET experiments. The empty vector pcDNA3.1 was used to equilibrate the total amount of transfected DNA. For extracellular signal-regulated kinase (ERK) experiments, HEK-293 cells were grown to 80% confluence and transfected by using linear polyethylenimine, MW 25 000 (PEI, Polysciences, Eppelheim, Germany) with 5 μg of cDNA corresponding to human H_3 receptors or human D_1 receptors or both cDNAs at the same time. The empty vector pcDNA3.1 was used to equilibrate the total amount of transfected DNA. Briefly, the plasmid DNA was diluted in 50 μL of medium containing no additives (serum, antibiotics or other protein), and PEI was added (ratio μg DNA : μg PEI, 1:7.5) and incubated for 8 min at room temperature. Medium with 10% FBS was added to the DNA/PEI complex, and the mixture was applied to the cultures. After 2 h incubation, the mixture was replaced for grown medium.

SK-N-MC cells were grown in Eagle's minimal essential medium, supplemented with 10% FBS, 50 units·mL^{-1} penicillin, 50 μg·mL^{-1} streptomycin, non-essential amino acids, 2 mmol·L^{-1} L-glutamine and 50 μg·mL^{-1} sodium pyruvate at 37°C in a humidified atmosphere of 5% CO_2 to 80% confluence. Cells were transiently transfected with 5 μg of cDNA corresponding to human D_1 receptors (SK-N-MC/D_1) using Lipofectamine™ 2000 (Invitrogen), according to the manufacturer's protocol. To obtain the SK-N-MC cells stably expressing human H_3 receptors and human D_1 receptors (SK-N-MC/D_1H_3), the SK-N-MC cells stably expressing the human H_3R (SK-N-MC/H_3) (provided by Johnson & Johnson Pharmaceutical Research & Development, L.L.C.) were grown to 30–40% confluence in 60 cm^2 dishes in presence of 600 μg·mL^{-1} G418 (Invitrogen) and transfected with the cDNA corresponding to human D_1 receptors using Lipofectamine™ 2000. SK-N-MC/D_1H_3 receptor cells were allowed to recover for 24 h before the addition of G418 and 300 μg·mL^{-1} hygromycin B (Invitrogen), and the colonies that survived selection were grown and tested by binding experiments and Western blotting.

Immunostaining

For immunocytochemistry, HEK-293 cells were grown on glass coverslips and transiently transfected with 0.1 μg of D_1 receptor–*RLuc* and 0.1 μg H_3 receptor–YFP constructs. After 48 h the cells were fixed in 4% paraformaldehyde for 15 min and washed with phosphate-buffered saline containing 20 mmol·L^{-1} glycine (buffer A) to quench the aldehyde groups. Then, after permeabilization with buffer A containing 0.05% Triton X-100 for 15 min, cells were treated with

phosphate-buffered saline containing 1% bovine serum albumin. After 1 h at room temperature, cells expressing D_1 receptor–*RLuc* were labelled with the primary rat monoclonal anti-D_1 receptor antibody (1:200, Sigma, St. Louis, MO, USA) for 1 h, washed and stained with the secondary antibody Alexa Fluor®350 Goat anti-rat (1:1000, Invitrogen). The H_3 receptor–YFP construct was detected by its fluorescence properties. Samples were rinsed and observed in a Leica SP5 confocal microscope (Leica Microsystems, Mannheim, Germany).

Bioluminescence Resonance Energy Transfer (BRET)

HEK-293 cells were transfected with 250 ng·well^{-1} of the cDNA construct coding for D_1 receptor–*RLuc*, acting as BRET donor, and increasing amounts (0.5–9 μg·well^{-1}) of the cDNA construct coding for the BRET acceptor H_3 receptor–YFP or the negative control H_4 receptor–YFP. After 48 h of transfection cells were washed twice with Hanks' balanced salt solution HBSS (137 mmol·L^{-1} NaCl, 5 mmol·L^{-1} KCl, 0.34 mmol·L^{-1} $Na_2HPO_4.12H_2O$, 0.44 mmol·L^{-1} KH_2PO_4, 1.26 mmol·L^{-1} $CaCl_2.2H_2O$, 0.4 mmol·L^{-1} $MgSO_4.7H_2O$, 0.5 mmol·L^{-1} $MgCl_2$, 10 mmol·L^{-1} HEPES, pH 7.4) supplemented with 0.1% glucose (w·v^{-1}), detached by gently pipetting and resuspended in the same buffer. Sample protein concentration was determined to control cell number, using a Bradford assay kit (Bio-Rad, Munich, Germany) using bovine serum albumin dilutions as standards. Cell suspension (20 μg of protein) was dispensed in duplicates into 96-well black microplates with a transparent bottom (Porvair, King's Lynn, UK), and the fluorescence was measured using a Mithras LB940 fluorescence-luminiscence detector (Berthold, Bad Wildbad, Germany) with an excitation filter of 485 nm and an emission filter of 535 nm. For BRET measurement, 20 μg of cell suspension were distributed in duplicates into 96-well white opaque microplates (Porvair), and coelenterazine H (Molecular Probes Europe, Leiden, The Netherlands) was added at a final concentration of 5 μmol·L^{-1}. After 1 min the readings were collected by using sequential integration of signals detected at 440–500 nm and 510–590 nm. The same samples were incubated for 10 min, and the luminescence was measured. Cells expressing BRET donors alone were used to determine background. The BRET ratio is defined as [(emission at 510–590)/(emission at 440–500)]–Cf where Cf corresponds to (emission at 510–590)/(emission at 440–500) for the D_1 receptor–*RLuc* construct expressed alone in the same experiment. Curves were fitted by using a non-linear regression equation, assuming a single phase with GraphPad Prism software (San Diego, CA, USA).

Membrane preparation and protein determination

SK-N-MC/D_1H_3 receptor or transfected HEK-293 cells were harvested by centrifugation at 1500× *g* for 5 min. Cell pellet was washed twice with phosphate-buffered saline and resuspended in 10 volumes of 50 mmol·L^{-1} Tris-HCl buffer, pH 7.4. Cell suspensions were disrupted with a Polytron homogenizer (PTA 20 TS rotor, setting 3; Kinematica, Basel, Switzerland) for three 5 s periods, and membranes were obtained by centrifugation at 105 000× *g* (40 min, 4°C). The pellet was resuspended and centrifuged under the same conditions, stored at –80°C until use. Membranes were washed once more as described above and resuspended in 50 mmol·L^{-1} Tris-HCl buffer for immediate use. Protein was quantified by the bicinchoninic acid method (Pierce Chemical Co., Rockford, IL, USA) using bovine serum albumin dilutions as standard.

Radioligand binding experiments

Membrane suspensions (0.3 mg of protein per millilitre) were incubated for 1 h at 25°C in 50 mmol·L^{-1} Tris-HCl buffer, pH 7.4, containing 10 mmol·L^{-1} $MgCl_2$ with the indicated radioligand in the presence or absence of competing ligands. To obtain competition curves, membranes were incubated with 2.2 nmol·L^{-1} of the D_1 receptor antagonist [^{3}H]SCH 23390 (NEN Perkin Elmer, Wellesley, MA, USA) or with 2.0 nmol·L^{-1} of the H_3 receptor agonist [^{3}H]R-α-methyl histamine ([^{3}H]RAMH, Amersham, Buckinghamshire, UK) and increasing concentrations of the D_1 receptor agonist SKF 38393 (Tocris, Ellisville, MO, USA) or H_3 receptor agonist R-α-methyl histamine (RAMH) (triplicates of 13 different competitor concentrations from 0.1 nmol·L^{-1} to 10 μmol·L^{-1}) in the absence or the presence of 10 nmol·L^{-1} of the H_3 receptor agonist RAMH or 100 nmol·L^{-1} of the D_1 receptor agonist SKF 38393 respectively. In all cases, non-specific binding was determined in the presence of an excess of unlabeled ligand [10 μmol·L^{-1} SCH 23390 (Sigma) for [^{3}H]SCH 23390 binding or 10 μmol·L^{-1} RAMH for [^{3}H]RAMH binding], and in competition experiments it was confirmed that the value was the same as calculated by extrapolation of the competition curves. Free and membrane-bound ligand were separated by rapid filtration of 500 μL aliquots in a cell harvester (Brandel, Gaithersburg, MD, USA) through Whatman GF/C filters (Brandel) soaked in 0.3% PEI, which were subsequently washed for 5 s with 5 mL of ice-cold Tris-HCl buffer. The filters were incubated with 10 mL of Ecoscint H scintillation cocktail (National Diagnostics, Atlanta, GA, USA) overnight at room temperature, and radioactivity counts were determined by using a Tri-Carb 1600 scintillation counter (PerkinElmer, Boston, MA, USA) with an efficiency of 62%.

Binding data analysis

Due to the homodimeric nature of D_1 receptors (O'Dowd *et al.*, 2005; Kong *et al.*, 2006) and H_3 receptors (Bakker *et al.*, 2006), binding data from competition experiments were analysed by non-linear regression using the commercial Grafit curve-fitting software (Erithacus Software, Surrey, UK), by fitting data to the two-state dimer receptor model (Franco *et al.*, 2005; 2006; Casadó *et al.*, 2007) and not to the classical two-independent-site model for monomeric receptors that considers two binding sites (high and low affinity binding sites). To calculate the macroscopic equilibrium dissociation constants involved in the binding of the agonist SKF 38393 or RAMH to the D_1 receptor or H_3 receptor dimer respectively, the following equation for a competition binding experiment (Casadó *et al.*, 2007) was considered:

$$A_{\text{bound}} = (K_{DA2}A + 2A^2 + K_{DA2}AB/K_{DAB})R_T/[K_{DA1}K_{DA2} + K_{DA2}A + A^2 + K_{DA2}AB/K_{DAB} + K_{DA1}K_{DA2}B/K_{DB1} + K_{DA1}K_{DA2}B^2/(K_{DB1}K_{DB2})] \quad (1)$$

where A represents the radioligand (the D_1 receptor antagonist [^{3}H]SCH 23390 or the H_3 receptor agonist [^{3}H]RAMH)

concentration, R_T is the total amount of receptor dimers and K_{DA1} and K_{DA2} are the macroscopic dissociation constants describing the binding of the first and the second radioligand molecule (*A*) to the dimeric receptor; *B* represents the assayed competing compound (the D_1 receptor agonist SKF 38393 or the H_3 receptor agonist RAMH) concentration, and K_{DB1} and K_{DB2} are, respectively, the equilibrium dissociation constants of the first and second binding of *B*; K_{DAB} can be described as a hybrid equilibrium dissociation constant, which is the dissociation constant of *B* binding to a receptor dimer semi-occupied by *A*.

Because the radioligand *A* ([^{3}H]RAMH or [^{3}H]SCH 23390) showed non-cooperative behaviour (Franco *et al.*, 2006); (Casadó *et al.*, 2007), Eqn 1 was simplified to Eqn 2 due to the fact that $K_{DA2} = 4K_{DA1}$ (see Casadó *et al.*, 2007):

$$A_{bound} = (4K_{DA1}A + 2A^2 + 4K_{DA1}AB/K_{DAB})R_T/[4K_{DA1}^2 + 4K_{DA1}A + A^2 + 4K_{DA1}AB/K_{DAB} + 4K_{DA1}^2B/K_{DB1} + 4K_{DA1}^2B^2/(K_{DB1}K_{DB2})] \quad (2)$$

The dimer homotropic cooperativity (D_C) index for the competing ligand *B* (the agonist SKF 38393) was calculated (see Casadó *et al.*, 2007; Gracia *et al.*, 2008) according to the following expression:

$$D_{CB} = \log(4K_{DB1}/K_{DB2})$$

Goodness of fit was tested according to reduced χ^2 value given by the non-linear regression programme. The test of significance for two different model population variances was based upon the *F*-distribution (see Casadó *et al.*, 1990, for details). Using this *F*-test, a probability greater than 95% ($P < 0.05$) was considered the criterion to select a more complex model (cooperativity) over the simplest one (non-cooperativity). In all cases, a probability of less than 70% ($P > 0.30$) resulted when one model was not significantly better than the other.

cAMP determination

The SK-N-MC or transfected HEK-293 cells were grown in 25 cm^2 flasks to 80% confluence and incubated in serum-free medium for 16 h before the experiment. The day of experiment the cells were pre-incubated with 50 μmol·L^{-1} zardaverine (a phosphodiesterase inhibitor; Tocris) for 10 min at 37°C and treated for 10 min with 100 nmol·L^{-1} RAMH or 1 μmol·L^{-1} SKF 81297 (Tocris) in the presence or the absence of 10 μmol·L^{-1} forskolin (Sigma). When indicated, the H_3 receptor antagonist thioperamide (Sigma) or the D_1 receptor antagonist SCH 23390 (Tocris) were added at 10 μmol·L^{-1} final concentration and pre-incubated for 5 min before agonist addition. To stop the reaction cells were placed on ice and washed with ice-cold phosphate-buffered saline. The cells were incubated with 200 μL of $HClO_4$ (4%) for 30 min, 1.5 mol·L^{-1} KOH was added to reach neutral pH, and samples were centrifuged. The supernatant was frozen at –20°C. The accumulation of cAMP was measured with cyclic AMP (^{3}H) assay system (Amersham Biosciences, Uppsala, Sweden) as described in the manual from the manufacturer.

ERK phosphorylation assay

Cells were grown in 25 cm^2 flasks to 80% confluence and cultured in serum-free medium for 16 h before the addition of any agent. Cells were treated or not with 10 μmol·L^{-1} SCH 23390 or 10 μmol·L^{-1} thioperamide for 30 min before the addition of the agonists 1 μmol·L^{-1} RAMH or 1 μmol·L^{-1} SKF 81297 for 2 min. In experiments evaluating *Pertussis* toxin (PTX), cells were pretreated with the toxin (100 ng·mL^{-1}) for 16 h before ligand addition and in experiments evaluating cholera toxin (CTX), cells were pretreated with the toxin (1 μg·mL^{-1}) for 30 min before ligand addition. At the end of the incubation periods, cells were rinsed with ice-cold phosphate-buffered saline and lysed by the addition of 500 μL of ice-cold lysis buffer (50 mmol·L^{-1} Tris-HCl pH 7.4, 50 mmol·L^{-1} NaF, 150 mmol·L^{-1} NaCl, 45 mmol·L^{-1} β-glycerophosphate, 1% Triton X-100, 20 μmol·L^{-1} phenylarsine oxide, 0.4 mmol·L^{-1} $NaVO_4$ and protease inhibitor cocktail). The cellular debris was removed by centrifugation at 13 000× *g* for 5 min at 4°C, and the protein was quantified by the bicinchoninic acid method by using bovine serum albumin dilutions as standard. To determine the level of ERK1/2 phosphorylation, equivalent amounts of protein (10 μg) were separated by electrophoresis on a denaturing 7.5% SDS-polyacrylamide gel and transferred onto PVDF membranes. The membranes were then probed with a mouse anti-phospho-ERK1/2 antibody (Sigma, 1:5000). In order to rule out that the differences observed were due to the application of unequal amounts of lysates, PVDF blots were stripped and probed with a rabbit anti-ERK1/2 antibody that recognizes both, phosphorylated and non-phosphorylated ERK1/2 (Sigma, 1:40 000). Bands were visualized by the addition of anti-mouse HRP conjugated (Dako, Glostrup, Denmark) or anti-rabbit HRP conjugated (Sigma) secondary antibodies, respectively, and SuperSignal West Pico Chemiluminescent Substrate (Pierce). Bands densities were quantified with a LAS-3000 (Fujifilm, Madrid, Spain), and the level of phosphorylated ERK1/2 isoforms was normalized for differences in loading using the total ERK protein band intensities. Quantitative analysis of detected bands was performed by Image Gauge V4.0 software.

Data analysis

Results are given as mean ± SEM. Differences between group means have been tested for significance ($P < 0.05$) by using Student's *t*-test for unpaired samples.

Results

Dopamine D_1–histamine H_3 receptor heteromerization

The BRET approach was used to demonstrate the ability of H_3 receptors to heteromerize with D_1 receptors. BRET measurements were performed in transiently co-transfected HEK-293 cells by using a constant amount of D_1 receptor–*RLuc* and increasing amounts of H_3 receptor–YFP. The subcellular localization of fusion proteins was investigated and the D_1 receptor–*RLuc* and H_3 receptor–YFP membrane expression and co-localization is shown in Figure 1A. Fusion of *RLuc* and YFP to D_1 receptors or to H_3 receptors did not modify receptor binding parameters (results not shown) or receptor function as determined by cAMP assays (Figure 1B). The correlation between properly folded receptors, determined by ligand

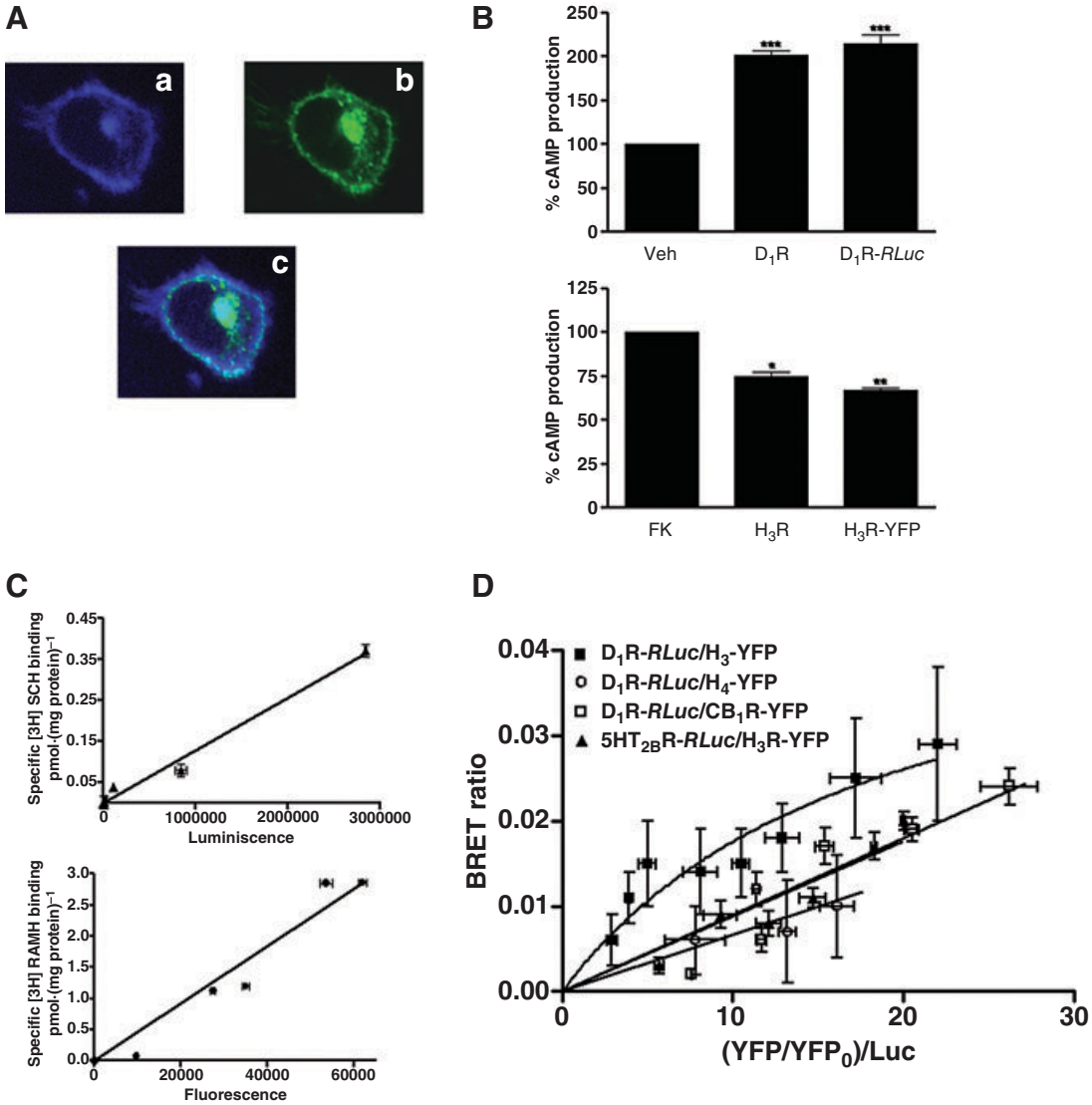

Figure 1 Heteromerization of functional D_1 and H_3 receptors. (A) Confocal microscopy images of HEK-293 cells expressing D_1 receptor–*RLuc* (0.1 μg plasmid) and H_3 receptor–YFP (0.1 μg plasmid). Proteins were identified by fluorescence or by immunocytochemistry. D_1 receptor–*RLuc* immunoreactivity in shown in blue (a), H_3 receptor–YFP fluorescence in shown in green (b) and co-localization of D_1 receptor–*RLuc* and H_3 receptor–YFP is shown in light blue (c). (B) Functionality of D_1 receptor–*RLuc* (D_1R–*RLuc*) and H_3 receptor–YFP (H_3R–YFP) constructs. HEK-293 cells transfected with 5 μg of cDNA corresponding to D_1 receptors or D_1 receptor–*RLuc* were stimulated with the D_1 receptor agonist SKF 81297 (10 μmol·L^{-1}), and HEK-293 cells transfected with 5 μg of cDNA corresponding to H_3 receptors or H_3 receptor–YFP were treated with 10 μmol·L^{-1} forskolin plus the H_3 receptor agonist RAMH (0.1 μmol·L^{-1}). Results (mean ± SEM; $n = 2$–4) are expressed as percentage over basal (upper panel) or over forskolin (FK) alone (lower panel); significantly different compared with the basal for D_1 receptors and D_1 receptor–*RLuc* or compared with forskolin alone for H_3 receptors or H_3 receptor–YFP, (non-paired Student's *t*-test: $^*P < 0.05$, $^{**}P < 0.01$ and $^{***}P < 0.001$). (C) Correlation between 2.1 nmol·L^{-1} [^{3}H]SCH 23390 binding and luminiscence expression (upper panel) or 1.9 nmol·L^{-1} [^{3}H]RAMH binding and fluorescence expression (lower panel) in HEK-293 cell transfected with increasing amounts of cDNA for D_1 receptor–*RLuc* (upper panel) or H_3 receptor–YFP (lower panel) (D) D_1–H_3 receptor heteromerization in HEK-293 cells. BRET experiments were performed with HEK-293 cells co-expressing D_1 receptor–*RLuc* and H_3 receptor–YFP, D_1 receptor–*RLuc* and CB_1 receptor–YFP, $5HT_{2B}$ receptor–*RLuc* and H_3 receptor–YFP or D_1 receptor–*RLuc* and H_4 receptor–YFP constructs. Co-transfections were performed with increasing amounts of plasmid–YFP (0.5–9 μg cDNA) whereas the plasmid–*RLuc* construct was maintained constant (250 ng cDNA). Both fluorescence and luminiscence of each sample were measured before every experiment to confirm similar donor expressions (about 250 000 luminescent units) while monitoring the increase acceptor expression (5000–80 000 fluorescent units). The relative amount of BRET is given as the ratio between the fluorescence of the acceptor and the luciferase activity of the donor. YFP_0 corresponds to the fluorescence value of cells expressing the donor alone. BRET data are expressed as means ± SD of 3–13 different experiments grouped as a function of the amount of BRET acceptor. [^{3}H]RAMH, [^{3}H]R-α-methyl histamine; BRET, Bioluminescence Resonance Energy Transfer; HEK, human embryonic kidney; *RLuc, Renilla* luciferase; Veh, vehicle.

binding, and fluorescence or luminescence is shown in Figure 1C. The expression level of the fusion proteins was in the range of 0.05 pmol·mg^{-1} protein for D_1 receptor–*RLuc* and between 0.3 and 4.5 pmol·mg^{-1} protein for the different amounts of the transfected cDNA corresponding to H_3 receptor–YFP. These data demonstrate that the fusion proteins are not strongly over-expressed at $BRET_{50}$. A positive and saturable BRET signal was found for the pair D_1 receptor–*RLuc*

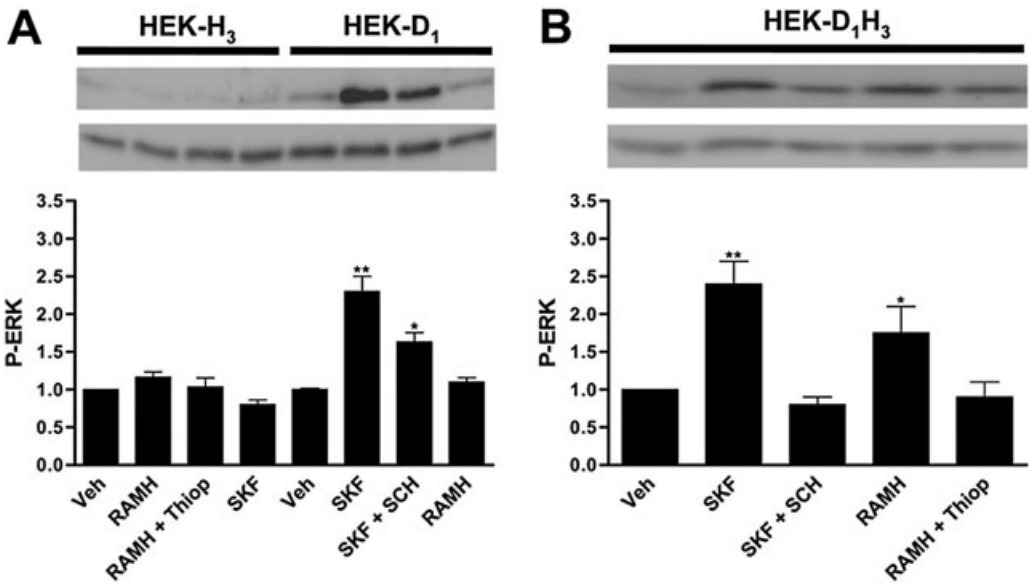

Figure 2 Crosstalk between H_3 receptors and D_1 receptors in HEK-293 cells. HEK-293 cells transiently expressing H_3 receptors (HEK-H_3) or D_1 receptors (HEK-D_1) (A) or both (HEK-D_1H_3) (B) were treated for 2 min with the H_3 receptor agonist RAMH (1 $\mu mol \cdot L^{-1}$) or with the D_1 receptor agonist SKF 81297 (1 $\mu mol \cdot L^{-1}$, SKF), in the presence or in the absence of the H_3 receptor antagonist thioperamide (10 $\mu mol \cdot L^{-1}$, Thiop) or the D_1 receptor antagonist SCH 23390 (10 $\mu mol \cdot L^{-1}$, SCH), and ERK1/2 phosphorylation (P-ERK) was determined as indicated in *Methods*. A representative Western blot is shown in each panel. The immunoreactive bands from three independent experiments were quantified, and values represent the mean ± SEM of fold increase of phosphorylation over the basal levels found in untreated cells. Significant differences with respect to the treatment with vehicle, were calculated by Student's *t*-test for unpaired samples (*$P < 0.05$ and **$P < 0.01$). ERK, extracellular signal-regulated kinase; HEK, human embryonic kidney; RAMH, R-α-methyl histamine; Veh, vehicle.

and H_3 receptor–YFP (Figure 1D). From the saturation curve, a $BRET_{max}$ of 0.034 ± 0.005 units and a $BRET_{50}$ of 10 ± 4 were calculated. As the human histamine H_4 receptor is closely related to the human H_3 receptor [31% sequence identity at the protein level, which increases to 54% in the transmembrane region; de Esch *et al*. (2005)], the pair D_1 receptor–*RLuc* and H_4 receptor–YFP was used as a negative control. Also as negative controls the BRET pairs D_1 receptor–*RLuc* and cannabinoid CB_1 receptor–YFP or $5HT_{2B}$ receptor–*RLuc* and H_3 receptor–YFP were used. As shown in Figure 1D the negative controls gave a linear non-specific BRET signal, thus confirming the specificity of the interaction between D_1 receptor–*RLuc* and H_3 receptor–YFP in HEK-293 cells.

Intracellular crosstalk between histamine H_3 and dopamine D_1 receptors in HEK-293 cells

To investigate potential functional consequences of D_1–H_3 receptor heteromerization, HEK-293 cells expressing the human D_1 receptor and/or the human H_3 receptor at amounts giving approximately maximum BRET (Figure 1D) were treated with dopamine or histamine receptor agonists, and signalling was assayed by ERK1/2 phosphorylation. When cells expressing H_3 receptors were treated with the selective H_3 receptor agonist RAMH, no phosphorylation of ERKs was found (Figure 2A). On the other hand, when cells expressing D_1 receptors were activated with the selective D_1 receptor agonist SKF 81297, we observed a significant level of ERK1/2 phosphorylation, which was antagonized by the selective D_1 receptor antagonist SCH 23390 (Figure 2A). When HEK-293 cells were transfected simultaneously with D_1 receptors and H_3 receptors, the D_1 receptor agonist also activated the mitogen-activated protein kinase (MAPK) pathway, and this effect was blocked by SCH 23390 (Figure 2B). Interestingly, the H_3 receptor agonist was also able to induce a significant ERK1/2 phosphorylation in co-transfected cells expressing D_1–H_3 receptor heteromers (Figure 2B). The specificity of the effect was proven by the blockade of the RAMH-induced effect by the H_3 receptor antagonist, thioperamide (Figure 2B). These results indicate that the H_3 receptor is able to couple to the MAPK-signalling pathway only in HEK-293 cells expressing D_1 receptors and H_3 receptors.

D_1–H_3 receptor heteromers in human neuroblastoma cells

For some receptor pairs it is possible to detect the heteromer receptor fingerprint (Ferré *et al*., 2007; Franco *et al*., 2007). This fingerprint often consists of intramembrane receptor–receptor interactions, in which changes in ligand binding characteristics of one receptor are obtained when the partner receptor is activated by using membrane preparations in which no intracellular crosstalk occurs (Agnati *et al*., 2003; El-Asmar *et al*., 2005; Ferré *et al*., 2007; Springael *et al*., 2007; Vilardaga *et al*., 2008). We investigated the possible existence of D_1–H_3 receptor intramembrane receptor interactions in SK-N-MC cells as a neuronal cell model. SK-N-MC cells have been used as a good model to transfect H_3 receptors (Bongers *et al*., 2007); nevertheless, some authors have described the presence of D_1 receptors in SK-N-MC cells (Sidhu *et al*., 1999; Chen *et al*., 2003; Moussa *et al*., 2006; Robinson *et al*., 2008) and some controversy exists about the functionality of these receptors, whether they couple to different G proteins

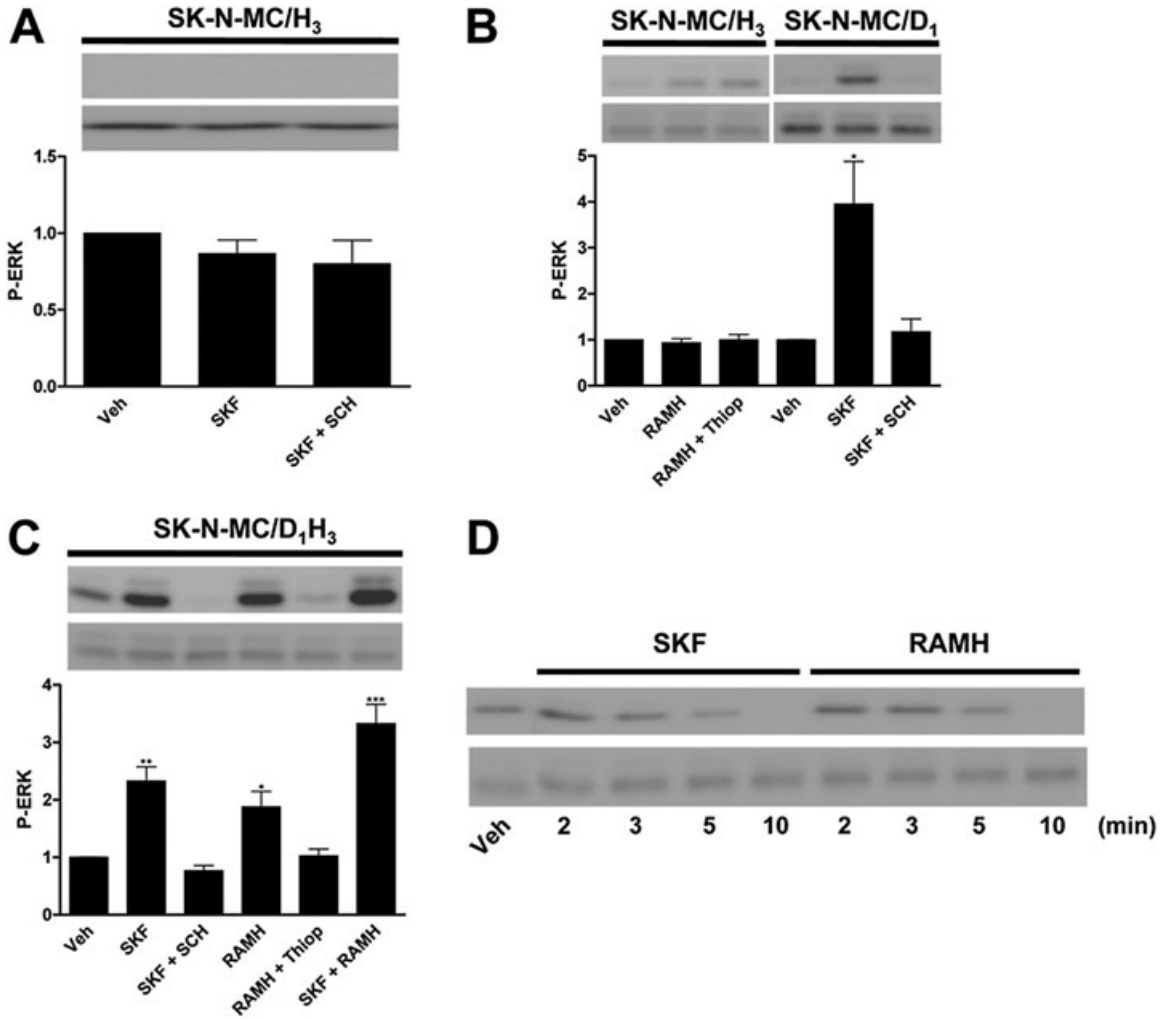

Figure 3 ERK1/2 phosphorylation (P-ERK) via the D_1–H_3 receptor heteromer in human neuroblastoma cells. SK-N-MC cells expressing H_3 receptors (SK-N-MC/H_3) or D_1 receptors (SK-N-MC/D_1) or both (SK-N-MC/D_1H_3) were treated with the H_3 receptor agonist, RAMH (1 μmol·L^{-1}), or with the D_1 receptor agonist, SKF 81297 (1 μmol·L^{-1}, SKF) alone or in combination, in the presence or in the absence of the H_3 receptor antagonist, thioperamide (10 μmol·L^{-1}, Thiop) or the D_1 receptor antagonist, SCH 23390 (10 μmol·L^{-1}, SCH). ERK1/2 phosphorylation was determined as indicated in *Methods* after 2 min of agonist treatment (A, B and C). In (D) a time–course response of ERK1/2 phosphorylation induced by 1 μmol·L^{-1} SKF 81297 or 1 μmol·L^{-1} RAMH in SK-N-MC/D_1H_3 cells is shown. A representative Western blot is shown in each panel. The immunoreactive bands from three to four experiments were quantified, and values represent the mean ± SEM of fold increase of phosphorylation over the basal levels found in untreated cells. Significant differences were calculated by Student's *t*-test for unpaired samples (*$P < 0.05$, **$P < 0.01$, ***$P < 0.001$). ERK, extracellular signal-regulated kinase; RAMH, R-α-methyl histamine; Veh, vehicle.

(Kimura *et al*., 1995) and whether they signal (Chen *et al*., 2004) or not (Chan *et al*., 2005) towards the MAPK cascade. Our SK-N-MC cell clone expresses less than 0.030 pmol·(mg protein)$^{-1}$ of D_1 receptors [0.009 ± 0.004 pmol·(mg protein)$^{-1}$ in the parental cell clone and 0.026 ± 0.005 pmol·(mg protein)$^{-1}$ in the SK-N-MC/H3 cell clone], determined as [^{3}H]SCH 23390 maximum binding, that is, at near saturating (>90%) concentrations of the radioligand. It should be noted that the D_1 receptor agonist did not induce ERK1/2 phosphorylation neither in SK-N-MC/H3 (Figure 3A) or in parental cells (results not shown). Therefore it seems that different SK-N-MC cell clones may give different results.

Membranes prepared from SK-N-MC human neuroblastoma cells stably expressing human versions of H_3 receptors and D_1 receptors (SK-N-MC/D_1H_3 cells) were used in binding competition experiments with [^{3}H]SCH 23390 (2.2 nmol·L^{-1}) as radioligand and increasing concentrations of SKF 38393 as competitor in the presence and in the absence of RAMH (10 nmol·L^{-1}). Binding data were fitted to the two-state dimer receptor model (Franco *et al*., 2005; 2006; Casadó *et al*., 2007), to calculate the macroscopic equilibrium dissociation constants and the cooperativity index. The competition curve was biphasic in the absence of RAMH (significantly better than monophasic; *F*-test: $P < 0.05$), showing cooperativity in the D_1 receptor agonist binding, but monophasic in the presence of RAMH. Variations in binding parameter values are shown in Table 1. These results indicate that an intramembrane crosstalk occurs between these receptors by which H_3 receptor activation induces a shift from a cooperative to a non-cooperative binding and an overall decrease of affinity for the D_1 receptor agonist binding. In contrast, D_1 receptor stimulation did not influence the agonist binding to H_3 recep-

Table 1 Parameter values from competition experiments of [^{3}H]SCH 23390 versus SKF 38393 in the presence and in the absence of RAMH (two-state dimer model)

Agonists	*Parameters*			
	R_T *[pmol·(mg protein)$^{-1}$]*	K_{DB1} *(nmol·L^{-1})*	K_{DB2} *(μmol·L^{-1})*	D_{CB}
SKF 38393	0.436 ± 0.011	41 ± 3	1.3 ± 0.1	–0.85
SKF 38393 + RAMH	0.404 ± 0.007	95 ± 9*	–	0

Data are mean ± SEM values of three experiments; D_{CB}, dimer cooperativity index for the binding of SKF 38393; K_{DB1} and K_{DB2}, equilibrium dissociation constants for the first and second bindings of SKF 38393; RAMH, R-α-methyl histamine; R_T, total amount of receptor dimers.
*Significantly different compared with the K_{DB1} value of SKF 38393 alone, $P < 0.05$.

tor. In fact, competition experiments of 2 nmol·L^{-1} [^{3}H]RAMH binding versus increasing RAMH concentrations, performed as indicated in *Methods*, gave similar R_T and K_{DB1} values for the non-cooperative RAMH binding both in the absence [0.46 ± 0.05 pmol·(mg protein)$^{-1}$ and 2.9 ± 0.3 nmol·L^{-1}] or presence [0.42 ± 0.04 pmol·(mg protein)$^{-1}$ and 3.0 ± 0.3 nmol·L^{-1}] of 100 nmol·L^{-1} SKF 38393.

Signal transduction via D_1–H_3 receptor heteromers in human neuroblastoma cells

As described above, in HEK-293 cells, H_3 receptors were able to mediate activation of the MAPK signalling pathway only through D_1–H_3 receptor heteromerization, demonstrated by BRET. This characteristic of the heteromer can also be used as a signalling fingerprint to identify the D_1–H_3 receptor heteromers. Thus, similar biochemical experiments were performed in SK-N-MC/D_1H_3 cells and cells transfected with only one receptor. As shown in Figure 3B, cells expressing D_1 receptors are able to induce ERK1/2 phosphorylation in response to the treatment with the D_1 receptor agonist SKF 81297, an effect that was blocked by SCH 23390. In SK-N-MC/H_3 cells, RAMH had no effect on ERK1/2 phosphorylation (Figure 3B). However, in SK-N-MC/D_1H_3 cells both RAMH and SKF 81297 were able to activate the MAPK pathway, and co-activation of the two receptors did not result in synergism (Figure 3C). As shown in Figure 3D, there was no change in the time course of ERK1/2 phosphorylation when the agonists for D_1 receptors or H_3 receptors were used individually in SK-N-MC/D_1H_3 cells; the maximum phosphorylation was reached at 2 min and disappeared after 10 min stimulation. Overall the results were qualitatively identical to those obtained by using transiently transfected HEK-293 cells, demonstrating D_1–H_3 receptor heteromerization in neuroblastoma cells. These results also indicate that H_3 receptors are able to couple to the MAPK pathway only in neuroblastoma cells expressing D_1–H_3 receptor heteromers. Similar experiments were performed by using a mutant version of H_3 receptors (R3.50A; Arg 132 substituted by Ala) that is neither able to bind full agonists nor to signal (Appendix S1; Figure S1). The D_1 receptor agonist was not able to provide any ERK1/2 phosphorylation signal when D_1 receptors were co-expressed with the H_3 R3.50A receptors (data not shown). This indicates that the D_1 receptor signals towards MAPK via H_3 receptors in cells co-expressing both receptors. Interestingly, in SK-N-MC/D_1H_3 cells, SKF 81297-induced ERK1/2 phosphorylation was reversed not only by SCH 23390, the specific D_1 receptor antagonist, but also by thioperamide, the H_3 receptor antagonist. Furthermore, RAMH-induced ERK1/2 phosphorylation in these cells was not only antagonized by thioperamide but also by SCH 23390 (Figure 4). It should be noted that both SKF 81297 and SCH 23390 are specific ligands for D_1 receptors and do not appreciably interact with H_3 receptors, as in SK-N-MC/H_3 cells they were not able to reduce the 1.9 nmol·L^{-1} [^{3}H]RAMH binding [0.61 ± 0.02 vs. 0.57 ± 0.02 and 0.54 ± 0.04 pmol·(mg protein)$^{-1}$ in the presence of 10 μmol·L^{-1} SKF 81297 or 10 μmol·L^{-1} SCH 23390, respectively]. Analogously, thioperamide and RAMH are specific H_3 receptor ligands, as they were not able to reduce the 1.9 nmol·L^{-1} [^{3}H]SCH 23390 binding to SK-N-MC/D_1H_3 cells [0.72 ± 0.03 vs. 0.71 ± 0.02 and 0.73 ± 0.01 pmol·(mg protein)$^{-1}$ in the presence of 10 μmol·L^{-1} thioperamide or 10 μmol·L^{-1} RAMH, respectively].

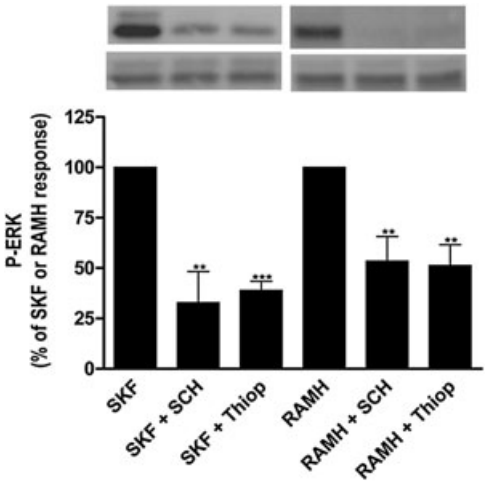

Figure 4 Effect of receptor antagonists on ERK1/2 phosphorylation (P-ERK) via the D_1–H_3 receptor heteromer in human neuroblastoma cells. SK-N-MC cells expressing H_3 receptors and D_1 receptors (SK-N-MC/D_1H_3) were treated with the H_3 receptor agonist, RAMH (1 μmol·L^{-1}), or the D_1 receptor agonist, SKF 81297 (1 μmol·L^{-1}. SKF), in the presence or in the absence of the H_3 receptor antagonist, thioperamide (10 μmol·L^{-1}, Thiop) or the D_1 receptor antagonist, SCH 23390 (10 μmol·L^{-1}, SCH). ERK1/2 phosphorylation was determined as indicated in *Methods* after 2 min of agonist treatment. A representative Western blot is shown. The immunoreactive bands from four experiments were quantified, and values represent the mean ± SEM of percentage of phosphorylation of agonist-treated cells. Significant differences were calculated by Student's *t*-test for unpaired samples (**$P < 0.01$, ***$P < 0.001$). ERK, extracellular signal-regulated kinase; RAMH, R-α-methyl histamine.

As expected from the known coupling of H_3 receptor to heterotrimeric G_i proteins (Lovenberg *et al.*, 1999; Drutel

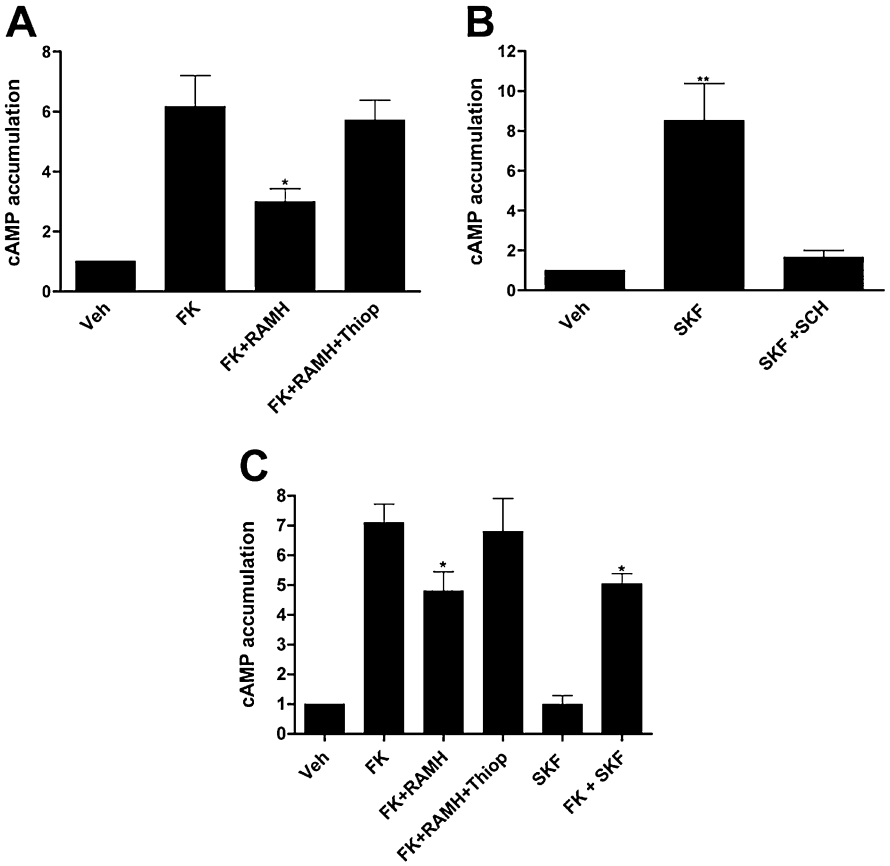

Figure 5 cAMP production by D_1–H_3 receptor heteromer in human neuroblastoma cells. SK-N-MC cells expressing (A) H_3 receptors (SK-N-MC/H_3) or (B) D_1 receptors (SK-N-MC/D_1) or (C) both (SK-N-MC/D_1H_3) were treated or not with 10 μmol·L^{-1} forskolin (FK) and the H_3 receptor agonist, RAMH (0.1 μmol·L^{-1}), and/or the D_1 receptor agonist, SKF 81297 (1 μmol·L^{-1}, SKF). The effect of the H_3 receptor antagonist, thioperamide (10 μmol·L^{-1}, Thiop) or the D_1 receptor antagonist, SCH 23390 (10 μmol·L^{-1}, SCH) was also assayed. cAMP levels were determined as indicated in *Methods*. Results are expressed as fold increase over basal levels obtained in untreated cells (mean ± SEM of three to five experiments). Significant differences were calculated by Student's *t*-test for unpaired samples (*$P < 0.05$, **$P < 0.01$). RAMH, R-α-methyl histamine; Veh, vehicle.

et al., 2001; Leurs *et al*., 2005), RAMH markedly inhibited the 10 μmol·L^{-1} forskolin-stimulated production of cAMP in SK-N-MC/H_3 cells, and this effect was effectively blocked by thioperamide (Figure 5A), showing that in these neuroblastoma cells the H_3 receptors are functional. Consistent with the very low D_1 receptor expression in parental SK-N-MC cells and with the reported coupling of D_1 receptors to G_s proteins (Neve *et al*., 2004), SKF 81297 was not able to increase cAMP in our SK-N-MC cell clone but was able to increase the intracellular levels of cAMP in SK-N-MC/D_1 cells, an effect that was fully blocked by SCH 23390 (Figure 5B). Interestingly, in SK-N-MC/D_1H_3 cells, RAMH was still able to inhibit the cAMP accumulation induced by forskolin, and thioperamide blocked this action. In the same cell clone, which co-expresses the two receptors, SKF 81297 did not have any significant effect on cAMP production but reduced the forskolin-induced cAMP levels (Figure 5C). This suggests that D_1 receptors are signalling in the D_1–H_3 receptor heteromer by coupling to an inhibitory G protein.

Based on the data described above, it is likely that a single heterotrimeric G protein, probably of the $G_{i/o}$ type, is transducing the signal generated by either dopamine or histamine receptor agonists through the H_3–D_1 receptor heteromer. To check for this possibility SK-N-MC/D_1H_3 cells were pretreated with PTX, which specifically inactivates G_i/G_o-mediated signalling pathways, or with CTX, which activates adenylyl cyclase by catalysing ADP-ribosylation of the stimulatory $G\alpha_s$ protein. After pretreatment with these toxins, H_3 receptors and D_1 receptors were activated by using respectively RAMH or SKF 81297. Whereas PTX inhibited the phosphorylation of ERK1/2 induced by RAMH and SKF 81297, CTX had no significant effect on the activation induced by any of the agonists (Figure 6). These results suggest that the activation of MAPK pathway through any of the two receptors in the D_1–H_3 receptor heteromer depends on G_i coupling.

Discussion

It seems that most, if not all, members of the GPCR superfamily can exist as homodimers (Bouvier, 2001; Devi, 2001; Marshall, 2001; Rios *et al*., 2001; George *et al*., 2002; Franco *et al*., 2003; Terrillon and Bouvier, 2004; Prinster *et al*., 2005; Milligan, 2006). The first indication of the existence of GPCR heteromers was obtained with radioligand binding experiments, which showed the existence of biochemical interac-

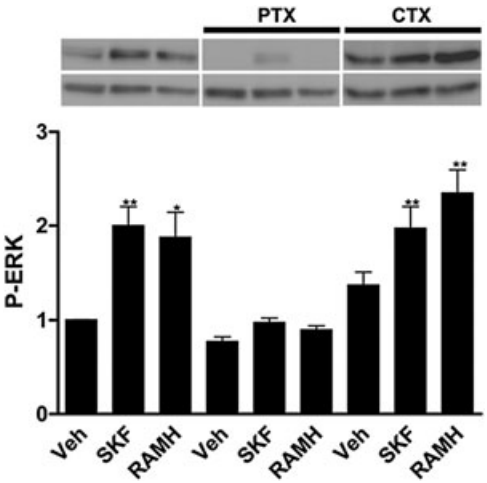

Figure 6 Effect of PTX and CTX on SKF- or RAMH-induced ERK1/2 phosphorylation (P-ERK). SK-N-MC cells expressing H_3 receptors and D_1 receptors (SK-N-MC/D_1H_3) were treated with PTX (100 ng·mL^{-1}) for 16 h or with CTX (1 μg·mL^{-1}) for 30 min prior to the addition of the H_3 receptor agonist, RAMH (1 μmol·L^{-1}), or the D_1 receptor agonist, SKF 81297 (1 μmol·L^{-1}, SKF). ERK1/2 phosphorylation was determined as indicated in *Methods*. A representative Western blot is shown. The immunoreactive bands from four experiments were quantified, and values represent the mean ± SEM of fold increase of phosphorylation over basal levels found in untreated cells. Significant differences were calculated by Student's *t*-test for unpaired samples (*$P < 0.05$ and **$P < 0.01$). CTX, cholera toxin; ERK, extracellular signal-regulated kinase; RAMH, R-α-methyl histamine; PTX, *Pertussis* toxin; Veh, vehicle.

tions between different GPCRs in brain membrane preparations (Agnati *et al.*, 2003). In this kind of interactions, initially known as 'intramembrane receptor–receptor interactions', stimulation of one receptor changes the binding characteristics of another receptor for endogenous or exogenous ligands in crude membrane preparations (Agnati *et al.*, 2003). This implied the lack of involvement of intracellular signalling and suggested some kind of allosteric interaction between adjacent receptors. Thus, at the beginning of the 90s, it was hypothesized that this intramembrane interaction could result from an intermolecular crosstalk, implying receptor heteromerization (Zoli *et al.*, 1993). This is now considered as a biochemical fingerprint of a receptor heteromer (Ferré *et al.*, 2007; Franco *et al.*, 2007). Here we show that D_1 receptors and H_3 receptors are able to form D_1–H_3 receptor heteromers by BRET, in transiently transfected human embryonic cells, and by radioligand experiments in SK-N-MC/D_1H_3 cells, in which a specific H_3 receptor agonist led to the disappearance of the cooperative D_1 receptor agonist binding and to a significant change in the affinity of the D_1 receptor for the agonist.

The crosstalk occurring via receptor heteromers has different components. One of them is the above discussed change in binding characteristics of one receptor upon activation of the partner receptor. Another is the crosstalk at the level of second messengers. For heteromers in which one of the constituent receptors is coupled to $G_{i/o}$ whereas the other is coupled to G_s proteins, co-activation of the receptors would result not in a functional antagonism but in contradictory messages for the cell. Recent reports are providing clues to solve this conundrum. Significant advances in the case of heteromers for the same neurotransmitter have been achieved (Jordan and Devi, 1999; George *et al.*, 2000; Fan *et al.*, 2005; Ciruela *et al.*, 2006; Rashid *et al.*, 2007). Recent data indicate that in neurons co-expressing D_1 receptors, a G_s-coupled receptor, and D_2 receptors, a G_i-coupled receptor, D_1–D_2 receptor heteromers are formed that couple to a G_q protein (Rashid *et al.*, 2007). This makes possible that a single neurotransmitter may increase cAMP levels, decrease cAMP levels or modify intracellular calcium levels depending on whether a given neuron (or microdomain in a neuron) expresses, respectively, the D_1 receptor, the D_2 receptor or the D_1–D_2 receptor heteromer. Two different neurotransmitters, dopamine and histamine, can interact with D_1–H_3 receptor heteromers. In neuroblastoma cells co-expressing D_1 receptors and H_3 receptors there is a change in the D_1 receptor coupling from the G_s to the G_i protein, to which H_3 receptors are already coupled. In fact, in the presence of the H_3 receptor, D_1 receptors were no longer coupled to G_s, and could not activate adenylyl cyclase, but were coupled to G_i, which transduced the signal towards the MAPK pathway. On the other hand, H_3 receptors in cells co-expressing the two receptors could signal through both adenylyl cyclase (inhibiting enzyme activity) and MAPK (increasing ERK1/2 phosphorylation). These results indicate that D_1–H_3 receptor heteromers constitute unique devices to direct dopaminergic and histaminergic signalling towards the MAPK pathway in a G_s-independent and G_i-dependent manner. In the SK-N-MC cell clone stably expressing the human H_3 receptors near to physiological receptor densities [0.1–1 pmol·(mg protein)$^{-1}$], the H_3 receptor agonist did not promote ERK1/2 phosphorylation unless the D_1 receptor was co-expressed. It has been described that agonist binding to H_3 receptors expressed at high densities in Chinese hamster ovary or in COS-7 cells can phosphorylate ERK1/2 (Drutel *et al.*, 2001; Gbahou *et al.*, 2003). In contrast to the cAMP response, the H_3 receptor did not exhibit constitutive activation of the MAPK pathway (Gbahou *et al.*, 2003). Whether ERK1/2 phosphorylation in these cells is solely due to the action of $G_{\beta\gamma}$ subunits or to crosstalk with another receptor in these cells remains to be elucidated. *In vivo*, the first evidence of a positive correlation between ERK phosphorylation and memory improvement was given by Giovannini *et al.* (2003), who demonstrated an improvement in fear memory by H_3 receptor-elicited ERK2 phosphorylation in hippocampal CA3 neurons in which the D_1 receptor is co-expressed (Pantazopoulos *et al.*, 2004)

Our results would be in agreement with the recently suggested 1:2 stoichiometry for the G protein: receptor interaction (Herrick-Davis *et al.*, 2005). The results obtained by co-expressing D_1 receptors and the mutant version of H_3 receptors unable to activate MAPK indicate that GPCR activation results from a dynamic intersubunit interplay as shown in dimeric metabotropic glutamate receptors (Brock *et al.*, 2007). The possibility that better explains the overall results is that D_1 receptors are able to signal to the MAP kinase in the absence of the H_3 receptor, but that in the presence of this receptor the signalling to ERK is mediated by the H_3 receptor and not via the D_1 receptor. Then, in the presence of non-functional H_3 receptors, D_1 receptor agonists are unable to produce ERK phosphorylation. Interestingly, not only the

antagonist of their respective receptors but also the antagonist of the partner receptor counteracted the effect of D_1 receptor or H_3 receptor activation. Thus, an antagonist of one of the receptor units in the D_1–H_3 receptor heteromer can induce conformational changes in the other receptor unit and block specific signals originating in the heteromer. This fact broadens the therapeutic potential for GPCR antagonists.

Acknowledgements

This work was supported by Grants from Spanish Ministerio de Ciencia y Tecnología (SAF2005-00170 to E.I.C. SAF2006-05481 to R.F), Grant 060110 from Fundació La Marató de TV3 (RF) and by the intramural funds of the National Institute on Drug Abuse (SF). We acknowledge Dr Timothy A Esbenshade (Abbott Laboratories) for the kind gift of [^{3}H]-A-349821. Sergi Ferré is employed by NIDA-NIH. No claim to US government work.

Conflict of interest

The authors state no conflict of interest.

References

Agnati LF, Ferré S, Lluis C, Franco R, Fuxe K (2003). Molecular mechanisms and therapeutical implications of intramembrane receptor/receptor interactions among heptahelical receptors with examples from the striatopallidal GABA neurons. *Pharmacol Rev* **55**: 509–550.

Agnati LF, Fuxe K, Ferré S (2005). How receptor mosaics decode transmitter signals. Possible relevance of cooperativity. *Trends Biochem Sci* **30**: 188–193.

Alexander SPH, Mathie A, Peters JA (2008). Guide to Receptors and Channels (GRAC), 3rd edn (2008 revision). *Br J Pharmacol* **153** (Suppl. 2): S1–S209.

Anichtchik OV, Peitsaro N, Rinne JO, Kalimo H, Panula P (2001). Distribution and modulation of histamine H(3) receptors in basal ganglia and frontal cortex of healthy controls and patients with Parkinson's disease. *Neurobiol Dis* **8**: 707–716.

Arias-Montano JA, Floran B, Garcia M, Aceves J, Young JM (2001). Histamine H(3) receptor-mediated inhibition of depolarization-induced, dopamine D(1) receptor-dependent release of [(3)H]-gamma-aminobutryic acid from rat striatal slices. *Br J Pharmacol* **33**: 165–171.

Bakker RA, Lozada AF, van Marle A, Shenton FC, Drutel G, Karlstedt K *et al*. (2006). Discovery of naturally occurring splice variants of the rat histamine H3 receptor that act as dominant-negative isoforms. *Mol Pharmacol* **69**: 1194–1206.

Bockaert J, Fagni L, Dumuis A, Marin P (2004). GPCR interacting proteins (GIP). *Pharmacol Ther* **103**: 203–221.

Bongers G, Sallmen T, Passani MB, Mariottini C, Wendelin D, Lozada A *et al*. (2007). The Akt/GSK-3beta axis as a new signaling pathway of the histamine H(3) receptor. *J Neurochem* **103**: 248–258.

Bouvier M (2001). Oligomerization of G-protein-coupled transmitter receptors. *Nat Rev Neurosci* **2**: 274–286.

Brock C, Oueslati N, Soler S, Boudier L, Rondard P, Pin JP (2007). Activation of a dimeric metabotropic glutamate receptor by intersubunit rearrangement. *J Biol Chem* **282**: 33000–33008.

Brown RE, Stevens DR, Haas HL (2001). The physiology of brain histamine. *Prog Neurobiol* **63**: 637–672.

Casadó V, Cantí C, Mallol J, Canela EI, Lluís C, Franco R (1990). Solubilization of A_1 adenosine receptor from pig brain. Characterization and evidence of the role of the cell membrane on the coexistence of the high and low-affinity states. *J Neurosci Res* **26**: 461–473.

Casadó V, Cortés A, Ciruela F, Mallol J, Ferré S, Lluis C et al. (2007). Old and new ways to calculate the affinity of agonists and antagonists interacting with G-protein-coupled monomeric and dimeric receptors: the receptor-dimer cooperativity index. *Pharmacol Ther* **116**: 343–354.

Chan AS, Yeung WW, Wong YH (2005). Integration of G protein signals by extracellular signal-regulated protein kinases in SK-N-MC neuroepithelioma cells. *J Neurochem* **94**: 1457–1470.

Chen J, Wersinger C, Sidhu A (2003). Chronic stimulation of D1 dopamine receptors in human SK-N-MC neuroblastoma cells induces nitric-oxide synthase activation and cytotoxicity. *J Biol Chem* **278**: 28089–28100.

Chen J, Rusnak M, Luedtke RR, Sidhu A (2004). D1 dopamine receptor mediates dopamine-induced cytotoxicity via the ERK signal cascade. *J Biol Chem* **279**: 39317–33930.

Ciruela F, Casadó V, Rodrigues RJ, Lujan R, Burgueno J, Canals M et al. (2006). Presynaptic control of striatal glutamatergic neurotransmission by adenosine A1-A2A receptor heteromers. *J Neurosci* **26**: 2080–2087.

Devi LA (2001). Heterodimerization of G-protein-coupled receptors: pharmacology, signaling and trafficking. *Trends Pharmacol Sci* **22**: 532–537.

Drutel G, Peitsaro N, Karlstedt K, Wieland K, Smit MJ, Timmerman H et al. (2001). Identification of rat H3 receptor isoforms with different brain expression and signaling properties. *Mol Pharmacol* **59**: 1–8.

El-Asmar L, Springael JY, Ballet S, Andrieu EU, Vassart G, Parmentier M (2005). Evidence for negative binding cooperativity within CCR5-CCR2b heterodimers. *Mol Pharmacol* **67**: 460–469.

de Esch IJ, Thurmond RL, Jongejan A, Leurs R (2005). The histamine H4 receptor as a new therapeutic target for inflammation. *Trends Pharmacol Sci* **26**: 462–469.

Fan T, Varghese G, Nguyen T, Tse R, O'Dowd BF, George SR (2005). A role for the distal carboxyl tails in generating the novel pharmacology and G protein activation profile of mu and delta opioid receptor hetero-oligomers. *J Biol Chem* **280**: 38478–38488.

Ferré S, Ciruela F, Woods AS, Lluis C, Franco R (2007). Functional relevance of neurotransmitter receptor heteromers in the central nervous system. *Trends Neurosci* **30**: 440–446.

Ferré S, Baler R, Bouvier M, Caron MG, Devi LA, Durroux T *et al*. (2009). Building a new conceptual framework for receptor heteromers. *Nat Chem Biol* **5**: 131–134.

Franco R, Canals M, Marcellino D, Ferré S, Agnati L, Mallol J et al. (2003). Regulation of heptaspanning-membrane-receptor function by dimerization and clustering. *Trends Biochem Sci* **28**: 238–243.

Franco R, Casadó V, Mallol J, Ferré S, Fuxe K, Cortés A et al. (2005). Dimer-based model for heptaspanning membrane receptors. *Trends Biochem Sci* **30**: 360–366.

Franco R, Casadó V, Mallol J, Ferrada C, Ferré S, Fuxe K et al. (2006). The two-state dimer receptor model: a general model for receptor dimers. *Mol Pharmacol* **69**: 1905–1912.

Franco R, Casadó V, Cortés A, Ferrada C, Mallol J, Woods A et al. (2007). Basic concepts in G-protein-coupled receptor homo- and heterodimerization. *Sci World J* **7**: 48–57.

Gbahou F, Rouleau A, Morisset S, Parmentier R, Crochet S, Lin JS et al. (2003). Protean agonism at histamine H3 receptors *in vitro* and *in vivo*. *Proc Natl Acad Sci USA* **100**: 11086–11091.

George SR, Fan T, Xie Z, Tse R, Tam V, Varghese G et al. (2000). Oligomerization of mu- and delta-opioid receptors. Generation of novel functional properties. *J Biol Chem* **275**: 26128–26135.

George SR, O'Dowd BF, Lee SP (2002). G-protein-coupled receptor

oligomerization and its potential for drug discovery. *Nat Rev Drug Discov* **1**: 808–820.

Gerfen CR (2004). Basal ganglia. In: Paxinos G (ed.). *The Rat Nervous System*. Elsevier Academis Press: Amsterdam, pp. 445–508.

Giovannini MG, Efoudebe M, Passani MB, Baldi E, Bucherelli C, Giachi F et al. (2003). Improvement in fear memory by histamine-elicited ERK2 activation in hippocampal CA3 cells. *J Neurosci* **23**: 9016–9023.

Gracia E, Cortés A, Meana JJ, García-Sevilla J, Herhsfield MS, Canela EI et al. (2008). Human adenosine deaminase as an allosteric modulator of human A adenosine receptor: abolishment of negative cooperativity for [H](R)-PIA binding to the caudate nucleus. *J Neurochem* **107**: 161–170.

Herrick-Davis K, Grinde E, Harrigan TJ, Mazurkiewicz JE (2005). Inhibition of serotonin 5-hydroxytryptamine 2C receptor function through heterodimerization: receptor dimers bind two molecules of ligand and one G-protein. *J Biol Chem* **280**: 40144–40151.

Jordan M, Schallhorn A, Wurm FM (1996). Transfecting mammalian cells: optimization of critical parameters affecting calcium-phosphate precipitate formation. *Nucleic Acids Res* **24**: 596–601.

Jordan BA, Devi LA (1999). G-protein-coupled receptor heterodimerization modulates receptor function. *Nature* **399**: 697–700.

Kimura K, White BH, Sidhu A (1995). Coupling of human D-1 dopamine receptors to different guanine nucleotide binding proteins. Evidence that D-1 dopamine receptors can couple to both Gs and G(o). *J Biol Chem* **270**: 14672–14678.

Kong MM, Fan T, Varghese G, O'Dowd BF, George SR (2006). Agonist-induced cell surface trafficking of an intracellularly sequestered D1 dopamine receptor homo-oligomer. *Mol Pharmacol* **70**: 78–89.

Leurs R, Bakker RA, Timmerman H, de Esch IJ (2005). The histamine H3 receptor: from gene cloning to H3 receptor drugs. *Nat Rev Drug Discov* **4**: 107–120.

Lovenberg TW, Roland BL, Wilson SJ, Jiang X, Pyati J, Huvar A et al. (1999). Cloning and functional expression of the human histamine H3 receptor. *Mol Pharmacol* **55**: 1101–1107.

Marshall FH (2001). Heterodimerization of G-protein-coupled receptors in the CNS. *Curr Opin Pharmacol* **1**: 40–44.

Milligan G (2006). G-protein-coupled receptor heterodimers: pharmacology, function and relevance to drug discovery. *Drug Discov Today* **11**: 541–549.

Moussa CE, Tomita Y, Sidhu A (2006). Dopamine D1 receptor-mediated toxicity in human SK-N-MC neuroblastoma cells. *Neurochem Int* **48**: 226–234.

Neve KA, Seamans JK, Trantham-Davidson H (2004). Dopamine receptor signaling. *J Recept Signal Transduct Res* **24**: 165–205.

O'Dowd BF, Ji X, Alijaniaram M, Rajaram KD, Kong MM, Rashid A et al. (2005). Dopamine receptor oligomerization visualized in living cells. *J Biol Chem* **280**: 37225–33735.

Pillot C, Heron A, Cochois V, Tardivel-Lacombe J, Ligneau X, Schwartz JC et al. (2002). A detailed mapping of the histamine H(3) receptor and its gene transcripts in rat brain. *Neuroscience* **114**: 173–193.

Pantazopoulos H, Stone D, Walsh J, Benes FM (2004). Differences in the cellular distribution of D1 receptor mRNA in the hippocampus of bipolars and schizophrenics. *Synapse* **54**: 147–155.

Pollard H, Moreau J, Arrang JM, Schwartz JC (1993). A detailed autoradiographic mapping of histamine H3 receptors in rat brain areas. *Neuroscience* **52**: 169–189.

Prinster SC, Hague C, Hall RA (2005). Heterodimerization of G protein-coupled receptors: specificity and functional significance. *Pharmacol Rev* **57**: 289–298.

Rashid AJ, So CH, Kong MMC, Furtak T, El-Ghundi M, Cheng R et al. (2007). D1–D2 dopamine receptor heterooligomers with unique pharmacology are coupled to rapid activation of Gq/11 in the striatum. *Proc Natl Acad Sci USA* **104**: 654–659.

Rios CD, Jordan BA, Gomes I, Devi LA (2001). G-protein-coupled receptor dimerization: modulation of receptor function. *Pharmacol Ther* **92**: 71–87.

Robinson P, Lebel M, Cyr M (2008). Dopamine D1 receptor-mediated aggregation of N-terminal fragments of mutant huntingtin and cell death in a neuroblastoma cell line. *Neuroscience* **153**: 762–772.

Ryu JH, Yanai K, Iwata R, Ido T, Watanabe T (1994). Heterogeneous distributions of histamine H3, dopamine D1 and D2 receptors in rat brain. *Neuroreport* **5**: 621–624.

Sanchez-Lemus E, Arias-Montano JA (2004). Histamine H3 receptor activation inhibits dopamine D1 receptor-induced cAMP accumulation in rat striatal slices. *Neurosci Lett* **364**: 179–184.

Sidhu A, Olde B, Humblot N, Kimura K, Gardner N (1999). Regulation of human D1 dopamine receptor function and gene expression in SK-N-MC neuroblastoma cells. *Neuroscience* **9**: 537–547.

Springael JY, Urizar E, Costagliola S, Vassart G, Parmentier M (2007). Allosteric properties of G protein-coupled receptor oligomers. *Pharmacol Ther* **115**: 410–418.

Terrillon S, Bouvier M (2004). Roles of G-protein-coupled receptor dimerization. *EMBO Rep* **5**: 30–34.

Vilardaga JP, Nikolaev VO, Lorenz K, Ferrandon S, Zhuang Z, Lohse MJ (2008). Conformational cross-talk between alpha2A-adrenergic and mu-opioid receptors controls cell signaling. *Nat Chem Biol* **4**: 126–131.

Zoli M, Agnati LF, Hedlund PB, Li XM, Ferré S, Fuxe K (1993). Receptor-receptor interactions as an integrative mechanism in nerve cells. *Mol Neurobiol* **7**: 293–334.

Supporting Information

Additional Supporting Information may be found in the online version of this article:

Appendix S1

Figure S1 Binding and signalling of wild type or mutant (R3.50A) H_3R in transfected HEK-293 cells. (A, B) HEK-293 cells co-transfected with pTATAlucNEO/CRE121-3 (pTLNC121-3) CRE-luciferase reporter gene, and either the wild type or the mutant version of human H_3R (Arg 132 substituted by Ala; see *Methods*) were treated with a full (R-α-methyl histamine) or an inverse (A-349821) agonist and the activity of the reporter gene was recorded (see *Methods*). (C, D) Binding to membranes from cells transfected with either the wild type or the mutant version of human H_3R were performed by using (see *Methods*) either radiolabelled full (NAMH) or inverse (A-349821) agonists.

Please note: Wiley-Blackwell are not responsible for the content or functionality of any supporting materials supplied by the authors. Any queries (other than missing material) should be directed to the corresponding author for the article.

Marked changes in signal transduction upon heteromerization of dopamine D1 and histamine H3 receptors

Carla Ferrada, Estefanía Moreno, Vicent Casadó, Gerold Bongers, Antoni Cortés, Josefa Mallol, Enric I Canela, Rob Leurs, Sergi Ferré, Carmen Lluís and Rafael Franco (rfranco@ub.edu)

Supporting Information

Generation of a mutant of H_3R (R132A) defective in signal transduction. The human H_3R was cloned from the human male PAC clone RP5-1005F21 with the following primers for the three exons of the receptor: forward primer GCCATGGAGCGCGCGCCGCC and reverse primer CGACGAGGAAGTCGGA were used for exon 1, forward primer TCCGACTTCCTCGTCGGCGCCTTCTGCATCCC and reverse primer CGCTCGGGTGACCGAC were used for exon 2 and forward primer GTCGGTCACCCGAGCGGTCTCATACCGGGCCC and reverse primer ATGGAGCGCGCGCCGCCCGA were used for exon 3. Subsequently, exon 1 and exon 2 were joined by PCR with forward primer AAGGTACCGCCACCATGGAGCGCGCGCCGCCCG and reverse primer CGCTCGGGTGACCGAC and exon 2 and exon 3 were joined by PCR with forward primer TCCGACTTCCTCGTCGGCGCCTTCTGCATCCC and reverse primer AATCTAGATATCTCACTTCCAGCAGTGCTCC. These two fragments were joined by PCR with forward primer AAGGTACCGCCACCATGGAGCGCGCGCCGCCCG and reverse primer AATCTAGATATCTCACTTCCAGCAGTGCTCC. The subsequent fragment was cloned into pcDNA3.1/V5-HisTOPO vector by TOPO TA cloning (Invitrogen, Breda, The Netherlands) and subsequently subcloned into the pCIneo expression vector. The cloned receptor was confirmed to be identical to the published H_3R sequence (GenBank accession number AF140538; see ref. 16 from the main text). The human H_3R R3.50A receptor cDNA was synthesized by HD Bioscience (Shanghai, China) verified by dideoxy sequencing and inserted in pCIneo. Wild type but not the mutant protein was able to signal in response to the full agonists RAMH or the inverse agonist A-349821 as tested by the reporter gene, CRE, activity (Fig. 1 A, B). To test whether the receptor was expressed, binding assays were performed. Cells were scraped from their dishes, centrifuged (3 minutes, 1000 rpm) and pellets were homogenized in 50 mM Tris, pH 7.4 (for N^{α}-[methyl-^{3}H]histamine and [^{3}H]A-349821) for 2 seconds (40 Watt, Labsonic 1510). Cell homogenates (10-20 µg) were incubated for 60 minutes at 25°C with or without competing ligands in a total volume of 200 µl. The incubation was terminated by rapid filtration over polyethylenimine (0.3 %) pretreated Unifilter GF/C filterplates with two subsequent washes with ice cold 50 mM Tris-HCl (pH 7.4). Radioactivity retained on the filter was determined by liquid scintillation counting on the Microbeta Trilux with 25 µl Microscint "O". The H_3R R3.50A mutant was not able to bind the agonist NAMH, but still bound the inverse agonist A-349821 (Fig. 1 C, D). These data are in accordance with the known (in)sensitivity of the N^{α}-[methyl-^{3}H]histamine and [^{3}H]A-349821 binding to G-protein coupling (Witte et al., 2006, *Br J Pharmacol* 148, 657–670) and show that the H_3R R3.50A receptor protein molecule is expressed, but unable to signal.

Reporter-Gene Assay. HEK-293 cells transiently cotransfected with pTATAlucNEO/CRE121-3 (pTLNC121-3) CRE-luciferase reporter gene (Fluhmann et al., 1998; 10 µg/$1\cdot10^6$ cells), pCIneo/hH_3R (2.5 µg/$1\cdot10^6$ cells) (2.5 µg/$1\cdot10^6$ cells) were seeded in 96-well white plates (Greiner Bio-one, Wemmel, Belgium) in serum-free culture medium. After 48 hours, cells were stimulated and assayed for luminescence by aspiration of the medium and the addition of 25 µL/well luciferase assay reagent (0.83 mM ATP, 0.83 mM D-luciferin, 18.7 mM $MgCl_2$, 0.78 µM $Na_2H_2P_2O_7$, 38.9 mM Tris, pH 7.8, 0.39% (v/v) glycerol, 0.03% (v/v) Triton X-100, and 2.6 µM dithiothreitol). After 5 min, luminescence was measured for 1 sec./well on a Victor^2 (PerkinElmer Wallac, Gaithersburg, MD).

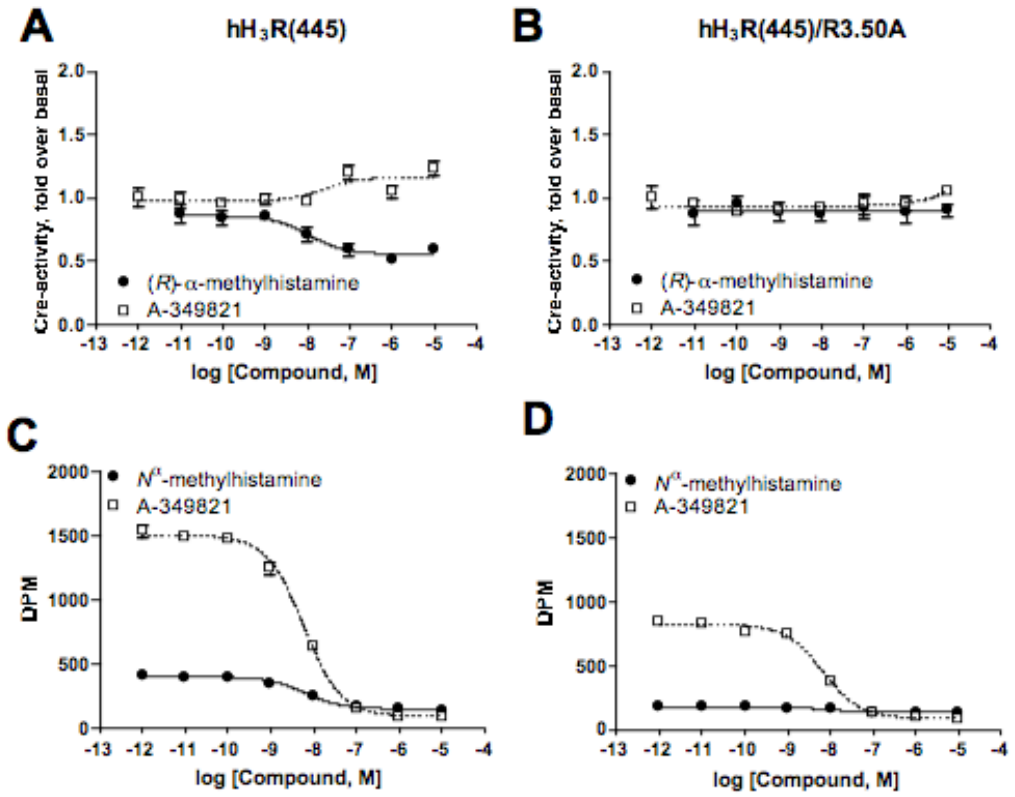

Figure 1
Binding and signalling of wild type or mutant (R3.50A) H_3R in transfected HEK-293 cells. Panels A, B. HEK-293 cells cotransfected with pTATAlucNEO/CRE121-3 (pTLNC121-3) CRE-luciferase reporter gene and either the wild type or the mutant version of human H_3R (Arg 132 substituted by Ala; see Methods) were treated with a full (RAMH) or a inverse (A-349821) agonist and the activity of the reporter gene was recorded (see Methods). Panels C, D. Binding to membranes from cells transfected with either the wild type or the mutant version of human H_3R were performed using (see Methods) either radiolabeled full (NAMH) or inverse (A-349821) agonists.

3.3 Los heterómeros de los receptores de dopamina D_1 e histamina H_3 direccionan de manera selectiva la señalización histaminérgica a la vía de las MAP cinasas en neuronas GABAérgicas de la vía estriatal directa

Estefanía Moreno[‡], Hanne Hoffmann[§¶], Marta Gonzalez-Sepúlveda[§], Gemma Navarro[‡], Vicent Casado´[‡], Antoni Cortés[‡], Josefa Mallol[‡], Michel Vignes[¶], Peter J. McCormick[‡1], Enric I. Canela[‡], Carme Lluís[‡], Rosario Moratalla[‖], Sergi Ferre´[**], Jordi Ortiz[§2], and Rafael Franco[‡ ‡‡2]

[2]Codirectores del manuscrito

[‡]Centro de Investigación Biomédica en Red sobre Enfermedades Neurodegenerativas, y Departamento de Bioquímica y Biología Molecular, Facultad de Biología, Universidad de Barcelona, Diagonal 645, 08028 Barcelona, España,
[§]Instituto de Neurosciencias y Departamento de Bioquímica y Biología Molecular, Facultad de Medicina, Universitat Autónoma de Barcelona, 08193 Bellaterra, España,
[¶]UMR 5247 The Max Mousseron Biomolecules Institute, CNRS, University of Montpellier 1 and 2, University of Montpellier 2, 34095 Montpellier, France,
[‖]Instituto Cajal, Consejo Superior de Investigaciones Científicas, Madrid, España,
[**]the National Institute on Drug Abuse, Intramural Research Program, National Institutes of Health, Department of Health and Human Services, Baltimore, Maryland 21224,
[‡‡]Centro de Investigación Médica Aplicada, Universidad de Navarra, Pio XII 55, 31008 Pamplona, España.

Manuscrito publicado en Journal of Biological Chemistry, (2011 Feb); ***286(7):*** *5846-54.*

Previamente, utilizando modelos celulares heterólogos, identificamos heterómeros entre receptores D_1 o D_2 de dopamina y receptores H_3 de histamina y estudiamos las características bioquímicas de los heterómeros D_1-H_3. En este trabajo hemos ampliado este estudio para demostrar que los heterómeros de los receptores D_1 de dopamina y H_3 de histamina se expresan en el cerebro y sirven para mediar la señalización por la vía de las MAP cinasas (MAPK) en neuronas GABAérgicas de la vía estriatal directa. Utilizando las características bioquímicas descritas previamente, demostramos que la capacidad del receptor H_3 de histamina para activar la vía MAPK fosforilando ERK 1/2 se observa únicamente en cortes estriatales de ratones que expresan los receptores D_1 de dopamina, pero no en ratones deficientes en este receptor. Por otro lado, los antagonistas de los receptores D_1 y H_3 bloquearon la activación de la vía MAPK inducida por cualquiera de los agonistas de los receptores D_1 y H_3 en cortes estriatales. Todos estos resultados muestran la existencia de heterómeros D_1-H_3 en el estriado y lo que es más importante, demuestran que la fosforilación de ERK 1/2 inducida por el agonista del receptor H_3 en cortes estriatales está mediada por heterómeros D_1-H_3. Además, las ERK 1/2 fosforiladas por agonistas del receptor H_3 se detectaron en neuronas que expresaban el receptor D_1, pero no en neuronas que expresaban el receptor D_2. Estos resultados indican que los heterómeros D_1-H_3 funcionan como procesadores que integran las señales de la dopamina y la histamina involucradas en el control de la función de neuronas en la vía estriatal directa.

THE JOURNAL OF BIOLOGICAL CHEMISTRY VOL. 286, NO. 7, pp. 5846–5854, February 18, 2011
Printed in the U.S.A.

Dopamine D_1-histamine H_3 Receptor Heteromers Provide a Selective Link to MAPK Signaling in GABAergic Neurons of the Direct Striatal Pathway*[S]

Received for publication, July 7, 2010, and in revised form, December 16, 2010 Published, JBC Papers in Press, December 20, 2010, DOI 10.1074/jbc.M110.161489

Estefanía Moreno[‡], Hanne Hoffmann[§¶], Marta Gonzalez-Sepúlveda[§], Gemma Navarro[‡], Vicent Casadó[‡], Antoni Cortés[‡], Josefa Mallol[‡], Michel Vignes[¶], Peter J. McCormick[‡1], Enric I. Canela[‡], Carme Lluís[‡], Rosario Moratalla[‖], Sergi Ferré[**], Jordi Ortiz[§2], and Rafael Franco[‡ ‡‡2,3]

From the [‡]Centro de Investigación Biomédica en Red sobre Enfermedades Neurodegenerativas, and Department of Biochemistry and Molecular Biology, Faculty of Biology, University of Barcelona, Diagonal 645, 08028 Barcelona, Spain, the [§]Neuroscience Institute and Department of Biochemistry and Molecular Biology, Faculty of Medicine, Universitat Autónoma de Barcelona, 08193 Bellaterra, Spain, [¶]UMR 5247 The Max Mousseron Biomolecules Institute, CNRS, University of Montpellier 1 and 2, University of Montpellier 2, 34095 Montpellier, France, [‖]Instituto Cajal, Consejo Superior de Investigaciones Científicas, Madrid, Spain, the [**]National Institute on Drug Abuse, Intramural Research Program, National Institutes of Health, Department of Health and Human Services, Baltimore, Maryland 21224, and the [‡‡]Centro de Investigación Médica Aplicada, Universidad de Navarra, Pio XII 55, 31008 Pamplona, Spain

Previously, using artificial cell systems, we identified receptor heteromers between the dopamine D_1 or D_2 receptors and the histamine H_3 receptor. In addition, we demonstrated two biochemical characteristics of the dopamine D_1 receptor-histamine H_3 receptor heteromer. We have now extended this work to show the dopamine D_1 receptor-histamine H_3 receptor heteromer exists in the brain and serves to provide a novel link between the MAPK pathway and the GABAergic neurons in the direct striatal efferent pathway. Using the biochemical characteristics identified previously, we found that the ability of H_3 receptor activation to stimulate p44 and p42 extracellular signal-regulated MAPK (ERK 1/2) phosphorylation was only observed in striatal slices of mice expressing D_1 receptors but not in D_1 receptor-deficient mice. On the other hand, the ability of both D_1 and H_3 receptor antagonists to block MAPK activation induced by either D_1 or H_3 receptor agonists was also found in striatal slices. Taken together, these data indicate the occurrence of D_1-H_3 receptor complexes in the striatum and, more importantly, that H_3 receptor agonist-induced ERK 1/2 phosphorylation in striatal slices is mediated by D_1-H_3 receptor heteromers. Moreover, H_3 receptor-mediated phospho-ERK 1/2 labeling co-distributed with D_1 receptor-containing but not with D_2 receptor-containing striatal neurons. These results indicate that D_1-H_3 receptor heteromers work as processors integrating dopamine- and histamine-related signals involved in controlling the function of striatal neurons of the direct striatal pathway.

The striatum is the main input structure of the basal ganglia, which are subcortical structures involved in the processing of information related to the performance and learning of complex motor acts. It is widely accepted that dopamine receptor subtypes, which are fundamental for motor control and are implicated in numerous neuropsychiatric disorders, are largely segregated in the two subtypes of medium spiny neurons (MSNs),[4] the most populated neuronal type in the striatum. Dopamine D_2 receptors (D_2Rs) are mostly localized in the striatopallidal MSNs, which express the peptide enkephalin and which gives rise to the indirect striatal efferent pathway, whereas dopamine D_1 receptors (D_1Rs) are mostly expressed by the striatonigral MSNs, which express substance P and dynorphin and constitute the direct striatal efferent pathway (1, 2). Dopaminergic drugs activate the ERK transduction pathway, which is involved in basic physiological processes and in synaptic plasticity (3). In the dopamine-depleted striatum, ERK signaling is implicated in the development of L-DOPA-induced dyskinesia. Thus, in dopamine-denervated mice, L-DOPA activates ERK signaling specifically in D_1Rs containing striatonigral MSNs but not in D_2Rs containing striatopallidal MSNs (4). This regulation may result in ERK-dependent changes in striatal plasticity leading to dyskinesia.

Histamine is an important regulatory transmitter in the nervous system involved in the sleep/wake cycle, attention, memory, and other functions. Four histamine receptor types (H_1R–H_4R) have been cloned. H_3Rs are expressed in abundance in the brain and high densities are particularly found in the striatum (5–7). H_3Rs were first identified as autoreceptors (8), but they were later found to act as heteroreceptors (9).

* This study was supported by Grants SAF2008-00146, SAF2008-03229-E, SAF2009-07276, SAF2006-08240, and SAF2009-12510 from the Spanish Ministerio de Ciencia y Tecnología, the Centre National de la Recherche Scintifique, the French Ministry of Research and Higher Education, Red de Transtornos Adictivos RD06/0001/0015, Grant 060110 from Fundació La Marató de TV3 and the Intramural Funds of the National Institute on Drug Abuse.

[S] The on-line version of this article (available at http://www.jbc.org) contains supplemental Fig. 1.

[1] A Ramon y Cajal investigator.

[2] Both authors contributed equally to this article.

[3] To whom correspondence should be addressed: Centro de Investigación Médica Aplicada, University of Navarra, Pio XII, 55, 31008 Pamplona, Italy. Tel.: 34-948194700; Fax: 34-948194715; E-mail: rfranco@unav.es.

[4] The abbreviations used are: MSN, medium spiny neurons; D_2R, dopamine D_2 receptor; H_1R, histamine H_1 receptor; D_1R, dopamine D_1 receptor; RAMH, R(−)-α-methylhistamine dihydrochloride.

The major localization of striatal H_3Rs is postsynaptic (5, 10), and most probably in both subtypes of MSNs (6, 10). Histamine, by means of interactions with striatal H_3Rs, plays an important role in the modulation of dopamine neurotransmission (11–14). At the behavioral level, it was shown that stimulation of postsynaptic H_3R counteracts the motor activation induced by D_1R and D_2R agonists in reserpinized mice (14). These interactions may be related to the ability of H_3Rs to form heteromers with dopamine receptors. In fact, D_1R-H_3R and D_2R-H_3R heteromerization was demonstrated by biophysical techniques in mammalian cells (14, 15). However, their presence in the brain remained to be demonstrated. In addition, if H_3Rs form heteromers with both D_1R and D_2R, is there a functional difference between these two receptor heteromer pairs? One might expect that because the D_1R and D_2R receptors are found in two different neuronal pathways that the different heteromers might confer different properties. Here, we have explored this idea by taking advantage of unique properties of the D_1R-H_3R heteromers to provide evidence for their presence in rodent brain. Previously, using an *in vitro* cell system, we found an important feature of the D_1R-H_3R heteromer is that H_3R agonists only activate ERK 1/2 in a receptor heteromer context, but not in cells expressing H_3Rs without D_1R (15). Here, by taking advantage of this distinct ERK 1/2 signaling characteristic, we demonstrate the occurrence of D_1R-H_3R heteromers in rodent striatum. Despite H_3Rs being expressed in both D_1R and D_2R containing neurons, histamine-receptor-mediated phosphorylation of the ERK 1/2 kinase occurred only in neurons expressing D_1R and not in those with D_2R. Thus, D_1-H_3 receptor heteromers confer a direct link to MAPK activation within the GABAergic neurons of the direct striatal efferent pathway.

EXPERIMENTAL PROCEDURES

Animals—Sprague-Dawley male rats, 7–9 weeks old and weighing 200–250 g, were provided by the Animal Service of the Universidad Autónoma de Barcelona (Barcelona, Spain). Six-to-eight-month-old wild-type littermates and dopamine D_1 receptor knock-out C57BL6 male mice, weighing 25–30 g, were provided by Instituto Cajal (Consejo Superior de Investigaciones Científicas; Madrid, Spain) and generated by homologous recombination as described previously (16). Rats (2 per cage) or mice (five per cage) were housed in a temperature (21 ± 1 °C) and humidity-controlled (55 ± 10%) room with a 12:12 h light/dark cycle (light between 08:00 and 20:00 h) with food and water *ad libitum*. Animal procedures were conducted according to standard ethical guidelines (European Communities Council Directive 86/609/EEC) and approved by the local (Universidad Autónoma de Barcelona or Consejo Superior de Investigaciones Científicas) ethical committee.

Cell Culture and Membrane Preparation—SK-N-MC/H_3 cells were grown in Eagle's minimal essential medium, supplemented with 10% FBS, 50 units/ml penicillin, 50 μg/ml streptomycin, nonessential amino acids, 2 mmol/liter L-glutamine, and 50 μg/ml sodium pyruvate at 37 °C in a humidified atmosphere of 5% CO_2 to 80% confluence. The SK-N-MC cells stably expressing the human H_3R (SK-N-MC/H_3) were provided by Johnson & Johnson Pharmaceutical Research & Development, L.L.C. Cells were disrupted with a Polytron homogenizer (PTA 20 TS rotor, setting 3; Kinematica, Basel, Switzerland) in 50 mM Tris-HCl buffer, pH 7.4, containing a protease inhibitor mixture (1/1000; Sigma). The cellular debris was removed by centrifugation at 13,000 × *g* for 5 min at 4 °C, and membranes were obtained by centrifugation at 105,000 × *g* for 1 h at 4 °C. Membranes were lysed in 50 mM Tris-HCl, pH 7.4, containing 50 mM NaF, 150 mM NaCl, 45 mM β-glycerophosphate, 1% Triton X-100, 20 μM phenylarsine oxide, 0.4 mM $NaVO_4$, and protease inhibitor mixture to be processed by Western blot.

Brain Slice Preparation—Rats and mice were decapitated with a guillotine, and the brains were rapidly removed and placed in ice-cold oxygenated (O_2/CO_2: 95/5%) Krebs-HCO_3^- buffer (124 mM NaCl, 4 mM KCl, 1.25 mM NaH_2PO_4, 1.5 mM $MgCl_2$, 1.5 mM $CaCl_2$, 10 mM glucose, and 26 mM $NaHCO_3$, pH 7.4). The brains were sliced at 4 °C in a brain matrix (Zivic Instruments, Pittsburgh, PA) into 0.5-mm coronal slices. Slices were kept at 4 °C in Krebs-HCO_3^- buffer during the dissection of the striatum. Each slice was transferred into an incubation tube containing 1 ml of ice-cold Krebs-HCO_3^- buffer. The temperature was raised to 23 °C and after 30 min, the medium was replaced by 2 ml Krebs-HCO_3^- buffer (23 °C). The slices were incubated under constant oxygenation (O_2/CO_2: 95/5%) at 30 °C for 4–5 h in an Eppendorf Thermomixer (5 Prime, Inc., Boulder, CO). The media was replaced by 200 μl of fresh Krebs-HCO_3^- buffer and incubated for 30 min before the addition of ligands.

ERK Phosphorylation Assays—Striatal slices were incubated in the presence of the indicated concentrations of histamine H_3 or dopamine D_1 receptor ligands, prepared in Krebs-HCO_3^- buffer. After the indicated incubation period, the solution was discarded, and slices were frozen on dry ice and stored at −80 °C. Slices were lysed by the addition of 500 μl of ice-cold lysis buffer (50 mM Tris-HCl pH 7.4, 50 mM NaF, 150 mM NaCl, 45 mM β-glycerophosphate, 1% Triton X-100, 20 μM phenylarsine oxide, 0.4 mM $NaVO_4$, and protease inhibitor mixture). Cellular debris was removed by centrifugation at 13,000 × *g* for 5 min at 4 °C, and protein was quantified by the bicinchoninic acid method using bovine serum albumin dilutions as standard. To determine the level of ERK1/2 phosphorylation, equivalent amounts of protein (10 μg) were separated by electrophoresis on a denaturing 10% SDS-polyacrylamide gel and transferred onto PVDF-FL membranes. Odyssey blocking buffer (LI-COR Biosciences, Lincoln, Nebraska) was then added, and membranes were rocked for 90 min. Membranes were then probed with a mixture of a mouse antiphospho-ERK 1/2 antibody (1:2500, Sigma) and rabbit anti-ERK 1/2 antibody (1:40,000, Sigma) for 2–3 h. The 42 and 44 kDa bands corresponding to ERK 1 and ERK 2 were visualized by the addition of a mixture of IRDye 800 (anti-mouse) antibody (1:10,000, Sigma) and IRDye 680 (anti-rabbit) antibody (1:10,000, Sigma) for 1 h and scanned by the Odyssey infrared scanner (LI-COR Biosciences). Bands densities were quantified using the scanner software and exported to Microsoft Excel. The level of phosphorylated ERK 1 and phosphorylated ERK 2 was normalized for differences in loading using the total ERK 1/2 protein band intensities.

Immunohistochemistry—Striatal slices were incubated with the indicated H_3R ligands in Krebs-HCO_3^- buffer for 10 min and fixed with 4% paraformaldehyde solution (Antigenfix, DiaPath) for 1 h at room temperature with gentle agitation. The slices were then washed in TBS (50 mM Tris-HCl, 0.9% NaCl, pH 7.8), treated 5 min with 1% Na_2BH_4 dissolved in TBS, followed by successive TBS washes until all Na_2BH_4 was eliminated. Finally, the slices were cryopreserved in a 30% sucrose solution overnight at 4 °C and stored at −20 °C until sectioning. 15-μm-thick coronal sections were cut on a freezing cryostat (Leica Jung CM-3000) and mounted on slide glass (three control and three treated coronal sections in each slide; STAR FROST PLUS, DELTALAB). Coronal sections were thawed at 4 °C, washed in TBS, and rocked in 7% normal donkey serum (SND, Sigma) in TBS for 1 h at 37 °C in a humidified atmosphere. Coronal sections were then incubated overnight at 4 °C in a humidified atmosphere with the primary antibodies: rabbit antiphospho-Thr^{202}/Tyr^{204} ERK 1/2 antibody (1:300, Cell Signaling Technology, Danvers, MA), guinea pig anti-D_1 antibody (1:100, Frontier Institute, Ishikari, Hokkaido, Japan) or guinea pig anti-D_2 antibody (1:100, Frontier Institute, Ishikari, Hokkaido, Japan) alone or in combination in a solution with 0.1% TBS-Tween, 0.1% BSA-acetylated (Aurion), 7% SND (250 μl per slide). The specificity of these dopamine receptor antibodies has been previously shown by preabsorption tests with the antigen peptides and by mutually exclusive pattern and triple labeling in immunohistochemistry (17) and by Western blot (see "Results"). Coronal sections were washed in 0.05% TBS-T and left for 2 h at room temperature in a humidified atmosphere with the corresponding secondary antibodies: chicken anti-rabbit (1:200, Alexa Fluor 594, Invitrogen) and goat anti-guinea pig (1:200, Alexa Fluor 488, Invitrogen) in a solution with TBS-Tween 0.1%, BSA acetylated 0.1%, SND 7%, and then washed in TBS-T 0.05%, followed by a single wash in TBS before mounting in Mowiol medium (Calbiochem), covered with a glass, and left to dry at 4 °C for 24 h. Single and double immunostained slices were observed and imaged in a Leica SP2 confocal microscope (Leica Microsystems, Mannheim, Germany). Images were opened and processed with ImageJ confocal microscopy program and a Adobe Photoshop program (version 5.5; Seattle, WA). Double-labeled cells (cells stained for phospho-ERK 1/2 and D_1 or D_2 receptors) were counted in a total of two to three nonoverlapping fields of 45 coronal sections from 4 to 5 slices treated with medium (control), 1 μM RAMH, or 1 μM imetit.

Coronal sections from nontreated slices (six control coronal sections in each slide) were used for double-immunohistochemistry using rabbit anti-H_3R antibody (1:200, Chemicon, Billerica, MA) and guinea pig anti-D_1R antibody or guinea pig anti-D_2R antibody as primary antibodies and goat anti-rabbit-peroxidase (1:200, Thermo Scientific, Fremont, CA) and goat anti-guinea pig (1:200, Alexa Fluor 488, Invitrogen) as secondary antibodies by the same procedure as described above. In this case, the amplification system for the red fluorophore, TSA-cyanine 3 (1:100, Tyramide Signal Amplification, PerkinElmer Life Science) was used as described in the TSA Plus fluorescence amplification kit, before mounting in Mowiol medium. Double-labeled cells (cells stained for H_3 and D_1 or D_2 receptors) were counted in a total of two to three nonoverlapping fields of 15 coronal sections from four to five slices. In all cases, we did not observe staining in the absence of the primary antibodies.

Coimmunoprecipitation—The rat striatal tissue was disrupted with a Polytron homogenizer in 50 mM Tris-HCl buffer, pH 7.4, containing a protease inhibitor mixture (1/1000, Sigma). The cellular debris was removed by centrifugation at 13,000 × *g* for 5 min at 4 °C, and membranes were obtained by centrifugation at 105,000 × *g* for 1 h at 4 °C. Membranes were washed two more times at the same conditions and were solubilized by homogenization in ice-cold immunoprecipitation buffer (phosphate-buffered saline, pH 7.4, containing 1% (v/v) Nonidet P-40) and incubated for 30 min on ice before centrifugation at 105,000 × *g* for 1 h at 4 °C. The supernatant (1 mg/ml of protein) was processed for immunoprecipitation as described in immunoprecipitation protocol using a Dynabeads® Protein G kit (Invitrogen). Protein was quantified by the bicinchoninic acid method (Pierce) using bovine serum albumin dilutions as standard. Immunoprecipitates were carried out with rat anti-D_1 receptor antibody (1:1000, Sigma) or rabbit anti-D_2 receptor antibody (1:1000, Millipore, Billerica, MA) As negative control anti-calnexin antibody was used (1:1000, BD Biosciences Pharmingen). Immunoprecipitates were separated on a denaturing 10% SDS-polyacrylamide gel and transferred onto PVDF membranes. Membranes were proved with the primary antibodies guinea pig anti-D_1 antibody (1:1000, Frontier Institute, Ishikari, Hokkaido, Japan), guinea pig anti-D_2 antibody (1:1000, Frontier Institute) or goat anti-H_3R antibody (1:500, Santa Cruz Biotechnology, Santa Cruz, CA) and the secondary antibodies goat anti-guinea pig-peroxidase (1:20,000, Sigma) and donkey anti-goat-peroxidase (1:20,000, Jackson ImmunoResearch Laboratories, West Grove, PA). Bands were visualized with a LAS-3000 (Fujifilm). Analysis of detected bands was performed by Image Gauge software (version 4.0) and Multi Gauge software (version 3.0).

RESULTS

D_1R and H_3R Are Functionally Coupled to MAPK Signaling Pathway in Brain Striatal Slices—To establish whether D_1R and H_3R are functionally coupled to the MAPK pathway in rat striatum, slices were treated with a D_1R or an H_3R agonist, and ERK 1/2 phosphorylation was assayed as described under "Experimental Procedures." The time response curve obtained after treatment with 10 μM SKF 38393 (D_1R agonist) or 0.1 μM imetit (H_3R agonist) showed that phosphorylation peaked at 10 min (Fig. 1*a*). Therefore, all subsequent assays were analyzed at 10 min of drug treatment. Dose-response curves for different D_1R or H_3R agonists are displayed in Fig. 1*b*. Both SKF 81297 and SKF 38393 (full and partial D_1R agonists, respectively) were able to increase ERK 1/2 phosphorylation; SKF 81297 was more potent than SKF 39393. RAMH and imetit (H_3R agonists) also increased ERK 1/2 phosphorylation, with imetit being more potent than RAMH. The results show that striatal slices contain D_1R and H_3R functionally coupled to MAPK signaling.

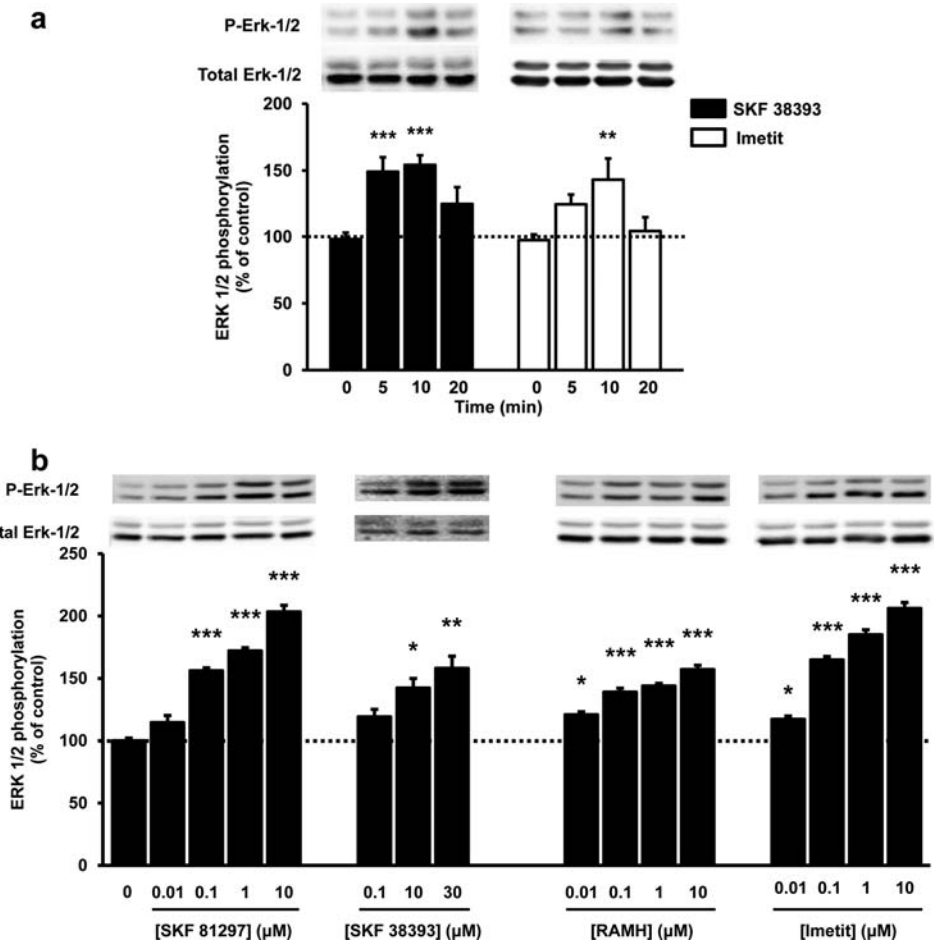

FIGURE 1. **H_3R and D_1R agonists induced ERK 1/2 phosphorylation in rat striatal slices.** *a*, slices were treated with 10 μM SKF 38393 (*black*) or 1 μM imetit (*white*). *b*, slices were treated for 10 min with different SKF 81297, SKF 38393, RAMH, or imetit concentrations. ERK 1/2 phosphorylation was determined as described under "Experimental Procedures." The immunoreactive bands from five to 27 (*a*) or 19 to 24 (*b*) slices obtained from three to 14 (*a*) or six to nine (*b*) animals were quantified, and values represent the mean ± S.E. of the percentage of phosphorylation relative to basal levels of untreated slices (100%). Significant differences were calculated by one-way analysis of variance with post hoc Bonferroni's multiple tests and *, **, and *** correspond to $p < 0.05$, $p < 0.01$, and $p < 0.001$, respectively, as compared with nontreated samples (control). A representative Western blot is shown in each panel (*top*).

H_3R Agonist-induced ERK 1/2 Phosphorylation in Striatal Slices Is Mediated by D_1R-H_3R Heteromers—A cross-antagonism between D_1Rs and H_3Rs has been demonstrated previously in heterologous cell systems. This cross-antagonism only occurs in D_1R-H_3R-heteromer-containing cells and consists of both the ability of D_1R antagonists to block the effect of H_3R agonists and, conversely, the ability of H_3R antagonists to block the effect of D_1R agonists (15). To test whether this phenomenon also occurs *in vivo*, rat striatal slices were incubated with D_1R or H_3R agonists (SKF 81297 or RAMH, respectively) in the presence of either D_1R or H_3R antagonists (SCH 23390 or thioperamide, respectively). The results reproduced the cross-antagonism found in the heterologous cell system (Fig. 2). ERK 1/2 phosphorylation induced by RAMH (0.1 μM) was not only blocked by thioperamide (10 μM) but also by SCH 23390 (10 μM) (Fig. 2*a*). Similarly, ERK 1/2 phosphorylation induced by SKF 81297 (0.1 μM) was blocked by both SCH23390 and thioperamide (10 μM in both cases) (Fig. 2*b*). As a control, activation of striatal serotonin receptors (with 0.2 μM of serotonin) significantly induced ERK 1/2 phosphorylation, but the effect was not modified by either SCH23390 or thioperamide (10 μM in both cases) (Fig. 2, *c* and *d*). These results provide evidence for the expression D_1R-H_3R heteromers in the striatum. Another characteristic of the D_1R-H_3R heteromer is that it allows H_3R agonists to activate MAPK signaling (15). We decided to investigate whether this heteromer characteristic persisted *in vivo* using transgenic mice lacking D_1Rs. When H_3R-mediated MAPK signaling was investigated in striatal slices from transgenic mice lacking the D_1Rs and in wild-type littermate controls displaying the same genetic background, RAMH (0.1 μM) was unable to induce ERK 1/2 phosphorylation, whereas a strong signal was obtained in slices from wild-type littermate controls displaying the same genetic background (Fig. 3). In addition in wild-type animals, RAMH-induced ERK 1/2 phosphorylation was blocked by both thioperamide (10 μM) and SCH 23390 (10 μM) (Fig. 3). These results indicate that H_3R agonist-induced ERK 1/2 phosphorylation in striatal slices is mediated by D_1R-H_3R heteromers.

To provide further insight on the function of striatal D_1R and H_3R receptors coexpressed in striatal neurons, ERK 1/2

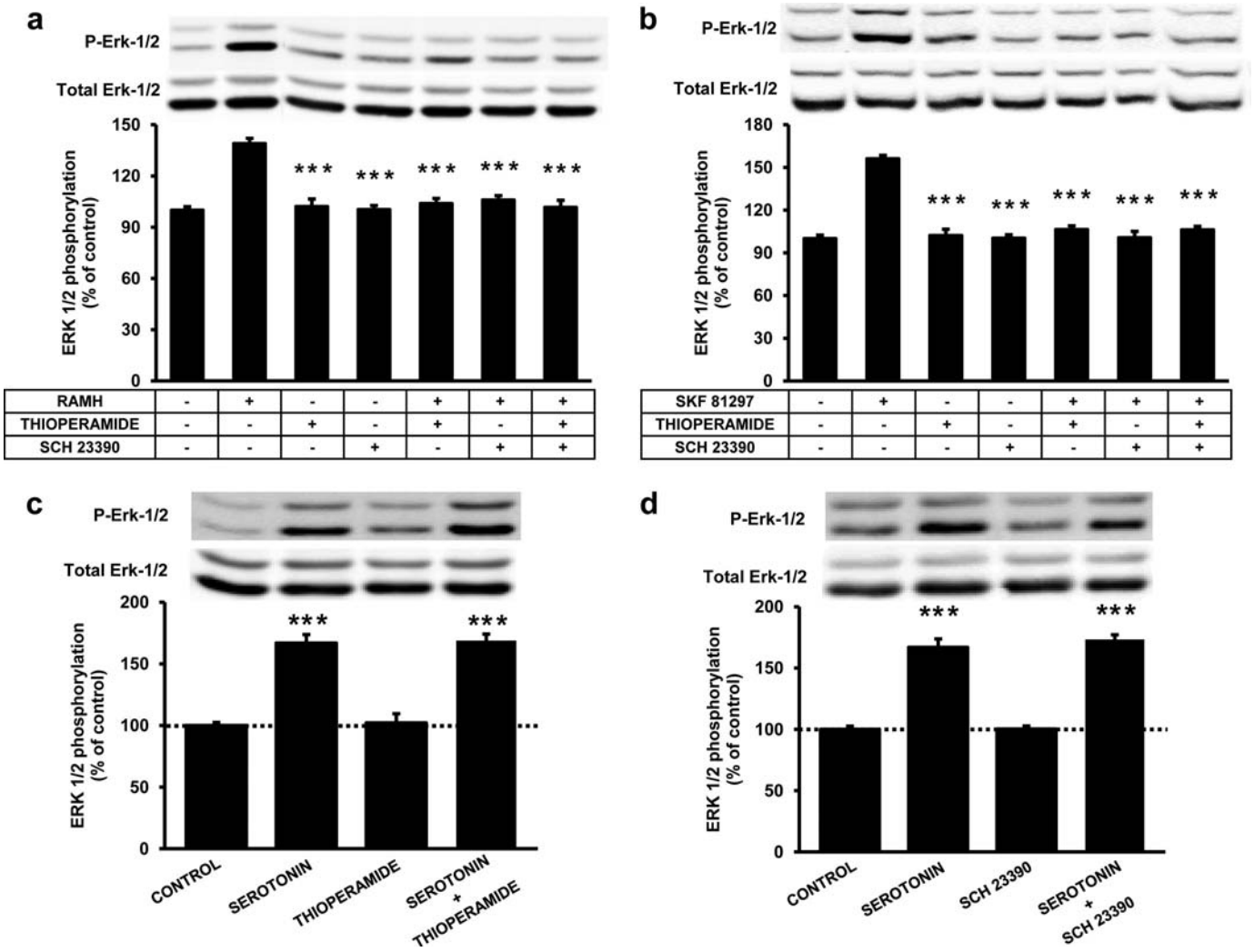

FIGURE 2. **Effect of H_3R and D_1R antagonists on agonist-induced ERK 1/2 phosphorylation in rat striatal slices.** Slices were preincubated with medium or with 10 μM thioperamide, 10 μM SCH 23390, or both for 20 min prior to the addition of 0.1 μM RAMH (*a*) or 0.1 μM SKF 81297 (*b*) followed by a further incubation of 10 min. In *c* and *d*, slices were preincubated for 20 min with medium or with 10 μM thioperamide (*c*) or 10 μM SCH 23390 (*d*) prior to the addition of 0.2 μM serotonin followed by a further incubation of 10 min. ERK1/2 phosphorylation was determined as described under "Experimental Procedures." The immunoreactive bands from 12 to 21 (*a* and *b*) or 10 to 14 (*c* and *d*) slices obtained from 8 to 10 (*a* and *b*) or 4 to 6 (*c* and *d*) animals were quantified, and values represent the mean ± S.E. of the percentage of phosphorylation relative to basal levels found in untreated slices (100%). Significant differences were calculated by one-way analysis of variance with post hoc Bonferroni's multiple tests (***, $p < 0.001$, as compared with the first treatment in *a* and *b*, or to the basal in *c* and *d*). A representative Western blot is shown in each panel (*top*).

activation was studied in rat striatal slices in the presence of agonists for the two receptors. This would mimic the situation when the two neurotransmitters histamine and dopamine are simultaneously impacting a given GABAergic neuron. Interestingly, the effect of the D_1R agonist SKF 81297 (10 μM) was significantly counteracted by the H_3R agonist, RAMH (1 μM). Furthermore, the combination of RAMH (10 μM) and SKF 81297 (1 μM) produced a significantly weaker effect than that of either drug alone (Fig. 4), indicating the existence in striatal neural circuits of an agonist-induced D_1R-H_3R reciprocal negative cross-talk.

Selective D_1R-H_3R Heteromer-mediated Effects only in Striatal Neurons of Direct Pathway—Dopamine receptors are segregated in the two main types of GABAergic striatal efferent neurons: dynorphinergic neurons of the direct pathway expressing D_1Rs and enkephalinergic neurons of the indirect pathway expressing dopamine D_2Rs. Evidence supporting the presence of H_3R in both types of neurons had been obtained previously by autoradiography and lesion studies (5) and by *in situ* hybridization (10). Accordingly, by double immunohistochemistry using H_3R and either D_1R or D_2R antibodies, we found H_3R immunostaining in cells labeled with either D_1R or D_2R antibodies (Fig. 5). In fact, 95 ± 12% of D_1R stained neurons or 89 ± 15% of D_2R stained neurons showed H_3R staining (Fig. 6*a*). Thus, co-expression of D_1R and H_3R in GABAergic neurons of the direct pathway and co-expression of D_2R and H_3R in GABAergic neurons of the indirect pathway was found. We have described previously that both D_1R and D_2R may form heteromers with H_3R in living cells (14, 15). To test D_1R-H_3R and D_2R-H_3R heteromer expression in the rat striatum, co-immunoprecipitation experiments were carried out. The immunoprecipitates with the anti-D_1R antibody (Fig. 7*a*) or with the anti-D_2R antibody (Fig. 7*b*) were not stained in a Western blot using anti-D_2R or anti-D_1R anti-

bodies respectively, showing the specificity of the antibodies. Interestingly, specific H_3R staining was detected by Western blot in both immunoprecipitates using anti-D_1R or anti-D_2R antibodies but not with an irrelevant antibody (Fig. 7*c*). These results corroborate the expression of D_1R-H_3R heteromers in the neurons of the direct pathway and suggest the expression of D_2R-H_3R heteromers in the neurons of the indirect pathway.

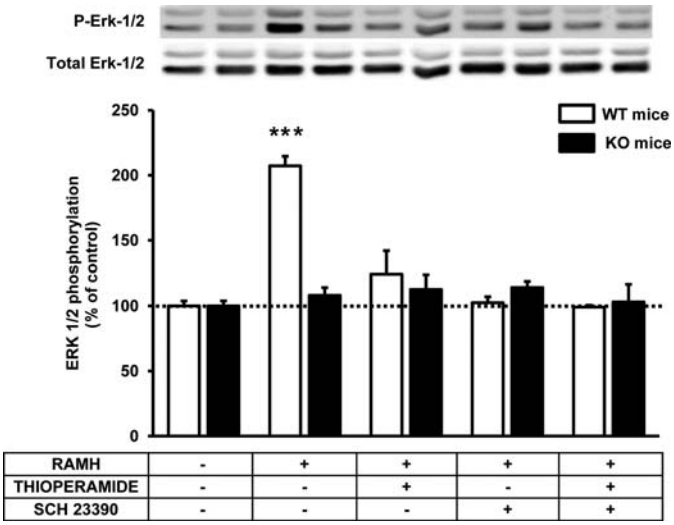

FIGURE 3. **H_3R agonist-induced ERK 1/2 phosphorylation in striatal slices from wild-type and dopamine D_1R knock-out mice.** Wild-type (*white*) or D_1R knock-out mice (*black*) slices were treated for 10 min with 0.1 μM RAMH or for 10 min with 10 μM thioperamide and/or 10 μM SCH 23390 prior to the addition of 0.1 μM RAMH and incubation for further 10 min. ERK 1/2 phosphorylation was determined as described under "Experimental Procedures." For each treatment, the immunoreactive bands from four to six slices from a total six wild-type and nine knock-out animals were quantified, and values represent the mean ± S.E. of the percentage of phosphorylation relative to basal levels found in untreated slices (100%). No significant differences were obtained between the basal levels of the wild-type and the D_1R knock-out mice, and no significant differences were observed between basal and slices treated (20 min) with 10 μM thioperamide or 10 μM SCH 23390. Significant treatment and genotype effects were analyzed by a bifactorial analysis of variance followed by post hoc Bonferroni's tests. There were significant genotype, treatment, and interaction effects, explained by the ability of RAMH to strongly and selectively induce ERK 1/2 phosphorylation in wild-type mice (***, $p < 0.001$, as compared with knock-out mice). A representative Western blot is also displayed (*top*).

In striatal slices incubated with 1 μM imetit and subjected to immunohistochemistry, we observed that imetit-induced ERK 1/2 phosphorylation occurs in a high number of neurons stained using the anti-D_1R antibody, but only in a small number of neurons stained using the anti-dopamine D_2R antibody (Fig. 8). In fact, 85 ± 7% of phospho-ERK 1/2-positive neurons displayed specific D_1 receptor immunostaining, whereas only 23 ± 5% of phospho-ERK 1/2-positive neurons were positive for D_2 receptor labeling (Fig. 6*b*). It should be noted that despite D_2R-H_3R heteromers may play a role in this signaling pathway, neurons containing both the D_1R and D_2R may exist in the striatum (18). Similar results were obtained in striatal slices incubated with 1 μM RAMH (results not shown). Furthermore, the effect of H_3R agonists in striatal slices was independent of changes in presynaptic neurotransmitter release (*e.g.* dopamine or histamine), which could potentially contribute to trigger ERK 1/2 phosphorylation in D_1R-expressing cells. In fact, the presence of 1 μM tetrodotoxin affected neither the D_1R agonist nor the H_3R agonist-induced ERK 1/2 phosphorylation (supplemental Fig. 1). Collectively, these results demonstrate that histamine-induced MAPK pathway activation in striatal slices is specifically mediated by the D_1R and H_3R heteromers present in neurons of the direct pathway, but not by the H_3Rs localized in the indirect pathway or as autoreceptors or heteroceptors in neighboring nerve terminals.

DISCUSSION

We have previously described that not only D_1R but also D_2R may form heteromers with H_3R in living cells (14, 15). Here, it is demonstrated that both D_1R and D_2R co-immunoprecipitate H_3R from rat striatum supporting the expression

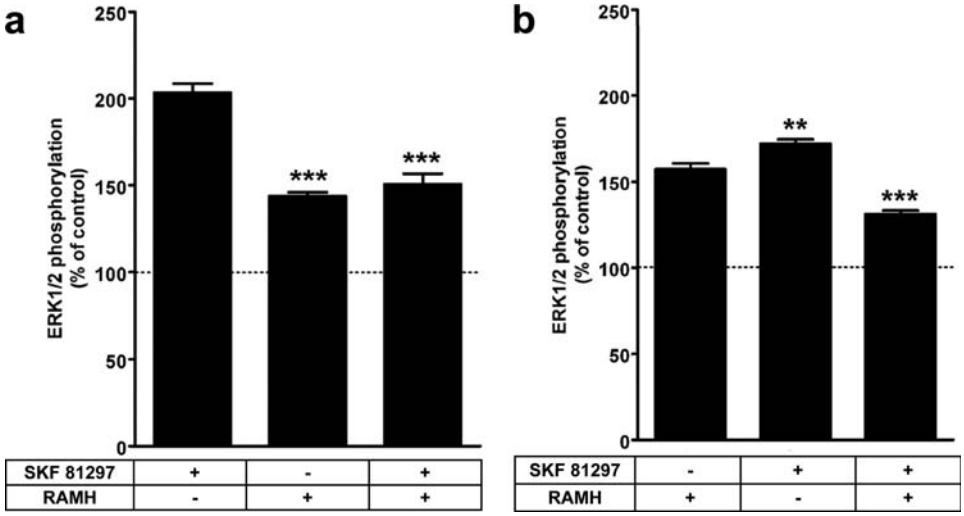

FIGURE 4. **Negative cross-talk between D_1Rs and H_3R receptors on ERK 1/2 phosphorylation in rat striatal slices.** Slices were treated for 10 min with 10 μM SKF 81297 and/or 1 μM RAMH (*a*) or 10 μM RAMH and/or 1 μM SKF 81297 (*b*). ERK 1/2 phosphorylation was determined as described under "Experimental Procedures." The immunoreactive bands from 10 to 24 (*a*) or eight to 23 (*b*) slices obtained from four to six animals were quantified, and values represent the mean ± S.E. of the percentage of phosphorylation relative to basal levels found in untreated slices (100%). Significant differences were calculated by one-way analysis of variance with post hoc Bonferroni's multiple tests. (** and ***, $p < 0.01$ and $p < 0.001$, respectively, as compared with 10 μM SKF 81297 in (*a*) or 10 μM RAMH in (*b*)).

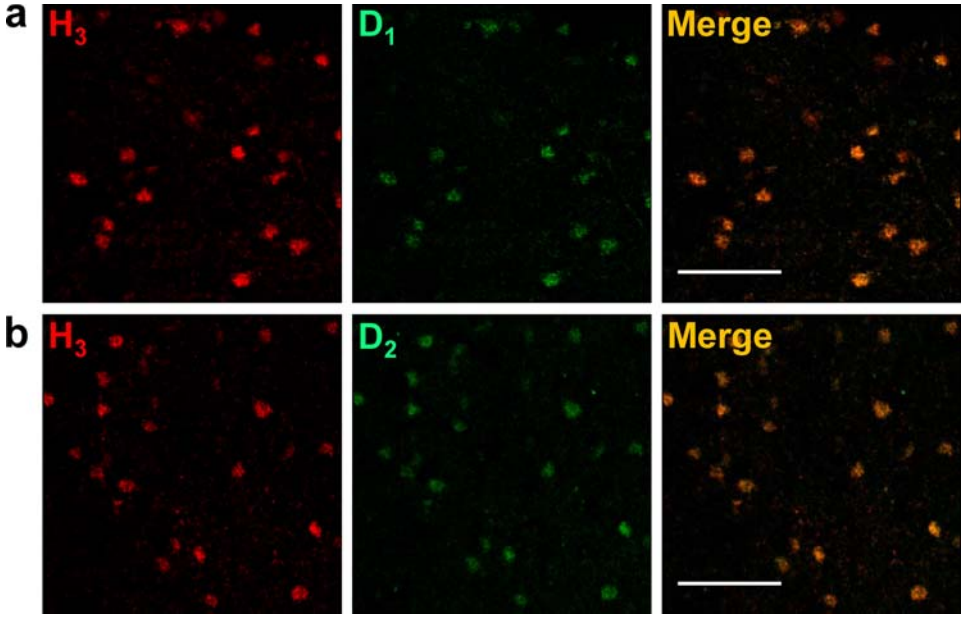

FIGURE 5. **Co-localization between H_3R and D_1R or D_2R in striatal MSNs.** Confocal microscope representative images of coronal sections from striatal slices are shown. Slices were labeled with anti-H_3R antibody (*red*). Labeling (*green*) using an anti-D_1R antibody (*a*) or an anti-D_2R antibody (*b*) is also shown. In *a* and *b*, colocalization is shown in *yellow*. *Scale bars*, 60 μm.

of D_1R-H_3R and D_2R-H_3R heteromers in the neurons of the direct and indirect striatal efferent pathways, respectively. From our earlier work, it was unclear whether D_1R-H_3R and D_2R-H_3R heteromers were engaging similar signaling pathways in the two different neuronal populations or whether there was a functional difference that might help delineate the direct and indirect pathways of the striatum via the existence of these heteromers. The data presented in this paper indicate that D_1R-H_3R heteromers in the striatonigral GABAergic neurons of the direct pathway, but not the H_3R receptors in the indirect pathway, allow direct histaminergic activation of the MAPK pathway.

Biophysical techniques can provide strong support for the existence of receptor heteromers in artificial cell systems (19, 20), but, as these techniques are difficult to perform in intact tissues, obtaining evidence for naturally occurring heteromer expression remains a significant challenge. For many receptor heteromers, we depend on an indirect approach for their identification in native tissues, which relies on the discovery of a characteristic signature of the heteromer. This characteristic, which is usually identified in a heterologous cell system, may be then used as a "fingerprint" to demonstrate the presence of the heteromer in the native tissue (21–24). A specific characteristic of the D_1R-H_3R heteromer, previously identified in transfected cells is cross-antagonism (15), *i.e.* the ability of both D_1R and H_3R antagonists to block the effect of either D_1R or H_3R agonists. This phenomenon, in which an antagonist of one of the receptor units in the receptor heteromer blocks signaling originated by ligand binding to the other receptor unit in the heteromer, has also been observed with other receptor heteromers, such as the cannabinoid CB_1-orexin OX_1 receptor heteromer (25). Significantly, the same D_1R-H_3R cross-antagonism on MAPK signaling, which was described in transfected cells (15), was observed in rat striatal slices (Fig. 2), strongly supporting the occurrence of D_1R-H_3R heteromers in the rodent striatum. Of note, a further characteristic of the D_1R-H_3R heteromer is its ability to allow the activation of the MAPK cascade by H_3R-selective agonists, which otherwise cannot drive this signaling pathway (15). In fact, H_3R agonist-induced ERK 1/2 phosphorylation was demonstrated in striatal slices of wild-type but not of D_1R knockout mice, indicating the occurrence of D_1R-H_3R heteromers in the rodent striatum. As the H_3R agonist was unable to activate MAPK signaling in slices from D_1R-deficient mice (Fig. 3) it is likely that only neurons containing both H_3R and D_1R are able to link histaminergic neurotransmission to the MAPK cascade. Interestingly, although H_3R were found to be co-expressed with D_1R- and D_2R-containing neurons, the H_3R-mediated phospho-ERK labeling only co-distributed with D_1R- but not with D_2R-containing neurons (Figs. 5 and 8) and was not dependent on neurotransmitter release from neighboring cells.

The results obtained with co-administration of D_1R and H_3R agonists suggest that the D_1R-H_3R heteromer works as a processor that integrates dopamine and histamine-related signals, and its output consists of quantitatively different activation of the MAPK pathway. Strong MAPK signaling was obtained with either D_1R or H_3R activation, but a significantly weaker MAPK signaling was obtained upon co-activation of both receptors. Thus, at very low dopamine concentrations, histamine can foster MAPK signaling by activating H_3Rs in D_1R-H_3R-coexpressing neurons. In contrast, when the two neurotransmitters are present, the MAPK activation in the striatonigral MSN would be repressed. Because the MAPK pathway is considered critical to activity-dependent changes underlying synaptic strengthening (26), our results predict that not only dopamine but also histamine plays an important role in MAPK-dependent neuroplasticity in the striatonigral MSN.

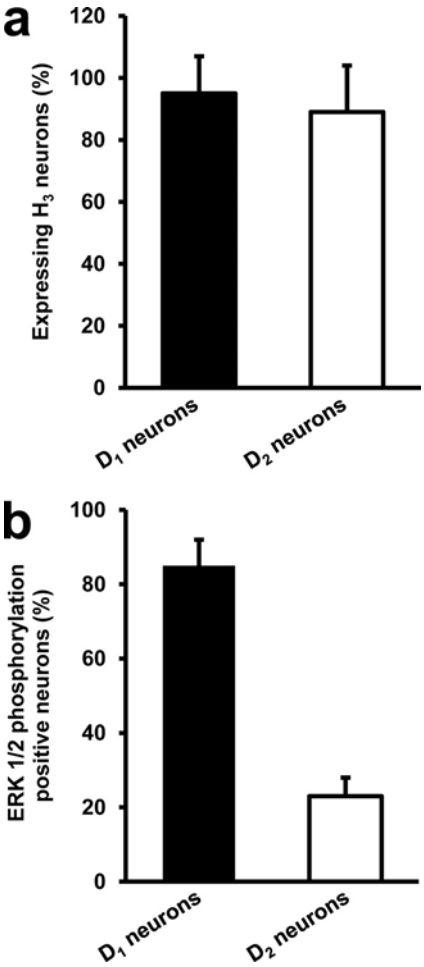

FIGURE 6. **Quantification of colocalization in confocal microscope images.** Quantification of H_3R expression (*a*) or 1 μM imetit-induced ERK 1/2 phosphorylation (*b*) in neurons expressing D_1R (D_1 neurons) or D_2R (D_2 neurons). Values are mean ± S.E. of the percentage of double-labeled cells (cells stained for $H_3R$and D_1Ror D_2R in *a* or cells stained for imetit-induced phospho-ERK 1/2 and D_1Ror D_2R in *b*) were counted in a total of two to three nonoverlapping fields of 15 (*a*) or 45 (*b*) coronal sections from four to five slices.

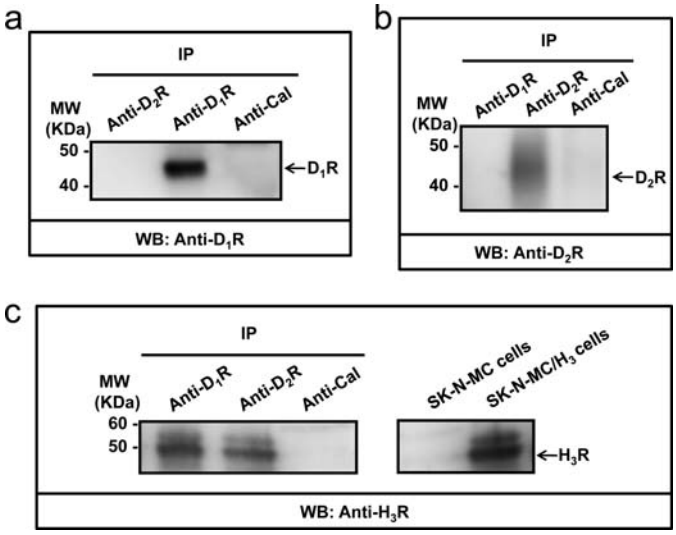

FIGURE 7. **Co-immunoprecipitation of H_3R and D_1R or D_2R.** Rat striatal membranes were solubilized and processed for immunoprecipitation as described under "Experimental Procedures" using rat anti-D_1R antibody, rabbit anti-D_2R antibody, or rabbit anti-calnexin antibody as negative control. As positive controls and to test the specificity of dopamine receptors antibodies, immunoprecipitates were analyzed by SDS-PAGE and immunoblotted using guinea pig anti-D_1R antibody (*a*) or guinea pig anti-D_2R antibody (*b*). To test the co-immunoprecipitation, immunoprecipitates were blotted with goat anti-H_3R antibody (*c*). The *right panel* in *c* corresponds to solubilized membranes from SK-N-MC and SK-N-MC/H_3 cells analyzed by SDS-PAGE and blotted with anti-H_3R antibody to test the specificity of the antibody. *IP*, immunoprecipitation; *MW*, molecular mass.

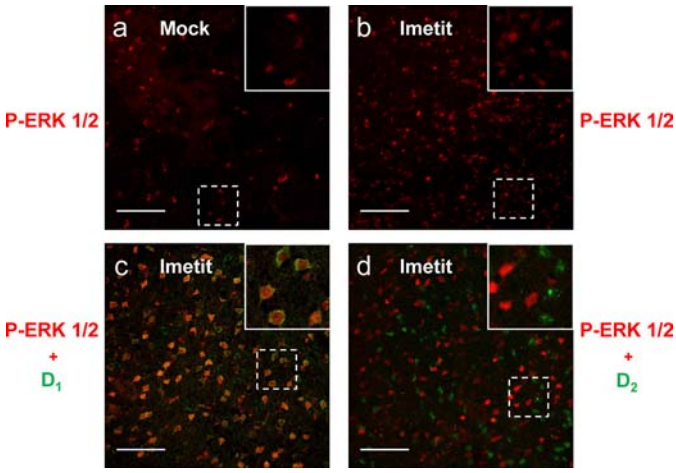

FIGURE 8. **Imetit-induced ERK 1/2 phosphorylation in rat striatal GABAergic neurons.** Confocal microscopy images of coronal sections from striatal slices were treated with medium (*a*) or treated with 1 μM imetit (*b*–*d*). Slices were labeled with antiphospho-ERK 1/2 antibody (*red*). Labeling (*green*) using an anti-D_1 receptor antibody (*c*), or an anti-D_2 receptor antibody (*d*) is also shown. *Insets* in *c* and *d* are 2× magnification of the indicated parts of the figure. *Scale bars*, 100 μm (*a* and *b*) or 80 μm (*c* and *d*). Representative images of coronal sections are displayed.

A negative cross-talk between striatal D_1R and H_3R has also been described for the adenylyl cyclase-induced signaling pathway, as histamine H_3R activation inhibits D_1R-mediated cAMP accumulation in striatal slices (27). Additional examples of H_3R-mediated responses able to inhibit D_1R-mediated effects are the ability of H_3R agonists to inhibit the effects of D_1R agonists on GABA release in striatal slices (12) and motor activation in reserpinized mice (14). Overall, these results are consistent with an antagonism at the level of adenylyl cyclase between H_3R and D_1R that would not require heteromer formation. In fact, it is known that H_3R and D_1R couple to G_i and G_s, respectively (9, 28–30). Although it is difficult to confirm these results in living animals, studies in transfected cells indicate that D_1R-H_3R heteromers couple to G_i, but not to G_s, to direct histaminergic input toward the MAPK pathway.

Taken together, it appears that histamine and dopamine antagonism mediated by D_1Rs and H_3Rs may rely on balancing ERK activation in GABAergic neurons where D_1R and H_3R are co-expressed and where D_1R-H_3R heteromerization is likely occurring. Heteromers not only allow neurons to differentially "sense" a given neurotransmitter, but they serve to process the different signals impacting them at a given time frame (31, 32). Therefore D_1R-H_3R receptor heteromers would be actively involved in controlling the response of striatal neurons of the direct striatal efferent pathway. The qualitative and quantitative output on ERK 1/2 phosphorylation would largely depend on the concentrations of histamine and dopamine impacting neurons expressing D_1R-H_3R complexes.

Acknowledgments—We acknowledge the technical help obtained from Jasmina Jiménez (Molecular Neurobiology Laboratory, Barcelona University) and Mar Castillo (Neuroscience Institute, Universidad Autónoma de Barcelona).

REFERENCES

1. Albin, R. L., Young, A. B., and Penney, J. B. (1995) *Trends Neurosci.* **18,** 63–64
2. Gerfen, C. R. (2004) in *The Rat Nervous System* (Paxinos G., ed) pp. 445–508, Elsevier Academic Press, Amsterdam
3. Thomas, G. M., and Huganir, R. L. (2004) *Nat. Rev. Neurosci.* **5,** 173–183
4. Santini, E., Alcacer, C., Cacciatore, S., Heiman, M., Hervé, D., Greengard, P., Girault, J. A., Valjent, E., and Fisone, G. (2009) *J. Neurochem.* **108,** 621–633
5. Ryu, J. H., Yanai, K., Iwata, R., Ido, T., and Watanabe, T. (1994) *Neuroreport* **5,** 621–624
6. Pillot, C., Heron, A., Cochois, V., Tardivel-Lacombe, J., Ligneau, X., Schwartz, J. C., and Arrang, J. M. (2002) *Neuroscience* **114,** 173–193
7. Hamill, T. G., Sato, N., Jitsuoka, M., Tokita, S., Sanabria, S., Eng, W., Ryan, C., Krause, S., Takenaga, N., Patel, S., Zeng, Z., Williams, D., Jr., Sur, C., Hargreaves, R., and Burns, H. D. (2009) *Synapse* **63,** 1122–1132
8. Arrang, J. M., Garbarg, M., and Schwartz, J. C. (1983) *Nature* **302,** 832–837
9. Leurs, R., Bakker, R. A., Timmerman, H., and de Esch, I. J. (2005) *Nat. Rev. Drug Discov.* **4,** 107–120
10. Pillot, C., Ortiz, J., Héron, A., Ridray, S., Schwartz, J. C., and Arrang, J. M. (2002) *J. Neurosci.* **22,** 7272–7280
11. García-Ramírez, M., Aceves, J., and Arias-Montaño, J. A. (2004) *Behav. Brain Res.* **154,** 409–415
12. Arias-Montaño, J. A., Floran, B., Garcia, M., Aceves, J., and Young, J. M. (2001) *Br. J. Pharmacol.* **133,** 165–171
13. Hussain, N., Flumerfelt, B. A., and Rajakumar, N. (2002) *Neuroscience* **112,** 427–438
14. Ferrada, C., Ferré, S., Casadó, V., Cortés, A., Justinova, Z., Barnes, C., Canela, E. I., Goldberg, S. R., Leurs, R., Lluis, C., and Franco, R. (2008) *Neuropharmacology* **55,** 190–197
15. Ferrada, C., Moreno, E., Casadó, V., Bongers, G., Cortés, A., Mallol, J., Canela, E. I., Leurs, R., Ferré, S., Lluís, C., and Franco, R. (2009) *Br. J. Pharmacol.* **157,** 64–75
16. Xu, M., Moratalla, R., Gold, L. H., Hiroi, N., Koob, G. F., Graybiel, A. M., and Tonegawa, S. (1994) *Cell* **79,** 729–742
17. Narushima, M., Uchigashima, M., Hashimoto, K., Watanabe, M., and Kano, M. (2006) *Eur. J. Neurosci.* **24,** 2246–2252
18. Hasbi, A., Fan, T., Alijaniaram, M., Nguyen, T., Perreault, M. L., O'Dowd, B. F., and George, S. R. (2009) *Proc. Natl. Acad. Sci. U.S.A.* **106,** 21377–21382
19. Milligan, G., and Bouvier, M. (2005) *FEBS J.* **272,** 2914–2925
20. Pfleger, K. D., and Eidne, K. A. (2006) *Nat. Meth.* **3,** 165–174
21. Franco, R., Casadó, V., Cortés, A., Mallol, J., Ciruela, F., Ferré, S., Lluis, C., and Canela, E. I. (2008) *Br. J. Pharmacol.* **153,** S90-S98
22. Ferré, S., Ciruela, F., Woods, A. S., Lluis, C., and Franco, R. (2007) *Trends Neurosci.* **30,** 440–446
23. Ferré, S., Baler, R., Bouvier, M., Caron, M. G., Devi, L. A., Durroux, T., Fuxe, K., George, S. R., Javitch, J. A., Lohse, M. J., Mackie, K., Milligan, G., Pfleger, K. D., Pin, J. P., Volkow, N. D., Waldhoer, M., Woods, A. S., and Franco, R. (2009) *Nat. Chem. Biol.* **5,** 131–134
24. Casadó, V., Cortés, A., Mallol, J., Pérez-Capote, K., Ferré, S., Lluis, C., Franco, R., and Canela, E. I. (2009) *Pharmacol. Ther.* **124,** 248–257
25. Ellis, J., Pediani, J. D., Canals, M., Milasta, S., and Milligan, G. (2006) *J. Biol. Chem.* **281,** 38812–38824
26. Sánchez-Lemus, E., and Arias-Montaño, J. A. (2004) *Neurosci. Lett.* **364,** 179–184
27. Torrent, A., Moreno-Delgado, D., Gómez-Ramírez, J., Rodríguez-Agudo, D., Rodríguez-Caso, C., Sánchez-Jiménez, F., Blanco, I., and Ortiz, J. (2005) *Mol. Pharmacol.* **67,** 195–203
28. Moreno-Delgado, D., Torrent, A., Gómez-Ramírez, J., de Esch, I., Blanco, I., and Ortiz, J. (2006) *Neuropharmacology* **51,** 517–523
29. Missale, C., Nash, S. R., Robinson, S. W., Jaber, M., and Caron, M. G. (1998) *Physiol. Rev.* **78,** 189–225
30. Rashid, A. J., So, C. H., Kong, M. M., Furtak, T., El-Ghundi, M., Cheng, R., O'Dowd, B. F., and George, S. R. (2007) *Proc. Natl. Acad. Sci. U.S.A.* **104,** 654–659
31. Franco, R. (2009) *Br. J. Pharmacol.* **158,** 23–31
32. Hasbi, A., O'Dowd, B. F., and George, S. R. (2010) *Curr. Op. Pharmacol.* **10,** 93–99

Supplementary Figure 1

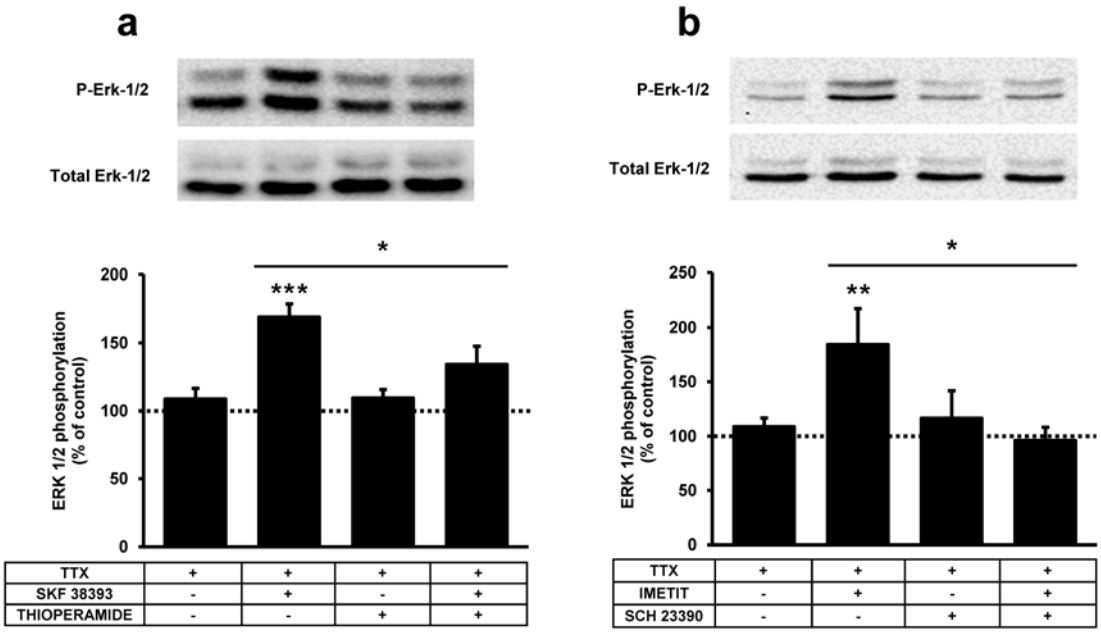

Tetrodotoxin effect on D_1R or H_3R agonist-mediated ERK 1/2 phosphorylation. Rat striatal slices were treated for 10 min with 1 µM tetrodotoxin before addition of ligands. Slices were incubated in the absence or in the presence of 10 µM thioperamide (a) or 10 µM SCH 23390 (b) prior to the addition of medium or 1 µM SKF 38393 (a) or 1 µM imetit (b) and incubated further (10 min). ERK1/2 phosphorylation was determined as indicated in Materials and Methods. The immunoreactive bands from 7 to 16 (a) or 5 to 16 (b) slices obtained from 3 to 8 animals were quantified and values represent as mean ± S.E.M. of the percentage of phosphorylation relative to basal levels found in untreated slices (100 %). Significant differences were calculated by one-way ANOVA with post-hoc Bonferroni's multiple tests (* $p< 0.05$, ** $p< 0.01$, *** $p <0.001$, as compared to TTX alone or as indicated by bar).

3.4 Participación directa de los receptores σ-1 en los efectos de la cocaína mediados por el receptor D_1 de dopamina

Gemma Navarro[a], Estefanía Moreno[a], Marisol Aymerich[b], Daniel Marcellino[c], Peter J. McCormick[a], Josefa Mallol[a], Antoni Cortés[a], Vicent Casadó[a], Enric I. Canela[a], Jordi Ortiz[d], Kjell Fuxe[c], Carmen Lluís[a], Sergi Ferré[e], and Rafael Franco[a,b]

[a]Centro de Investigación Biomédica en Red sobre Enfermedades Neurodegenerativas, y Departamento de Bioquímica y Biología Molecular, Facultad de Biología, Universidad de Barcelona, Barcelona, España,
[b]Centro de Investigación Médica Aplicada, Universidad de Navarra, 31008 Pamplona, España,
[c]Department of Neuroscience, Karolinska Institutet, 17177 Stockholm, Sweden,
[d]Instituto de Neurosciencias y Departmento de Bioquímica y Biología Molecular, Facultad de Medicina, Universitat Autónoma de Barcelona, 08193 Bellaterra, España,
[e]National Institute on Drug Abuse, Intramural Research Program, National Institutes of Health, Department of Health and Human Services, Baltimore, MD 21224.

*Manuscrito publicado en Proceedings of the National Academy of Sciences of USA (2010 Oct); **107(43)**: 18676-81.*

Es bien conocido que la cocaína bloquea el transportador de dopamina. Este mecanismo debería llevar a un incremento generalizado en la neurotransmisión dopaminérgica y, aun así, se conoce que los receptores D_1 de dopamina (D_1Rs) juegan un papel mucho más significativo en los efectos comportamentales de la cocaína que cualquier otro subtipo de receptores de dopamina. La cocaína también se une a los receptores σ-1, el papel fisiológico de esta interacción es totalmente desconocido. En este trabajo, hemos descubierto que D_1R y σ-1 heteromerizan en células transfectadas, donde la cocaína potencia la activación de la adenilato ciclasa mediada por D_1R, induce la activación de la vía de las MAP cinasas por sí misma y contrarresta la activación de las MAP cinasas mediada por D_1Rs de forma independiente del transportador de dopamina y de forma dependiente del receptor σ-1. Algunos de estos efectos se han demostrado también en cortes estriatales de ratón no modificado pero no en ratones deficientes en el receptor σ-1, proporcionando evidencias de la existencia de heterómeros D_1R-σ-1 en el estriado cerebral. En conjunto, estos resultados aportan una explicación molecular por la cual los heterómeros D_1R-σ-1 desempeñan un papel importante en los efectos comportamentales de la cocaína y proporcionan una nueva perspectiva para entender las bases moleculares involucradas en la adicción a la cocaína.

Direct involvement of σ-1 receptors in the dopamine D_1 receptor-mediated effects of cocaine

Gemma Navarro[a], Estefanía Moreno[a], Marisol Aymerich[b], Daniel Marcellino[c], Peter J. McCormick[a], Josefa Mallol[a], Antoni Cortés[a], Vicent Casadó[a], Enric I. Canela[a], Jordi Ortiz[d], Kjell Fuxe[c], Carmen Lluís[a], Sergi Ferré[e,1], and Rafael Franco[a,b]

[a]Centro de Investigación Biomédica en Red sobre Enfermedades Neurodegenerativas, and Department of Biochemistry and Molecular Biology, Faculty of Biology, University of Barcelona, 08028 Barcelona, Spain; [b]Centro de Investigación Médica Aplicada, Universidad de Navarra, 31008 Pamplona, Spain; [c]Department of Neuroscience, Karolinska Institutet, 17177 Stockholm, Sweden; [d]Neuroscience Institute and Department of Biochemistry and Molecular Biology, Faculty of Medicine, Universitat Autónoma de Barcelona, 08193 Bellaterra, Spain; and [e]National Institute on Drug Abuse, Intramural Research Program, National Institutes of Health, Department of Health and Human Services, Baltimore, MD 21224

Edited by Leslie Lars Iversen, University of Oxford, Oxford, United Kingdom, and approved September 10, 2010 (received for review June 22, 2010)

It is well known that cocaine blocks the dopamine transporter. This mechanism should lead to a general increase in dopaminergic neurotransmission, and yet dopamine D_1 receptors (D_1Rs) play a more significant role in the behavioral effects of cocaine than the other dopamine receptor subtypes. Cocaine also binds to σ-1 receptors, the physiological role of which is largely unknown. In the present study, D_1R and σ_1R were found to heteromerize in transfected cells, where cocaine robustly potentiated D_1R-mediated adenylyl cyclase activation, induced MAPK activation per se and counteracted MAPK activation induced by D_1R stimulation in a dopamine transporter-independent and σ_1R-dependent manner. Some of these effects were also demonstrated in murine striatal slices and were absent in σ_1R KO mice, providing evidence for the existence of σ_1R-D_1R heteromers in the brain. Therefore, these results provide a molecular explanation for which D_1R plays a more significant role in the behavioral effects of cocaine, through σ_1R-D_1R heteromerization, and provide a unique perspective toward understanding the molecular basis of cocaine addiction.

receptor heteromer | drug addiction

A key molecular mechanism contributing to the development of addiction by drugs of abuse consist of the increase of the extracellular levels of dopamine in the striatum, particularly in its ventral portion, the nucleus accumbens (1, 2). Cocaine causes a rapid and strong increase in striatal extracellular dopamine by its ability to bind with high affinity to the dopamine transporter (DAT) and to inhibit its function (3–5). In the striatum, dopamine signaling is mediated mainly by dopamine D_1 and D_2 receptors (D_1Rs and D_2Rs, respectively), which are mostly segregated in two phenotypically different subtypes of GABAergic medium-sized spiny neurons (MSNs) (6). Activation of D_1Rs is an absolute requirement for the induction of many of the cellular and behavioral responses to cocaine, as deduced from studies performed in D_1R KO mice and from experiments with transgenic mice in which D_1R- or D_2R-expressing MSNs are visualized by the expression of fluorescent proteins (7–11).

The σ-1 receptor, originally proposed as a subtype of opioid receptors, is now considered to be a nonopioid receptor with two transmembrane domains, one extracellular loop and cytosolic N and C termini (12). The σ_1R is highly expressed in the brain, including the striatum, and its association with neurons is well established (12, 13). However, its biological function and even its main endogenous neurotransmitter remain enigmatic (12). Cocaine interacts with σ_1Rs at pharmacologically relevant concentrations (12, 14). In fact, reducing brain σ_1R levels with antisense oligonucleotides attenuates the convulsive and locomotor stimulant actions of cocaine (15, 16), and σ_1R antagonists mitigate the actions of cocaine in animal models (12, 14). A recent study showed that σ_1R agonists not only potentiate the reinforcing effects of cocaine, but they may be self-administered (17). In the current study, we explored the existence of molecular and functional interactions between σ_1R and D_1R, which could underlie these pharmacological interactions.

Using bioluminescence resonance energy transfer-based techniques, we report a molecular interaction in living cells between σ_1R and D_1R. Cocaine was able to bind to a receptor heteromer constituted by at least one σ_1R and two D_1R units and promoted structural changes in the heteromer that led to significant modifications in D_1R function. Cocaine effects on D_1R function did not occur in cells transfected with σ_1R siRNA or in striatal slices of σ_1R KO mice. Altogether, the findings indicate that σ_1R-D_1R heteromer-mediated alterations of dopaminergic neurotransmission constitutes a previously uncharacterized mechanism of cocaine action.

Results

Heteromerization of σ_1R and D_1R. We explored the possibility that σ_1R might interact directly with D_1R. BRET measurements were performed in HEK-293T cells expressing a constant amount of D_1R fused to *Renilla Luciferase* (Rluc) and increasing amounts of σ_1R fused to yellow fluorescence protein (YFP). A positive and saturable BRET signal was obtained ($BRET_{max}$, 44 ± 4; $BRET_{50}$, 18 ± 3; Fig. 1*A*). The pair constituted by the adenosine A_1 receptor fused to Rluc, and the σ_1R-YFP was used as a negative control. As shown in Fig. 1*A*, the negative control gave a linear nonspecific BRET signal, thus confirming the specificity of the interaction between D_1R–Rluc and σ_1R–YFP. Because one of the limitations of BRET is that it cannot distinguish between two or three interacting proteins, and because homomerization seems to be a requirement for the normal membrane expression of D_1R (18), we investigated the possible formation of receptor heteromers constituted by σ_1R and D_1R homomers by combining BRET with bimolecular fluorescence complementation (BiFC, Fig.1*C*) (19). Cells were cotransfected with cDNAs for σ_1R–Rluc, D_1R–nYFP and D_1R–cYFP, and BRET between σ_1R-Rluc receptor as donor and reconstituted D_1R–nYFP–D_1R–cYFP homomer as acceptor was evaluated. σ_1R–D_1R–D_1R heterotrimerization could be demonstrated by a positive and saturable BRET signal ($BRET_{max}$, 46 ± 6; $BRET_{50}$, 21 ± 5; Fig. 1*B*). Cells expressing σ_1R, D_1R–cYFP and nYFP or σ_1R, D_1R–nYFP and cYFP did not provide any significant fluorescent signal or positive BRET. An additional negative control was performed using $GABA_{B2}$ receptor fused to Rluc, which did not

Author contributions: G.N., D.M., P.J.M., J.M., V.C., E.I.C., J.O., K.F., C.L., S.F., and R.F. designed research; G.N., E.M., M.A., A.C., and V.C. performed research; G.N., E.M., C.L., and S.F. analyzed data; and G.N., K.F., C.L., S.F., and R.F. wrote the paper.

The authors declare no conflict of interest.

This article is a PNAS Direct Submission.

[1]To whom correspondence should be addressed. E-mail: sferre@intra.nida.nih.gov.

This article contains supporting information online at www.pnas.org/lookup/suppl/doi:10.1073/pnas.1008911107/-/DCSupplemental.

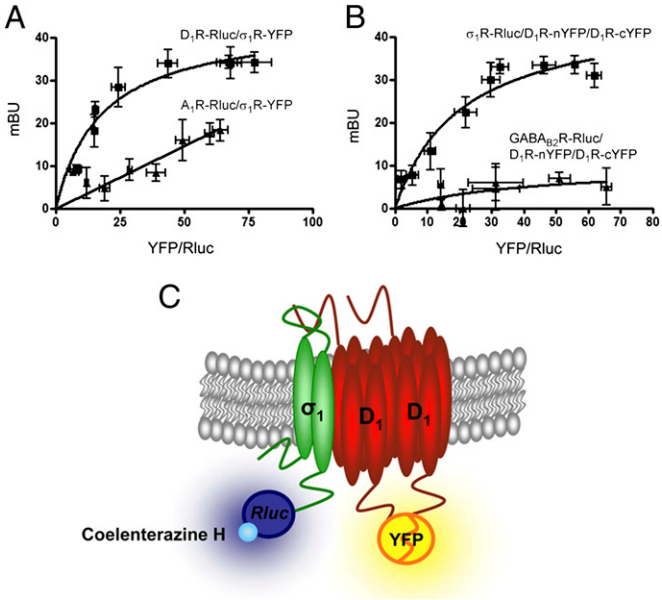

Fig. 1. Heteromerization of D_1R and σ_1R in living cells. (*A*) BRET saturation experiments performed with HEK-293T cells transfected with D_1R–Rluc cDNA (0.6 μg; ■) or A_1R–Rluc cDNA as negative control (0.4 μg; ▲) and increasing amounts of σ_1R-YFP cDNA (0.2–2 μg cDNA). (*B*) BRET saturation curve was obtained using HEK-293T cells cotransfected with σ_1R-Rluc cDNA (0.4 μg, ■) or $GABA_{B2}R$-Rluc cDNA as negative control (0.5 μg; ▲) and increasing equal amounts of D_1R–nYFP and D_1R–cYFP cDNAs (0.5–4 μg cDNA). BRET data are expressed as means ± SD of five to six different experiments grouped as a function of the amount of BRET acceptor. (*C*) Schematic representation of BiFC. A receptor-Rluc acts as BRET donor and, as BRET acceptor, one receptor is fused to an YFP N-terminal fragment (nYFP) and another receptor is fused to the remaining YFP C-terminal fragment (cYFP). Upon coexpression, fluorescence indicates reconstitution of YFP from both fragments and therefore a close receptor–receptor interaction.

interact with D_1R homodimers (Fig. 1*B*). Collectively, these results indicate that σ_1R–D_1R heteromers occur in cells coexpressing both receptors.

Cocaine Induces Modifications of Subcellular Distribution of σ_1R. It is known that the majority of σ_1R are found in the endoplasmic reticulum membrane (12). The possibility that cocaine binding to the σ_1R may alter the cell surface levels of putative σ_1R-D_1R heteromers was therefore explored. HEK-293T cells were used in the assays, because they constitutively express σ_1R, but not DAT (Fig. 2 *A* and *B*). By means of immunofluorescence a punctate σ_1R staining in naïve HEK cells was detected, which is the expected pattern for an endoplasmic reticulum-associated protein (Fig. 2*C, Left,* top images). Expression of D_1R induced in HEK-293T cells an increase in the localization of σ_1R at the plasma membrane (Fig. 2*C, Left,* bottom images), suggesting that heteromerization with D_1R facilitates translocation of σ_1R to the plasma membrane. Cocaine (150 μM; 30 min) produced an increase of σ_1R expression at the plasma membrane in nontransfected cells (Fig. 2*C, Right*, top images) and an increase in the colocalization of σ_1Rs and D_1Rs in transfected cells (Fig. 2*C, Right,* bottom images), suggesting that cocaine induces an increase in the amount of σ_1R-D_1R heteromers at the plasma membrane.

Cocaine Induces Modifications of Quaternary Structure of D_1R Homomers in σ_1R-D_1R Heteromer. The observed changes in the plasma membrane expression of σ_1R-D_1R heteromers in the presence of cocaine suggested that cocaine binding might be altering the interaction between D_1Rs and σ_1Rs. Such a change

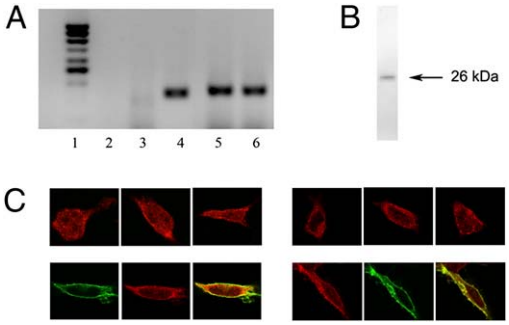

Fig. 2. Expression and subcellular distribution of σ_1R. (*A*) RT-PCR was performed using total RNA from HEK-293T cells (lanes 2, 3, 5, and 6) or RNA from human striatum as DAT positive control (lane 4), and primers specific for the human σ_1R gene (lane 5), for the human DAT gene (lanes 3 and 4), or for human GADPH (lane 6). RNA from cells without primers (lane 2) was included as negative control. Molecular mass markers are shown in lane 1. (*B*) HEK cell membranes were analyzed by SDS/PAGE and immunoblotted with the anti-σ_1R antibody. (*C*) Confocal microscopy images of HEK-293T cells transfected (*Lower*) or not transfected (*Upper*) with D_1R–YFP cDNA, treated (right images) or not treated (left images) with 150 μM cocaine for 30 min. The σ_1R (red) and D_1R (green) were identified by immunocytochemistry. Colocalization is shown in yellow.

should be detectable using an energy transfer-based approach. In HEK-293T cells expressing D_1R–Rluc and D_1R–YFP, the BRET saturation curve corresponding to D_1R–Rluc–D_1R–YFP pair was drastically reduced in the presence of cocaine (Fig. 3*A*). This effect was specific for the D_1R, because it did not occur for the A_1R-Rluc and A_1R-YFP pair (Fig. 3*B*) and was dose dependent (Fig. 3*C*) and time dependent (Fig. 3d). Although the BRET signal for the D_1R–Rluc–D_1R–YFP pair was negligible at 180 min

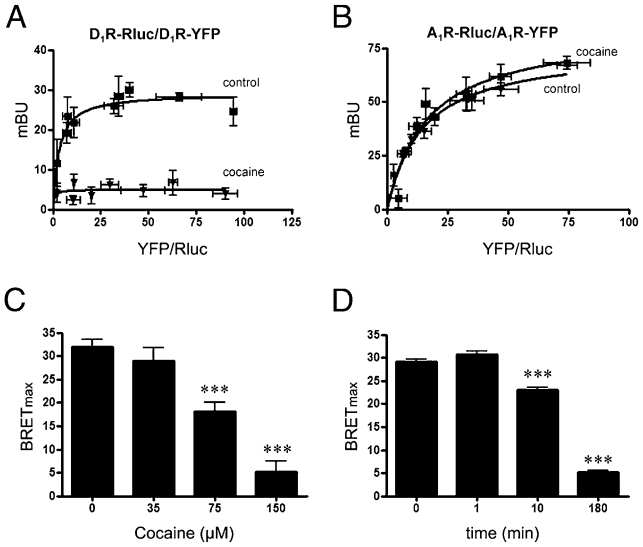

Fig. 3. Effects of cocaine on D_1R homomers. BRET was measured in HEK-293T cells cotransfected with D_1R–Rluc cDNA (0.6 μg) and increasing amounts of D_1R–YFP cDNA (*A*) or A_1R-Rluc cDNA (0.4 μg) and increasing amounts of A_1R-YFP cDNA (*B*), treated (▼) or not treated (■) with 150 μM cocaine for 180 min. BRET data are expressed as means ± SD of four to six different experiments grouped as a function of the amount of BRET acceptor. (*C*) Cells were treated for 180 min with the indicated concentrations of cocaine before the determination of BRET. (*D*) Cells were treated with 150 μM cocaine for the indicated times before the determination of BRET. $BRET_{max}$ data are expressed as means ± SEM of four to six different experiments. ***Significantly different ($P < 0.001$) compared with cocaine 0 μM or 0 min (one-way ANOVA followed by Bonferroni post hoc tests).

NEUROSCIENCE

of cocaine treatment, there was no real disruption of D_1R homomerization, because cocaine did not modify the amount of fluorescence in HEK 293 cells expressing D_1R–cYFP–D_1R–nYFP dimers. These results strongly suggest that cocaine binding to σ_1R alters the quaternary structure of the σ_1R–D_1R–D_1R heteromer, resulting from separation of the C-termini of the D_1R protomers fused to Rluc and YFP. The participation of σ_1R on the cocaine-mediated alteration of the quaternary structure of D_1R was demonstrated in experiments performed in cells the σ_1R expression of which was knocked down using an RNAi approach. By RNA interference (RNAi), using a specific small interfering RNA (siRNA), a robust silencing of σ_1R expression was obtained without significantly altering the expression of D_1R (Figs. 4 *A* and *B*). The treatment with the specific siRNA completely abolished the effect of cocaine on the BRET saturation curve obtained with D_1R–Rluc and D_1R–YFP (Fig. 4*C*). Finally, the selective σ_1R agonist PRE084 also modified the BRET saturation curve corresponding to D_1R–Rluc–D_1R–YFP pair (200 nM; 10 min) (Fig. S1).

Cocaine Binding to σ_1R Modulates D_1R Function in Living Cells. To study how cocaine affects D_1R–mediated signaling, CHO cells were used, as they provided a lower baseline of signaling for which to detect downstream changes. CHO cells were also shown to constitutively express σ_1Rs but not DAT or D_1Rs (Fig. 5 *A* and *B*). As expected, in CHO cells expressing D_1Rs, the full D_1R agonist SKF 81297 dose-dependently increased cAMP production (Fig. 5*C*). Treatment with cocaine (150 μM; 10 min) did not induce a significant increase in cAMP, but robustly enhanced D_1R agonist-induced cAMP accumulation (Fig. 5*C*). This was completely counteracted by silencing expression of σ_1R via RNAi (Fig. 5*C*), indicating that this effect of cocaine was mediated by σ_1R. SKF 81297 also produced a dose-dependent MAPK activation (ERK1/2 phosphorylation; Fig. 6*A*) with a maximum response at 2 min (Fig. 6*B*). SKF 81297-induced ERK1/2 phosphorylation was inhibited by the D_1R antagonist SCH 23390 (10 μM) and also by the σ_1R antagonist PD144.418 (1 μM; Figs. 6 *A* and *B*), indicating that σ_1R modulates a D_1R-mediated MAP kinase pathway in addition to the cAMP pathway.

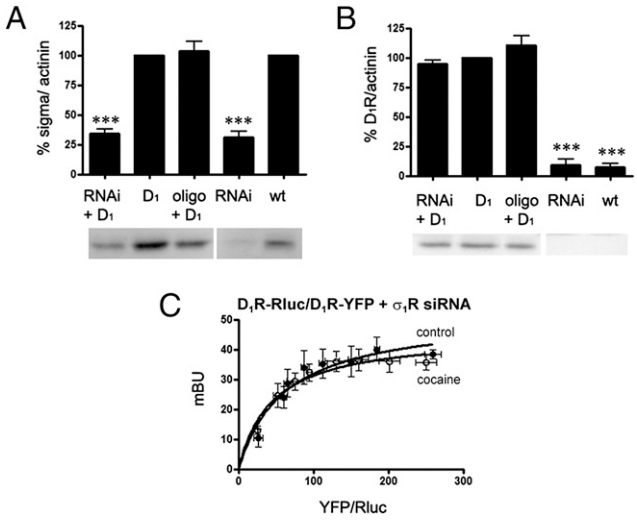

Fig. 4. Effect of cocaine on D_1R homomers was mediated by σ_1R. (*A* and *B*) HEK-293T cells were transfected or not transfected (wt, nontranfected cells) with σ_1R siRNA, irrelevant oligonucleotides (oligo) and/or D_1R cDNA (D_1). Cell membranes were analyzed by SDS/PAGE and immunoblotted with the anti-σ_1R (*A*) or D_1R (*B*) antibody. Values are mean ± SEM of three experiments, and a representative Western blot for σ_1R (*A*) or D_1R (*B*) is shown. ***P < 0.001 compared with D_1R cDNA transfected cells (one-way ANOVA followed by Bonferroni post hoc tests). (*C*) BRET saturation experiments were performed in HEK-293T cells cotransfected with σ_1R siRNA (50 pmol), D_1R–Rluc receptor cDNA (0.5 μg), and increasing amounts of D_1R–YFP cDNA (0.3–3 μg cDNA), treated (open symbols) or not (filled symbols) with 150 μM cocaine for 30 min. BRET data are expressed as mean ± SD of four to six different experiments grouped as a function of the amount of BRET acceptor.

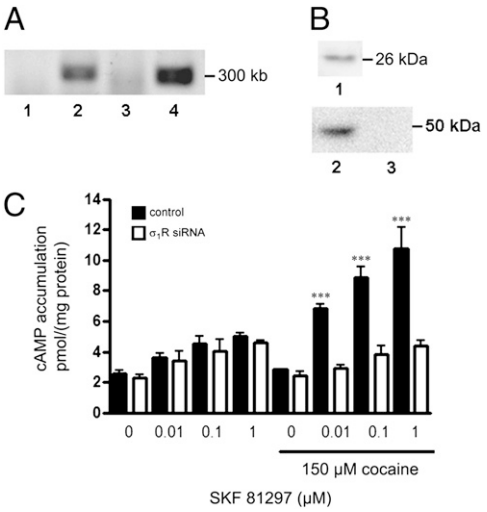

Fig. 5. Effect of cocaine on D_1R-mediated cAMP production. (*A*) RT-PCR was performed using total RNA from CHO cells (lanes 1–4) and primers for Chinese hamster σ_1R (lane 2), DAT (lane 3), or GAPDH (lane 4). RNA from cells without primers (lane 1) was included as negative control. (*B*) CHO cell membranes were analyzed by SDS/PAGE and immunoblotted with the anti-σ_1R antibody (top blot) or anti-D_1R antibody (bottom blot, lanes 1 and 2: cells transfected or not transfected with D_1R cDNA, respectively). (*C*) CHO cells transfected with D_1R cDNA (1.5 μg, filled bars) or cotransfected with D_1 receptor cDNA and 125 pmol σ_1R siRNA (open bars) were treated with increasing concentrations of D_1R agonist SKF 81297 for 10 min in the absence or presence of 150 μM cocaine or with cocaine alone. Results are mean ± SEM of three to six independent experiments performed in triplicate. Bifactorial ANOVA of results of samples without or with siRNA transfection showed significant effect of SKF (P < 0.0001 and P < 0.001, respectively), but only in samples without siRNA transfection was there a highly significant effect of cocaine (***P < 0.0001, compared with samples with the same concentration of SKF 81297 and without RNAi transfection and in the absence of cocaine; Bonferroni post hoc tests).

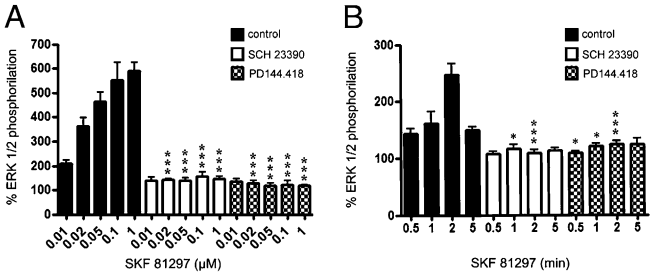

Fig. 6. Effect of σ_1R ligands on D_1R-mediated ERK1/2 phosphorylation. CHO cells transfected with D_1R cDNA (1.5 μg) were stimulated with increasing concentrations of the D_1R agonist SKF 81297 for 2 min (*A*) or with 100 nM SKF 81297 for increasing periods of time (*B*) in the absence (filled bars) or presence of 10 μM D_1R antagonist SCH 23390 (open bars) or 1 μM σ_1R specific ligand PD144.418 (cross-hatched bars). ERK1/2 phosphorylation is represented as percentage over basal levels (100%). Results are a mean ± SEM of four independent experiments performed in duplicate. Bifactorial ANOVA showed a significant effect of SKF 81297 (P < 0.0001 in *A* and P < 0.001 in *B*), and Bonferroni post hoc tests showed a significant SCH 23390-mediated or PD144.418-mediated counteraction of the effect SKF 81297 (*P < 0.05 and ***P < 0.001, compared with control samples with the same concentration and exposure time of SKF 81297).

Importantly, cocaine per se dose-dependently (Fig. 7*A*) and time-dependently (Fig. 7*B*) activated ERK1/2 phosphorylation. Again, this effect was mediated by σ_1R, as it was strongly diminished in cells transfected with the σ_1R siRNA (Fig. 7 *A* and *B*). Furthermore, a similar effect could be obtained with the selective σ_1R agonist PRE084 (Fig. S1). Cocaine-induced ERK1/2 phosphorylation seemed to be dependent on D_1R expression, because the increase in ERK1/2 phosphorylation was not found in CHO cells lacking D_1R expression (Fig. S2). Moreover, cocaine-induced ERK1/2 phosphorylation in cells expressing σ_1R and D_1R was not only counteracted by PD144.418 (1 μM), which therefore acted as a σ_1R antagonist, but also by SCH 23390 (10 μM, Fig. 7 *C* and *D*). All of these results suggest that cocaine binding to σ_1R or SKF 81297 binding to D_1R in the D_1R–σ_1R heteromer induce ERK1/2 phosphorylation that is equally counteracted by σ_1R or D_1R antagonists. Finally, we found a strong and reciprocal antagonistic interaction between σ_1R and D_1R on MAPK signaling. Thus, SKF 81297-induced ERK1/2 phosphorylation was drastically counteracted by increasing concentrations of cocaine (Fig. 8*A*), and cocaine-induced ERK1/2 phosphorylation was also counteracted in the presence of increasing concentrations of SKF 81297 (Fig. 8*B*). Again the same qualitative effects were obtained with the selective σ_1R agonist PRE084 (Fig. S1).

Cocaine Binding to σ_1R Modulates D_1R Function in Mouse Brain Striatum. To explore whether our results above using cultured cells could be extrapolated to the level of the organism, we took tissue from WT and s_1R KO mice and examined the effects of cocaine on signaling. Previous in vivo studies have shown that pharmacologically significant doses of cocaine produce striatal levels of the drug at a low micromolar range (20). Those measurements reflect free, rather than bound, concentrations of cocaine, and it is well established that higher drug concentrations need to be applied in brain slice preparations, to allow diffusion into the tissue. Because, in cotransfected CHO cells, a strong and significant effect of cocaine was observed at 30 μM (Fig. 8*A*), a fivefold higher concentration, 150 μM, was then used to see clear effects in slices of mouse striatum (Fig. 8*C*). On one hand, both the D_1R agonist SKF 81297 (1 μM) and cocaine (150 μM) induced ERK1/2 phosphorylation in striatal slices of WT mice after 10-min activation (Fig. 8*C*). On the other hand, in striatal slices of WT mice, SKF 81297-induced ERK1/2 phosphorylation was significantly reduced with pretreatment with cocaine for 30 min (Fig. 8*C*). The antagonistic interaction between σ_1R and D_1R on MAPK signaling is therefore detected in cotransfected cells and in striatal samples from WT mice. When similar experiments were performed in striatal slices from mice lacking the σ_1R, cocaine was unable to induce ERK1/2 phosphorylation (Fig. 8*C*) and SKF 81297-induced ERK1/2 phosphorylation was not modified by pretreatment with cocaine (Fig. 8*C*). These results strongly support the existence of σ_1R-D_1R heteromers in

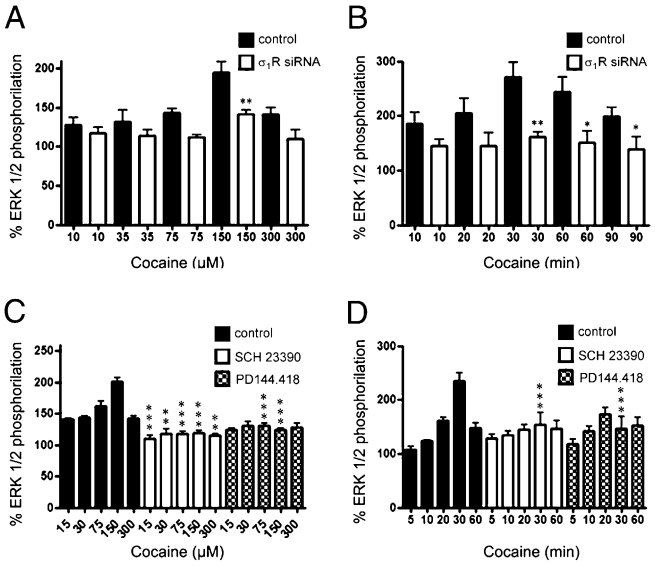

Fig. 7. Cocaine-induced σ_1R-mediated ERK1/2 phosphorylation. CHO cells transfected with D_1 receptor cDNA (1.5 μg, filled bars) or cotransfected (open bars) with D_1R cDNA and σ_1R siRNA (125 pmol) were incubated with increasing concentrations of cocaine for 30 min (*A*) or with 150 μM cocaine for increasing time periods (*B*). (C and *D*) CHO cells were transfected only with D_1 receptor cDNA (1.5 μg) and were treated (30 min) with increasing concentrations of cocaine (*C*) or with 150 μM cocaine for different periods of time (*D*), in the absence (filled bars) or presence of 10 μM of the D_1R antagonist SCH 23390 (open bars) or 1 μM σ_1R antagonist PD144.418 (cross-hatched bars). ERK1/2 phosphorylation is represented as percentage over basal levels (100%). Results are mean ± SEM of four to seven independent experiments performed in duplicate. In all samples, bifactorial ANOVA showed a significant ($P < 0.0001$ in *A–C*; $P < 0.001$ in *D*) effect of cocaine, and Bonferroni post hoc tests showed a significant counteraction of cocaine effect by siRNA (*A* and *B*, $*P < 0.05$ and $**P < 0.01$ compared with sample with the same treatment and without siRNA transfection) and a significant SCH 23390-mediated or PD144.418-mediated counteraction of the cocaine effect for some concentrations and exposure times (*C* and *D*, $*P < 0.05$, $**P < 0.01$, and $***P < 0.001$ compared with control samples with the same treatment).

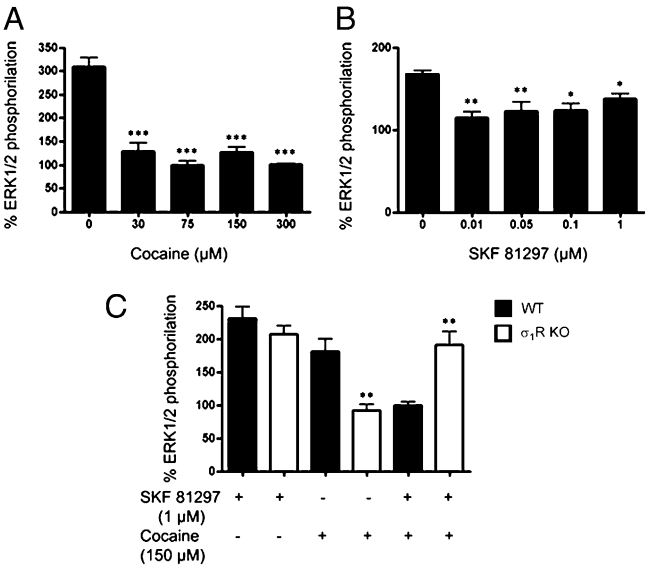

Fig. 8. Antagonistic interaction between cocaine and the D_1R agonist SKF 81297 on ERK1/2 phosphorylation. (*A* and *B*) CHO cells transfected with D_1R cDNA (1.5 μg) were treated or not treated for 30 min with increasing concentrations of cocaine (*A*) or with 150 μM cocaine (*B*) and, during the last 2 min, the additon of 100 nM (*A*) or increasing concentrations (*B*) of D_1 receptor agonist SKF 81297. ERK1/2 phosphorylation is represented as percentage over basal levels (100%). Results are mean ± SEM of four independent experiments performed in duplicate. One-way ANOVA followed by Bonferroni post hoc tests showed a significant cocaine-mediated counteraction of SKF 81297 and a significant SKF 81297-mediated counteraction of cocaine-induced ERK1/2 phosphorylation ($*P < 0.05$, $**P < 0.01$, and $***P < 0.001$ compared with control, without cocaine or SKF 81297 exposure). (*C*) WT (filled bars) and σ_1R KO (open bars) mouse striatal slices were treated with SKF 81297 for 10 min, with cocaine for 30 min or with cocaine for 30 min and, during the last 10 min, the addition of SKF 81297. Immunoreactive bands from six slices obtained from five WT or five KO animals were quantified for each condition. Values represent mean ± SEM of percentage of phosphorylation relative to basal levels found in untreated slices. Significant differences respect to corresponding treatment in WT mouse slices were calculated by bifactorial ANOVA followed by post hoc Bonferroni tests ($**P < 0.01$).

NEUROSCIENCE

the brain and indicate that all detected cocaine effects are dependent on σ_1R.

Discussion

The role of σ_1R in cell-signaling is not well understood and its main endogenous ligand has not been identified (12, 15). It has been suggested that σ_1R may possess a constitutive biological activity, and that σ_1R ligands may just be modulators of its innate activity (12). The best- characterized acute effects of σ_1R ligands at the cellular level are their ability to modulate the function of several ion channels (K^+ channels, NMDA receptors, IP3 receptors) (12). In the present study a mechanism by which σ_1R modulates the function of a G-protein–coupled receptor, the D_1R, is reported. This modulation depends on protein–protein interactions, which were detected by BRET assays. In agreement with the oligomeric nature of D_1R (18), the existence of heteromers constituted by a minimum of a D_1R homodimer and a σ_1R was demonstrated by BRET/BiFC.

The σ_1R, which is found mainly at the membrane of the endoplasmic reticulum, may modulate the activity of plasma membrane-located ion channels by its ability to translocate to the plasma membrane (12, 21). Coexpression of σ_1R and D_1R resulted in an alteration of σ_1R subcellular distribution because, in the presence of D_1R, σ_1R was more abundant at the plasma membrane that in intracellular membranes. Importantly, coexpression of σ_1R and D_1R also led to heteromerization of the receptors, as measured by energy transfer in the absence of ligands. Acute administration of σ_1R ligands, including cocaine, without coactivation of other receptors or channels may cause σ_1R translocation to the plasma membrane (12). Apart from the increase in plasma membrane σ_1R expression, cocaine led to an increase of σ_1R-D_1R colocalization. Taken together, these data suggest that heteromerization occurs between these receptors at steady state in the absence of ligands, but the presence of cocaine might induce an increase of the amount of receptor heteromers constituted by σ_1Rs and D_1Rs homomers at the level of the plasma membrane, perhaps through some stabilization of a given receptor conformation.

Although further studies will be required to understand how cocaine acts on the receptor monomers, homomers or heteromers and the specific effects at a protein level, we were able to observe that cocaine binding to σ_1R led to a structural modification, detected as a separation between the C termini of the D_1Rs in the σ_1R–D_1R–D_1R heterotrimer. This was evidenced by a pronounced decrease (Fig. 3*C*) in the BRET signal due to a decrease in the energy transfer between Rluc and YFP (located in the C-terminal domains of D_1Rs). These structural changes, which did not result from dimer disruption, correlated with changes in D_1R function, as demonstrated by means of assays performed in both heterologous cells and in slices from mouse striatum. Importantly, cocaine binding to σ_1R robustly enhanced D_1R agonist-induced cAMP accumulation. This synergy is probably underlying the predominant role of D_1R versus D_2R in the behavioral effects of cocaine (discussed earlier here). These results are also strong evidence that cocaine effects are not adequately addressed by assuming that the drug is just increasing the synaptic dopamine concentration by a DAT-dependent mechanism. In fact, the reported effects were not dependent on DAT, because cell lines lacking this protein were used. It is thus expected that cocaine is acting by at least two different but interrelated mechanisms, one dependent on DAT and leading to an increase in dopamine levels and another dependent on σ_1R and leading to an enhancement of D_1R-mediated neurotransmission.

Unexpectedly, cocaine was able to induce ERK1/2 phosphorylation per se, although this effect depended on the presence of both the D_1R and σ_1R. As these particular effects were reproduced by the selective σ_1R agonist (17) and counteracted by the putative σ_1R antagonist PD144.418 (22), these results indicate that cocaine acts as a σ_1R agonist. In living cells, cocaine-induced ERK1/2 phosphorylation was seen at short times of cocaine exposure (10 min); but the maximum effect was reached at 30 min, suggesting an involvement of cocaine-induced translocation of σ_1R to the plasma membrane, with a consequent increase in cell surface σ_1R-D_1R heteromers. Both cocaine-induced and D_1R-mediated ERK1/2 phosphorylation were counteracted by D_1R or σ_1R antagonists. The ability of an antagonist of one of the receptors in a receptor heteromer to block signals originated by stimulation of the partner receptor is a biochemical characteristic that has been described for other receptor heteromers, such as the D_1R-histamine H_3 receptor heteromer (23). Importantly, cocaine-induced ERK1/2 phosphorylation could also be demonstrated in mouse striatal slices, but not in striatal slices from σ_1R KO mice. Because cocaine-induced ERK1/2 phosphorylation seems to be a biochemical characteristic of σ_1R-D_1R heteromers, these results provide evidence for the presence of these heteromers in the brain. Furthermore, we also found reciprocal antagonistic interactions between σ_1R and D_1R on MAPK activation, both in transfected cells and in mouse striatal slices. The D_1R agonist-induced ERK1/2 phosphorylation was counteracted when agonist stimulation was performed in slices pretreated with cocaine and, conversely, cocaine-induced ERK1/2 phosporylation was counteracted by D_1R agonist treatment. The cocaine-induced antagonistic modulation of D_1R-mediated MAPK activation was shown to be dependent on σ_1R, as demonstrated in cells transfected with σ_1R siRNA and in striatal slices of σ_1R KO mice. The qualitative similar results observed in transfected cells and in striatal slices support again the existence of σ_1R-D_1R heteromers in the brain.

We have described a previously uncharacterized mechanism by which cocaine binding to σ_1R may significantly influence dopaminergic neurotransmission. Our results show that σ_1R and D_1R heteromerize in living cells and strongly suggest that σ_1R-D_1R heteromers are present in the striatum. Furthermore, our results shed light on the mechanisms behind the behavioral effects of cocaine that are dependent on σ_1R. These data suggest that σ_1R-D_1R heteromers may be considered as targets for the treatment of cocaine addiction and that σ_1R antagonists could counteract some of the behavioral and perhaps the addictive properties of cocaine. It will be important to determine the molecular determinants responsible for this heteromerization. This would allow the development of transgenic animals with mutated receptors not able to form σ_1R-D_1R receptor heteromers and therefore would allow one to better determine the role of σ_1R-D_1R receptor heteromerization in cocaine addiction.

Materials and Methods

Fusion Proteins and Expression Vectors. The N-terminal truncated (nYFP) and the C-terminal truncated (cYFP) version of YFP were made as previously indicated (24). Human cDNAs for D_1R, A_1R, $GABA_{B2}$R, or σ_1R cloned in pcDNA3.1 were amplified without their stop codons and subcloned in an Rluc-expressing vector (pRluc-N1; PerkinElmer), or in a variant of GFP (EYFP-N3; enhanced yellow variant of GFP; Clontech), to give the plasmids that express D_1R, A_1R, $GABA_{B2}$R or σ_1R fused to either Rluc or YFP on the C-terminal end of the receptor (D_1R–Rluc, D_1R–YFP, σ_1R–Rluc, σ_1R–YFP, A_1R–Rluc, A_1R–YFP or $GABA_{B2}$R–Rluc). Human cDNA for D_1R was subcloned in pcDNA3.1–cYFP or pcDNA3.1–nYFP to give the plasmids that express D_1R fused to either nYFP or cYFP on the C-terminal end of the receptor (D_1R–cYFP and D_1R–nYFP). When analyzed by confocal microscopy, it was observed that all fusion proteins showed similar subcellular distribution than naïve receptors. Fusion of Rluc and YFP to D_1R did not modify receptor function as previously determined by cAMP assays.

Cell Culture and Transient Transfection. HEK-293T and CHO cells, grown as previously described (23, 24), were transiently transfected with the corresponding cDNAs by PEI (PolyEthylenImine; Sigma) method as previously described (25) or with siRNA by lipofectamine (Invitrogen) method following the instructions of the supplier. Human and Chinese hamster σ_1R siRNA and scrambled siRNA were designed and synthesized by Invitrogen (HSS 145543).

Cells were used 48 h after transfection. To control for cell number, sample protein concentration was determined by a Bradford assay kit (Bio-Rad).

Immunostaining. Immunocytochemistry assays were performed as previously described (24) using the primary antibodies mouse monoclonal anti-σ_1R (1/200; Chemicon) or rat anti-D_1R (1/200; Chemicon) and stained with the secondary antibodies Cyn3 donkey anti-mouse (1/100; Jackson Immunoresearch Laboratories) or Cyn2 goat antirat (1/100; Jackson Immunoresearch Laboratories). D_1R fused to YFP protein was detected by its fluorescence properties. Samples were observed in a Leica SP2 confocal microscope (Leica Microsystems). Heterodimers of receptors fused to complementary fragments of YFP were detected directly by their fluorescence properties using a Zeiss 510 Meta confocal microscope.

RT-PCR. Total cellular RNA was isolated from HEK-293T or CHO cells using QuickPrep Total RNA Extraction Kit (Amersham Biosciences). Total RNA (1 μg) was reverse transcribed by random priming using M-MLV Reverse Transcriptase, RNase H Minus, Point Mutant, following the protocol of Two-Step RT-PCR provided by the manufacturer (Promega). The resulting single-stranded cDNA was used to perform PCR amplification for σ_1R, DAT and GAPDH as an internal control of PCR technique using Taq DNA Polymerase (Promega). Common primers to amplify human and Chinese hamster σ_1R gene were used: 5′-CCTGGCTGTCGCAGCGGTGCTG-3′ (forward) and 5′-GGTGCCAGAGATGATGGTATCC-3′ (reverse). To amplify human and Chinese hamster DAT, the primers used were 5′-TTCATCATCTACCCGGAAGC-3′ (forward) and 5′-CACCATAGAACCAGGCCACT-3′ (reverse). To amplify human GAPDH, the primers used were 5′-TTCATCATCTACCCGGAAGC-3′ (forward) and 5′-CACCATAGAACCAGGCCACT-3′ (reverse). To amplify Chinese hamster GAPDH, the primers used were 5′-TTCATCATCTACCCGGAAGC-3′ (forward) and 5′- CACCATAGAACCAGGCCACT-3′ (reverse). RNA without reverse transcriptions did not yield any amplicons, indicating that there was no genomic DNA contamination.

BRET Assays. HEK-293T cells were cotransfected with a constant amount of cDNA encoding for the receptor fused to Rluc and with increasingly amounts of cDNA encoding to the receptor fused to YFP to measure BRET, as previously described (25). For BRET assays with bimolecular fluorescence-complemented proteins, HEK-293T cells were cotransfected with a constant amount of cDNA encoding for σ_1R-Rluc or $GABA_{B2}$R-Rluc receptors and with increasingly equal amounts of cDNA corresponding to D_1R–nYFP and D_1R–cYFP, and fluorescence complementation and BRET were determined as previously indicated (25, 26). Both fluorescence and luminescence for each sample were measured before every experiment to confirm similar donor expressions (≈100,000 bioluminescence units) while monitoring the increase in acceptor expression (1,000–10,000 fluorescence units). In each BRET saturation curve, the relative amount of acceptor is given as the ratio between the fluorescence of the acceptor (YFP) and the luciferase activity of the donor (Rluc).

cAMP Determination. CHO cells were treated for 10 min with the indicated concentrations of D_1R agonist SKF 81297 (Sigma), in the absence or presence of 150 μM cocaine (cocaine-HCl, Spanish Agencia del Medicamento no: 2003C00220) or with cocaine alone and cAMP was determined by cAMP (^{3}H) assay kit (Amersham Biosciences).

ERK1/2 Phosphorylation Assays. Brains from WT littermates and σ_1R KO CD1 male albino Swiss mice (8 wk of age, 25 g) were generously provided by Laboratorios Esteve (Barcelona, Spain) (27). Striatal slices were obtained as previously indicated (28), treated with the indicated concentrations of ligands for the indicated time, frozen on dry ice, and stored at −80 °C. Transfected CHO cells were cultured in serum-free medium for 16 h before the addition of the indicated concentration of ligands for the indicated time. Both cells and slices were lysed in ice-cold lysis buffer (24, 28), and ERK1/2 phosphorylation was determined as indicated elsewhere (24, 28).

ACKNOWLEDGMENTS. We thank Hanna Hoffmann (Universitat Autónoma de Barcelona) for assistance with brain striatal slices and Jasmina Jiménez (University of Barcelona) for technical assistance. Brains from σ_1R KO and wild-type littermates CD1 albino Swiss male mice were generously provided by Laboratorios Esteve (Barcelona, Spain). This study was supported by Grants SAF2008-00146, SAF2008-03229-E, and SAF2009-07276 from Spanish Ministerio de Ciencia y Tecnología, Grant 060110 from Fundació La Marató de TV3, and by Intramural Funds of the National Institute on Drug Abuse.

1. Kalivas PW, Volkow ND (2005) The neural basis of addiction: A pathology of motivation and choice. *Am J Psychiatry* 162:1403–1413.
2. Di Chiara G, Bassareo V (2007) Reward system and addiction: What dopamine does and doesn't do. *Curr Opin Pharmacol* 7:69–76.
3. Giros B, Jaber M, Jones SR, Wightman RM, Caron MG (1996) Hyperlocomotion and indifference to cocaine and amphetamine in mice lacking the dopamine transporter. *Nature* 379:606–612.
4. Chen R, et al. (2006) Abolished cocaine reward in mice with a cocaine-insensitive dopamine transporter. *Proc Natl Acad Sci USA* 103:9333–9338.
5. Beuming T, et al. (2008) The binding sites for cocaine and dopamine in the dopamine transporter overlap. *Nat Neurosci* 11:780–789.
6. Gerfen CR (2004) Basal Ganglia. *The Rat Nervous System*, ed Paxinos G (Elsevier Academic Press, Amsterdam), pp 445–508.
7. Xu M, et al. (1994) Elimination of cocaine-induced hyperactivity and dopamine-mediated neurophysiological effects in dopamine D1 receptor mutant mice. *Cell* 79: 945–955.
8. Bertran-Gonzalez J, et al. (2008) Opposing patterns of signaling activation in dopamine D1 and D2 receptor-expressing striatal neurons in response to cocaine and haloperidol. *J Neurosci* 28:5671–5685.
9. Weiss F, et al. (2001) Compulsive drug-seeking behavior and relapse. Neuroadaptation, stress, and conditioning factors. *Ann N Y Acad Sci* 937:1–26.
10. Wolf ME, Mangiavacchi S, Sun X (2003) Mechanisms by which dopamine receptors may influence synaptic plasticity. *Ann N Y Acad Sci* 1003:241–249.
11. Anderson SM, Pierce RC (2005) Cocaine-induced alterations in dopamine receptor signaling: Implications for reinforcement and reinstatement. *Pharmacol Ther* 106: 389–403.
12. Hayashi T, Su TP (2005) The sigma receptor: Evolution of the concept in neuropsychopharmacology. *Curr Neuropharmacol* 3:267–280.
13. Alonso G, et al. (2000) Immunocytochemical localization of the sigma(1) receptor in the adult rat central nervous system. *Neuroscience* 97:155–170.
14. Matsumoto RR, Liu Y, Lerner M, Howard EW, Brackett DJ (2003) Sigma receptors: Potential medications development target for anti-cocaine agents. *Eur J Pharmacol* 469:1–12.
15. Matsumoto RR, et al. (2001) Conformationally restricted analogs of BD1008 and an antisense oligodeoxynucleotide targeting sigma1 receptors produce anti-cocaine effects in mice. *Eur J Pharmacol* 419:163–174.
16. Matsumoto RR, McCracken KA, Pouw B, Zhang Y, Bowen WD (2002) Involvement of sigma receptors in the behavioral effects of cocaine: Evidence from novel ligands and antisense oligodeoxynucleotides. *Neuropharmacology* 42:1043–1055.
17. Hiranita T, Soto PL, Tanda G, Katz JL (2010) Reinforcing effects of sigma-receptor agonists in rats trained to self-administer cocaine. *J Pharmacol Exp Ther* 332:515–524.
18. Kong MM, Fan T, Varghese G, O'dowd BF, George SR (2006) Agonist-induced cell surface trafficking of an intracellularly sequestered D1 dopamine receptor homo-oligomer. *Mol Pharmacol* 70:78–89.
19. Gandía J, Lluís C, Ferré S, Franco R, Ciruela F (2008) Light resonance energy transfer-based methods in the study of G protein-coupled receptor oligomerization. *Bioessays* 30:82–89.
20. Pettit HO, Pan HT, Parsons LH, Justice JB, Jr. (1990) Extracellular concentrations of cocaine and dopamine are enhanced during chronic cocaine administration. *J Neurochem* 55:798–804.
21. Su TP, Hayashi T (2001) Cocaine affects the dynamics of cytoskeletal proteins via sigma(1) receptors. *Trends Pharmacol Sci* 22:456–458.
22. Akunne HC, et al. (1997) The pharmacology of the novel and selective sigma ligand, PD 144418. *Neuropharmacology* 36:51–62.
23. Ferrada C, et al. (2009) Marked changes in signal transduction upon heteromerization of dopamine D1 and histamine H3 receptors. *Br J Pharmacol* 157:64–75.
24. Navarro G, et al. (2009) Interactions between calmodulin, adenosine A2A, and dopamine D2 receptors. *J Biol Chem* 284:28058–28068.
25. Carriba P, et al. (2008) Detection of heteromerization of more than two proteins by sequential BRET-FRET. *Nat Methods* 5:727–733.
26. Gandia J, et al. (2008) Detection of higher-order G protein-coupled receptor oligomers by a combined BRET-BiFC technique. *FEBS Lett* 582:2979–2984.
27. Langa F, et al. (2003) Generation and phenotypic analysis of sigma receptor type I (sigma 1) KO mice. *Eur J Neurosci* 18:2188–2196.
28. Navarro G, et al. (2010) Interactions between intracellular domains as key determinants of the quaternary structure and function of receptor heteromers. *J Biol Chem* 285:27346–27359.

Supporting Information

Navarro et al. 10.1073/pnas.1008911107

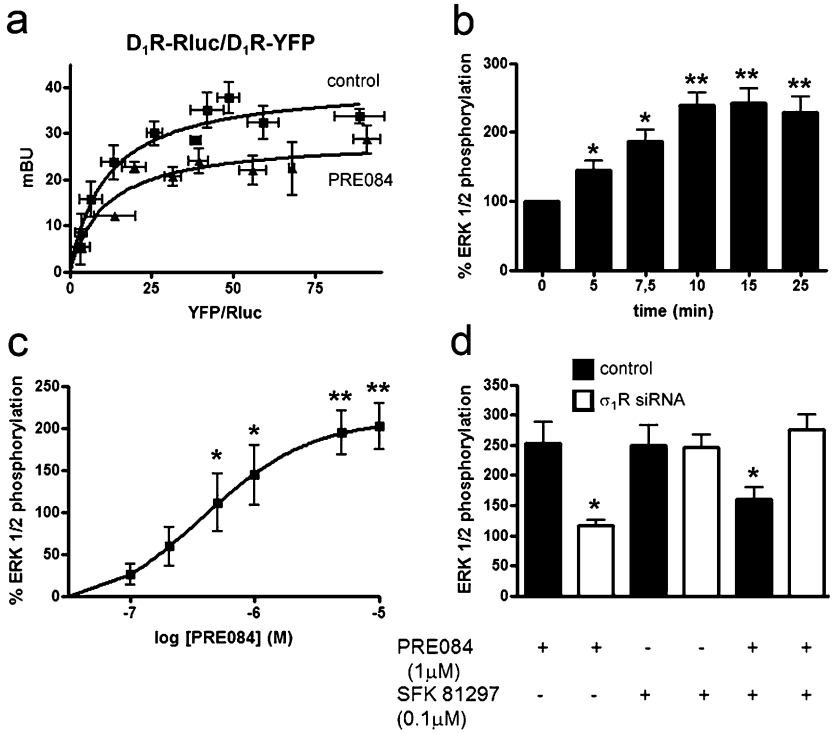

Fig. S1. Effect of s_1R agonist PRE084 on D_1R homomerization and function. (*A*) BRET was measured in HEK-293T cells transfected with D_1R–Rluc cDNA and increasing amounts of D_1R–YFP cDNA treated with (▲) or without (■) 200 nM PRE084 for 10 min. Relative amounts of BRET acceptor are expressed as ratio between fluorescence of acceptor (YFP) and luciferase activity of donor (Rluc). BRET data are expressed as means ± SD of five different experiments grouped as a function of the amount of BRET acceptor. (*B* and *C*) CHO cells transfected with D_1R cDNA were treated or not treated with 200 nM PRE084 for increasing length of time (*B*) or for 10 min with increasing concentrations of PRE084 (*C*) $*P < 0.05$ and $**P < 0.01$, compared with time "0" (*B*) or 100 nM (*C*); one-way ANOVA followed by Bonferroni post hoc tests. (*D*) CHO cells were transfected with D_1R cDNA (filled bars) or cotransfected with D_1R and σ_1R siRNA (open bars) and were treated or not treated for 10 min with 1 μM PRE084 and, during the last 2 min, the addition of 100 nM SKF 81297 or medium. ERK 1/2 phosphorylation is represented as percentage of basal levels (100%). $*P < 0.05$ compared with PRE084-treated samples; one-way ANOVA followed by Bonferroni post hoc tests. Values are mean ± SEM of five experiments.

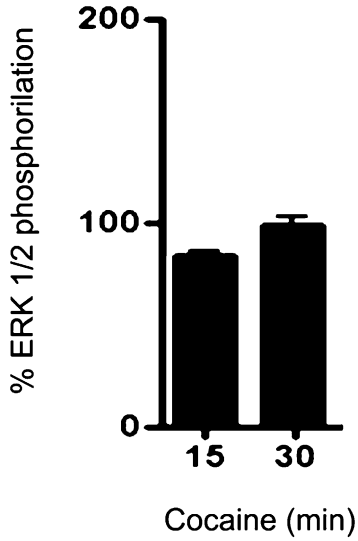

Fig. S2. Effect of cocaine on ERK1/2 phosphorylation in nontransfected CHO cells. CHO cells were incubated with 150 μM cocaine for 15 or 30 min. ERK 1/2 phosphorylation is represented as percentage over basal levels (100%). Results are mean ± SEM of four independent experiments performed in duplicate.

3.5 La cocaína a través de heterómeros de receptores sigma-1 y D_2 de dopamina inhibe la señalización del receptor D_2

Gemma Navarro[1], Estefanía Moreno[1], Jordi Bonaventura[1], Marc Brugarolas[1], Daniel Farré[1], Josefa Mallol[1], Antoni Cortés[1], Vicent Casadó[1], Carme Lluís[1], Sergi Ferre[2], Rafael Franco[3], Enric Canela[1*], Peter J. McCormick[1*]

[*]Codirectores del manuscrito.

[1]Centro de Investigación Biomédica en Red sobre Enfermedades Neurodegenerativas, Departamento de Bioquímica y Biología Molecular, Facultad de Biología, Universidad de Barcelona, Barcelona, España,
[2]National Institute on Drug Abuse, Intramural Research Program, National Institutes of Health, Department of Health and Human Services, Baltimore, MD, USA,
[3]Centro de Investigación Médica Aplicada, Universidad de Navarra, Pamplona, España.

Manuscrito enviado para su publicación a *Proceedings of the National Academy of Sciences of USA*.

En el estudio del efecto de la cocaína sobre la funcionalidad del receptor D_2 de dopamina, presentado en este trabajo, demostramos la interacción molecular y funcional del receptor σ_1 con los receptores D_2 de dopamina. Mediante aproximaciones biofísicas y bioquímicas, hemos descubierto que los receptores D_2 de dopamina (la isoforma larga del receptor D_2) pueden formar heterómeros con los receptores σ_1, siendo esta interacción específica de los receptores D_2, ya que otros miembros de la familia de receptores D_2-like, D_3 y D_4, no forman heterómeros. Los heterómeros σ_1-D_2 están constituidos por oligómeros de orden superior, con una estructura mínima de heterotetrámeros, σ_1-σ_1-D_2-D_2. Hemos demostrado que los heterómeros σ_1-D_2 se expresan en estriado de ratón y se demuestra que la cocaína, a través de la unión a los heterómeros σ_1-D_2, inhibe la señalización de los receptores D_2 tanto en cultivos celulares como en estriado de ratón. En conjunto, todos estos resultados proporcionan un nuevo mecanismo por el cual la cocaína puede disminuir la señalización de la vía indirecta (neuronas que expresan el receptor D_2) alterando el delicado balance entre las neuronas que expresan receptores D_1 y D_2 en el estriado.

Cocaine inhibits D_2 receptor signalling via sigma-1-dopamine D_2 receptor heteromers

Gemma Navarro[1], Estefanía Moreno[1], Jordi Bonaventura[1], Marc Brugarolas[1], Daniel Farré[1], Josefa Mallol[1], Antoni Cortés[1], Vicent Casadó[1], Carme Lluís[1], Sergi Ferre[2], Rafael Franco[3]*, Enric Canela[1]*, Peter J. McCormick[1]*

[1]Centro de Investigación Biomédica en Red sobre Enfermedades Neurodegenerativas, and Department of Biochemistry and Molecular Biology, Faculty of Biology, University of Barcelona, Barcelona, 08028 Spain; [2]National Institute on Drug Abuse, Intramural Research Program, National Institutes of Health, Department of Health and Human Services, Baltimore, MD, 21224 USA; [3]Centro de Investigación Médica Aplicada, Universidad de Navarra, Pamplona, 31008 Spain

*These authors contributed equally to this work

Running Title: Sigma-1 and dopamine D_2 receptor heteromers

ABSTRACT

Exploring the effect of cocaine on dopamine D_2 receptors function, we present evidence of σ_1 receptor molecular and functional interaction with dopamine D_2 receptors. Using biophysical and biochemical approaches, we discovered that D_2 receptors (the long isoform of the D_2 receptor) can form heteromers with σ_1 receptors, a result that is specific to D_2 receptors, as the other members of the D_2-like receptor family, D_3 and D_4 receptors, did not form heteromers. The σ_1-D_2 receptor heteromers consist of higher order oligomers with a minimal structure of σ_1-σ_1-D_2-D_2 receptor heterotetramers. We demonstrate that these σ_1-D_2 receptor heteromers are found in mouse striatum and show that cocaine, by binding to σ_1-D_2 receptor heteromers, inhibits downstream signaling in both cultured cells and in mouse striatum. Taken together, these data illuminate the mechanism by which cocaine can inhibit signaling via the indirect (D_2 receptor containing neurons) pathways, destabilizing the delicate balance of D_1 and D_2 neurons in the brain.

Keywords: Cocaine /Dopamine receptors / Heteromers / GPCRs / Sigma-1/dopamine signaling

INTRODUCTION

The mechanisms leading to cocaine addiction are multifaceted, but a major player in the pathogenesis of addiction is the dopaminergic pathway particularly the striatal efferent neurons *(1, 2)*. GABAergic striatal efferent neurons constitute more than 95% of the striatal neuronal population *(3)*. There are two major subtypes of GABAergic striatal efferent neurons: GABAergic dynorphinergic neurons, which express the peptide dynorphin and dopamine D_1 receptors and GABAergic enkephalinergic neurons, which express the peptide enkephalin and dopamine D_2 receptors *(3)*. Originally it was thought that the major player in cocaine addiction was the dopamine D_1 receptor and the neurons that express it as the activation of D_1 receptors is an absolute requirement for the induction of the cellular and behavioral responses to cocaine, as demonstrated by studies performed in D_1 receptor knockout mice *(4)*. These results are supported by studies using transgenic mice in which dopamine D_1 or D_2 receptors containing GABAergic neurons are visualized by the expression of fluorescent proteins, showing that the acute cellular response to cocaine mostly engage D_1 receptor-expressing neurons *(5)*. However more recent data has pointed out that both dopamine D_1 and D_2 containing neurons play a role in addiction. It has been shown that D_2 receptor is required to enhance the rewarding properties of cocaine *(6)*. In addition, the release of dopamine evoked by cocaine injection is dramatically higher in D_2 −/− mutants compared to WT animals *(7)*, and an intact D_2-mediated signaling is thought to be required to elicit the rewarding and reinforcing effects of cocaine *(7)*. These studies and others point out a role for both presynaptic and postsynaptic D_2 receptors in cocaine-induced effects *(8, 9)*. In a study looking at how cocaine alters neuromodulatory effects, there was a switch from D_2 to a D_1 mediated increase on $GABA_A$-IPSC in cocaine treated rats *(11)*, and in long-term models of cocaine addiction it has been shown that D_1 increases and D_2 levels decrease *(12)*. Thus, this begs the question, if D_2 is required for cocaine addiction and yet it seems to decrease in expression in relation to D_1 over time, are the effects of D_2 accomplished at the initial stages of cocaine exposure?

The initial mechanistic steps of cocaine binding and its effects on these two populations of neurons (D_1 and D_2 receptor containing neurons) are not well understood. What is known is cocaine is able to exert part of its behavioural and cellular effect by elevating dopamine levels in the striatum *(8)*. It achieves this by binding to and inhibiting the presynaptic dopamine transporter (DAT) *(13)*. DAT mediates reuptake of dopamine from the synaptic cleft and controls the termination of dopaminergic signaling. Cocaine is a high-affinity inhibitor of DAT and upon binding to DAT cocaine causes a rapid increase in extracellular dopamine levels. Thus, upon drug intake, DAT is inhibited, transport of dopamine into the cell is blocked, the amount of extracellular dopamine increases, and dopamine signaling, controlled by any of the five dopamine receptors, is strongly activated leading to stimulation or inhibition of signaling pathways. Signaling through the D_1-like receptor family (eg. D_1 or D_5 receptors) or D_2-like receptor family, (D_2, D_3 and D_4 receptors), translates into activation/inhibition of specific neurons and circuitries. In addition, to binding to DAT, cocaine can also bind to a receptor heteromer made up of the D_1-like receptor family member, D_1 and the σ_1-receptor *(14)*. Through this latter interaction, cocaine robustly potentiated D_1 receptor-mediated adenylyl cyclase activation, induced ERK1/2 phosphorylation and counteracted the MAPK activation induced by D_1 receptor stimulation *(14)*. Although the early effects of cocaine binding to D_1 containing neurons via σ_1 receptor heteromers are now clear the initial mechanistic steps of cocaine binding and its effects on the D_2 receptor if any are unknown. Here we explore the initial molecular events after cocaine exposure on the dopamine receptor D_2 like family. We report a molecular interaction between σ_1 and D_2 receptors but not the other dopamine D_2-like receptors. Cocaine was able to bind to a receptor heteromer, consisting of at least two interacting σ_1 receptor and D_2 receptor homodimers, and promoted structural changes in the heteromer that led to significant modifications in D_2 receptor signaling. Cocaine binding to σ_1-D_2 receptor heteromer diminishes the ability of D_2 receptors to signal through G_i protein or to induce ERK 1/2 phosphorylation, effects that might have implications on establishing addiction. Altogether, these findings indicate that σ_1-D_2 receptor heteromer-mediated alterations of dopaminergic neurotransmission constitute an important initial mechanistic step of cocaine action.

RESULTS

σ_1 receptors form heteromers with dopamine D_2 receptors but not with the other D_2-like receptor family members

We first examined whether the receptors of the D_2R-like family could directly interact with σ_1 receptors and thus be a target for cocaine binding. To do this we used the Bioluminescence Resonance Energy Transfer (BRET) technology in HEK-293T cells expressing a constant amount of D_2 (long isoform), D_3 or D_4 dopamine receptors fused to *Renilla Luciferase* (RLuc) and increasing amounts of σ_1 receptors fused to Yellow Fluorescence Protein (YFP). Clear BRET saturation curves were obtained in cells expressing D_2-RLuc receptors and increasing amounts of σ_1-YFP receptors with a $BRET_{max}$ of 55±7 mBU and a $BRET_{50}$ of 28±6 (Fig. 1a). In contrast, in cells expressing D_3-RLuc or D_4-RLuc and σ_1-YFP receptors a low and linear non-specific BRET signal was obtained thus confirming the specificity of the interaction between D_2-RLuc and σ_1-YFP receptors (Fig. 1b). As a further control, cells were cotranfected with σ_1-YFP receptors and adenosine A_{2A}-Rluc receptors and no specific BRET signal was obtained (Fig. 1a). These results indicate that σ_1 receptors selectively interact with dopamine D_2 receptors and not with the other members of the D_2-like receptor family.

It is known that σ_1 receptors are predominantly found in the endoplasmic reticulum membrane, and also in the plasma membrane *(15)*. The expression of σ_1 and D_2 receptors at the plasma membrane level was explored by analyzing the co-localization of both receptors by confocal microscopy. HEK-293T cells were used in the assays since they constitutively express σ_1 receptors, but not DAT *(14)*. As expected, a punctate σ_1 receptor staining in naïve HEK cells was detected (Fig. 1c left panel, top images). After transfection of the cDNA corresponding to D_2 receptors, a co-localization of σ_1 receptor and D_2 receptors was detected at the plasma membrane level in cells not treated with cocaine (Fig. 1c left panel, bottom images) or in cells treated with 30 μM cocaine for 30 min (Fig. 1c right panels).

Higher order complex formation between σ_1 receptors and dopamine D_2 receptors

It is known that many membrane receptors are expressed as oligomers (homomers) with a minimal structural unit of homodimers *(16–22)*. Taking this into account, we investigated the possible formation of receptor heteromers constituted by σ_1 and D_2 receptor homomers. In the case of dopamine D_2 receptors it has been described that they are expressed as homodimers *(23–27)*, however dimerization of σ_1-receptors has not been reported. First, we tested if σ_1 receptors can form homomers by BRET experiments in HEK-293T cells expressing a constant amount of σ_1-RLuc receptors and increasing amounts of σ_1-YFP receptors. A positive and saturable BRET signal was obtained with a $BRET_{max}$ of 165±35 mBU and a $BRET_{50}$ of 22±12 (Fig. 2a) indicating that a σ_1-σ_1 homodimers can exist and demonstrating, for the first time, the oligomerization of σ_1 receptors. Next, we tested whether D_2 receptor homomers could interact with σ_1-receptors by a combined BRET and FRET assay termed Sequential Resonance Energy Transfer (SRET) *(28)*. This assay involves two sequential energy transfer events, one BRET process between Rluc and a blue shifted GFP^2 and a second FRET process between excited GFP^2 and YFP (see Fig. 2b top scheme). In HEK-293T cells expressing a constant amount of D_2-RLuc and D_2-GFP^2 receptors and increasing amounts of σ_1-YFP receptors, a net SRET saturation curve was obtained with a $SRET_{max}$ of 269±33 SU and a $SRET_{50}$ of 92±24 (Fig. 2b). Cells expressing constant amounts of adenosine A_{2A}-RLuc and A_{2A}-GFP^2 receptors and increasing amounts of σ_1-YFP receptors provided very low and linear SRET, according to the lack of interaction between A_{2A} receptors and σ_1 receptors. These results demonstrate that σ_1 receptors are able to form heteromers with D_2-D_2 receptor homomers. A net SRET saturation curve was also obtained using HEK 293T cells expressing constant amounts of σ_1-Rluc and D_2-GFP^2 and increasing amounts of σ_1-YFP ($SRET_{max}$: 140±8 SU; $SRET_{50}$: 9±3; Fig. 2c) but not when D_2-GFP^2 receptor was replaced by A_2-GFP^2 receptor. These results demonstrate that D_2 receptors are able to form heteromers with σ_1-σ_1 receptor homomers. Finally, we tested for a higher order

interaction of receptor heteromers constituted by σ_1 and D_2 receptor homomers (σ_1-σ_1-D_2-D_2). This was done using a modified BRET assay that involves a double complementation assay *(27)*. An explanatory diagram showing BRET with luminescence/fluorescence complementation approach (BRET with BiFC assay; see Methods) is shown in Figure 2d (top panel). Briefly, one receptor fused to the N-terminal fragment (nRluc8) and another receptor fused to the C-terminal fragment (cRluc8) of the Rluc8 act as BRET donor after Rluc8 reconstitution by a close receptor-receptor interaction and one receptor fused to an YFP Venus N-terminal fragment (nVenus) and another receptor fused to the YFP Venus C-terminal fragment (cVenus), act as BRET acceptor after YFP Venus reconstitution by a close receptor-receptor interaction. Accordingly, cells were co-transfected with a constant amount of the two cDNAs corresponding to D_2-nRLuc8 and D_2-cRLuc8 (equal amounts of the two cDNAs) and with increasing amounts of the two cDNAs corresponding to σ_1-nVenus and σ_1-cVenus (equal amounts of the two cDNAs). Specific BRET would only be possible if RLuc reconstituted by D_2-nRLuc8-D_2-cRLuc8 dimerization is close enough to YFP Venus reconstituted by σ_1-nVenus-σ_1-cVenus dimerization. Higher order heterotetramers were in fact observed as evidenced by a positive BRET signal (Fig. 2d). As negative controls, cells expressing only three fusion proteins and the fourth receptor not fused provided neither a significant fluorescent signal nor a positive BRET (Figure 2d). Collectively these results indicate that σ_1-D_2 receptor heteromers seem to be constituted by the interaction of receptor homomers and the minimal structural unit is the σ_1-σ_1-D_2-D_2 receptor heterotetramer.

Effect of σ_1 receptor ligands on σ_1-D_2 receptor heterotetramer.

It is known that cocaine can bind to σ_1 *(29, 30)*. We sought to measure the effect of cocaine binding to σ_1 receptors on σ_1-D_2 receptor heteromers. We performed BRET experiments in HEK-293T cells expressing a constant amount of D_2-RLuc receptors and increasing amounts of σ_1-YFP receptors in the presence or in the absence of both cocaine and the σ_1 ligand PRE084. The BRET saturation curve was reduced when cells were treated for 10 min with 100 nM of the selective σ_1 receptor agonist PRE084 ($BRET_{max}$: 40±8 mBU; $BRET_{50}$: 31±6) or with 30 μM of cocaine ($BRET_{max}$: 35±6 mBU; $BRET_{50}$: 26±8) (Fig. 3a) indicating that ligand binding to σ_1 receptors induces structural changes in the σ_1-D_2 receptor heteromer. To know if structural changes in σ_1-σ_1 receptor homomers or in D_2-D_2 receptor homomers can account for the ligand-induced effect on σ_1-D_2 receptor heteromers, we performed BRET experiments in cells expressing σ_1-RLuc and σ_1–YFP receptors as indicated in Fig. 2a, treating cells for 10 min with 100 nM of PRE084 or for 30 min with 30 μM of cocaine. As shown in Fig. 3b, no significant changes in $BRET_{max}$ or $BRET_{50}$ were observed. In contrast, the BRET saturation curve obtained in cells expressing a constant amount of D_2-RLuc receptors and increasing amounts of D_2-YFP receptors ($BRET_{max}$: 44±3 mBU; $BRET_{50}$: 12±4) changed in cells treated for 10 min with 100 nM of PRE084 ($BRET_{max}$: 27±5 mBU; $BRET_{50}$: 11±4) or 30 min with 30 μM of cocaine ($BRET_{max}$: 29±2 mBU; $BRET_{50}$: 19±5) (Fig. 3c). To test whether the effect of cocaine on D_2-D_2 heteromers is be due to the presence of σ_1 receptors, assays were performed in cells whose σ_1 receptor expression was knocked-down using an RNAi approach (Fig. 3d). When we transfected a specific small interfering RNA (siRNA), a robust silencing of σ_1 receptor expression was obtained (Supplementary Fig. 1). The treatment with the specific siRNA completely abolished the effect of cocaine or PRE084 on the BRET saturation curve (Fig. 3d). These results suggest that ligand binding to σ_1 receptors induces strong changes in the structure of the D_2-D_2 receptor homomers in the σ_1-D_2 receptor heteromers.

Cocaine binding to σ_1 receptors modulate the D_2 receptor signaling in transfected cells

The cocaine-induced modifications of the quaternary structure of D_2 receptor homomers in the σ_1-D_2 receptor heteromer described above suggest that cocaine can modulate the functionality of D_2 receptors. To study how cocaine affects D_2 receptor-mediated signaling, Chinese hamster ovary (CHO) cells were used as they provided a lower baseline of signalling for which to detect downstream changes.

CHO cells have been shown to constitutively express σ_1 receptors but not DAT *(14)*. The effect of cocaine on D_2 receptor agonist-induced, G protein-mediated signalling was measured using a label free assay that measures changes in cell impedance in response to stimulation. In CHO cells stably expressing D_2 receptors, increasing cocaine concentrations (10 nM to 100 μM) did not give any G protein-mediated signaling, neither $G_{i/0}$, G_S or G_q (Fig. 4a) as compared to known control receptors (Supplementary Fig. 2). The signaling obtained upon D_2 receptor activation with the agonist quinpirole (0.1 nM to 1 μM) showed a G_i profile (increases in impedance) that was completely blocked when cells were treated with the G_i specific pertussis toxin (PTx) (Fig. 4b). We observed a small but significant decrease in the G_i activation induced by quinpirole when cells where pre-treated for 1h with cocaine (Fig. 4c). These results indicate that cocaine by itself is not able to induce a G protein-mediated signaling but can partially inhibit the ability of D_2 receptors to signal through G_i. A downstream consequence of G_i mediated signaling is the ability to suppress cAMP signaling. In addition to the label free experiments above we determined the levels of cAMP in CHO cells stably expressing D_2 receptors using forskolin and then measured whether cocaine was able to decrease the forskolin-induced cAMP formation. We found cocaine alone could not decrease the levels of cAMP after treatement with forskolin compared to the D_2 agonist quinpirole (Fig 4d). However, cocaine significantly dampened the quinpirole-induced decreases of forskolin-mediated increases in cAMP levels (Fig. 4d). This effect was blocked when cells were transfected with siRNA against the σ_1 receptor (Fig. 4d), demonstrating that cocaine's ability to counteract the action of quinpirole was mediated by σ_1 receptors. Similar results were obtained when instead of cocaine the σ_1 receptor agonist PRE084 was used (Supplementary Fig. 3) reinforcing the concept that σ_1 receptor ligands induce a significant decrease in the ability of D_2 receptors to signal through G_i.

Apart from G protein-mediated signaling, many GPCRs are able to signal in a G protein-independent way *(31–35)*. ERK 1/2 phosphorylation is one of the MAPK pathways that has been described to be activated in a G protein-independent and arrestin-dependent mechanism *(34)*. Several reports have highlighted the importance of ERK 1/2 activation in D_2 receptors containing neurons for the effects of cocaine *(36–38)*. We sought to understand how cocaine might influence σ_1-D_2 receptor heteromer-mediated ERK 1/2 signaling. Varying concentrations of cocaine and varying time of treatment did not lead to any significant change in ERK 1/2 phosphorylation in response to cocaine in cells not expressing D_2 receptors (Supplementary Fig. 4). Importantly, cocaine *per se* dose-dependently (Fig. 5a) and time-dependently (Fig. 5b) activated ERK 1/2 phosphorylation in cells expressing D_2 receptors. This effect was mediated by σ_1 receptors since it was strongly diminished in cells transfected with the σ_1 receptors siRNA (Figs. 5a and 5b). The D_2 receptor agonist quinpirole was also dose-dependently (Fig 5c) and time-dependently (Fig. 5d) able to activate ERK 1/2 phosphorylation but, as expected, this effect was not mediated by σ_1 receptors since it was not diminished in cells transfected with the σ_1 receptors siRNA (Figs. 5c and 5d). These results point out that σ_1 or D_2 receptor activation in the σ_1-D_2 receptor heteromer induces ERK 1/2 phosphorylation. Thus, cocaine, like quinpirole, may be considered an agonist at the MAPK activation level for the heteromer.

A property of some receptor heteromers is the ability of the antagonist of one receptor to block the function of the agonist of the partner receptor, a property defined as cross-antagonism *(39)*. In cells expressing D_2 receptors we looked for cross-antagonism among σ_1-D_2 receptor heteromers. Indeed we found the cocaine-induced ERK 1/2 phosphorylation was counteracted not only by the σ_1 receptor antagonist PD144.418 (1 μM) but also by the D_2 receptor antagonist raclopride (10 μM) (Fig. 6a). Analogously the D_2 receptor agonist quinpirole-induced ERK 1/2 phosphorylation was blocked by raclopride but also by PD144.418 (Fig. 6b). Interestingly, the effect of PD144.418 on quinpirole-induced ERK1/2 phosphorylation was not observed when cells were transfected with the siRNA for σ_1 receptors (Fig. 6b). These results indicate that there is a cross-antagonism between σ_1 and D_2 receptors. By definition an antagonist cannot signal on its own, therefore this cross-antagonism can only derive from the direct protein-protein interactions established between the receptors in the σ_1-D_2 receptor heteromer.

As mentioned above cocaine can inhibit DAT and increase the dopamine concentration in the striatum; so, in the presence of cocaine both receptors in the σ_1-D_2 receptor heteromer could be activated. Therefore we asked, what happens to ERK 1/2 phosphorylation after co-activation of both receptors? Surprisingly, a negative cross-talk was detected. When cells expressing D_2 receptors were treated with both 1 μM quinpirole and 30 μM cocaine there was a decrease in ERK 1/2 phosphorylation compared to quinpirole alone (Fig 7a). This difference was not seen if the cells were depleted of σ_1 receptors via siRNA (Fig. 7a).

Cocaine binding to σ_1 receptors modulates the D_2 receptor signaling in mouse brain striatum

The above described negative cross-talk is a characteristic of the σ_1-D_2 receptor heteromers that may be exploited as a fingerprint to look for the existence of σ_1-D_2 receptor heteromers in the striatum. Striatum slices from wild-type (WT) and σ_1 knockout (KO) mice were tested for the effects of cocaine on ERK 1/2 phosphorylation. In co-transfected cells a strong and significant effect of cocaine was observed at 15 μM (see Fig. 5), a striatal level of the drug reached after pharmacologically significant doses of cocaine *(40)*. To allow diffusion into the tissue a ten-fold higher cocaine concentration, 150 μM, was then used to see clear effects in slices of mouse striatum (Fig. 7b). Both the D_2 receptor agonist quinpirole (1 μM) and cocaine (150 μM) induced ERK 1/2 phosphorylation in striatal slices of WT mice after 10 min activation (Supplementary Fig. 5) or after 30 min activation (Fig. 7b). More interestingly, in striatal slices of WT mice, the co-activation with quinpirole and cocaine blocked ERK 1/2 phosphorylation (Fig. 7b and Supplementary 5). Thus, the negative cross-talk between σ_1 and D_2 receptors on MAPK signaling detected in cotransfected cells was also observed in striatal samples from WT mice, meaning that the same biochemical fingerprint seen in transfected cells was also found in WT mice. When similar experiments were performed in striatal slices from mice lacking the σ_1 receptors, cocaine was unable to induce ERK 1/2 phosphorylation (Fig. 7b and Supplementary 5) and quinpirole-induced ERK 1/2 phosphorylation was not modified by cocaine (Fig. 7b and Supplementary 5). These results strongly support the existence of σ_1-D_2 receptor heteromers in the striatum and indicate that all detected cocaine effects are dependent on σ_1 receptors expression.

DISCUSSION

The data presented in this paper lead to several major conclusions on the role of D_2 receptors on the initial events upon cocaine exposure. First, D_2 receptors can form heteromers with σ_1 receptors, a result that is specific to D_2 receptors as the other members of the D_2-like family, D_3 and D_4 receptors, did not form heteromers. Second, σ_1-D_2 receptor heteromers consist of higher order oligomers with a minimal structure of σ_1-σ_1-D_2-D_2 receptor heterotetramers. Third, these σ_1-D_2 receptor heteromers are found in mouse striatum. Finally, cocaine, by binding to σ_1-D_2 receptor heteromers, inhibits downstream signaling in both cultured cells and in mouse striatum. Cocaine intake elevates dopamine levels in the striatum, particularly in its more ventral part, the nucleus acccumbens, which has been shown to be a preferential anatomical substrate for reward *(41, 42)*. Cocaine exploits the dopaminergic system to elicit part of its behavioral and cellular effects *(8)*. Earlier studies have suggested that the presynaptic dopamine transporter (DAT) is the primary target for cocaine effects *(43–46)*. However, not all cocaine effects are mediated by a dopamine increase derived by the cocaine inhibition of DAT. Indeed, cocaine interacts with many proteins, and it is now well established that cocaine interacts with σ_1 receptors at concentrations that are neuroactive *(47, 48)*. In fact, reducing brain σ_1 receptor levels with antisense oligonucleotides attenuates the convulsive and locomotor stimulant actions of cocaine *(49, 50)* and antagonists for σ_1 receptors have also been shown to mitigate the actions of cocaine in animal models *(47)*. σ_1 receptors are highly expressed in the brain *(15, 51)*. Within the caudate-putamen and nucleus accumbens (the dorsal and ventral parts of the striatum, respectively), brain regions that mediate the long-term effects of cocaine, it was demonstrated that repeated cocaine administration induces up-regulation of σ_1 receptors, a process mediated by dopamine D_1 receptors *(52)*. Indeed, we have demonstrated earlier the

importance of the σ_1 and D_1 receptor interaction on the initial events upon cocaine exposure *(14)*. Through σ_1-D_1 receptor heteromers, cocaine robustly potentiated D_1 receptor-mediated adenylyl cyclase activation, providing a mechanism for D_1 receptor-mediated effects of cocaine *(14)*. In addition to DAT and D_1 receptors, our work here highlights an additional player in the early events of cocaine exposure, the dopamine D_2 receptor. We found that σ_1 and D_2 receptors interact at both molecular and functional levels. At the molecular level, by using new developed techniques based on resonance energy transfer, we demonstrated the oligomerization of σ_1 receptors in cell cultures and that σ_1 and D_2 receptors combine into heteromers consisting of at least one σ1 receptor homodimer and one D_2 receptor homodimer. Cocaine binding to the σ_1 receptor in the heteromer promotes structural changes in the heteromer that lead to significant modifications in D_2 receptor function. Cocaine by itself is not able to induce a G protein-mediated signaling, but by acting on the σ_1-D_2 heteromer it can decrease the ability of D_2 receptors to signal through G_i. Thus, the D_2 receptor-mediated inhibition of cAMP production was significantly reduced by cocaine binding to σ_1-D_2 receptor heteromers, resulting in a cocaine-induced inhibition of D_2 receptor signaling. Moreover, cocaine by itself activated ERK 1/2 phosphorylation, as an initial event, in a process that requires both σ_1 and D_2 receptors. These results indicate that cocaine acts as an agonist of σ_1-D_2 receptor heteromers at the MAPK activation level. Importantly, cocaine-induced ERK 1/2 phosphorylation could also be demonstrated in mouse striatal slices, but not in striatal slices from σ_1 receptor KO mice. Since cocaine-induced ERK 1/2 phosphorylation seems to be a biochemical characteristic of σ_1-D_2 receptor heteromers, these results provide evidence for their presence in the striatum. In addition, cocaine inhibited the D_2 receptor-induced ERK 1/2 phosphorylation. In summary, the cocaine binding to σ_1-D_2 receptor heteromers dampened D_2 receptor signaling.

The cocaine effect on σ_1-D_2 receptor heteromer signaling is in contrast with the cocaine effect on σ_1-D_1 receptor heteromer signaling described by Navarro et al*(13)*. In the last case, the D_1 receptor-mediated activation of cAMP production was significantly increased by cocaine binding to σ_1 protomer in the σ_1-D_1 receptor heteromers, resulting in a cocaine-induced increase in cAMP production. The results here described and those described by Navarro et al *(13)*, point to a scenario where cocaine selectively leads to increased dopamine-induced signaling through the cAMP pathway in D_1 receptor-containing neurons and to depressed dopamine-induced inhibition of cAMP formation in D_2 receptor-containing neurons. Simultaneously, cocaine disrupts the initial ERK 1/2 phosphorylation signaling induced by dopamine in both D_1 receptor and D_2 receptor-containing neurons. These findings suggest that cocaine exposure leads to a deregulation of a normally balanced D_1/D_2 dopamine receptor signaling. The balance of D_1 and D_2 inputs is designed to avoid addictive behavior, thus its disruption would have long term consequences. The data presented in this paper support a key role of σ_1 receptors in determining the acute effects of cocaine by increasing the D_1 receptor-mediated cAMP production and dampening the D_2 receptor signaling in σ_1-D_2 receptor heteromers,pushing the balance of inputs towards the D_1 containing direct pathway. Our data has support to the results described by Bateup et al. *(53)* since they found that the locomotor response to acute cocaine was reduced after selective deletion of DARPP-32 in striatonigral neurons, indicating an essential role for the direct pathway in this behavior while, the authors also reported, that D_2 receptor-expressing striatopallidal neurons oppose the locomotor activation induced by cocaine. More recently, Luo et al *(54)*, have found in vivo evidence for the existence of D_1 and D_2 receptor-mediated cellular effects of cocaine (D_1 receptor-mediated increase in Ca^{2+} influx and D_2 receptor-mediated decrease in Ca^{2+} influx, using in vivo optical microprobe Ca^{2+} influx imaging), with a significantly slower dynamics of the effect mediated by D_2 receptors. Taking into account our findings, the observations of Luo et al could in fact be related to the signaling brake imposed by cocaine on the sigma σ_1-D_2 receptor heteromer. Cocaine binding to σ_1 receptors in σ_1-D_2 receptor heteromers may significantly influence dopaminergic neurotransmission. In summary the results described here provide insight on a novel molecular mechanism by which cocaine affects differently the direct (D_1 containing) and indirect (D_2 containing) pathways.

MATERIALS AND METHODS

Fusion proteins and expression vectors.

Sequences encoding amino acids residues 1-155 and 155-238 of YFP Venus protein, and amino acids residues 1-229 and 230-311 of RLuc8 protein were subcloned in pcDNA3.1 vector to obtain the YFP Venus (nVenus, cVenus) and RLuc8 (nRLuc8, cRLuc8) hemi-truncated proteins expressed in pcDNA3.1 vector. The human cDNA for the long isoform of dopamine D_2 receptors (D_2 receptors), adenosine A_{2A} or σ_1 receptors cloned in pcDNA3.1 were amplified without their stop codons using sense and antisense primers harboring either unique *EcoRI* and *BamHI* sites (or *EcoRI* and *KpnI* sites for σ_1 receptor). The fragments were then subcloned to be in-frame with Rluc, EYFP or GFP^2 into the *EcoRI* and *BamHI* or *KpnI* restriction site of an Rluc-expressing vector (pRluc-N1, PerkinElmer, Wellesley, MA), an EYFP expressing vector (EYFP-N3; enhanced yellow variant of GFP; Clontech, Heidelberg, Germany) or an GFP^2 expressing vector (GFP^2-N2, Clontech) respectively, to give the plasmids that express receptors fused to either RLuc, YFP or GFP^2 on the C-terminal end of the receptor (D_2-RLuc, D_2-YFP, D_2-GFP^2, σ_1-Rluc, σ_1-YFP, A_{2A}-RLuc or A_{2A}-YFP receptors respectively). The human cDNAs for D_2 and σ_1 receptors cloned in pcDNA3.1 were amplified without its stop codon using sense and antisense primers harboring unique *KpnI* and *EcoRI* sites to clone D_2 and σ_1 receptors in pcDNA3.1-cVenus, pcDNA3.1-nVenus, pcDNA3.1-cRLuc8 or pcDNA3.1-nRLuc8. The amplified fragments were subcloned to be in-frame with the multiple cloning sites of the vectors to give the plasmids that express D_2 and σ_1 receptors fused to either nVenus, cVenus, nRLuc8 or cRLuc8 on the C-terminal end of the receptor (D_2-cVenus, D_2-nVenus, D_2-cRLuc8, D_2-nRLuc8, σ_1-nVenus, σ_1-cVenus, σ_1-nRluc8 or σ_1-cRluc8, respectively). When analysed by confocal microscopy, it was observed that all fusion proteins showed similar subcellular distribution than naïve receptors (see results and results not shown). Fusion of RLuc and YFP to D_2 or A_{2A} receptors did not modify receptor function as previously determined by cAMP assays *(54)*.

Cell Culture and transient transfection

HEK-293T cells were grown in Dulbecco's modified Eagle's medium (DMEM) supplemented with 2 mM L-glutamine, 100 U/ml penicillin/streptomycin, and 5% (v/v) heat inactivated Foetal Bovine Serum (FBS) (all supplements were from Invitrogen, Paisley, Scotland, UK). CHO cell lines were maintained in α-MEM medium without nucleosides, containing 10% fetal calf serum, 50 µg/mL penicillin, 50 µg/mL streptomycin, and 2 mM L-glutamine (300 µg/mL). Cells were maintained at 37ºC in an atmosphere of 5% CO_2, and were passaged when they were 80-90% confluent, i.e. approximately twice a week. HEK-293T or CHO cells were transiently transfected with the corresponding cDNAs by PEI (PolyEthylenImine, Sigma, Steinheim, Germany) method as previously described (2) or the corresponding siRNA by lipofectamine (Invitrogen™, Carlsbad, USA) method following the instructions of the supplier. Human and Chinese hamster σ_1 siRNA and scrambled siRNA were designed and synthesized by Invitrogen (HSS 145543).

Immunostaining

For immunocytochemistry, cells were fixed in 4% paraformaldehyde for 15 min and washed with PBS containing 20 mM glycine (buffer A) to quench the aldehyde groups. Then, after permeabilization with buffer A containing 0.2% Triton X-100 for 5 min, cells were treated with PBS containing 1% bovine serum albumin. After 1 h at room temperature, cells were labelled with the primary mouse monoclonal anti-Rluc receptor antibody (1/200, Millipore, CA, USA) or mouse monoclonal anti-σ_1 receptor antibody (1/200; Chemicon) for 1 h, washed, and stained with the secondary Cyn3 donkey anti-mouse antibody (1/200, Jackson Immunoresearch Laboratories, Baltimore, PA, USA). D_2 receptors fused to YFP protein were detected by their fluorescence properties. Samples were rinsed and observed in a Leica SP2 confocal microscope (Leica Microsystems, Mannheim, Germany).

BRET and BRET with BiLFC assays.

HEK-293T cells growing in six-well plates were transiently co-transfected with a constant amount of cDNA encoding for the receptor fused to RLuc or nRLuc8 and cRLuc8 proteins and with increasingly amounts of cDNA corresponding to the receptor fused to YFP or nVenus and cVenus proteins (see figure legends). To quantify receptor-YFP expression or receptor-reconstituted YFP Venus expression, cells (20 µg protein) were distributed in 96-well microplates (black plates with a transparent bottom) and fluorescence was read in a Fluoro Star Optima Fluorimeter (BMG Labtechnologies, Offenburg, Germany) equipped with a high-energy xenon flash lamp, using a 10nm bandwidth excitation filter at 400 nm reading. Receptor-fluorescence expression was determined as fluorescence of the sample minus the fluorescence of cells expressing the BRET donor alone. For BRET or BRET with BiLFC measurements, the equivalent of 20 µg of cell suspension were distributed in 96-well microplates (Corning 3600, white plates; Sigma) and 5 µM coelenterazine H (Molecular Probes, Eugene, OR) was added. After 1 minute for BRET or after 5 min for BRET with BiLFC of adding coelenterazine H, the readings were collected using a Mithras LB 940 that allows the integration of the signals detected in the short-wavelength filter at 485 nm (440-500 nm) and the long-wavelength filter at 530 nm (510-590 nm). To quantify receptor-RLuc or receptor-reconstituted RLuc8 expression luminescence readings were also performed after 10 minutes of adding 5µM coelenterazine H. Both fluorescence and luminiscence of each sample were measured before every experiment to confirm similar donor expressions (about 150,000 luminescent units) while monitoring the increase acceptor expression (10,000–70,000 fluorescent units). The net BRET is defined as [(long-wavelength emission)/(short-wavelength emission)]-Cf where Cf corresponds to [(long-wavelength emission)/(short-wavelength emission)] for the donor construct expressed alone in the same experiment. BRET is expressed as mili BRET units, mBU (net BRET x 1000).

SRET assays.

HEK-293T cells growing in six-well plates were transiently co-transfected with constant amounts of cDNAs encoding for both receptor fused to RLuc and GFP^2 proteins and with increasingly amounts of cDNA corresponding to the receptor fused to YFP protein and SRET was detemined as previously described using a Mithras LB 40 *(27)*.

cAMP determination.

Non transfected or transiently transfected CHO cells (see figure legends) were treated for 10 min with the indicated concentrations of D_2 receptor agonist quinpirole (Sigma, MO, USA), 30 µM cocaine (cocaine-HCl, Spanish Agencia del Medicamento nº: 2003C00220) or 100 nM of the sigma-1 antagonist PRE-084 (Tocris,Bristol, UK) alone or in combination. cAMP production was determined using [^{3}H]cAMP kit (Amersham Biosciences, Uppsala, Sweden) following the instructions from the manufacturer.

ERK 1/2 phosphorylation assays

Brains from WT littermates and sigma-1 receptor knock out CD1 albino Swiss male mice (8 weeks old, 25 g of weight) were generously provided by Laboratorios Esteve (Barcelona, Spain) *(55)*. Brains were rapidly removed from animals and striatal slices were obtained as previously indicated *(13, 56)*. Slices were treated for the indicated time with the indicated concentrations of cocaine and/or D_2 receptor ligands, frozen on dry ice and stored at −80°C. When ERK1/2 phosphorylation assays were performed in cell cultures, CHO cells (48 h after transfection) were cultured in serum-free medium for 16 h before the addition of the indicated concentration of cocaine or/and D_2 receptor ligands for the indicated time. Both, cells and slices were lysed in ice-cold lysis buffer (50 mM Tris-HCl pH 7.4, 50 mM NaF, 150 mM NaCl, 45 mM β-glycerophosphate, 1% Triton X-100, 20 µM phenyl-arsine oxide, 0.4 mM $NaVO_4$ and protease inhibitor cocktail) and ERK 1/2 phosphorylation was determined as indicated elsewhere *(13, 38)*.

CellKey label-free assays.

The CellKey system provides a universal, label-free, cell-based assay platform that uses cellular dielectric spectroscopy (CDS) to measure endogenous and transfected receptor activation in real time in live cells *(57)*. Changes in the complex impedance (DZ or dZ) of a cell monolayer in response to receptor stimulation were measured. Impedance (Z) is defined by the ratio of voltage to current as described by Ohm's law (Z=V/I). CHO cell clones stably expressing D_2 receptors were grown to confluence in a CellKey Standard 96 well microplate that contains electrodes at the bottom of each well. For untreated cells or for cells preincubated (overnight at 37ºC) with PTx (10 ng/ml), medium was replaced by HBSS buffer (Gibco) suplemented with 20mM HEPES 30 minutes prior to running the cell equilibration protocol. A baseline was recorded for 5 minutes and then cells were treated with increasing concentrations of the D_2 receptor agonist quinpirole or cocaine alone or in combination and data was acquired for the following 10 minutes. To calculate the impedance, small voltages at 24 different measurement frequencies were applied to treated or non-treated cells. At low frequencies, extracellular currents (iec) that pass around individual cells in the layer were induced. At high frequencies, transcellular currents (itc) that penetrate the cellular membrane were induced and the ratio of the applied voltage to the measured current for each well is the impedance. The data shown refer to the maximum complex impedance induced extracellular currents (Ziec) response to the ligand addition.

ACKNOWLEDGEMENTS

We would like to thank Jasmina Jiménez for technical help (University of Barcelona). We thank Laboratorios Esteve (Barcelona, Spain) for providing σ_1 receptor KO and WT littermates mice brains. This study was supported by grants from the Spanish Ministerio de Ciencia y Tecnología (SAF2009-07276, SAF2010-18472, SAF2008-00146), and by Intramural Funds of the National Institute on Drug Abuse. PJM is a Ramón y Cajal Fellow. The authors declare that they have no conflict of interest.

AUTHOR CONTRIBUTIONS

GN, EM, MB, DF, JM, AC, and JB performed the experiments. CL, EC, VC and PJM designed the experiments and drafted the manuscript. RF and SF, provided essential reagents and edited the manuscript.

REFERENCES

1. P. W. Kalivas, N. D. Volkow, The neural basis of addiction: a pathology of motivation and choice, *Am J Psychiatry* **162**, 1403-1413 (2005).

2. G. Di Chiara, V. Bassareo, Reward system and addiction: what dopamine does and doesn't do, *Current Opinion in Pharmacology* **7**, 69-76 (2007).

3. C. R. Gerfen, in *The Rat Nervous System (Third Edition)*, (Academic Press, Burlington, 2004), pp. 455-508.

4. M. Xu *et al.*, Elimination of cocaine-induced hyperactivity and dopamine-mediated neurophysiological effects in dopamine D1 receptor mutant mice, *Cell* **79**, 945-955 (1994).

5. J. Bertran-Gonzalez *et al.*, Opposing patterns of signaling activation in dopamine D1 and D2 receptor-expressing striatal neurons in response to cocaine and haloperidol, *J. Neurosci* **28**, 5671-5685 (2008).

6. M. Welter *et al.*, Absence of dopamine D2 receptors unmasks an inhibitory control over the brain circuitries activated by cocaine, *Proceedings of the National Academy of Sciences of the United States of America* **104**, 6840-6845 (2007).

7. F. Rougé-Pont *et al.*, Changes in extracellular dopamine induced by morphine and cocaine: Crucial control by D2 receptors, *Journal of Neuroscience* **22**, 3293-3301 (2002).

8. C. De Mei, M. Ramos, C. Iitaka, E. Borrelli, Getting specialized: presynaptic and postsynaptic dopamine D2 receptors, *Curr Opin Pharmacol* **9**, 53-58 (2009).

9. S. Asensio *et al.*, Striatal dopamine D2 receptor availability predicts the thalamic and medial prefrontal responses to reward in cocaine abusers three years later, *Synapse* **64**, 397-402 (2010).

10. M. Krawczyk *et al.*, A Switch in the Neuromodulatory Effects of Dopamine in the Oval Bed Nucleus of the Stria Terminalis Associated with Cocaine Self-Administration in Rats, *The Journal of Neuroscience* **31**, 8928 -8935 (2011).

11. D. Thompson, L. Martini, J. L. Whistler, Altered ratio of D1 and D2 dopamine receptors in mouse striatum is associated with behavioral sensitization to cocaine, *PLoS ONE* **5**, e11038 (2010).

12. T. Beuming *et al.*, The binding sites for cocaine and dopamine in the dopamine transporter overlap, *Nat. Neurosci* **11**, 780-789 (2008).

13. G. Navarro *et al.*, Direct involvement of sigma-1 receptors in the dopamine D1 receptor-mediated effects of cocaine, *Proc. Natl. Acad. Sci. U.S.A* **107**, 18676-18681 (2010).

14. T. Hayashi, T. Su, The sigma receptor: evolution of the concept in neuropsychopharmacology, *Curr Neuropharmacol* **3**, 267-280 (2005).

15. F. Ciruela *et al.*, G protein-coupled receptor oligomerization for what?, *J. Recept. Signal Transduct. Res* **30**, 322-330 (2010).

16. L. Prezeau *et al.*, Functional crosstalk between GPCRs: with or without oligomerization, *Curr Opin Pharmacol* **10**, 6-13 (2010).

17. J. A. Hern *et al.*, Formation and dissociation of M1 muscarinic receptor dimers seen by total internal reflection fluorescence imaging of single molecules, *Proceedings of the National Academy of Sciences* **107**, 2693-2698 (2010).

18. R. Rozenfeld, L. A. Devi, Exploring a role for heteromerization in GPCR signalling specificity, *Biochem. J* **433**, 11-18 (2010).

19. R. S. Kasai *et al.*, Full characterization of GPCR monomer–dimer dynamic equilibrium by single molecule imaging, *The Journal of Cell Biology* **192**, 463 -480 (2011).

20. I. Gomes, A. P. Ijzerman, K. Ye, E. L. Maillet, L. A. Devi, G protein-coupled receptor heteromerization: a role in allosteric modulation of ligand binding, *Mol. Pharmacol* **79**, 1044-1052 (2011).

21. V. Casadó *et al.*, Old and new ways to calculate the affinity of agonists and antagonists interacting with G-protein-coupled monomeric and dimeric receptors: the receptor-dimer cooperativity index, *Pharmacol. Ther* **116**, 343-354 (2007).

22. G. Y. K. Ng *et al.*, Dopamine D2 Receptor Dimers and Receptor-Blocking Peptides, *Biochemical and Biophysical Research Communications* **227**, 200-204 (1996).

23. S. P. Lee *et al.*, Inhibition of Cell Surface Expression by Mutant Receptors Demonstrates that D2 Dopamine Receptors Exist as Oligomers in the Cell, *Molecular Pharmacology* **58**, 120 -128 (2000).

24. D. Armstrong, P. G. Strange, Dopamine D2 Receptor Dimer Formation, *Journal of Biological Chemistry* **276**, 22621 -22629 (2001).

25. W. Guo, L. Shi, J. A. Javitch, The Fourth Transmembrane Segment Forms the Interface of the Dopamine D2 Receptor Homodimer, *Journal of Biological Chemistry* **278**, 4385 -4388 (2003).

26. W. Guo *et al.*, Dopamine D2 receptors form higher order oligomers at physiological expression levels, *EMBO J* **27**, 2293-2304 (2008).

27. P. Carriba *et al.*, Detection of heteromerization of more than two proteins by sequential BRET-FRET, *Nat. Methods* **5**, 727-733 (2008).

28. J. Sharkey, K. A. Glen, S. Wolfe, M. J. Kuhar, Cocaine binding at [sigma] receptors, *European Journal of Pharmacology* **149**, 171-174 (1988).

29. T. Maurice, T.-P. Su, The pharmacology of sigma-1 receptors, *Pharmacol. Ther* **124**, 195-206 (2009).

30. L. M. Luttrell *et al.*, Beta-arrestin-dependent formation of beta2 adrenergic receptor-Src protein kinase complexes, *Science* **283**, 655-661 (1999).

31. S. K. Shenoy, R. J. Lefkowitz, Multifaceted roles of beta-arrestins in the regulation of seven-membrane-spanning receptor trafficking and signalling, *Biochem. J* **375**, 503-515 (2003).

32. J.-M. Beaulieu *et al.*, An Akt/[beta]-Arrestin 2/PP2A Signaling Complex Mediates Dopaminergic Neurotransmission and Behavior, *Cell* **122**, 261-273 (2005).

33. S. K. Shenoy *et al.*, beta-arrestin-dependent, G protein-independent ERK1/2 activation by the beta2 adrenergic receptor, *J Biol Chem* **281**, 1261-73 (2006).

34. S. M. DeWire, S. Ahn, R. J. Lefkowitz, S. K. Shenoy, β-Arrestins and Cell Signaling, *Annu. Rev. Physiol.* **69**, 483-510 (2007).

35. E. Valjent *et al.*, Involvement of the Extracellular Signal-Regulated Kinase Cascade for Cocaine-Rewarding Properties, *J. Neurosci.* **20**, 8701-8709 (2000).

36. L. Lu, E. Koya, H. Zhai, B. Hope, Y. Shaham, Role of ERK in cocaine addiction, *Trends in Neurosciences* **29**, 695-703 (2006).

37. M. K. Lobo *et al.*, Cell Type-Specific Loss of BDNF Signaling Mimics Optogenetic Control of Cocaine Reward, *Science* **330**, 385-390 (2010).

38. E. Moreno *et al.*, Dopamine-Galanin Receptor Heteromers Modulate Cholinergic Neurotransmission in the Rat Ventral Hippocampus, *J Neurosci* **31**, 7412-7423 (2011).

39. H. O. Pettit, H. T. Pan, L. H. Parsons, J. B. Justice Jr, Extracellular concentrations of cocaine and dopamine are enhanced during chronic cocaine administration, *J. Neurochem.* **55**, 798-804 (1990).

40. G. F. Koob, The neurobiology of addiction: a neuroadaptational view relevant for diagnosis, *Addiction* **101 Suppl 1**, 23-30 (2006).

41. G. Di Chiara, V. Bassareo, Reward system and addiction: what dopamine does and doesn't do, *Curr Opin Pharmacol* **7**, 69-76 (2007).

42. M. C. Ritz, R. J. Lamb, S. R. Goldberg, M. J. Kuhar, Cocaine receptors on dopamine transporters are related to self-administration of cocaine, *Science* **237**, 1219-1223 (1987).

43. B. Giros, M. Jaber, S. R. Jones, R. M. Wightman, M. G. Caron, Hyperlocomotion and indifference to cocaine and amphetamine in mice lacking the dopamine transporter, *Nature* **379**, 606-612 (1996).

44. R. Chen *et al.*, Abolished cocaine reward in mice with a cocaine-insensitive dopamine transporter, *Proc. Natl. Acad. Sci. U.S.A* **103**, 9333-9338 (2006).

45. A. Ferragud *et al.*, A dopamine transport inhibitor with markedly low abuse liability suppresses cocaine self-administration in the rat, *Psychopharmacology (Berl.)* **207**, 281-289 (2009).

46. R. R. Matsumoto, Y. Liu, M. Lerner, E. W. Howard, D. J. Brackett, Sigma receptors: potential medications development target for anti-cocaine agents, *Eur. J. Pharmacol* **469**, 1-12 (2003).

47. E. J. Cobos, J. M. Entrena, F. R. Nieto, C. M. Cendán, E. Del Pozo, Pharmacology and therapeutic potential of sigma(1) receptor ligands, *Curr Neuropharmacol* **6**, 344-366 (2008).

48. R. R. Matsumoto *et al.*, Conformationally restricted analogs of BD1008 and an antisense oligodeoxynucleotide targeting sigma1 receptors produce anti-cocaine effects in mice, *Eur. J. Pharmacol* **419**, 163-174 (2001).

49. R. R. Matsumoto, K. A. McCracken, B. Pouw, Y. Zhang, W. D. Bowen, Involvement of sigma receptors in the behavioral effects of cocaine: evidence from novel ligands and antisense oligodeoxynucleotides, *Neuropharmacology* **42**, 1043-1055 (2002).

50. G. Alonso *et al.*, Immunocytochemical localization of the sigma(1) receptor in the adult rat central nervous system, *Neuroscience* **97**, 155-170 (2000).

51. D. Zhang *et al.*, Repeated cocaine administration induces gene expression changes through the dopamine D1 receptors, *Neuropsychopharmacology* **30**, 1443-1454 (2005).

52. H. S. Bateup *et al.*, Distinct subclasses of medium spiny neurons differentially regulate striatal motor behaviors, *Proc. Natl. Acad. Sci. U.S.A.* **107**, 14845-14850 (2010).

53. Z. Luo, N. D. Volkow, N. Heintz, Y. Pan, C. Du, Acute Cocaine Induces Fast Activation of D1 Receptor and Progressive Deactivation of D2 Receptor Striatal Neurons: In Vivo Optical Microprobe [Ca2+]i Imaging, *The Journal of Neuroscience* **31**, 13180 -13190 (2011).

54. M. Canals *et al.*, Adenosine A2A-Dopamine D2 Receptor-Receptor Heteromerization, *Journal of Biological Chemistry* **278**, 46741-46749 (2003).

55. F. Langa *et al.*, Generation and phenotypic analysis of sigma receptor type I (σ1) knockout mice, *European Journal of Neuroscience* **18**, 2188-2196 (2003).

56. E. Moreno *et al.*, Dopamine D1-histamine H3 receptor heteromers provide a selective link to MAPK signaling in GABAergic neurons of the direct striatal pathway, *J. Biol. Chem* **286**, 5846-5854 (2011).

57. R. Schroder *et al.*, Applying label-free dynamic mass redistribution technology to frame signaling of G protein-coupled receptors noninvasively in living cells, *Nat. Protocols* **6**, 1748-1760 (2011).

FIGURES AND FIGURE LEGENDS

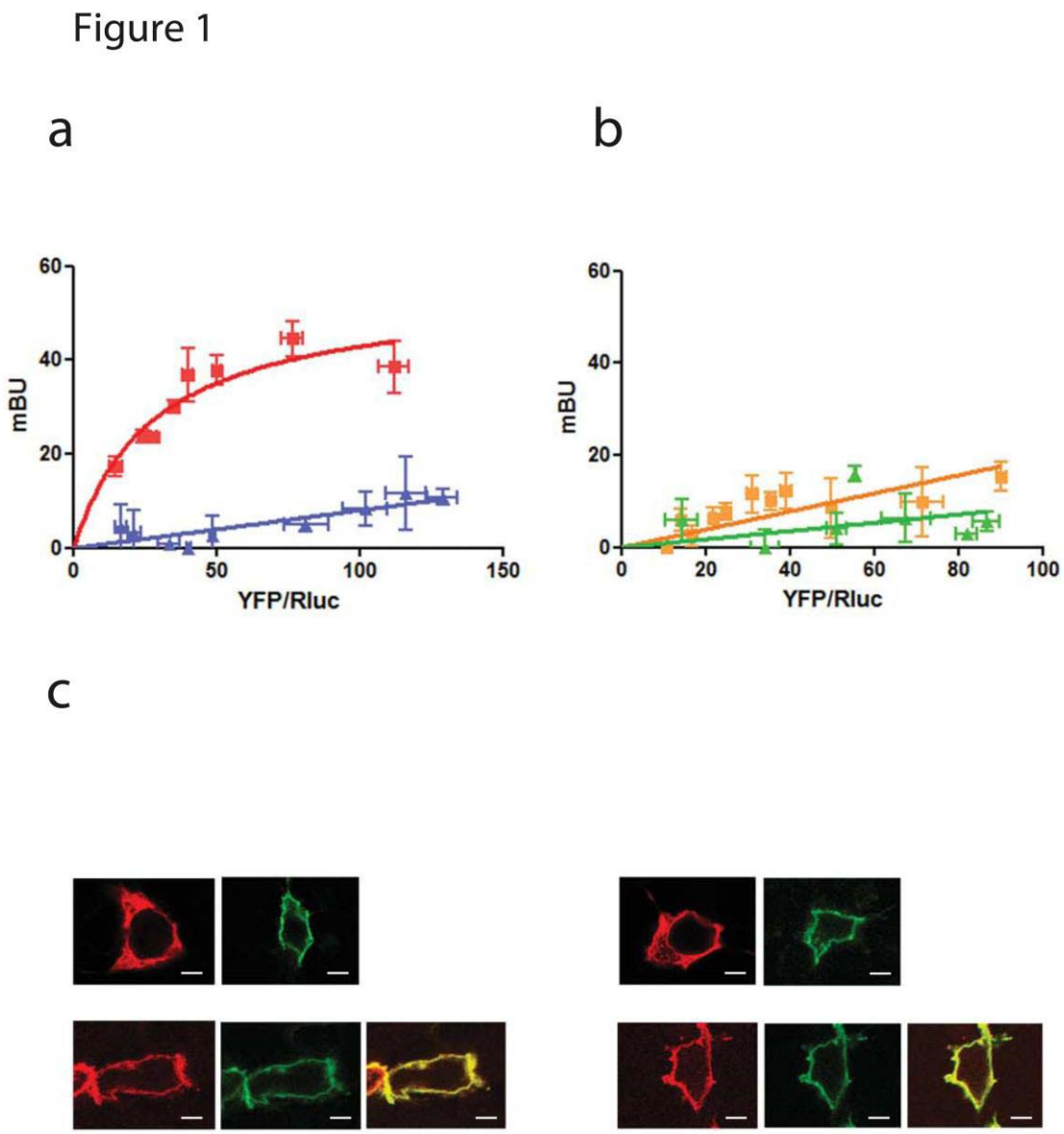

Figure 1. Molecular interaction between σ_1 receptors and D_2 receptors in living cells. BRET saturation experiments were performed with HEK-293T cells co-transfected with: **(a)** D_2-RLuc cDNA (0.4 µg, squares) or adenosine A_{2A}-RLuc cDNA as negative control (0.2 µg, triangles) and increasing amounts of σ_1-YFP cDNA (0.1 to 1 µg cDNA), **(b)** D_3-RLuc cDNA (0.5 µg, squares) or D_4-RLuc cDNA (0.5 µg, triangles) and increasing amounts of σ_1-YFP cDNA (0.1 to 1 µg cDNA). The relative amount of BRET acceptor is given as the ratio between the fluorescence of the acceptor minus the fluorescence detected in cells only expressing the donor, and the luciferase activity of the donor (YFP/Rluc). BRET data are expressed as means ± S.D. of five to six different experiments grouped as a function of the amount of BRET acceptor. In **(c)** confocal microscopy images of HEK-293T cells transfected with D_2-YFP or σ_1-RLuc (top panels) or co-transfected with D_2-YFP and σ_1-RLuc (bottom panels), treated (right images) or not (left images) with 30 µM cocaine for 30 min. σ_1 receptors (red) were identified by immunocytochemistry and D_2 receptors (green) were identified by its own fluorescence. Co-localization is shown in yellow. Scale bar: 10 µm.

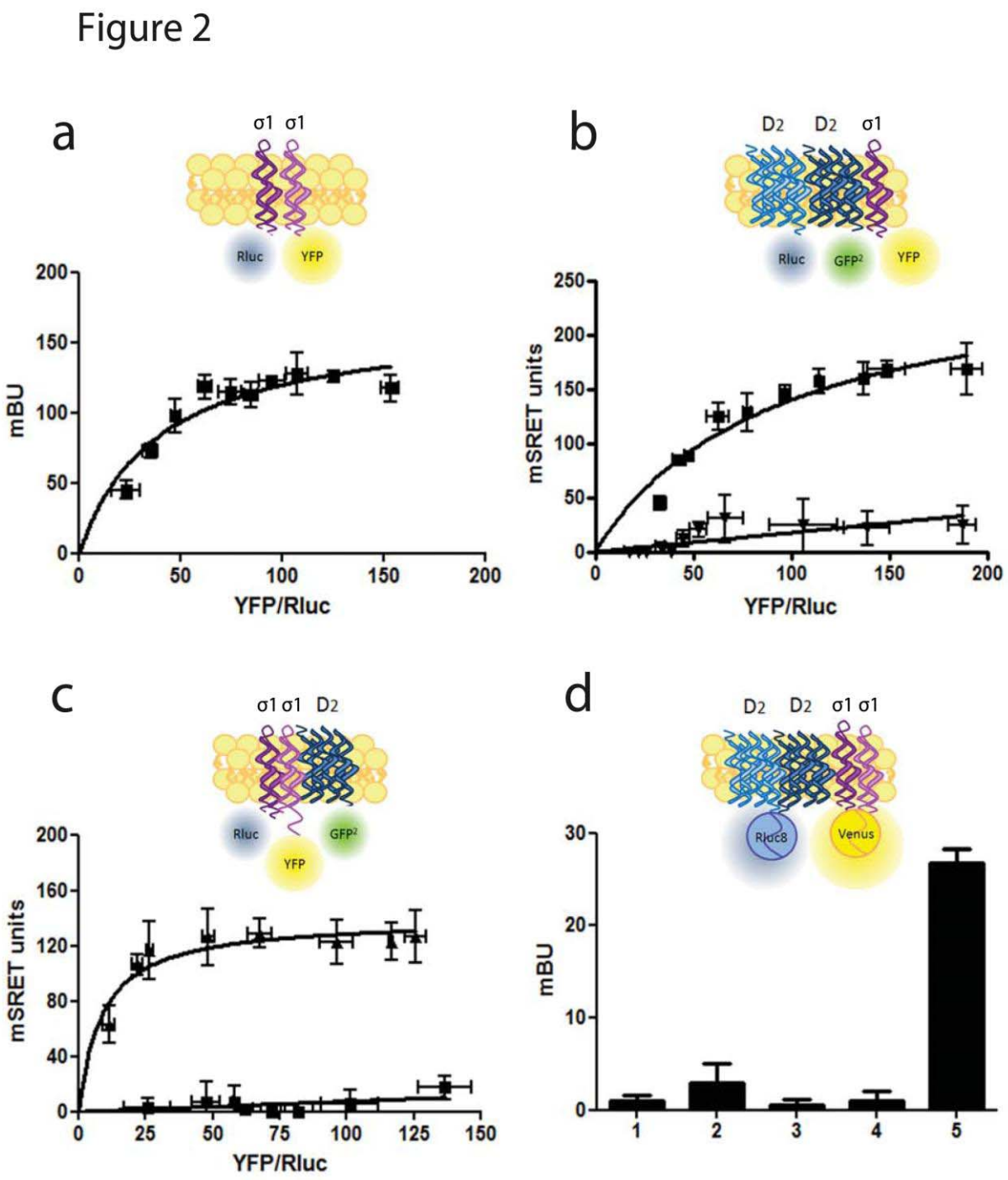

Figure 2. Higher order complex formation between σ_1 receptors and dopamine D_2 receptors in living cells. In **(a)** BRET saturation experiments were performed with HEK-293T cells co-transfected with σ_1-RLuc cDNA (0.2 µg) and increasing amounts of σ_1-YFP cDNA (0.1 to 0.6 µg cDNA). A schematic representation of a BRET process is shown at top in which the receptor fused to RLuc acts as donor and the receptor fused to YFP acts as acceptor. In **(b)** and **(c)** SRET saturation experiments were performed with HEK-293T cells co-transfected with: (b) a constant amount of D_2-RLuc (0.6 µg) and D_2-

GFP^2 (1 μg) receptor cDNA (squares) or A_{2A}-RLuc (0.3 μg) and A_{2A}-GFP^2 (0.5 μg) receptor cDNA, as negative control (triangles), and increasing amounts of σ_1-YFP receptor (0.2 to 1.5 μg cDNA), (c) a constant amount of σ_1-Rluc (0.3 μg) and D_2-GFP^2 (1 μg) (triangles) or A_2-GFP^2 (0.5 μg) as negative control (squares) receptor cDNA and increasing amounts of σ_1-YFP receptor cDNA (0.2 to 1.5 μg). The relative amount of acceptor is given as the ratio between the fluorescence of the acceptor minus the fluorescence detected in cells only expressing the donor, and the luciferase activity of the donor (YFP/Rluc). A schematic representation of a SRET process is shown at top images in which two sequential energy transfer events between Rluc and GFP^2 (BRET process) and between GFP^2 and YFP (FRET process) occurs. In **(d)** BRET with luminescence/fluorescence complementation approach was performed measuring BRET in cells co-transfected with 1 μg of the two cDNAs corresponding to D_2-nRLuc8 and D_2-cRLuc8 and with 1.5 μg of the two cDNAs corresponding to σ_1-nVenus and σ_1-cVenus (5). As negative controls, cells transfected with the same amount of cDNA corresponding to D_2-nRLuc8, D_2-cRLuc8, σ_1-nVenus and cVenus (1), D_2-nRLuc8, D_2-cRLuc8, σ_1-cVenus and nVenus (2), D_2-nRLuc8, σ_1-nVenus, σ_1-cVenus and cRLuc8 (3), or D_2-cRLuc8, σ_1-nVenus, σ_1-cVenus and nRLuc8 (4) did not display any significant luminescence or positive BRET. A schematic representation of a BRET with luminescence/fluorescence complementation approach is given at the top image in which one receptor fused to the N-terminal fragment (nRluc8) and another receptor fused to the C-terminal fragment (cRluc8) of the Rluc8 act as BRET donor after Rluc8 reconstitution by a close receptor-receptor interaction and one receptor fused to an YFP Venus N-terminal fragment (nVenus) and another receptor fused to the YFP Venus C-terminal fragment (cVenus), act as BRET acceptor after YFP Venus reconstitution by a close receptor-receptor interaction. BRET or SRET data are expressed as means ± S.D. of five to six different experiments grouped as a function of the amount of BRET or SRET acceptor.

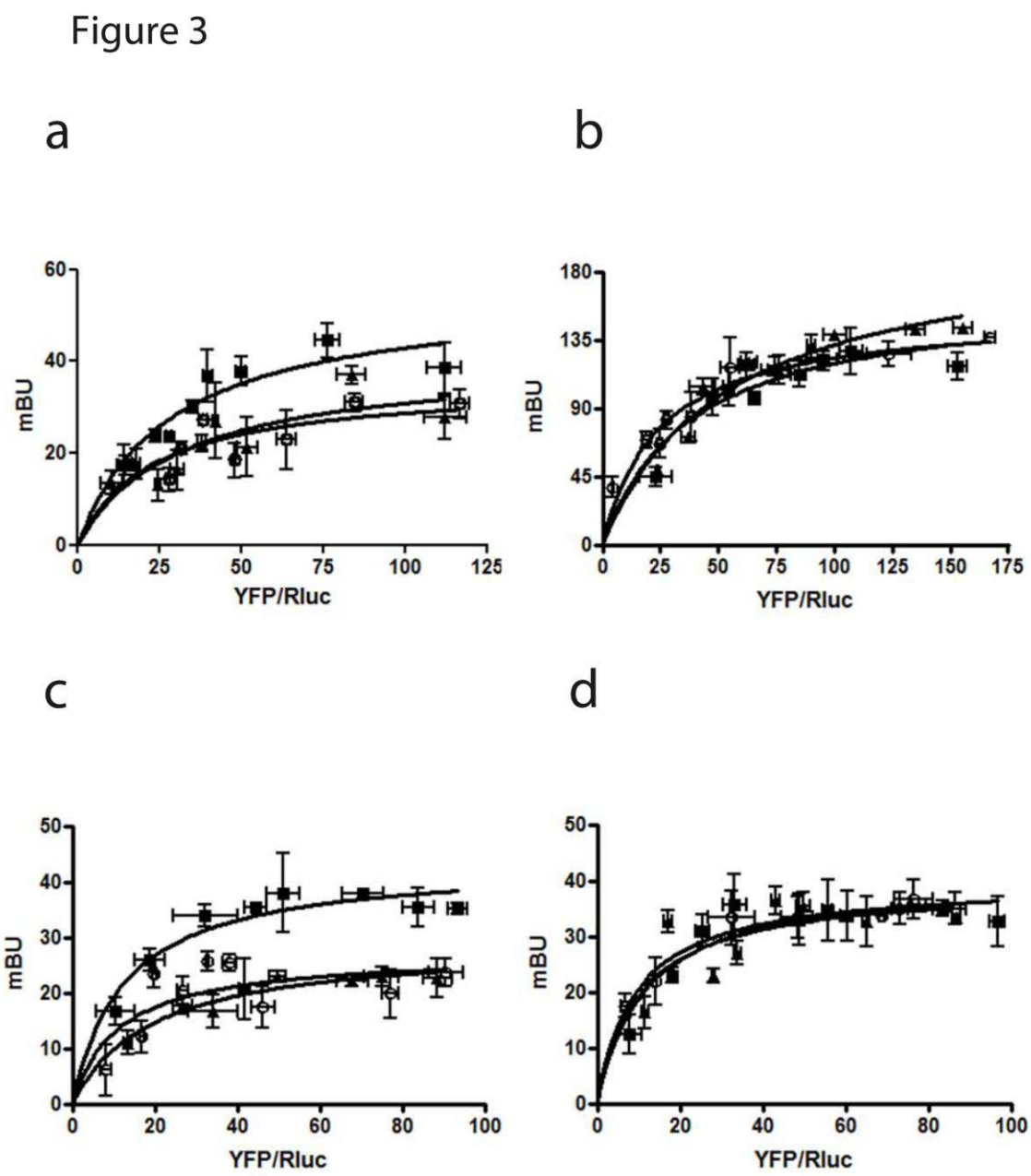

Figure 3. Effect of σ_1 receptor ligands on σ_1-D_2 receptor heteromer. BRET was measured in HEK-293T cells cotransfected with: **(a)** D_2–Rluc cDNA (0.4 µg) and increasing amounts of σ_1-YFP receptor cDNA (0.1 to 1 µg), **(b)** σ_1–Rluc cDNA (0.2 µg) and increasing amounts of σ_1-YFP receptor cDNA (0.1 to 1 µg), **(c)** D_2–Rluc cDNA (0.4 µg) and increasing amounts of D_2-YFP receptor cDNA (0.2 to 2 µg) or **(d)** siRNA corresponding to σ1 receptor (see Methods), D_2–Rluc cDNA (0.4 µg) and increasing amounts of D_2-YFP receptor cDNA (0.2 to 2 µg)**,** not treated (squares) or treated with 30 µM cocaine (circles) or 100 nM PRE084 (triangles**).** The relative amount of BRET acceptor is given as the ratio between the fluorescence of the acceptor minus the fluorescence detected in cells only expressing the donor, and the luciferase activity of the donor (YFP/Rluc). BRET data are expressed as means ± SD of four to six different experiments grouped as a function of the amount of BRET aceptor.

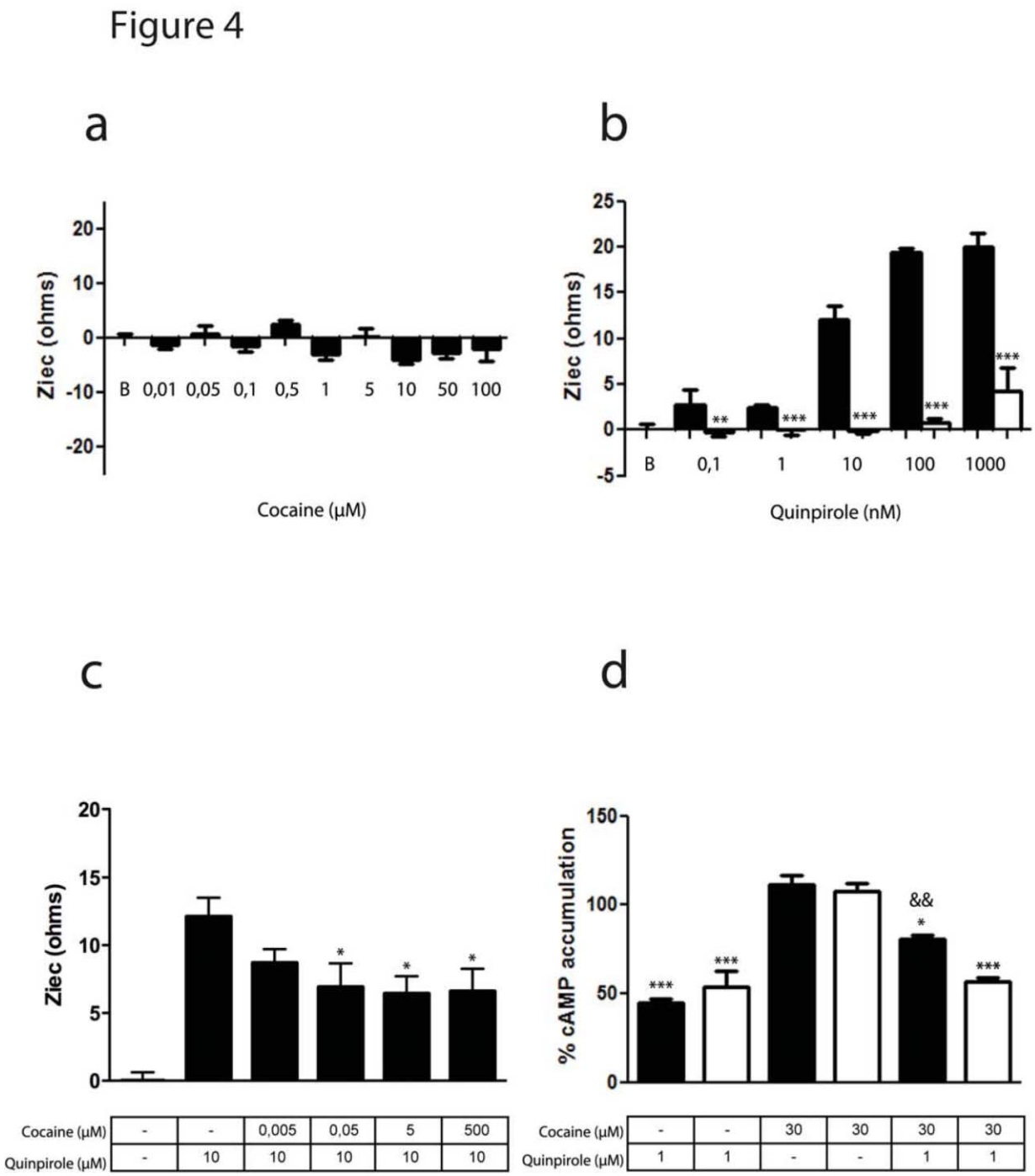

Figure 4. Cocaine binding to σ_1 receptor modulates the G_i-dependent D_2 receptor signaling in transfected cells. In (**a** to **c**) CellKey label-free assays were performed in CHO cells stable expressing D_2 receptors. In (a) cells were stimulated with buffer (B) or with increasing concentrations of cocaine. In (b) cells were preincubated (black columns) or not (white columns) with PTx (10 ng/ml) overnight and stimulated with buffer (B) or increasing concentrations of quinpirole. In (c) cells were stimulated with 1

μM quinpirole in the absence or in the presence of cocaine. In (**d**) cAMP production was determined in CHO cells stable expressing D_2 receptors not transfected (black columns) or transfected (white columns) with siRNA corresponding to σ_1 receptor (6.25 μg of oligonucleotides) and stimulated with 5 μM forskoline in absence (100%) or presence of 1 μM quinpirole, 30 μM cocaine alone or in combination. Percent of cAMP produced respect to 5 μM forkoline treatment was represented. Results are as mean ± S.E.M from 4-8 independent experiments. Statistical significance was calculated by one way ANOVA followed by Bonferroni multiple comparison test; in b **$p<0.01$ and ***$p<0.005$ compared with cells not transfected with siRNA, in c *$p<0.05$ compared with cells only treated with quinpirole, in d $^{\&\&}p<0.01$ compared to the corresponding quinpirole-treated cells and *$p<0.05$ and ***$p<0.005$ compared with forskoline-treated cells (100%).

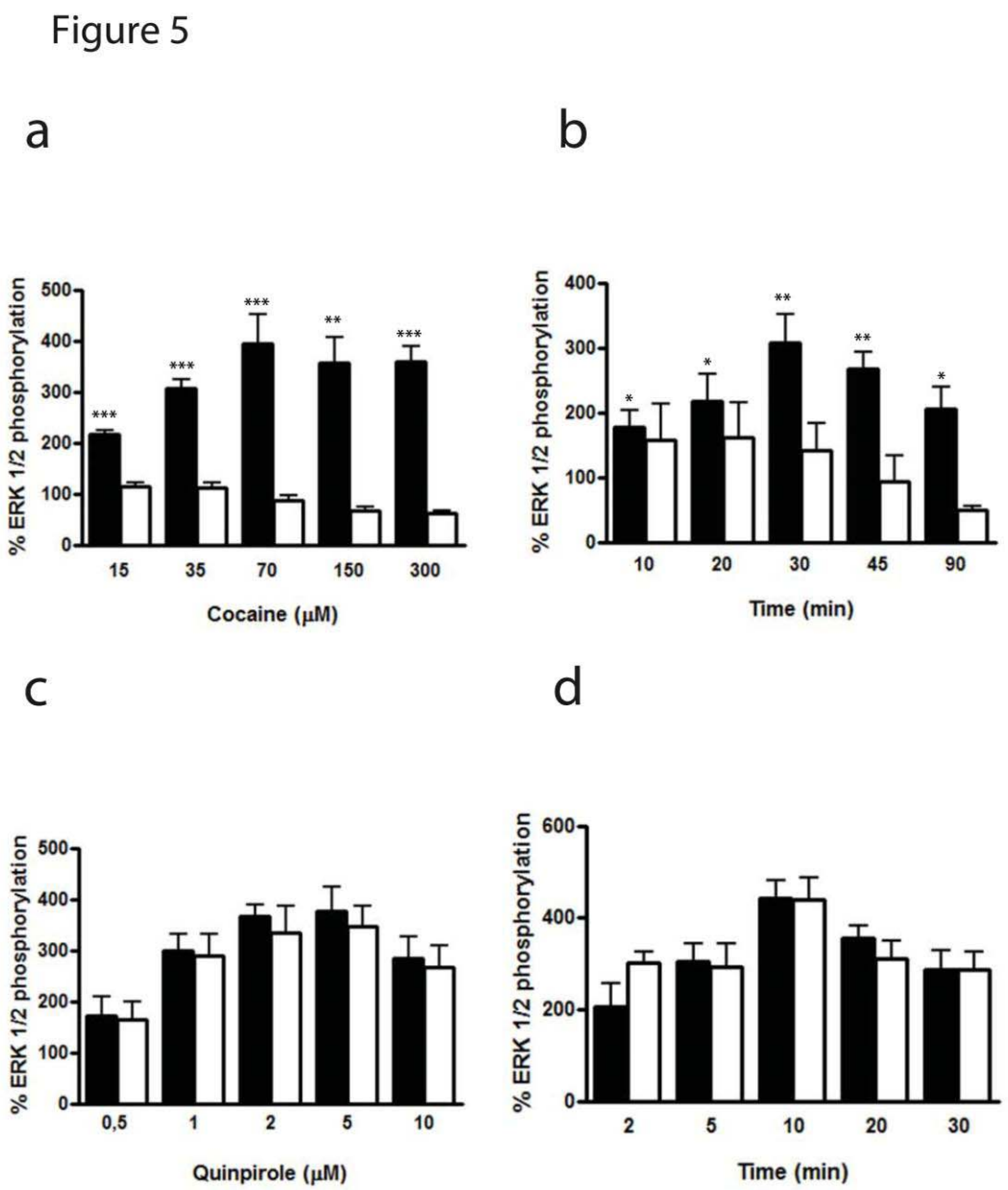

Figure 5. Cocaine-induced σ_1-D_2 receptor heteromer-mediated ERK 1/2 phosphorylation in transfected cells. CHO cells transfected with D_2 receptor cDNA (1 μg, black bars) or cotransfected (white bars) with D_2 receptor cDNA and σ_1 receptor siRNA (6.25 μg of oligonucleotides) were incubated with increasing cocaine concentrations for 30 min (a), with 30 μM cocaine for increasing time periods (b), with increasing quinpirole concentrations for 10 min (c) or with 1 μM quinpirole for increasing time periods (d)**.** ERK1/2 phosphorylation is represented as percentage over basal levels (100%). Results are mean ± SEM of four to six independent experiments performed in duplicate. In all samples in (c) and (d) and samples without siRNA transfection in (a) and (b), bifactorial ANOVA showed a significant ($p < 0.01$) effect of cocaine or quinpirole over basal, and Bonferroni post hoc tests showed a significant counteraction of cocaine effect by siRNA (*$p < 0.05$, **$p < 0.01$ and ***$p < 0.005$ compared with sample with the same treatment and with siRNA transfection).

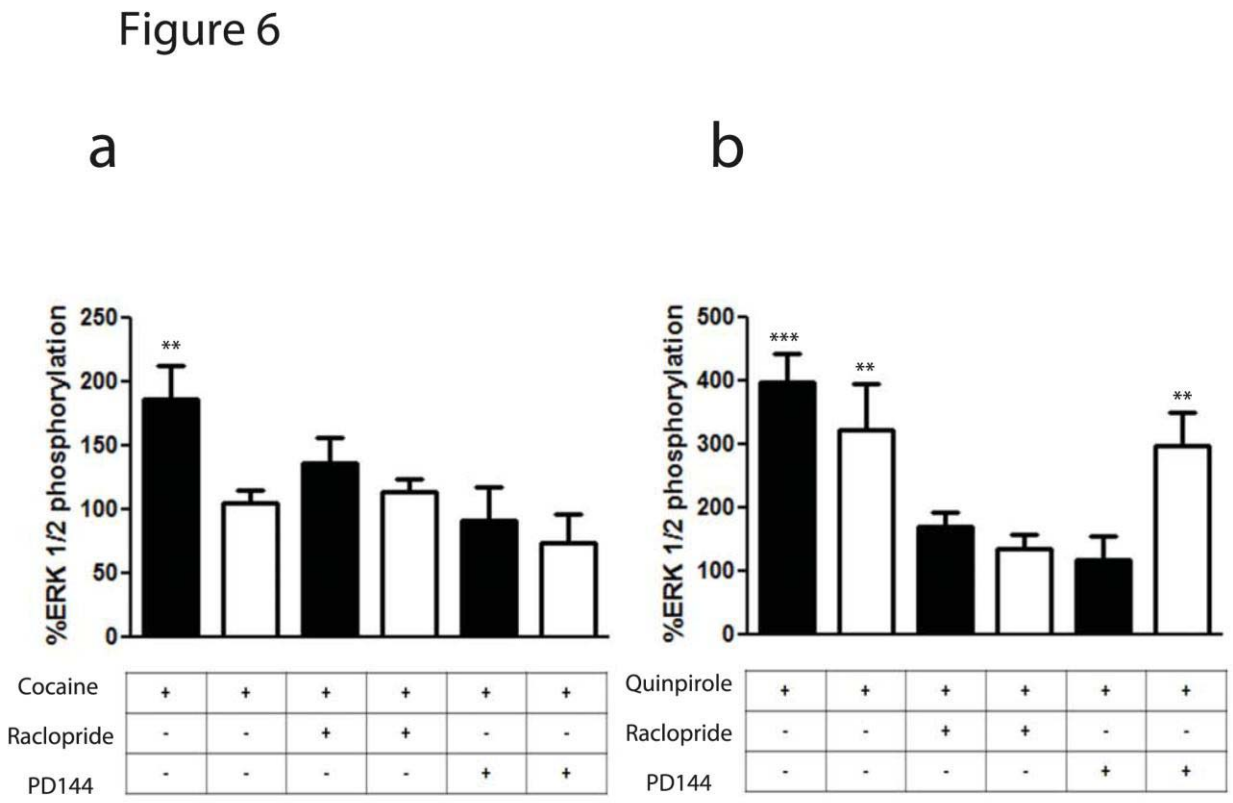

Figure 6. Cross-antagonism among σ_1-D_2 receptor heteromers. CHO cells were transfected with D_2 receptor cDNA (1 µg, black bars) or cotransfected (white bars) with D_2 receptor cDNA and σ_1 receptor siRNA (6.25 µg of oligonucleotides). Cells were incubated for 30 min (a) or 10 min (b) with medium (basal) or with 30 µM cocaine (a) or 1 µM quinpirole (b) in the absence or in the presence of 10 µM raclopride or 100 nM PRE084. ERK1/2 phosphorylation is represented as percentage over basal levels (100%). Results are mean ± SEM of six to eight independent experiments performed in duplicate. Bifactorial ANOVA showed a significant (**$p < 0.01$ and ***$P < 0.005$) effect over basal.

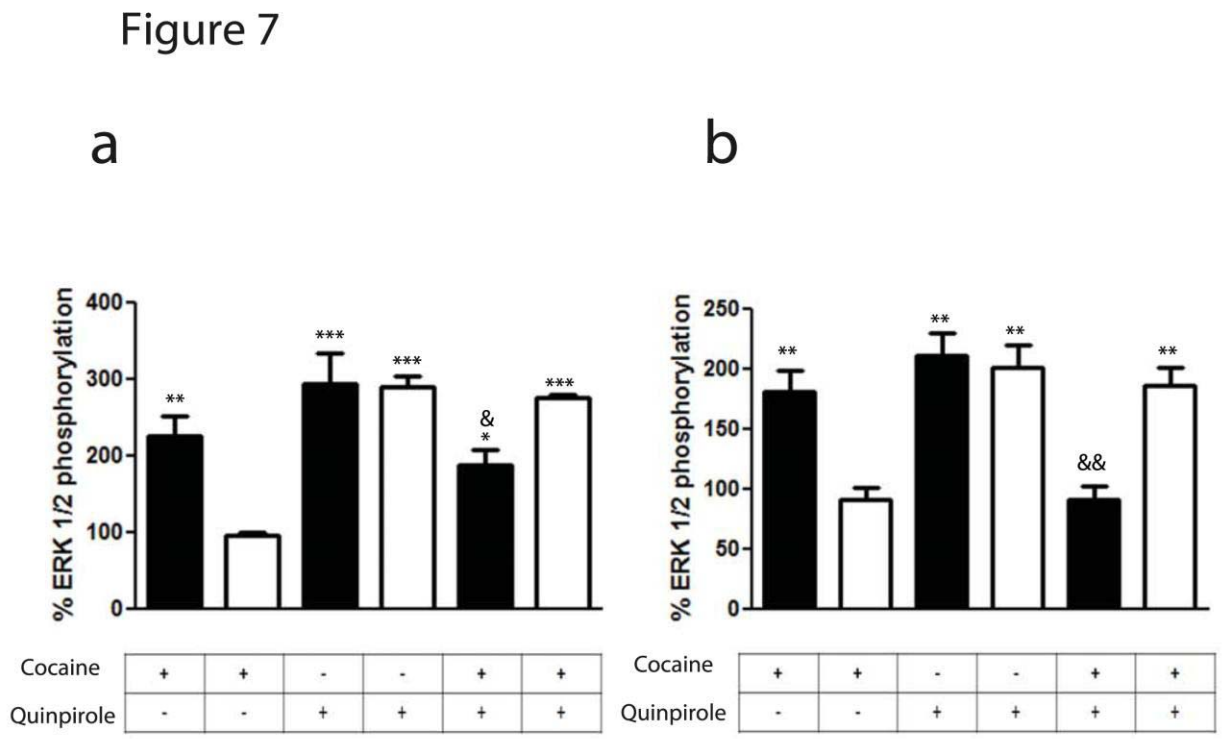

Figure 7. Negative cross-talk between cocaine and the D_2 receptor agonist quinpirole on ERK 1/2 phosphorylation in living cells and in mice stiatum. In (**a**) CHO cells were transfected with D_2 receptor cDNA (1 µg, black bars) or cotransfected (white bars) with D_2 receptor cDNA and σ_1 receptor siRNA (6.25 µg of oligonucleotides). Cells were treated with medium (basal), 30 µM cocaine for 30 min, 1 µM quinpirole for 10 min or 30 µM cocaine for 30 min and, during the last 10 min, with 1 µM quinpirole. ERK 1/2 phosphorylation is represented as percentage over basal levels (100%). Results are mean ± SEM of six independent experiments performed in duplicate. In (**b**) WT (black bars) and σ_1 receptor KO (white bars) mouse striatal slices were treated with 1 µM quinpirole for 10 min, with 150 µM cocaine for 30 min or with cocaine for 30 min and, during the last 10 min, with quinpirole. Immunoreactive bands from six slices obtained from five WT or five KO animals were quantified for each condition. Values represent mean ± SEM of percentage of phosphorylation relative to basal levels found in untreated slices. No significant differences were obtained between the basal levels of the WT and the σ_1 receptor KO mice. Bifactorial ANOVA showed a significant (*$p < 0.05$, **$p < 0.01$, ***$p < 0.005$) effect over basal. One-way ANOVA followed by Bonferroni post hoc tests showed a significant cocaine-mediated counteraction of quinpirole ($^{\&}p < 0.05$, $^{\&\&}p < 0.01$).

FIGURES AND SUPPLEMENTARY FIGURE LEGENDS

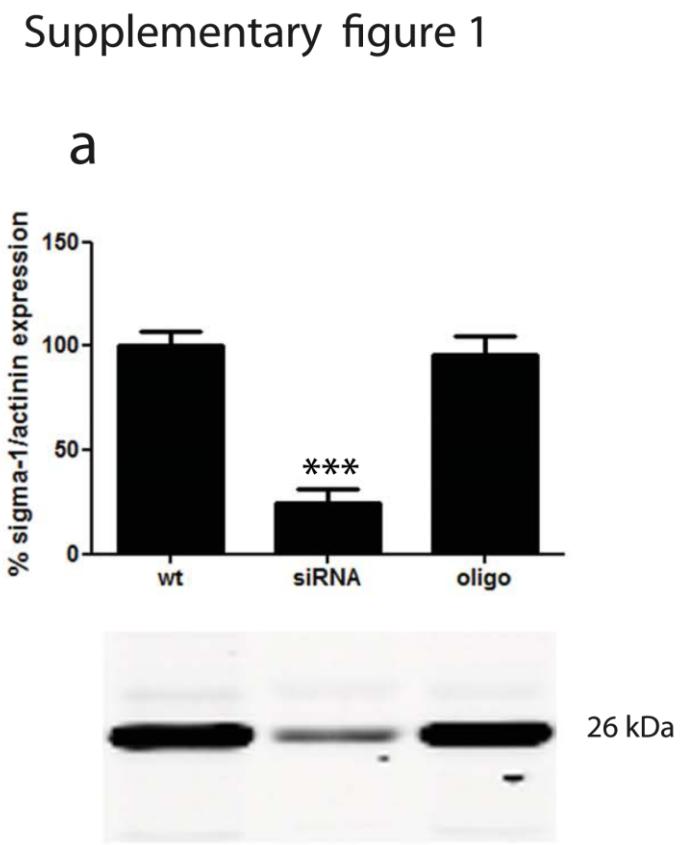

Supplementary Figure 1. Effect of σ_1 receptor siRNA transfection on σ_1 receptor expresión. Membranes from non-transfected HEK-293T cells (wt) or cells transfected with σ_1 receptor siRNA (6.25 µg of oligonucleotides) or irrelevant oligonucleotides (oligo, 6.25 µg of oligonucleotides) were analyzed by SDS/PAGE and immunoblotted with the anti-σ_1 receptor antibody. Values are mean ± SEM of three experiments. ***P <0.001 compared with non-transfected cells (one-way ANOVA followed by Bonferroni post hoc tests).

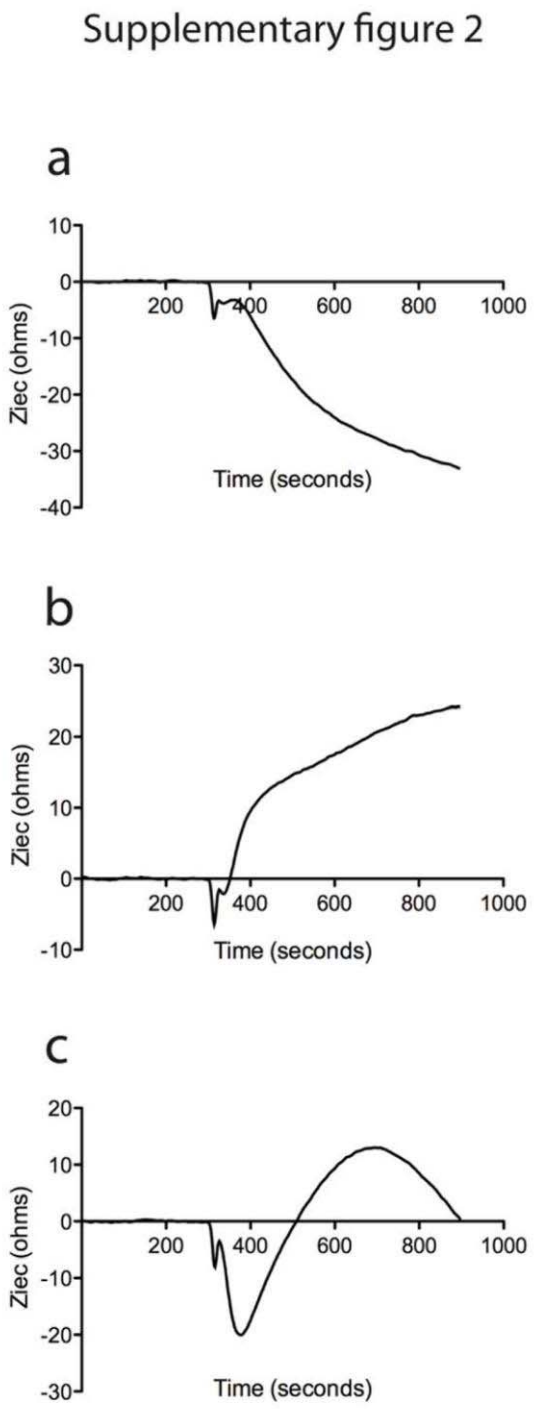

Supplementary Figure 2. Control CellKey label-free assays. HEK-293T cells were stably transfected with the G_s protein-coupled adenosine A_{2A} receptor (a), the G_i protein-coupled adenosine A_1 receptor (b) or untransfected (c) in 96 well Cell-Key plates. Impedence changes were measured upon addition of 10 nM CGS 21680 (A_{2A} receptor agonist) in (a), 10 nM CPA (A_1 receptor agonist) in (b) or 50 nM thrombin (the agonist for the endogenous G_q protein-couples thrombin receptors) in (c). Plot shapes are consistent with the expected results for the respective G-proteins.

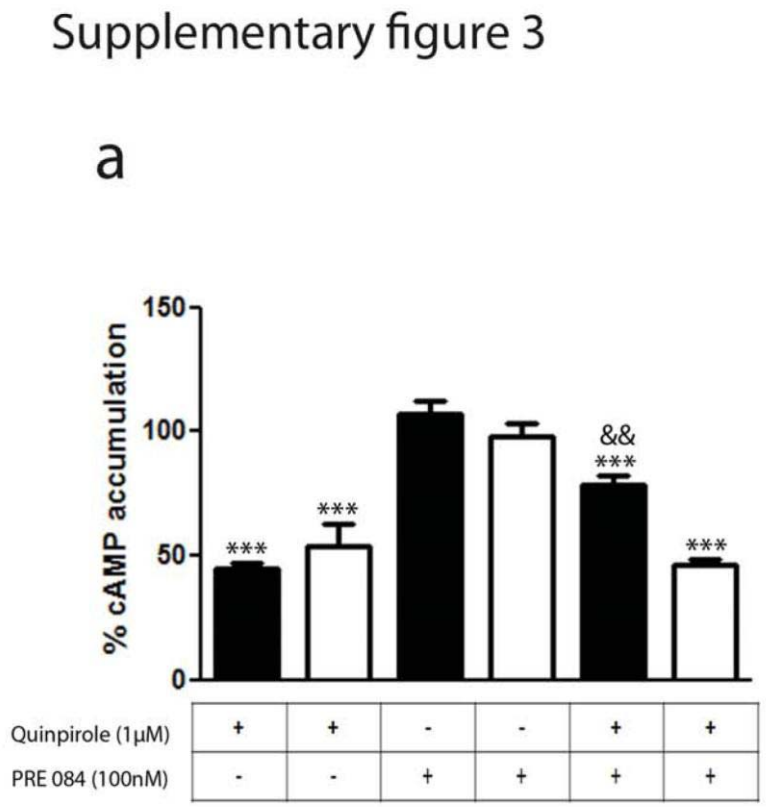

Supplementary Figure 3. σ_1 receptor agonist modulates the D_2 receptor-mediated cAMP decreases. cAMP production was determined in CHO cells stable expressing D_2 receptors not transfected (black columns) or transfected (white columns) with siRNA corresponding to σ_1 receptor (6.25 μg of oligonucleotides). Cells were stimulated with 5 μM forskoline in absence (100%) or presence of 1 μM quinpirole, 100 nM PRE084 alone or in combination. Percent of cAMP produced respect to forkoline treatment was represented. Results are as mean ± S.E.M from five independent experiments. Statistical significance was calculated by one way ANOVA followed by Bonferroni multiple comparison test; ***$p<0.005$ compared with forskoline-treated cells (100%) and $^{\&\&}$ $p<0.01$ compared with the corresponding only quinpirole-treated cells.

Supplementary figure 4

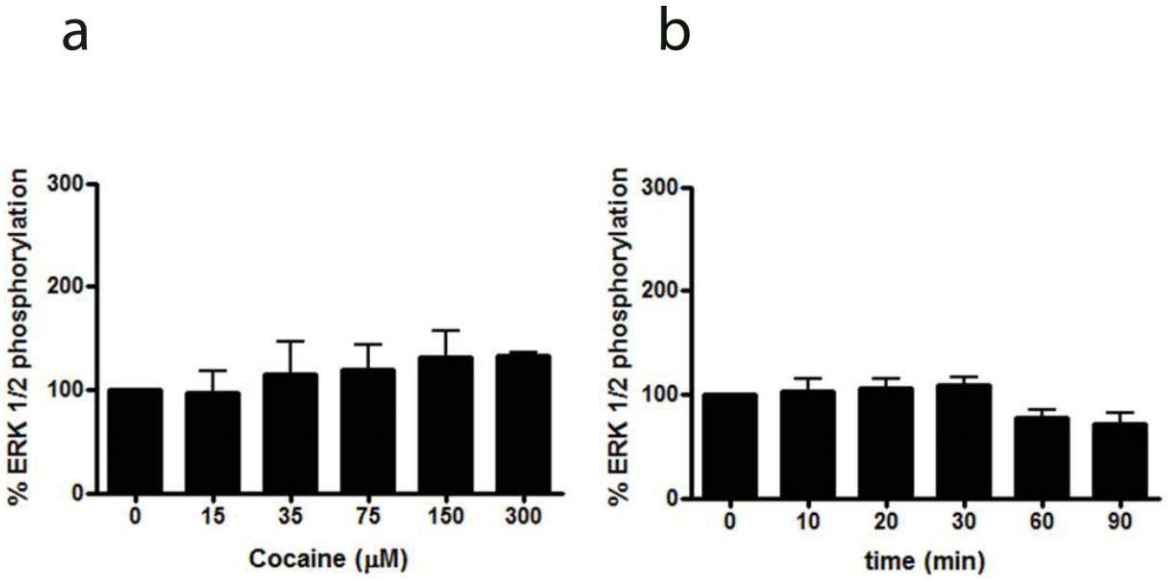

Supplementary Figure 4. Cocaine effect on ERK 1/2 phosphorylation in cells not expressing D_2 receptors. CHO cells were incubated with increasing cocaine concentrations for 30 min (a) or with 30 μM cocaine for increasing time periods (b). ERK1/2 phosphorylation is represented as percentage over basal levels (100%, non-treated cells). Results are mean ± SEM of three to four independent experiments performed in duplicate.

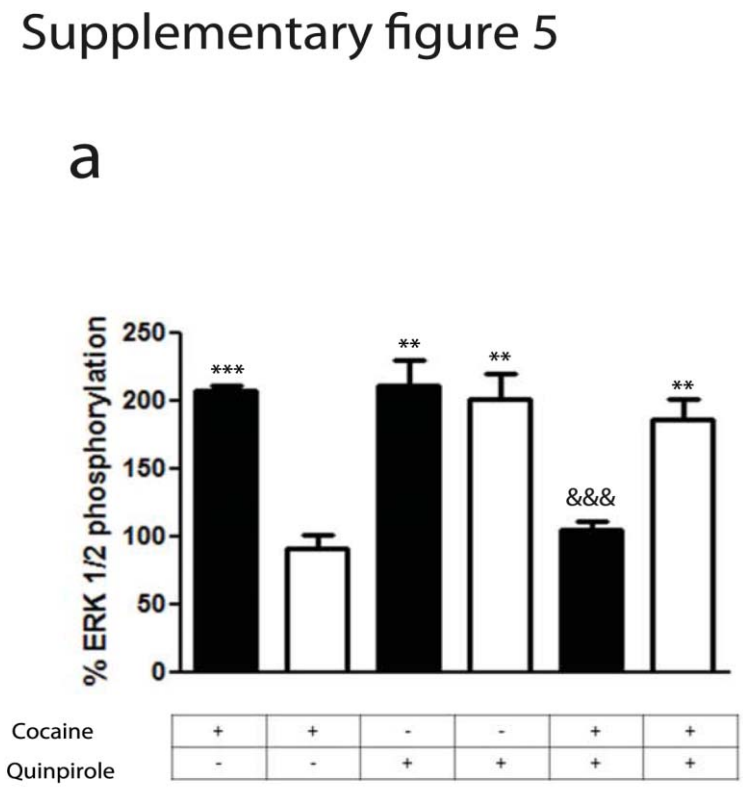

Supplementary Figure 5. Negative cross-talk between cocaine and the D_2 receptor agonist quinpirole on ERK 1/2 phosphorylation in mouse striatum. WT (black bars) and σ_1 receptor KO (white bars) mouse striatal slices were treated for 10 min with 1 μM quinpirole, with 150 μM cocaine or with both. Immunoreactive bands from six slices obtained from five WT or five KO animals were quantified for each condition. Values represent mean ± SEM of percentage of phosphorylation relative to basal levels found in untreated slices. No significant differences were obtained between the basal levels of the wild-type and the KO mice. Bifactorial ANOVA showed a significant (**$p < 0.01$, ***$p < 0.005$) effect over basal. One-way ANOVA followed by Bonferroni post hoc tests showed a significant cocaine-mediated counteraction of quinpirole ($^{\&\&\&}P < 0.005$)

3.6 El receptor D_4 de dopamina, pero no la variante $D_{4.7}$ asociada a ADHD, forma heterómeros funcionales con el receptor D_{2S} de dopamina en el cerebro

Sergio González[1], Claudia Rangel-Barajas[2], Marcela Peper[3], Ramiro Lorenzo[3], Estefanía Moreno[1], Francisco Ciruela[4], Janusz Borycz[5], Jordi Ortiz[6], Carme Lluís[1], Rafael Franco[1,7], Peter J. McCormick[1], Nora D. Volkow[8], Marcelo Rubinstein[3], Benjamín Floran[2] and Sergi Ferré[5]

[1]Centro de Investigación Biomédica en Red sobre Enfermedades Neurodegenerativas, y Departamento de Bioquímica y Biología Molecular, Facultad de Biología, Universidad de Barcelona, Barcelona, España,
[2]Departamento de Fisiología, Biofísica y Neurociencias, Centro de Investigación y de Estudios Avanzados del Instituto Politécnico Nacional, México D.F., México,
[3]Instituto de Investigaciones en Ingeniería Genética y Biología Molecular, Consejo Nacional de Investigaciones Científicas y Técnicas, Buenos Aires, Argentina,
[4]Unitat de Farmacologia, Departament Patologia i Terapèutica Experimental, Facultat de Medicina, Universitat de Barcelona, L'Hospitalet de Llobregat, Barcelona, Spain,
[5]National Institute on Drug Abuse, Intramural Research Program, National Institutes of Health, Department of Health and Human Services, Baltimore, MD, USA,
[6]Instituto de Neurosciencias y Departamento de Bioquímica y Biología Molecular, Facultad de Medicina, Universitat Autónoma de Barcelona, 08193 Bellaterra, España,
[7]Centro de Investigación Médica Aplicada, Universidad de Navarra, Pamplona, España,
[8]National Institute on Drug Abuse, National Institutes of Health, Department of Health and Human Services, Bethesda MD, USA.

Manuscrito publicado en Molecular Psychiatry, (2011 Aug); 1-13: 1359-4184/11.

Las variantes polimórficas del receptor D_4 de dopamina se han asociado con el trastorno por déficit de atención e hiperactividad (ADHD). Sin embargo, la importancia funcional del riesgo del polimorfismo (número variable de repeticiones en tándem en el exón 3) todavía es incierta. En este estudio mostramos que mientras que las variantes más frecuentes de 4 repeticiones ($D_{4.4}$) y 2 repeticiones ($D_{2.2}$) forman heterómeros funcionales con la isoforma corta del receptor D_2 (D_{2S}) de dopamina, la variante del alelo de riesgo de 7 repeticiones ($D_{4.7}$) no interacciona con este receptor. La activación del receptor D_{2s} en el heterómero D_{2S}-D_4 potencia la señalización a través de la vía de las MAP cinasas mediada por el receptor D_4 en células transfectadas y en el estriado, pero no en células que expresan la variante $D_{4.7}$ del receptor D_4 o en el estriado de ratones *knockin* portadores de la variante de 7 repeticiones ($D_{4\text{-}7}$) en el tercer bucle intracelular del receptor D_4. En el estriado, los receptores D_4 se localizan en terminales glutamatérgicas corticoestriatales, donde modulan de forma selectiva la neurotransmisión glutamatérgica interaccionando con los receptores D_{2S}. Esta interacción muestra las mismas características cualitativas que la señalización a través de la vía de las MAP cinasas mediada por el heterómero D_{2S}-D_4. La activación del receptor D_{2S} potencia la inhibición de la liberación de glutamato estriatal mediada por el receptor D_4. Por lo tanto, proponemos que la falta de heterómeros D_{2S}-$D_{4.7}$ funcionales puede alterar, a nivel presináptico, el control dopaminérgico de la neurotransmisión glutamatérgica corticoestriatal y explicar algunos de los déficits funcionales asociados a ADHD.

Molecular Psychiatry (2011), 1–13

www.nature.com/mp

ORIGINAL ARTICLE

Dopamine D_4 receptor, but not the ADHD-associated $D_{4.7}$ variant, forms functional heteromers with the dopamine D_{2S} receptor in the brain

S González[1], C Rangel-Barajas[2], M Peper[3], R Lorenzo[3], E Moreno[1], F Ciruela[4], J Borycz[5], J Ortiz[6], C Lluís[1], R Franco[7], PJ McCormick[1], ND Volkow[8], M Rubinstein[3], B Floran[2] and S Ferré[5]

[1]*Department of Biochemistry and Molecular Biology, Centro de Investigación Biomédica en Red sobre Enfermedades Neurodegenerativas, University of Barcelona, Barcelona, Spain;* [2]*Departamento de Fisiología, Biofísica y Neurociencias, Centro de Investigación y de Estudios Avanzados del Instituto Politécnico Nacional, México D.F., México;* [3]*Departamento de Fisiología y Biología Molecular y Celular, Instituto de Investigaciones en Ingeniería Genética y Biología Molecular, Consejo Nacional de Investigaciones Científicas y Técnicas, Buenos Aires, Argentina;* [4]*Unitat de Farmacologia, Departament Patologia i Terapèutica Experimental, Universitat de Barcelona, L'Hospitalet de Llobregat, Barcelona, Spain;* [5]*CNS Receptor-Receptor Interactions Unit, National Institute on Drug Abuse, Intramural Research Program, National Institutes of Health, Baltimore, MD, USA;* [6]*Department of Biochemistry and Molecular Biology, Neuroscience Institute, Universitat Autónoma de Barcelona, Bellaterra, Spain;* [7]*Departamento de Neurociencias, Centro de Investigación Médica Aplicada, Universidad de Navarra, Pamplona, Spain and* [8]*National Institute on Drug Abuse, National Institutes of Health, Bethesda MD, USA*

Polymorphic variants of the dopamine D_4 receptor have been consistently associated with attention-deficit hyperactivity disorder (ADHD). However, the functional significance of the risk polymorphism (variable number of tandem repeats in exon 3) is still unclear. Here, we show that whereas the most frequent 4-repeat ($D_{4.4}$) and the 2-repeat ($D_{4.2}$) variants form functional heteromers with the short isoform of the dopamine D_2 receptor (D_{2S}), the 7-repeat risk allele ($D_{4.7}$) does not. D_2 receptor activation in the D_{2S}–D_4 receptor heteromer potentiates D_4 receptor-mediated MAPK signaling in transfected cells and in the striatum, which did not occur in cells expressing $D_{4.7}$ or in the striatum of knockin mutant mice carrying the 7 repeats of the human $D_{4.7}$ in the third intracellular loop of the D_4 receptor. In the striatum, D_4 receptors are localized in corticostriatal glutamatergic terminals, where they selectively modulate glutamatergic neurotransmission by interacting with D_{2S} receptors. This interaction shows the same qualitative characteristics than the D_{2S}–D_4 receptor heteromer-mediated mitogen-activated protein kinase (MAPK) signaling and D_{2S} receptor activation potentiates D_4 receptor-mediated inhibition of striatal glutamate release. It is therefore postulated that dysfunctional D_{2S}–$D_{4.7}$ heteromers may impair presynaptic dopaminergic control of corticostriatal glutamatergic neurotransmission and explain functional deficits associated with ADHD.
Molecular Psychiatry advance online publication, 16 August 2011; doi:10.1038/mp.2011.93

Keywords: dopamine receptors; receptor heteromers; ADHD; striatum; glutamate

Introduction

Dopamine D_4 receptors are expressed in the prefrontal cortex, in GABAergic interneurons and in glutamatergic pyramidal neurons, including their striatal projections.[1–3] D_4 receptors have been implicated in attention-deficit hyperactivity disorder (ADHD).[1,4–6] In fact, the prefrontal cortex and associated fronto-striatal circuits are critical for executive function and are involved in ADHD.[5] The gene encoding the human D_4 receptor contains a large number of polymorphisms in its coding sequence.[4] The most extensive polymorphism is found in exon 3, a region that codes for the third intracellular loop (3IL) of the receptor. This polymorphism consists of a variable number of tandem repeats in which a 48-bp sequence exists as 2- to 11-fold repeats.[7] The three most common variants contain 2, 4 and 7 repeats ($D_{4.2}$, $D_{4.4}$ and $D_{4.7}$, respectively). $D_{4.4}$ constitutes the most frequent variant, with a global frequency of 64%, followed by $D_{4.7}$ (21%) and $D_{4.2}$ (8%).[8] Importantly, a high prevalence of the $D_{4.7}$ variant has been demonstrated in children diagnosed with ADHD.[5] Though stimulation of the $D_{4.7}$ variant has been reported to be less potent at inhibiting cAMP than $D_{4.2}$ or $D_{4.4}$,[9] the functional significance of these variants are poorly understood.

Correspondence: Dr S Ferré, National Institute on Drug Abuse, Intramural Research Program, National Institutes of Health, 251 Bayview Boulevard, Baltimore, MD 21224, USA.
E-mail: sferre@intra.nida.nih.gov
Received 25 March 2011; revised 27 June 2011; accepted 7 July 2011

Receptor heteromers are becoming the focus of extensive research in the field of G-protein-coupled receptors.[10] A receptor heteromer is currently defined as a macromolecular complex composed of at least two (functional) receptor units with biochemical properties that are demonstrably different from those of its individual components.[10] In some cases, receptor heteromers provide a framework in which to understand the role of receptors with no clear functional significance, and example being the D_3 receptor, which forms heteromers with the D_1 receptor and modifies its function.[11] A recent study showed that in mammalian transfected cells, the long isoform of the D_2 receptor (D_{2L}) heteromerizes with the three main D_4 receptor variants, $D_{4.2}$, $D_{4.4}$ and $D_{4.7}$.[12] Interestingly, results from the same study suggested that $D_{4.7}$ was less effective in forming heteromers with D_{2L} receptors.[12] In view of the reported evidence of predominant co-localization of D_4 receptors with the short isoform of the D_2 receptor (D_{2S}) in corticostriatal glutamatergic terminals,[2,3,13] we first investigated if any of the three main human variants of the D_4 receptor could interact both physically and functionally with D_{2S}. By using the Bioluminescence Resonance Energy Transfer (BRET) technique, here we show evidence for the formation of heteromers between D_{2S} and $D_{4.2}$ and $D_{4.4}$ variants of the D_4 receptor. In contrast, the $D_{4.7}$ variant failed to form heteromers with the D_{2S} receptor. In transfected cells, we found a biochemical property of the D_{2S}–D_4 receptor heteromer, which consists of the ability of D_{2S} receptor activation to potentiate D_4 receptor-mediated mitogen-activated protein kinase (MAPK) signaling. A similar result was observed in striata from wild-type (WT) mice, a species that expresses D_4 receptors with a short 3IL comparable to human $D_{4.2}$. In contrast, potentiation of D_4 receptor-mediated MAPK signaling was not observed in transfected cells expressing $D_{4.7}$ or in striata taken from *knockin* mice carrying a humanized 7-repeat intracellular loop identical to that found in human $D_{4.7}$. Finally, analyzing neurotransmitter release in striatal slices and with *in vivo* microdialysis in rats, evidence was obtained for a key role of D_2–D_4 receptor interaction in the modulation of striatal glutamatergic neurotransmission.

Materials and methods

Fusion proteins and expression vectors

The synthetic cDNAs for the human $D_{4.2}$, $D_{4.4}$ and, $D_{4.7}$ receptor gene (kindly provided by TP Sakmar, Rockefeller University, USA) were amplified using sense oligonucleotide primer (5′-TCAACGGGACTTTCCA AAATGT-3′) and antisense primer (5′-CTCCGAGAT CAACTTCTGCTCGCTTCGGTTACCC-3′), resulting in a cDNA fragment of 200 bp. A second product was generated using the sense oligonucleotide primer (5′-AAGTTGATCTCGGAGGAAGATACAGCAGATGC AG-3′) and antisense primer (5′- GCGAATTCGCAGC AAGCACGTAGAGCCTTACG-3′), resulting in a cDNA fragment of 1500 bp. Equimolar quantities of both fragments were used to produce a third product corresponding to the myc-$D_{4.2}$, myc-$D_{4.4}$ or myc-$D_{4.7}$-tagged gene using the sense primer (5′-GTGCTCGAG CACCATGGGTAACCGAAGCACAG-3′) and antisense primer without its stop codon (5′-GCGAATTCTCAG CAGCAAGCACGTAGAGCCTTACG-3′), harboring unique *Xho*I and *Eco*RI restriction sites, respectively. The fragments were then subcloned in-frame into *Xho*I/*Eco*RI sites of the pcDNA3.1 vector (Invitrogen, Paisley, Scotland, UK). Next, the human cDNAs for the adenosine A_1 receptor and dopamine $D_{4.2}$, $D_{4.4}$, $D_{4.7}$ and D_{2S} receptors, cloned in *pcDNA3.1* were amplified without their stop codons using sense and antisense primers harboring unique *Xho*I and *Eco*RI sites to clone A_1, $D_{4.2}$, $D_{4.4}$ and $D_{4.7}$ receptors in the RLuc and the yellow fluorescent protein (YFP) corresponding vectors, and *Hin*dIII and *Bam*HI to clone D_{2S} in the RLuc and the YFP corresponding vectors. The mouse cDNAs for the D_4 and D_{2S} receptors, cloned in pCMV-SPORT6 (American Type Culture Collection, Manassas, USA) and pReceiver-M16 vectors, respectively (GeneCopoeia, Rockville, MD, USA), were amplified without their stop codons using sense and antisense primers harboring unique *Xho*I and *Eco*RV sites to clone D_4 receptor in the RLuc corresponding vector, and *Xho*I and *Kpn*I to clone D_{2S} receptor in the RLuc and the YFP corresponding vectors. The amplified fragments were subcloned to be in-frame into restriction sites of the multiple cloning sites of EYFP-N3 vector (enhanced yellow variant of YFP; Clontech, Heidelberg, Germany) or the mammalian humanized pRluc-N1 vectors (Perkin-Elmer, Waltham, MA, USA) to give the plasmids that express the receptors fused to either Rluc or YFP on the C-terminal end of the receptor ($D_{4.2}$-RLuc, $D_{4.4}$-RLuc, $D_{4.7}$-Rluc, D_{2S}-RLuc and A_1-RLuc or D_{2S}-YFP, $D_{4.7}$-YFP and D_1-YFP, respectively). All constructs were verified by nucleotide sequencing and the fusion proteins are functional and expressed at the membrane level (see Results).

Cell culture and transient transfection

HEK (human embryonic kidney)-293T cells were grown in DMEM (Dulbecco's modified Eagle's medium) (Gibco Paisley, Scotland, UK) supplemented with 2 mM L-glutamine, 100 U ml^{-1} penicillin/streptomycin and 5% (*v*/*v*) heat-inactivated fetal bovine serum (all supplements were from Invitrogen). CHO cell lines were maintained in á-MEM medium without nucleosides, containing 10% fetal calf serum, 50 μg ml^{-1} penicillin, 50 μg ml^{-1} streptomycin and 2 mM L-glutamine (300 μg ml^{-1}). Cells were maintained at 37°C in an atmosphere of 5% CO_2, and were passaged when they were 80–90% confluent, twice a week. HEK-293T or CHO cells growing in six-well dishes or in 25 cm^2 flasks were transiently transfected with the corresponding fusion protein cDNA by the PEI (PolyEthylenImine; Sigma, Steinheim, Germany) method as previously described.[14]

Immunostaining
For immunocytochemistry, HEK-293T cells were grown on glass coverslips and transiently transfected with 1 μg of cDNA corresponding to human $D_{4.2}$-RLuc, $D_{4.4}$-RLuc or $D_{4.7}$-RLuc and 0.5 μg of cDNA corresponding to human D_{2S}-YFP or 0.8 μg of cDNA corresponding to mouse D_4-RLuc and 0.5 μg of cDNA corresponding to mouse D_{2S}-YFP. After 48 h of transfection, cells were fixed in 4% paraformaldehyde for 15 min and washed with phosphate-buffered saline contraining 20 mM glycine to quench the aldehyde groups. After permeabilization with phosphate-buffered saline containing 0.05% Triton X-100 for 15 min, cells were treated with phosphate-buffered saline containing 1% bovine serum albumin. After 1 h at room temperature, cells were labeled with the primary rabbit monoclonal anti-human D_4 receptor (1/10 000; Abcam, Cambridge, UK) or with the primary goat polyclonal anti-D_4 receptor (1/500; Santa Cruz Biotechnology, Santa Cruz, CA, USA) for 1 h, washed and stained with the secondary antibody Cy3 anti-rabbit (1/200; Jackson ImmunoResearch, Baltimore, PA, USA) or with the secondary antibody Cy3 anti-goat (1/200; Jackson ImmunoResearch). The D_{2S}-YFP construct was detected by its fluorescence properties. Samples were rinsed and observed in an Olympus confocal microscope.

BRET assay
HEK-293T cells were co-transfected with a constant amount of cDNA encoding for the receptor fused to RLuc and with increasingly amounts of cDNA encoding to the receptor fused to YFP to measure BRET as previously described.[14] Both fluorescence and luminescence for each sample were measured before every experiment to confirm similar donor expressions (~100 000 bioluminescence units) while monitoring the increase in acceptor expression (2000–20 000 fluorescence units). The relative amounts of BRET acceptor are expressed as the ratio between the net fluorescence of the acceptor and the luciferase activity of the donor being the net fluorescence the fluorescence of the acceptor minus the fluorescence detected in cells only expressing the donor. The BRET ratio is defined as [(emission at 510–590)/(emission at 440–500)]−Cf, where Cf corresponds to (emission at 510–590)/(emission at 440–500) for the D_4-RLuc or D_{2S}-RLuc constructs expressed alone in the same experimental conditions. Curves were fitted by using a non-linear regression equation, assuming a single phase with GraphPad Prism software (San Diego, CA, USA).

Generation of knockin mutant mice carrying human expansions in the 3IL of the D_4 receptor
A targeting vector was designed such that coding sequences of the 3IL of mouse *Drd4* were replaced by human ortholog sequences corresponding to the most frequent 7-variable number of tandem repeat human variant allele (see Figure 4). The vector included a selectable PGK-*neo* cassette, flanked by two loxP sites, placed just downstream of *Drd4* polyadenylation site and an herpes simplex virus-thymidine kinase cassette placed at one of the extremes of the targeting vector to select for the absence of random integrations. A long and short arm of *Drd4* homology were inserted flanking the swapped sequence and the selectable marker, respectively. The linearized vector was used to electroporate hybrid 129svev/C57BL/6 ES cells (inGenious Targeting Laboratory, Stony Brook, NY, USA) and homologous recombinant clones were selected in the presence of G418 and gancyclovir. Two selected clones carrying the human 7-variable number of tandem repeat were used to microinject C57BL/6J blastocysts and one high percentage chimeric male mouse was used to produce heterozygote $Drd4^{+/7repeat.neo}$ mice. The neo cassette was excissed from the recombinant allele by crossing mutant mice with transgenic mice expressing Cre recombinase from an EIIa promoter (Jackson Laboratories; Cat. No. 003724). The resulting heterozygote $Drd4^{+/7repeat}$ ($D_{4.7}$ knockin) mice were successively bred to C57BL/6J mice to obtain a congenic heterozygote strain ($n = 10$) that was used to establish a breeding colony. Homozygous $D_{4.7}$ knockin mice and their WT littermates were used for the experiments. Knockin animals were characterized as indicated in Figure 4.

Mouse striatal slices preparation
Mice were housed five per cage in a temperature (21 ± 1 °C) and humidity-controlled (55 ± 10%) room with a 12:12-h light/dark cycle (light between 0800 and 2000 hours) with food and water *ad libitum*. All animal procedures were conducted according to the standard ethical guidelines (National Institutes of Health Animal care guidelines and European Communities Council Directive 86/609/EEC) and approved by the Local Ethical and Animal Care Committees. Transgenic mice and littermattes were decapitated with a guillotine and the brains were rapidly removed and placed in ice-cold oxygenated (O_2/CO_2:95%/5%) Krebs-HCO_3^- buffer (124 mM NaCl, 4 mM KCl, 1.25 mM NaH_2PO_4, 1.5 mM $MgCl_2$, 1.5 mM $CaCl_2$, 10 mM glucose and 26 mM $NaHCO_3$, pH 7.4). The brains were sliced at 4 °C in a brain matrix (Zivic Instruments, Pittsburgh, PA, USA) into 0.5 mm coronal slices. Slices were kept at 4 °C in Krebs-HCO_3^- buffer during the dissection of the striatum. Each slice was transferred into an incubation tube containing 1 ml of ice-cold Krebs-HCO_3^- buffer. The temperature was raised to 23 °C and after 30 min, the media was replaced by 2 ml Krebs-HCO_3^- buffer (23 °C).

ERK phosphorylation assay
Striatal slices from transgenic mice and littermattes were incubated under constant oxygenation (O_2/CO_2:95%/5%) at 30 °C for 4–5 h in an Eppendorf Thermomixer (5 Prime, Boulder, CO, USA) with Krebs-HCO_3^- buffer. The media was replaced by 200 μl of fresh Krebs-HCO_3^- buffer and incubated for 30 min before the addition of ligands. Transfected CHO cells were cultured in serum-free medium for

16 h before the addition of the indicated concentration of ligands for the indicated time. Both, cells and slices were lysed in ice-cold lysis buffer (50 mM Tris-HCl pH 7.4, 50 mM NaF, 150 mM NaCl, 45 mM β-glycerophosphate, 1% Triton X-100, 20 μM phenylarsine oxide, 0.4 mM $NaVO_4$ and protease inhibitor cocktail). Cellular debris was removed by centrifugation at 13 000 *g* for 5 min at 4 °C and protein was quantified by the bicinchoninic acid method using bovine serum albumin dilutions as standard. To determine the level of extracellular signal-regulated kinases 1 and 2 (ERK1/2) phosphorylation, equivalent amounts of protein (10 μg) were separated by electrophoresis on a denaturing 10% sodium dodecyl sulfate-polyacrylamide gel and transferred onto polyvinylidene fluoride for fluorescence membranes. Odyssey blocking buffer (LICOR Biosciences, Lincoln, NE, USA) was then added and membranes were blocked for 90 min. Membranes were then probed with a mixture of a mouse anti-phospho-ERK1/2 antibody (1:2500; Sigma) and rabbit anti-ERK1/2 antibody (1:40 000; Sigma) for 2–3 h. Bands were visualized by the addition of a mixture of IRDye 800 (anti-mouse) antibody (1:10 000; Sigma) and IRDye 680 (anti-rabbit) antibody (1:10 000; Sigma) for 1 h and scanned by the Odyssey infrared scanner (LICOR Biosciences). Bands densities were quantified using the scanner software and exported to Excel (Microsoft, Redmond, WA, USA). The level of phosphorylated ERK1/2 isoforms was normalized for differences in loading using the total ERK protein band intensities.

In vivo *microdialysis in rat striatum*

Male Sprague-Dawley rats (Charles River Laboratory, Wilmington, MA, USA), weighing 300–350 g were used. Concentric microdialysis probes with 2 mm long dialysis membranes were prepared as described previously.[15] Animals were anesthetized with Equithesin (NIDA Pharmacy, Baltimore, MD, USA) and microdialysis probes were implanted in the ventral striatum (core of the nucleus accumbens); coordinates with respect to bregma: A 1.7, L +1.2 and V −7.6 mm. The experiments were performed on freely moving rats 24 h after the probe implantation. A Ringer solution (in mmol l^{-1}) of 147 NaCl, 4 KCl and 2.2 $CaCl_2$ was pumped through the dialysis probe at a constant rate of 1 μl per minute. After a washout period of 90 min, samples were collected at 20 min intervals and split into two fractions of 10 μl, to separately measure glutamate and dopamine contents. Each animal was used to study the effect of one treatment by local administration (perfusion by reverse dialysis) of the D_4 receptor agonist RO-10-5824 or the D_4 receptor antagonist L-745 870. At the end of the experiment, rats were killed with an overdose of Equithesin and methylene blue was perfused through the probe. The brain was removed and placed in a 10% formaldehyde solution, and coronal sections were cut to verify the probe location. Dopamine content was measured by reverse high-performance liquid chromatography coupled to an electrochemical detector, as described in detail previously. Glutamate content was measured by high-performance liquid chromatography coupled to a flourimetric detector, as described before.[16] The limit of detection (which represents three times baseline noise levels) for dopamine and glutamate was 0.5 and 50 nM, respectively. Dopamine and glutamate values were transformed as percentage of the mean of the three values before the stimulation and transformed values were statistically analyzed with one-way repeated measures analysis of variance followed by Newman–Keuls tests, to compare glutamate and dopamine values of the samples obtained after drug perfusion with those obtained just before drug perfusion.

Neurotransmitter release in rat striatal slices

Rat brain slices were obtained from male Wistar rats weighing 180–220 g. After rapid killing of the rat, the brain was immersed in oxygenated ice-cold artificial cerebrospinal fluid (ACSF) solution, and coronal brain slices (300 μm thick) were obtained with a vibratome. The striatum (caudate-putamen and nucleus accumbens) was microdissected under a stereoscopic microscope and the slices were incubated for 30 min at 37 °C in ACSF (in mM: NaCl 118.25, KCl 1.75, $MgSO_4$ 1, KH_2PO_4 1.25, $NaHCO_3$ 25, $CaCl_2$ 2 and D-glucose 10), gassed continuously with O_2/CO_2 (95:5, v/v). For γ-aminobutyric acid (GABA) release, the slices were then incubated for 30 min with 8 nM [^{3}H]GABA in 2 ml solution containing 10 μM aminooxyacetic acid (to inhibit GABA transaminase, thus preventing degradation of the labeled GABA). At the end of this period, excess radiolabeled compound was removed by washing twice with ACSF containing, in addition to aminooxyacetic acid and 10 μM nipecotic acid (to prevent the reuptake of the released [^{3}H]GABA). Both compounds were present in the perfusion solution for the rest of the experiment. For dopamine release, the slices were labeled with 77 nM [^{3}H]dopamine in Krebs–Henseleit solution containing 10 μM pargyline, 0.57 mM ascorbic acid and 0.03 mM EDTA, which were present in the solutions for the rest of the experiment. For glutamate release, the tissues were incubated for 30 min with 100 nM [^{3}H]glutamate in 2 ml of ACSF containing 200 μM aminooxyacetic acid (to inhibit glutamate decarboxylase and prevent the conversion of glutamate to GABA) and 200 μM dihydrokainic acid (to prevent the uptake of [^{3}H]glutamate by astrocytes). Dihydrokainic acid was present in the medium only during the incubation period. At the end of this period, the excess radiolabeled compound was removed by washing twice with ACSF. Methods for measuring [^{3}H]neurotransmitter release and data analysis used in the present work were the same as those described previously.[17,18] The slices were apportioned randomly between the chambers (usually three slices per chamber) of a superfusion system (volume of each chamber 80 μl; 20 chambers in parallel) and perfused with the ACSF at a flow rate of 0.5 ml per minute for 1 h. Basal release of

[^{3}H]neurotransmitter was measured by collecting four fractions of the superfusate (total volume 2 ml) before depolarizing the slices with a solution in which the [K^+] was raised to 25 mM. The composition of the high K^+ solution was (in mM): NaCl 101.25, KCl 23.75, $MgSO_4$ 1, KH_2PO_4 1.25, $NaHCO_3$ 25, $CaCl_2$ 2 and D-glucose 10. Six more fractions were collected in the high K^+ medium. All drugs were added to the medium at fraction 2, before changing the superfusion to the high K^+ medium, to explore effects on basal release. To determine the total amount of tritium remaining in the tissue, the slices were collected, treated with 1 ml of 1 M HCl and allowed to stand for 1 h before adding the scintillator. The [^{3}H]neurotransmitter release was expressed initially as a fraction of the total amount of tritium remaining in the tissue. The effect of drugs on the basal release of [^{3}H]neurotransmitter was assessed by comparing the fractional release in fraction 2 (immediately before exposure of the tissue to the drug) and fraction four (immediately before exposure to 25 mM of K^+), using Student's paired *t*-test. Changes in depolarization-induced [^{3}H]GABA release by drugs and treatments were assessed by comparing the area under the appropriate release curves between the first and last fractions collected after the change to high K^+. The significance of drug effects was assessed by one-way analysis of variance and Tukey–Kramer test, using Prism Graph Pad Software 4.0 (Graph Pad Software). To obtain an unbiased estimate of IC_{50} values, concentration-response data were fitted by non-linear regression using the same software.

Statistical analysis

Statistical analyses were performed with Prism Graph Pad Software 4.0 (Graph Pad Software). See above and figure legends (Figure 1 to Figure 7) for details.

Results

D_{2S} and D_4 receptors form heteromers in transfected cells

BRET experiments were performed where one of the receptor is fused to the bioluminescent protein *Renilla Luciferase* (RLuc) and the other receptor is fused to a YFP. The fusion proteins were functional (Supplementary Figure 1) and expressed at the membrane level (Figure 1c). Clear BRET saturation curves were obtained in cells expressing $D_{4.2}$-RLuc or $D_{4.4}$-RLuc receptors and increasing amounts of D_{2S}-YFP (Figure 1a), but not in cells expressing $D_{4.2}$-RLuc or $D_{4.4}$-RLuc receptors and increasing amounts of D_1-YFP (Figure 1a), indicating that the $D_{4.2}$ and the $D_{4.4}$ form heteromers with D_{2S} but not with D_1 receptors. Interestingly, in cells expressing the $D_{4.7}$-Rluc variant and D_1-YFP or D_{2S}-YFP (Figure 1a) low linear BRET was detected, which was qualitatively similar to the results obtained with the negative control, with adenosine A_1-RLuc and D_{2S}-YFP receptors (Figure 1a). This result was not due to the particular BRET donor and acceptor chosen, as low and linear BRET were obtained when we swapped the fused proteins, that is, in cells co-expressing D_{2S}-Rluc and $D_{4.7}$-YFP (Figure 1a). These results strongly suggest that the human $D_{4.7}$ polymorphic variant does not form heteromers with the human D_{2S} receptor or if heteromers are formed, the fusion proteins are not properly oriented or are not within proximity to allow energy transfer (<10 nm). One way to test if the receptors are indeed forming heteromers in such a way that impedes energy transfer is to titrate one receptor in the presence of the heteromer and look for changes in the BRET signal. In BRET displacement experiments, $D_{4.2}$, but not $D_{4.7}$ receptors were able to compete with $D_{4.4}$-Rluc and alter heteromer formation with D_{2S}-YFP (Figure 1b), meaning that $D_{4.2}$ and $D_{4.4}$, but not $D_{4.7}$ receptors use the same molecular determinants to establish intermolecular interactions with D_{2S} receptor and strongly suggesting that $D_{4.7}$ receptors are unable to form heteromers with D_{2S}.

D_{2S}–D_4 receptor heteromer signals through MAPK

To investigate the function of the D_{2S}–D_4 receptor heteromer, MAPK signaling (ERK1/2 phosphorylation) was determined. RO-10-5824 and quinelorane, selective D_4 and $D_{2/3}$ receptor agonists respectively,[19,20] selectively stimulated MAPK in cells transfected with D_4 or D_{2S} receptors, respectively (Supplementary Figure 2). Dose-response experiments with RO-10-5824 showed no significant differences between cells transfected with $D_{4.2}$, $D_{4.4}$ or $D_{4.7}$ receptors (Supplementary Figure 2). However, in co-transfected cells, stimulation of D_{2S} receptors potentiated D_4 receptor-mediated MAPK activation, but not the other way around. Importantly, this functional interaction only occurred in cells transfected with D_{2S} and $D_{4.2}$ or $D_{4.4}$, but not in cells expressing $D_{4.7}$ receptors (Figure 2). Since disruption of D_{2S}–D_4 receptor heteromers (by substituting $D_{4.2}$ or $D_{4.4}$ with the $D_{4.7}$ variant) is associated with the loss of the D_{2S}–D_4 receptor interaction at the MAPK level, this interaction constitutes a specific biochemical property of the D_{2S}–D_4 receptor heteromer and can be used as a biochemical fingerprint to detect the heteromer in native tissues.[10]

D_{2S}–D_4 receptor heteromers in the mouse brain

D_4 receptors are preferentially expressed in limbic areas and the prefrontal cortex, where they can be found in interneurons and also projecting neurons.[1] In corticostriatal neurons, D_4 receptors have also been localized at their nerve terminals,[2,3] where they can co-localize with D_{2S} receptors.[13] We therefore investigated the existence of D_{2S}–D_4 receptor heteromers in the striatum. Biophysical techniques cannot be easily applied in native tissues, but indirect methods can be used, such as the identification of a biochemical property of the heteromer (biochemical fingerprint).[10] In this case, the biochemical fingerprint would be the potentiation by D_{2S} receptor activation of D_4 receptor-mediated MAPK activation, which should not occur

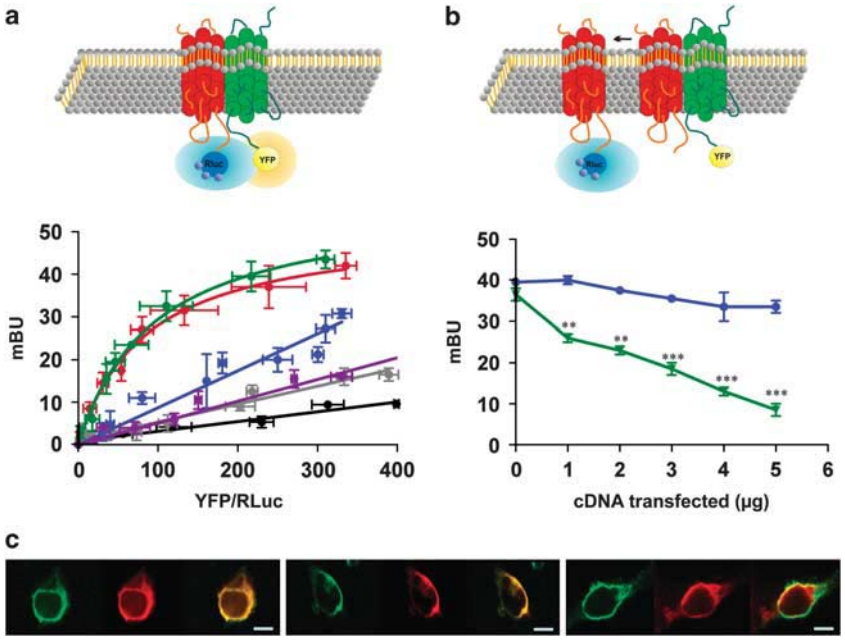

Figure 1 Human D_{2S} and D_4 receptors form heteromers in transfected cells. (**a**) Bioluminescence Resonance Energy Transfer (BRET) saturation curves were obtained from experiments with cells co-expressing, top to bottom, D_{2S}-YFP (yellow fluorescent protein) and $D_{4.2}$-RLuc (red), $D_{4.4}$-RLuc (green) or $D_{4.7}$-Rluc (blue), D_{2S}-RLuc and $D_{4.7}$-YFP (purple), A_1-RLuc and D_{2S}-YFP (black) or $D_{4.4}$-RLuc and D_1-YFP (gray). Co-transfections were performed with a constant amount of cDNA corresponding to the receptor-RLuc construct (2 μg of cDNA for D_4-RLuc or 1 μg of cDNA for A_1-RLuc) and increasing amounts of cDNA corresponding to the receptor-YFP construct (0.2–6 μg of cDNA for D_{2S}-YFP or 1–4 μg of cDNA for D_1-YFP). Both fluorescence and luminescence of each sample were measured before every experiment to confirm equal expression of Rluc (about 100 000 luminescence units) while monitoring the increase of YFP expression (2000–20 000 fluorescence units). BRET data are expressed as mean values ± s.d. of four to nine different experiments grouped as a function of the amount of BRET acceptor. (**b**) BRET displacement experiments were performed in cells expressing constant amounts of $D_{4.4}$-RLuc (2 μg cDNA transfected) and D_{2S}-YFP (2 μg cDNA transfected) and increasing amounts (1–5 μg of cDNA transfected) of $D_{4.7}$ (blue) or $D_{4.2}$ (green). Both fluorescence and luminescence of each sample were measured before every experiment to confirm no changes in the expression of $D_{4.4}$-RLuc and D_{2S}-YFP. BRET data are expressed as mean values ± s.d. of five different experiments grouped as a function of the amount of BRET acceptor. Significant differences with respect to the samples without $D_{4.2}$ or $D_{4.7}$ were calculated by one-way analysis of variance (ANOVA) and Bonferroni's test (**$P<0.01$ and ***$P<0.001$). In (**a**, **b**), the relative amounts of BRET acceptor are expressed as the ratio between the fluorescence of the acceptor minus the fluorescence detected in cells only expressing the donor, and the luciferase activity of the donor. In the top, schematic representations of BRET (**a**) or BRET displacement (**b**) are shown. (**c**) Confocal microscopy images of cells transfected with 1 μg of cDNA corresponding to, left to right, $D_{4.2}$-RLuc, $D_{4.4}$-RLuc or $D_{4.7}$-RLuc and 0.5 μg cDNA corresponding to D_{2S}-YFP. Proteins were identified by fluorescence or by immunocytochemistry. D_4-RLuc receptors are shown in red, D_{2S}-YFP is shown in green and co-localization is shown in yellow. Scale bar: 5 μm.

with the human $D_{4.7}$ variant. Before these experiments with mouse brain, we demonstrated by BRET saturation experiments in transfected cells that the mouse D_{2S} receptor forms heteromers with the mouse D_4 receptor (which has an amino-acid sequence in the 3IL similar to that from the human $D_{4.2}$). Mouse fusion proteins were expressed in the plasma membrane of transfected cells (Figure 3a) and shown to be functional (Supplementary Figure 3). Like the human receptors, mouse D_{2S} receptors were found to form heteromers with mouse D_4 receptors and also with human $D_{4.4}$ receptors, but not with human $D_{4.7}$ receptors (Figure 3b). Furthermore, it was also shown that, in co-transfected cells, stimulation of the mouse D_{2S} receptor potentiates the effect of the mouse D_4, but not the human $D_{4.7}$, on MAPK signaling (Figures 3c and d). This result was not reciprocal (Supplementary Figure 4) and mirrors the results obtained with human D_4 and D_{2S} receptors (Figure 2). We next analyzed the effects of D_2 and D_4 receptor agonists on MAPK signaling on striatal slices taken from knockin mice carrying the 7 repeats of the human $D_{4.7}$ in replacement of the mouse region and from WT littermates (Figure 4). Neither quinelorane nor RO-10-5824 induced a significant ERK1/2 phosphorylation in striatal slices of WT mice when administered alone, but co-administration of both agonists produced a significant dose-dependent effect with an increase of up to fourfold (Figure 3e). This synergistic interaction between D_2 and D_4 receptors, which constitutes the biochemical fingerprint of the D_{2S}–D_4 receptor heteromer, was completely absent in the $D_{4.7}$ mutant mouse (Figure 3e), confirming both the existence of D_{2S}–D_4 receptor heteromers and the

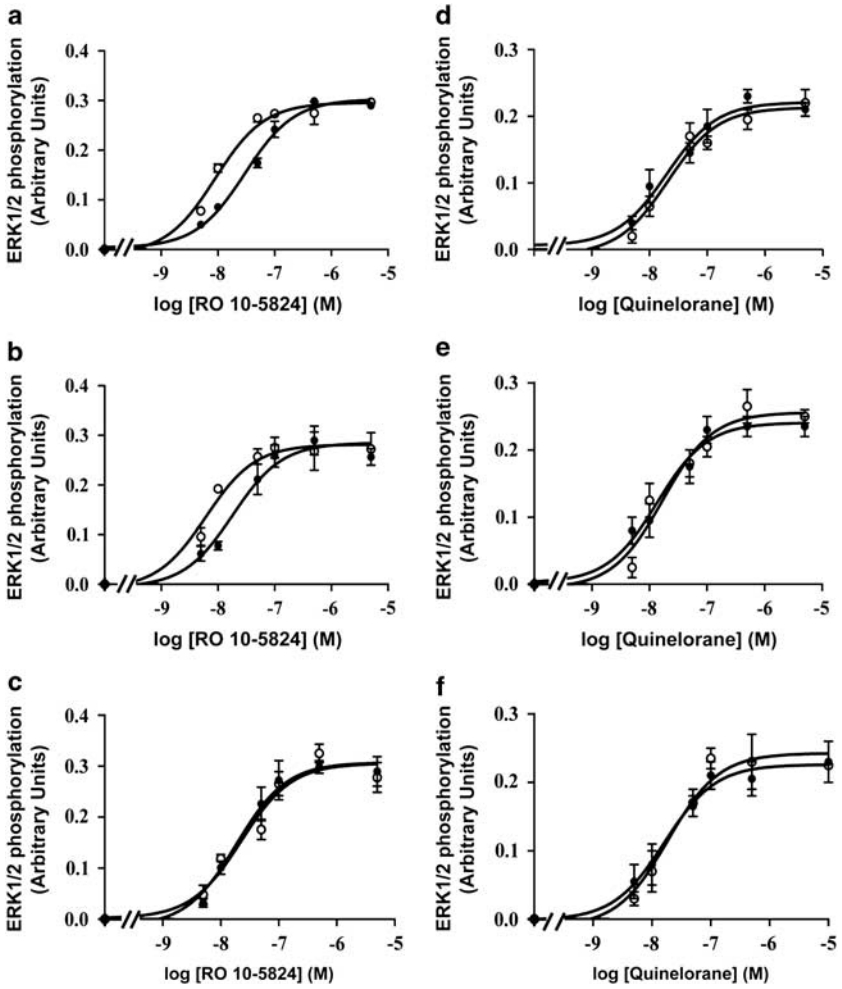

Figure 2 Crosstalk between human D_4 and D_{2S} receptors in ERK1/2 phosphorylation. Cells were transiently co-transfected with 2.5 μg of cDNA corresponding to D_{2S} and 2.5 μg of cDNA corresponding to $D_{4.2}$ (**a**, **d**), $D_{4.4}$ (**b**, **e**) or $D_{4.7}$ (**c**, **f**). In (**a–c**), cells were treated for 10 min with increasing concentrations of RO-10-5824 in the presence (○) or in the absence (●) of quinelorane (50 nM). In (**d–f**), cells were treated for 10 min with increasing concentrations of quinelorane in the presence (○) or in the absence (●) of RO-10-5824 (50 nM). The immunoreactive bands, corresponding to ERK1/2 phosphorylation, of three to six experiments were quantified and expressed as arbitrary units. For each curve, EC_{50} values were calculated as mean ± s.e.m. and statistical differences between curves obtained in the presence or in the absence of quinelorane (**a–c**) or RO-10-5824 (**d–f**) were determined by Student's *t*-test. EC_{50} with and without quinelorane: (**a**) 9 ± 1 and 26 ± 1 nM ($P < 0.01$), (**b**) 7 ± 1 and 23 ± 1 nM ($P < 0.01$), (**c**) 18 ± 1 and 22 ± 1 nM (N.S.). EC_{50} with and without RO-10-5824: (**d**) 22 ± 1 and 20 ± 1 nM (N.S.), (**e**) 20 ± 1 and 17 ± 1 nM (N.S.), (**f**) 18 ± 1 and 13 ± 1 nM (N.S.). N.S., non-statistical differences.

absence of functional interactions between D_2 and $D_{4.7}$ receptors in the brain.

D_2–D_4 receptor interactions modulate striatal glutamate release

To investigate the functional significance of D_4 receptor activation, we determined D_4 receptor-mediated modulation of striatal glutamate release by *in vivo* microdialysis in freely moving rats. The local perfusion of the D_4 receptor agonist RO-10-5824 in the ventral striatum (in the nucleus accumbens) produced a dose-dependent decrease in the striatal extracellular concentration of glutamate and a concomitant increase in the extracellular concentration of dopamine (Figures 5a and 5b), which were counteracted by co-perfusion with the selective D_4 receptor antagonist L-745 870 (which was inactive when perfused alone) (Figures 5a–c). These results suggest that inhibitory D_4 receptors are located in glutamatergic terminals, whose activation decreases basal striatal glutamate release. The increase in dopamine concentration can best be explained by a decreased activation of striatal GABAergic efferent neurons that tonically inhibit dopaminergic mesencephalic neurons. This interpretation could be confirmed in experiments with striatal slices, where dopamine should not be modified due to the interruption of the striatal-mesencephalic loop. In fact, in slices of dorsal or ventral rat striatum, the D_4 receptor agonist RO-10-5824 decreased K^+-induced glutamate release, an effect that was counteracted by the selective D_4 receptor antagonist L-745 870, but did not change

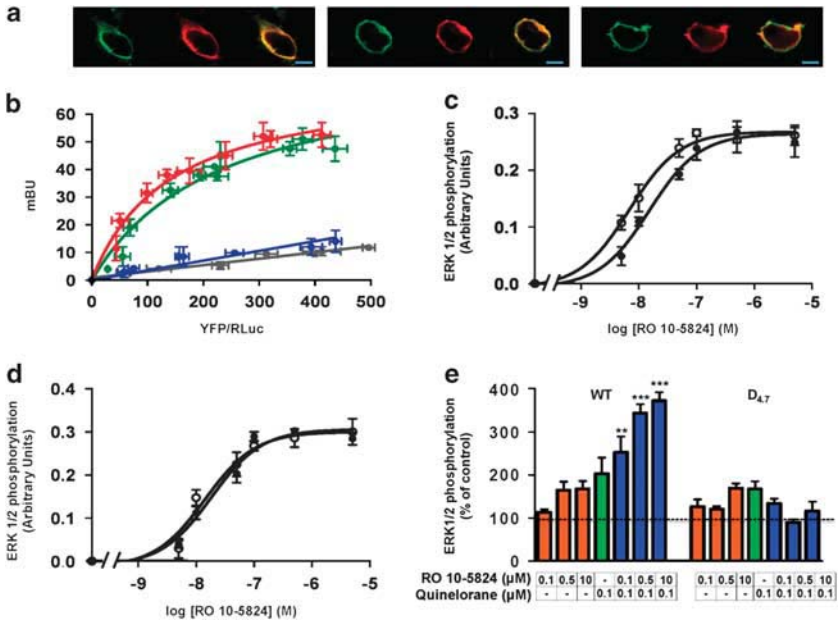

Figure 3 D_{2s}–D_4 receptor heteromers in the mouse brain. (**a**) Confocal microscopy images of cells transfected with 1 μg of cDNA corresponding to, left to right, mouse D_4-RLuc, human $D_{4.4}$-RLuc and human $D_{4.7}$-RLuc and 0.5 μg of cDNA corresponding to D_{2S}- yellow fluorescent protein (YFP). Proteins were identified by fluorescence or by immunocytochemistry. D_4-RLuc receptors are shown in red, D_{2S}-YFP is shown in green and co-localization is shown in yellow. Scale bar: 5 μm. (**b**) Mouse D_{2S} receptor heteromerization with mouse and human D_4 receptors. Bioluminescence Resonance Energy Transfer (BRET) saturation curves were obtained from cells co-expressing mouse D_4-Rluc (green), human $D_{4.4}$-RLuc (red), human $D_{4.7}$-RLuc (blue) or human A_1-RLuc (gray) and mouse D_{2S}-YFP receptors. Co-transfections were performed with a constant amount of cDNA corresponding to the receptor-RLuc construct (2 μg of cDNA for mouse D_4-RLuc, 2.5 μg of cDNA for human D_4-RLuc or 1 μg of cDNA for A_1-RLuc) and increasing amounts of cDNA corresponding to the receptor-YFP construct (0.2–6 μg cDNA). Both fluorescence and luminescence of each sample were measured before every experiment to confirm equal expression of Rluc (about 100 000 luminescence units) while monitoring the increase of YFP expression (2000–20 000 fluorescence units). The relative amounts of BRET acceptor are expressed as the ratio between the fluorescence of the acceptor minus the fluorescence detected in cells only expressing the donor, and the luciferase activity of the donor. BRET data are expressed as mean values ± s.d. of three to six different experiments grouped as a function of the amount of BRET acceptor. (**c**, **d**) Crosstalk between mouse D_{2S} receptors and mouse or human D_4 receptors in ERK1/2 phosphorylation. Cells transiently co-expressing mouse D_{2S} receptors and mouse D_4 receptors (**c**) or human $D_{4.7}$ receptors (**d**) were treated for 10 min with increasing RO-10-5824 concentrations in the presence (○) or in the absence (●) of quinelorane (50 nM) before the ERK1/2 phosphorylation determination. The immunoreactive bands of three experiments (mean ± s.e.m.; $n = 3$) were quantified and expressed as arbitrary units. EC_{50} values with or without quinelorane were: (**c**) 7 ± 0.1 and 15 ± 0.1 nM (Student's *t*-test: $P < 0.01$) or (**d**) 18 ± 0.1 and 15 ± 0.1 nM (Student's *t*-test: N.S.). (**e**) Striatal slices from wild-type (WT) or $D_{4.7}$ mutant mice were treated for 10 min with the indicated concentrations of RO-10-5824 (orange) or quinelorane (green) or with RO-10-5824 plus quinelorane (blue) and ERK1/2 phosphorylation was determined. For each treatment, the immunoreactive bands from four to six slices from a total 10 WT and 10 $D_{4.7}$ mutant animals were quantified and values represent the mean ± s.e.m. of the percentage of phosphorylation relative to basal levels found in untreated slices (100%). No significant differences were obtained between the basal levels of the WT and the $D_{4.7}$ mutant mice. Significant treatment and genotype effects were shown by a bifactorial analysis of variance (ANOVA) followed by *post hoc* Bonferroni's tests (**$P < 0.01$ and ***$P < 0.001$, as compared with the lowest concentration of RO-10-5824).

dopamine or GABA release (Figure 6), indicating that striatal D_4 receptors selectively and locally modulate glutamate release. This role of D_4 receptors in the striatum can also explain previous results obtained with D_4 receptor KO mice, which show an increase and decrease in the striatal extracellular concentration of glutamate and dopamine, respectively.[21,22]

As mentioned before, there is evidence for co-localization of both D_2 and D_4 receptors in corticostriatal glutamatergic terminals[2,3,13] and previous studies have demonstrated that presynaptic D_2-like receptors have an inhibitory role in the modulation of striatal glutamate release.[13,23] However, since those studies did not use selective compounds, they could not distinguish between effects due to D_2 or D_4 receptor stimulation. Therefore, in this study we tested the effect of quinelorane alone and in combination with RO-10-5824 on glutamate release in rat striatal slices. To eliminate endogenous dopamine, rats were treated with reserpine, and the experiments performed in the presence of the D_1-like receptor antagonist SCH-23390. Quinelorane significantly decreased K^+-induced glutamate release, whereas the co-application of quinelorane with RO-10-5824 showed a more significant effect (Figure 7a). Dopamine strongly decreased K^+-induced glutamate

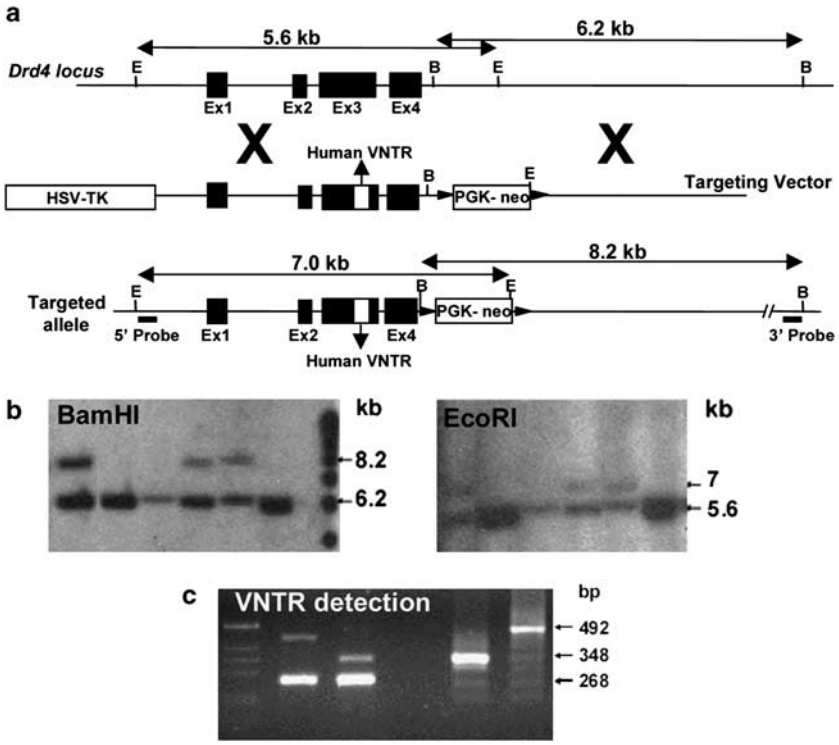

Figure 4 Targeted insertion of human variable number of tandem repeats (VNTRs) carrying 7 repeats into the mouse *Drd4* exon 3 by homologous recombination in ES cells. (**a**) Structure of the *Drd4 locus*, targeting vector and targeted allele. (**b**) Southern blot analysis detected double homologous recombination events at the 5′ and 3′ ends using external probes after digestion with *Bam*HI or *Eco*RI. (**c**) The presence of inserted human VNTR was verified by PCR using mouse primers flanking the expansion.

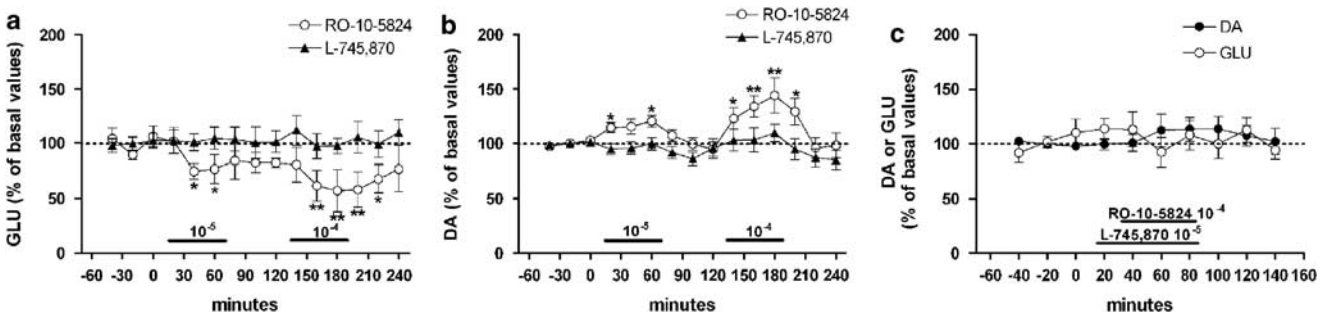

Figure 5 *In vivo* D_4 receptor-mediated modulation of basal extracellular levels of glutamate in the rat ventral striatum. Effects of the local perfusion with the D_4 receptor agonist RO-10-5824 and the D_4 receptor antagonist L-745 870 on the basal extracellular concentrations of glutamate (GLU) and dopamine (DA) in the ventral striatum (core of the nucleus accumbens). Horizontal bars show the periods of drug perfusion (concentrations are indicated in M). Data represent mean values ± s.e.m. of the percentage of the mean of the three basal values before the first drug perfusion ($n = 6$–8 per group): $^*P < 0.05$ and $^{**}P < 0.01$, compared with the values previous in time '0' (repeated measures analysis of variance (ANOVA) followed by Newman–Keuls tests).

release, an effect partially counteracted by the D_2 receptor antagonist L-741 626 or by the D_4 receptor antagonist L-745 870, but completely counteracted by the simultaneous application of both antagonists (Figure 7b). In agreement with the reported higher *in vitro* affinity of D_4 versus D_2 receptor for dopamine,[24] the IC_{50} of dopamine-mediated inhibition of K^+-induced glutamate release was significantly higher in the presence of the D_4 receptor antagonist (D_2-mediated effect) than in the presence of the D_2 receptor antagonist (D_4-mediated effect) (Figure 7b). Finally, and more importantly, the D_2 receptor agonist quinelorane synergistically potentiated the inhibitory effect of the D_4 receptor agonist RO-10-5824 on K^+-induced glutamate release (significant decrease in IC_{50} value) (Figure 7c), but not the other way around (Figure 7d). These results therefore show the same kind of D_2–D_4 receptor interaction demonstrated by

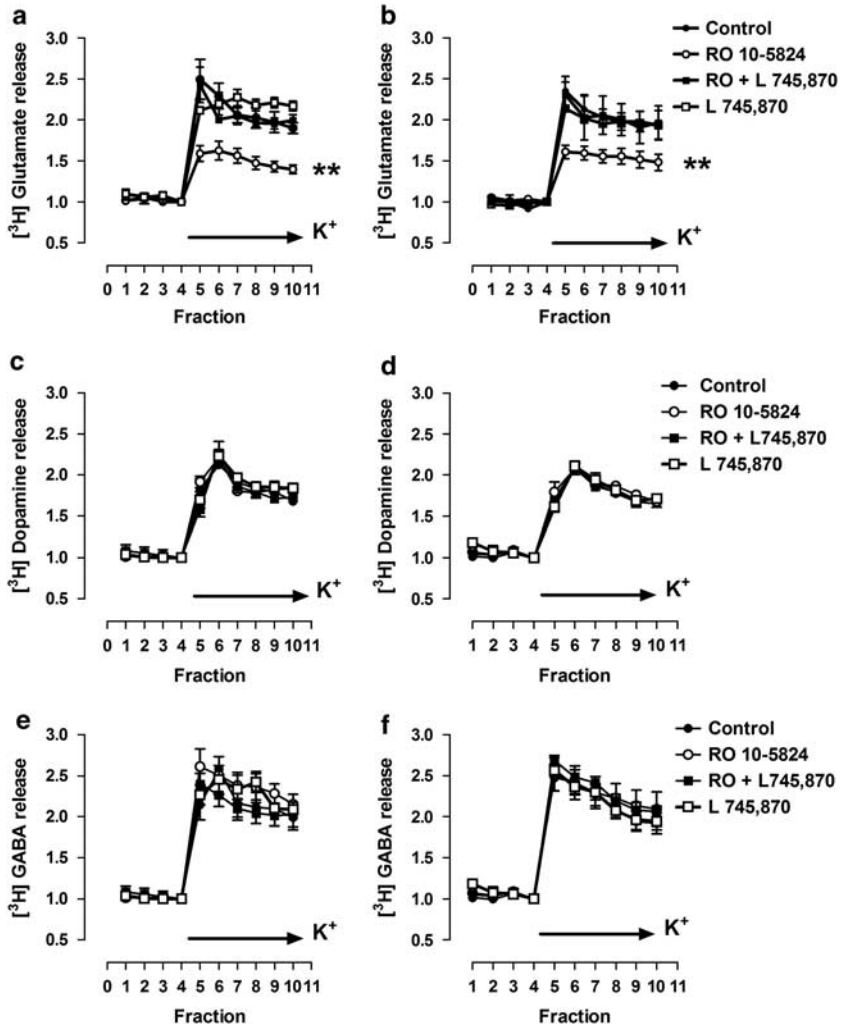

Figure 6 D_4 receptor-mediated modulation of [^{3}H]glutamate, but not [^{3}H]dopamine or [^{3}H]GABA release from slices of dorsal and ventral striatum. Slices from the dorsal striatum (caudate-putamen; **a**, **c**, **e**) or the ventral striatum (nucleus accumbens; **b**, **d**, **f**) of reserpine-treated rats were treated with the D_4 receptor agonist RO-10-5824 (100 nM) or with the D_4 receptor antagonist L-745 870 (10 nM) alone or in combination and the time course of K^+-stimulated [^{3}H]glutamate (**a**, **b**), [^{3}H]dopamine (**c**, **d**) or [^{3}H]GABA (**e**, **f**) release was determined. The RO-10-5824-induced effect (open circles) was prevented by the antagonist L-745 870 (dark squares), which itself had no effect (open squares). Values are mean ± s.e.m. of samples from three different animals performed in four replicates. Drug effect was assessed by comparing the relative area under the curve for each condition. $^{**}P<0.01$ with respect to the control (analysis of variance (ANOVA) followed by Tukey–Kramer multiple comparison *post hoc* test).

D_{2S}–D_4 receptor heteromers in transfected cells with MAPK signaling. Our combined *in vitro* and *in vivo* data strongly suggest that D_{2S}–D_4 receptor heteromers are likely to have a key role in dopamine-mediated modulation of striatal glutamate release.

Discussion

The present study shows that dopamine D_{2S} and $D_{4.2}$ or $D_{4.4}$ receptors, but not the ADHD-associated human $D_{4.7}$ variant, form functional heteromers in transfected cells and in the rodent brain. Co-stimulation of D_{2S} and D_4 receptors in the D_{2S}–D_4 receptor heteromer has a synergistic effect on MAPK signaling, which could be demonstrated in transfected cells and in the mouse striatum, but not in cells expressing $D_{4.7}$ or in the striatum of a mutant mouse carrying the 7 repeats of the human $D_{4.7}$ in the 3IL of the D_4 receptor. These results provide a significant functional difference of one of the human receptor variants, $D_{4.7}$, compared with the $D_{4.2}$ and $D_{4.4}$ variants, which can have important implications for the understanding of the pathogenesis of ADHD. Importantly, we also demonstrated, for the first time, that D_{2S}–D_4 receptor interactions modulate striatal glutamate release, suggesting that the D_{2S}–D_4 receptor heteromer allows dopamine to fine-tune glutamate neurotransmission.

The molecular mechanism involved in preventing heteromer formation between D_{2S} and $D_{4.7}$ receptors is not yet known. Indeed, the control of heteromer

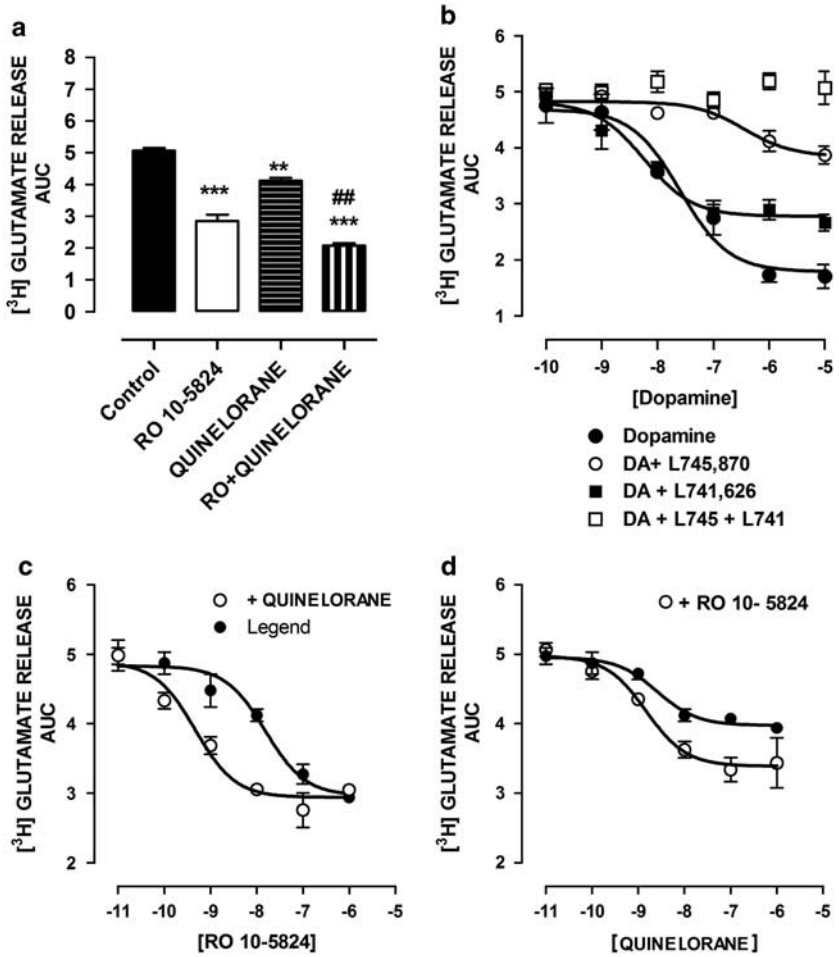

Figure 7 D_2 and D_4 receptor interactions in the modulation of striatal [^{3}H]glutamate release. Striatal slices (dorsal striatum) from reserpine-treated rats were incubated with SCH-23390 (100 nM) to block D_1 receptor activation. In (**a**), slices were treated for 32 min (fraction 2 to fraction 10) with medium (control), with the D_4 receptor agonist RO-10-5824 (100 nM), with the $D_{2/3}$ receptor agonist quinelorane (100 nM) or with both and K^+-stimulated [^{3}H]glutamate release was determined. Values are mean ± s.e.m. of samples from three different animals performed in four replicates. Drug effects were assessed by comparing the relative area under the curve for each condition. $^{**}P<0.01$ and $^{***}P<0.001$ with respect to the control and $^{\#\#}P<0.01$ with respect to slices treated with RO-10-5824 or quinelorane alone (analysis of variance (ANOVA) followed by Tukey–Kramer multiple comparison *post hoc* test). In (**b**), slices were treated for 32 min with increasing dopamine concentrations in the absence (dark circles) or in the presence of the D_4 receptor antagonist L-45 870 (10 nM, dark squares), the D_2 receptor antagonist L-741 626 (10 nM, open circles) or both (open squares) and K^+-stimulated [^{3}H]glutamate release was determined. Values are mean ± s.e.m. of samples from three different animals performed in four replicates. Drug effects were assessed by comparing the relative area under the curve for each condition. The IC_{50} values were: 25.25 nM (C.I.: 9.63–66.20 nM) for dopamine alone, 5.75 nM (2.12–15 nM) for dopamine in the presence of L-741 626 and 357.27 nM (C.I.: 73.40–1739 nM) for dopamine in the presence of L-745 870. In (**c**), slices were treated for 32 min with increasing concentrations of RO-10-5824 in the absence (black circles) or in the presence (open circles) of quinelorane (10 nM) and K^+-stimulated [^{3}H]glutamate release was determined. In (**d**), slices were treated for 32 min with increasing concentrations of quinelorane in the absence (black circles) or in the presence (open circles) of RO-10-5824 (10 nM) and K^+-stimulated [^{3}H]glutamate release was determined. In (**c**, **d**), values are mean ± s.e.m. of samples from three different animals performed in four replicates. The IC_{50} values were (**c**) 15 nM (35.15–6.55 nM) for RO-10-5824 alone and 0.05 nM (1.21–0.02 nM) for RO-10-5824 in the presence of quinelorane (Student's *t*-test: $P<0.01$) and (**d**) 2.55 nM (7.31–0.89 nM) for quinelorane alone and 1.48 nM (4.5–0.45 nM) for quinelorane in the presence of RO-10-5824 (Student's *t*-test; N.S.).

formation between G-protein-coupled receptors is still a large question in the field. Since the $D_{4.7}$ receptor variant has the longest 3IL and is the only polymorphic form not forming heteromers with the D_{2S} receptor, steric hindrance of the 3IL of $D_{4.7}$ receptor is a probable mechanism responsible for this lack of heteromerization, but other mechanisms cannot be ruled out. Using two-hybrid methodologies as well as proteomic studies, interactions between dopamine receptors and a cohort of DRIPs (dopamine receptor interacting proteins) have been demonstrated, forming signaling complexes or signalplexes.[25,26] Some of these DRIPs show selectivity for some dopamine receptor subtypes. For example, filamin or protein 4.1 N

interact with D_2 and D_3 receptors but not with D_1, D_5 or D_4 receptors,[27,28] the PDZ domain-containing protein, GIPC (GAIP interacting protein, C terminus) interacts with D_2 and D_3 receptor but not with the D_4 receptor subtype[29] and paralemmin interacts exclusively with D_3, but not with D_2 or D_4 receptors.[30] All of these interactions modulate receptor targeting, trafficking and signaling. Proline-rich sequences of the D_4 receptor, mainly located in the polymorphic region of the 3IL, constitute putative SH3 binding domains, which can potentially interact with adapter proteins like Grb2 and Nck, which do not have any known catalytic activity but are capable of recruiting multiprotein complexes to the receptor.[24] It can be hypothetized that differences in DRIPs recruitment by $D_{4.7}$ and the other D_4 polymorphic forms can influence the $D_{4.7}$ ability to form heteromers, but future studies will be required.

Previous experiments indicated that locally in the striatum, dopamine inhibits glutamate release by activating D_2 receptors (predominantly D_{2S}) localized in glutamatergic terminals.[13,15] Other studies also indicate that striatal postsynaptic D_2 receptors (predominantly D_{2L}) indirectly modulate glutamate release by retrograde endocannabinoids signaling.[31] The present results indicate that D_4 receptors also have a key role in the modulation of striatal glutamate release, likely through its ability to form heteromers with presynaptic D_{2S} receptors. In the striatal D_{2S}–D_4 receptor heteromer, low concentrations of dopamine should bind to the D_4 receptor, which has more affinity for dopamine than the D_{2S} receptor,[24] causing a certain degree of inhibition of glutamate release. However, at higher concentrations, dopamine should also bind to the D_{2S} receptor and under these conditions, the synergistic interaction in the D_{2S}–D_4 receptor heteromer will produce an even stronger inhibition of glutamate release. Therefore, the D_{2S}–D_4 receptor heteromer seems to act as a concentration-dependent device that establishes two different degrees of presynaptic dopaminergic control over striatal glutamatergic neurotransmission. Since the strong modulation observed with higher concentrations of dopamine depends on D_{2S}–D_4 receptor heteromerization, the existence of a $D_{4.7}$ variant implies a weaker control of glutamatergic neurotransmission, which could be a main mechanism involved in the pathogenesis of ADHD. This could also explain at least part of the so far not understood successful effect of psychostimulants in ADHD, which amplify dopaminergic signaling and these medications appear to be more effective in ADHD patients with the $D_{4.4}$ than with the $D_{4.7}$ variants.[32,33] We have to take into account that the existence of a $D_{4.7}$ variant does not imply ADHD is the result of this variant, but rather that it is one factor that contributes to its development. In fact, the $D_{4.7}$ variant might constitute a successful evolutionary trait under the appropriate environmental exposure.[7,34] The present study provides a new element of interest in the field of receptor heteromes, which now become new targets to be studied when dealing with functional differences associated with polymorphisms of G-protein-coupled receptor genes.

Conflict of interest

The authors declare no conflict of interest.

Acknowledgments

We thank the technical help from Jasmina Jiménez (University of Barcelona). The study was supported by the NIDA IRP funds and from Grants from Spanish Ministerio de Ciencia y Tecnología (SAF2008-03229-E, SAF2009-07276, SAF2010-18472, SAF2008-01462 and Consolider-Ingenio CSD2008-00005) and from Consejo Nacional de Ciencia y Tecnología de México (50428-M). PJM is a Ramón y Cajal Fellow.

References

1 Lauzon NM, Laviolette SR. Dopamine D4-receptor modulation of cortical neuronal network activity and emotional processing: implications for neuropsychiatric disorders. *Behav Brain Res* 2010; **208**: 12–22.
2 Tarazi FI, Campbell A, Yeghiayan SK, Baldessarini RJ. Localization of dopamine receptor subtypes in corpus striatum and nucleus accumbens septi of rat brain: comparison of D1-, D2-, and D4-like receptors. *Neuroscience* 1998; **83**: 169–176.
3 Svingos AL, Periasamy S, Pickel VM. Presynaptic dopamine D(4) receptor localization in the rat nucleus accumbens shell. *Synapse* 2000; **36**: 222–232.
4 LaHoste GJ, Swanson JM, Wigal SB, Glabe C, Wigal T, King N *et al.* Dopamine D4 receptor gene polymorphism is associated with attention deficit hyperactivity disorder. *Mol Psychiatry* 1996; **1**: 121–124.
5 Swanson JM, Kinsbourne M, Nigg J, Lanphear B, Stefanos GA, Volkow N *et al.* Etiologic subtypes of attention-deficit/hyperactivity disorder: brain imaging, molecular genetics and environmental factors and the dopamine hypothesis. *Neuropsychol Rev* 2007; **17**: 39–59.
6 Casey BJ, Nigg JT, Durston S. New potential leads in the biology and treatment of attention deficit-hyperactivity disorder. *Curr Opin Neurol* 2007; **20**: 119–124.
7 Wang E, Ding YC, Flodman P, Kidd JR, Kidd KK, Grady DL *et al.* The genetic architecture of selection at the human dopamine receptor D4 (DRD4) gene locus. *Am J Hum Genet* 2004; **74**: 931–944.
8 Chang FM, Kidd JR, Livak KJ, Pakstis AJ, Kidd KK. The worldwide distribution of allele frequencies at the human dopamine D4 receptor locus. *Hum Genet* 1996; **98**: 91–101.
9 Asghari V, Sanyal S, Buchwaldt S, Paterson A, Jovanovic V, Van Tol HH. Modulation of intracellular cyclic AMP levels by different human dopamine D4 receptor variants. *J Neurochem* 1995; **65**: 1157–1165.
10 Ferré S, Baler R, Bouvier M, Caron MG, Devi LA, Durroux T *et al.* Building a new conceptual framework for receptor heteromers. *Nat Chem Biol* 2009; **5**: 131–134.
11 Marcellino D, Ferré S, Casadó V, Cortés A, Le Foll B, Mazzola C *et al.* Identification of dopamine D1-D3 receptor heteromers. Indications for a role of synergistic D1-D3 receptor interactions in the striatum. *J Biol Chem* 2008; **283**: 26016–26025.
12 Borroto-Escuela DO, Van Craenenbroeck K, Romero-Fernandez W, Guidolin D, Woods AS, Rivera A *et al.* Dopamine D2 and D4 receptor heteromerization and its allosteric receptor-receptor interactions. *Biochem Biophys Res Commun* 2011; **404**: 928–934.
13 De Mei C, Ramos M, Iitaka C, Borrelli E. Getting specialized: presynaptic and postsynaptic dopamine D2 receptors. *Curr Opin Pharmacol* 2009; **9**: 53–58.

14 Carriba P, Navarro G, Ciruela F, Ferré S, Casadó V, Agnati L *et al.* Detection of heteromerization of more than two proteins by sequential BRET-FRET. *Nat Methods* 2008; **5**: 727–733.
15 Pontieri FE, Tanda G, Di Chiara G. Intravenous cocaine, morphine, and amphetamine preferentially increase extracellular dopamine in the 'shell' as compared with the 'core' of the rat nucleus accumbens. *Proc Natl Acad Sci USA* 1995; **92**: 12304–12308.
16 Quarta D, Ferré S, Solinas M, You ZB, Hockemeyer J, Popoli P *et al.* Opposite modulatory roles for adenosine A1 and A2A receptors on glutamate and dopamine release in the shell of the nucleus accumbens. Effects of chronic caffeine exposure. *J Neurochem* 2004; **88**: 1151–1158.
17 Garcia M, Floran B, Arias-Montaño JA, Young JM, Aceves J. Histamine H3 receptor activation selectively inhibits dopamine D1 receptor-dependent [3H]GABA release from depolarization-stimulated slices of rat substantia nigra pars reticulata. *Neuroscience* 1997; **80**: 241–249.
18 Cortés H, Paz F, Erlij D, Aceves J, Florán B. GABA(B) receptors modulate depolarization-stimulated [ǂH]glutamate release in slices of the pars reticulata of the rat substantia nigra. *Eur J Pharmacol* 2010; **649**: 161–167.
19 Powell SB, Paulus MP, Hartman DS, Godel T, Geyer MA. RO-10-5824 is a selective dopamine D4 receptor agonist that increases novel object exploration in C57 mice. *Neuropharmacology* 2003; **44**: 473–481.
20 Gackenheimer SL, Schaus JM, Gehlert DR. [3H]-quinelorane binds to D2 and D3 dopamine receptors in the rat brain. *J Pharmacol Exp Ther* 1995; **274**: 1558–1565.
21 Thomas TC, Kruzich PJ, Joyce BM, Gash CR, Suchland K, Surgener SP *et al.* Dopamine D4 receptor knockout mice exhibit neurochemical changes consistent with decreased dopamine release. *J Neurosci Meth* 2007; **166**: 306–314.
22 Thomas TC, Grandy DK, Gerhardt GA, Glaser PE. Decreased dopamine D4 receptor expression increases extracellular glutamate and alters its regulation in mouse striatum. *Neuropsychopharmacology* 2008; **34**: 436–445.
23 Bamford NS, Zhang H, Schmitz Y, Wu NP, Cepeda C, Levine SM *et al.* Heterosynaptic dopamine neurotransmission selects sets of corticostriatal terminals. *Neuron* 2004; **42**: 653–663.
24 Rondou P, Haegeman G, Van Craenenbroeck K. The dopamine D4 receptor: biochemical and signalling properties. *Cell Mol Life Sci* 2010; **67**: 1971–1986.
25 Kabbani N, Levenson R. A proteomic approach to receptor signaling: molecular mechanisms and therapeutic implications derived from discovery of the dopamine D2 receptor signalplex. *Eur J Pharmacol* 2007; **572**: 83–93.
26 Yao WD, Spealman RD, Zhang J. Dopaminergic signaling in dendritic spines. *Biochem Pharmacol* 2008; **75**: 2055–2069.
27 Lin R, Karpa K, Kabbani N, Goldman-Rakic P, Levenson R. Dopamine D2 and D3 receptors are linked to the actin cytoskeleton via interaction with filamin A. *Proc Natl Acad Sci USA* 2001; **98**: 5258–5263.
28 Binda AV, Kabbani N, Lin R, Levenson R. D2 and D3 dopamine receptor cell surface localization mediated by interaction with protein 4.1N. *Mol Pharmacol* 2002; **62**: 507–513.
29 Jeanneteau F, Diaz J, Sokoloff P, Griffon N. Interactions of GIPC with dopamine D2, D3 but not D4 receptors define a novel mode of regulation of G protein-coupled receptors. *Mol Biol Cell* 2004; **15**: 696–705.
30 Basile M, Lin R, Kabbani N, Karpa K, Kilimann M, Simpson I *et al.* Paralemmin interacts with D3 dopamine receptors: implications for membrane localization and cAMP signaling. *Arch Biochem Biophys* 2006; **446**: 60–68.
31 Yin HH, Lovinger DM. Frequency-specific and D2 receptor-mediated inhibition of glutamate release by retrograde endocannabinoid signaling. *Proc Natl Acad Sci USA* 2006; **103**: 8251–8256.
32 Cheon KA, Kim BN, Cho SC. Association of 4-repeat allele of the dopamine D4 receptor gene exon III polymorphism and response to methylphenidate treatment in Korean ADHD children. *Neuropsychopharmacology* 2007; **32**: 1377–1383.
33 Hamarman S, Fossella J, Ulger C, Brimacombe M, Dermody J. Dopamine receptor 4 (DRD4) 7-repeat allele predicts methylphenidate dose response in children with attention-deficit/hyperactivity disorder: a pharmacogenetic study. *J Child Adolesc Psychopharmacol* 2004; **14**: 564–574.
34 Ding YC, Chi HC, Grady DL, Morishima A, Kidd JR, Kidd KK *et al.* Evidence of positive selection acting at the human dopamine receptor D4 gene locus. *Proc Natl Acad Sci USA* 2002; **99**: 309–314.

Supplementary Information accompanies the paper on the Molecular Psychiatry website (http://www.nature.com/mp)

FIGURES AND SUPPLEMENTARY FIGURE LEGENDS

Supp Figure 1

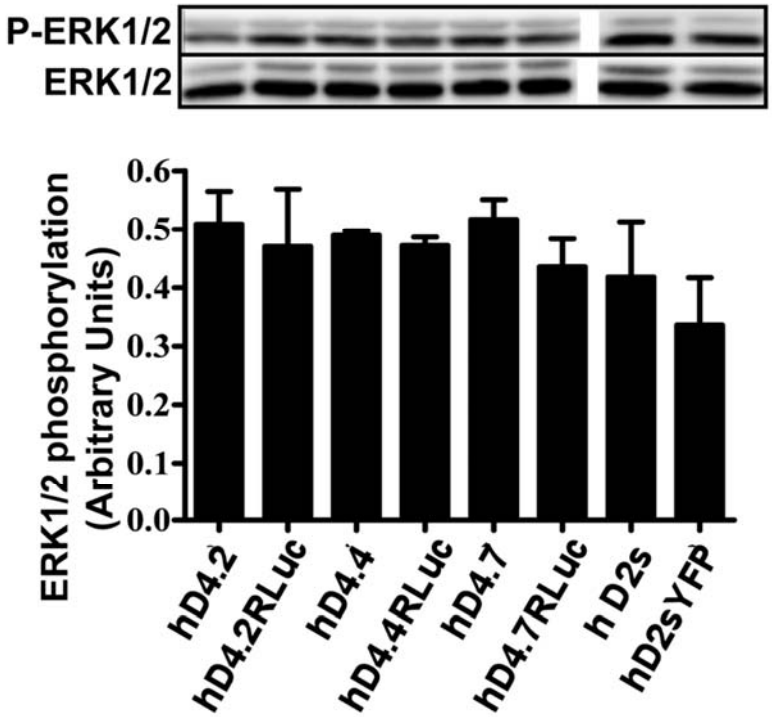

Suppl. Fig. 1. Functionality of the human fusion proteins. Cells were transfected with 2.5 µg of cDNA corresponding to the human $D_{4.2}$, $D_{4.4}$, $D_{4.7}$ or D_{2S} dopamine receptors or to the corresponding fusion proteins $D_{4.2}$-RLuc, $D_{4.4}$-RLuc, $D_{4.7}$-RLuc or D_{2S}-YFP. 48 h post-transfection, cells expressing D_4 or D_4-RLuc receptors were treated for 10 minutes with RO 10-5824 (100 nM) and cells expressing D_{2S} or D_{2S}-YFP receptors were treated for 10 min with quinelorane (300 nM) and ERK1/2 phosphorylation was determined. The immunoreactive bands of three to four experiments were quantified and expressed as arbitrary units. A representative Western blot is shown at the top.

Supp Figure 2

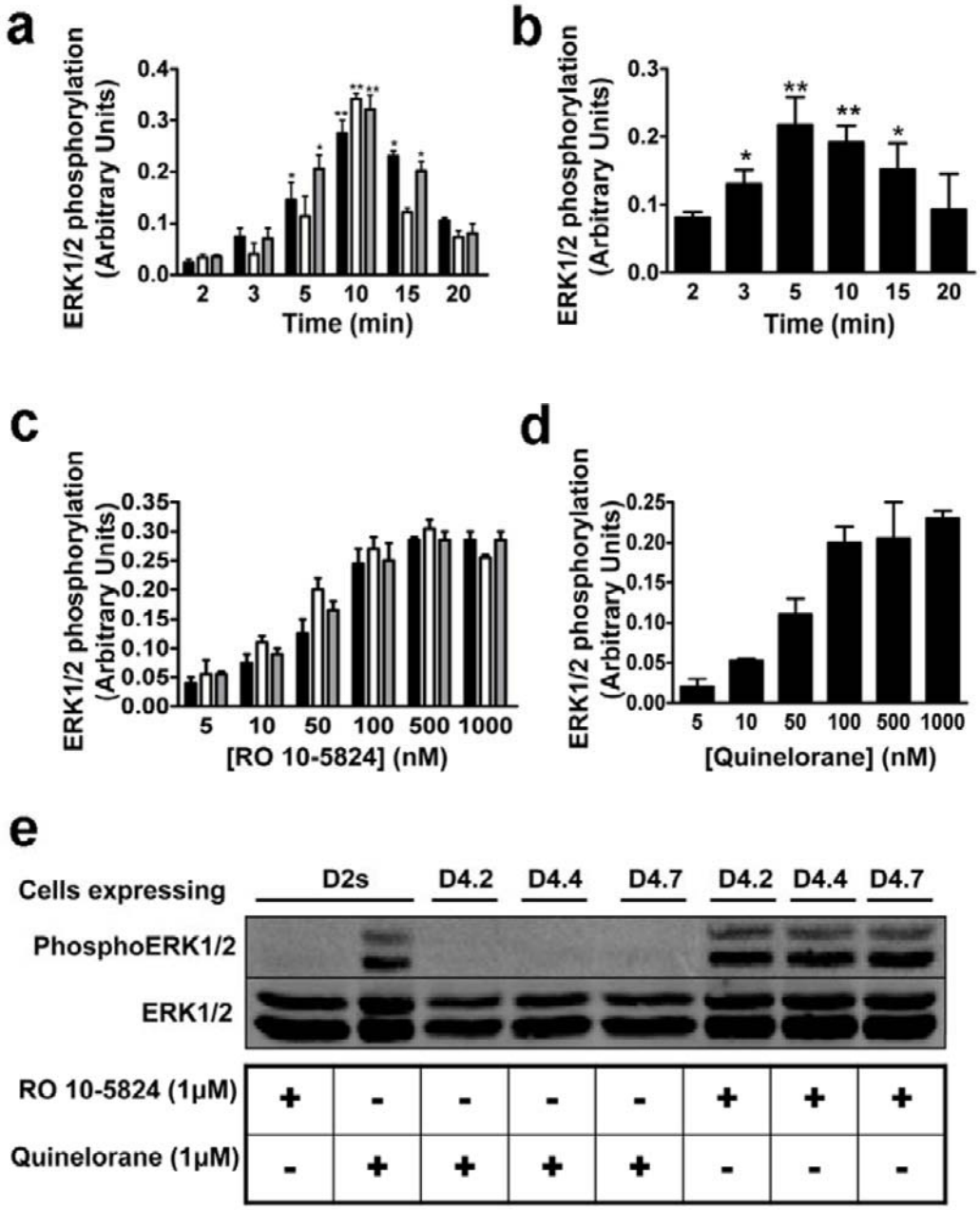

Suppl. Fig. 2. Agonist selectivity and time-response of ERK1/2 phosphorylation in cells transfected with D_4 or D_2 receptors. In **(a)** and **(c)** cells were transfected with 2.5 μg of cDNA corresponding to the human $D_{4.2}$ (black), $D_{4.4}$ (white) or $D_{4.7}$ (gray) dopamine receptors. 48 h post-transfection, cells were treated for increasing time **(a)** or for 10 min **(c)** with 500 nM **(a)** or increasing concentrations **(c)** of RO 10-5824. In **(b)** and **(d)** cells were transfected with 2 μg of cDNA corresponding to the human D_{2S} receptor and 48 h post-transfection, cells were treated for increasing time **(b)** or for 10 min **(d)** with 300 nM **(a)** or increasing concentrations **(d)** of quinelorane. In all cases the immunoreactive bands of three to four experiments were quantified and expressed as arbitrary units. Statistical differences with respect to non-treated cells were determined by Student's *t* test (*$p<0.05$ and **$p<0.01$). In **(e)** the selectivity of RO-10-5824 and quinelorane was proved by the lack of ERK1/2 phophorylation observed in cells not expressing D_4 receptors or D_{2S} receptors, respectively, when stimulated by high concentrations (1 μM) of these agonists.

Supp Figure 3

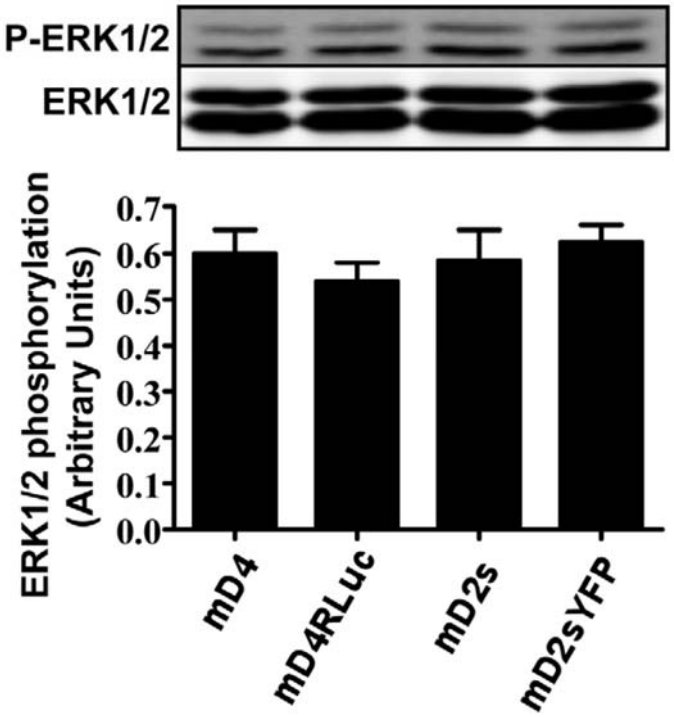

Suppl. Fig. 3. Functionality of the mouse fusion proteins. Cells were transfected with 2.5 µg of cDNA corresponding to mouse D_4 or D_{2S} dopamine receptors or to the corresponding fusion proteins D_4-RLuc or D_{2S}-YFP. 48 h post-transfection, cell expressing D_4 or D_4-RLuc receptors were treated for 10 minutes with RO 10-5824 (100 nM) and cells expressing D_{2S} or D_{2S}-YFP receptors were treated for 10 min with quinelorane (300 nM) and ERK1/2 phosphorylation was determined. The immunoreactive bands of three to four experiments were quantified and expressed as arbitrary units. A representative Western blot is shown at the top.

Supp Figure 4

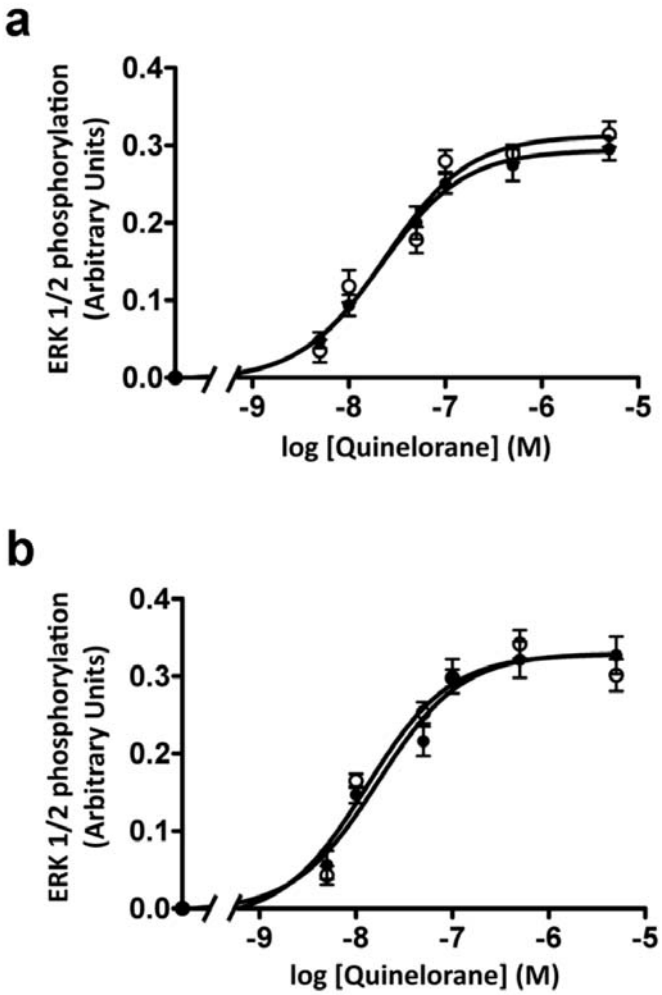

Suppl. Fig. 4. Crosstalk between mouse D_2 receptors and mouse or human D_4 receptors. Cells transiently co-expressing mouse D_{2S} receptors and mouse D_4 receptors **(a)** or human $D_{4.7}$ receptors **(b)** were treated for 10 minutes with increasing quinolerane concentrations in the presence (○) or in the absence (●) of RO 10-5824 (50 nM) prior to the ERK1/2 phosphorylation determination. The immunoreactive bands of three experiments (mean ± SEM; n = 3) were quantified and expressed as arbitrary units. EC50 values with or without RO 10-5824 were: (**a**) 23.8 ± 0.1 and 21.4 ± 0.1 nM (Student's t test: N.S.) or **(b)** 15.2 ± 0.1 and 18.2 ± 0.1 nM (Student's t test: NS).

3.7 La heteromerización de receptores adrenérgicos y receptores D_4 de dopamina asociada a los ritmos circadianos modula la síntesis y liberación de melatonina en la glándual pineal

Sergio González[1], David Moreno-Delgado[1], Estefanía Moreno[1], Kamil Pérez-Capote[1], Rafael Franco[1$], Josefa Mallol[1], Antoni Cortés[1], Vicent Casadó[1], Carme Lluís[1], Jordi Ortiz[2], Sergi Ferré[3], Enric Canela[1*], Peter J. McCormick[1*]

[*]Codirectores del manuscrito.

[1]Centro de Investigación Biomédica en Red sobre Enfermedades Neurodegenerativas (CIBERNED), y Departamento de Bioquímica y Biología Molecular, Facultad de Biología, Universidad de Barcelona, Barcelona, España,
[2]Instituto de Neurosciencias y Departamento de Bioquímica y Biología Molecular, Facultad de Medicina, Universitat Autónoma de Barcelona, 08193 Bellaterra, España,
[3]National Institute on Drug Abuse, Intramural Research Program, National Institutes of Health, Department of Health and Human Services, Baltimore, MD 21224,
[$]Present address: Centro de Investigación Médica Aplicada (CIMA), Universidad de Navarra, Pamplona, España.

Manuscrito enviado para su publicación a *Plos Biology*

El papel de la glándula pineal es traducir los ritmos cíclicos de día y noche codificados por la retina en señales hormonales transmitidas al resto de los sistemas neuronales en forma de síntesis y liberación de serotonina y melatonina. En este estudio describimos que la producción y secreción de serotonina y melatonina por la glándula pineal está regulada por la heteromerización de los receptores adrenégicos y receptores D_4 de dopamina asociada al ritmo circadiano. A través de la heteromerización de los receptores $alfa_{1B}$-D_4 y $beta_1$-D_4, la dopamina inhibe la señalización de los receptores adrenérgicos y bloquea la síntesis y liberación de melatonina inducida por los ligandos de los receptores adrenérgicos. Estos datos proporcionan una nueva perspectiva sobre la función de la dopamina y constituye el primer ejemplo de un heterómero de receptores controlado por el ritmo circadiano. Esta heteromerización no descrita con anterioridad entre receptores adrenérgicos y receptores D_4 de dopamina proporciona un mecanismo de retroalimentación en el sistema hormonal neuronal, siendo la dopamina un controlador de los ritmos circadianos.

Circadian-related heteromerization of adrenergic and dopamine D_4 receptors modulates melatonin synthesis and release in the pineal gland

Sergio González[1], David Moreno-Delgado[1], Estefanía Moreno[1], Kamil Pérez-Capote[1], Rafael Franco[1$], Josefa Mallol[1], Antoni Cortés[1], Vicent Casadó[1], Carme Lluís[1], Jordi Ortiz[2], Sergi Ferré[3], Enric Canela[1], Peter J. McCormick[1]**

[1]Centro de Investigación Biomédica en Red sobre Enfermedades Neurodegenerativas (CIBERNED), and Department of Biochemistry and Molecular Biology, Faculty of Biology, University of Barcelona, Avda. Diagonal 645, 08028 Barcelona, Spain. [2]Neuroscience Institute and Department of Biochemistry and Molecular Biology, Faculty of Medicine, Universitat Autònoma de Barcelona, 08193 Bellaterra, Spain; [3]National Institute on Drug Abuse, Intramural Research Program, National Institutes of Health, Department of Health and Human Services, Baltimore, MD 21224

Corresponding author: Peter J. McCormick, Department of Biochemistry and Molecular Biology, Faculty of Biology, University of Barcelona, Avda. Diagonal 645, 08028 Barcelona, Spain. Tel +(93)4021208; Fax +(93)4021559 pmccormick@ub.edu

Additional Footnotes:

- * Both authors contributed equally to the manuscript.
- [$] Present address: Centro de Investigación Médica Aplicada (CIMA), University of Navarra, Pamplona, Spain

Running Title: Pineal gland α_{1B}-D_4 and β_1-D_4 receptor heteromers

Introduction

Dopamine receptors are G protein-coupled receptors (GPCRs) and consist of two major families, the D_1-like and D_2-like receptors. D_1-like receptors include D_1 and D_5 subtypes that are known to stimulate adenylate cyclase activity via a Gs mechanism and D_2-like receptors include D_2, D_3 and D_4 subtypes that inhibit adenylate cyclase activity via a Gi mechanism [1]. Of these subtypes, D_1 and D_2 and their heteromers constitute the most abundant in the brain [2–4]. The function of the other dopamine receptor subtypes has been more difficult to determine. The dopamine D_4 receptor was discovered twenty years ago and initially drew a lot of attention in view of its significantly higher affinity for the atypical antipsychotic clozapine compared to the previously discovered D_2 and D_3 receptors [5,6]. It was also found that the human D_4 receptor gene contains a large number of polymorphisms in its coding sequence, one of which was related to attention deficit hyperactivity disorder [7]. In the retina, D_4 receptors modulate phototransduction through a mechanism that requires cAMP [8]. It has been described that *Drd4* is the dominant dopamine receptor gene expressed in the rat pineal gland and that it is expressed in pinealocytes and retina at levels which are greater than in other tissues [9]. Rat pineal *Drd4 mRNA* expression was found to be circadian in nature and under photoneural control [9,10]. In the pineal gland, the mRNA expression for D_4 receptors has been shown to be tightly regulated and stimulated by norepinephrine through a mechanism involving thyroid hormone [9]. Nevertheless, nothing was known about D_4 receptor protein expression or function in the pineal gland. In the current study, the primary issue under consideration is whether or not dopamine receptor D_4 is active within the pineal gland and what is the physiological role of agonist binding to D_4 receptors with respect to pineal gland function.

The role of the pineal gland is to translate the light inputs from the retina into chemical signals for the rest of the body. This is achieved via production and secretion of melatonin by the pineal gland. Melatonin production occurs on a night / day cycle and is heavily dependent on the concentration of serotonin (5-HT)[11–15]. The β_1 and α_{1B} adrenergic receptors are the main receptors that control melatonin production by different mechanisms. One of them is to control the availability of 5-HT, the melatonin precursor, by increasing both the activity of tryptophan hydroxylase (TPH) and the release of 5-HT. Another is via a strict regulation of the enzyme that converts 5-HT to melatonin, the aromatic amino-acid N-acetyl transferase (AANAT)[16–19]. Despite tight regulation by the adrenergic receptors it is unclear what limits the nighttime and daytime rates of melatonin and 5-HT production. We hypothesized that one important role of dopamine D_4 receptors in the pineal gland can be the modulation of β_1 and α_{1B} adrenergic receptor function. One possibility for such a modulation could be through a concept becoming widely accepted for GPCRs, and that is the modulation of function through receptor heteromer formation [20–24]. A receptor heteromer is a macromolecular complex composed of at least two functional receptor units with biochemical properties that are demonstrably different from those of its individual receptors [25]. Here, using a combination of different approaches including biophysical, molecular and cellular biology, and metabolic assays from cultured cells to whole, intact, pineal gland, we explored the possibility that D_4 might modify adrenergic receptor function through direct receptor-receptor interaction. We report the first heteromer between dopamine and adrenergic receptors, provide new data that adrenergic receptor control of 5-HT levels can be modulated via the D_4 receptor, and show that D_4-adrenergic regulation can alter melatonin production from the pineal gland.

Results

D_4 receptors are functional in the pineal gland.

The expression of D_4 receptor mRNA in the pineal gland during the last part of the dark period has been described but the functional role of the protein is unknown [9,26]. Thus we first assessed if the receptor was active in the pineal gland. Pineal gland dissected from rats 1 h from the start of the light period were stimulated with increasing concentrations of dopamine or with the D_4 receptor agonist RO 10-5824 and the levels of p-ERK 1/2 and p-Akt/PKB were

determined. As shown in Figure 1A and B, dopamine increased both p-ERK 1/2 and p-Akt/PKB in a similar extent to RO 10-5824. Moreover, primary cultures of pinealocytes stimulated with RO 10-5824, the adrenergic α_1 receptor agonist phenylephrine or the adrenergic β receptor agonist isoproterenol showed signaling via p-ERK 1/2 (Fig. 1C). The subcellular distribution of the pinealocyte marker S-arrestin in the absence of ligands was diffuse, suggesting cytosolic, and in the presence of ligands was found in punctate structures, indicating recruitment to membrane structures. In addition, these punctate structures colocalized with the p-ERK 1/2, confirming receptor activation as endosomes containing receptor-arrestin complexes are known to serve as a signaling platform for p-ERK 1/2 [27] (Fig. 1C). Thus, in both intact pineal gland and isolated pinealocytes D_4 receptors are functional.

D_4 receptors form heteromers with α_{1B} and β_1 receptors in transfected cells.

The adrenergic receptors α_{1B} and β_1 are essential drivers of pineal gland function [28]. In addition, previous work has shown that dopamine receptors are able to influence other non-adrenergic receptor function by forming heteromers [29,30]. With this in mind we decided to test whether D_4 receptors might form heteromers with the adrenergic receptors α_{1B} and β_1. We first examined this possibility using transfected cells. The best assay for detecting an interaction between two membrane receptors in transfected cell is through biophysical means using Bioluminescence Resonance Energy Transfer (BRET) assays. BRET experiments were performed by fusing one of the receptors to the bioluminescent protein *Renilla Luciferase* (RLuc) and the other to a yellow fluorescent protein (YFP) (Experimental Procedures). Prior to BRET experiments we first confirmed that the fusion proteins were able to activate p-ERK 1/2 in the same manner as the native protein (Figure 2A) and that all receptors were properly trafficked to the cell membrane as observed by confocal microscopy (Fig. 2B and C). Clear BRET saturation curves were obtained in cells expressing D_4-RLuc receptors and increasing amounts of α_{1B} -YFP or β_1-YFP receptors (Fig. 2D) with $BRET_{max}$ values of 74 ± 4 mBU and 120 ± 10 mBU respectively and $BRET_{50}$ values of 37 ± 2 and 61 ± 4, indicating that the two receptors are indeed forming a higher order structure that allows energy transfer. In contrast, a low and linear BRET was detected in cells expressing α_{1B}-RLuc and increasing amounts of β_1-YFP (Fig. 2D gray line) which was qualitatively similar to the results obtained with the negative control, cells expressing D_4-RLuc receptors and increasing amounts of D_1-YFP (Fig. 2D green line). Taken together, these results strongly suggest that the D_4 receptor forms heteromers with both, α_{1B} and β_1 receptors, but heteromers are not formed between α_{1B} and β_1 receptors.

Although these results show that α_{1B} and β_1 do not form heteromers in cells not expressing D_4 receptors, they do not count out the possibility that there are heterotrimers between D_4, α_{1B} and β_1 in cells expressing the three receptors, as has been previously reported for other GPCRs [31]. If α_{1B}-β_1-D_4 heterotrimers are formed, the molecular determinants on the D_4 receptor to interact with α_{1B} receptor must be different than those required to interact with β_1 receptors. On the contrary, if α_{1B} and β_1 receptors interact with the same molecular determinants on the D_4 receptor, α_{1B}-β_1-D_4 receptor heterotrimers can not be formed. We discarded α_{1B}-β_1-D_4 receptor heterotrimers formation by showing that α_{1B} and β_1 share the same binding surface on D_4 receptor. In fact, when we titrated β_1 receptors in cells expressing a constant amount of D_4-RLuc and α_{1B}-YFP (Fig. 2E) or when we titrated α_{1B} receptors in cells expressing a constant amount of D_4-RLuc and β_1-YFP (Fig. 3F), we found in either case that α_{1B} and β_1 receptors were both able to alter heteromer formation, as measured by a decrease in BRET, between D_4-RLuc and β_1-YFP or α_{1B}-YFP showing that α_{1B} and β_1 receptors interact with the same or at least heavily overlapping molecular determinants on the D_4 receptor.

Functional consequences of α_{1B}-D_4 and β_1-D_4 receptor heteromer formation in transfected cells.

A common and often essential attribute of receptor heteromers is the ability to modify the downstream signaling versus the single constituent receptors. This type of receptor-receptor interaction has been observed for several receptor heteromers [29,32–34]. To understand the function of α_{1B}-D_4 and β_1-D_4 receptor heteromers, we investigated whether there were changes in MAPK (ERK 1/2 phosphorylation) and Akt/PKB (Ser-473 Akt phosphorylation) signaling when heteromers were co-stimulated with both agonists or blocked with antagonists. First, the selectivity of receptor agonists, RO 10-5824, phenylephrine and isoproterenol was tested in cells only expressing D_4, α_{1B} or β_1 receptors (Fig. 3A). In addition we confirmed that RO 10-5824 did not modify ERK 1/2 or Akt/PKB phosphorylation induced by phenylephrine or isoproterenol in cells transfected with α_{1B} or β_1 receptors alone (Fig. 3B). Using selective agonist in time-response assays we found an increase in ERK 1/2 and Akt/PKB phosphorylation in cells only expressing D_4, α_{1B} or β_1 receptors (Fig. S1). We next explored whether any cross-talk between the receptors could be detected in cells co-expressing the receptors. In α_{1B}-D_4 and β_1-D_4 receptor co-expressing cells, stimulation of D_4 receptors for 7 min with the D_4 specific ligand RO 10-5824 inhibited α_{1B} and β_1 receptor-mediated ERK 1/2 and Akt/PKB activation induced by increasing amounts of phenylephrine and isoproterenol (Fig 3 C to F). We saw an almost complete block in the amount of p-ERK 1/2 induced by adrenergic agonists in the presence of RO 10-5824 (Fig. 3C and E) indicating that D_4 activation inhibited the α_{1B} and β_1 receptor-mediated ERK 1/2 phosphorylation. In addition, a complete block of p-Akt production was observed in the presence of both adrenergic receptor agonist and D_4 receptor agonist (Fig. 3D and F), demonstrating that D_4 activation inhibited the α_{1B} and β_1 receptor-mediated Akt/PKB phosphorylation and vice-versa. These results are not due to a change in the time in which the signaling peaks since differences were not observed in time-response curves when co-transfected cells were activated with one or both agonists (Fig. S2).

Although these data, coupled with the energy transfer experiments above, are suggestive of heteromer function they could be explained via simple downstream signaling cross-talk rather than via physical interaction between receptors. One way to test whether cross-talk occurs via receptor-receptor interaction is to look for cross-antagonism. Antagonists, by definition do not signal; thus, cross-antagonism, any change in α_{1B} or β_1 mediated signaling caused by an antagonist of D_4 receptors, could only be due to protein-protein contact between the receptors. Prior to looking for cross-antagonism we investigated the selectivity of D_4, α_{1B} and β_1 receptor antagonists by measuring MAPK and Akt/PKB signaling in cells transfected with only D_4, α_{1B} or β_1 receptors and stimulated or not with agonist and treated with the selective D_4, α_{1B} and β_1 receptor antagonists L-745,870, REC 15/2615 and CGP 20712, respectively. All antagonists behaved as classical antagonists, as none demonstrated any signaling properties on transfected cells (Fig. S3). Importantly, all antagonists were selective as expected and were able to attenuate agonist-induced signaling in only their respective receptors (Fig. S3). Next, cells co-expressing α_{1B}-D_4 and β_1-D_4 receptors were treated with antagonists prior to activation with agonist. We obtained a striking cross-antagonism in MAPK and Akt/PKB activation (Fig. 4). In both cases, the D_4 receptor antagonist, L-745,870 was able to completely block the signaling caused by isoproterenol or phenylephrine. Moreover, the signaling induced by the D_4 receptor agonist was blocked by the adrenergic receptor antagonist REC 15/2615 and CGP 20712. These results demonstrate that the dopamine receptor D_4 is able to modify α_{1B} and β_1 function via receptor heteromers and vice-versa. In addition, this cross-antagonism constitutes a specific biochemical property of the α_{1B}-D_4 and β_1-D_4 receptor heteromers and can be used as a biochemical fingerprint to detect the heteromers in native tissues.

Functional α_{1B}-D_4 and β_1-D_4 receptor heteromers in the pineal gland.

We next sought to detect α_{1B}-D_4 and β_1-D_4 receptor heteromers in the pineal gland. We looked for the heteromer biochemical property identified above, the cross-antagonism, as an initial demonstration of the existence of α_{1B}-D_4 and β_1-D_4 receptor heteromers in the pineal gland. Thus, whole pineal glands were isolated one hour after starting the light period and stimulated with the respective D_4, α_{1B} and β_1 agonists RO 10-5824, phenylephrine and isoproterenol and p-ERK 1/2 (Fig. 4E) and p-Akt (Fig. 4F) signaling were measured with respect to basal levels. As can be seen in Figure 4E and F, all three receptors showed robust signaling that could be attenuated with the respective antagonist (L-745,870, REC 15/2615, and CGP 20712). We also detected a cross-antagonism in MAPK and Akt/PKB activation. In both cases, the D_4 receptor antagonist, L-745,870, was able to completely block the signaling caused by isoproterenol or phenylephrine and the signaling induced by the D_4 receptor agonist was blocked by the adrenergic receptor antagonist REC 15/2615 and CGP 20712 (Fig 4E and F). These results matched the cross-antagonism observed in transfected cells strongly indicating that D_4 receptors form functional heteromers with α_{1B} and β_1 receptors in the pineal gland.

Direct detection of α_{1B}-D_4 and β_1-D_4 receptor heteromers in the pineal gland.

Biophysical techniques to directly detect heteromers cannot be easily applied in native tissue, but other direct methods can be used. One example is the application of the newly developed proximity ligation assay (PLA). This technique has been successfully employed to detect protein dimers in cells and in tissue [35]. Prior to performing PLA, we first confirmed the antibody specificity. The antibody against D_4, α_{1B} or β_1 receptor, only stained cells expressing the corresponding receptor but not non-transfected cells and cells expressing D_4 receptors were not stained by antibodies against adrenergic receptors and cells expressing α_{1B} or β_1 receptors are not stained with anti-D_4 receptors antibody (Fig. S4). The selectivity for anti-D_4 antibody was also demonstrated by taking advantage of the fact that rat pineal *Drd4 mRNA* expression was found to be circadian in nature being high at the last part of the dark period and very low during the light period [9,10]. Thus, without the need of genetically manipulated animals, we observed that the anti-D_4 antibody was able to stain pinealocytes from pineal glands extracted just after the darkness period (Fig. 5A) but not pinealocytes from glands extracted at the end of the light period (Fig. 5B). After testing the expression of the individual receptors using immunofluorescence in pinealocytes (Fig. 5A to F), we next looked for evidence of expression of α_{1B}-D_4 and β_1-D_4 receptor heteromers in pineal gland using the proximity ligation assay. This direct method requires that both receptors be close enough to allow the two different antibody-probes to be able to ligate (<30nm). If the receptors are within proximity, a punctate fluorescent signal can be detected by confocal microscopy (see Experimental Procedures). We found that the endogenously expressed D_4 receptors indeed form heteromers with the endogenous expressed α_{1B} and β_1 receptors in a primary culture of pinealocytes obtained from a pineal gland dissected 1 h after the start of the light period (Fig 5G, punctate pattern of fluorescence) but we did not observe receptor interaction in the form of a fluorescent signal for negative controls performed in the absence of primary antibodies (Fig. S5) or for α_{1B} - β_1 receptors (Fig. 5G), results that were consistent with the BRET experiments in Fig. 2 and demonstrated α_{1B}-D_4 and β_1-D_4 receptor heteromers expression in pinealocytes. As we observed a severe depletion of D_4 receptor expression in pinealocytes from glands isolated at the end of the light period, we performed the PLA experiments also with glands isolated at the end of the light period. As expected no α_{1B}-D_4 and β_1-D_4 receptor heteromers were detected (Fig 5H). These results not only confirm the specificity of the results in fig. 5G, but also demonstrate the circadian nature of heteromer formation.

Functional consequences of α_{1B}-D_4 and β_1-D_4 receptor heteromer formation in the pineal gland.

To test the effect of receptor co-activation in α_{1B}-D_4 and β_1-D_4 receptor heteromers in the p-ERK 1/2 and p-Akt/PKB production, pineal glands, isolated at 9:00h, one hour after the start of the light period (at sunrise), were stimulated with RO 10-5824, phenylephrine or isoproterenol alone or in combination. Co-activation with RO 10-5824 and phenylephrine or with RO 10-5824 and isoproterenol induced a significant decrease of p-ERK 1/2 production compared with the stimulation with one agonist alone (Fig 6A) and completely blocked the p-Akt/PKB production with respect to the that obtained with RO 10-5824, phenylephrine or isoproterenol (Fig. 6B). These results indicate that there is a negative cross-talk between D_4 and α_{1B} or β_1 not only in transfected cells but also in the pineal gland. To be sure that the data reflected a true negative cross-talk between D_4 and α_{1B} or β_1, and not a time displacement of the signaling, we performed time-response experiments with pineal glands (Fig. S6). The effect of co-activation with RO 10-5824 and phenylephrine or with RO 10-5824 and isoproterenol on α_{1B} and β_1 signaling was not due to a change in timing of the signal with maximal signal obtained at 10 min. In addition, at all times examined no p-Akt/PKB signal was detected in the presence of both adrenergic agonists and RO 10-5824. These data support that the result observed in Figure 6A and B were indeed due to a true negative cross-talk.

As the expression of D_4 receptor in the pineal gland is regulated by a cycle of light/dark, we reasoned if we isolated pineal gland after 12 hours of light (at sunset) when the levels of D_4 are low, then we should now lose the negative cross-talk seen in Fig. 6 A and B. To test this, we stimulated pineal gland extracted at 20:00 h and compared signaling after stimulation with RO 10-5824 in the presence or absence of phenylephrine and isoproterenol. As shown in Fig. 6C and D, there was no inhibition of α_{1B} and β_1 receptor-mediated MAPK and Akt/PKB activation by the D_4 receptor agonist RO 10-5824 in glands isolated at the end of the light period (sunset), a time of low D_4 receptors expression. This was in contrast to signaling in glands extracted at 9:00h, just after the dark period (sunrise) where D4 receptors are expressed and negative cross-talk in agonist-induced signaling was observed (Fig 6 A and B).

The metabolic consequences of α_{1B}-D_4 and β_1-D_4 receptor heteromers activation in the pineal gland.

Finally, we sought to understand how α_{1B}-D_4 and β_1-D_4 receptor heteromers might modulate pineal gland function. A major role of the pineal gland is controlling the levels of melatonin and its precursor 5-HT synthesized and released. The α_{1B} receptor controls 5-HT and melatonin release via potentiation the calcium-induced exocitosis, while the β_1 receptors modify the synthesis of 5-HT via tryptophan hydroxylase and serotonin N-acetyltransferase activation and the synthesis of melatonin mainly via aromatic amino-acid N-acetyl transferase (AANAT) activation [16–19]. Taking this in mind, we tested the role of the α_{1B}-D_4 and β_1-D_4 receptor heteromers in 5HT and melatonin synthesis and release. Ideally to test the physiological importance of heteromers one would like to create a targeted knockout animal lacking one of the partner receptors in the tissue of interest to be compared with wild type animals. However in the case of D_4 receptor expression in the pineal gland nature provided a suitable alternative. We decided to take advantage of fact that D_4 expression is altered by the cycle of light and dark and compare results obtained with pineal gland extracted at the end of the light period (sunset) when D_4 receptors are not expressed with those obtained with glands extracted at the end of the dark period (sunrise) when D_4 receptors are expressed.

We treated pineal glands, isolated at 20:00h, when α_{1B}-D_4 and β_1-D_4 receptor heteromers are not expressed, with specific agonists or/and antagonists and measured the amount of 5-HT synthesized (Fig. 7A and C) or released (Fig.7B and D) and the amount of melatonin synthesized (Fig. 7E and G) or released (Fig.7F and H). As can be seen in Fig. 7A to H, treatment with the D_4 specific agonist, RO 10-5824, showed no increase in either 5HT or

melatonin synthesis or release compared to basal levels. In contrast, we observed a large increase in melatonin synthesis and release when the glands were treated with the β_1 receptor agonist isoproterenol or the α_{1B} agonist phenylephrine respectively (Fig. 7E to H) and a significant increase in 5HT synthesis and release when the glands were treated with isoproterenol or phenylephrine (Fig 7A to D). The increases in 5-HT and melatonin synthesis and release could be only blocked by the corresponding specific antagonists of adrenergic receptors but not by the D_4 receptor antagonist L-745,870 (Fig. 7A, B, E and F) demonstrating a lack of cross-antagonism according to the lack of heteromers expression. In addition, when we treated the glands with either phenylephrine or isoproterenol in the presence of the dopamine D_4 receptor agonist RO 10-5824 (Fig. 7C, D, G and H) any negative cross-talk between dopamine D_4 and adrenergic receptors could be detected and the role of adrenergic receptors is represented in Fig. 7I. In contrast and very interesting, when pineal glands were isolated at 9:00h, at sunrise (when D_4 receptor expression increases and α_{1B}-D_4 and β_1-D_4 receptor heteromers are expressed) and were stimulated as before with agonists of both α_{1B} and β_1 receptors in the presence of either the pertinent antagonist or the D_4 antagonist, we observed that 5HT and melatonin synthesis and release could be blocked not only by the corresponding specific antagonists of adrenergic receptors but also by the D_4 receptor antagonist L-745,870 (Fig. 7J, K, N and O) demonstrating a clear cross-antagonism. In addition, when we treated the glands with either phenylephrine or isoproterenol in the presence of the dopamine D_4 receptor agonist RO 10-5824, a complete block in the ability of either ligand to increase 5-HT or melatonin synthesis or release was observed (Fig. 7L, M, P and Q) showing that, in these conditions, a negative cross-talk between dopamine D_4 and adrenergic receptors exists in the pineal gland. The influence of dopamine in 5-HT and melatonin synthesis and release in these conditions is represented in Fig. 7R. These data provide strong evidence that the role of the dopamine D_4 receptor via either α_{1B}-D_4 and β_1-D_4 receptor heteromers is to modify the melatonin metabolic pathway in the pineal gland.

Discussion

In the present study we identified a previously unknown mechanism for how dopamine can regulate adrenergic receptor function in a circadian fashion. By applying a number of different experimental approaches, we were able to identify: 1) That functional dopamine D_4 receptors form heteromers with both α_{1B}- and β_1 adrenergic receptors in transfected cells and in the pineal gland; 2) that the α_{1B}-D_4 and β_1-D_4 receptor heteromers allow for direct modulation of the adrenergic agonist-induced MAPK and Akt signaling by the D_4 receptor agonist and antagonist in transfected cells and in the pineal gland; 3) that the synthesis of melatonin and its precursor 5-HT, promoted by adrenergic receptor stimulation in the pineal gland, can be controlled by D_4 receptors activation via α_{1B}-D_4 and β_1-D_4 receptor heteromers and 4) that this D_4 receptor heteromer-mediated modulation is dependent on the circadian light/dark cycle. This is the first example of a circadian-dependent modulation of receptor heteromerization. Together these findings point to a new role for the D_4 receptor in the pineal gland where D_4 receptor activation modifies α_{1B}- and β_1 adrenergic receptor function by a direct receptor-receptor interaction which can limit the levels of melatonin secreted by the pineal gland.

The adrenergic receptors are the mainstay receptors of pineal gland function. They form the bridge between the circadian controlled release of norepinephrine by the surrounding sympathetic nerve terminals and melatonin production of the pineal gland. The adrenergic receptors are thought to control the production of melatonin through a variety of mechanisms, including control of the levels of the melatonin precursor 5-HT [16,17]. Dopamine is also present in the afferent sympathetic nerves in the pineal gland, not only as a precursor of norepinephrine, but also co-released to a lesser extent with norepinephrine [9].

The 'receptor heteromer' concept, in which receptors of the same and different gene families can combine among themselves to generate new and unique biochemical and functional characteristics, is becoming widely accepted for GPCRs and constitutes an emerging area in the

field of GPCR signaling and function regulation [25]. To date there has been no demonstration of heteromers involving dopamine and the adrenergic receptors. Here, by means of BRET experiments in transfected cells and by proximity ligation assays in pinealocytes, we present direct evidence that the D_4 receptor forms heteromers with both the α_{1B} and β_1 adrenergic receptors. The formation of α_{1B}-D_4 and β_1-D_4 receptor heteromers in the pineal gland manifests itself in the form of cross-antagonism. We observed that a D_4 receptor specific antagonist was able to block the signaling through both α_{1B}- and β_1 adrenergic receptors. α_{1B}- and β_1 adrenergic receptors specific antagonists were also able to block signaling through D_4 receptors. This is a clear example of cross-antagonism in a receptor heteromer [36–38]. Since, by definition an antagonist is not able to induce intracellular signaling, a statement a propos in our case as none of the antagonists used here demonstrated any signaling activity, the more straightforward way to explain the effect of a D_4 receptor antagonist on α_{1B} and β_1 receptor activation and vice-versa, is through a direct protein-protein interaction between both receptors.

The functional consequences of this protein-protein interaction is a negative cross-talk between both receptors in the α_{1B}-D_4 and β_1-D_4 receptor heteromers, i.e. the block in the amount of p-ERK 1/2 induced by adrenergic agonists in the presence of D_4 receptor agonist and the complete block of p-Akt production when both receptors in the heteromer were co-stimulated. In the pineal gland, D_4 receptor mRNA expression is tightly regulated so that it is highest during the last part of the dark period [9]. Accordingly, we show that the D_4 receptor is expressed and is functional in pineal gland isolated at sunrise and we saw no activity and no expression when pineal glands were isolated at sunset, the end of the light period. Our finding that the D_4 receptor can modify the downstream signaling of the α_{1B} and β_1 adrenergic receptors is particularly interesting as D_4 receptor expression was found to be modified by an increase in norepinephrine levels [9]. Norepinephrine levels are also known to increase at night and it is through its binding to the adrenergic receptors that the level of D_4 receptor mRNA is thought to reach the maximum at the end of the dark period [9]. Thus, the mechanism we describe may represent a feedback inhibition, where increased expression of D_4 receptor via adrenergic signaling leads to an increase of α_{1B}-D_4 and β_1-D_4 receptor heteromers which then inhibit adrenergic-induced signaling through the above described cross-talk.

We also studied the metabolic consequences of α_{1B}-D_4 and β_1-D_4 receptor heteromer activation at the level of melatonin synthesis and release, as well as the precursor of melatonin, 5-HT. Melatonin levels are increased at night while 5-HT levels fluctuate in the opposite manner, with production and secretion increasing during the day with the levels of AANAT, the enzyme in the last step to melatonin synthesis. Through mass action, large changes in AANAT activity at night can rapidly decrease the levels of 5-HT yielding large increases in melatonin [39]. It is important to point out that 5-HT synthesis is thought to occur both during the day and at night and nocturnal synthesis and release of 5-HT is required for maximal adrenergic stimulation of melatonin synthesis [40,41]. Extracellular 5-HT is either taken up by surrounding sympathetic nerves or binds $5HT_{2C}$ receptors on the pineal gland, which in turn can lead to increased melatonin synthesis and release [40,42]. To date it has not been entirely clear what limits the maximum nighttime and minimum daytime rates of melatonin production. Our data suggest that α_{1B}-D_4 and β_1-D_4 receptor heteromers may play an important role in this process. In pineal glands, isolated at the end of the light period (sunset) when the expression of D_4 receptor is negligible, treated with adrenergic ligands, we have seen a large increase in melatonin and a moderate increase in 5HT synthesis mediated by β_1 receptors and release mediated by α_{1B} receptors (Fig. 7I). In this case neither synthesis nor release of 5HT or melatonin were blocked by treating the gland simultaneously with a D_4 agonist or were modified in the presence of D_4 antagonist. In these conditions pineal gland is starting the melatonin production during the dark period. In pineal glands, isolated at the end of the dark period (sunrise) when the D_4 receptor is expressed, treated with adrenergic ligands, we have also seen a large increase in melatonin and 5-HT synthesis mediated by β_1 receptors and release mediated by α_{1B} receptors and, interestingly, both synthesis and release were blocked by treating the gland simultaneously with

a D_4 receptor agonist (Figure 7). This block could simply be due to cross-talk at the signaling level. However, a D_4 antagonist also led to a block in both adrenergic receptor-mediated synthesis and release of melatonin or 5-HT. Because antagonists do not signal on their own, this block must be due to protein-protein interactions via the heteromer. Thus, dopamine appears to be able to regulate the melatonin and 5-HT levels as seen in Figure 7R. This suggests that dopamine, via α_{1B}-D_4 and β_1-D_4 receptor heteromers, may serve both as a buffer to control the amount of 5-HT that can be made and released during the light period, limiting total melatonin production, and be partially responsible for the block of melatonin production after the dark period. During the day, D_4 receptors would begin to be down-regulated, less α_{1B}-D_4 and β_1-D_4 receptor heteromers would be formed, AANAT would be also down regulated maintaining a reduced melatonin production, 5-HT levels would gradually increase, and the cycle could repeat. These findings provide the first report of a role for the D_4 receptor in the pineal gland and suggest a new area of research on how dopamine receptors, by means of a circadian-related heteromerization with adrenergic receptors, may help maintain the circadian rhythm signals emulating from the pineal gland.

Experimental Procedures

Fusion proteins and expression vectors. The cDNA for dopamine D_4, and adrenergic α_{1B} and β_1 receptor genes expressed in the *pcDNA3.1* vector were amplified without its stop codon using sense and antisense primers to be cloned in the mammalian humanized pRluc-N1 or in the EYFP-N3 vectors (*See Supplementary Experimental Procedures*).

Cell culture and transient transfection. CHO or HEK-293T cells were grown in supplemented α-MEM or Dulbecco's modified Eagle's medium (DMEM) medium, respectively, and they were transfected by the polyethylenimine (PEI) method. (*See Supplementary Experimental Procedures*).

Immunostaining. HEK-293T cells were grown on glass coverslips and transiently transfected. After 48h of transfection, cells were fixed and labeled with the corresponding antibodies. (*See Supplementary Experimental Procedures*).

BRET assay. HEK-293T cells were co-transfected with a constant amount of cDNA encoding for the receptor fused to Rluc and with increasingly amounts of cDNA encoding to the receptor fused to YFP to measure BRET as previously described by Carriba et al. (2008) (*See Supplementary Experimental Procedures)*.

Pineal glands dissection and culture. Male Sprague Dawley rats (3 month old, ≈350g), receiving water and food *ad libitum,* were obtained from the animal facility of the Faculty of Biology (University of Barcelona). 4% Isoflurane (2-chloro-2-(difluoromethoxy)-1,1,1-trifluoro-ethane) anesthetized animals were killed by decapitation at 9:00h (just after the dark period) or at 20:00h (after light period) and pineal glands were immediately dissected. All procedures were approved by the Catalan Ethical Committee for Animal Use (CEAA/ DMAH 4049 and 5664). Rat pineal glands were cultured in defined culture medium (BGJb, Invitrogen, Carlsbad, CA) containing 10% (v/v) fetal bovine serum (heat- inactivated) for 24-36h and cultured in serum-free medium for 16 h before the addition of agonists and/or antagonist for signaling experiments or over-night cultured in HBSS medium (137 mM NaCl, 5 mM KCl, 0.34 mM $Na_2HPO_4.12H_2O$, 0.44 mM KH_2PO_4, 1.26 mM $CaCl_2.2H_2O$, 0.4 mM $MgSO_4.7H_2O$, 0.5 mM $MgCl_2$, 10 mM HEPES, pH 7.4), supplemented with 0,1% glucose, 100 U/ml penicillin/streptomycin and 1mg/ml bovine serum albumin, containing agonist and/or antagonist for serotonin synthesis and release determination .

MAPK and Akt/PKB determination. Transfected cells or pineal glands were cultured in serum-free medium before the addition of the indicated concentration of ligands for the indicated time. Both, cells and pineal glands were rised and lysed. MAPK (ERK1/2) or

Akt/PKB phosphorylation protein were separated by electrophoresis and bands densities were quantified (*See Supplementary Experimental Procedures).*

Pinealocyte culture, signaling and immunocytochemistry. Pinealocytes were prepared from rat pineal glands as previously described by Silveira Cruz-Machado et al. (2010). For signaling experiments, pinealocytes were treated with specific agonist, fixed with paraformaldehyde and treated with the corresponding antibodies (*See Supplementary Experimental Procedures)*.

In situ Proximity Ligation Assay (PLA). The primary cultures of pinealocytes were fixed and permeabilized as described above. The receptor-receptor molecular interaction was detected using the Duolink II in situ PLA detection Kit (*See Supplementary Experimental Procedures)*.
Serotonin synthesis and release determination. After 36 h of culture in BGJb medium, pineal glands were incubated in supplemented HBSS medium for 12 h with specific agonist and/or antagonist and radioactive [^{14}C]-Tryptophan (10 μM). Medium and pineal glands were collected separately and [^{14}C]-serotonin in medium or in homogenized glands, was separated by HPLC chromatography coupled to detection by fluorescence and counted in a liquid scintillation counter (*See Supplementary Experimental Procedures)*.

Melatonin synthesis and release determination. After 36 h of culture in BGJb medium, the pineal glands were incubated for 12h with specific agonist and/or antagonist in supplemented HBSS medium. After incubation, mediums were collected into eppendorf tubes and pineal glands were homogenized by sonication in a Dynatech/Sonic Dismembrator (Dynatech Labs, Chantilly, VA) for 15 seconds. An aliquot was reserved for protein quantification by the Lowry method and cellular debris were removed by centrifugation at 10,000 g for 10 min at 4ºC. Melatonin was quantified using a radioimmunoassay kit with [^{125}I]-melatonin (DiaSource, Belgique) following the instructions of the supplier.

Acknowledgments

We would like to thank D.C. Klein for helpful suggestions. We thank Jasmina Jiménez for technical help (University of Barcelona). We would like to thank S. Lefrancois for critical reading of the manuscript. This study was supported by grants from the Spanish Ministerio de Ciencia y Tecnología (SAF2010-18472, SAF2008-01462). PJM is a Ramón y Cajal Fellow.

References

1. Missale C, Nash SR, Robinson SW, Jaber M, Caron MG (1998) Dopamine receptors: from structure to function. Physiol Rev 78: 189–225.

2. Rashid AJ, O'Dowd BF, Verma V, George SR (2007) Neuronal Gq/11-coupled dopamine receptors: an uncharted role for dopamine. Trends Pharmacol Sci 28: 551–555. doi:10.1016/j.tips.2007.10.001.

3. Hasbi A, O'Dowd BF, George SR (2010) Heteromerization of dopamine D2 receptors with dopamine D1 or D5 receptors generates intracellular calcium signaling by different mechanisms. Curr Opin Pharmacol 10: 93–99. doi:10.1016/j.coph.2009.09.011.

4. Perreault ML, O'Dowd BF, George SR (2011) Dopamine receptor homooligomers and heterooligomers in schizophrenia. CNS Neurosci Ther 17: 52–57. doi:10.1111/j.1755-5949.2010.00228.x.

5. Van Tol HH, Bunzow JR, Guan HC, Sunahara RK, Seeman P, et al. (1991) Cloning of the gene for a human dopamine D4 receptor with high affinity for the antipsychotic clozapine. Nature 350: 610–614. doi:10.1038/350610a0.

6. Rondou P, Haegeman G, Van Craenenbroeck K (2010) The dopamine D4 receptor: biochemical and signalling properties. Cell Mol Life Sci 67: 1971–1986. doi:10.1007/s00018-010-0293-y.

7. LaHoste GJ, Swanson JM, Wigal SB, Glabe C, Wigal T, et al. (1996) Dopamine D4 receptor gene polymorphism is associated with attention deficit hyperactivity disorder. Mol Psychiatry 1: 121–124.

8. Ivanova TN, Alonso-Gomez AL, Iuvone PM (2008) Dopamine D4 receptors regulate intracellular calcium concentration in cultured chicken cone photoreceptor cells: relationship to dopamine receptor-mediated inhibition of cAMP formation. Brain Res 1207: 111–119. doi:10.1016/j.brainres.2008.02.025.

9. Kim J-S, Bailey MJ, Weller JL, Sugden D, Rath MF, et al. (2010) Thyroid hormone and adrenergic signaling interact to control pineal expression of the dopamine receptor D4 gene (Drd4). Mol Cell Endocrinol 314: 128–135. doi:10.1016/j.mce.2009.05.013.

10. Bai L, Zimmer S, Rickes O, Rohleder N, Holthues H, et al. (2008) Daily oscillation of gene expression in the retina is phase-advanced with respect to the pineal gland. Brain Research 1203: 89–96. doi:16/j.brainres.2008.01.073.

11. Delgado MJ, Vivien-Roels B (1989) Effect of environmental temperature and photoperiod on the melatonin levels in the pineal, lateral eye, and plasma of the frog, Rana perezi: importance of ocular melatonin. Gen Comp Endocrinol 75: 46–53.

12. Alonso-Gómez AL, Tejera M, Alonso-Bedate M, Delgado MJ (1990) Response to pinealectomy and blinding in vitellogenic female frogs (Rana perezi) subjected to high temperature in autumn. Can J Physiol Pharmacol 68: 94–98.

13. Ganguly S, Coon SL, Klein DC (2002) Control of melatonin synthesis in the mammalian pineal gland: the critical role of serotonin acetylation. Cell Tissue Res 309: 127–137. doi:10.1007/s00441-002-0579-y.

14. Velarde E, Cerdá-Reverter JM, Alonso-Gómez AL, Sánchez E, Isorna E, et al. (2010) Melatonin-synthesizing enzymes in pineal, retina, liver, and gut of the goldfish (Carassius): mRNA expression pattern and regulation of daily rhythms by lighting conditions. Chronobiol Int 27: 1178–1201. doi:10.3109/07420528.2010.496911.

15. Klein DC, Bailey MJ, Carter DA, Kim J-so, Shi Q, et al. (2010) Pineal function: impact of microarray analysis. Mol Cell Endocrinol 314: 170–183. doi:10.1016/j.mce.2009.07.010.

16. Gonzalez-Brito A, Troiani ME, Menendez-Pelaez A, Delgado MJ, Reiter RJ (1990) mRNA transcription determines the lag period for the induction of pineal melatonin synthesis in the Syrian hamster pineal gland. J Cell Biochem 44: 55–60. doi:10.1002/jcb.240440105.

17. Zheng W, Cole PA (2002) Serotonin N-acetyltransferase: mechanism and inhibition. Curr Med Chem 9: 1187–1199.

18. Klein DC (2007) Arylalkylamine N-acetyltransferase: “the Timezyme.” J Biol Chem 282: 4233–4237. doi:10.1074/jbc.R600036200.

19. Ho AK, Chik CL (2010) Modulation of Aanat gene transcription in the rat pineal gland. J Neurochem 112: 321–331. doi:10.1111/j.1471-4159.2009.06457.x.

20. Ferré S, Ciruela F, Woods AS, Lluis C, Franco R (2007) Functional relevance of neurotransmitter receptor heteromers in the central nervous system. Trends Neurosci 30: 440–446. doi:10.1016/j.tins.2007.07.001.

21. Terrillon S, Bouvier M (2004) Roles of G-protein-coupled receptor dimerization. EMBO Rep 5: 30–34. doi:10.1038/sj.embor.7400052.

22. Bulenger S, Marullo S, Bouvier M (2005) Emerging role of homo- and heterodimerization in G-protein-coupled receptor biosynthesis and maturation. Trends Pharmacol Sci 26: 131–137. doi:10.1016/j.tips.2005.01.004.

23. Waldhoer M, Fong J, Jones RM, Lunzer MM, Sharma SK, et al. (2005) A heterodimer-selective agonist shows in vivo relevance of G protein-coupled receptor dimers. Proc Natl Acad Sci USA 102: 9050–9055. doi:10.1073/pnas.0501112102.

24. Smith NJ, Milligan G (2010) Allostery at G protein-coupled receptor homo- and heteromers: uncharted pharmacological landscapes. Pharmacol Rev 62: 701–725. doi:10.1124/pr.110.002667.

25. Ferré S, Baler R, Bouvier M, Caron MG, Devi LA, et al. (2009) Building a new conceptual framework for receptor heteromers. Nat Chem Biol 5: 131–134. doi:10.1038/nchembio0309-131.

26. Klitten LL, Rath MF, Coon SL, Kim J-S, Klein DC, et al. (2008) Localization and regulation of dopamine receptor D4 expression in the adult and developing rat retina. Exp Eye Res 87: 471–477. doi:10.1016/j.exer.2008.08.004.

27. DeWire SM, Ahn S, Lefkowitz RJ, Shenoy SK (2007) β-Arrestins and Cell Signaling. Annu Rev Physiol 69: 483–510. doi:10.1146/annurev.physiol.69.022405.154749.

28. Maronde E, Stehle JH (2007) The mammalian pineal gland: known facts, unknown facets. Trends Endocrinol Metab 18: 142–149. doi:10.1016/j.tem.2007.03.001.

29. Moreno E, Hoffmann H, Gonzalez-Sepúlveda M, Navarro G, Casadó V, et al. (2011) Dopamine D1-histamine H3 receptor heteromers provide a selective link to MAPK signaling in GABAergic neurons of the direct striatal pathway. J Biol Chem 286: 5846–5854. doi:10.1074/jbc.M110.161489.

30. Moreno E, Vaz SH, Cai N-S, Ferrada C, Quiroz C, et al. (2011) Dopamine-Galanin Receptor Heteromers Modulate Cholinergic Neurotransmission in the Rat Ventral Hippocampus. J Neurosci 31: 7412–7423. doi:10.1523/JNEUROSCI.0191-11.2011.

31. Navarro G, Carriba P, Gandía J, Ciruela F, Casadó V, et al. (2008) Detection of heteromers formed by cannabinoid CB1, dopamine D2, and adenosine A2A G-protein-coupled receptors by combining bimolecular fluorescence complementation and bioluminescence energy transfer. ScientificWorldJournal 8: 1088–1097. doi:10.1100/tsw.2008.136.

32. Jiang H, Betancourt L, Smith RG (2006) Ghrelin Amplifies Dopamine Signaling by Cross Talk Involving Formation of Growth Hormone Secretagogue Receptor/Dopamine Receptor Subtype 1 Heterodimers. Mol Endocrinol 20: 1772–1785. doi:10.1210/me.2005-0084.

33. Sohy D, Parmentier M, Springael J-Y (2007) Allosteric Transinhibition by Specific Antagonists in CCR2/CXCR4 Heterodimers. Journal of Biological Chemistry 282: 30062–30069. doi:10.1074/jbc.M705302200.

34. Levoye A, Balabanian K, Baleux F, Bachelerie F, Lagane B (2009) CXCR7 heterodimerizes with CXCR4 and regulates CXCL12-mediated G protein signalling. Blood. Available:http://www.ncbi.nlm.nih.gov/pubmed/19380869. Accessed 1 May 2009.

35. Trifilieff P, Rives M-L, Urizar E, Piskorowski RA, Vishwasrao HD, et al. (2011) Detection of antigen interactions ex vivo by proximity ligation assay: endogenous dopamine D2-adenosine A2A receptor complexes in the striatum. BioTechniques 51: 111–118. doi:10.2144/000113719.

36. Carriba P, Navarro G, Ciruela F, Ferré S, Casadó V, et al. (2008) Detection of heteromerization of more than two proteins by sequential BRET-FRET. Nat Methods 5: 727–733. doi:10.1038/nmeth.1229.

37. Ferrada C, Moreno E, Casadó V, Bongers G, Cortés A, et al. (2009) Marked changes in signal transduction upon heteromerization of dopamine D1 and histamine H3 receptors. Br J Pharmacol 157: 64–75. doi:10.1111/j.1476-5381.2009.00152.x.

38. Navarro G, Moreno E, Aymerich M, Marcellino D, McCormick PJ, et al. (2010) Direct involvement of sigma-1 receptors in the dopamine D1 receptor-mediated effects of cocaine. Proc Natl Acad Sci USA 107: 18676–18681. doi:10.1073/pnas.1008911107.

39. Klein DC, Coon SL, Roseboom PH, Weller JL, Bernard M, et al. (1997) The melatonin rhythm-generating enzyme: molecular regulation of serotonin N-acetyltransferase in the pineal gland. Recent Prog Horm Res 52: 307–357; discussion 357–358.

40. Miguez JM, Simonneaux V, Pevet P (1997) The role of the intracellular and extracellular serotonin in the regulation of melatonin production in rat pinealocytes. J Pineal Res 23: 63–71.

41. Simonneaux V, Ribelayga C (2003) Generation of the Melatonin Endocrine Message in Mammals: A Review of the Complex Regulation of Melatonin Synthesis by Norepinephrine, Peptides, and Other Pineal Transmitters. Pharmacological Reviews 55: 325–395. doi:10.1124/pr.55.2.2.

42. Sugden D (1990) 5-Hydroxytryptamine amplifies beta-adrenergic stimulation of N-acetyltransferase activity in rat pinealocytes. J Neurochem 55: 1655–1658.

FIGURES AND FIGURE LEGENDS

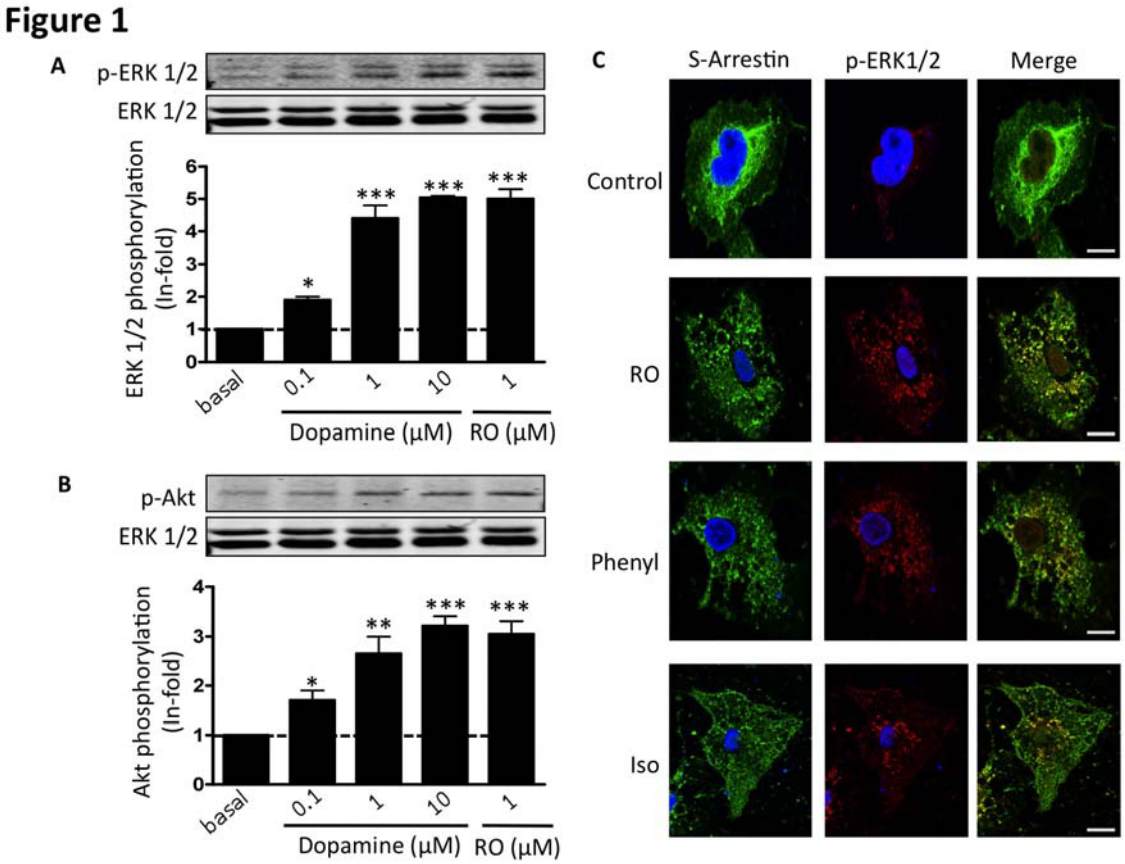

Figure 1. Functionality of dopamine D_4 receptors in pineal gland and pinealocytes. Pineal glands extracted at 9:00h were treated for 10 min with increasing amounts of dopamine or with 1 μM of RO 10-5824 (RO). The immunoreactive bands, corresponding to ERK 1/2 phosphorylation **(A)** and Akt phosphorylation **(B)**, of two separate experiments performed in duplicate were quantified and values represent the mean ± S.E.M. of in-folds relative to basal found in untreated cells. Significant differences with respect to basal were determined by Student's *t* test (*p<0.05, **p<0.01 and ***p<0.001). A representative Western blot is shown at the top (see Experimental Procedures). **(C)** Pinealocytes were isolated from pineal glands extracted at 9:00h and were treated with 1 μM of RO 10-5824 (RO), 1 μM phenylephrine (Phenyl) or 1 μM isoproterenol (Iso) for 10 min before labeling with anti-S-arrestin and anti-phospho-Thr^{202}/Tyr^{204} ERK1/2 as indicated in Experimental Procedures. Scale bar: 5 μm.

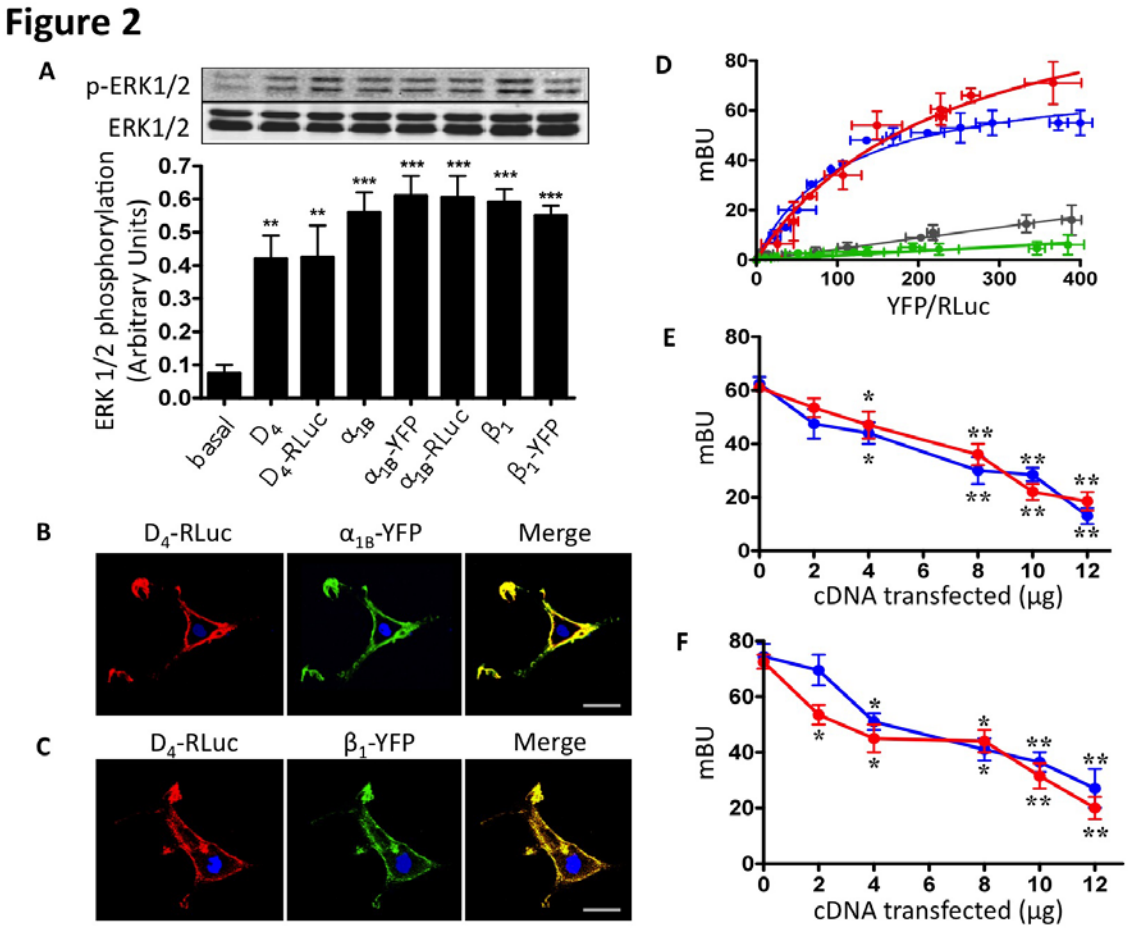

Figure 2. D_4 receptors form heteromers with α_{1B} and β_1 receptors in transfected cells. (A) Functionality of the fusion proteins in cells transfected with 2 µg of cDNA corresponding to the D_4 receptor or with 3 µg of cDNA corresponding to the adrenergic α_{1B} or β_1 receptors or to the corresponding fusion proteins D_4-RLuc, α_{1B}-YFP, α_{1B}-RLuc or β_1-YFP. 48 h post-transfection, cells expressing D_4 or D_4-RLuc receptors were treated for 7 min with 500 nM RO 10-5824, cells expressing α1B, α_{1B}-YFP or α_{1B}-RLuc receptors were treated for 7 min with 1µM phenylephrine and cells expressing β1 or β_1-YFP were treated for 7 min with 1µM isoproterenol and ERK1/2 phosphorylation was determined. The immunoreactive bands of three experiments performed in duplicates were quantified and expressed as mean ± S.E.M. of arbitrary units. A representative Western blot is shown at the top. Significant differences respect to basal were calculated by one-way ANOVA and Bonferroni's test. (**$p < 0.01$ and ***$p < 0.001$). **(B and C)** Confocal microscopy images of cells transfected with 1 µg of cDNA corresponding to D_4-RLuc and 0.5 µg cDNA corresponding to α_{1B}-YFP **(B)** or to β_1-YFP **(C)**. Proteins were identified by fluorescence or by immunocytochemistry. D_4-RLuc receptor is shown in red, α_{1B}-YFP and β_1-YFP receptors are shown in green and co-localization is shown in yellow. Scale bar: 5 µm. **(D)** BRET saturation curves were performed in cells co-expressing a constant amount D_4-RLuc construct (2 µg cDNA transfected) and increasing amounts α_{1B}-YFP construct (0.4-5 µg cDNA transfected) (blue), β_1-YFP construct (0.4-5 µg cDNA transfected, red) or D_1-YFP construct (1-4 µg cDNA transfected) (green) or with cells co-expressing a constant amount of α_{1B}-RLuc construct (3 µg cDNA transfected) and increasing amounts of β_1-YFP construct (0.4-5 µg cDNA transfected) (gray). Both fluorescence and luminescence of each sample were measured prior to every experiment to confirm equal expression of Rluc (about 100,000 luminescence units) while monitoring the increase of YFP expression (2000 to 40,000 fluorescence units). BRET data are expressed as means ± S.D. of five different experiments

grouped as a function of the amount of BRET acceptor. **(E and F)** BRET was determined in cells expressing a constant amount of D_4-RLuc (2 µg cDNA transfected) and **(E)** α_{1B}-YFP (4µg cDNA tranfected) or **(F)** β_1-YFP (4µg cDNA tranfected) and increasing amounts (2-12 µg of cDNA transfected) of **(E)** α_{1B} (red) or β_1 (blue) or **(F)** β_1 (red) or α_{1B} (blue). Both fluorescence and luminescence of each sample were measured prior to every experiment to confirm no changes in the expression of D_4-RLuc, α_{1B}-YFP or β_1-YFP. BRET data are expressed as means ± S.D. of three different experiments grouped as a function of the amount of BRET acceptor. Significant differences with respect to cells not expressing α_{1B} or β_1 were calculated by one-way ANOVA and Bonferroni's test. (*$p < 0.05$ and **$p < 0.01$).

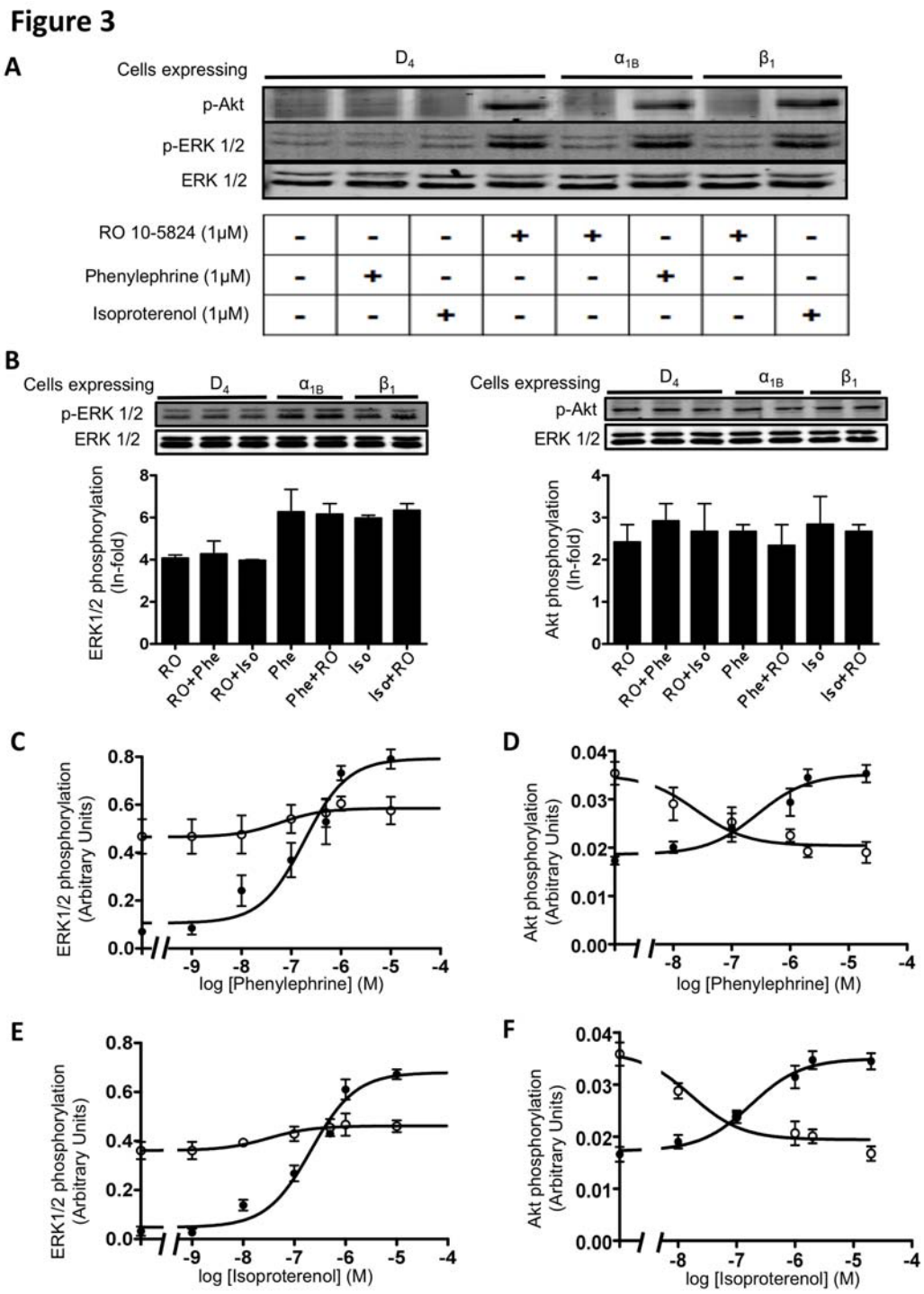

Figure 3. Functional characteristics of α_{1B}-D_4 and β_1-D_4 receptor heteromers in transfected cells. CHO cells were transfected with 2 μg of cDNA corresponding to D_4 receptors or with 3 μg of cDNA corresponding to α_{1B} receptors or to β_1 receptors alone **(A and B)** or in combination **(C to F)**. In **(A and B)** the selectivity of ligands was proved by measuring ERK1/2 and Akt phosphorylation in cells expressing D_4, α_{1B} or β_1 receptors, treated for 7 min with 1 μM RO 10-5824, phenylephrine or isoproterenol alone (A) or in combination (B) as indicated. In (C to F), cells expressing D_4 and α_{1B} receptors **(C and D)** or D_4 and β_1 receptors **(E and F)** were treated for 7 min with increasing concentrations of phenylephrine **(C and D)** or isoproterenol **(E and F)** in the presence (○) or in the absence (●) of 500 nM RO 10-5824. The immunoreactive bands, corresponding to ERK 1/2 **(C and E)** and Akt phosphorylation **(D and F)** of four experiments were quantified and expressed as mean ± S.E.M. of arbitrary units.

Figure 4

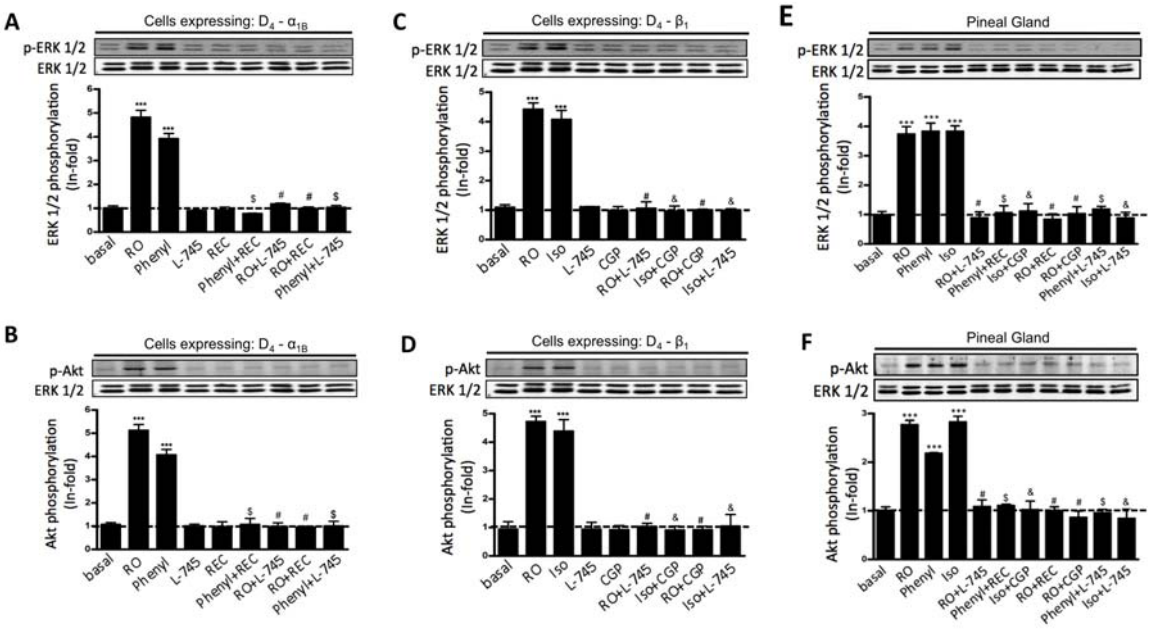

Figure 4. Cross-antagonism between D_4 and α_{1B} or β_1 receptors in transfected cells and in pineal gland. In (**A to D**) CHO cells were transiently co-transfected with 2 μg of cDNA corresponding to D_4 receptors and with 3 μg of cDNA corresponding to α_{1B} receptors **(A and B)** or β_1 receptors **(C and D).** In **(E and F)** rat pineal glands were extracted at 9:00h and processed as indicated in Experimental Procedures. Cells were treated for 7 min and pineal glands were treated for 10 min with 500 nM of RO 10-5824 (RO), phenylephrine (Phenyl) or isoproterenol (Iso) or with 1 μM of L-745,870 (L-745), REC 15/2615 (REC) or CGP 20712 (CGP), alone or in combination. The immunoreactive bands, corresponding to ERK 1/2 phosphorylation **(A, C and E)** and Akt phosphorylation **(B, D and F)** of four experiments were quantified and values represent the mean ± S.E.M. of in-fold respect to basal levels found in untreated cells. Significant differences respect to basal or to the treated samples were calculated by a bifactorial ANOVA followed by post-hoc Bonferroni's tests (***$p<0.001$, as compared to the basal. $^{\#}p<0.001$, as compared to the sample treated with RO 10-5824. $^{\$}p<0.001$, as compared to the sample treated with phenylephrine. $^{\&}p<0.001$, as compared to the sample treated with isoproterenol). A representative Western blot is shown at the top of each panel.

Figure 5

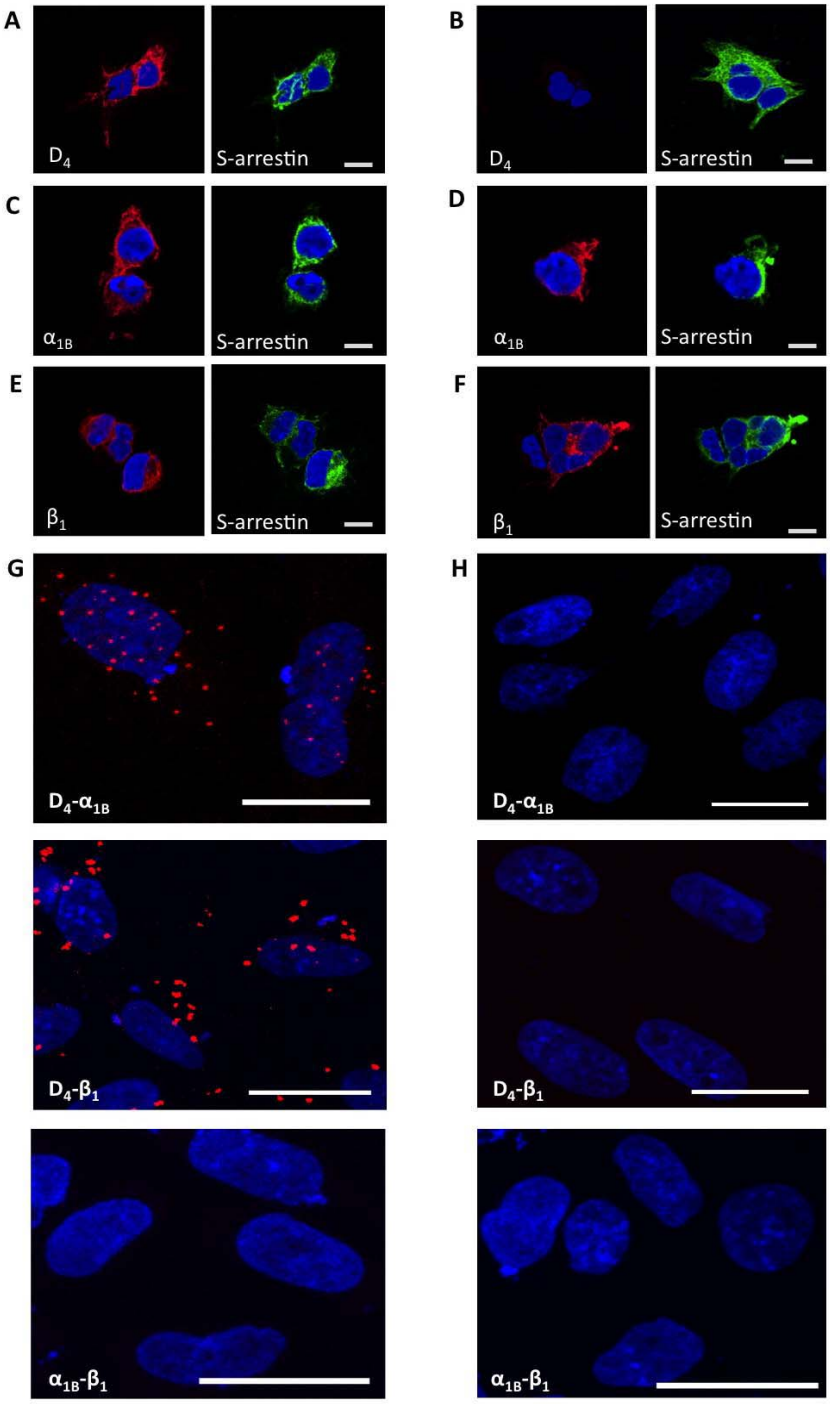

Figure 5. D_4 receptors form heteromers with α_{1B} and β_1 receptors in the pineal gland. Pinealocytes were isolated from pineal glands extracted at 9:00 h **(A, C, E and G)** or at 20:00 h **(B, D, F and H).** In **(A to F)** pinealocytes were stained using anti-S-arrestin antibodies (green) and anti-D_4 (**A and B**), anti α_{1B} (**C and D**) or anti β_1 (**E and F**) antibodies (red) as indicated in Experimental Procedures. In **(G and H)** pinealocytes were prepared as indicated in Experimental Procedures and the expression of α_{1B}-D_4 (top panels) and β_1-D_4 (middle panels) receptor heteromers was visualized as a punctate red fluorescent spots detected by confocal microscopy using the proximity ligation assay (see Experimental procedures). Any expression of α_{1B}-β_1 receptor heteromers was seen (bottom panels). Scale bar 20 μm.

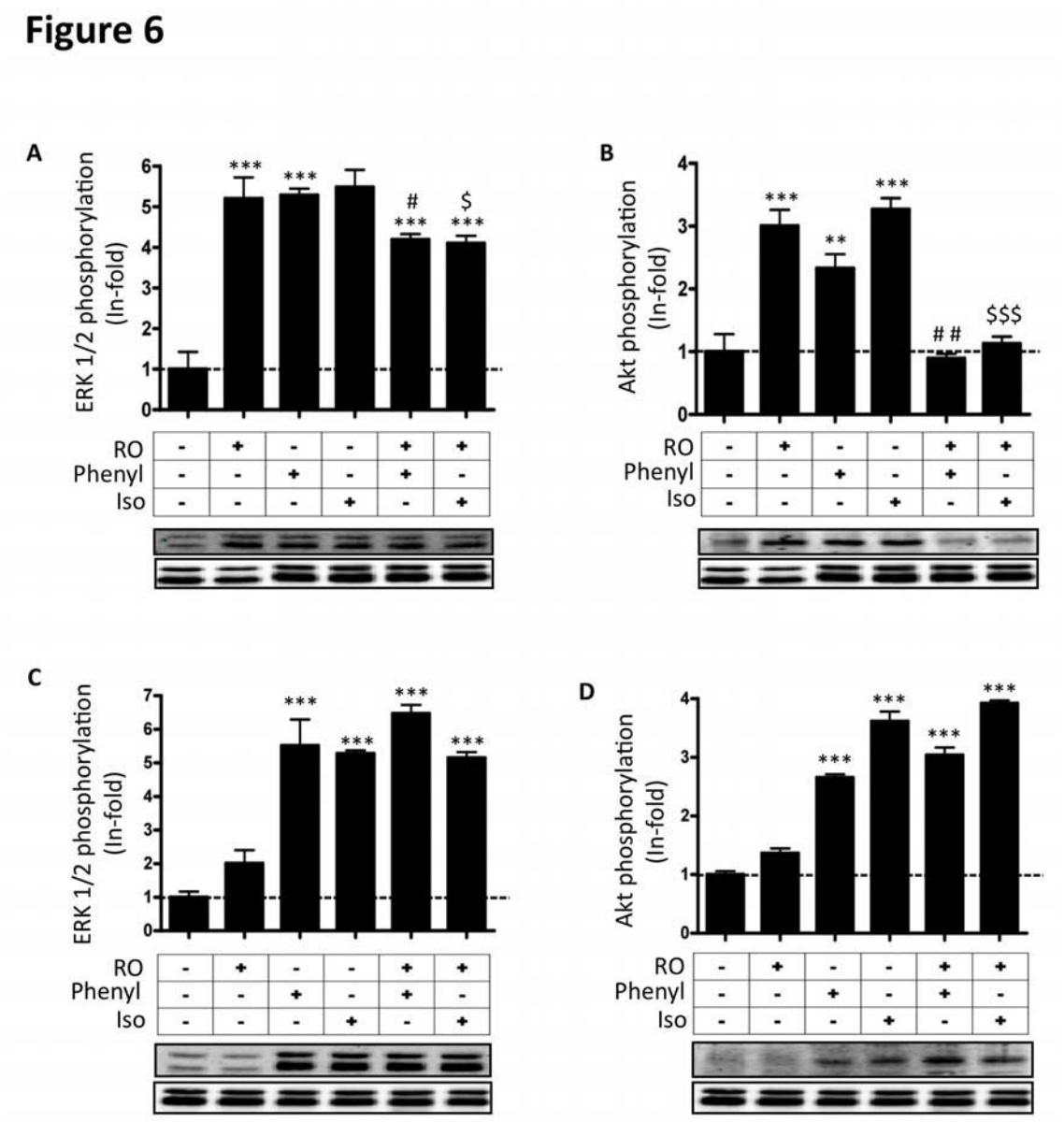

Figure 6. Functional characteristics of α_{1B}-D_4 and β_1-D_4 receptor heteromers in pineal gland. Pineal glands extracted at 9:00 h **(A and B)** or at 20:00 h **(C and D)** were treated for 10 min with RO 10-5824, phenylephrine or isoproterenol at 1 μM concentration alone or in combination. The immunoreactive bands, corresponding to ERK 1/2 phosphorylation **(A and C)** or Akt phosphorylation **(B and D),** of three experiments performed in duplicates were quantified and values represent the mean ± S.E.M. of in-folds respect to basal levels found in untreated pineal glands. Significant differences were calculated by a bifactorial ANOVA followed by post-hoc Bonferroni's tests (**p<0.01 and ***p<0.001, as compared to the basal. $^{\#}$p<0.05 and $^{\#\#}$p<0.01, as compared to the sample treated with phenylephrine. $^{\$}$p<0.05 and $^{\$\$\$}$p<0.001, as compared to the sample treated with isoproterenol). A representative Western blot is shown at the bottom of each panel.

Figure 7

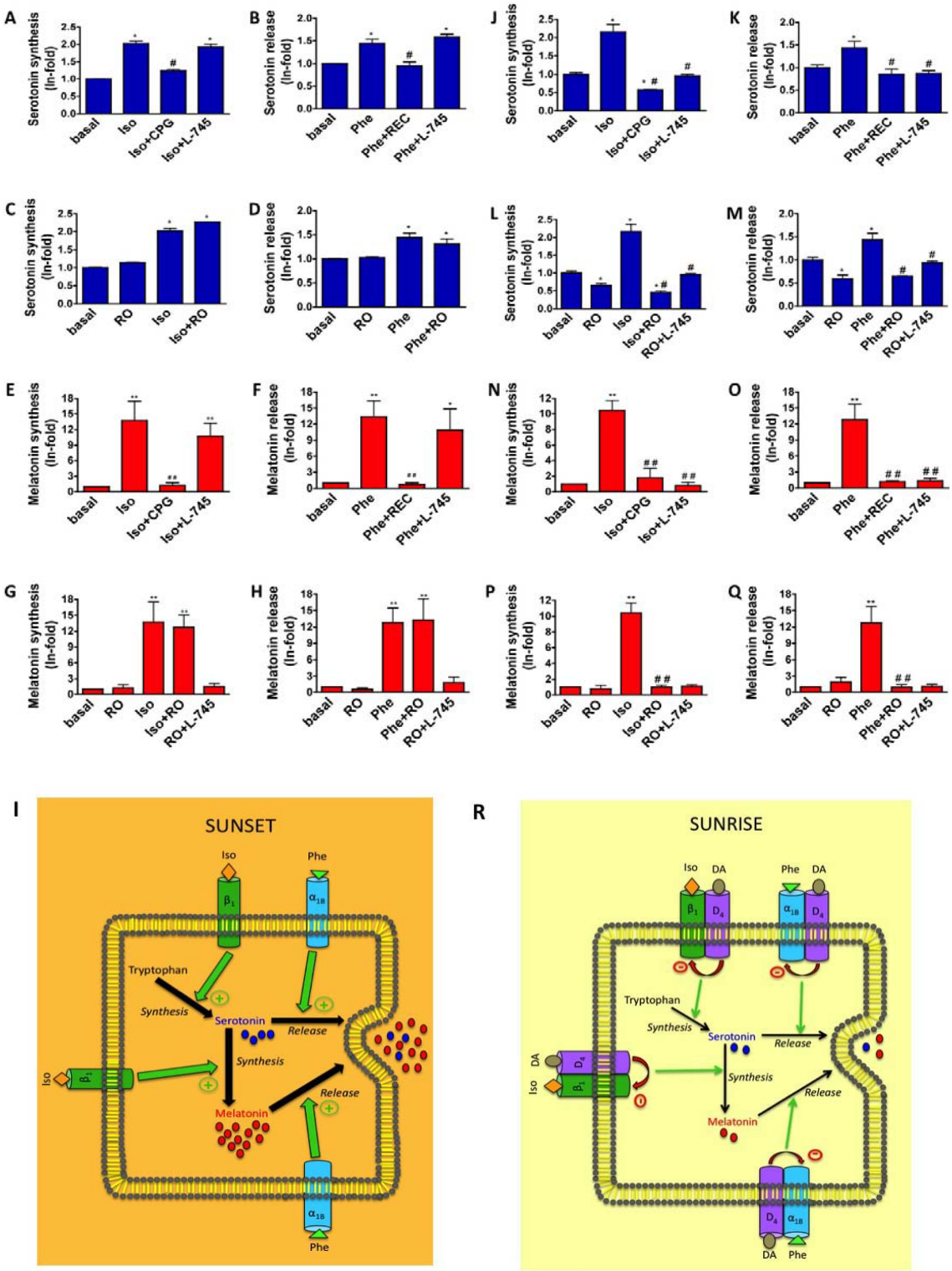

Figure 7. Metabolic consequences of α_{1B}-D_4 and β_1-D_4 receptor heteromers activation. 5HT synthesis (**A, C, J, L**) and release (**B, D, K, M**) and melatonin synthesis (**E,G, N, P**) and release (**F, H,O, Q**) were measured as described in Experimental Procedures in pineal gland extracted

at 20:00 h (**A to H**) or at 9:00 h (**J to Q**). Pineal glands were not treated (basal) or treated with 500 nM RO 10-5824 (RO), 500 nM phenylephrine (Phe), 500 nM isoproterenol (Iso), 1 μM L-745,870 (L-745), 1 μM REC 15/2615 (REC) or 1 μM CGP 20712 (CGP), alone or in combination. Three experiments were quantified and values represent the mean ± S.E.M. of in-folds respect to basal levels found in untreated pineal glands. Significant differences were calculated by a bifactorial ANOVA followed by post-hoc Bonferroni's tests (*$p<0.01$ as compared to the basal. $^{\#}p<0.005$ as compared to the sample treated with isoproterenol or with phenylephrine). In (**I and R**) the overall results are presented as a scheme.

FIGURES AND SUPPLEMENTARY FIGURE LEGENDS

Figure S1

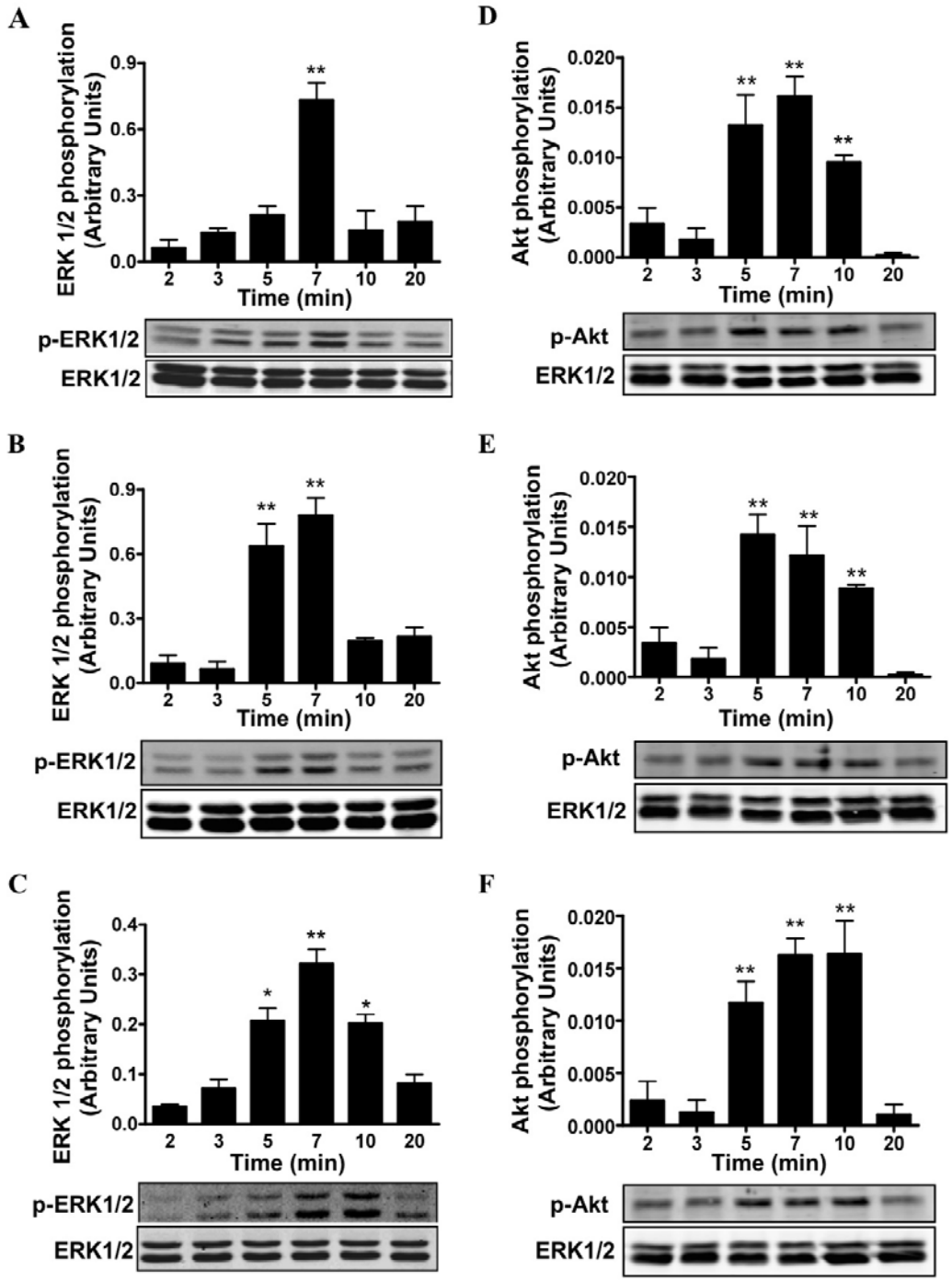

Fig. S1. ERK 1/2 and Akt phosphorylation in cells transfected with D_4, α_{1B} or β_1 receptors. CHO cells were transfected with 2 µg of cDNA corresponding to the D_4 receptor **(A, D)**, 3 µg of cDNA corresponding to the α_{1B} receptor **(B, E)** or 3 µg of cDNA corresponding to the β_1 receptor **(C, F)**. 48 h post-transfection, cells were treated for increasing time with 500 nM RO 10-5824 **(A**, **D)**, 1µM phenylephrine **(B, E)** or 1µM isoproterenol **(C, F)**. The immunoreactive bands, corresponding to ERK 1/2 **(A to C)** and Akt **(D to F)** phosphorylation of three experiments were quantified and expressed as arbitrary units. Statistical differences over non-treated cells were determined by Student's *t* test (*p<0.05 and **p<0.01).

Figure S2

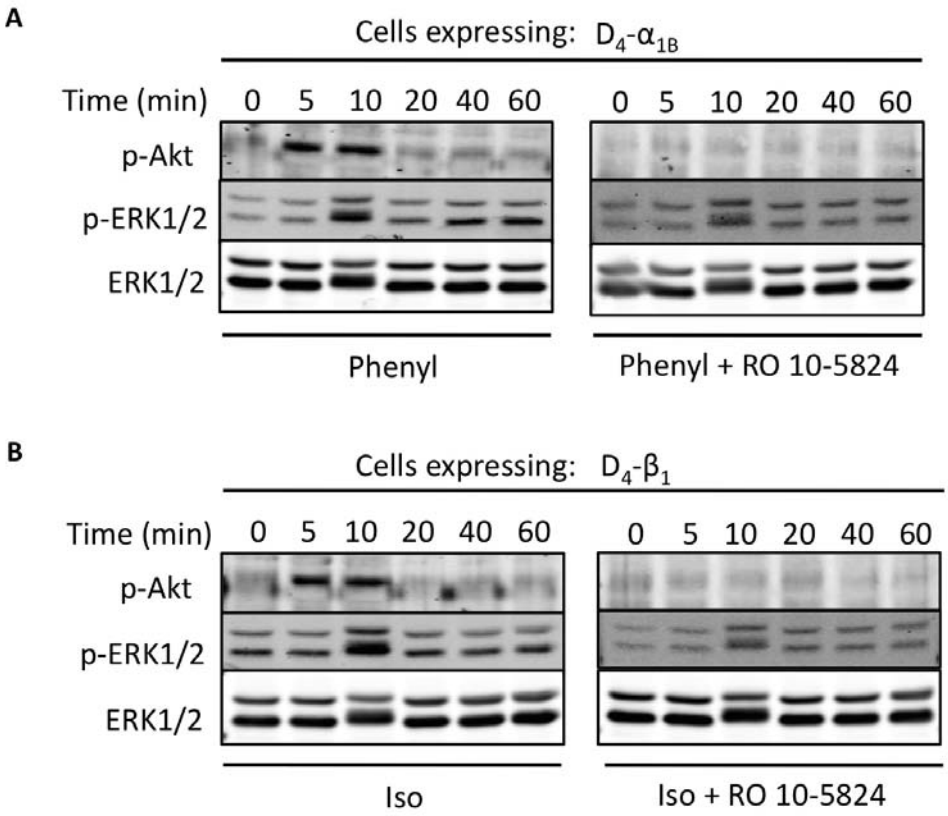

Fig. S2. Time-response on ERK 1/2 and Akt phosphorylation by co-activation of α_{1B}-D_4 and β_1-D_4 receptor heteromers in cell cultures. CHO cells were transfected with 2 μg of cDNA corresponding to the D_4 receptor and 3 μg of cDNA corresponding to the α_{1B} receptor **(A)** or the β_1 receptor **(B).** 48 h post-transfection, cells were treated with 1 μM phenylephrine (Phenyl, **A**) or 1 μM isoproterenol (Iso, **B**) alone or in the presence of 1 μM RO 10-5824 for different times. A representative Western blot is shown.

Figure S3

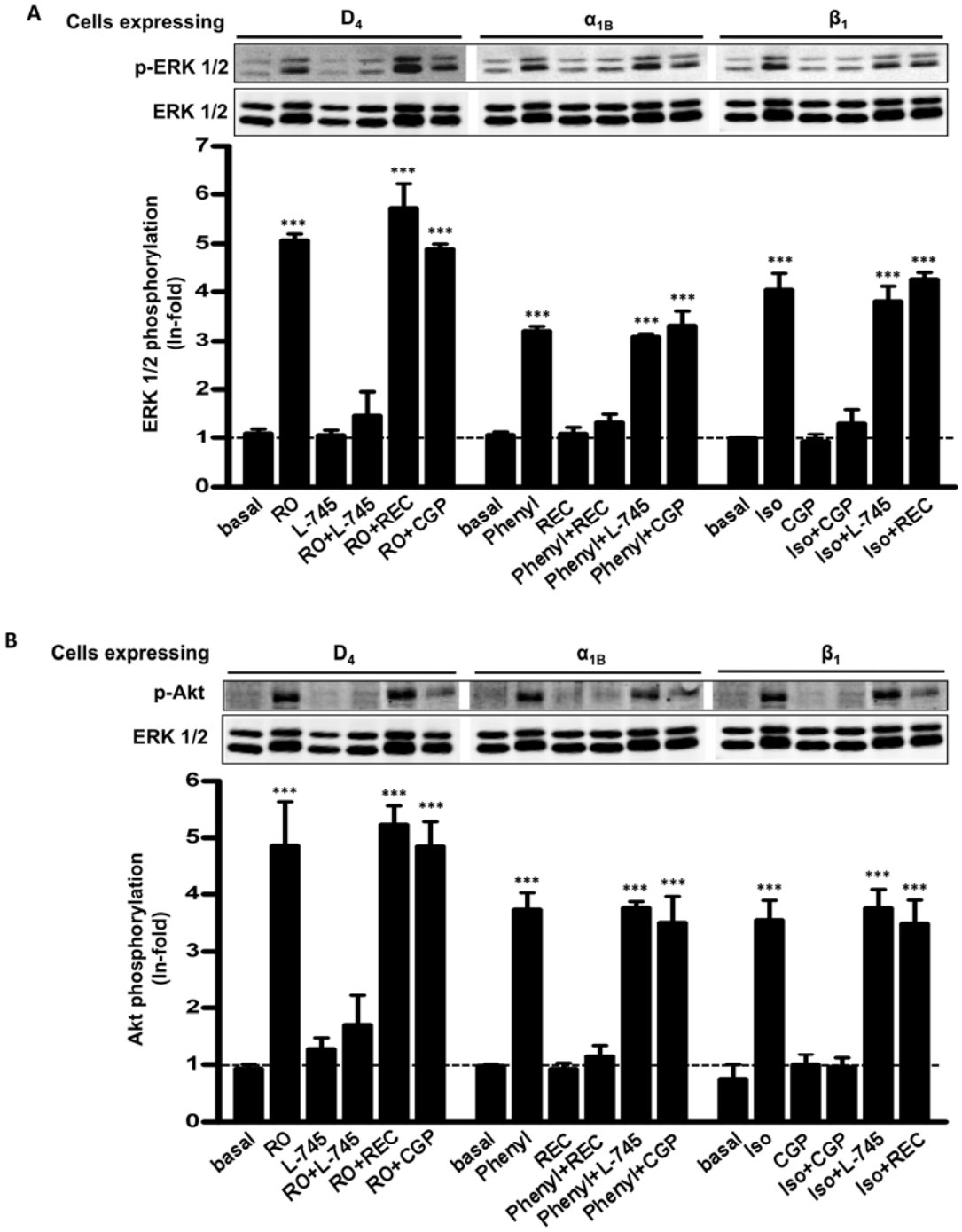

Fig. S3. Selectivity of D_4, α_{1B} or β_1 receptor antagonists. CHO cells were transfected with 2 µg of cDNA corresponding to the D_4 receptor or with 3 µg of cDNA corresponding to α_{1B} or β_1 receptors. 48 h post-transfection, cells were treated for 7 min with 500 nM RO 10-5824 (RO), 500 nM phenylephrine (Phenyl), 500 nM isoproterenol (Iso), 1 µM L-745,870 (L-745), 1 µM REC 15/2615 (REC) or 1 µM CGP 20712 (CGP) alone or in combination. The immunoreactive bands, corresponding to ERK 1/2 phosphorylation **(A)** and Akt phosphorylation **(B)**, of three experiments were quantified and values represent the mean ± S.E.M. of in-folds over basal levels found in untreated cells (basal). Significant differences over basal were determined by Student's *t* test (***p<0.001). A representative Western blot is shown at the top.

Figure S4

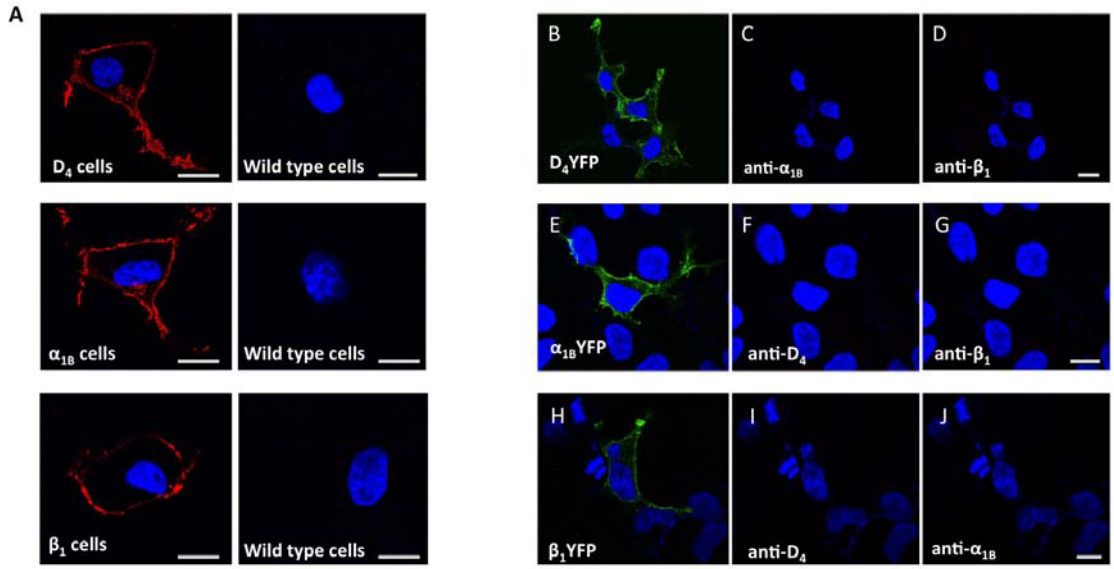

Fig. S4. Specificity of the antibodies tested by immunocytochemistry. In **(A)** non transfected HEK-293T cells (right panels) and cells transfected with, top to bottom, 1 µg of cDNA corresponding to D_4 receptor, 0.5 µg cDNA corresponding to α_{1B} receptor or 0.5 µg cDNA corresponding to β_1 receptor (left panels) were stained using, top to bottom, anti-D_4, anti-α_1 or anti-β_1 antibodies as indicated in Experimental Procedures. Scale bar: 5 µm. In **(B to J)**, cells were transfected with 1 µg of cDNA corresponding to D_4-YFP receptor **(B to D)**, 0,5 µg cDNA corresponding to α_{1B}-YFP receptor **(E to G)** or 0.5 µg cDNA corresponding to β_1-YFP receptor **(H to J).** The expression of the receptors was detected by its own YFP fluorescence (**B, E and H**) and cells were stained using anti-α_1 **(C and J)**, anti-β_1 **(D and G)** or anti-D_4 **(F and I)** antibodies. Scale bar: 5 µm.

Figure S5

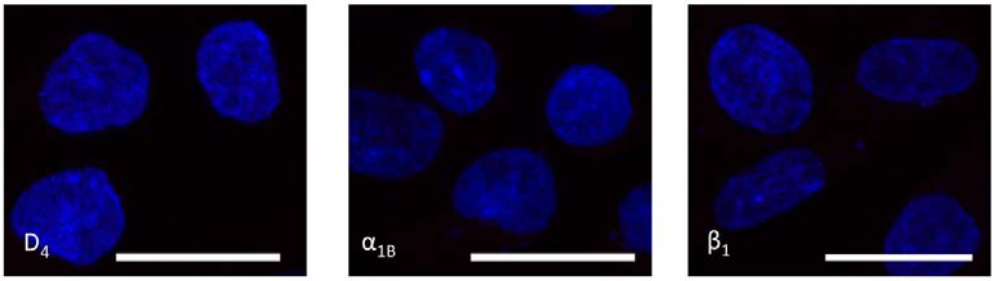

Fig. S5. Negative controls for in situ proximity ligation assays. Negative controls for in situ proximity ligation assays (PLA) were shown as not punctuated red fluorescence staining in pinealocytes in the absence of primary antibodies, left to right, anti-D_4, anti-α_1 or anti-β_1 antibodies. Scale bar: 20 µm.

Figure S6

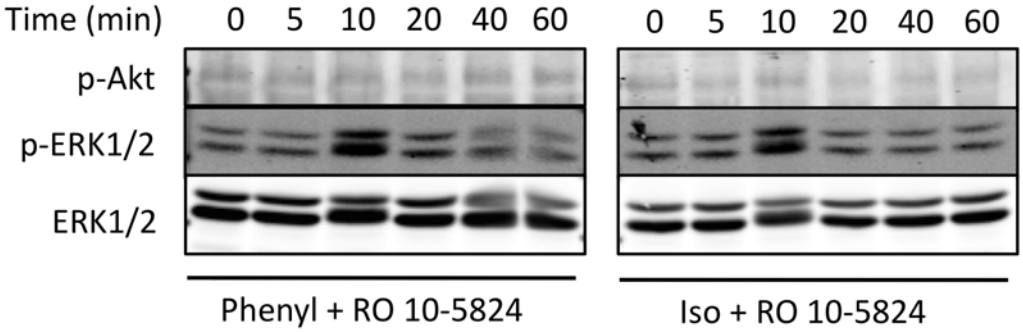

Fig. S6. Time-response on ERK 1/2 and Akt phosphorylation by co-activation of α_{1B}-D_4 and β_1-D_4 receptor heteromers in pineal gland. Pineal glands extracted at 9:00 h were treated with 1 µM phenylephrine (Phenyl) or 1 µM isoproterenol (Iso) in the presence of 1 µM RO 10-5824 for different times. A representative Western blot is shown.

Supplementary Experimental Procedures

Fusion proteins and expression vectors. The cDNA for the dopamine D_4 receptor expressed in the *pcDNA3.1* vector (Invitrogen, Paisley, Scotland, UK) was amplified without its stop codon using sense and antisense primers harboring unique XhoI and EcoRI sites to be cloned it in the mammalian humanized pRluc-N1 vectors (Perkin-Elmer, Waltham, MA, USA). The cDNA for the adrenergic α_{1B} receptor gene, cloned in pOmicsLink ORF Expression Clone (GeneCopoeia, Maryland, USA) was amplified without its stop codon using sense and antisense primers harbouring unique KpnI and ApaI restriction sites, to be subcloned into KpnI/ApaI sites of the *pcDNA3.1* vector, the pRluc-N1 vector or the EYFP-N3 vector (enhanced yellow variant of YFP; Clontech, Heidelberg, Germany). Finally, the cDNA for the adrenergic β_1 receptor gene, (kindly provided by Dr. S. Dorsch, University of Wuerzburg, Germany) and D_1 receptor cloned in *pcDNA3.1* vector were amplified without their stop codon using sense and antisense primers harboring unique BamHI and HindIII sites or EcoRI and KpnI, respectively to be cloned in the EYFP-N3 vector. The resulting plasmids express the receptors fused to either Rluc or YFP on the C-terminal end of the receptor (D_4-RLuc, α_{1B}-RLuc, α_{1B}-YFP, β_1-YFP, and D_1-YFP, respectively). All constructs were verified by nucleotide sequencing and the fusion proteins were functional and expressed at the membrane level (see Results).

Cell culture and transient transfection. CHO cell were maintained in α-MEM medium without nucleosides (Invitrogen), containing 10% fetal calf serum, 50 µg/ml penicillin, 50 µg/ml streptomycin and 2 mM L-glutamine. Human embryonic kidney (HEK)-293T cells were grown in Dulbecco's modified Eagle's medium (DMEM) supplemented with 2 mM L-glutamine, 100 U/ml penicillin/streptomycin, and 5% (v/v) heat inactivated Foetal Bovine Serum (FBS) (all from Invitrogen). Cells were maintained at 37ºC in an atmosphere of 5% CO_2, and were passaged every 3 or 4 days when they were 80-90% confluent. HEK-293T or CHO cells growing in 6-well dishes or in 25 cm^2 flasks were transiently transfected with the corresponding fusion protein cDNA by the polyethylenimine (PEI) (PolyEthylenImine, Sigma, Steinheim, Germany) method as previously described (Carriba et al. 2008, Nat. Methods, 5, 727-733).

Immunostaining. For immunocytochemistry, HEK-293T cells were grown on glass coverslips and transiently transfected as indicated in Figure legends. After 48h of transfection cells were fixed in 4% paraformaldehyde for 15 min and washed with phosphate-buffered saline (PBS) containing 20 mM glycine to quench the aldehyde groups. After permeabilization with PBS containing 0.05% Triton X-100 for 15 min, cells were incubated 1 h at room temperature with PBS containing 1% bovine serum albumin and were labeled with the primary goat polyclonal anti-D_4 receptor antibody (1/500, Santa Cruz Biotechnology), rabbit anti-α_1 receptor antibody (1:100, Abcam, Cambridge, UK) or rabbit anti-β_1 receptor antibody (1:100, Santa Cruz Biotechnology) for 1 h, washed and stained with the secondary antibody Cy3 labeled anti-goat (1/200, Jackson ImmunoResearch, Baltimore, PA) or Cy3 labeled anti-rabbit (1/200, Jackson ImmunoResearch, Baltimore, PA). The D_4-YFP, α_{1B}-YFP and β_1-YFP constructs were detected by monitoring fluorescence emission at 530 nm. Samples were rinsed and observed using an Olympus FV1000 confocal microscope.

BRET assay. HEK-293T cells were co-transfected with a constant amount of cDNA encoding for the receptor fused to Rluc and with increasingly amounts of cDNA encoding to the receptor fused to YFP to measure BRET as previously described by Carriba et al. (2008). Both fluorescence and luminescence for each sample were measured at 530 nm and 480 nm respectively before every experiment to confirm similar donor expressions (approximately 100,000 bioluminescence units) while monitoring the increase in acceptor expression (2000 to 40,000 fluorescence units). The relative amounts of BRET acceptor are expressed as the ratio between the net fluorescence of the acceptor and the luciferase activity of the donor being the net fluorescence the fluorescence of the acceptor minus the fluorescence detected in cells only expressing the donor. The BRET ratio is defined as [(emission at 510-590)/(emission at 440-500)] - Cf, where Cf corresponds to (emission at 510-590)/(emission at 440-500) for the D_4-

RLuc construct expressed alone in the same experimental conditions. BRET was expressed as mili BRET Units (mBU, BRET ratio x 1000). Curves were fitted by using a non-linear regression equation, assuming a single phase with GraphPad Prism software (San Diego, CA, USA).

MAPK and Akt/PKB determination. Transfected CHO cells or pineal glands were cultured in serum-free medium for 16h before the addition of the indicated concentration of ligands for the indicated time. Both, cells and pineal glands were rinsed with ice-cold PBS and lysed by the addition of 300µl of ice-cold lysis buffer (50mM Tris-HCl pH 7.4, 50mM NaF, 150 mM NaCl, 45 mM β-glycerophosphate, 1% Triton X-100, 20 mM phenylarsine oxide, 0.4 mM $NaVO_4$ and protease inhibitor cocktail) and by shaking (cells) or sonicating (pineal glands, Branson Digital Sonifier S-250 from Branson Ultrasonic Corporation, Dambury, USA with an amplitude of 10% for 10 seconds). Cellular debris was removed by centrifugation at 13,000 g for 5 min at 4ºC and protein was quantified by the bicinchoninic acid method using bovine serum albumin as a standard. To determine the level of MAPK (ERK1/2) and Akt/PKB phosphorylation, equivalent amounts of protein (10µg) were separated by electrophoresis on a denaturing 10% SDS-polyacrylamide gel and transferred onto PVDF-FL membranes. Odyssey blocking buffer (LICOR Biosciences, Lincoln, Nebraska, USA) was then added and membranes were blocked for 90 min. Membranes were then probed for 2-3 h with a mixture of a mouse anti-phospho-ERK 1/2 antibody (1:2500, Sigma, Steinheim, Germany), a rabbit anti-phospho-Ser473-Akt antibody (1/2500, SAB Signalway Antibody, Pearland, USA) and a rabbit anti-ERK 1/2 antibody (1:40000, Sigma, Steinheim, Germany) to control differences in loading. Bands were visualized by the addition of a mixture of IRDye 800 (anti-mouse) antibody (1:10000, Sigma) and/or IRDye 680 (anti-rabbit) antibody (1:10000, Sigma) for 1 h and scanned by the Odyssey infrared scanner. Bands densities were quantified using the scanner software and exported to Excel (Microsoft, Redmond, WA, USA). The level of phosphorylated ERK 1/2 isoforms or phosphorylated Akt in the same membrane were normalized for differences in loading using the total ERK protein band intensities.

Pinealocyte culture, signaling and immunocytochemistry. Pinealocytes were prepared from rat pineal glands as previously described by Silveira Cruz-Machado et al. (2010). Briefly, pinealocytes were obtained by trypsinization (0.25%, 37°C, 15 min) followed by mechanical dispersion in the presence of fetal bovine serum. Cells were pelleted and resuspended in BGJb medium supplemented with 10% v/v fetal bovine serum (heat- inactivated), 100 U/mL penicillin/streptomycin (pH 7.4). The total number of cells and fractional survival was estimated by Trypan blue exclusion. Cells (200.000 x well) were plated on polylysine coated 6-well chamber plate and maintained at 37°C, 5% CO_2 for 48 h prior to use. For signalling experiments, pinealocytes were treated with specific agonist for 10 min, fixed in 4% paraformaldehyde for 15 min and washed with PBS containing 20 mM glycine. After permeabilization with PBS containing 0.05% Triton X-100 for 15 min, pinealocytes were treated 1 h at room temperature with PBS containing 1% bovine serum albumin and were labeled with the mouse monoclonal anti-S-arrestin 2 (1/100, Thermo Scientific, Rockford, USA) and the rabbit polyclonal anti-phospho-Thr^{202}/Tyr^{204} ERK1/2 (1/300, Cell Signaling Technology, Danvers, MA) for 1 h, washed and stained with the secondary chicken anti-rabbit (1/200, Alexa Fluor 594, Invitrogen) and goat anti-mouse (1/200, Alexa Fluor 488, Invitrogen). For D_4, α_{1B} or β_1 receptor staining pinealocytes were labeled with the goat anti D_4 receptor antibody (1:100, Santa Cruz Biotechnology, Heidelberg, Germany), rabbit anti-α_1 receptor antibody (1:100, Abcam, Cambridge, UK) or rabbit anti-β_1 receptor antibody (1:100, Santa Cruz Biotechnology) and mouse monoclonal anti-S-arrestin 2 (1/100, Thermo Scientific) and the secondary antibody Cy3 labeled anti-goat (1/200, Jackson ImmunoResearch, Baltimore, PA) or Cy3 labeled anti-rabbit (1/200, Jackson ImmunoResearch) and Cy3 labeled anti-mouse (1/200, Jackson ImmunoResearch. Samples were rinsed and observed in a Leica SP2 confocal microscope.

In Situ Proximity Ligation Assay (PLA). The primary cultures of pinealocytes were fixed and permeabilized as described above. The receptor-receptor molecular interaction was detected using the Duolink II in situ PLA detection Kit (OLink; Bioscience, Uppsala, Sweden). After 1 h incubation at 37°C with the blocking solution in a pre-heated humidity chamber, pinealocytes were incubated overnight with the primary antibodies: goat anti-D_4 antibody (1:100, Santa Cruz Biotechnology, Heidelberg, Germany) and rabbit anti-α_1 antibody (1:100, Abcam, Cambridge, UK) to detect α_{1B}-D_4 receptor heteromers, goat anti-D_4 antibody and rabbit anti β_1 antibody (1:100, Santa Cruz Biotechnology) to detect β_1-D_4 receptor heteromers or rabbit anti-α_1 antibody and goat anti-β_1 antibody (1:100, Abcam) to detect α_{1B}-β_1 receptor heteromers, in the antibody diluent medium. The pinealocytes were washed with wash buffer A at room temperature and incubated for 2 h in a pre-heated humidity chamber at 37°C with PLA probes detecting rabbit or goat antibodies (Duolink II PLA probe anti-Rabbit plus and Duolink II PLA probe anti-Goat minus diluted in the antibody diluent to a concentration of 1:5). After washing with wash buffer A at room temperature, pinealocytes were incubated in a pre-heated humidity chamber for 30 min at 37°C, with the ligation solution (Duolink II Ligation stock 1:5 and Duolink II Ligase 1:40). Detection of the amplified probe was done with the Duolink II Detection Reagents Red Kit. After exhaustively washing at room temperature with wash buffer B, the pinealocytes were mounted using the mounting medium with DAPI. The samples were observed in a Leica SP2 confocal microscope. As negative controls for the technique, the same procedure was done but omitting the primary antibodies. As negative control for heteromerization, heteromers between α_{1B} and β_1 receptors were tested.

Serotonin synthesis and release determination. After 36 h of culture in BGJb medium (Invitrogen, Carlsbad, CA), the pineal glands were incubated in HBSS medium supplemented with 0,1% glucose, 100 U/ml penicillin/streptomycin and 1mg/ml bovine serum albumin for 12 h with specific agonist and/or antagonist and radioactive [^{14}C]-Tryptophan (10 μM). After incubation, medium and pineal glands were collected separately into eppendorf tubes with 35 μl of trichloroacetic acid (TCA 1%) and were kept at 4ºC. Pineal glands were homogenized in a Dynatech/Sonic Dismembrator (Dynatech Labs, Chantilly, VA) for 15 seconds. An aliquot was reserved for protein quantification by the Lowry method and cellular debris were removed by centrifugation at 10,000 g for 10 min at 4ºC. [^{14}C]-Serotonin present in the supernatant was separated from [^{14}C]-Tryptophan by HPLC coupled to detection by fluorescence (excitation: 252nm; emission:382). The chromatography system consisted of a reverse-phase C18 column (2.5μm particle Fortis C18, 100 x 4.6, Sugelabor, Spain) and an ion-pair mobile phase, made up of 500mM sodium acetate, 500mM citric acid, 1mM EDTA, 5 mM octanesulfonic acid plus 20% methanol (v/v) , pH 3.8. The flow rate was 1ml/min. Serotonin fractions were recovered in scintillation vials, mixed with Optiphase HiSafe III cocktail, and [^{14}C]-serotonin was quantified in a liquid scintillation counter.

Rafael Franco Fernández y Carme Lluís Biset
Grupo de Neurobiología Molecular
Departamento de Bioquímica y Biología Molecular
Av. Diagonal, 643
Edificio Nuevo, Planta-2
08028 Barcelona

La tesis doctoral de Estefanía Moreno Guillén **"Heterómeros de receptores de dopamina. Nuevos mecanismos para la regulación de la transmisión dopaminérgica"** se presenta como un compendio de publicaciones.

En el apartado de **RESULTADOS** se presentan los siguientes trabajos:

El manuscrito "**Dopamine–Galanin Receptor Heteromers Modulate Cholinergic Neurotransmission in the Rat Ventral Hippocampus**" ha sido publicado en *Journal of Neuroscience.* Esta revista tiene un factor de impacto de 7.271 y se encuentra en el primer decil, (17/239), del área *Neurosciences*. El manuscrito "**Marked changes in signal transduction upon heteromerization of dopamine D_1 and histamine H_3 receptors**" ha sido publicado en *British Journal of Pharmacology.* Esta revista tiene un factor de impacto de 4.925, y se encuentra en el primer decil, (19/252), del área *Pharmacology and Pharmacy*. El manuscrito "**Dopamine D_1-histamine H_3 Receptor Heteromers Provide a Selective Link to MAPK Signaling in GABAergic Neurons of the Direct Striatal Pathway**" ha sido publicado en *Journal of Biological Chemistry,* revista con un factor de impacto de 5.328, que se encuentra en el primer cuartil, (50/286), dentro de *Biochemistry and Molecular Biology*. El manuscrito "**Direct involvement of σ-1 receptors in the dopamine D_1 receptor-mediated effects of cocaine**" ha sido publicado en *Proceedings of the National Academy of Sciences of USA.* Esta revista tiene un factor de impacto de 9.771 y se encuentra en el primer decil, (3/59), del área *Multidisciplinary Sciences*. El manuscrito "**Cocaine inhibits D_2 receptor signalling via sigma-1-dopamine D_2 receptor heteromers**" ha sido enviado a *Proceedings of the National Academy of Sciences of USA*, revista con un factor de impacto de 9.771, que se encuentra en el primer decil, (3/59), dentro de *Multidisciplinary Sciences*. El manuscrito "**Dopamine D_4 receptor, but not the ADHD-associated $D_{4.7}$ variant, forms functional heteromers with the dopamine D_{2S} receptor in the brain**" ha sido publicado en *Molecular Psychiatry.* Esta revista tiene un factor de impacto de 15.470, y se encuentra en el primer decil, (5/286, 4/239 y 1/128), de las áreas *Biochemistry and Molecular Biology*, *Neurosciences* y *Psychiatry*. El manuscrito "**Circadian-related heteromerization of adrenergic and dopamine D_4 receptors modulates melatonin synthesis and release in the pineal gland**" ha sido enviado a *Plos Biology*, revista con un

factor de impacto de 12.472, que se encuentra en el primer decil, (9/286, 1/86), de las áreas *Biochemistry and Molecular Biology* y *Biology.*

El trabajo "**Dopamine–Galanin Receptor Heteromers Modulate Cholinergic Neurotransmission in the Rat Ventral Hippocampus**", la doctoranda es co-primer autor del trabajo junto con Sandra H. Vaz. La doctoranda Estefanía Moreno ha realizado la totalidad del trabajo experimental exceptuando los experimentos de *pull-down*, los experimentos de liberación de acetilcolina en sinaptosomas y los experimentos de determinación de potenciales postsinápticos excitatorios.

En el trabajo "**Marked changes in signal transduction upon heteromerization of dopamine D_1 and histamine H_3 receptors**", la doctoranda Estefanía Moreno ha realizado una parte de los experimentos de transferencia de energía de resonancia bioluminiscente, de los experimentos de unión de radioligandos y de los experimentos de determinación de AMPc.

En el trabajo "**Dopamine D_1-histamine H_3 Receptor Heteromers Provide a Selective Link to MAPK Signaling in GABAergic Neurons of the Direct Striatal Pathway**", la doctoranda Estefanía Moreno ha realizado la totalidad del trabajo experimental.

En el trabajo "**Direct involvement of σ-1 receptors in the dopamine D_1 receptor-mediated effects of cocaine**", Estefanía Moreno ha realizado los experimentos de determinación de AMPc y los experimentos de señalización efectuados con muestras de ratones.

En el trabajo "**Cocaine inhibits D_2 receptor signalling via sigma-1-dopamine D_2 receptor heteromers**", la doctoranda ha realizado una parte de los experimentos de transferencia de energía de resonancia bioluminiscente y los experimentos de señalización efectuados con muestras de ratones.

En el trabajo "**Dopamine D_4 receptor, but not the ADHD-associated $D_{4.7}$ variant, forms functional heteromers with the dopamine D_{2S} receptor in the brain**", la doctoranda Estefanía Moreno ha realizado los experimentos de señalización efectuados con muestras de ratones.

En el trabajo "**Circadian-related heteromerization of adrenergic and dopamine D_4 receptors modulates melatonin synthesis and release in the pineal gland**", la doctoranda Estefanía Moreno ha realizado los experimentos de *In Situ Proximity Ligation Assay* (PLA).

La Dra. Carla Ferrada ha utilizado una primera versión del manuscrito "**Marked changes in signal transduction upon heteromerization of dopamine D_1 and histamine H_3 receptors**" para la elaboración de su tesis doctoral. La Dra. Hanne Hoffmann ha utilizado una primera versión del manuscrito "**Dopamine D_1-histamine H_3 Receptor Heteromers Provide a Selective Link to MAPK Signaling in GABAergic Neurons of the Direct Striatal Pathway**" para la elaboración de su tesis doctoral. La Dra. Gemma Navarro ha utilizado una primera

versión del manuscrito "**Direct involvement of σ-1 receptors in the dopamine D_1 receptor-mediated effects of cocaine**" para la elaboración de su tesis doctoral.

En el apartado de **ANEXOS** se presentan los siguientes manuscritos:

El manuscrito "**Production of functional recombinant G-protein coupled receptors for heteromerization studies**" ha sido publicado en *Journal of Neuroscience Methods* con un factor de impacto de 2.100, esta revista se encuentra en el tercer cuartil, (158/239), del área *Neurosciences*. El manuscrito "**Interactions between Intracellular Domains as Key Determinants of the Quaternary Structure and Function of Receptor Heteromers**" ha sido publicado en *Journal of Biological Chemistry*, revista con un factor de impacto de 5.328, que se encuentra en el primer cuartil, (50/286), en el área *Biochemistry and Molecular Biology*. El manuscrito "**A_{2A} adenosine receptor ligand binding and signalling is allosterically modulated by adenosine deaminase**" ha sido publicado en *Biochemical Journal*. Esta revista tiene un factor de impacto de 5.016 y se encuentra en el primer cuartil, (55/286), en el área *Biochemistry and Molecular Biology*. El manuscrito "**Homodimerization of adenosine A_1 receptors in brain cortex explains the biphasic effects of caffeine**" ha sido enviado a *Biochemical Pharmacology,* revista con un factor de impacto de 4.889 y se encuentra en el primer cuartil (20/252), del área *Pharmacology and Pharmacy*.

En el trabajo "**Production of functional recombinant G-protein coupled receptors for heteromerization studies**", la doctoranda ha realizado parte del trabajo de obtención de las proteínas de fusión.
En el trabajo "**Interactions between Intracellular Domains as Key Determinants of the Quaternary Structure and Function of Receptor Heteromers**", Estefanía Moreno ha llevado a cabo los experimentos de señalización realizados con muestras de ratones.
En el trabajo "**A_{2A} adenosine receptor ligand binding and signalling is allosterically modulated by adenosine deaminase**", la doctoranda ha realizado los experimentos de transferencia de energía de resonancia bioluminiscente.
El trabajo "**Homodimerization of adenosine A_1 receptors in brain cortex explains the biphasic effects of caffeine**" la doctoranda es co-primer autor del trabajo junto con el Dr. Eduardo Gracia. Estefanía Moreno ha realizado la totalidad del trabajo experimental exceptuando los experimentos de unión de radioligandos.

La Dra. Gemma Navarro ha utilizado una primera versión del manuscrito "**Interactions between Intracellular Domains as Key Determinants of the Quaternary Structure and Function of Receptor Heteromers**" para la elaboración de su tesis doctoral. El Dr. Eduardo

Gracia ha utilizado los manuscritos "**A_{2A} adenosine receptor ligand binding and signalling is allosterically modulated by adenosine deaminase**" y "**Homodimerization of adenosine A_1 receptors in brain cortex explains the biphasic effects of caffeine**" para la elaboración de su tesis doctoral.

Barcelona, a 13 de Febrero de 2012

Dr. Rafael Franco Fernández

Dra. Carme Lluís Biset

RESUMEN DE RESULTADOS Y DISCUSIÓN

4. RESUMEN DE RESULTADOS Y DISCUSIÓN

A pesar de una cierta resistencia inicial por parte de la comunidad científica, la existencia de heterómeros entre diversos receptores de neurotransmisores y neuromoduladores es, hoy por hoy, un hecho aceptado. La heteromerización implica cambios en la forma de entender la neurotransmisión. Así, los receptores no pueden considerarse como una única unidad funcional, sino como agregados multimoleculares localizados en el plano de la membrana plasmática (Franco *et al.* 2003). La heteromerización confiere a los receptores propiedades bioquímicas distintas de los componentes individuales, como cambios en la funcionalidad y en las propiedades farmacológicas (Terrillon and Bouvier 2004). Los ensayos de doble híbrido, pull-down o coinmunoprecipitación han hecho posible la construcción de mapas de las redes moleculares formadas por interacciones proteína-proteína entre las proteínas citosólicas; sin embargo, estas técnicas se ven limitadas cuando se analizan proteínas de membrana. Recientemente, el desarrollo de las técnicas biofísicas basadas en la transferencia de energía de resonancia, como BRET y FRET han facilitado la demostración de la homodimerización y heterodimerización de proteínas de membrana y especialmente GPCR, en células vivas, siendo hoy en día un hecho aceptado el que los GPCR pueden existir como complejos oligoméricos (Bouvier 2001; Agnati *et al.* 2003; Franco *et al.* 2003; Milligan *et al.* 2004; Pfleger *et al.* 2006; Ferré *et al.* 2007). Dado que los heterómeros se definen como complejos macromoleculares compuestos al menos por dos receptores funcionales distintos y que presentan propiedades bioquímicas que son diferentes a las de los receptores individuales que los constituyen, se pueden considerar como nuevas entidades funcionales que hay que tener en cuenta como nuevas dianas para el desarrollo de fármacos. Los resultados descritos en esta Tesis ponen de manifiesto la formación de heterómeros entre receptores de dopamina y otros receptores que están implicados en la regulación de la transmisión dopaminérgica, como receptores de galanina, histamina, adrenérgicos o receptores σ-1 y muestran el papel fundamental que alguno de estos heterómeros puede desempeñar en el hipocampo, en el estriado o en la glándula pineal.

Teniendo en cuenta que tanto la galanina como la dopamina modulan la liberación de acetilcolina en el hipocampo, se ha investigado, en primer lugar, si los receptores de dopamina de la familia D_1 (receptores D_1 y D_5) pueden formar heterómeros con los receptores de galanina y se ha estudiado la función de estos heterómeros en la liberación de acetilcolina en el hipocampo. A través de una aproximación multidisciplinar, en el trabajo ***"Dopamine–Galanin Receptor Heteromers Modulate Cholinergic Neurotransmission in the Rat Ventral Hippocampus"*** se muestra, por primera vez, que los receptores de dopamina de la familia D_1

(receptores D_1 y D_5) forman heterómeros con los receptores de galanina Gal_1 pero no con los receptores Gal_2, tanto en células transfectadas como en el hipocampo ventral de rata. La activación con agonistas y el bloqueo con antagonistas de los receptores de dopamina en los heterómeros D_1-Gal_1 y D_5-Gal_1, potencia y contrarresta, respectivamente, la activación de la vía de las MAPK inducida por la estimulación del receptor Gal_1, mientras que los ligandos del receptor Gal_1 no modifican la activación de la vía de las MAPK mediada por los receptores de dopamina. Un resultado interesante de este trabajo es la demostración de que la dopamina y la galanina funcionan coordinadamente para modular la neurotransmisión colinérgica en el hipocampo ventral y que esta modulación puede darse vía heterómeros entre receptores D_1 o D_5 y receptores Gal_1.

La capacidad de los receptores de dopamina D_1 y D_5 para formar heterómeros con los receptores de galanina Gal_1, pero no con los receptores Gal_2, se ha demostrado mediante la técnica de BRET utilizando células transfectadas con ambos receptores. Desde el punto de vista estructural, la selectividad para formar heterómeros con los receptores Gal_1 y no con los Gal_2 no es sorprendente si se considera que estos dos receptores de galanina presentan una similitud relativamente baja en sus secuencias aminoacídicas (Branchek *et al.* 2000). Los receptores de dopamina D_1 y D_5, son capaces de competir para heteromerizar con el receptor Gal_1, lo que sugiere que ambos receptores interaccionan con los mismos dominios, o dominios muy relacionados, del receptor de galanina. Por otro lado, tan solo el extremo C-terminal del receptor D_5, pero no del receptor D_1, ha sido capaz de precipitar al receptor Gal_1 a partir de preparaciones de membrana de células transfectadas. Ello sugiere que en la formación de los heterómeros están involucradas regiones adicionales al extremo C-terminal de los receptores de dopamina y que existen diferencias entre los receptores D_1 y D_5 en las regiones implicadas en la heteromerización con los receptores Gal_1.

Uno de los principales retos en el estudio de las interacciones moleculares entre receptores de membrana es la identificación de heterómeros en tejidos nativos. Una aproximación es la co-inmunoprecipitación a partir de membranas tisulares. Sin embargo, problemas de solubilidad de los receptores, así como la falta de anticuerpos fiables, dificultan la interpretación de los experimentos de co-inmunoprecipitación. Por otro lado, las aproximaciones espectroscópicas actuales, con pocas excepciones, carecen de la resolución apropiada para una aproximación *in situ* a nivel molecular. Estas limitaciones hacen que se requieran aproximaciones indirectas para validar la presencia de heterómeros en tejidos nativos, tales como la determinación de una propiedad bioquímica del heterómero, la cual puede ser usada como una huella dactilar (*fingerprint*) para su localización tisular (Ferré *et al.* 2009). El antagonismo cruzado (*cross-antagonism)*, en el que un antagonista de los receptores $D_{1/5}$ es

capaz de bloquear el efecto de un agonista del receptor Gal_1, es difícil de explicar mediante un mecanismo que no implique la heterodimerización de receptores, teniendo en cuenta que un antagonista no induce señalización intracelular. Este antagonismo cruzado se ha utilizado como huella dactilar de los heterómeros $D_{1/5}$-Gal_1 para su localización en el hipocampo. Utilizando este criterio y evaluando la activación de la vía de las MAPK, se han podido identificar heterómeros de receptores $D_{1/5}$-Gal_1 en el hipocampo ventral, pero no en el hipocampo dorsal donde la expresión de receptores Gal_2 predomina sobre la de Gal_1.

Otra característica importante de los heterómeros entre receptores de dopamina y galanina es que la estimulación de los receptores D_1 o D_5 en células transfectadas potencia la activación de receptores Gal_1 pero no de Gal_2 por sus agonistas, pero la estimulación del receptor Gal_1 no modifica la señal mediada por los receptores D_1 o D_5. En preparaciones sinaptosomales de hipocampo, ni la estimulación de los receptores Gal_1 ni la de los receptores $D_{1/5}$ a concentraciones nanomolares de sus agonistas, produce ninguna modificación en la liberación de acetilcolina inducida por K^+; no obstante, la activación previa de receptores $D_{1/5}$ desencadena que la galanina facilite la liberación de acetilcolina. También de manera paralela a lo que ocurre en células transfectadas, la galanina no modifica el que los agonistas de los receptores $D_{1/5}$ no ejerzan ningún efecto sobre la liberación de acetilcolina. Como los receptores D_5 predominan sobre los receptores D_1 en el hipocampo (Ciliax *et al.* 2000) y como se ha descrito previamente que los receptores D_5 están implicados en la modulación de la liberación de acetilcolina en el hipocampo (Hersi *et al.* 2000; Laplante *et al.* 2004b), es probable que el subtipo D_5 de la familia de receptores D_1 forme heterómeros con el receptor Gal_1 en las terminales colinérgicas del hipocampo ventral.

En estudios previos se había descrito que la galanina inhibía la neurotransmisión colinérgica hipocampal (Fisone *et al.* 1987; Ögren *et al.* 1998; Laplante *et al.* 2004a). En muchos de estos estudios se han aplicado técnicas de microdiálisis *in vivo* en las que se han utilizado concentraciones muy altas (micromolar) de galanina (Ögren *et al.* 1998; Laplante *et al.* 2004a) y una concentración de acetilcolina extracelular incrementada artificialmente por la adición de inhibidores de la acetilcolinesterasa en el medio de perfusión. El uso de estos inhibidores en el medio de diálisis ha suscitado polémica respecto a la posibilidad de que los resultados sean artefactuales no sólo de forma cuantitativa si no también cualitativa (DeBoer and Abercrombie 1996; Acquas and Fibiger 1998). Se ha descrito que a nivel de las sinapsis glutamatérgicas *Schaffer-CA1* del hipocampo ventral, las concentraciones pequeñas (nanomolar) de galanina tienen un efecto inhibidor, siempre y cuando los receptores de dopamina no esten activados. Este resultado concuerda con la expresión de receptores Gal_1 en el área *CA1* del hipocampo ventral (O'Donnell *et al.* 1999) y el efecto depresor de la galanina,

independiente de acetilcolina, puede estar relacionado con su capacidad de reducir la neurotransmisión glutamatérgica en el hipocampo (Zini *et al.* 1993; Mazarati *et al.* 2000). En este trabajo nosotros observamos que el agonista de los receptores $D_{1/5}$, inefectivo administrado por sí solo, cambiaba el efecto inhibidor de la galanina a un efecto activador. Este fenómeno es dependiente de la neurotransmisión colinérgica ya que se bloquea por un antagonista del receptor muscarínico de acetilcolina. A partir de los resultados obtenidos con preparaciones sinaptosomales de hipocampo ventral y de cortes hipocampales, se propone un modelo sobre el papel de la galanina en las sinapsis de *Schaffer-CA1* en el hipocampo ventral: un incremento aislado de la actividad de las señales colinérgicas en el septohipocampo produce una modesta liberación de acetilcolina y galanina. Esta modesta liberación de galanina debería ser suficiente para inhibir la excitabilidad de las sinapsis glutamatérgicas actuando sobre los receptores de galanina pre- o post-sinápticos. Sin embargo, teniendo en cuenta que se puede producir el incremento simultáneo en la actividad del área tegmental ventral (VTA) con el consiguiente incremento dopaminérgico en el hipocampo, la coactivación de los receptores $D_{1/5}$ y los receptores de galanina localizados en las terminales colinérgicas inducen una fuerte liberación de acetilcolina, la cual supera el efecto inhibidor de la galanina y lleva a un incremento de la excitabilidad en las sinapsis glutamatérgicas.

Las interacciones descritas en este trabajo ocurren en el hipocampo ventral pero no en el dorsal. Estas dos áreas hipocampales presentan conexiones eferentes distintas con respecto al resto del cerebro, es decir, que mientras el hipocampo dorsal está conectado principalmente con la neocorteza, el hipocampo ventral está conectado con estructuras subcorticales, como el hipotálamo y la amígdala (Naber and Witter 1998). Puesto que la amígdala y el hipotálamo controlan la actividad del eje hipotálamo-pituitaria-adrenal, no debe sorprender que la función principal del hipocampo ventral sea el procesamiento de la información relacionada con comportamientos emotivos, como recientemente se ha demostrado (Segal *et al.* 2010). Cabe destacar que una inyección de acetilcolina en el hipocampo ventral, pero no en el dorsal, reduce la ansiedad (Degroot and Treit 2004). Es posible especular que la activación inducida por la galanina, dependiente de acetilcolina, en las sinapsis excitatorias de Schaffer-CA1 (el último punto de la señal eferente excitatoria del hipocampo) puede influir en el control de la ansiedad y de la memoria emocional.

En conjunto, nuestros resultados sugieren claramente que los heterómeros de los receptores $D_{1/5}$-Gal_1 localizados en las terminales nerviosas colinérgicas juegan un papel importante en la modulación de la neurotransmisión colinérgica en el hipocampo ventral. Este trabajo proporciona un claro ejemplo de que los heterómeros de receptores actúan como un procesador que integra señales de diferentes neurotransmisores y modulan la señalización

celular y la función neuronal. Ya que los heterómeros de receptores están siendo, cada vez más, considerados como dianas farmacológicas (George *et al.* 2002; Ferré *et al.* 2010), los heterómeros de los receptores D_1-Gal_1 y D_5-Gal_1 podrían ser considerados dianas para fármacos utilizados en la enfermedad de Alzheimer, teniendo en cuenta la implicación del sistema colinérgico septohipocampal en la enfermedad (Mitsukawa *et al.* 2008; Ögren *et al.* 2010). De manera relevante, los receptores D_1, D_5 y Gal_1 colocalizan en otras zonas del cerebro además de en el hipocampo, como en la sustancia negra o la VTA (Schilström *et al.* 2006; Picciotto 2008). Si los heterómeros de los receptores $D_{1/5}$-Gal_1 están también presentes en células mesencefálicas dopaminérgicas, podrían resultar dianas en el tratamiento de desórdenes neuropsiquiátricos relacionados con la dopamina, incluida la adicción a drogas. Finalmente, la capacidad de los receptores de galanina de heterodimerizar con otros GPCRs en otras regiones del SNC podría esclarecer hallazgos farmacológicos que hasta este momento han sido difíciles de explicar, como el conocido efecto bifásico dosis-dependiente de la galanina en la nocicepción (Xu *et al.* 2008).

Aparte del hipocampo, los receptores de dopamina desempeñan un papel muy relevante en el estriado. Los receptores D_1 y D_2 están predominantemente localizados en las neuronas GABAérgicas dinorfinérgicas y GABAérgicas encefalinérgicas, respectivamente (Starr *et al.* 1987; Rubinstein *et al.* 1988; Ferré *et al.* 1991a; Ferré *et al.* 1994). Las neuronas GABAérgicas dinorfinérgicas y GABAérgicas encefalinérgicas dan origen a dos sistemas estriatales eferentes que conectan el estriado con las estructuras de salida de los ganglios basales: la sustancia nigra pars reticulata y el segmento interno del globus pallidus (núcleo entopeduncular en roedores) (Gerfen 2004) y que se denomina vía directa y vía indirecta, respectivamente. La vía directa está constituida por neuronas GABAérgicas dinorfinérgicas, las cuales conectan directamente el estriado con las estructuras de salida. La vía indirecta está constituida por neuronas GABAérgicas encefalinérgicas que conectan el estriado con el segmento externo del globus pallidus (globus pallidus en roedores), por neuronas GABAérgicas que conectan el globus pallidus con el núcleo subtalámico y por las neuronas glutamatérgicas que conectan el núcleo subtalámico con las estructuras de salida (Gerfen 2004). La estimulación de la vía directa resulta en la activación motora y la estimulación de la vía indirecta produce la inhibición motora. La dopamina y los agonistas dopaminérgicos inducen la activación motora por activación de la vía directa (actuando sobre los receptores D_1 activadores de las neuronas GABAérgicas dinorfigénicas) y por depresión de la vía indirecta (actuando sobre los receptores D_2 inhibidores de las neuronas GABAérgicas encefalinérgicas) (Gerfen 2004). Por otra parte, el estriado contiene una alta densidad postsináptica de receptores de histamina H_3, los cuales están colocalizados con los receptores D_1 o D_2 en las neuronas GABAérgicas dinorfigénicas y las neuronas GABAérgicas encefalinérgicas respectivamente (Ryu *et al.* 1994a; Pillot *et al.* 2002).

Además de los receptores H_3 postsinápticos se ha descrito la existencia de receptores H_3 presinápticos en las terminales glutamatérgicas y dopaminérgicas, donde inhiben la liberación de glutamato y dopamina (Schlicker *et al.* 1993; Molina-Hernandez *et al.* 2000; Doreulee *et al.* 2001; Molina-Hernandez *et al.* 2001; Munzar *et al.* 2004). A pesar de la codistribución de receptores de histamina y de dopamina en el estriado, al iniciarse esta Tesis no estaba claro si existía una interacción entre ambos receptores y cual podía ser la naturaleza de esta interacción. Se habían descrito interacciones antagónicas entre los receptores H_3 y D_1 que podían explicarse por una interacción antagónica a nivel de la producción de AMPc. Sin embargo, no se podía descartar la existencia de una interacción molecular entre ambos receptores en las membranas de las neuronas GABAérgicas dinorfinérgicas y que los receptores H_3 y D_1 pudiesen heteromerizar de manera similar a como lo hacen los receptores H_3 y D_2 (Ferrada *et al.* 2008). Por todo ello, en esta Tesis se ha investigado la heteromerización de receptores H_3 y D_1 utilizando un modelo celular neuronal. En el trabajo ***"Marked changes in signal transduction upon heteromerization of dopamine D_1 and histamine H_3 receptors"***, se ha demostrado que cuando los receptores D_1 y H_3 se coexpresan son capaces de formar el heterómeros. La heteromerización de estos receptores se ha demostrado mediante la técnica de BRET en células transfectadas de manera transitoria con ambos receptores y, también, mediante ensayos de unión de radioligandos (*heteromer fingerprint*) en neuroblastomas humanos SK-N-MC/D_1H_3, en los cuales el agonista específico del receptor H_3 produce la desaparición de la cooperatividad y un cambio significativo en la afinidad en la unión del agonista del receptor D_1.

Al parecer, muchos, sino todos, los miembros de la superfamilia de los GPCRs pueden existir en forma de homodímeros (Bouvier 2001; Devi 2001; Marshall 2001; Rios *et al.* 2001; George *et al.* 2002; Franco *et al.* 2003; Terrillon and Bouvier 2004; Prinster *et al.* 2005; Milligan 2006). Una de las características de la homodimerización es que la unión de un ligando a un receptor puede modificar la afinidad del ligando por el segundo receptor en el homodímero, produciéndose un fenómeno de cooperatividad. La primera evidencia de la existencia de heterómeros de GPCRs fue obtenida a través de experimentos de unión de radioligandos, poniendo de manifiesto la existencia de interacciones bioquímicas entre diferentes GPCRs en preparaciones de membrana de cerebro (Agnati *et al.* 2003). Hoy en día se contempla la posibilidad de que los heterómeros estén constituidos, al menos, por la interacción de homodímeros (Cristóvão-Ferreira *et al.* 2011). En este tipo de interacciones, conocidas inicialmente como "interacciones receptor-receptor intramembrana", la estimulación de un homómero altera las características de unión de ligando al otro homómero en preparaciones de membrana, pudiendo alterar tanto la afinidad por el ligando como la cooperatividad (Agnati *et al.* 2003). La utilización de preparados de membrana implica la ausencia de la maquinaria de señalización intracelular y sugiere algún tipo de interacción alostérica entre receptores

(homómeros) adyacentes. Actualmente, esto se considera una característica bioquímica del heterómero (Ferré *et al.* 2007; Franco *et al.* 2007a; Ferré *et al.* 2009). En este trabajo, mediante la técnica de BRET en células embrionarias humanas transfectadas transitoriamente y mediante experimentos de unión de radioligandos en neuroblastomas SK-N-MC/D_1H_3, se ha demostrado que los receptores de dopamina D_1 y de histamina H_3 son capaces de formar heterómeros. La unión de un agonista específico al receptor H_3 produce la desaparición de la cooperatividad en la unión del agonista del receptor D_1, además de producir un cambio significativo en la afinidad del receptor D_1 para su agonista.

La interacción que se da vía heterómeros de receptores presenta diferentes componentes. Uno de ellos son los cambios farmacológicos, es decir, cambios en las características de unión de un receptor ante la activación del receptor adyacente. El otro componente es la interacción a nivel de segundos mensajeros. En heterómeros en los que uno de los receptores constituyentes está acoplado a proteína $G_{i/0}$, mientras que el otro está acoplado a proteína G_s, como ocurre para el heterómero H_3-D_1, la coactivación de los receptores puede dar lugar no solo a un antagonismo funcional, sino a mensajes contradictorios para la célula. En algunos casos se ha determinado que la heteromerización solventa este problema, ya que modifica la señalización respecto a los receptores que no heteromerizan. El cambio en la señalización se ha descrito para heterómeros de un mismo neurotransmisor (Jordan and Devi 1999; George *et al.* 2000; Fan *et al.* 2005; Ciruela *et al.* 2006; Rashid *et al.* 2007). En neuronas que coexpresan receptores D_1, acoplados a proteína G_s, y receptores D_2, acoplados a proteína $G_{i/0}$, los heterómeros de receptores D_1-D_2 se acoplan a proteína G_q (Rashid *et al.* 2007). Esto hace posible que un único neurotransmisor pueda aumentar o disminuir los niveles de AMPc o modificar los niveles de calcio intracelular dependiendo de que una neurona (o microdominio de una neurona), exprese receptores D_1, receptores D_2 o heterómeros de receptores D_1-D_2 de dopamina, respectivamente. Hoy en día es evidente que los heterómeros son mecanismos que añaden diversidad al efecto de un neurotransmisor; sin embargo, el papel de la heteromerización de receptores para dos neurotransmisores diferentes, acoplados a proteína $G_{i/o}$ y a G_s, era todavía materia de debate.

Con los heterómeros de receptores D_1-H_3 pueden interactuar dos neurotransmisores diferentes, dopamina e histamina. En células de neuroblastoma que co-expresan los receptores D_1 y H_3, no se detecta un cambio a un tipo diferente de proteína G como ocurre en el heterómero D_1-D_2 (Rashid *et al.* 2007) sino que se produce un cambio en la proteína G que se acopla al receptor D_1, pasando de G_s a G_i, a la cual los receptores H_3 ya están unidos. De hecho, en presencia del receptor H_3, el receptor D_1 no está acoplado a proteína $G_{s,}$ de manera que no pueden activar a la adenilato ciclasa y al estar acoplado a G_i la inhibe. De este modo, en

modelos celulares, la dopamina, vía el heterómero D_1-H_3, no es capaz de incrementar los niveles de AMPc, pero si puede desencadenar eventos mediados por G_i. Por otro lado, en células que co-expresan los dos receptores, el receptor H_3 puede señalizar a través de la adenilato ciclasa (inhibiendo la actividad de la enzima) y también por la vía MAPK (incrementando la fosforilación de ERK 1/2). La activación de los receptores H_3 no produce señalización a través de la vía de la MAP cinasa a menos que los receptores H_3 se coexpresen con los receptores de dopamina D_1. Estos resultados indican que los heterómeros de receptores D_1-H_3 constituyen un "dispositivo" único para dirigir las señalización dopaminérgica e histaminérgica hacia la vía MAPK, de forma independiente de la proteína G_s y dependiente de la proteína G_i. Se observa que en clones de células SK-N-MC transfectadas de forma estable con el receptor H_3, expresado a niveles fisiológicos (0.1-1 pmol-(mg proteina)$^{-1}$), el agonista de este receptor no promueve la fosforilación de ERK 1/2 a menos que se co-exprese el receptor D_1.

Nuestros resultados concuerdan con la estequiometria 1:2 (proteína G: interacción de receptores) descrita por Herrick-Davis *et al.* 2005. Si se considera que los GPCR son monoméricos, es lógico pensar que un GPCR interactúa con una proteína G; sin embargo, estos autores observaron que la coexpresión del receptor de serotonina 5-HT_{2C} con una forma mutada de este receptor, que no era capaz de unir ligando ni de estimular la señalización a través de inositol fosfato pero formaba dímeros con 5-HT_{2C}, no tenía efecto en la unión de ligando al receptor no mutado, pero producía la inhibición de la producción de inositol fosfato. Por lo tanto, el receptor de serotonina 5-HT_{2C} inactivo inhibía la función del receptor nativo por la formación de una especie dimérica no funcional, lo que sugería un modelo en el que un dímero de GPCR une dos moléculas de ligando y una única proteína G (Herrick-Davis *et al.* 2005). Análogamente, cuando expresamos receptores D_1 y una versión mutada del receptor H_3, que no es capaz de unir agonista ni de señalizar, la activación del receptor D_1 por su agonista específico no activa la vía de las MAPK. Estos resultados sugieren que la señal de D_1 a través de la vía de la MAP cinasa está mediada por el receptor H_3 en células que coexpresan ambos receptores, indicando que en la activación de GPCR se produce una interacción dinámica entre protómeros del heterómero tal como demostró Brock para dímeros del receptor metabotrópico de glutamato (Brock *et al.* 2007). La explicación más adecuada para los resultados obtenidos, sería que los receptores D_1 serían capaces de señalizar a través de la vía de las MAPK en ausencia de los receptores H_3, pero en presencia de estos, la señalización a través de ERK 1/2 estaría mediada por los receptores H_3 y no por los receptores D_1. Por otra parte, los resultados mostrados en esta Tesis son consistentes con la evidencia de que en la activación de un homo- o un heterodímero interviene un único protómero, tal como ha sido demostrado para receptores metabotrópicos de glutamato (Hlavackova *et al.* 2005). Para estos últimos receptores se forman dímeros de manera constitutiva y su actividad no disminuye al bloquear uno de los dominios heptahelicoidales en

su estado inactivo. Los resultados de esta Tesis sugieren que podría estar operando un mecanismo similar en heterómeros formados por otros miembros de la superfamilia de GPCR, ya que en el heterómero de receptores D_1-H_3 no solo el antagonista de cada uno de los receptores, sino que el antagonista del receptor adyacente puede contrarrestar el efecto de la activación de los receptores D_1 o de los receptores H_3. Así, el antagonista de una de las unidades del heterómero D_1-H_3 puede inducir cambios conformacionales en la otra unidad del heterómero y bloquear señales específicas originadas en el heterómero. Este hecho amplia las posibles terapias para antagonistas de los GPCR.

Los resultados comentados anteriormente indican que, en células transfectadas, los heterómeros D_1-H_3 constituyen un mecanismo único para la señalización dopaminérgica e histaminérgica a través de la vía de la MAP cinasa de manera independiente de proteína G_s y dependiente de proteína G_i. Sin embargo, para establecer el significado fisiológico de estos heterómeros es necesario conocer previamente si se expresan en tejidos nativos. Como se ha mencionado anteriormente, las técnicas biofísicas de BRET o FRET producen muy buenos resultados en células transfectadas (Milligan and Bouvier 2005; Pfleger and Eidne 2006) pero son de difícil aplicación in vivo, por lo que hay que utilizar técnicas indirectas para la detección de heterómeros en tejidos nativos. Una de las características del heterómero H_3-D_1 es que únicamente en el heterómero los agonistas del receptor H_3 inducen la fosforilación de ERK 1/2 y que ésta puede ser inhibida tanto por antagonistas del receptor H_3 como del receptor D_1. Puesto que ésta es una característica bioquímica específica del heterómero H_3-D_1, se puede utilizar como una huella dactilar (*fingerprint*) para determinar si este heterómero existe in vivo. Por ello se ha estudiado la fosforilación de ERK 1/2 inducida por agonistas de receptores H_3 y/o D_1 en cortes de caudado-putamen de cerebro de rata y se ha analizado el efecto de antagonistas de ambos receptores sobre esta señalización. Estos resultados se recogen en el trabajo ***"Dopamine D_1-histamine H_3 Receptor Heteromers Provide a Selective Link to MAPK Signaling in GABAergic Neurons of the Direct Striatal Pathway"*** donde se demuestra la expresión de heterómeros de los receptores D_1-H_3 en las neuronas GABAérgicas estriatonigrales de la vía directa. La activación de los receptores H_3 en estas neuronas, pero no en las neuronas de la vía indirecta donde los receptores H_3 y D_2 colocalizan, produce la activación histaminérgica de la vía de las MAPK.

Una característica específica del heterómero D_1-H_3, previamente identificada en células transfectadas, es el antagonismo cruzado, la capacidad tanto de antagonistas de D_1 como de H_3 de bloquear el efecto de los agonistas de D_1 y de H_3. Este fenómeno, en el que un antagonista de uno de los receptores unidos al heterómero bloquea la señalización originada por la unión del ligando al otro receptor unido al heterómero, también ha sido observada con otros heterómeros,

como el heterómero cannabinoide CB_1 – orexina OX_1 (Ellis *et al.* 2006). El mismo antagonismo cruzado descrito para la señalización de la vía de las MAPK en células transfectadas (véase más arriba) se ha observado en cortes de estriado de rata, indicando la presencia de heterómeros D_1-H_3 en el estriado de roedor. De hecho, la fosforilación de ERK 1/2 inducida por agonistas del receptor H_3 se detecta en cortes de estriado de ratones no modificados pero no en ratones deficientes para el receptor D_1. Debido a que los agonistas del receptor H_3 no son capaces de activar la vía MAPK en cortes estriatales procedentes de ratones deficientes en el receptor D_1, se formuló la hipótesis de que tan sólo las neuronas que expresen tanto el receptor D_1 como el receptor H_3 son capaces de unir la neurotransmisión histaminérgica a la vía MAPK. De hecho, se ha demostrado que el receptor H_3 se expresa tanto en neuronas que contienen los receptores D_1 como las que contienen el receptor D_2; sin embargo, el marcaje de fosfo-ERK 1/2 mediado por el receptor H_3 sólo codistribuye con el receptor D_1, pero no con las neuronas que expresan el receptor D_2 y no depende de la liberación de neurotransmisor por parte de las células vecinas.

El heterómero D_1-H_3 trabaja como un procesador que integra señales mediadas por la dopamina y la histamina, activando la vía de las MAPK de manera diferente según la combinación hormonal. De la activación tanto del receptor D_1 como del receptor H_3 se obtiene una fuerte activación de MAPK, aunque de la coactivación de los dos receptores a la vez se obtiene una señal menor. De este modo, a muy bajas concentraciones de dopamina, la histamina puede promover señalización por MAPK mediante la activación de los receptores H_3 en las neuronas que coexpresen D_1-H_3. Por el contrario, cuando los dos neurotransmisores están presentes, la activación de MAPK en la vía estriatonigral es reprimida. Debido a que la vía MAPK es considerada crítica en la consolidación de las sinapsis (Sanchez-Lemus and Arias-Montano 2004), nuestros resultados predicen que no solo la dopamina sino también la histamina juega un papel importante en la neuroplasticidad dependiente de MAPK en la vía estriatonigral. De forma global, parece que el antagonismo de histamina y dopamina mediado por los receptores D_1 y H_3 puede depender del equilibrio de la activación de ERK en neuronas GABAérgicas, donde los receptores D_1 y H_3 se coexpresan y en las que se da la heteromerización de D_1-H_3. Los heterómeros no solo permiten a las neuronas diferenciar entre acciones de un neurotransmisor dado, sino que también sirven para procesar las diferentes señales que reciben en un mismo intervalo de tiempo (Franco 2009; Hasbi *et al.* 2010). Por tanto, los heterómeros de los receptores D_1-H_3 podrían estar activamente implicados en el control de la respuesta de las neuronas de la vía estriatal directa eferente. Las señales eferentes tanto a nivel cuantitativo como cualitativo derivadas de la fosforilación de ERK podrían depender fuertemente de concentraciones de dopamina e histamina que impacten en neuronas que expresen heterómeros D_1-H_3.

Una interacción negativa entre los receptores D_1 y H_3 a nivel de estriado ha sido también descrita para la vía de señalización de la adenilato ciclasa. La activación del receptor H_3 inhibe la acumulación de AMPc mediada por el receptor D_1 en cortes de estriado (Torrent *et al.* 2005). Otros ejemplos sobre la capacidad del receptor H_3 para inhibir los efectos mediados por el receptor D_1 son la capacidad de agonistas del receptor H_3 de inhibir los efectos de agonistas del receptor D_1 en la liberación de GABA en cortes de estriado (Arias-Montano *et al.* 2001) y la activación motora en ratones reserpinizados (Ferrada *et al.* 2008). En conjunto, estos resultados son consistentes con un antagonismo a nivel de la adenilato ciclasa entre los receptores D_1 y H_3 que no requiere necesariamente la formación de heterómeros.

Los receptores de dopamina están implicados en multitud de funciones estriatales, por ejemplo, están implicados en el control de los sistemas de recompensa. Las vías dopaminérgicas y especialmente la señalización mediada por los receptores D_1 y D_2 de dopamina, están profundamente implicadas en la adicción a cocaína (Kalivas 2007). Una gran parte de los efectos mediados por la cocaína se atribuyen a una sobre estimulación de la señalización de los receptores de dopamina debida al incremento de dopamina ocasionado por la inhibición del transportador de dopamina (DAT) por cocaína. Sin embargo, la cocaína, además de interaccionar con DAT, puede unirse a otras proteínas como los receptores σ_1. En este contexto, es interesante conocer si los receptores σ_1 pueden modular la funcionalidad de los receptores de dopamina D_1 y D_2 mediante un proceso de heteromerización. Teniendo en cuenta estas consideraciones, en esta Tesis se ha estudiado si los receptores D_1 y D_2 de dopamina pueden formar heterómeros con los receptores σ_1 y se ha investigado el efecto que ejerce la cocaína, mediado por estos heterómeros, en la transmisión dopaminérgica. Los resultados de estas investigaciones se recogen en los trabajos ***"Direct involvement of σ_1 receptors in the dopamine D_1 receptor-mediated effects of cocaine"*** y ***"Cocaine inhibits D_2 receptor signalling via sigma-1-dopamine D_2 receptor heteromers".***

Es bien sabido que la cocaína exhibe múltiples efectos sobre la transmisión dopaminérgica. Estos conocimientos se han adquirido, básicamente, en el campo de la drogadicción, analizándose la conducta (abstinencia, deseo, necesidad…) y los efectos bioquímicos (cambios en la transducción de señal) y genéticos (cambios en la actividad de algunos genes específicos) que pueden aparecer después de una toma de cocaína más o menos prolongada en humanos y en modelos animales. Mediante este tipo de investigación, se ha conseguido mejorar considerablemente el conocimiento sobre la acción a largo plazo de la cocaína, aunque se sabe muy poco sobre los primeros mecanismos moleculares que tienen lugar con la presencia de cocaína, con la excepción de la interacción de la cocaína con DAT. En este contexto, nos propusimos estudiar si la cocaína era capaz de modular la transmisión

dopaminérgica mediante la interacción con una de sus proteínas de unión, el receptor σ_1. Aunque originalmente se propuso como un subtipo de receptor opioide, actualmente, se ha confirmado que el receptor σ_1 es un receptor no-opioide que se une a distintas clases de drogas psicotrópicas incluyendo la cocaína (Mesangeau *et al.* 2008). Aun así, el papel de los receptores σ_1 en la señalización celular no es totalmente conocido y su principal ligando endógeno no ha sido identificado (Matsumoto *et al.* 2001b; Hayashi and Su 2005). En el trabajo ***"Direct involvement of σ_1 receptors in the dopamine D_1 receptor-mediated effects of cocaine"*** se describe un mecanismo por el cual los receptores σ_1 modulan la actividad del receptor D_1 de dopamina. Esta modulación depende de interacciones proteína-proteína, detectadas por ensayos de BRET. Mediante experimentos de BRET se ha demostrado que los receptores σ_1 y los receptores D_1 de dopamina pueden heteromerizar en células vivas. De acuerdo con la naturaleza oligomérica de los receptores D_1 de dopamina (Kong *et al.* 2006), la existencia de heterómeros constituidos por un mínimo de un homodímero de receptores D_1 de dopamina y un receptor σ_1 se ha demostrado por las técnicas BRET/BiFC. La unión de la cocaína al receptor σ_1 modula la función del receptor D_1 de dopamina no tan solo en células vivas, sino también en cortes de estriado de cerebro.

Los receptores σ_1 se encuentran principalmente en la membrana del retículo endoplasmático (Alonso *et al.* 2000), donde pueden modular la actividad de canales iónicos de la membrana plasmática, gracias a su capacidad de translocarse a la membrana plasmática (Su and Hayashi 2001; Hayashi and Su 2005). En este trabajo, describimos un mecanismo similar mediante el cual los receptores σ_1 modulan a los receptores D_1. La coexpresión de los receptores D_1 y σ_1 produce una alteración de la distribución subcelular del receptor σ_1, ya que en presencia del receptor D_1 de dopamina, el receptor σ_1 se expresa más en la membrana plasmática que en membranas intracelulares. De acuerdo con que la presencia de ligandos de los receptores σ_1, incluyendo la cocaína, puede causar la translocación de los receptores σ_1 a la membrana plasmática (Hayashi and Su 2005), en este trabajo hemos observado que además de un incremento en la expresión de los receptores σ_1 en la membrana, la cocaína incrementa la colocalización de los receptores D_1 y σ_1. Por otra parte, los receptores σ_1 y D_1 forman heterómeros constituidos por la interacción de σ_1 con homómeros de receptores D_1, como se ha demostrado por técnicas de BRET. En conjunto, estos resultados sugieren que la heteromerización entre estos receptores ocurre en ausencia de ligandos, pero la presencia de cocaína puede inducir un incremento en la cantidad de heterómeros en la membrana plasmática, posiblemente mediante la estabilización de una conformación determinada de los receptores.

La unión de la cocaína a los receptores σ_1 causa una modificación en la estructura cuaternaria del heterómero que implica la separación de los extremos C-terminal de los

receptores D_1 en el heterotrímero σ_1-D_1-D_1 y que es detectada por una marcada reducción en la señal de BRET. Estos cambios estructurales se correlacionan con los cambios en la función de los receptores D_1, tal y como se demuestra en los ensayos realizados en sistemas de expresión heteróloga y en cortes de estriado de ratón. Efectivamente, la unión de la cocaína a los receptores σ_1 incrementa de forma muy significativa la acumulación de AMPc mediada por agonistas del receptor D_1. Este efecto sinérgico sobre el receptor D_1, puede constituir, al menos en parte, la base molecular mediante la cual la cocaína potencia la señal mediada por el receptor D_1 sobre la mediada por el receptor D_2. Además, estos resultados son una clara evidencia de que los efectos de la cocaína no se pueden explicar adecuadamente asumiendo que la cocaína únicamente aumenta la concentración sináptica de dopamina por un mecanismo dependiente de los transportadores de dopamina (DAT). De hecho, se muestra que los efectos observados no dependen de DAT, ya que se han utilizado líneas celulares deficientes en esta proteína. Por lo tanto, es posible que la cocaína actúe a través de dos mecanismos diferentes e interrelacionados, uno dependiente de DAT, que lleva a un incremento de los niveles de dopamina, y otro dependiente del receptor σ_1, que lleva a un incremento en la neurotransmisión dependiente del receptor D_1 de dopamina.

Se ha observado que la cocaína también es capaz de modular la fosforilación de ERK 1/2 inducida por agonistas del receptor D_1. La cocaína incrementa la fosforilación de ERK 1/2 por sí misma, aunque este efecto es dependiente de la presencia de ambos receptores σ_1 y D_1. Este efecto de la cocaína es emulado por un agonista selectivo del receptor σ_1 (Hiranita *et al.* 2010) y contrarrestado por un antagonista putativo de este mismo receptor, PD144.148 (Akunne *et al.* 1997), lo que indica que la cocaína actúa como un agonista del heterómero σ_1-D_1. En células vivas, la cocaína induce la fosforilación de ERK 1/2 a tiempos bajos de estimulación (10 min), pero el efecto máximo se observa a 30 minutos, sugiriendo, no sólo que en esta activación se ve involucrada la interacción de la cocaína con el receptor σ_1, sino también, la translocación del receptor σ_1 a la membrana plasmática inducida por la cocaína, con el consecuente incremento en la formación de los heterómeros σ_1-D_1. La fosforilación de ERK 1/2 inducida tanto por la cocaína como por la estimulación del receptor D_1 se bloquea por los antagonistas de ambos receptores, σ_1 y D_1, lo que constituye un fenómeno de antagonismo cruzado (véase más arriba). Estos resultados sugieren que la unión de un antagonista a una de las unidades del heterómero puede inducir cambios conformacionales en las otras unidades y bloquear las señales específicas generadas en el heterómero. Es importante destacar que la fosforilación inducida por la cocaína se produce, también, en cortes estriatales de ratón, pero no en cortes estriatales de ratones deficientes para el receptor σ_1. Dado que la fosforilación de ERK 1/2 por cocaína parece ser una característica bioquímica de los heterómeros σ_1-D_1, estos resultados proveen evidencias de la presencia de estos heterómeros en el cerebro. Es importante resaltar

que se detecta una interacción negativa entre agonistas de los receptores σ_1 y los receptores D_1 de dopamina en la activación de las MAPK tanto en células transfectadas como en cortes estriatales de ratón. La fosforilación de ERK 1/2 inducida por el agonista del receptor D_1 se inhibe cuando los cortes se tratan previamente con cocaína, e inversamente, la fosforilación de ERK 1/2 inducida por cocaína se contrarresta por la presencia previa del agonista del receptor D_1 en las muestras. Todos estos fenómenos son dependientes del receptor σ_1, ya que no se observan en células transfectadas con sondas siRNA del receptor σ_1 y en cortes estriatales de ratones deficientes para el receptor σ_1. Los resultados observados tanto en células transfectadas como en cortes estriatales apoyan de nuevo la existencia de los heterómeros σ_1-D_1 en el cerebro.

En resumen, el hecho más destacable de este trabajo es que se ha descrito un mecanismo previamente no caracterizado, por el cual la unión de la cocaína a los receptores σ_1 puede modular significativamente la neurotransmisión dopaminérgica. Nuestros resultados muestran, por primera vez, la heteromerización de los receptores σ_1 y D_1 en células vivas y evidencian la presencia de estos heterómeros en el estriado, lo que constituye la base mediante la cual la cocaína puede modular la estructura y funcionalidad de los receptores de dopamina D_1. Mediante su interacción con los receptores σ_1, un efecto a corto plazo de la cocaína es el de focalizar la señalización de los receptores D_1 hacia la vía del AMPc y, consecuentemente, inducir un incremento en la actividad de las neuronas que proyectan del núcleo accumbens al área ventral-tegmental, que se encuentran estrictamente limitadas a las neuronas que expresan el receptor D_1 (Anderson and Pierce 2005) y así, podrían activarse otras vías de señalización involucradas en los efectos a largo plazo de la cocaína. En conjunto, nuestros resultados describen un nuevo mecanismo mediante el cual los efectos de la cocaína pueden modular a corto plazo la transmisión dopaminérgica. Todos estos datos sugieren que los heterómeros σ_1-D_1 pueden considerarse dianas terapéuticas para el tratamiento de la adicción a la cocaína y que los antagonistas de los receptores σ_1 podrían contrarrestar algunas de las propiedades comportamentales y posiblemente adictivas de la cocaína.

Si bien los resultados comentados anteriormente ponen de manifiesto el importante papel que pueden desempeñar los heterómeros σ_1-D_1 en focalizar las acciones immediatas de la cocaina hacia la activación de las neuronas que expresan receptores D_1, también abren un interrogante sobre cual es el papel de las neuronas que expresan receptores D_2. El caudado-putamen y el núcleo acumbens (las partes dorsales y ventrales del estriado, respectivamente), son regiones cerebrales que median los efectos a largo plazo de la cocaína y en las que abundan tanto receptores D_1 como D_2; se ha demostrado que la administración continua de cocaína en estas zonas induce el incremento de los receptores σ_1, un proceso mediado por los receptores D_1 de dopamina (Zhang *et al.* 2005). Como hemos comentado anteriormente, hemos demostrado la

importancia de los receptores σ_1 y los receptores D_1 de dopamina en los eventos iniciales que causa la exposición a la cocaína (véase más arriba). De hecho, a través de los heterómeros σ_1-D_1, la cocaína potencia de forma significativa la activación de la adenilato ciclasa a través del receptor D_1. Sin embargo, no se ha descrito la posibilidad de que los receptores σ_1 puedan modular también la función de los receptores D_2 de dopamina. Con objeto de estudiar los efectos de la cocaína sobre la función de los receptores D_2 se ha llevado a cabo la investigación que se reseña en el estudio ***"Cocaine inhibits D_2 receptor signalling via sigma-1-dopamine D_2 receptor heteromers".*** En primer lugar, se ha demostrado que los receptores D_2 de dopamina (concretamente, la isoforma larga del receptor) puede formar heterómeros con los receptores σ_1, interacción que es específica ya que otros miembros de esta familia, los receptores D_3 y D_4, no forman heterómeros. En segundo lugar, se ha descubierto que los heterómeros σ_1-D_2 están constituidos por oligómeros de orden superior, con una estructura mínima de heterotetrámeros σ_1-σ_1-D_2-D_2. En tercer lugar, se ha descrito que los heterómeros σ_1-D_2 se encuentran en el estriado de ratón. Finalmente, se demuestra que la cocaína, a través de la unión con los heterómeros σ_1-D_2, inhibe la señalización de segundos mensajeros tanto en cultivos celulares como en estriado de ratón.

Se ha demostrado que los receptores σ_1 y D_2 interaccionan a nivel molecular y a nivel funcional. Mediante el desarrollo de nuevas técnicas basadas en la transferencia de energía por resonancia, se ha demostrado la oligomerización de los receptores σ_1 en cultivos celulares y que los receptores σ_1 y D_2 pueden formar heterómeros constituidos al menos por un homómero de receptor σ_1 y un homómero de receptor D_2. La unión de la cocaína al receptor σ_1 en el heterómero promueve cambios estructurales en el heterómero que llevan a modificaciones significativas en la función del receptor D_2. La cocaína por sí sola no es capaz de inducir la señalización mediada por proteína G, pero, actuando a través del heterómero σ_1-D_2, puede disminuir la capacidad del receptor D_2 para señalizar a través de la proteína G_i. De este modo, la inhibición de la producción de AMPc mediada por el receptor D_2 se reduce significativamente por la unión de la cocaína al heterómero de receptores σ_1-D_2. Además, la cocaína por sí sola, activa la fosforilación de ERK 1/2, un proceso que requiere ambos receptores σ_1 y D_2. Estos resultados indican que la cocaína es un agonista del heterómero σ_1-D_2 a nivel de la activación de la vía de las MAPK. Paralelamente a lo que ocurre en modelos celulares, la fosforilación de ERK 1/2 mediada por la cocaína se detecta en cortes estriatales de ratón, pero no en cortes estriatales de ratón deficientes en el receptor σ_1. Dado que la fosforilación de ERK 1/2 inducida por la cocaína parece ser una característica bioquímica de los heterómeros σ_1-D_2, estos resultados proporcionan evidencias de su presencia en el estriado. Además, se ha descrito que la cocaína puede inhibir la fosforilación de ERK 1/2 mediada por el receptor D_2. Todos estos datos indican que la unión de la cocaína al heterómero σ_1-D_2 inhibe la señalización del receptor D_2.

El efecto de la cocaína en la señalización del heterómero σ_1-D_2 es opuesta al efecto de ésta en la señalización del heterómero σ_1-D_1 descrita anteriormente (véase más arriba). En el caso del heterómero σ_1-D_1, la producción de AMPc mediada por el receptor D_1 se incrementa significativamente por la unión de la cocaína a σ_1, mientras que para el heterómero σ_1-D_2, la disminución de la producción de AMPc mediada por el receptor D_2 se inhibe significativamente por la unión de la cocaína a σ_1. El conjunto de estos resultados, indica que la cocaína produce un incremento selectivo de la señalización inducida por la dopamina a través de la ruta de la formación de AMPc en neuronas que expresan el receptor D_1 a la vez que inhibe la función mediada por el receptor D_2 en neuronas que expresan el receptor D_2. De forma simultánea, la cocaína altera la señalización a través de la fosforilación de ERK 1/2 inducida por la dopamina en neuronas que expresan el receptor D_1 y en neuronas que expresan el receptor D_2. Estos hallazgos sugieren que la exposición a la cocaína lleva a la desregulación de la señalización de los receptores D_1/D_2 que está balanceada en situaciones normales. Los datos presentados en este trabajo apoyan un papel importante de los receptores σ_1, por lo menos durante los efectos agudos de la cocaína, no sólo incrementando la producción de AMPc mediada por los receptores D_1, sino también impidiendo la señalización del receptor D_2 en los heterómeros σ_1-D_2. Estos desequilibrios entre la vía directa e indirecta, pueden sustentar los hallazgos descritos por Bateup *et al*. (2010), que encontraron que la respuesta locomotora inducida por tratamiento agudo con cocaína disminuye después de la eliminación de DARP-32 en neuronas nigroestriatales, indicando un papel esencial de la vía directa en este comportamiento. En contraposición, las neuronas estriopalitales que expresan los receptores D_2 reducen la activación locomotora inducida por la cocaína. Más recientemente, Luo *et al.* (2011) han demostrado *in vivo* la existencia de efectos agudos de la cocaína mediados tanto por los receptores D_1 como por receptores D_2 de dopamina (incrementos en el flujo de Ca^{2+} mediado por el receptor D_1 y disminuciones en el flujo de Ca^{2+} mediado por el receptor D_2), con una disminución significativa en la dinámica de los efectos mediados por el receptor D_2. Teniendo en cuenta nuestros datos, las observaciones de Luo y colaboradores podrían estar relacionadas con la disminución en la señalización impuesta por la cocaína a través del heterómero σ_1-D_2. En resumen, los resultados sugieren que tanto la vía directa como la indirecta ejercen un papel importante en el comportamiento motor inducido por la cocaína. En conjunto, todos estos datos proporcionan un nuevo mecanismo global por el cual la cocaína, al unirse a heterómeros σ_1-D_1 y σ_1-D_2 afecta las vías directa (D_1) e indirecta (D_2) de manera contrapuesta, proporcionando, al menos en parte, las bases moleculares para explicar por qué en los efectos de la cocaína hay un papel prevalente del receptor D_1 respecto al receptor D_2.

Todos los receptores de la familia D_2 (D_2, D_3 y D_4) se expresan en el estriado aunque los receptores D_4 lo hacen de manera minoritaria respecto a los otros miembros. Sin embargo, los

receptores D_4 en humanos tienen un interés especial ya que son los únicos que presentan formas polimórficas, las más comunes $D_{4.4}$, $D_{4.2}$ y $D_{4.7}$. Existe una clara relación entre la forma polimorfica $D_{4.7}$ del receptor D_4 humano con el trastorno de hiperactividad y déficit de atención. No existen muchas diferencias funcionales entre las formas polimórficas por lo que no se conoce cuales son las repercusiones bioquímicas de expresar una u otra forma. En esta Tesis se ha estudiado si podían existir diferencias entre las isoformas en la capacidad de formar heterómeros con otros receptores de dopamina como el D_2 y se ha investigado si estos heterómeros podrían modular la liberación de glutamato en el estriado, lo que podría ser relevante en el trastorno de hiperactividad y déficit de atención. Los resultados obtenidos se describen en el trabajo ***"Dopamine D_4 receptor, but not the ADHD-associated $D_{4.7}$ variant, forms functional heteromers with the dopamine D_{2S} receptor in the brain".*** En este trabajo se muestra que los receptores de dopamina D_{2S}, $D_{4.2}$ y $D_{4.4}$, pero no la variante $D_{4.7}$ asociada con el trastorno por déficit de atención y hiperactividad (ADHD), forman heterómeros funcionales en células transfectadas y en cerebro de ratón. La coestimulación de los receptores D_{2S} y D_4 en el heterómero D_{2S}-D_4 tiene un efecto sinérgico en la señalización, hecho que no ocurre en células que expresaban la variante $D_{4.7}$ o en el estriado de ratones mutados (*knock-in)* portadores de la variante de 7 repeticiones ($D_{4.7}$) en el tercer bucle intracelular del receptor D_4 de dopamina. Estos resultados indican una diferencia funcional de la variante $D_{4.7}$ del receptor D_4 respecto a las variantes $D_{4.2}$ y $D_{4.4}$, la cual puede tener implicaciones importantes para la comprensión de la patogénesis de ADHD. Se ha demostrado por primera vez que las interacciones entre los receptores D_{2S}-D_4 modulan la secreción de glutamato en el estriado, hecho que sugiere que los heterómeros de receptores D_{2S}-D_4 permiten a la dopamina ejercer una modulación más precisa en la neurotransmisión glutamatérgica.

Puesto que la variante $D_{4.7}$ del receptor D_4 de dopamina posee el tercer bucle intracelular (IL3) más largo y es la única variante polimórfica que no forma heterómeros con el receptor D_{2S}, el impedimento estérico de este bucle del receptor D_4 podría ser el mecanismo responsable de obstaculizar la heteromerización, aunque no se pueden descartar otros mecanismos, como la intervención de otras proteínas intracelulares en la formación de los heterómeros. Utilizando metodologías de proteómica, se han demostrado interacciones entre receptores de dopamina y DRIPS (*dopamine receptor interacting proteins*), formando complejos de señalización o "*signalplexes"* (Kabbani and Levenson 2007; Yao *et al.* 2008). Algunas de las proteínas DRIPS muestran selectividad hacia algunos subtipos de receptores de dopamina. Por ejemplo, la filamina o la proteína 4.1N interacciona con los subtipos D_2 y D_3, pero no lo hace con los subtipos D_1, D_5 o D_4 (Lin *et al.* 2001; Binda *et al.* 2002), las proteínas con dominios PDZ, como GIPC (GAIP *interacting protein, C terminus*) interaccionan con los subtipos D_2 y D_3, pero no lo hacen con los subtipos D_4 (Jeanneteau *et al.* 2004) y la proteína

paralemmin interacciona exclusivamente con el receptor D_3, pero no con los receptores D_2 y D_4 (Basile *et al.* 2006). Todas estas interacciones modulan la especificidad del receptor, el tráfico y la señalización. Las secuencias ricas en prolina del receptor D_4, principalmente localizadas en la región polimórfica del IL3, constituyen los supuestos dominios de unión que, potencialmente, pueden interaccionar con proteínas "adaptadoras" como Grb2 y Nck, que no tienen ninguna actividad catalítica conocida pero son capaces de reclutar complejos multiproteicos con el receptor (Rondou *et al.* 2010). Se podría hipotetizar que las diferencias en el reclutamiento de DRIP´s por el receptor $D_{4.7}$ y otras variantes polimórficas podrían influenciar la habilidad del receptor $D_{4.7}$ para formar heterómeros, pero serían necesarios más estudios para corroborar esta hipótesis.

Experimentos previos indicaban que la dopamina en el estriado inhibe la secreción de glutamato activando los receptores D_2, predominantemente el receptor D_{2S} localizado en terminales glutamatérgicas (Pontieri *et al.* 1995; De Mei *et al.* 2009). Otros estudios también indicaban que los receptores estriatales postsinápticos, predominantemente el receptor D_{2L}, modulan de forma indirecta la liberación de glutamato por un mecanismo de señalización retrogrado mediado por endocannabinoides (Yin and Lovinger 2006). Los resultados de esta Tesis indican que los receptores D_4 tienen un papel muy importante en la modulación de la secreción de glutamato en el estriado, muy posiblemente a través de su capacidad para formar heterómeros con receptores D_{2S} presinápticos. Los resultados sugieren que a través de los heterómeros D_{2S}-D_4, la dopamina, a concentraciones bajas, se unirían al receptor D_4, el cual tiene mayor afinidad para la dopamina que el receptor D_{2S} (Rondou *et al.* 2010), causando un cierto nivel de inhibición en la secreción de glutamato. Sin embargo, a altas concentraciones, la dopamina debería unirse también al receptor D_{2S} y, en estas condiciones, el efecto sinérgico de la interacción de los receptores D_{2S}-D_4 en el heterómero produciría una mayor inhibición de la liberación de glutamato. Por lo tanto, el heterómero de los receptores D_{2S}-D_4 podría actuar a través de un mecanismo dependiente de la concentración de dopamina para establecer dos niveles de control dopaminérgico presináptico sobre la neurotransmisión estriatal glutamatérgica. Dado que la potente modulación sinérgica observada depende de la heteromerización de los receptores D_{2S}-D_4, la existencia de la variante $D_{4.7}$ implicaría un control más débil de la neurotransmisión glutamatérgica, lo cual podría constituir un mecanismo involucrado en la patogénesis de ADHD. Este hecho también podría explicar en parte los efectos, hasta estos momentos poco claros, de los psicoestimulantes en ADHD, los cuales amplifican la señalización dopaminérgica y la efectividad de este tipo de tratamientos en pacientes ADHD con la variante $D_{4.4}$ y no así con la variante $D_{4.7}$ (Hamarman *et al.* 2004; Cheon *et al.* 2007). Hay que tener en cuenta que la existencia de la variante $D_{4.7}$ no implica que ésta sea la causante de ADHD, sino que puede ser un factor que contribuye a su desarrollo. De hecho, la

variante $D_{4.7}$ podría constituir una característica evolutiva exitosa bajo la exposición adecuada al medio (Ding *et al.* 2002; Wang *et al.* 2004). El presente estudio aporta un nuevo elemento de interés en el campo de los heterómeros, los cuales son nuevas dianas para el estudio de diferencias funcionales asociadas a polimorfismos de los genes de los receptores acoplados a proteína G.

Otra particularidad del receptor de dopamina D_4 es que es el único receptor dopaminérgico en la glándula pineal de rata sin que se conozca cual es su función a pesar de que se expresa de manera circadiana. Por tanto, la glándula pineal de rata es una región del cerebro en donde es interesante investigar las características del receptor D_4. Dado que la glándula pineal está bajo el control de los receptores α_{1B} y β_1 adrenérgicos, de cuya activación depende la regulación del ritmo circadiano y la síntesis y liberación de serotonina y melatonina, una posibilidad es que los receptores de dopamina D_4, que en animales no presenta formas polimórficas, puedan modular la función de los receptores adrenérgicos de la glándula pineal mediante un proceso de heteromerización. Esta posibilidad se ha estudiado en esta Tesis y los resultados aparecen en el trabajo ***"Circadian-related heteromerization of adrenergic and dopamine D_4 receptors modulates melatonin synthesis and release in the pineal gland"***. En este trabajo se ha identificado un nuevo mecanismo que describe como la dopamina regula la función de los receptores adrenérgicos durante el ritmo circadiano. Utilizando diversas técnicas experimentales se ha puesto de manifiesto que: 1) los receptores D_4 de dopamina forman heterómeros con receptores adrenérgicos α_{1B} y β_1 en células transfectadas y en la glándula pineal 2) los heterómeros α_{1B}-D_4 y β_1-D_4 permiten la modulación inducida por agonistas y antagonistas del receptor D_4 de la activación de MAPK y Akt mediada por agonistas de los receptores adrenérgicos en células transfectadas y en la glándula pineal 3) la síntesis y la liberación de serotonina y melanina, promovida por la estimulación de los receptores adrenérgicos en la glándula pineal, está controlada por el receptor D_4 a través de la activación de los heterómeros α_{1B}-D_4 y β_1-D_4, y 4) la modulación de los heterómeros a través de los receptores D_4 depende de los ciclos circadianos de día/noche. Este es el primer ejemplo de la modulación de la heteromerización de receptores dependiente de ritmos circadianos. Todos estos resultados apuntan un nuevo papel del receptor D_4 en la glándula pineal que lleva a la reducción de la función de los receptores α_{1B} y β_1 adrenérgicos a través de una interacción directa receptor-receptor.

Los receptores adrenérgicos son el sostén principal de la función en la glándula pineal. Forman el puente entre la secreción de noradrenalina por las terminaciones nerviosas del sistema nervioso simpático controlado por ritmos circadianos y la producción de melatonina en la glándula pineal. Los receptores adrenérgicos son los responsables de la producción de

melatonina a través de varios mecanismos, incluyendo el control de los niveles del precursor serotonina (5-HT) (Gonzalez-Brito *et al.* 1990; Zheng and Cole 2002). La dopamina también está presente en los nervios simpáticos aferentes en la glándula pineal, no solo como un precursor de la noradrenalina, sino que también es co-secretada junto con la noradrenalina (Kim *et al.* 2010). En la glándual pineal de rata la noradrenalina ejerce sus funciones por interacción con los receptores α_{1B} y β_1 y la dopamina actúa activando a los receptores D_4. Hasta este momento no existía ningún indicio de interacción entre los receptores de dopamina y los receptores adrenérgicos. En este trabajo a través de experimentos de BRET en células transfectadas y ensayos de ligación por proximidad (PLA, *proximity ligation assays)* en pinealocitos, se muestran evidencias directas de la formación de heterómeros de los receptores D_4 y receptores α_{1B} y β_1. La formación de heterómeros α_{1B}-D_4 y β_1-D_4 en la glándula pineal se ha demostrado, también, por determinación de antagonismo cruzado. Se observa que un antagonista específico del receptor D_4 es capaz de bloquear la señalización mediada por los receptores α_{1B} y β_1 y que los antagonistas de los receptores α_{1B} y β_1 son también capaces de bloquear la señalización mediada por el receptor D_4. Ya que por definición un antagonista es incapaz de inducir la señalización intracelular, la forma más sencilla de explicar el efecto de un antagonista del receptor D_4 sobre los receptores α_{1B} y β_1 y viceversa, es a través de una interacción proteína-proteína directa entre ambos receptores.

Hemos podido establecer que las consecuencias funcionales de la heteromerización son una interacción negativa cuando los dos receptores del heterómero se co-activan. En los heterómeros α_{1B}-D_4 y β_1-D_4, se produce la inhibición de fosforilación de ERK 1/2 y el bloqueo total de la fosforilación de Akt inducidas por los agonistas adrenérgicos en presencia de agonistas del receptor D_4. El hecho de que el receptor D_4 pueda modificar la señalización de los receptores α_{1B} y β_1 adrenérgicos es particularmente interesante ya que la expresión del receptor D_4 está regulada por el incremento de los niveles de norepinefrina (Kim *et al.* 2010). El mecanismo que describimos puede representar una inhibición por retroceso (*feedback* negativo) donde el incremento de la expresión del receptor D_4 a través de la señalización adrenérgica da lugar a un incremento de la formación de heterómeros α_{1B}-D_4 y β_1-D_4, los cuales inhiben la señalización mediada por los receptores adrenérgicos a través de la interacción negativa descrita anteriormente.

La expresión de ARNm del receptor D_4 en la glándula pineal está estrictamente regulada y alcanza sus máximos niveles en la última parte del período oscuro y no se expresa en medio del periodo de luz (Kim *et al.* 2010). Se ha observado que el receptor D_4 se expresa y es funcional en la glándula pineal cuando ésta se disecciona en las primeras horas del período de luz, y no se observó actividad ni expresión cuando las glándulas pineales fueron aisladas al final

del período de luz. Ello significa que la modulación ejercida por el receptor D_4 está bajo control circadiano.

Se han estudiado las consecuencias metabólicas de la activación de los heterómeros α_{1B}-D_4 y β_1-D_4 en la síntesis y secreción de 5-HT y de melatonina. Los niveles de 5-HT incrementan durante el día, mientras que los niveles de melatonina fluctúan de manera opuesta, incrementando su producción y secreción por la noche a través de la activación del enzima AANAT, enzima involucrada en las últimas etapas de su síntesis. A través de la acción de masas, el incremento significativo en la actividad de AANAT por la noche pueden reducir rápidamente los niveles de 5-HT (Klein *et al.* 1997). Es importante destacar que la síntesis de 5-HT parece ocurrir tanto durante el día como durante la noche, y la síntesis y secreción nocturna de 5-HT es necesaria para la síntesis de melatonina a través de la estimulación adrenérgica (Miguez *et al.* 1997; Simonneaux and Ribelayga 2003). La 5-HT extracelular es absorbida por terminaciones nerviosas simpáticas o se une a los receptores $5HT_{2C}$ de la glándula pineal, que a su vez puede llevar a un incremento de la síntesis y secreción de melatonina (Sugden 1990; Miguez *et al.* 1997). Hasta este momento no está completamente claro como se limitan los niveles de producción de 5-HT y melatonina durante los ciclos día/noche. Nuestros datos sugieren que los heterómeros α_{1B}-D_4 y β_1-D_4 pueden jugar un papel importante en este proceso.

Cuando las glándulas pineales aisladas al final del período de luz, cuando la expresión del receptor D_4 es inapreciable, se tratan con ligandos adrenérgicos, se produce un incremento en la síntesis de 5-HT y un gran incremento en la síntesis de melatonina mediadas por el receptor β_1 y se detecta, también, un incremento en la secreción de 5-HT y un gran incremento en la secreción de melatonina mediadas por el receptor α_{1B}. En este caso cabe destacar que ni la síntesis ni la secreción se bloquean por el tratamiento simultáneo con el agonista del receptor D_4 cuya expresión en estas condiciones es muy baja. Por el contrario, se observa que al tratar con ligandos adrenérgicos glándulas pineales aisladas al principio del período de luz, cuando el receptor D_4 se expresa, el incremento en la síntesis de 5-HT y de melatonina mediado por los receptores β_1 y la secreción mediada por los receptores α_{1B} se inhiben drásticamente al tratar las glándulas simultáneamente con un agonista del receptor D_4. Este bloqueo podría ser debido a una interacción negativa a nivel de señalización. Sin embargo, se ha visto que un antagonista del receptor D_4 también produce inhibición tanto de la síntesis como de la secreción de 5-HT y melatonina mediada por los receptores adrenérgicos. Puesto que los antagonistas no pueden por si solos señalizar, este bloqueo debe ser causado por una interacción proteína-proteína a través de los heterómeros α_{1B}-D_4 y β_1-D_4.

El conjunto de resultados muestra que la dopamina parece que es capaz de regular los niveles de 5-HT y de melatonina. Esto sugiere que la dopamina, a través de los heterómeros α_{1B}-D_4 y β_1-D_4, puede servir como molécula reguladora para reducir la cantidad de melatonina sintetizada y secretada al principio del período de luz. Al anochecer, la ausencia de receptores D_4 favorecería la síntesis de 5-HT y una rápida transformación de serotonina en melatonina inducida por la noradrenalina. La progresiva aparición de ARNm durante la noche y el incremento de la expresión del receptor D_4 al amanecer facilitarían el bloqueo de la síntesis y liberación de la melatonina. Durante el día, los receptores D_4 "desaparecerían" de la membrana, por lo que los heterómeros α_{1B}-D_4 y β_1-D_4 tampoco se formarían. La actividad AANAT también disminuiría, y los niveles de 5-HT incrementarían gradualmente y el ciclo se repetiría. Estos resultados ponen de manifiesto el papel del receptor D_4 en la glándula pineal y abren una nueva área de investigación sobre el papel de los heterómeros entre receptores de dopamina y noradrenalina para mantener las señales de los ritmos circadianos de la glándula pineal.

CONCLUSIONES

5. CONCLUSIONES

Conclusiones respecto al Objetivo 1:

- Los receptores D_1 y D_5 de dopamina forman heterómeros con los receptores de galanina Gal_1 pero no con los Gal_2 en células transfectadas y en el hipocampo ventral de rata.

- En los heterómeros D_1-Gal_1 y D_5-Gal_1, los agonistas de los receptores de dopamina potencian y los antagonistas inhiben la fosforilación de ERK 1/2 inducida por agonistas de receptores Gal_1.

- En el hipocampo ventral de rata la galanina induce la liberación de acetilcolina únicamente si el receptor D_1 está estimulado. El heterómero modula la transmisión sináptica ya que los agonistas de los receptores de dopamina, que son inefectivos por si mismos, provocan un cambio de efecto inhibidor a excitador de la transmisión sináptica que requiere de la liberación de acetilcolina. Los heterómeros D_1-Gal_1 y D_5-Gal_1 actúan, por tanto, como procesadores que integran señales de dopamina y galanina para modular la liberación de acetilcolina en el hipocampo ventral.

Conclusiones respecto al Objetivo 2:

- Los receptores D_1 de dopamina forman heterómeros con los receptores H_3 de histamina en células de neuroblastoma humano.

- En el heterómero D_1-H_3 se produce un acoplamiento distinto a la maquinaria de señalización. Por un lado, la activación de los receptores H_3, que produce decremento en los niveles de AMPc, no produce fosforilación de ERK 1/2 a menos que los receptores H_3 formen heterómeros con los receptores D_1. Por otro lado, se produce un cambio en el acoplamiento del receptor D_1 de la proteína G_s a la proteína G_i, por lo que los agonistas D_1, vía el heterómero D_1-H_3, no aumentan los niveles de AMPc pero activan la vía de las MAPK por un proceso mediado por G_i.

- En cortes de tejido estriatal de rata se han identificado heterómeros D_1-H_3. La unión de agonistas del receptor H_3, en el heterómero D_1-H_3, produce la fosforilación de ERK 1/2 en las neuronas del estriado que expresan receptores D_1 pero no en las que expresan receptores D_2. Ello indica que los heterómeros D_1-H_3 actúan como procesadores integrando señales dopaminérgicas e histaminérgicas involucradas en el control de la vía directa estriatal.

Conclusiones respecto al Objetivo 3:

- Los receptores sigma-1 forman heterómeros con los receptores D_1 de dopamina y también con los receptores D_2 de dopamina pero no con los otros miembros de la familia D_2, los receptores D_3 o D_4. Estos heterómeros están constituidos como mínimo por la interacción de homodímeros de sus componentes y se expresan tanto en células transfectadas como en el estriado de ratón.

- La unión de la cocaína al receptor sigma-1 induce cambios estructurales y funcionales en los heterómeros sigma-1-D_1 y sigma-1-D_2. La cocaína, interaccionando con sigma-1, es capaz de incrementar la señalización inducida por agonistas de receptores D_1 de dopamina hacia la producción de AMPc e inhibir los decrementos de AMPc inducidos por agonistas del receptor D_2 y, simultáneamente, la cocaína es capaz de bloquear la fosforilación de ERK 1/2 inducida por agonistas de receptores D_1 y D_2. Esto podría resultar en una desregulación del balance entre las vías directa e indirecta del estriado que contienen neuronas que expresan receptores D_1 y D_2 respectivamente. Estos resultados constituyen nuevas perspectivas en el entendimiento de las acciones a corto plazo de esta droga.

Conclusiones respecto al Objetivo 4:

- En células transfectadas y en tejido estriatal de ratones transgénicos, la formas polimórficas $D_{4.2}$ y $D_{4.4}$ del receptor D_4 de dopamina humano, pero no la forma polimérica $D_{4.7}$ asociada a ADHD, forman heterómeros con el receptor D_{2s} de dopamina.

- La co-activación de los receptores D_{2s} y D_4 en los heterómeros tiene un efecto sinérgico en la activación de la vía de las MAPK. La interacción entre receptores D_{2s} y D_4 modula la liberación de glutamato en el estriado ya que la activación de los receptores D_{2s} potencia la inhibición de la liberación de glutamato inducida por la activación de los receptores D_4. Se concluye que la dopamina, a través de los heterómeros D_{2s}-D_4 ejerce una modulación muy precisa de la neurotransmisión glutamatérgica estriatal.

Conclusiones respecto al Objetivo 5:

- Los receptores D_4 de dopamina forman heterómeros con los receptores α_{1B} y β_1 adrenérgicos en células transfectadas. En la glándula pineal, la formación de estos heterómeros está regulada por el ritmo circadiano.

- La activación de los receptores D_4 en los heterómeros α_{1B}-D_4 y β_1-D_4 inhibe la fosforilación de ERK 1/2 y Akt/PKB inducida por los agonistas de los receptores adrenérgicos y también inhibe la síntesis y liberación de serotonina mediada por la activación de los receptores

adrenérgicos. Por tanto, los receptores D_4 en la glándula pineal modulan negativamente y de manera circadiana la funcionalidad de los receptores adrenérgicos en la vía metabólica de la síntesis de melatonina.

ANEXOS

6. ANEXOS

A lo largo del desarrollo de esta Tesis Doctoral se ha colaborado muy activamente en tres proyectos de investigación que han dado lugar a la publicación de cuatro trabajos que, al no estar incluidos dentro de los resultados que constituyen el núcleo central de esta Tesis Doctoral, se presentan como anexos. Estos proyectos están íntimamente relacionados con el estudio de homómeros y heterómeros de receptores acoplados a proteína G (GPCR) y por lo tanto dentro del marco general en el que se incluye esta Tesis.

El primer proyecto versa sobre la obtención de proteínas de fusión constituídas por GPCR y proteínas fluorescentes o bioluminiscentes que son necesarias para la aplicación de técnicas de transferencia de energía bioluminiscente o fluorescente como BRET o FRET. Los resultados de estos estudios han dado lugar al siguiente trabajo que se presenta como Anexo 6.1:

Production of functional recombinant G-protein coupled receptors for heteromerization studies. Milena Ĉavić, Carme Lluís, **Estefanía Moreno**, Jana Bakešová, Enric I. Canela, Gemma Navarro. *Journal of Neuroscience Methods (2011)* ***199****:258-264.*

El segundo proyecto versa sobre la relación estructura-función en los heterómeros entre receptores. La característica más notoria de los heterómeros de GPCR es que la funcionalidad de los receptores no es la misma si se encuentran expresados individualmente o formando heterómeros. Este cambio de funcionalidad por heteromerización tiene una importante repercusión en la búsqueda de nuevas terapias para las diversas enfermedades donde estos heterómeros puedan verse involucrados. Sin embargo, las bases estructurales implicadas en este cambio de funcionalidad son totalmente desconocidas, principalmente por que se conoce muy poco la estructura cuaternaria de los homo- y heterómeros. En este proyecto se ha investigado la estructura cuaternaria de los heterotrímeros de receptores A_{2A} de adenosina-CB_1 de cannabinoides-D_2 de dopamina y se ha analizado la relevancia de las interacciones estructurales en la funcionalidad del heterómero. Los resultados obtenidos han dado lugar al siguiente trabajo que se presenta como Anexo 6.2:

Interactions between Intracellular Domains as Key Determinants of the Quaternary Structure and Function of Receptor Heteromers. Gemma Navarro, Sergi Ferré, Arnau Cordomi, **Estefanía Moreno**, Josefa Mallol, Vicent Casado, Antoni Cortés, Hanne Hoffmann, Jordi Ortiz, Enric I. Canela, Carme Lluís, Leonardo Pardo, Rafael Franco, Amina S. Woods. *Journal of Biological Chemistry (2010)* ***285 (35)****: 27346-27359.*

La capacidad de las proteínas de autoensamblarse para formar homodímeros u oligómeros de orden superior o de interaccionar con otras proteínas para formar heterómeros, es una de las características importantes en la señalización intracelular. Un ejemplo paradigmático son los receptores de adenosina A_1, A_{2A} y A_{2B}. En el plano horizontal de la membrana, estos GPCRs se expresan como homómeros o como heterómeros con otros GPCRs. En el plano vertical, a través de la membrana, estos receptores interaccionan con las proteínas intracelulares encargadas de la señalización o de la regulación de la señalización, pero, también en este plano vertical, alguno de estos receptores, como los subtipos A_1 y A_{2B} son capaces de interaccionar con una proteína extracelular como el enzima adenosina desaminasa (ADA). Este enzima del metabolismo purínico es capaz de degradar adenosina con lo que regula la cantidad de hormona extracelular que se une a los receptores. En el tercer proyecto se ha estudiado cuál es el papel de la ADA en la homomerización de los receptores de adenosina A_1 y A_{2A}, y en la regulación de las propiedades farmacológicas de estos homómeros. Los resultados obtenidos en este proyecto han dado lugar a los dos trabajos que se reseñan a continuación y que se presentan como Anexo 6.3 y Anexo 6.4:

A_{2A} adenosine receptor ligand binding and signalling is allosterically modulated by adenosine deaminase. Eduard Gracia, Kamil Pérez-Capote, **Estefanía Moreno**, Jana Bakešová, Josefa Mallol, Carme Lluís, Rafael Franco, Antoni Cortés, Vicent Casadó, Enric I. Canela. *Biochemical Journal (2011)* ***435(3)****: 701-709.*

Homodimerization of adenosine A_1 receptors in brain cortex explains the biphasic effects of caffeine. Eduard Gracia*, **Estefanía Moreno***, Carme Lluís, Josefa Mallol, Peter J. McCormick, Enric I. Canela, Antoni Cortés, Vicent Casadó. Manuscrito enviado para su publicación a *Biochemical Pharmacology.*

6.1 Producción de receptores acoplados a proteína G recombinantes para estudios de heteromerización

Milena Čavić [a], Carme Lluis [b], Estefanía Moreno[b], Jana Bakešová[b], Enric I. Canela[b], Gemma Navarro[b]

[a]Department of Experimental Oncology, Institute of Oncology and Radiology of Serbia, Pasterova 14, 11000 Belgrade, Serbia,
[b]Centro de Investigación Biomédica en Red sobre Enfermedades Neurodegenerativas (CIBERNED), y Departamento de Bioquímica y Biología Molecular, Facultad de Biología, Universidad de Barcelona, Avda. Diagonal 645, 08028 Barcelona, España.

*Manuscrito publicado en Journal of Neuroscience Methods (2011 May); **199**:258-264.*

Los receptores acoplados a proteína G (GPCR) representan una diversa familia de receptores que transducen señales desde el espacio extracelular a moléculas intracelulares desencadenando varias respuestas celulares. Actualmente, está generalmente aceptado que los GPCR se expresan y funcionan como dímeros o muy probablemente como oligómeros compuestos por protómeros de más de dos receptores. El heterómero tiene características bioquímicas y farmacológicas diferentes a los monómeros, incrementando las respuestas funcionales de los GPCR. Los GPCR están involucrados en una gran variedad de enfermedades, y son diana de aproximadamente la mitad de fármacos en la actualidad. En el caso de la enfermedad de Parkinson, síndrome degenerativo que causa la desaparición gradual de neuronas dopaminergicas nigro-estriatales, se sospecha que la diana para su tratamiento debería ser heterómeros conteniendo receptores de dopamina. Las tecnologías basadas en el uso de receptores fusionados con proteínas fluorescentes o bioluminiscentes y sus adaptaciones a técnicas de transferencia de energía de resonancia, han sido muy útiles para la investigación de las interrelaciones funcionales entre receptores en heterómeros. En este estudio, se han clonado y caracterizado los receptores de adenosina A_{2A}, dopamina D_2 e histamina H_3 recombinantes fusionados a la proteína bioluminiscente *Renilla luciferasa* (Rluc) o a las proteínas fluorescentes GFP^2 y YFP para dar lugar a las proteínas de fusión A_{2A}-Rluc, D_2-GFP^2 y H_3-YFP. Estas proteínas constituyen la base para el posterior estudio de la heteromerización entre estos receptores, lo que permitiría profundizar en el conocimiento de la farmacología y las relaciones de estos tres receptores en el cerebro y posibilitar el diseño y evaluación de nuevas estrategias terapéuticas para la enfermedad de Parkinson.

Journal of Neuroscience Methods 199 (2011) 258–264

Contents lists available at ScienceDirect

Journal of Neuroscience Methods

journal homepage: www.elsevier.com/locate/jneumeth

Production of functional recombinant G-protein coupled receptors for heteromerization studies

Milena Čavić[a,*], Carme Lluís[b], Estefanía Moreno[b], Jana Bakešová[b], Enric I. Canela[b], Gemma Navarro[b]

[a] Department of Experimental Oncology, Institute of Oncology and Radiology of Serbia, Pasterova 14, 11000 Belgrade, Serbia
[b] Centro de Investigación Biomédica en Red sobre Enfermedades Neurodegenerativas (CIBERNED), and Department of Biochemistry and Molecular Biology, Faculty of Biology, University of Barcelona, Avda. Diagonal 645, 08028 Barcelona, Spain

ARTICLE INFO

Article history:
Received 6 May 2011
Accepted 24 May 2011

Keywords:
Heteromer
Adenosine
Dopamine
Histamine
Cloning
Parkinson's disease

ABSTRACT

G-protein-coupled receptors (GPCRs) represent a diverse protein family of receptors that transduce signals from the extracellular surrounding to intracellular signaling molecules evoking various cellular responses. It is now widely accepted that GPCRs are expressed and function as dimers or most probably as oligomers of more than two receptor protomers. The heteromer has different biochemical and pharmacological characteristics from the monomers, which increases the functional responses of GPCRs. GPCRs are involved in many diseases, and are also the target of around half of all modern medicinal drugs. In the case of Parkinson's disease, a degenerative process caused by gradual disappearance of dopaminergic nigrostriatal neurons, it is suspected that the targets for treatment should be dopamine-receptor-containing heteromers. Technologies based on the use of fluorescent- or luminescent-fused receptors and adaptations of resonance energy transfer (RET) techniques have been useful in investigating the functional inter-relationships between receptors in a heteromer. In this study functional recombinant adenosine A_{2A}-Rluc, dopamine D_2-GFP[2] and histamine H_3-YFP receptor fusion proteins were successfully cloned and characterized, producing the essential basis for heteromerization studies between these receptors. This might provide a better insight into their pharmacological and functional inter-relationships in the brain and enable the design and evaluation of new therapeutic strategies for Parkinson's disease.

1. Introduction

G-protein-coupled receptors (GPCRs) represent a diverse protein family of receptors that transduce signals from the extracellular surrounding to intracellular signaling molecules evoking various cellular responses. The chemical diversity of the ligands that bind and activate GPCRs is exceptional and they stimulate cytoplasmic and nuclear targets through heterotrimeric G-protein-dependent and independent pathways. Since the early 1980s, experimental data has accumulated suggesting that GPCRs may be expressed and function as dimers or most probably as oligomers of more than two receptor protomers (Fuxe et al., 2008). Both homo- and heteromers were found in a variety of studies (Bulenger et al., 2005). The heteromers have different biochemical and pharmacological characteristics from the monomers (Ferre et al., 2007), which considerably increases the possible functional responses of GPCRs affecting all aspects of receptor physiology and pharmacology.

G protein-coupled receptors are involved in many diseases, but are also the target of around half of all modern medicinal drugs (Gilchrist, 2010). Nevertheless, currently the developed drugs target only a small number of GPCRs, and the potential for drug discovery within this field is enormous. The discovery of physiologically relevant GPCR heteromers suggested that new, more selective, drugs can be developed by targeting the heteromers instead of the monomers thus increasing the breadth and depth of receptors available for therapeutic interventions. Such "designer" drugs currently include allosteric regulators, inverse agonists, and drugs targeting hetero-oligomeric complexes (Panetta and Greenwood, 2008).

When considering the nervous system, the existence of heteromers of neurotransmitter GPCRs contributes to the high degree of plasticity characteristic for such a highly organized and complex system. Neurotransmitter receptors are no more considered as single functional units, but as forming part of multimolecular aggregates localized in the plane of the plasma membrane which can contain other interacting proteins (Franco et al., 2007). In the case of Parkinson's disease, a degenerative process caused by a gradual disappearance of the dopaminergic nigrostriatal neurons, it is suspected that the real targets for treatment should be dopamine-receptor-containing heteromers, among which

* Corresponding author. Tel.: +381 112067284; fax: +381 112067294.
E-mail address: milena.cavic@ncrc.ac.rs (M. Čavić).

0165-0270/$ – see front matter © 2011 Elsevier B.V. All rights reserved.
doi:10.1016/j.jneumeth.2011.05.021

adenosine receptors have been extensively studied (Franco, 2009). At present there are different clinical trials in which synthetic A_{2A} receptor ($A_{2A}R$) antagonists are under evaluation, since there is a functional antagonism between $A_{2A}R$ and dopamine D_2 receptor (D_2R) in the striatum (Canals et al., 2003). Also, histamine H_3 receptor (H_3R) has been proposed as a promising candidate (Leurs et al., 2005; Ferrada et al., 2008; Moreno et al., 2011).

To fully appreciate the contribution of these heteromers to normal physiology of the brain and use them for selective drug targeting, it is necessary to investigate the functional inter-relationships between the receptors in a heteromer. Technologies based on the use of fluorescent-fused proteins and different adaptations of resonance energy transfer (RET) techniques have been very useful. RET consists of a nonradiative (dipole–dipole) transfer of energy from a chromophore in an excited state fused to receptor A (known as the "donor"), to a chromophore fused to receptor B (the "acceptor"). This results in reduction of the donor emission and a consequent increase of fluorescence emission by the acceptor. In fluorescence RET (FRET) the molecules are fluorescent, whereas in bioluminescence RET (BRET) the donor is a bioluminescent enzyme which excites the acceptor fluorophore in the presence of a substrate. If two receptors are positioned at a distance beneath 10 nm (i.e., form a heteromer) effective energy transfer can occur. To evaluate the existence of higher-order oligomers, a sequential BRET–FRET technique, called SRET, to identify heteromers formed by the physical interaction of three different proteins in living cells has recently been developed (Carriba et al., 2008).

GPCRs oligomerization is difficult to analyze in native cells, therefore, many cell lines in which receptor proteins can be efficiently expressed have been widely used as an accepted model. Cloning different GPCRs into fluorescent or luminescent vectors enables their easy detection and tracking, as well as the employment of various techniques for investigation of receptor heteromerization at the intramembrane (RET, radioligand binding. . .) and intracellular signaling level (cAMP, ERK. . .).

The aim of this study was the production and characterization of recombinant $A_{2A}R$-Rluc, D_2R-GFP^2 and H_3R-YFP receptors, which would in the future be used to provide better insight into their pharmacological and functional inter-relationships in the brain, and lead to the design of new drugs for the treatment of Parkinson's disease.

2. Materials and methods

2.1. Preparation of vectors and insert DNA

Renilla luciferase expressing vector pRluc-N1 and Green Fluorescent Protein 2 expressing vector pGFP^2-N3(h) were obtained from PerkinElmer, Boston, MA. The Enhanced Yellow variant of green Fluorescent Protein vector pEYFP-N1 was obtained from Clontech, Heidelberg, Germany. The lyophilized plasmid DNAs were reconstituted according to manufacturer's instructions.

The cDNA of human $A_{2A}R$ from a host plasmid pcDNA3.1 (10 ng/μL) was amplified without its stop codon using sense and antisense primers (10 μM) harboring EcoRI and BamHI sites, to be in-frame with Rluc in the pRluc-N1 vector. The cDNA of human D_2R from pcDNA3.1 (10 ng/μL) was amplified without its stop codon using sense and antisense primers (10 μM) harboring HindIII and KpnI, to be in-frame with GFP^2 in the pGFP^2-N3(h) vector. The cDNA of human H_3R from a host plasmid (Johnson & Johnson Pharmaceutical Research & Development, L.L.C., San Diego, CA, USA) was amplified without its stop codon using sense and antisense primers harboring EcoRI and BamHI, to be in frame with eYFP in the pEYFP-N1 vector. The obtained PCR products were analyzed by electrophoresis on a 1% agarose gel, and the detected bands were purified using PCR clean-up/gel extraction NS® Extract II kit (MACHEREY-NAGEL GmbH & Co. KG, Düren, Germany).

2.2. Cutting and ligation

The purified PCR products and target vectors were cut in separate tubes by the appropriate restriction enzymes, i.e., $A_{2A}R$ and pRluc-N1 with EcoRI and BamHI, D_2R and pGFP^2-N3(h) with HindIII and KpnI, and H_3R pEYFP-N1 with BamHI and EcoRI. The products were run on a 1% agarose gel with 2 mM guanosine. The obtained linear vectors and cDNAs were extracted from the gel using PCR clean-up/gel extraction NS® Extract II kit, and their concentrations were determined using NanoDrop spectrophotometer (ThermoFisher Scientific). Typically 100 ng of target vector DNA and a 3 to 6-fold molar excess of inserts were used with 100 IU of T4 DNA ligase (Promega, WI, USA) in a total volume of 10 μL in an overnight temperature gradient according to the manufacturer's recommendation.

2.3. Bacterial transformation

The ligation mixture was used to transform 100 μL of Dh5α chemically competent cells (Invitrogen, Paisley, UK). The tubes were incubated on ice for 30 min, heat shocked at 42 °C for 45 s and then returned to ice. After 5 min, 900 μL of Luria-Bertani (LB) medium was added to each transformation mixture and the tubes were placed in an incubator at 37 °C for 75 min, with shaking. After centrifugation (2500 rpm 2 min) the supernatant was discarded and 100 μL of fresh LB added to dissolve the pellet. The cultures were spread onto LB plates containing appropriate antibiotics (for pRluc-N1 kanamycin 100 μg/mL, for pGFP^2-N3(h) zeocin 25 μg/mL and for pEYFP-N1 kanamycin 100 μg/mL) and incubated at 37 °C overnight.

2.4. Plasmid DNA preparation

Several colonies were picked from each LB plate, and 5 mL of LB solution containing appropriate antibiotics was inoculated with a single colony in separate 15 mL falcons. The suspensions were grown at 37 °C for 6 h with shaking, then transferred to 250 mL of LB containing appropriate antibiotics in erlenmayers and further grown at 37 °C overnight with shaking. The next day, the suspensions were centrifuged for 20 min at 7500 rpm at room temperature, and plasmid DNA was isolated from the pellet using PureLink™ HiPure Plasmid Filter Maxiprep Kit (Invitrogen, Paisley, UK). After obtaining DNA in water solution, the samples were quantified, aliquoted and stored at −20 °C for further use.

All constructs were verified by restriction digestion and positive samples were sequenced to confirm the correct insertion of cDNA into the vectors.

2.5. Cell culture

Human embryonic kidney cells (HEK-293T, American Type Tissue Culture, Manassas, VA) and Chinese hamster ovary cells (CHO, ATCC) were cultured in Dulbecco's modified Eagle's medium (DMEM, Gibco, Paisley, UK) and in minimum essential medium (αMEM, Gibco, Paisley, UK), respectively, supplemented with 2 mM L-glutamine, 100 UI/mL penicillin/streptomycin and 5% (v/v) heat-inactivated fetal bovine serum (FBS) (all supplements were from Invitrogen, Paisley, UK). Cells were maintained at 37 °C in an atmosphere of 5% CO_2, and were passaged twice a week.

2.6. Transient transfection

Cells were grown in six-well dishes or 25 cm^2 flasks to 80% confluence and were transiently transfected with cDNA of $A_{2A}R$, $A_{2A}R$-Rluc, D_2R, D_2R-GFP^2, H_3R or H_3R-YFP depending on the experiment, using the PolyEthylenImine (PEI, Polysciences, Eppelheim, Germany) method. Cells were incubated with a mix containing cDNA, 5.47 mM PEI and 150 mM NaCl in a serum starved medium. After 4 h, medium was changed to a fresh complete medium, and further experiments were performed at appropriate times after transfection.

2.7. Expression of constructs

48 h after transfection, HEK-293 T cells were rapidly washed twice in Hanks' balanced salt solution (HBSS – 137 mM NaCl, 5 mM KCl, 0.34 mM $Na_2HPO_4 \cdot 12H_2O$, 0.44 mM KH_2PO_4, 1.26 mM $CaCl_2 \cdot 2H_2O$, 0.4 mM $MgSO_4 \cdot 7H_2O$, 0.5 mM $MgCl_2$, 10 mM HEPES, pH 7.4) with 10 mM glucose, detached by gently pipetting and resuspended in the same buffer. To control the cell number, sample protein concentration was determined using a Bradford assay kit (Bio-Rad, Munich, Germany) using bovine serum albumin dilutions as standards. To quantify the luminescence of $A_{2A}R$-Rluc, cell suspension (20 μg of protein) was distributed in triplicates in 96-well microplates (Corning 3600, white plates with white bottom). 5 mM coelenterazine H (Invitrogen Molecular Probes, Eugene, OR, USA) was added and the luminescence of Rluc quantified after 10 min using a Mithras LB 940 fluorescence-luminescence detector (Berthold Technologies, DLReady, Germany) detecting the light emitted by the Rluc (440–500 nm). To quantify the fluorescence of H_3R-YFP, cell suspension (20 μg of protein) was distributed in duplicates into 96-well black microplates with a transparent bottom (Porvair, King's Lynn, UK) and read in a Mithras LB940 equipped with an excitation filter of 485 nm and an emission filter of 530 nm. To quantify the fluorescence of D_2R-GFP^2, plates were read in a Fluostar Optima Fluorimeter (BMG Labtechnologies, Offenburg, Germany) equipped with a high energy xenon flash lamp, using a 10-nm bandwidth excitation filter at 400 nm (393–403 nm), and 10-nm bandwidth emission filters corresponding to 506–515 nm filter (Ch 1) and 527–536 nm filter (Ch 2). Rluc, YFP or GFP^2 data was calculated as the signal of the sample minus the signal of non-transfected cells, and is given in relative luminescence (RLU) and relative fluorescence (RFU) units.

2.8. Confocal microscopy

HEK-293T cells transiently transfected with various amounts of cDNA of $A_{2A}R$-Rluc, D_2R-GFP^2 and H_3R-YFP were grown in six-well dishes on 15-mm glass coverslips. At 60% confluence, cells were rinsed with phosphate-buffered saline PBS, fixed in 4% paraformaldehyde for 15 min, and washed with PBS containing 20 mM glycine to quench the aldehyde groups. Cells were permeabilized with PBS containing 20 mM glycine, 1% bovine serum albumin (BSA) (buffer A) and 0.05% Triton X-100 during 5 min. After that the cells were blocked with buffer A for 1 h at room temperature. Cells were labeled for 1 h with the primary mouse monoclonal anti-Rluc antibody (Millipore, Bedford, USA). The cover slips were then washed and stained for 1 h with the secondary antibody cyanine 3-conjugated affinity purified donkey antimouse IgG (Jackson ImmunoResearch, West Grove, USA). Negative control of the secondary antibody was performed for each sample. The coverslips were rinsed for 30 min in buffer A and fixed with Mowiol mounting medium. Microscopic observations of the pattern of expression of the fusion proteins were made using Olympus FV 300 confocal scanning laser microscope (Leica Lasertechnik, Leica Microsystems, Mannheim, Germany). Detection of the D_2R-GFP^2 and H_3R-YFP constructs was performed using their fluorescent properties.

2.9. ERK phosphorylation assay

CHO cells were transiently transfected with 0.5 μg of $A_{2A}R$-Rluc cDNA, 1 μg of D_2R-GFP^2 cDNA and 2.5 μg of H_3R-YFP cDNA. Cells were treated (or not) with 1 μM ZM241385 ($A_{2A}R$ antagonist), 1 μM YM091502 (D_2R antagonist) or 1 μM thioperamide (H_3R antagonist) for 30 min before the addition of the agonists 200 nM CGS21680, 1 μM quinpirole or 50 nM (R)-α-methylhistamine (RAMH), respectively, for 5 min. All drugs were provided by CHDI Foundation Inc. (Los Angeles, CA, US). At the end of the incubation periods, cells were rinsed with ice-cold PBS and lysed by the addition of 500 μL of ice-cold lysis buffer (50 mM Tris–HCl pH 7.4, 50 mM NaF, 150 mM NaCl, 45 mM, β-glycerophosphate, 1% Triton X-100, 20 mM phenylarsine oxide, 0.4 mM $NaVO_4$ and protease inhibitor cocktail). The cellular debris was removed by centrifugation at 13,000 × g for 5 min at 4 °C, and the proteins were quantified by the bicinchoninic acid (BCA) method using bovine serum albumin dilutions as standard (Pierce Chemical Co., Rockford, IL, USA). To determine the level of ERK1/2 phosphorylation, equal amounts of protein (10 μg) were separated by electrophoresis on a denaturing 10% SDS-polyacrylamide gel and transferred onto Immobilon-FL PVDF membrane (Millipore, Bedford, USA). After blocking the membranes in Odyssey Blocking Buffer (LI-COR, Lincoln, NE, USA) they were probed with a combination of mouse anti-phosphoERK1/2 antibody (Sigma, 1:2500) and rat anti-ERK1/2 antibody (Sigma, 1:40,000) that recognizes both phosphorylated and non-phosphorylated ERK1/2 in order to rule out that the differences observed were due to the application of unequal amounts of lysates.

The 42 and 44 kDa bands corresponding to ERK 1 and ERK 2 were visualized by the addition of a mixture of IRDye 800 (anti-mouse) antibody and IRDye 680 (anti-rabbit) antibody (1:10,000, Sigma) for 1 h and scanned by the Odyssey Infrared Scanner (LI-COR Biosciences, Lincoln, NE, USA). Bands densities were quantified using the Odyssey V3.0 software and exported to Excel (Microsoft, Redmond, WA, USA). The level of phosphorylated ERK1/2 isoforms was normalized for differences in loading using the total ERK protein band intensities. As a basal value (standardized to 1) activation of ERKs in transfected nontreated cells was used, while non-transfected cells were used as blank.

3. Results and discussion

The progress of the cloning process was monitored electrophoretically (Fig. 1). PCR products of insert cDNA were run on a 1% agarose gel, and distinctive bands around 1.3 kb corresponding to $A_{2A}R$, D_2R and H_3R were visible on the gel as expected (Fig. 1A). After purification, the PCR products and vectors were subjected to double digestion with the corresponding restrictive enzymes and subsequently ligated. After transformation of Dh5α cells with the ligation mixtures intact circular plasmids were obtained, with $A_{2A}R$ inserted into pRluc-N1, D_2R into $pGFP^2$-N3 and H_3R into pEYFP-N1 (Fig. 1B). All constructs were verified by double digestion, and the products were analyzed on 1% agarose gel. Clones were regarded as positive if they produced two bands, of 1.3 kb for $A_{2A}R$ and 4.9 kb for linearized pRluc-N1, 1.3 kb for D_2R and 4.3 kb for linearized $pGFP^2$-N3 and 1.3 kb for H_3R and 4.7 kb for linearized pEYFP-N1 (Fig. 1C). The correct insertion of cDNA into the vectors of the positive samples was confirmed by sequencing. Nucleotide sequences showed that the obtained constructs $A_{2A}R$-Rluc, D_2R-GFP^2 and H_3-YFP express Rluc, GFP^2 and EYFP on the C-terminal ends of the receptors, respectively. One confirmed clone for each receptor was

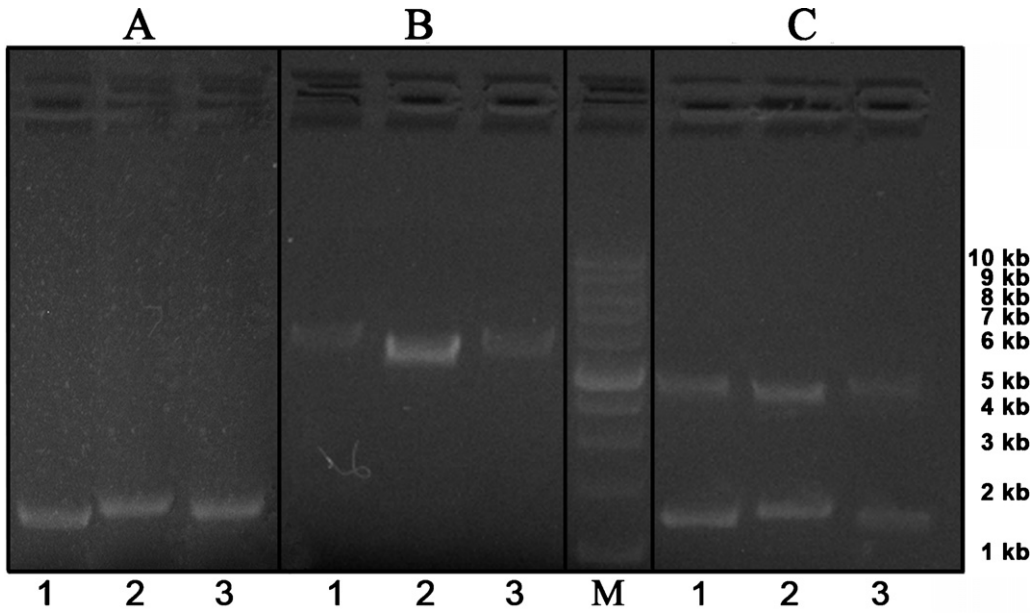

Fig. 1. Agarose gel electrophoresis of starting PCR products (A), intact plasmids (B) and digested plasmids (C). (A1) $A_{2A}R$, (A2) D_2R, (A3) H_3R; (B1) $A_{2A}R$-Rluc-N1, (B2) D_2R-GFP^2-N3, (B3) H_3R-EYFP-N1; (C1) $A_{2A}R$ and linearized pRluc-N1, (C2) D_2R and linearized $pGFP^2$-N3, (C3) H_3R and linearized pEYFP-N1; M, molecular weight marker.

used for transfection into HEK-293T and CHO cells. All expression and functional experiments were initially performed in both HEK-293T and CHO cell lines, to verify the validity of the obtained data. The same pattern of results for the localization, level of expression and functionality of the constructs was obtained in both cell lines. Expression and localization data from HEK cells is presented, as they consistently gave lower fluorescence and luminescence background signals. In the case of ERK1/2 phosphorylation studies, data obtained from CHO cells is presented, as they showed less variability of the level of ERK phosphorylation in repeated assays.

After transient transfection into HEK-293T cells increasing expression levels of the cloned receptors were detected (Fig. 2). Results are given in relative luminescence or relative fluorescence units by subtracting the value of untransfected cells and represent mean ± s.e.m. of three to five independent experiments. The receptor constructs gave increasing signals of Rluc (Fig. 2A), GFP^2 (Fig. 2B) and YFP (Fig. 2C) with increasing amounts of transfected cDNA, usually reaching a plateau at some higher concentration. From the curves, it was determined that the optimal amounts for transfection were 0.5 μg of cDNA for $A_{2A}R$-Rluc, 1 μg of cDNA for D_2R-GFP^2 and 2.5 μg of cDNA for H_3R-YFP, so the signal they produce in cells would be sufficient for detecting, while minimizing overexpression. These amounts of the constructs were determined as optimal to decrease the likelihood of false positive/negative results in further heteromerization studies.

Spatial expression of the receptors was observed by confocal microscopy at different times after transient transfection into HEK-293T cells. Representative images from three to four inde-

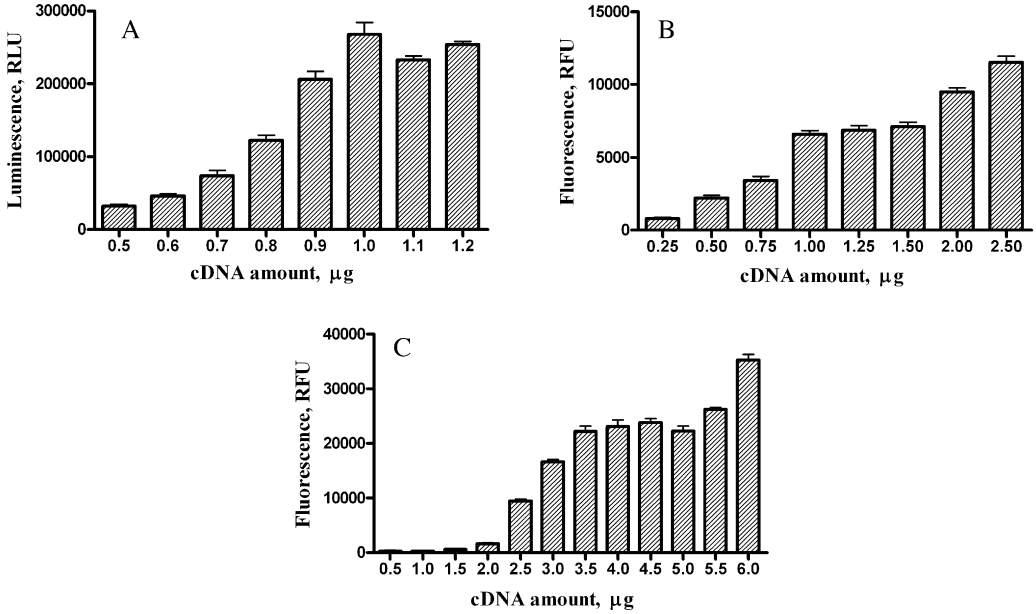

Fig. 2. Expression of $A_{2A}R$-Rluc (A), D_2R-GFP^2 (B) and H_3R-YFP (C) constructs. Results are obtained by subtracting the value of untransfected cells and represent mean ± s.e.m. of three to five independent experiments. RLU, relative luminescence units, RFU, relative fluorescence units.

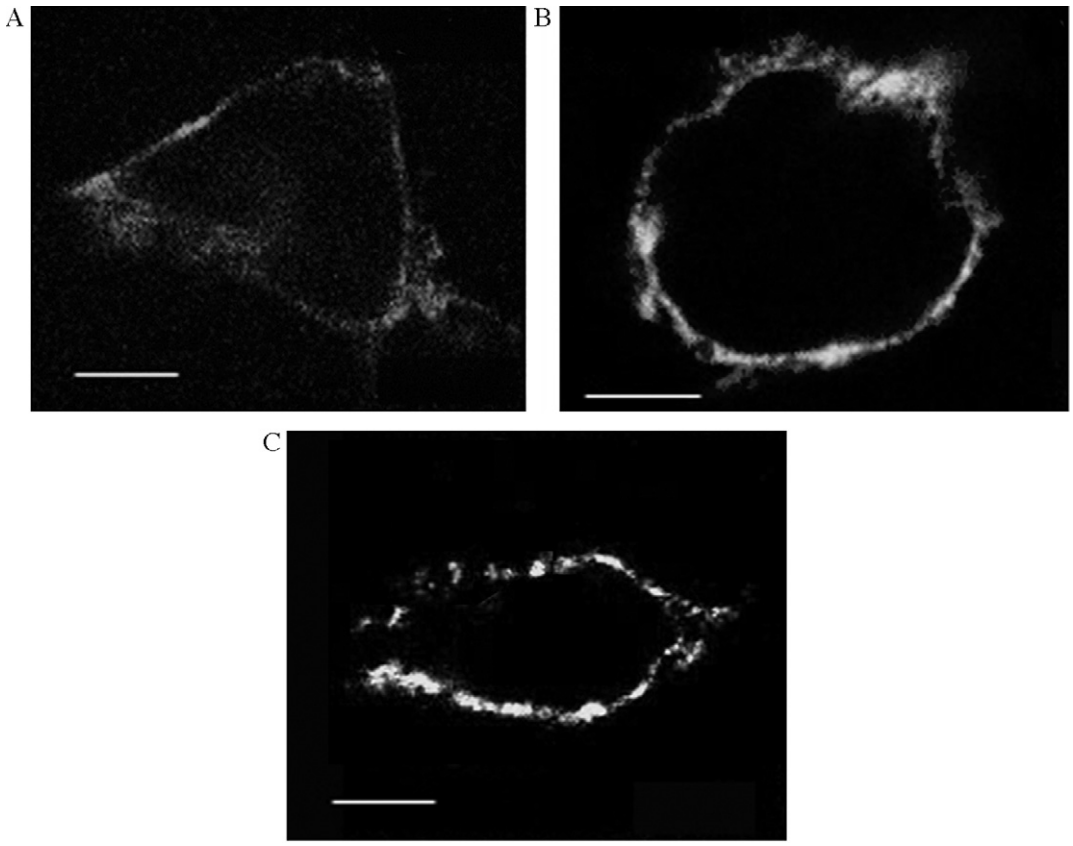

Fig. 3. Confocal microscopy images of HEK-293 T cells expressing A_{2A}R-Rluc (A, 0.5 μg of cDNA), D_2R-GFP^2 (B, 1 μg of cDNA) and H_3R-YFP (C, 2.5 μg of cDNA) constructs. Representative images from three to four independent experiments are shown. Scale bars, 10 μm.

pendent experiments for each construct are shown, considering the fact that the localization of the constructs was the same in over 90% of cells in each experiment (Fig. 3). The localization of A_{2A}R (Fig. 3A) was determined by detecting its Rluc tag with a monoclonal anti-Rluc antibody labeled with Cy3 dye, while the localization of D_2R (Fig. 3B) and H_3R (Fig. 3C) was determined by detecting their fluorescent GFP^2 and YFP tags, respectively. Controls using non-transfected cells and cells transfected only with empty vectors pRluc-N1, pGFP^2-N3 and pEYFP-N1 were employed in each experiment. While nontransfected cells gave no specific fluorescent signal, empty-vector transfected cells gave a fluorescent signal which was not localized in the plasma membrane, even after 72 h. When the cloned A_{2A}R-Rluc, D_2R-GFP^2 and H_3R-YFP were transfected, it was noted that 24 h after transfection the receptors were abundant in the endoplasmatic reticulum, but also begining to migrate to the plasma membrane. The optimal time needed for their expression in the plasma membrane was determined to be 48 h after transfection. This time frame was used in all subsequent experiments, to be certain that the GPCRs have been correctly placed in the plasma membrane. Using confocal microscopy it was shown that the cloned receptors express correctly in the cells and travel to the plasma membrane as their corresponding wild-type couples.

The functionality of the constructs was compared to their respective non-fluorescent couples measuring the phosphorylation of extracellular signal-regulated kinases 1 and 2 (ERK1/2) upon ligand stimulation in transiently transfected CHO cells. Controls using non-transfected cells and cells transfected only with empty vectors stimulated with ligands for A_{2A}, D_2 and H_3 receptors were employed in each experiment. No specific increase in ERK1/2 phosphorylation upon agonist stimulation was observed in neither non-transfected (Fig. 4) nor empty-vector transfected cells, which suggested that CHO cells did not have a significant level of endogenously expressed A_{2A}, D_2 and H_3 receptors. Cells transfected with cDNA of A_{2A}R (Fig. 5A) or A_{2A}R-Rluc (Fig. 5B) were treated or not with the A_{2A}R agonist CGS21680 in the presence or absence of the A_{2A}R antagonist ZM241385. Cells transfected with cDNA of

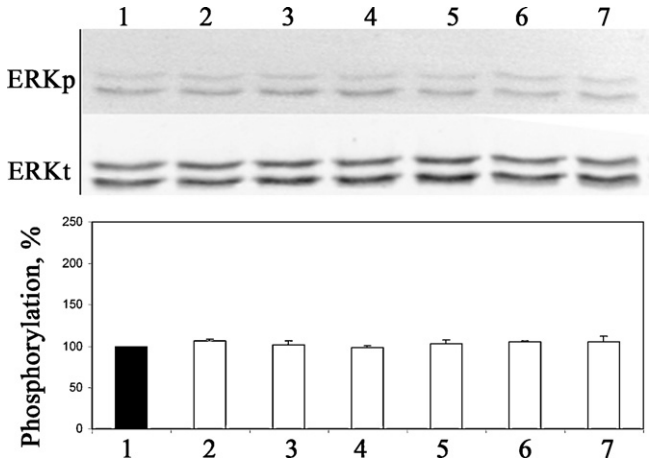

Fig. 4. Ligand-induced ERK phosphorylation in non-transfected CHO cells. Non-transfected CHO cells were treated or not (1) with the A_{2A}R agonist CGS21680 (200 nM) in the absence (2) or in the presence (3) of the A_{2A}R antagonist ZM241385 (1 μM), and with the D_2R agonist quinpirole (1 μM) in the absence (4) or in the presence (5) of the D_2R antagonist YM091502 (1 μM), and with the H_3R agonist RAMH (50 nM) in the absence (6) or in the presence (7) of the H_3R antagonist thioperamide (1 μM). In the top panel a representative Western blot is shown. In the bottom panel band density quatification results are expressed as a percentage of phosphorylation of the non-treated cells and represent mean ± s.e.m. of three independent experiments.

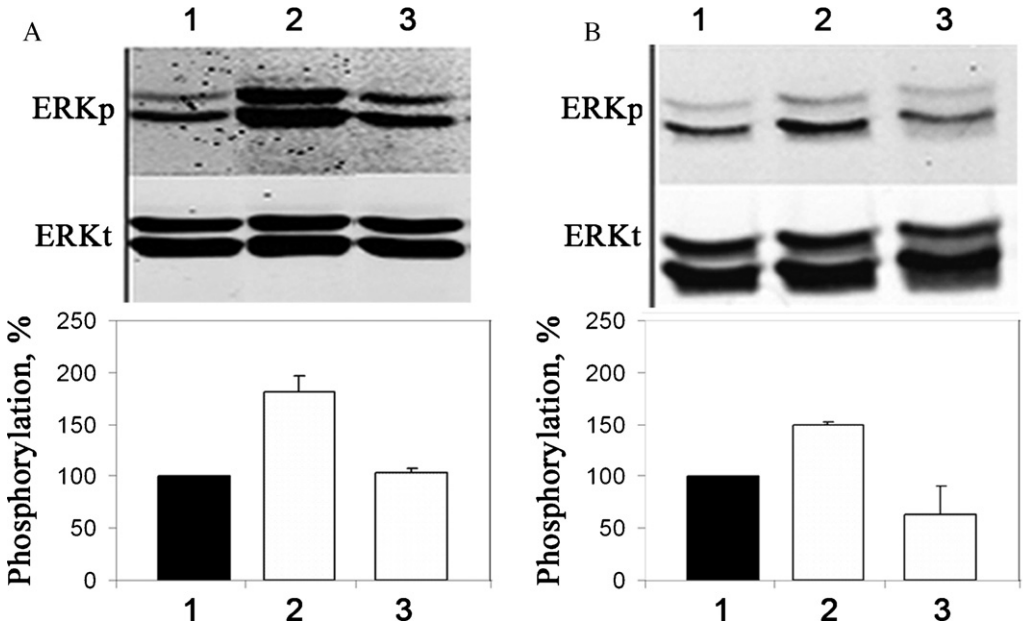

Fig. 5. $A_{2A}R$ (A) and $A_{2A}R$-Rluc (B) agonist-induced ERK phosphorylation. CHO cells transfected with 0.5 μg of cDNA of $A_{2A}R$ or $A_{2A}R$-Rluc were treated or not (1) with the $A_{2A}R$ agonist CGS21680 (200 nM) in the absence (2) or in the presence (3) of the $A_{2A}R$ antagonist ZM241385 (1 μM). In the top panel representative Western blots are shown. In the bottom panel band density quatification results are expressed as a percentage of phosphorylation of the non-treated cells and represent mean ± s.e.m. of three independent experiments.

D_2R (Fig. 6A) or D_2R-GFP^2 (Fig. 6B) were treated or not with the D_2R agonist quinpirole in the presence or absence of the D_2R antagonist YM091502. Cells transfected with cDNA of H_3R (Fig. 7A) or H_3R-YFP (Fig. 7B) were treated or not with the H_3R agonist RAMH in the presence or absence of the H_3R antagonist thioperamide. After quantification and normalization of data for differences in loading, results were expressed as a percentage of the value of transfected untreated cells and represent mean ± s.e.m. of three to five independent experiments. Upon stimulation with the corresponding agonists, cells expressing the wild type and the cloned receptors were able to induce ERK1/2 phosphorylation, and this effect was blocked by the corresponding antagonists. As this effect

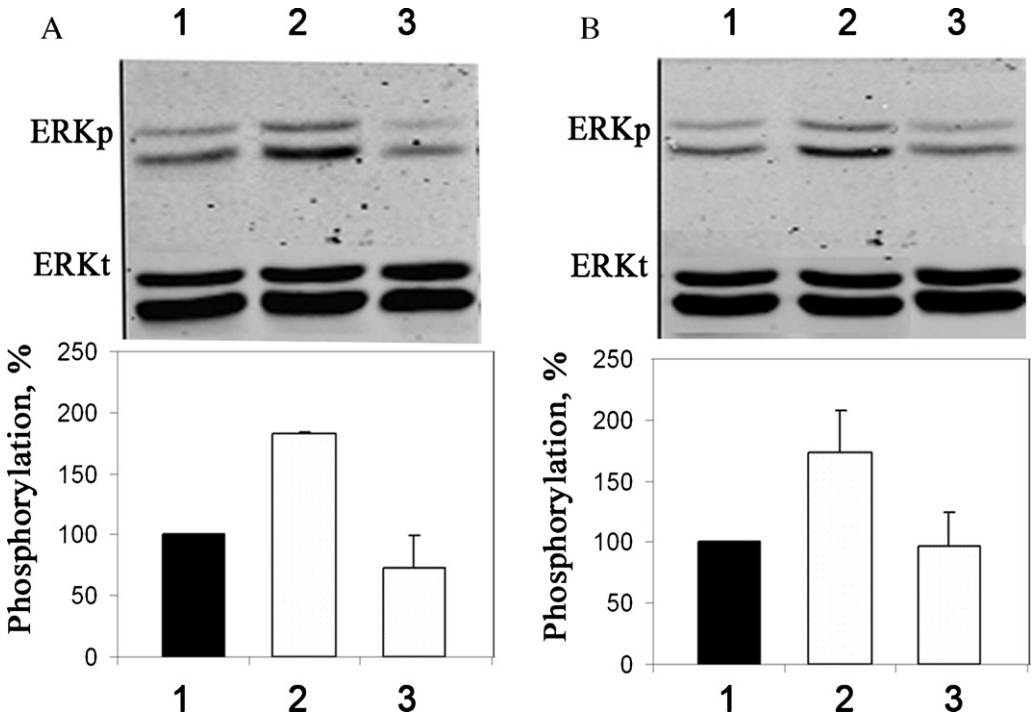

Fig. 6. D_2R (A) and D_2R-GFP^2 (B) agonist-induced ERK phosphorylation. CHO cells transfected with 1 μg of cDNA of D_2R or D_2R-GFP^2 were treated or not (1) with the D_2R agonist quinpirole (1 μM) in the absence (2) or in the presence (3) of the D_2R antagonist YM091502 (1 μM). In the top panel representative Western blots are shown. In the bottom panel band density quatification results are expressed as a percentage of phosphorylation of the non-treated cells and represent mean ± s.e.m. of three independent experiments.

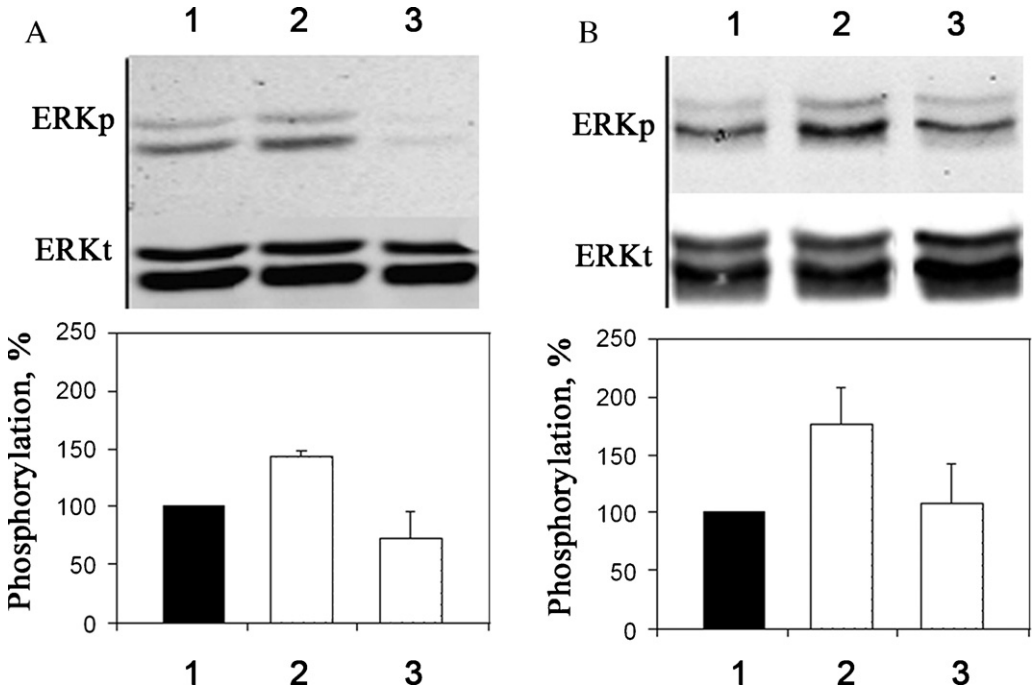

Fig. 7. H_3R (A) and H_3R-YFP (B) agonist-induced ERK phosphorylation. CHO cells transfected with 2.5 μg of cDNA of H_3R or H_3R-YFP were treated or not (1) with the H_3R agonist RAMH (50 nM) in the absence (2) or in the presence (3) of the H_3R antagonist thioperamide (1 μM). In the top panel representative Western blots are shown. In the bottom panel band density quatification results are expressed as a percentage of phosphorylation of the non-treated cells and represent mean ± s.e.m. of three independent experiments.

was not observed in non-transfected nor empty-vector transfected cells, it was concluded that specific changes in ERK1/2 phosphorylation were induced by the expression of the transfected receptors. Also, the cloned constructs exhibited a similar pattern (potency) of phosphorylation of ERKs upon ligand stimulation of $A_{2A}R$-Rluc, D_2R-GFP2 and H_3R-YFP and $A_{2A}R$, D_2R and H_3R, respectively. These results indicated that the cloned receptors are functional and can be used in experiments for determining the response of cells to different stimuli that affect the signaling pathway of ERK kinases. This method is extensively used to determine the impact of receptor heteromerization on cellular signaling response upon multiple stimulation.

4. Conclusion

The previous experiments confirmed that the cloned $A_{2A}R$-Rluc, D_2R-GFP[2] and H_3R-YFP constructs are functional, express correctly in the plasma membrane and can be used in further experiments to elucidate the pharmacological and functional inter-relationships between adenosine A_{2A}, dopamine D_2 and histamine H_3 receptors in the brain. Hopefully, this will enable the design and evaluation of new therapeutic strategies for Parkinson's disease.

Acknowledgements

We acknowledge the technical help obtained from Jasmina Jiménez (Molecular Neurobiology Laboratory, Barcelona University, Spain). This study was supported by Grant SAF2008-00146 from Spanish Ministerio de Ciencia y Tecnología.

References

Bulenger S, Marullo S, Bouvier M. Emerging role of homo- and heterodimerization in G-protein-coupled receptor biosynthesis and maturation. Trends Pharmacol Sci 2005;26:131–7.
Canals M, Marcellino D, Fanelli F, Ciruela F, de Benedetti P, Goldberg SR, et al. Adenosine A2A-dopamine D2 receptor-receptor heteromerization: qualitative and quantitative assessment by fluorescence and bioluminescence energy transfer. J Biol Chem 2003;278:46741–9.
Carriba P, Navarro G, Ciruela F, Ferré S, Casadó V, Agnati L, et al. Detection of heteromerization of more than two proteins by sequential BRET–FRET. Nat Methods 2008;8:727–33.
Ferrada C, Ferré S, Casadó V, Cortés A, Justinova Z, Barnes C, et al. Interactions between histamine H3 and dopamine D2 receptors and the implications for striatal function. Neuropharmacology 2008;55:190–7.
Ferre S, Ciruela F, Quiroz C, Lujan R, Popoli P, Cunha RA, et al. Adenosine receptor heteromers and their integrative role in striatal function. ScientificWorldJournal 2007;7(S2):74–85.
Franco R, Casado V, Cortes A, Ferrada C, Mallol J, Woods A, et al. Basic concepts in G-protein-coupled receptor homo- and heterodimerization. ScientificWorldJournal 2007;7(S2):48–57.
Franco R. Neurotransmitter receptor heteromers in neurodegenerative diseases and neural plasticity. J Neural Transm 2009;116:983–7.
Fuxe K, Marcellino D, Guidolin D, Woods AS, Agnati LF. Heterodimers and receptor mosaics of different types of G-protein-coupled receptors. Physiology 2008;23:322–32.
Gilchrist A. GPCR molecular pharmacology and drug targeting: shifting paradigms and new directions. Hoboken, NJ: John Wiley & Sons, Inc; 2010. p. 191.
Leurs R, Bakker RA, Timmerman H, de Esch IJ. The histamine H3 receptor: from gene cloning to H3 receptor drugs. Nat Rev Drug Discov 2005;4:107–20.
Moreno E, Hoffmann H, Gonzalez-Sepúlveda M, Navarro G, Casadó V, Cortés A, et al. Dopamine D1-histamine H3 receptor heteromers provide a selective link to MAPK signaling in GABAergic neurons of the direct striatal pathway. J Biol Chem 2011;286:5846–54.
Panetta R, Greenwood MT. Physiological relevance of GPCR oligomerization and its impact on drug discovery. Drug Discov Today 2008;13:1059–66.

6.2 Interacciones entre dominios intracelulares como determinantes importantes de la estructura cuaternaria y la función de heterómeros de receptores

Gemma Navarro[‡], Sergi Ferré[§], Arnau Cordomi[¶], Estefanía Moreno[‡], Josefa Mallol[‡], Vicent Casadó[‡], Antoni Cortés[‡], Hanne Hoffmann[¶], Jordi Ortiz[¶], Enric I. Canela[‡], Carme Lluís[‡], Leonardo Pardo[¶], Rafael Franco[‡**], and Amina S. Woods[§]

[‡]Centro de Investigación Biomédica en Red Sobre Enfermedades Neurodegenerativas, Departamento de Bioquímica y Biología Molecular, Facultad de Biología, Universidad de Barcelona, Avda. Diagonal 645, 08028 Barcelona, España,
[§]The Intramural Research Program, National Institute on Drug Abuse, Department of Health and Human Services, Baltimore, Maryland 21224,
[¶]Laboratori de Medicina Computacional, Unitat de Bioestadística y Instituto de Neurosciencias y Departamento de Bioquímica y Biología Molecular, Facultad de Medicina, Universitat Autónoma de Barcelona, 08193 Bellaterra, España,
[**]Centro de Investigación Médica Aplicada, Universidad de Navarra, 31008 Pamplona, Spain.

Manuscrito publicado en Journal of biological chemistry (2010 Aug), ***285 (35)****: 27346-27359.*

Los heterómeros de receptores acoplados a proteína G (GPCR) son complejos macromoleculares con propiedades funcionales propias, diferentes a las unidades individuales de los protómeros que los forman. Se sabe muy poco sobre qué es lo que determina la estructura cuaternaria de los heterómeros de los GPCR, dando resultado a sus propiedades funcionales únicas. Mediante el uso de técnicas de trasferencia de energía de resonancia en experimentos con receptores mutados, en este trabajo se demuestra, por primera vez, que los dominios intracelulares de los receptores juegan un papel importante en la determinación de la estructura cuaternaria de los heterómeros de receptores A_{2A} de adenosina, CB_1 de cannabinoides y D_2 de dopamina. En estos dominios, epítopos ricos en arginina forman puentes salinos con residuos fosforilados de serina o treonina de zonas consenso de fosforilación por CK1/2. Cada uno de los receptores (A_{2A}, CB_1, y D_2) contiene dos dominios intracelulares conservados evolutivamente que establecen interacciones electrostáticas selectivas con dominios intracelulares de los otros dos receptores, sugiriendo que estas interacciones electrostáticas constituyen un mecanismo general para la heteromerización entre receptores. Los experimentos realizados con receptores mutados indican que las interacciones entre dominios intracelulares del receptor CB_1 con los receptores A_{2A} y D_2 son fundamentales para la correcta formación de la estructura cuaternaria necesaria para la señalización del heterómero A_{2A}-CB_1-D_2 por la vía de las MAPK. El análisis de esta vía de señalización en cortes estriatales de ratones control y *knockout* para el receptor CB_1 proporciona evidencias de la existencia del heterómero A_{2A}-CB_1-D_2 en el cerebro. Estos resultados nos permiten proponer el primer modelo molecular de estructura cuaternaria de un "heteromultímero" de receptores.

THE JOURNAL OF BIOLOGICAL CHEMISTRY VOL. 285, NO. 35, pp. 27346–27359, August 27, 2010
Printed in the U.S.A.

Interactions between Intracellular Domains as Key Determinants of the Quaternary Structure and Function of Receptor Heteromers*[S]

Received for publication, February 18, 2010, and in revised form, June 7, 2010 Published, JBC Papers in Press, June 18, 2010, DOI 10.1074/jbc.M110.115634

Gemma Navarro[‡], Sergi Ferré[§], Arnau Cordomi[¶], Estefania Moreno[‡], Josefa Mallol[‡], Vicent Casadó[‡], Antoni Cortés[‡], Hanne Hoffmann[‖], Jordi Ortiz[‖], Enric I. Canela[‡], Carme Lluís[‡], Leonardo Pardo[¶], Rafael Franco[‡], and Amina S. Woods[§1]**

*From the [‡]Centro de Investigación Biomédica en Red Sobre Enfermedades Neurodegenerativas, Department of Biochemistry and Molecular Biology, Faculty of Biology, University of Barcelona, 08028 Barcelona, Spain, the [§]Intramural Research Program, National Institute on Drug Abuse, Department of Health and Human Services, Baltimore, Maryland 21224, the [¶]Laboratori de Medicina Computacional, Unitat de Bioestadística, and [‖]Neuroscience Institute and Department of Biochemistry and Molecular Biology, Facultat de Medicina, Universitat Autónoma de Barcelona, 08193 Bellaterra, Spain, and the **Centro de Investigación Médica Aplicada, Universidad de Navarra, 31008 Pamplona, Spain*

G protein-coupled receptor (GPCR) heteromers are macromolecular complexes with unique functional properties different from those of its individual protomers. Little is known about what determines the quaternary structure of GPCR heteromers resulting in their unique functional properties. In this study, using resonance energy transfer techniques in experiments with mutated receptors, we provide for the first time clear evidence for a key role of intracellular domains in the determination of the quaternary structure of GPCR heteromers between adenosine A_{2A}, cannabinoid CB_1, and dopamine D_2 receptors. In these interactions, arginine-rich epitopes form salt bridges with phosphorylated serine or threonine residues from CK1/2 consensus sites. Each receptor (A_{2A}, CB_1, and D_2) was found to include two evolutionarily conserved intracellular domains to establish selective electrostatic interactions with intracellular domains of the other two receptors, indicating that these particular electrostatic interactions constitute a general mechanism for receptor heteromerization. Mutation experiments indicated that the interactions of the intracellular domains of the CB_1 receptor with A_{2A} and D_2 receptors are fundamental for the correct formation of the quaternary structure needed for the function (MAPK signaling) of the A_{2A}-CB_1-D_2 receptor heteromers. Analysis of MAPK signaling in striatal slices of CB_1 receptor KO mice and wild-type littermates supported the existence of A_1-CB_1-D_2 receptor heteromer in the brain. These findings allowed us to propose the first molecular model of the quaternary structure of a receptor heteromultimer.

Receptor heteromers are the focus of intense research, as through heteromerization receptors become unique functional entities with different properties from those of either receptor when not engaged in heteromerization resulting in new therapeutic targets (1–4). Their unique properties provide a "biochemical fingerprint" thus allowing their identification in native tissues (1, 3). There is already a long list of discovered heteromers with two different G protein-coupled receptors (GPCRs)[2] (2, 4). Furthermore, we recently obtained evidence for the existence of receptor heteromultimers, *i.e.* heteromers including more than two different receptors, and reported on heteromers, including the GPCRs adenosine A_{2A}, cannabinoid CB_1, and dopamine D_2 receptors, in transfected cells (5). Evidence of GPCR homomultimers has also been recently demonstrated in living cells (6, 7). Many important questions regarding receptor heteromers and heteromultimers remain unanswered. What is the arrangement of their GPCR units (quaternary structure)? What are the molecular determinants of their quaternary structure? Last but not least, what is their functional significance in native tissues?

It was inferred that different molecular mechanisms were involved in GPCR homo- and heteromerization. For family C GPCRs, disulfide bonds between extracellular domains as well as coiled-coil interactions between C-terminal domains seem to be necessary for the formation of functional homomeric or heteromeric receptors (8). For oligomerization of family A GPCRs, the helical transmembrane (TM) domains seem to be particularly important (7, 9–15). In this study, by using mutated A_{2A}, CB_1, and D_2 receptors, we investigated the relevance of electrostatic interactions (16) between intracellular domains in the determination of the quaternary structure of GPCR heteromers between A_{2A}, CB_1, and D_2 receptors. Our initial goal was to obtain evidence for multiple intracellular interactions in the A_{2A}-CB_1-D_2 receptor heteromultimer. Significantly, the same intracellular domains involved in A_{2A}-CB_1-D_2 receptor heteromultimerization were also involved in

* This work was supported, in whole or in part, by a National Institutes of Health grant from intramural funds to NIDA. This work was also supported by Spanish Ministerio de Ciencia y Tecnología Grants SAF2008-00146, SAF2006-05481, and SAF2008-03229-E/ for ERA-NET Coordination of Research Activities and Instituto de Salud Carlos III (RD07/0067/0008) Grant 060110 from Fundació La Marató de TV3.

[S] The on-line version of this article (available at http://www.jbc.org) contains supplemental Figs. 1 and 2 and Table 1.

[1] To whom correspondence should be addressed: National Institute on Drug Abuse, Intramural Research Program, Department of Health and Human Services, 333 Cassell Dr., Baltimore, MD 21224. Tel.: 443-740-2747; Fax: 443-740-2144; E-mail: awoods@intra.nida.nih.gov.

[2] The abbreviations used are: GPCR, G protein-coupled receptor; SRET, sequential resonance energy transfer; ANOVA, analysis of variance; PDB, Protein Data Bank; BRET, bioluminescence resonance energy transfer; TM, transmembrane; IL3, intracellular loop 3.

A_{2A}-D_2, A_{2A}-CB_1, and CB_1-D_2 receptor heteromerization. A three-dimensional model of the quaternary structure of the receptor heteromultimer was obtained by using the information from resonance energy transfer between A_{2A}, CB_1, and D_2 receptors in the receptor heteromultimer. Furthermore, a biochemical property of the receptor heteromultimer was found to be dependent on its correct quaternary structure, determined by the intracellular electrostatic interactions, which allowed its identification in rodent brain tissue.

EXPERIMENTAL PROCEDURES

Cell Culture—HEK-293T cells were grown in Dulbecco's modified Eagle's medium (DMEM) (Invitrogen) supplemented with 2 mM L-glutamine, 100 units/ml penicillin/streptomycin, and 5% (v/v) heat-inactivated fetal bovine serum (FBS) (all supplements were from Invitrogen). CHO cell lines were maintained in α-minimal essential medium without nucleosides, containing 10% fetal calf serum, 50 μg/ml penicillin, 50 μg/ml streptomycin, and 2 mM L-glutamine (300 μg/ml). Cells were maintained at 37 °C in an atmosphere of 5% CO_2 and were passaged when they were 80–90% confluent, twice a week.

Mutant Receptors—Ser^{374} in the C-terminal domain of the human A_{2A} receptor was mutated to Ala to obtain the $A_{2A}{}^{A374}$ receptor. The sequence ^{199}RIFLAA**RR**Q^{207} (boldface letters indicate the amino acid involved in the interaction between the receptors and the residues that were mutated) in the cytoplasm at the end of TM5 of human A_{2A} receptor was mutated to ^{199}RIFLAA**AA**Q^{207} to obtain the $A_{2A}{}^{A205\text{-}A206}$ receptor. The sequence ^{462}SVSTD**TS**AE^{470} in the C-terminal domain of human CB1 receptor was mutated to ^{462}SVSTD**AA**AE^{470} to obtain the $CB_1{}^{A467\text{-}A468}$ receptor. The sequence ^{321}**TS**EDGKVQVT^{330} in the third intracellular loop of human CB_1 receptor was mutated to ^{321}AAEDGKVQVT^{330} to obtain $CB_1{}^{A321\text{-}A322}$ receptor. Mutations were performed by site-directed mutagenesis (Cellogenetics, Ijamsville, MD).

Fusion Proteins and Expression Vectors—The human cDNAs of the A_{2A}, CB_1, and the mutant versions of these receptors or the human D_2, D_{2S}, and $D_{4.4}$ receptors, cloned in *pcDNA3.1*, were amplified without their stop codons using sense and antisense primers harboring unique EcoRI and BamHI sites to clone A_{2A}, $A_{2A}{}^{A374}$, and $A_{2A}{}^{A205\text{-}A206}$ receptors in the *Rluc* corresponding vector, EcoRI and KpnI to clone D_2 and D_{2S} receptors in the GFP^2 corresponding vector, BamHI and EcoRI to clone CB_1, $CB_1{}^{A467\text{-}A468}$, and $CB_1{}^{A321\text{-}A322}$ in the enhanced YFP corresponding vector, and XhoI and BamHI sites to clone $D_{4.4}$ receptor in the *Rluc* corresponding vector. The amplified fragments were subcloned to be in-frame into restriction sites of the multiple cloning sites of *pcDNA3.1-Rluc, pGFP*^{2}*-N3*(*h*), *pEYFP-N1* (Clontech) to give the plasmids corresponding to A_{2A}-*Rluc*, $A_{2A}{}^{A374}$-*Rluc* $A_{2A}{}^{A205\text{-}A206}$-*Rluc*, D_4-*Rluc*, D_2-GFP^2, D_{2S}-GFP^2, CB_1-YFP, $CB_1{}^{A467\text{-}A468}$-YFP, and $CB_1{}^{A321\text{-}A322}$-YFP receptor fusion proteins. The cDNA of the $5HT_{2B}$-YFP fusion protein was kindly provided by Dr. Irma Nardi (University of Pisa, Italy). Under these conditions, the fusion proteins are expressed at the membrane level, are not strongly overexpressed, and are quantitatively expressed in similar amounts (5).

Transient Transfection and Sample Preparation—HEK-293T or CHO cells growing in 6-well dishes were transiently transfected with the corresponding fusion protein cDNA by the polyethyleneimine method (Sigma). Cells were incubated (4 h) with the corresponding cDNA together with polyethyleneimine (5.47 mM in nitrogen residues) and 150 mM NaCl in a serum-starved medium. After 4 h, the medium was changed to a fresh complete culture medium. Forty eight hours after transfection, cells were washed twice in quick succession in Hanks' balanced salt solution with 10 mM glucose, detached, and resuspended in the same buffer containing 1 mM EDTA. To control the cell number, sample protein concentration was determined using a Bradford assay kit (Bio-Rad) using bovine serum albumin dilutions as standards. Cell suspension (20 μg of protein) was distributed into 96-well microplates; black plates with transparent bottom were used for FRET and fluorescence determinations, and white plates with white bottom were used for BRET and SRET experiments.

BRET Experiments—HEK-293T cells expressing the corresponding donor (receptor *Rluc*) and increasing amounts of the corresponding acceptor (receptor GFP^2 for $BRET^2$ or receptor YFP for $BRET^1$), as indicated in figure legends, were used. With aliquots of transfected cells (20 μg of protein), three different determinations were performed in parallel. (i) To quantify fluorescence proteins expression, cells were distributed in 96-well microplates (black plates with transparent bottom), and fluorescence was read in a Fluostar Optima Fluorimeter (BMG Labtechnologies, Offenburg, Germany) equipped with a high energy xenon flash lamp, using an excitation filter at 410 nm for receptor GFP^2 reading ($BRET^2$) or 485 nm for receptor YFP reading ($BRET^1$), and emission was detected using filters at 510 nm (for GFP^2) or 530 nm (for YFP). Receptor fluorescence expression was determined as fluorescence of the sample minus the fluorescence of cells expressing receptor *Rluc* alone. (ii) For $BRET^2$ and $BRET^1$ measurements, the equivalent of 20 μg of cell suspension was distributed in 96-well microplates (Corning 3600, white plates with white bottom), and 5 μM DeepBlueC ($BRET^2$) or coelenterazine H ($BRET^1$) (Molecular Probes, Eugene, OR) was added. For $BRET^2$ experiments, readings were collected immediately (~30 s) after addition of DeepBlueC using a Mithras LB 940 (Berthold Technologies, DLReady, Germany) that allows the integration of the signals detected in the short wavelength filter at 410 nm and the long wavelength filter at 510 nm. In $BRET^1$ after 1 min of adding coelenterazine H, the readings were collected using a Mithras LB 940 that allows the integration of the signals detected in the short wavelength filter at 485 nm and the long wavelength filter at 530 nm. (iii) To quantify receptor *Rluc* expression, luminescence readings were performed after 10 min of adding 5 μM coelenterazine H. The net BRET is defined as ((long wavelength emission)/(short wavelength emission)) − *Cf*, where *Cf* corresponds to ((long wavelength emission)/(short wavelength emission)) for the *Rluc* construct expressed alone in the same experiment.

FRET Experiments—HEK-293T cells expressing the corresponding donor (receptor GFP^2) and increasing amounts of the corresponding acceptor (receptor YFP), as indicated in figure legends, were used. Using aliquots of transfected cells (20 μg of protein), two different determinations were performed in par-

allel. (i) To quantify YFP fluorescence, due to receptor YFP expression, the same procedure as described for BRET experiments was used. (ii) For FRET measurements, the equivalent of 20 μg of cell suspension was distributed into 96-well microplates (black plates with a transparent bottom) and read in a Fluostar Optima fluorimeter equipped with a high energy xenon flash lamp, using an excitation filter at 410 nm and an emission filters at 510 nm (Ch_x) and 530 nm (Ch_y). Gain settings were identical for all experiments to keep the relative contribution of the fluorophores to the detection channels constant for spectral unmixing. The contribution of GFP^2 and YFP proteins alone to the two detection channels (spectral signature (17)) was measured in experiments with cells expressing only one of these proteins and normalized to the sum of the signal obtained in the two detection channels. The spectral signatures of the different receptors fused to either GFP^2 or YFP did not vary significantly from the determined spectral signatures of the fluorescent proteins alone. In determinations i and ii, linear unmixing was done taking into account the spectral signature as described by Zimmermann *et al.* (17) to separate the two emission spectra. For quantitation of the fluorescence emitted by each of two individual fluorophores (FluoA corresponding to the donor and FluoB corresponding to the acceptor) in FRET experiments, Equation 1 was applied,

$$\begin{aligned} &\text{FluoA} = S/(1 + 1/R) \\ &\text{FluoB} = S/(1 + R) \\ &\text{Being} \qquad\qquad\qquad\qquad \text{(Eq. 1)} \\ &S = Ch_x + Ch_y \\ &R = (B_yQ - B_x)/(A_x - A_yQ) \\ &Q = Ch_x/Ch_y \end{aligned}$$

where Ch_x and Ch_y represent the signals in detection channels x and y, and A_x, B_x and A_y, B_x represent the normalized contributions of FluoA or FluoB to channels x and y, as they are known from the spectral signatures of the fluorescent proteins.

Sequential Resonance Energy Transfer (SRET) Experiments—The recently introduced sequential BRET-FRET (SRET) technique (5) not only allows the demonstration of heteromerization of three proteins but can also provide information about the quaternary structure of the heterotrimeric complex. By transfecting three receptors separately fused to *Rluc*, GFP^2, and YFP, the detection of the $SRET^2$ signal demonstrates the physical interactions between the three receptors. In $SRET^2$, the oxidation of the *Rluc* substrate DeepBlueC triggers GFP^2 excitation ($BRET^2$), which triggers a subsequent excitation of YFP (FRET) (see Fig. 1). Emission of YFP after addition of DeepBlueC is only possible if the three fusion proteins are in close proximity (<10 nm), allowing bioluminescent and fluorescent SRET to occur. For SRET experiments, HEK-293T cells were transiently co-transfected with the indicated amounts of plasmid cDNAs corresponding to receptor *Rluc*, receptor GFP^2, and receptor YFP (see figure legends). In the experiments without casein kinase 1/2 inhibitors, cells were used 48 h post-transfection. When using casein kinase 1/2 inhibitors, cells were treated with casein kinase 1 inhibitor IC 261 (50 μM; Calbiochem) and casein kinase 2 inhibitor TBAC (10 μM; Calbiochem) 4 h after transfection, and after 24 h, the medium was changed to a fresh complete culture medium containing the same amount of inhibitors, and cells were used 48 h post-transfection. Using aliquots of transfected cells (20 μg of protein), different determinations were performed in parallel. (i) Quantification of protein-YFP expression was performed as indicated in FRET experiments. The sample fluorescence is the fluorescence calculated as described minus the fluorescence of cells expressing only protein-*Rluc* and protein-GFP^2. (ii) Quantification of protein-*Rluc* expression was by determination of the luminescence due to protein-*Rluc*. Cells were distributed in 96-well microplates (Corning 3600, white plates with white bottom), and luminescence was determined 10 min after addition of 5 μM coelenterazine H in a Mithras LB 940 multimode reader. (iii) BRET and FRET were combined to generate a technique called sequential BRET-FRET (SRET) that permits identification of heteromers formed by three different proteins. Cells were distributed in 96-well microplates (Corning 3600, white plates with white bottom), and 5 μM DeepBlueC (Molecular Probes, Eugene, OR) was added. The $SRET^2$ signal was collected using a Mithras LB 940 reader with detection filters for short wavelength (410 nm) and long wavelength (530 nm). By analogy with BRET, net $SRET^2$ is defined as ((long wavelength emission)/(short wavelength emission)) − *Cf*, where *Cf* corresponds to long wavelength emission/short wavelength emission for cells expressing protein-*Rluc* and protein-GFP^2. Linear unmixing was done for $SRET^2$ quantification, taking into account the spectral signature to separate the two fluorescence emission spectra (17). (iv) Using aliquots of cells transfected for SRET experiments, $BRET^1$, $BRET^2$, and FRET measurements were performed as indicated above. A $SRET^2$ saturation curve can be obtained determining $SRET^2$ as a function of increasing expression of the FRET acceptor (receptor YFP). From these saturation curves, an apparent $SRET_{max}$ was determined by fitting data to a monophasic saturation curve by nonlinear regression using the commercial Grafit curve-fitting software (Erithacus Software, Surrey, UK). These parameters have a similar meaning to these parameters when applied to BRET assays (5).

ERK Phosphorylation Assays—Wild-type littermates and CB_1 receptor knock-out CD1 albino Swiss male mice, 8 weeks old, weighing 25 g were used. The generation of mice lacking CB_1 receptor has been described elsewhere (18, 19). Mice were housed five per cage in a temperature- (21 ± 1 °C) and humidity-controlled (55 ± 10%) room with a 12:12 h light/dark cycle (light between 08:00 and 20:00 h) with food and water *ad libitum*. Animal procedures were conducted according to standard ethical guidelines (European Communities Council Directive 86/609/EEC) and approved by the Local Ethical Committee (IMAS-IMIM/UPF). Mice were decapitated with a guillotine, and the brains were rapidly removed and placed in ice-cold oxygenated (O_2/CO_2, 95:5%) Krebs-HCO_3^- buffer (124 mM NaCl, 4 mM KCl, 1.25 mM NaH_2PO_4, 1.5 mM $MgCl_2$, 1.5 mM $CaCl_2$, 10 mM glucose, and 26 mM $NaHCO_3$, pH 7.4). The brains were sliced at 4 °C in a brain matrix (Zivic Instruments, Pittsburgh, PA) into 0.5-mm coronal slices. Slices were kept at 4 °C in Krebs-HCO_3^- buffer during the dissection of the striatum.

Each slice was transferred into an incubation tube containing 1 ml of ice-cold Krebs-HCO_3^- buffer. The temperature was raised to 23 °C, and after 30 min, the media were replaced by 2 ml of Krebs-HCO_3^- buffer (23 °C). The slices were incubated under constant oxygenation (O_2/CO_2, 95:5%) at 30 °C for 4–5 h in an Eppendorf thermomixer (Eppendorf-5 Prime, Inc., Boulder, CO). The media were replaced by 200 μl of fresh Krebs-HCO_3^- buffer, and after 30 min, 1 μM of the A_{2A} receptor agonist CGS-21680, 1 μM of the D_2 receptor agonist quinpirole, or both prepared in Krebs-HCO_3^- buffer were added. After 10 min, the incubation solution was discarded, and slices were frozen on dry ice and stored at −80 °C. When ERK phosphorylation assays were performed in cell cultures, CHO cells (48 h after transfection) were cultured in serum-free medium for 16 h before the addition of any agent. Cells were resuspended in Hanks' balanced salt solution buffer and were treated for 5 min with CGS2168 (200 nM), quinpirole (1 μM), or a mixture of both ligands and rinsed with ice-cold phosphate-buffered saline. Both cells and slices were lysed by the addition of 500 μl of ice-cold lysis buffer (50 mM Tris-HCl, pH 7.4, 50 mM NaF, 150 mM NaCl, 45 mM β-glycerophosphate, 1% Triton X-100, 20 μM phenylarsine oxide, 0.4 mM $NaVO_4$, and protease inhibitor mixture). The cellular debris was removed by centrifugation at 13,000 × *g* for 5 min at 4 °C, and the protein was quantified by the bicinchoninic acid method using bovine serum albumin dilutions as standard. To determine the level of ERK1/2 phosphorylation, equivalent amounts of protein (10 μg) were separated by electrophoresis on a denaturing 7.5% SDS-polyacrylamide gel and transferred onto PVDF membranes. The membranes were then probed with a mouse anti-phospho-ERK1/2 antibody (Sigma, 1:2500). To rule out that the differences observed were due to the application of unequal amounts of lysates, PVDF blots were stripped and probed with a rabbit anti-ERK1/2 antibody that recognizes both phosphorylated and nonphosphorylated ERK1/2 (Sigma, 1:40,000). Bands were visualized by the addition of anti-mouse HRP-conjugated (Dako, Glostrup, Denmark) or anti-rabbit HRP-conjugated (Sigma) secondary antibodies, respectively, and SuperSignal West Pico chemiluminescent substrate (Pierce). Bands densities were quantified with LAS-3000 (Fujifilm), and the level of phosphorylated ERK1/2 isoforms was normalized for differences in loading using the total ERK protein band intensities. Quantitative analysis of detected bands was performed by Image Gauge version 4.0 software. Bifactorial ANOVA and post hoc Bonferroni tests were used for statistical comparisons.

Mass Spectometric Analysis—0.3 μl of equimolar solutions of the various peptides were deposited on the sample plate followed by 0.3 μl of matrix, a saturated solution of 2,4,6-trihydroxyacetophenone in 50% ethanol, and left to dry at room temperature. Spectra of each sample spot were acquired using a MALDI TOF-TOF instrument (Applied Biosystem 4700 proteomics analyzer, Framingham, MA) in positive ion mode. Each spectrum is the average of 1000 shots. All peptides were synthesized at The Johns Hopkins School of Medicine "Synthesis and Sequencing Facility."

Computational Models of D_2, CB_1, and A_{2A} Receptors—The amino acid sequences of the human D_2 receptor (accession number P14416), CB_1 receptor (P21554), and A_{2A} receptor (P29274) receptors were obtained from UniProt. Structural simulations of the A_{2A} receptor are based on its crystal structure (PDB code 3EML) (20). Simulations of the D_2 and CB_1 receptors are based on computational models constructed by homology modeling techniques using the crystal structure of the β_2-adrenergic receptor (PDB code 2RH1) (21, 22) as template. Because of the absence of P5.50 Ballesteros-Weinstein numbering (23) in the CB_1 receptor, we superimposed Tyr^{292}(5.58) and Lys^{300}(5.66) to Tyr^{219}(5.58) and Lys^{227}(5.66) of the β_2-adrenergic receptor. Tyr5.58 and Lys5.66 are structural and functional amino acids involved in the stabilization of the active state by interacting with Arg3.50 and Asp/Glu6.30, respectively, as revealed by the recent crystal structure of the ligand-free opsin, which contains several distinctive features of the active state (24). The highly conserved NP$XXYX_{n=5,6}$F(K/R) motif at the junction between TM7 and Hx8 is one residue shorter in the β_2-adrenergic receptor ($n = 5$) than in rhodopsin and D_2 or CB_1 receptors ($n = 6$). Thus, this junction in D_2 or CB_1 receptors was modeled as in rhodopsin (PDB codes 1GZM and 2Z73) (25, 26). The unambiguous assignment of the TM boundaries to a particular position is not possible. However, we have assumed that TM5 of A_{2A} extends to position Arg^{206}(5.67) as shown in the crystal structure (20), and TM5 of D_2 extends to position Arg^{220}(5.69) according to the β_2-based homology model (21, 22). These definitions of TM5 cause Arg^{205}(5.66)–Arg^{206}(5.67) of the A_{2A} receptor and ^{215}(5.64)VL**RRRRKR**VN^{224} of the D_2 receptor to be located at the end of TM5 in the cytoplasm. In contrast, the Swiss Protein Database assigns these epitopes of A_{2A} and D_2 in IL3. The crystal structure of squid rhodopsin (PDB code 2Z73) has shown that in addition to the conserved amphipathic Hx8 that runs parallel to the membrane, the C terminus expands toward TM6 (25). However, the structural homology, among GPCRs, probably does not extend to this C-tail domain because of its high variability in length and amino acid composition among the members of the family. This C-tail is formed by 59 amino acids in the CB_1 receptor (Ser^{414}–Leu^{472}), only 1 amino acid in the D_2 receptor (Cys^{443}), and 104 amino acids in the A_{2A} receptor (Arg^{309}–Ser^{412}). Nevertheless, Ser^{414}–Asn^{437} of the CB_1 receptor and Arg^{309}–Gly^{330} of the A_{2A} receptor, forming part of this C-tail sequence, were modeled, in an arbitrary manner, based on the structure of squid rhodopsin.

Computational Models of Receptor Heteromers—Cysteine cross-linking experiments have suggested that receptor oligomerization involves the surfaces of TM1, -4, and/or -5 (10, 12, 13). Thus, the structures of receptor heteromers were modeled in such a manner that substituted cysteines at position 1.35 could be cross-linked (TM1–TM1) (13); or positions 4.41, 4.44, 4.48, 4.51, and 4.59 (TM4-$TM4^{invago}$) (12); or positions 4.50, 4.54, and 4.58 (TM4-$TM4^{ago}$) (12); or position 5.41 (TM5-TM5) (12).

RESULTS

Quaternary Structure of the A_{2A}-CB_1-D_2 Receptor Heteromer—An obvious initial question about receptor heteromers made up of three different receptors is whether each receptor interacts with the other two or not, *i.e.* if they form a triangular or linear arrangement. As in a prior report (5), we first demonstrated the

ability of A_{2A}-*Rluc*, D_2-GFP^2, and CB_1-YFP receptors to form heteromers by determining the SRET saturation curve in transfected HEK-293T cells (Fig. 1*a*). In the same experimental preparation, we found significant BRET^2 and FRET signals between the A_{2A}-*Rluc*-D_2-GFP^2 receptor pair and the D_2-GFP^2-CB_1-YFP receptor pair, respectively (Fig. 1*b*). Furthermore, we also detected by BRET^1 assays a positive transfer of energy between A_{2A}-*Rluc* and CB_1-YFP receptors (Fig. 1*b*). These data and the positive SRET signal (Fig. 1*a*) in cells co-expressing A_{2A}-*Rluc*, D_2-GFP^2, and CB_1-YFP receptors suggest a triangular arrangement between the three receptors (Fig. 1*c*). In fact, taking into account the correlation between FRET efficiency and acceptor/donor distances and that *Rluc*, GFP^2, and YFP are fused to the end of the C terminus of the receptors, the distance between BRET donors and acceptors can be approximated (17). Considering the high FRET efficiency between D_2-GFP^2 and CB_1-YFP receptors (36 ± 3%), the range of the distance between GFP^2 and YFP in the heteromer is estimated to be 5.7–6.1 nm. Thus, a linear arrangement of the three receptors could give a positive SRET signal but a very much reduced or even nonsignificant BRET^1 signal between A_{2A}-*Rluc* and CB_1-YFP receptors, because there is a rapid dissipation of the energy transfer (to the 6th power of the distance). Therefore, assuming that the heterotrimer is the minimal unit, only a triangular arrangement of monomers (Fig. 1*c*) would make both SRET (Fig. 1*a*) and BRET^1 (Fig. 1*b*) possible between A_{2A}-*Rluc* and CB_1-YFP receptors.

Multiple Electrostatic Interactions in A_{2A}-CB_1-D_2 Receptor Heteromers—The amino acid sequence of the human CB_1 receptor contains two highly conserved epitopes with two adjacent Thr and Ser residues (supplemental Table 1), which have a high probability of CK1/2-dependent phosphorylation (Swiss Protein Database "Net Phos" program (27)). They are located in the distal portion of the C terminus (CT) of the CB_1 receptor (Thr^{467} and Ser^{468}) and in the middle portion of intracellular loop (IL) 3 (Thr^{321} and Ser^{322}). The initial working hypothesis was that these CB_1 receptor epitopes, with high probability of phosphorylation, would be relevant in determining the quaternary structure of the A_{2A}-CB_1-D_2 receptor heteromer, by establishing electrostatic interactions with Arg-rich epitopes located in the A_{2A} and D_2 receptors.

Electrostatic Interaction between Phosphorylated Thr^{467}–Ser^{468} in the C Terminus of the CB_1 Receptor and Arg^{205}(5.66)-Arg^{206}(5.67) in the Cytoplasm at the End of Transmembrane Helix 5 of the A_{2A} Receptor—We first looked at possible alterations in heteromerization between CB_1 and A_{2A} and between CB_1 and D_2 receptor in cells co-expressing a mutant CB_1 receptor in which Thr^{467}(CT) and Ser^{468}(CT) were replaced by Ala ($CB_1^{A467-A468}$ receptor). In cells co-expressing A_{2A}-*Rluc* and $CB_1^{A467-A468}$-YFP receptors, there was a reduction of BRET^1 values when compared with those obtained with cells expressing A_{2A}-*Rluc* and CB_1-YFP (Fig. 2*a*). On the other hand, these mutations did not modify the FRET values between D_2-GFP^2 and $CB_1^{A467-A468}$-YFP, when compared with cells expressing D_2-GFP^2 and CB_1-YFP (Fig. 2*b*). This mutated CB_1 receptor and all the mutant receptors described below were shown to be well expressed at the membrane level (results not shown). Furthermore, the fact that the mutated CB_1 receptor selectively

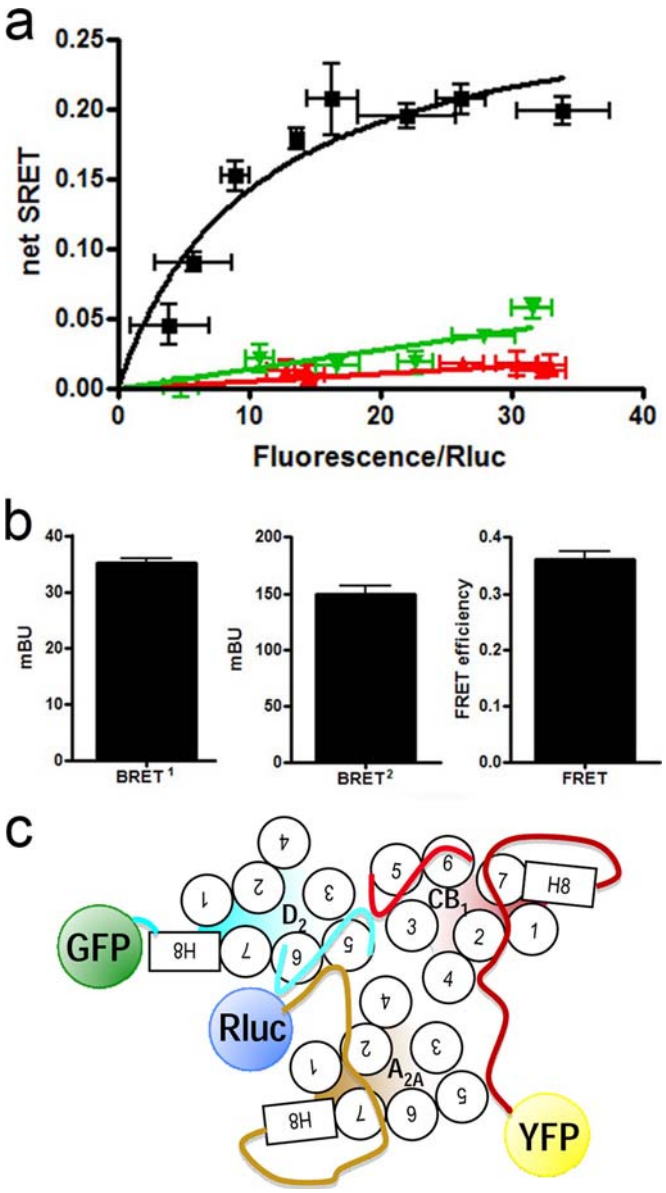

FIGURE 1. **A_{2A}-CB_1-D_2 receptor heteromerization in living cells.** Assays were performed 48 h post-transfection in cells expressing A_{2A}-*Rluc* receptor (1 μg of cDNA; ~100,000 luminescence units), D_2-GFP^2 receptor (3 μg of cDNA; ~6,000 fluorescence units), and increasing amounts of CB_1-YFP receptor cDNA (8,000–18,000 fluorescence units). In each sample fluorescence or luminescence was measured before every experiment to confirm similar donor expressions while monitoring the increased acceptor expression. *a* and *b*, aliquots of these cells were used. *a*, net SRET^2 was obtained by monitoring the YFP fluorescence emission after DeepBlueC addition, with subtraction of the value obtained with cells expressing the same amount of A_{2A}-*Rluc* and D_2-GFP^2 receptors. SRET saturation curves (*black*) were obtained for the coupling of A_{2A}-*Rluc*, D_2-GFP^2, and CB_1-YFP receptors, although negligible and linear SRET was obtained in cells expressing equivalent amounts of A_{2A}-*Rluc*, D_2-GFP^2, and $5HT_{2B}$-YFP receptors (*green*) or D_4-*Rluc*, A_{2A}-GFP^2, and CB_1-YFP receptors (*red*). SRET data are expressed as means ± S.D. of 5–8 different experiments grouped as a function of the amount of SRET acceptor. *b*, BRET^1 was obtained by monitoring the YFP fluorescence emission after coelenterazine H addition, with subtraction of the value obtained with cells expressing the same amount of A_{2A}-*Rluc* receptor. BRET^2 was obtained by monitoring the emission of GFP^2 fluorescence after DeepBlueC addition, with subtraction of the value obtained with cells expressing the same amount of A_{2A}-*Rluc* receptors. FRET was measured by monitoring the emission of YFP fluorescence after excitation of GFP^2 at 400 nm. Data are expressed as the mean ± S.E. of 5–8 independent experiments performed in duplicate. Linear unmixing of the emission signals was applied to BRET^2 and FRET values (*b*) and for YFP quantification in saturation curves (*a*). *c*, schematic representation of the putative triangular quaternary structure of the A_{2A}-CB_1-D_2 receptor heteromer. *mBu*, milli-BRET unit.

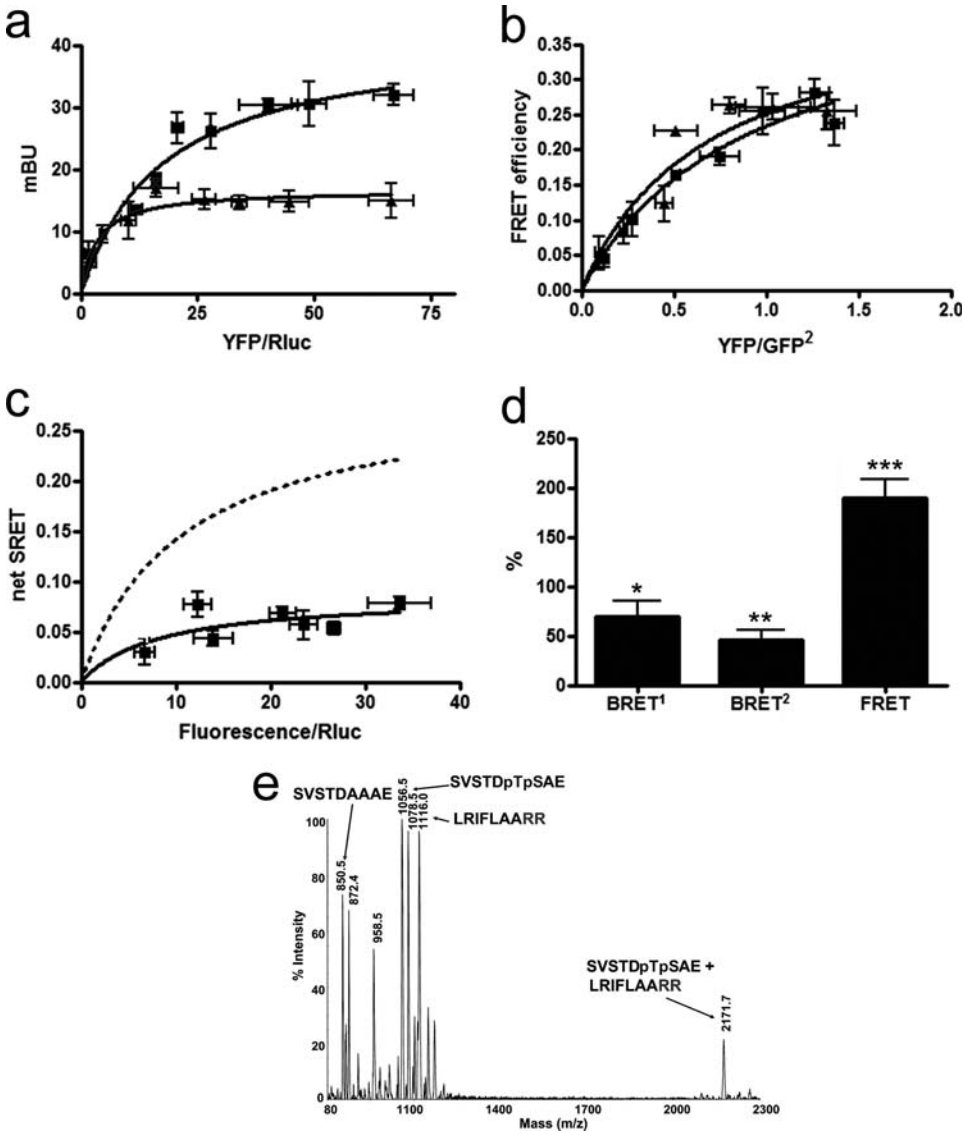

FIGURE 2. **A_{2A}-$CB_1^{A467-A468}$-D_2 receptor heteromerization in living cells.** Assays were performed 48 h post-transfection in cells expressing the following: *a*, A_{2A}-*Rluc* receptor (1 μg of cDNA; ~100,000 luminescence units) and increasing amounts of cDNA of the CB_1-YFP or $CB_1^{A467-A468}$-YFP receptors (8,000–18,000 fluorescence units); *mBu*, milli-BRET unit. *b*, D_2-GFP^2 (3 μg of the cDNA; ~6,000 fluorescence units) and increasing amounts of the cDNA for CB_1-YFP or $CB_1^{A467-A468}$-YFP; *c* and *d*, A_{2A}-*Rluc* receptor (1 μg of cDNA; ~100,000 luminescence units), D_2-GFP^2 receptor (3 μg of the cDNA; ~6,000 fluorescence units), and increasing amounts of cDNA of the $CB_1^{A467-A468}$-YFP receptor (8,000–18,000 fluorescence units). In each sample, fluorescence or luminescence was measured before every experiment to confirm similar donor expressions while monitoring the increased acceptor expression. *a*, $BRET^1$ saturation curves for the A_{2A}-*Rluc*-CB_1-YFP receptor pair (*squares*) and for the A_{2A}-*Rluc*-$CB_1^{A467-A468}$-YFP receptor pair (*triangles*) were obtained by monitoring the YFP fluorescence emission after coelenterazine H addition, with subtraction of the value obtained with cells expressing the same amount of A_{2A}-*Rluc* receptor. Data are expressed as means ± S.D. of five different experiments grouped as a function of the amount of $BRET^1$ acceptor. *b*, FRET saturation curves for the D_2-GFP^2-CB_1-YFP receptor pair (*triangles*) and for the D_2-GFP^2- $CB_1^{A467-A468}$-YFP receptor pair (*squares*) were obtained by monitoring the YFP fluorescence emission at 530 nm after excitation of GFP^2 at 400 nm, with subtraction of the value obtained with cells expressing the same amount of donor protein. Data are expressed as means ± S.D. of seven different experiments grouped as a function of the amount of FRET acceptor. *c*, net $SRET^2$ was obtained by monitoring the emission of YFP fluorescence after DeepBlueC addition, with subtraction of the value obtained with cells expressing the same amount of A_{2A}-*Rluc* and D_2-GFP^2 receptors. SRET saturation curves (*solid line*) were obtained for the coupling of A_{2A}-*Rluc*, D_2-GFP^2, and $CB_1^{A467-A468}$-YFP receptors and compared with the curve obtained for the coupling of A_{2A}-*Rluc*, D_2-GFP^2, and CB_1-YFP receptors (*dotted line*, see Fig. 1). SRET data are expressed as means ± S.D. of five different experiments grouped as a function of the amount of SRET acceptor. *d*, $BRET^1$, $BRET^2$, and FRET were measured as indicated in Fig. 1 legend. Data are expressed as % of values obtained in cells expressing A_{2A}-*Rluc*, D_2-GFP^2, and CB_1-YFP receptors (control, Fig. 1*b*), in mean ± S.E. of five independent experiments performed in duplicate. One-way ANOVA followed by Bonferroni test showed significant increases or decreases with respect to the control (*, $p < 0.05$; **, $p < 0.01$; ***, $p < 0.005$). Linear unmixing of the emission signals was applied to the data for $BRET^2$ and FRET values (*b* and *d*) and for YFP quantification in saturation curves (*a* and *c*). *e*, the spectrum of a mixture of the following three peptides SVSTDAAAE, SVSTD**pTpS**AE, and LRIFLAA**RR,** shows only one noncovalent complex between SVSTD**pTpS**AE and LRIFLAA**RR** at 2171.7 atomic mass units (see text).

altered the RET signal when co-expressed with A_{2A} but not with the D_2 receptors demonstrates that the results cannot be explained by changes in the membrane expression of the mutant receptor or its putative partner. These results therefore show that Thr^{467}(CT) and Ser^{468}(CT) of the CB_1 receptor are involved in the molecular interaction with the A_{2A} receptor in the A_{2A}-CB_1 receptor heteromer. The existence of measurable $BRET^1$ values in cells co-expressing A_{2A}-*Rluc* and $CB_1^{A467-A468}$-YFP receptors indicate that the $CB_1^{A467-A468}$ receptor is still able to interact physically with the A_{2A} receptor and that other domains, most likely TM domains (see Introduction). are also involved in A_{2A}-CB_1 receptor heteromerization. This CT epitope of the CB_1 receptor was also able to interact with the A_{2A} receptor in the A_{2A}-CB_1-D_2 receptor heteromer, as deduced from the low SRET values obtained when $CB_1^{A467-A468}$-YFP receptor was co-expressed with A_{2A}-*Rluc* and D_2-GFP^2 receptors (Fig. 2*c*). Furthermore, in cells expressing $CB_1^{A467-A468}$-YFP, A_{2A}-*Rluc,* and D_2-GFP^2 receptors, $BRET^1$ values between A_{2A}-*Rluc* and $CB_1^{A467-A468}$-YFP receptors and $BRET^2$ values between A_{2A}-*Rluc* and D_2-GFP^2 receptors were significantly reduced, and FRET values between D_2-GFP^2 and $CB_1^{A467-A468}$-YFP receptors were increased relative to cells expressing nonmutated receptors (Fig. 2*d*). Because the bioluminescent or fluorescent proteins are fused to the CT of the receptors, these results indicate that expression of $CB_1^{A467-A468}$-YFP receptors induced a modification of the quaternary structure of the A_{2A}-CB_1-D_2 heteromer, with separation of the CT of CB_1 and A_{2A} receptors and A_{2A} and D_2 receptors and approximation of the CT of CB_1 and D_2 receptors.

We then looked for the presence of adjacent Arg residues in intracellular domains of the A_{2A} receptor that could potentially interact with the phosphorylated Thr^{467}(CT) and Ser^{468}(CT) of CB_1

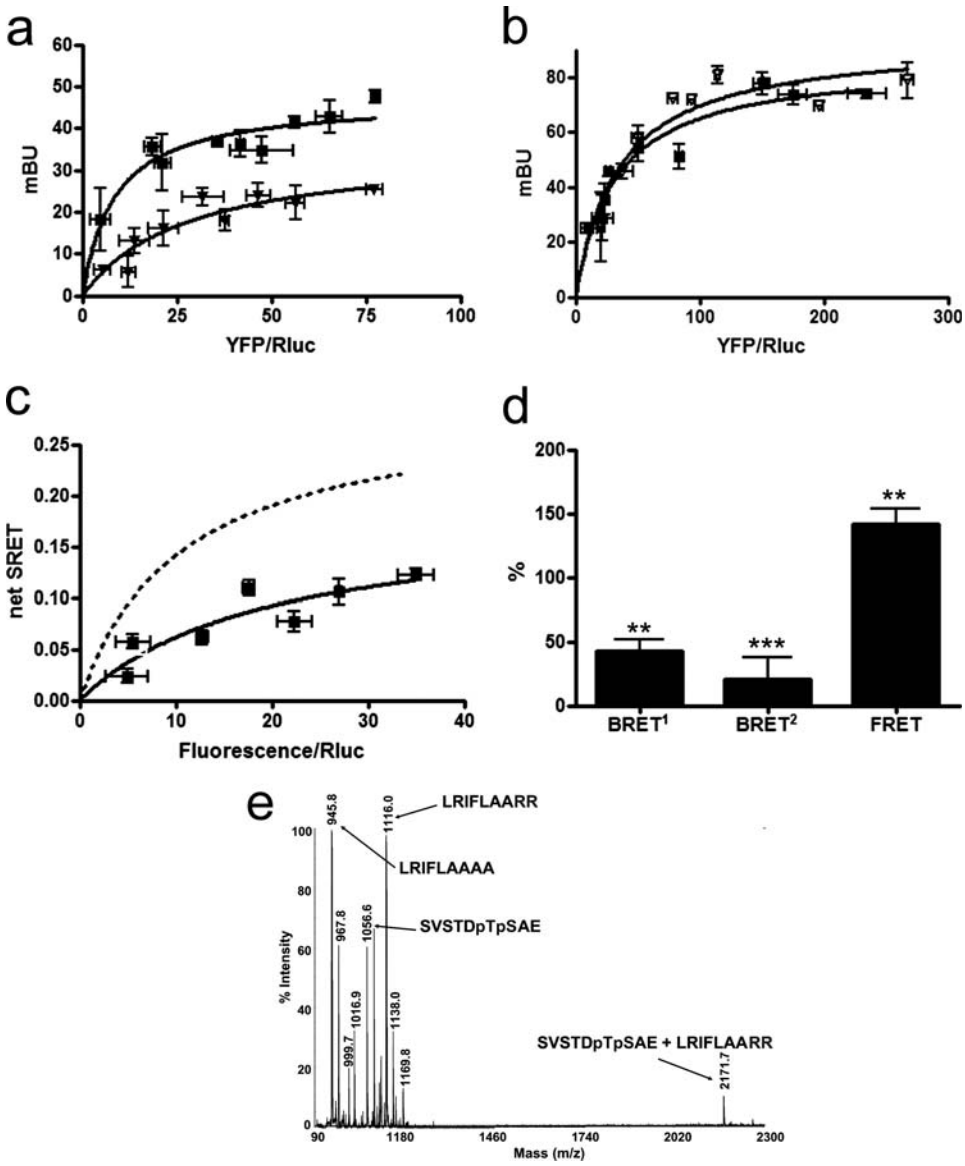

FIGURE 3. **$A_{2A}^{A205-A206}$-CB_1-D_2 receptor heteromerization in living cells.** Assays were performed 48 h post-transfection in cells expressing the following: *a*, A_{2A}-*Rluc* or $A_{2A}^{A205-A206}$-*Rluc* receptors (1 or 0.8 μg of cDNA respectively; ~100,000 luminescence units) and increasing amounts of the cDNA of the CB_1-YFP receptor (8,000–18,000 fluorescence units). *mBu*, milli-BRET unit. *b*, A_{2A}-*Rluc* or $A_{2A}^{A205-A206}$-*Rluc* (1 or 0.8 μg of cDNA, respectively; ~100,000 luminescence units) and increasing amounts of the cDNA for D_2-YFP. *c* and *d*, $A_{2A}^{A205-A206}$-*Rluc* receptor (1 μg of cDNA; ~100,000 luminescence units), D_2-GFP^2 receptor (3 μg of the cDNA; ~6,000 fluorescence units), and increasing amounts of cDNA of the CB_1-YFP receptor (8,000–18,000 fluorescence units). In each sample fluorescence or luminescence was measured before every experiment to confirm similar donor expressions while monitoring the increased acceptor expression. *a*, $BRET^1$ saturation curves for the A_{2A}-*Rluc*-CB_1-YFP receptor pairs (*squares*) and for the $A_{2A}^{A205-A206}$-*Rluc*-CB_1-YFP receptor pair (*triangles*) were obtained by monitoring the YFP fluorescence emission after coelenterazine H addition, with subtraction of the value obtained with cells expressing the same amount of donor. Data are expressed as means ± S.D. of five different experiments grouped as a function of the amount of $BRET^1$ acceptor. *b*, $BRET^1$ saturation curves for the A_{2A}-*Rluc*-D_2-YFP receptor pairs (*triangles*) and for the $A_{2A}^{A205-A206}$-*Rluc*-D_2-YFP receptor pair (*squares*) were obtained by monitoring the YFP fluorescence emission after coelenterazine H addition, with subtraction of the value obtained with cells expressing the same amount of donor. Data are expressed as means ± S.D. of five different experiments grouped as a function of the amount of $BRET^1$ acceptor. *c*, net $SRET^2$ was obtained by monitoring the YFP fluorescence emission after DeepBlueC addition, with subtraction of the value obtained with cells expressing the same amount of $A_{2A}^{A205-A206}$-*Rluc* and D_2-GFP^2 receptors. SRET saturation curves (*solid line*) were obtained for the coupling of $A_{2A}^{A205-A206}$*Rluc*, D_2-GFP^2, and CB_1-YFP receptors and compared with the curve obtained for the coupling of A_{2A}-*Rluc*, D_2R-GFP^2, and CB_1-YFP receptors (*dotted line*, see Fig. 1). SRET data are expressed as means ± S.D. of five different experiments grouped as a function of the amount of SRET acceptor. *d*, $BRET^1$, $BRET^2$, and FRET were measured as indicated in Fig. 1 legend. Data are expressed as % of values obtained in cells expressing A_{2A}-*Rluc*, D_2-GFP^2, and CB_1-YFP receptors (*control*, Fig. 1*b*), in mean ± S.E. of five independent experiments performed in duplicate. One-way ANOVA followed by Bonferroni test showed significant increases or decreases with respect to the control (**, $p < 0.01$; ***, $p < 0.005$). Linear unmixing of the emission signals was applied to the data for $BRET^2$ and FRET values (*d*) and for YFP quantification in saturation curves (*a*–*c*). *e*, spectrum of a mixture of the following three peptides LRIFLAAAA, LRIFLAA**RR,** and SVSTD**pTpS**AE, shows only one NCX between SVSTD**pTpS**AE and LRIFLAA**RR** at 2171.7 atomic mass units (see text).

receptor via electrostatic interactions. We found a highly conserved motif, Arg^{205}(5.66)–Arg^{206}(5.67) (supplemental Table 1), located in the cytoplasm at the end of TM5, according to the crystal structure (see "Experimental Procedures"). Mass spectrometric analysis demonstrated that a synthetic peptide corresponding to this A_{2A} receptor epitope, ^{198}LRIFLAA**RR**^{206}, and a phosphorylated peptide corresponding to the CT of the CB_1 receptor epitope, ^{462}SVSTD**pTpS**AE^{470}, form stable noncovalent complexes, and the Ala-containing peptides LRIFLAAAA and SVSTDAAAE do not (Figs. 2*e* and 3*e*). We then investigated whether the A_{2A} receptor epitope containing adjacent Arg could be involved in A_{2A}-CB_1 receptor heteromerization by using a mutant A_{2A} receptor in which Arg^{205}(5.66)–Arg^{206}(5.67) were replaced by Ala ($A_{2A}^{A205-A206}$ receptor). Cells co-expressing $A_{2A}^{A205-A206}$-*Rluc* and CB_1-YFP receptors showed lower $BRET^1$ values than those expressing WT receptors (Fig. 3*a*). On the other hand, the $BRET^1$ values between $A_{2A}^{A205-A206}$-*Rluc* and D_2-YFP receptors were similar to the values between A_{2A}-*Rluc* and D_2-YFP receptors (Fig. 3*b*). Hence, the quaternary structure of the A_{2A}-CB_1 receptor heteromer depends on an electrostatic interaction between epitopes located in the CT of the CB_1 receptor and in the cytoplasm at the end of TM5 of the A_{2A} receptor. Furthermore, this electrostatic interaction is also involved in A_{2A}-CB_1-D_2 receptor heteromerization (Fig. 3, *c* and *d*). In fact, low SRET values were obtained when the $A_{2A}^{A205-A206}$-*Rluc* receptor was co-transfected with D_2-GFP^2 and CB_1-YFP receptors (Fig. 3*c*). In cells co-expressing $A_{2A}^{A205-A206}$-*Rluc*, D_2-GFP^2, and CB_1-YFP receptors, $BRET^1$ and $BRET^2$ between the heteromer partners were significantly reduced, and FRET values between D_2-GFP^2 and CB_1-YFP receptors were increased, compared with cells co-expressing nonmutated receptors (Fig. 3*d*). Significantly,

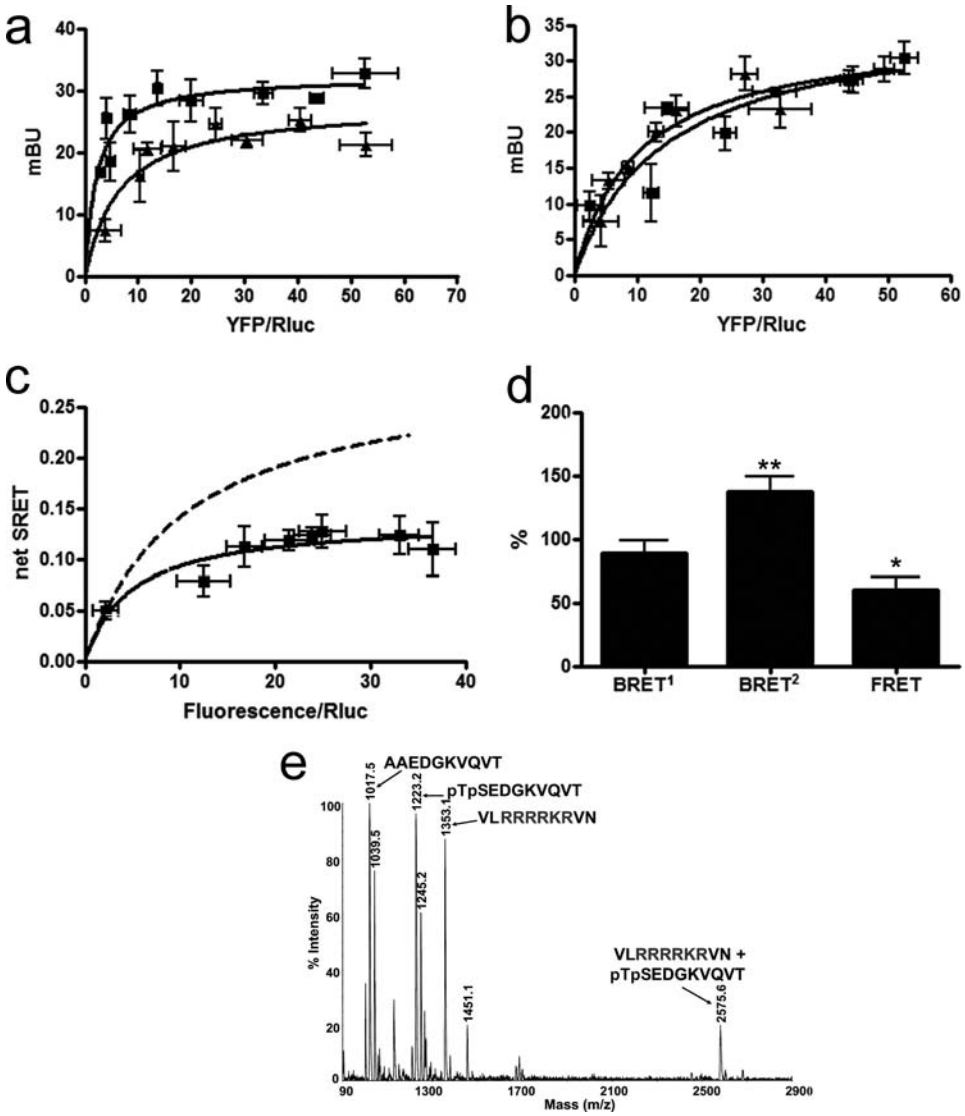

FIGURE 4. **A_{2A}-$CB_1^{A321-A322}$-D_2 receptor heteromerization in living cells.** Assays were performed 48 h post-transfection in cells expressing the following: *a*, D_2-*Rluc* receptor (1 μg of cDNA; ~100,000 luminescence units) and increasing amounts of the cDNA for CB_1-YFP or $CB_1^{A321-A322}$-YFP receptors (8,000–18,000 fluorescence units); *b*, A_{2A}-*Rluc* (1 μg of cDNA; ~100,000 luminescence units) and increasing amounts of the cDNA for CB_1-YFP or $CB_1^{A321-A322}$-YFP; *c* and *d*, A_{2A}-*Rluc* receptor (1 μg of cDNA; ~100,000 luminescence units), D_2-GFP^2 receptor (3 μg of the cDNA; ~6,000 fluorescence units), and increasing amounts of cDNA of the $CB_1^{A321-A322}$-YFP receptor (8,000–18,000 fluorescence units). In each sample fluorescence or luminescence was measured before every experiment to confirm similar donor expressions while monitoring the increased acceptor expression. *a*, $BRET^1$ saturation curves for the D_2-*Rluc*-CB_1-YFP receptor pair (*squares*) and for D_2-*Rluc*-$CB_1^{A321-A322}$-YFP receptor pair (*triangles*) were obtained by monitoring the YFP fluorescence emission after coelenterazine H addition, with subtraction of the value obtained with cells expressing the same amount of A_{2A}-*Rluc* receptor. Data are expressed as means ± S.D. of six different experiments grouped as a function of the amount of $BRET^1$ acceptor. *b*, $BRET^1$ saturation curves for the A_{2A}-*Rluc*-CB_1-YFP receptor pair (*triangles*) and for A_{2A}-*Rluc*-$CB_1^{A321-A322}$-YFP receptor pair (*squares*) were obtained by monitoring the YFP fluorescence emission after coelenterazine H addition, with subtraction of the value obtained with cells expressing the same amount of A_{2A}-*Rluc* receptor. Data are expressed as means ± S.D. of six different experiments grouped as a function of the amount of $BRET^1$ acceptor. *c*, net $SRET^2$ was obtained by monitoring the YFP fluorescence emission after DeepBlueC addition, with subtraction of the value obtained with cells expressing the same amount of A_{2A}-*Rluc* and D_2-GFP^2 receptors. SRET saturation curves (*solid line*) were obtained for the coupling of A_{2A}-*Rluc*, D_2-GFP^2, and $CB_1^{A321-A322}$-YFP receptors and compared with the curve obtained for the coupling of A_{2A}-*Rluc*, D_2-GFP^2, and CB_1-YFP receptors (*dotted line*, see Fig. 1). SRET data are expressed as means ± S.D. of six different experiments grouped as a function of the amount of SRET acceptor. *d*, $BRET^1$, $BRET^2$, and FRET were measured as indicated in Fig. 1*b* legend. Data are expressed as percent of values obtained in cells expressing A_{2A}-*Rluc*, D_2-GFP^2, and CB_1-YFP receptors (control, Fig. 1*b*), in mean ± S.E. of six independent experiments performed in duplicate. One-way ANOVA followed by Bonferroni test showed significant increases or decreases with respect to the control (*, $p < 0.05$; **, $p < 0.01$). Linear unmixing of the emission signals was applied to the data for $BRET^2$ and FRET values (*d*) and for YFP quantification in saturation curves (*a*–*c*). *e*, the spectrum of a mixture of the following three peptides AAEDGKVQVT, **pTpS**EDGKVQVT, and VL**RRRRKRV**N shows only one NCX between **pTpS**EDGKVQVT and VL**RRRRKR**VN at 2575.6 atomic mass units (see text). *mBu*, milli-BRET unit.

this outcome is qualitatively the same as the one shown in Fig. 2*d* with $CB_1^{A467-A468}$-YFP receptor, as it would be expected if both mutants disrupt the same intermolecular interaction.

Electrostatic Interaction between Phosphorylated Thr^{321}–Ser^{322} in Intracellular Loop 3 of the CB_1 Receptor and an Arg-rich Epitope in Intracellular Loop 3 of the D_2 Receptor—Because the Thr^{467}(CT)-Ser^{468}(CT)-containing epitope of the CB_1 receptor was found to interact with Arg^{205}(5.66)–Arg^{206}(5.67) of the A_{2A} receptor, it was expected that Thr^{321}(IL3)–Ser^{322}(IL3) of the CB_1 receptor could interact with the D_2 receptor. In fact, when co-expressing the mutant $CB_1^{A321-A322}$-YFP and D_2-*Rluc* receptors, the $BRET^1$ energy transfer between *Rluc* and YFP was reduced when compared with $BRET^1$ values obtained with CB_1-YFP and D_2-*Rluc* receptors (Fig. 4*a*). On the other hand, the $BRET^1$ values obtained in cells expressing $CB_1^{A321-A322}$-YFP and A_{2A}-*Rluc* receptors were similar to those obtained with cells expressing CB_1-YFP and A_{2A}-*Rluc* (Fig. 4*b*). These results therefore show that the Thr^{321}(IL3)–Ser^{322}(IL3) motif of the CB_1 receptor is selectively involved in the intermolecular interactions with the D_2 receptor in the CB_1-D_2 receptor heteromer. The fact that $BRET^1$ is still measurable between $CB_1^{A321-A322}$-YFP and D_2-*Rluc* receptors indicates that, once more, other epitopes are also involved in CB_1-D_2 receptor heteromerization. Also, the same Thr^{321}(IL3)–Ser^{322}(IL3) epitope of the CB_1 receptor interacted with the D_2 receptor in the A_{2A}-CB_1-D_2 receptor heteromer. Compared with nonmutated receptors, co-expression of $CB_1^{A321-A322}$-YFP receptor with A_{2A}-*Rluc* and D_2-GFP^2 receptors showed a reduction in SRET values (Fig. 4*c*), and FRET values were significantly decreased, and $BRET^2$ values were increased, whereas $BRET^1$ values were not modified (Fig. 4*d*). This suggests that replacement of

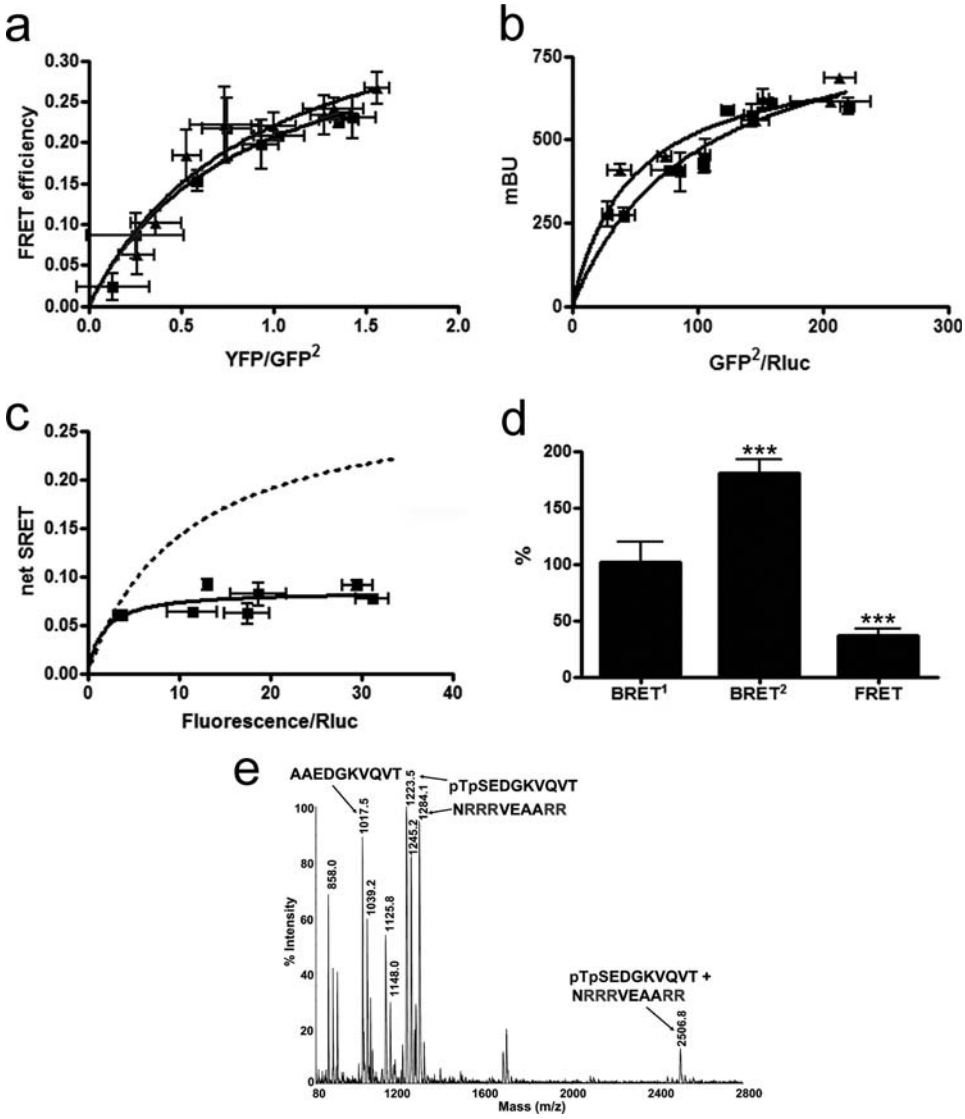

FIGURE 5. **A_{2A}-CB_1-D_{2S} receptor heteromerization in living cells.** Assays were performed 48 h post-transfection in cells expressing the following: *a,* D_{2S}-GFP^2 receptor (1.5 μg of cDNA; ~5,000 fluorescence units) or D_2-GFP^2 receptor (2 μg of cDNA; ~5,000 luminescence units), and increasing amounts of cDNA of CB_1-YFP receptor (8,000–18,000 fluorescence units); *b,* A_{2A}-*Rluc* (1 μg of cDNA; ~100,000 luminescence units) and increasing amounts of cDNA for D_2-GFP^2 or D_{2S}-GFP^2; *c* and *d,* A_{2A}-*Rluc* receptor (1 μg of cDNA; ~100,000 luminescence units), D_{2S}-GFP^2 receptor (3 μg of the cDNA; ~6,000 fluorescence units) and increasing amounts of the cDNA for CB_1-YFP receptor (8,000–18,000 fluorescence units). *mBu*, milli-BRET unit. In each sample fluorescence or luminescence was measured before every experiment to confirm similar donor expressions while monitoring the increased acceptor expression. *a*, FRET saturation curves for the D_2-GFP^2-CB_1-YFP receptor pair (*squares*) and for D_{2S}-GFP^2-CB_1-YFP receptor pair (*triangles*) were obtained by monitoring the YFP fluorescence emission at 530 nm after excitation of GFP^2 at 400 nm, with subtraction of the value obtained with cells expressing the same amount of donor protein. Data are expressed as means ± S.D. of seven different experiments grouped as a function of the amount of FRET acceptor. *b*, $BRET^2$ saturation curves for the A_{2A}-*Rluc*-D_2-GFP^2 receptor pair (*triangles*) and for A_{2A}-*Rluc*-D_{2S}-GFP^2 receptor pair (*squares*) were obtained by monitoring the YFP fluorescence emission after DeepBlueC addition, with subtraction of the value obtained with cells expressing the same amount of A_{2A}-*Rluc* receptor. Data are expressed as means ± S.D. of six different experiments grouped as a function of the amount of $BRET^2$ acceptor. *c*, net $SRET^2$ was obtained by monitoring the YFP fluorescence emission after DeepBlueC addition, with subtraction of the value obtained with cells expressing the same amount of A_{2A}-*Rluc* and D_{2S}-GFP^2 receptors. SRET saturation curves (*solid line*) were obtained for the coupling of A_{2A}-*Rluc*, D_{2S}-GFP^2, and CB_1-YFP receptors and compared with the curve obtained for the coupling of A_{2A}-*Rluc*, D_2-GFP^2, and CB_1-YFP receptors (*dotted line*, see Fig. 1). SRET data are expressed as means ± S.D. of five different experiments grouped as a function of the amount of SRET acceptor. *d*, $BRET^1$, $BRET^2$, and FRET were measured as indicated in Fig. 1 legend. Data are expressed as % of values obtained in cells expressing A_{2A}*Rluc*, D_2-GFP^2, and CB_1-YFP receptors (control, Fig. 1*b*), in mean ± S.E. of five independent experiments performed in duplicate. One-way ANOVA followed by Bonferroni test showed significant increases or decreases with respect to the control (***, $p < 0.005$). Linear unmixing of the emission signals was applied to the data for $BRET^2$ and FRET values (*a, b,* and *d*) and for YFP quantification in saturation curves (*a* and *c*). *e*, spectrum of a mixture of the following three peptides AAEDGKVQVT, **pTpS**EDGKVQVT, and N**RRR**VEAA**RR,** shows only one NCX between **pTpS**EDGKVQVT and N**RRR**VEAA**RR** at 2506.8 atomic mass units (see text).

Thr^{321}(IL3) and Ser^{322}(IL3) by Ala in CB_1 receptor induces a modification of the quaternary structure of the A_{2A}-CB_1-D_2 receptor heteromer with separation of the CT of the CB_1 and D_2 receptors and an approximation of the CT of the D_2 and A_{2A} receptors. Thus, CB_1 receptor uses two different CK1/2-dependent phosphorylatable epitopes, located in their CT (Thr^{467}–Ser^{468}) and IL3 (Thr^{321}–Ser^{322}) domains, to establish simultaneous electrostatic interactions with the A_{2A} and D_2 receptors, respectively, in the A_{2A}-CB_1-D_2 receptor heteromer.

Next step was finding out which intracellular epitope of the D_2 receptor is involved in CB_1-D_2 receptor heteromerization. D_2 receptor contains two highly conserved Arg-rich epitopes (supplemental Table 1), ^{215}(5.64)VL**RRRRKR**VN^{224}, located at the end of TM5 in the cytoplasm (according to the homology modeling using the β_2-adrenergic receptor as a template; see under "Experimental Procedures"), and ^{266}N**RRR**VEAA**RR**^{275}, in the middle of IL3. Because the VL**RRRRKR**VN epitope is most probably involved in A_{2A}-D_2 receptor heteromerization (28, 29), we explored the possibility that IL3 of the D_2 receptor could interact with IL3 of the CB_1 receptor (phosphorylated Thr^{321}–Ser^{322}), The D_2 short isoform (D_{2S}), an alternative splicing that lacks 29 amino acid residues of IL3 (30), including ^{266}N**RRR**VEAA**RR**^{275}, was used. SRET values were clearly reduced when D_{2S}-GFP^2 receptor was co-expressed with A_{2A}-*Rluc* and CB_1-YFP receptors (Fig. 5*c*). Significantly, the D_{2S} receptor led to the same qualitative modifications of the quaternary structure of the A_{2A}-CB_1-D_2 receptor heteromer as those induced by $CB_1^{A321-A322}$-YFP receptor (Fig. 5*d*). Thus, in cells expressing A_{2A}-*Rluc,* CB_1-YFP, and D_{2S}-GFP^2 receptors, FRET values between D_{2S}-GFP^2 and CB_1-YFP receptors were significantly decreased, whereas $BRET^2$ values between A_{2A}-*Rluc* and D_{2S}-GFP^2

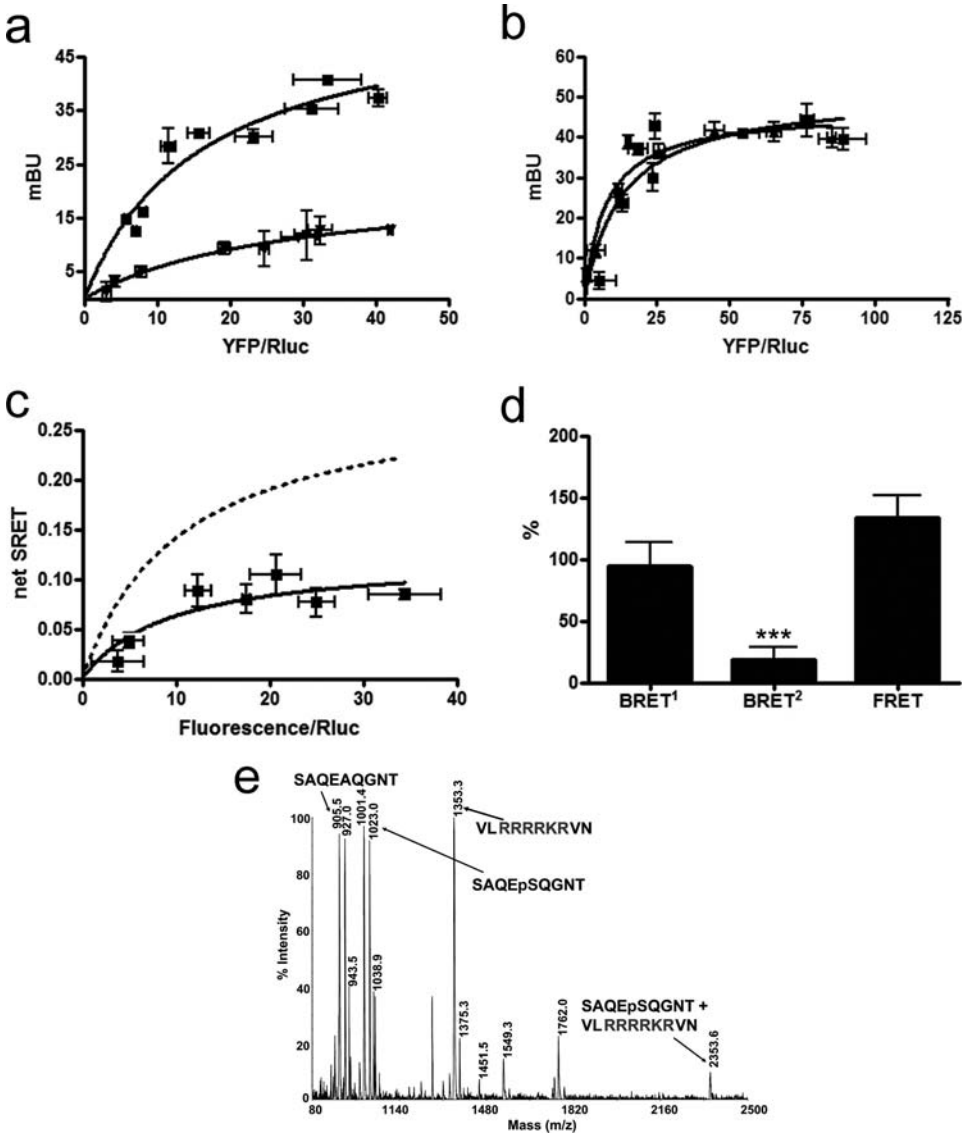

FIGURE 6. **A_{2A}^{A374}-CB_1-D_2 receptor heteromerization in living cells.** Assays were performed 48 h post-transfection in cells expressing the following: *a*, A_{2A}-*Rluc* or A_{2A}^{A374}-*Rluc* receptors (1 or 0.8 μg of cDNA respectively; ~100,000 luminescence units) and increasing amounts of cDNA of the D_2-YFP receptor (8,000–18,000 fluorescence units); *b*, A_{2A}-*Rluc* or A_{2A}^{A374}-*Rluc* (1 or 0.8 μg of cDNA respectively; ~100,000 luminescence units) and increasing amounts of the cDNA for CB_1R-YFP; *c* and *d*, A_{2A}^{A374}-*Rluc* receptor (1 μg of cDNA; ~100,000 luminescence units), D_2-GFP^2 receptor (3 μg of the cDNA; ~6,000 fluorescence units), and increasing amounts of cDNA of CB_1-YFP receptor (8,000–18,000 fluorescence units). In each sample fluorescence or luminescence was measured before every experiment to confirm similar donor expressions while monitoring the increased acceptor expression. *a*, $BRET^1$ saturation curves for the A_{2A}-*Rluc*-D_2-YFP receptor pair (*squares*) and for the A_{2A}^{A374}-*Rluc*-D_2-YFP receptor pair (*triangles*) were obtained by monitoring the YFP fluorescence emission after coelenterazine H addition, with subtraction of the value obtained with cells expressing the same amount of donor. Data are expressed as means ± S.D. of five different experiments grouped as a function of the amount of $BRET^1$ acceptor. *b*, $BRET^1$ saturation curves for the A_{2A}-*Rluc*-CB_1-YFP receptor pair (*triangles*) and for the A_{2A}^{A374}-*Rluc*-CB_1-YFP receptor pair (*squares*) were obtained by monitoring the YFP fluorescence emission after coelenterazine H addition, with subtraction of the value obtained with cells expressing the same amount of donor. Data are expressed as means ± S.D. of five different experiments grouped as a function of the amount of $BRET^1$ acceptor. *c*, net $SRET^2$ was obtained by monitoring the YFP fluorescence emission after DeepBlueC addition, with subtraction of the value obtained with cells expressing the same amount of A_{2A}^{A374}-*Rluc* and D_2-GFP^2 receptors. SRET saturation curves (*solid line*) were obtained for the coupling of A_{2A}^{A374}-*Rluc*, D_2-GFP^2, and CB_1-YFP receptors and compared with the curve obtained for the coupling of A_{2A}-*Rluc*, D_2-GFP^2, and CB_1-YFP receptors (*dotted line*, see Fig. 1). SRET data are expressed as mean ± S.D. of five different experiments grouped as a function of the amount of SRET acceptor. *d*, $BRET^1$, $BRET^2$, and FRET were measured as indicated in Fig. 1 legend. Data are expressed as % of values obtained in cells expressing A_{2A}-*Rluc*, D_2-GFP^2, and CB_1-YFP (control, Fig. 1*b*) in mean ± S.E. of five independent experiments performed in duplicate. One-way ANOVA followed by Bonferroni test showed significant increases or decreases with respect to the control (*, $p < 0.05$; **, $p < 0.01$; ***, $p < 0.005$). Linear unmixing of the emission signals was applied to the data for $BRET^2$ and FRET values (*e*) and for YFP quantification in saturation curves (*a* and *b*). *e*, spectrum of a mixture of the following three peptides SAQEAQGNT, SAQE**pSQGNT,** and VL**RRRRKRV**N shows only one NCX between SAQE**pSQGN**T and VL**RRRRKR**VN at 2353.6 atomic mass units (see text). *mBu*, milli-BRET unit.

receptors were increased, and $BRET^1$ values between A_{2A}-*Rluc* and CB_1-YFP receptors were not modified, when compared with cells co-expressing A_{2A}-*Rluc*, D_2-GFP^2, and CB_1-YFP receptors (Fig. 5*d*). These results indicate that in the A_{2A}-CB_1-D_2 receptor heteromer, CB_1 receptors interact with the Arg-rich domain located in IL3 of the D_2 receptor.

Notably, expression of D_{2S}-GFP^2 or D_2-GFP^2 receptors with either CB_1-YFP or A_{2A}-*Rluc* or receptors gives similar FRET (Fig. 5*a*) or $BRET^2$ (Fig. 5*b*) values, respectively. This indicates that in the absence of the ^{266}N**RRR**VEAA**RR**^{275} epitope in D_{2S}-GFP^2, the CB_1 receptor can potentially interact with the other Arg-rich domain, ^{215}(5.64)VL**R-RRRKR**VN^{224}, present in both isoforms of the D_2 receptor. As expected, mass spectrometric analysis demonstrated that a synthetic peptide of the epitope located in IL3 of the CB_1 receptor (^{321}**pTpS**EDGKVQVT^{330}), but not its equivalent Ala-containing peptide (AAEDGKVQVT), formed stable noncovalent complexes with the two Arg-rich epitopes of the D_2 receptor (^{215}(5.64)VL**R-RRRKR**VN^{224} and ^{266}N**RRR**VEA-A**RR**^{275}) (Figs. 4*e* and 5*e*).

Electrostatic Interaction between Phosphorylated Ser^{374} in the C Terminus of the A_{2A} Receptor and an Arg-rich Domain in the Cytoplasm at the End of Transmembrane Helix 5 of the D_2 Receptor—The ^{215}(5.64)VL**RRRRKR**VN^{224} epitope of the D_2 receptor was shown to be involved in A_{2A}-D_2 receptor heteromerization by interacting with the CT domain of the A_{2A} receptor (19, 20). We found a dramatic reduction of $BRET^1$ values in cells co-expressing a mutant A_{2A}-*Rluc* receptor, in which Ser^{374}(CT) was replaced by Ala (A_{2A}^{A374}-*Rluc* receptor), and D_2-YFP receptor (Fig. 6*a*). On the other hand, co-expression of A_{2A}^{A374}-*Rluc* and CB_1-YFP receptors gave similar $BRET^1$ values than WT receptors (Fig. 6*b*). These results confirm that Ser^{374}(CT) of the A_{2A} receptor is

involved in the molecular interaction with the D_2 receptor. Not surprisingly, Ser^{374}(CT) of the A_{2A} receptor was also found to be involved in providing the quaternary structure of the A_{2A}-CB_1-D_2 receptor heteromer. Low SRET values were obtained when $A_{2A}{}^{A374}$-*Rluc* was co-expressed with D_2-GFP^2 and CB_1-YFP receptors (Fig. 6*c*), compared with cells co-expressing the nonmutated receptors. From the analysis of $BRET^1$, $BRET^2$, and FRET occurring between partners in cells expressing $A_{2A}{}^{A374}$-*Rluc*, CB_1-YFP, and D_2-GFP^2 receptors, it was observed that $BRET^2$ values were significantly reduced, but FRET and $BRET^1$ values were not significantly modified (Fig. 6*d*). These results indicate that the CT-mutated A_{2A} receptor induces a modification of the quaternary structure of the A_{2A}-CB_1-D_2 receptor heteromer, with separation of the CT of the A_{2A} and D_2 receptors. Therefore, the A_{2A} receptor uses a double-Arg motif (Arg^{205}(5.66)–Arg^{206}(5.67)) located in the cytoplasm at the end of transmembrane helix 5 and a CK1/2-dependent phosphorylatable epitope located in CT (Ser^{374}) to establish selective electrostatic interactions with the CB_1 and D_2 receptors, respectively. Hence, mass spectrometric analysis of a mixture of peptides corresponding to the cytoplasmic epitope at the end of TM5 of the D_2 (^{215}(5.64)VL**RRRRKR**VN^{224}) and the CT epitopes of the A_{2A} receptor (^{370}SAQEpSQGNT^{378}) and the mutant A_{2A} receptor (^{370}SAQEAQGNT^{378}) resulted in noncovalent complexes between the D_2 and the A_{2A} receptor epitopes, but not in the case of the mutant A_{2A} receptor (Fig. 6*e*).

Role of Casein Kinase 1/2-mediated Phosphorylation in the Quaternary Structure of A_{2A}-CB_1-D_2 Receptor Heteromer—To demonstrate the actual involvement of casein kinase-induced phosphorylation in the electrostatic interactions between A_{2A}, CB_1, and D_2 receptors in the A_{2A}-CB_1-D_2 receptor heteromer, we studied the effects of co-administration of casein kinase 1 inhibitor IC 261 and casein kinase 2 inhibitor TBAC on SRET saturation experiments in HEK-293T cells co-transfected with A_{2A}-*Rluc*, D_2-GFP^2, and CB_1-YFP receptors. As expected, the casein kinase inhibitors significantly decreased SRET values (Fig. 7), supporting a role of casein kinases on maintaining a phosphorylated state of the intracellular domains of A_{2A} and CB_1 receptors involved in A_{2A}-CB_1-D_2 receptor heteromerization.

Computational Model of the Quaternary Structure of the A_{2A}-CB_1-D_2 Receptor Heteromer—Biochemical and biophysical studies have suggested that oligomerization of class A GPCRs primarily involves TM1, -4, and/or -5 (7, 9–15). Thus, the structure of the A_{2A}-CB_1-D_2 receptor heteromer was modeled using the following dimeric interfaces: TM1-TM1, TM4-$TM4^{invago}$, TM4-$TM4^{ago}$, and TM5-TM5 (see under "Experimental Procedures"). TM4-$TM4^{invago}$ and TM4-$TM4^{ago}$ stand for the proposed rearrangement of the oligomerization interface that has been observed for the dopamine D_2 receptor upon inverse agonist and agonist binding, respectively (12).

Modeling the CB_1-D_2 Receptor Heteromer—Initially, to discern which of these TM interfaces most favorably permits the proposed electrostatic interaction between phosphorylated Thr^{321}(IL3)–Ser^{322}(IL3) of CB_1 and ^{266}N**RRR**VEAA**RR**^{275}(IL3) of D_2 in the CB_1-D_2 receptor heteromer, all possible dimeric interfaces were constructed (supplemental Fig. 1). It is important to acknowledge the difficulty of modeling IL3 of either CB_1 or D_2 receptors unambiguously (see under "Experimental Procedures"); thus, the exact location of these epitopes in IL3 cannot be determined. Nevertheless, it seems clear to us that the TM1-TM1, TM4-$TM4^{invago}$, and TM4-$TM4^{ago}$ interfaces position IL3 of CB_1 and D_2 receptors in opposite sides of the TM bundles (supplemental Fig. 1, *a–c*), which makes the proposed electrostatic interaction difficult. In contrast, the TM5-TM5 interface places IL3 of the CB_1 receptor contiguous to IL3 of the D_2 receptor (supplemental Fig. 1*d*), facilitating their electrostatic interaction. It thus seems reasonable to propose that the Arg-rich epitope of the D_2 receptor located in the cytoplasm at the end of TM5 is involved in CB_1-D_2 receptor heteromerization.

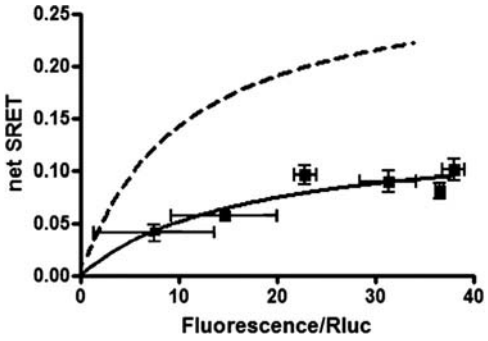

FIGURE 7. **A_{2A}-CB_1-D_2 receptor heteromerization in living cells treated with casein kinase 1/2 inhibitors.** $SRET^2$ saturation experiments were performed 48 h post-transfection in cells expressing A_{2A}-*Rluc* receptor (1 μg of cDNA), D_2-GFP^2 receptor (3 μg of cDNA),and increasing amounts of CB_1-YFP receptor cDNA, treated with the casein kinase 1 inhibitor IC 261 (50 μM) and casein kinase 2 inhibitor TBAC (10 μM) as described under "Experimental Procedures." In each sample fluorescence or luminescence was measured before every experiment to confirm similar donor expressions (~100,000 luminescence units) and similar GFP^2 fluorescence (~6,000 fluorescence units) while monitoring the increased acceptor expression (8,000–18,000 YFP fluorescence units). Net $SRET^2$ was obtained by monitoring the emission of YFP fluorescence after DeepBlueC addition, with subtraction of the value obtained with cells expressing the same amount of receptor *Rluc* and receptor GFP^2. $SRET^2$ saturation curves (*solid lines*) were compared with the curve obtained for the coupling of A_{2A}-*Rluc*, D_2-GFP^2, and CB_1-YFP receptors in cells not treated with casein kinase inhibitors (*dotted line*, see Fig. 1). SRET data are expressed as means ± S.D. of five different experiments grouped as a function of the amount of SRET acceptor.

Modeling the A_{2A}-CB_1 Receptor Heteromer—The A_{2A}-CB_1 receptor heteromer was also modeled through the entire set of TM interfaces (supplemental Fig. 2) to reproduce the electrostatic interaction between phosphorylated Thr^{467}–Ser^{468} in the CT of the CB_1 receptor and Arg^{205}(5.66)–Arg^{206}(5.67) in the cytoplasm at the end of TM5 of the A_{2A} receptor. CT of the CB_1 receptor is made of 59 amino acids (Ser^{414}–Leu^{472}), in addition to the conserved Hx8 that runs parallel to the membrane (Ser^{401}–Pro^{413}). It is thus difficult to determine with precision the position of Thr^{467}(CT)–Ser^{468}(CT). However, although GPCRs CT vary greatly in length and sequence, we have assumed that the CT of CB_1 unfolds toward TM6 as found in the crystal structure of squid rhodopsin (22). Taking these facts into account, TM4-$TM4^{invago}$, TM4-$TM4^{ago}$, and TM5-TM5 interfaces between CB_1 and A_{2A} receptors would allow the electrostatic interaction between Thr^{467}(CT)–Ser^{468}(CT) and Arg^{205}(5.66)–Arg^{206}(5.67) in the A_{2A} receptor (supplemental Fig. 2, *b–d*), whereas the TM1-TM1 interface would not (supplemental Fig. 2*a*).

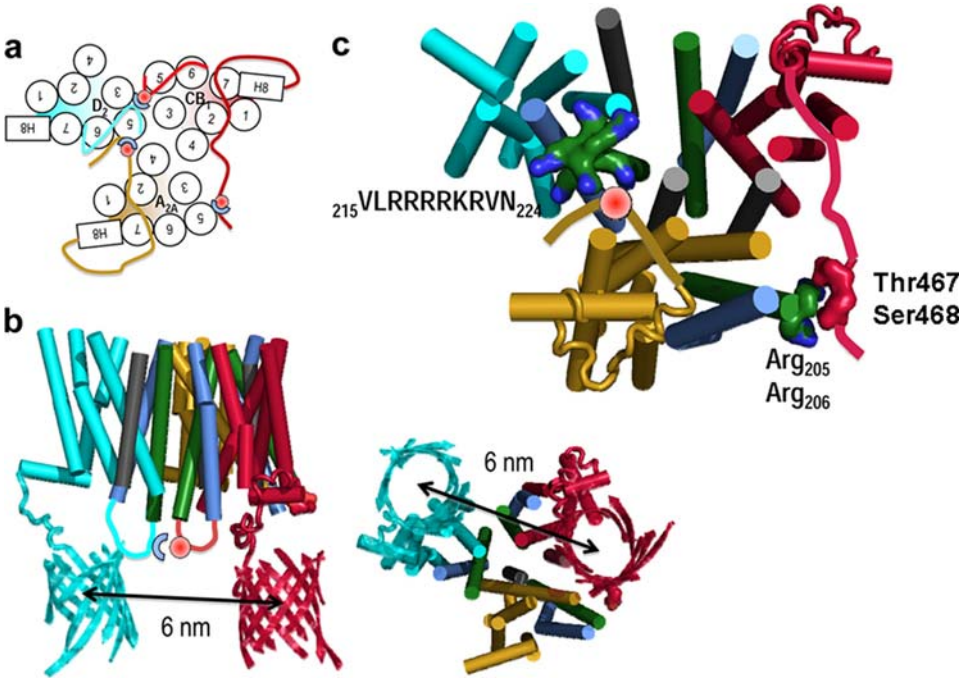

FIGURE 8. **Molecular model of the A_{2A}-CB_1-D_2 receptor heteromer.** *a,* schematic model of the heteromerization of A_{2A} (*gold*), CB_1 (*red*), and D_2 (*cyan*) receptors. *Solid lines* between TM5 and -6 symbolize IL3 of CB_1 (*red line*, 29 amino acids long) or D_2 (*cyan line*, 142 amino acids long) receptors, which were not modeled; *solid lines* after HX8 represent CT of CB_1 (*red line*) or A_{2A} (*gold line*), which were arbitrarily modeled as in squid rhodopsin; *red spheres* represent either phosphorylated Thr^{321}(IL3)–Ser^{322}(IL3) or Thr^{467}(CT)–Ser^{468}(CT) of CB_1 or phosphorylated Ser^{374}(CT) of A_{2A}; and *blue half-circles* represent either Arg^{205}(5.66)–Arg^{206}(5.67) of A_{2A} or the ^{215}(5.64)VL**RRRRKR**VN^{224} or ^{266}N**RRR**VEAA**RR**^{275}(IL3) epitopes of D_2. *b,* lateral and cytoplasmic views of the computational model of the A_{2A}-CB_1-D_2 receptor heteromer. GFP fused to Cys^{443}(CT) of the D_2 receptor (*cyan surface*) and YFP fused to Leu^{472}(CT) of the CB_1 receptor (*red surface*) are shown. IL3 of CB_1 (*red line*) and D_2 (*cyan line*) receptors are shown in *solid lines* to illustrate their proximity. *c,* cytoplasmic view of the computational model of the A_{2A}-CB_1-D_2 receptor heteromer. CT of the CB_1 receptor is depicted in the following manner: amino acids Ser^{414}–Asn^{437} of (*red tube ribbon*) are modeled as in the crystal structure of squid rhodopsin, amino acids Asn^{437}–Asp^{466} (not modeled) are shown as a *red solid line* to illustrate the position of Thr^{467}–Ser^{468}, and amino acids Ala^{469}–Leu^{472} (*red solid line*) are arbitrarily modeled to position YFP. CT of the A_{2A} receptor is depicted in the following manner: amino acids Ser^{305}–Gly^{328} (*golden tube ribbon*) are modeled as in the crystal structure of squid rhodopsin; amino acids Ser^{329}–Ser^{412} (not modeled) are shown as a *yellow solid line*, and phosphorylated Ser^{374} is shown as a *red circle*. Helices are shown as cylinders with the following color codes: TM4 in *gray*, TM5 in *green*, TM6 in *blue*, and the other helices in *yellow* for A_{2A}, in *red* for CB_1, and *cyan* for D_2 receptors.

Modeling the A_{2A}-CB_1-D_2 Receptor Heteromer—The quaternary structure of the A_{2A}-CB_1-D_2 heteromer was finally obtained by combining the CB_1-D_2 (TM5-TM5 interface) and CB_1-A_{2A} (TM4-TM4^{invago}) models described above (Fig. 8*a*). This combination of TM-TM interactions was selected among the others because it best reproduces the distance between GFP and YFP in the proposed A_{2A}-CB_1-D_2 receptor heteromer within the 5.7–6.1-nm range experimentally determined from FRET efficiencies (see above). Fig. 8*b* shows a molecular model of the A_{2A}-CB_1-D_2 heteromer, in which GFP was fused to Cys^{443}(CT) of the D_2 receptor at the end of the conserved Hx8; YFP was fused to Leu^{472}(CT) of the CB_1 receptor, only four amino acids apart from the phosphorylated Ser^{468}(CT); and Thr^{467}(CT)–Ser^{468}(CT) of the CB_1 receptor could interact with Arg^{205}(5.66)–Arg^{206}(5.67) of the A_{2A} receptor. In addition, this computational model of the A_{2A}-CB_1-D_2 receptor heteromer positioned the CT of the A_{2A} receptor toward the D_2 receptor epitope located in the cytoplasm at the end of TM5, so that phosphorylated Ser^{374}(CT) can interact with the (5.64) ^{215}VL**RRRRKR**VN^{224} epitope (Fig. 8, *a* and *c*).

As shown above, expression of the $CB_1^{A467\text{-}A468}$-YFP or A_{2A}^{A374}-*Rluc* mutant receptors leads to a separation of the CT of CB_1 from A_{2A} and the CT of A_{2A} from D_2, respectively. This clearly suggests that phosphorylated Thr^{467}(CT)–Ser^{468}(CT) in CB_1 or Ser^{374}(CT) in A_{2A} serves to maintain the large and flexible CT of the receptors in the proper conformation by interacting with the Arg-rich epitope of the corresponding promoter. It thus seems reasonable to suggest that the absence of Thr^{467}(CT)–Ser^{468}(CT) in CB_1 or Ser^{374}(CT) in A_{2A} modifies the CT of the mutant receptors, whereas the packing of the TMs in the A_{2A}-CB_1-D_2 heteromer remains similar.

Structure-Function Relationship in the A_{2A}-CB_1-D_2 Receptor Heteromer—We explored the possibility that changes in the quaternary structure of A_{2A}-CB_1-D_2 receptor heteromer after disruption of the electrostatic interactions could correlate with changes in the receptor heteromer function. We first looked for differences in signaling (activation of the MAPK pathway) in cells co-expressing A_{2A} and D_2 receptors in the absence and presence of CB_1 receptors (Fig. 9). In cells co-expressing A_{2A} and D_2 receptors, co-activation of both receptors with their respective selective agonists CGS 21680 (200 nM) and quinpirole (1 μM) produced a similar degree of ERK1/2 phosphorylation than activation of either A_{2A} or D_2 receptors. As shown in Fig. 9*a*, the additional co-expression of CB_1 receptor produced a qualitatively different pattern with a significantly higher effect of co-activation of A_{2A} and D_2 receptors compared with cells expressing only A_{2A} and D_2 receptors. We then demonstrated that this pattern of MAPK activation is a biochemical characteristic of the A_{2A}-CB_1-D_2 receptor heteromer, because it depends on the integrity of its quaternary structure. In fact, we found that it particularly depends on the integrity of the intracellular electrostatic interactions that the CB_1 receptor forms with the D_2 receptor in A_{2A}-CB_1-D_2 receptor heteromer. Thus, in cells expressing $CB_1^{A321\text{-}A321}$ or D_{2S} receptors (which lose the ability to establish electrostatic interactions with the D_2 or the CB_1 receptors, respectively, in the A_{2A}-CB_1-D_2 receptor heteromer), the pattern of MAPK activation was significantly altered and qualitatively similar to that observed in cells only co-expressing A_{2A} and D_2 receptors (Fig. 9*b*).

The pattern of MAPK activation could then be used as a biochemical fingerprint of the A_{2A}-CB_1-D_2 receptor heteromer to detect its presence in the brain (3). In fact, comparing the pattern of ERK1/2 phosphorylation upon activation of A_{2A} and D_2 receptors in striatal slices from wild-type mice and CB_1

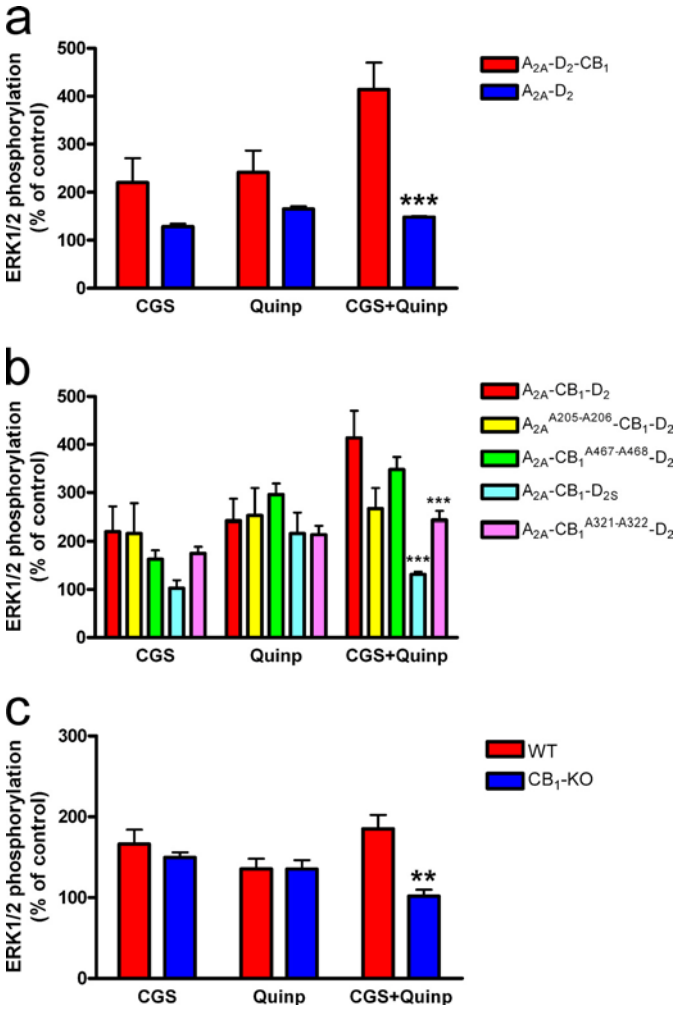

FIGURE 9. **Agonist-induced ERK1/2 phosphorylation by the A_{2A}-D_2-CB_1 receptor heteromer.** *a* and *b*, assays were performed 48 h post-transfection in cells expressing the indicated receptors (1.2 μg of cDNA of the A_{2A} or the $A_{2A}^{A205-A206}$ receptors, 1 μg of cDNA of the D_2, 0.8 μg of cDNA of the D_{2S} receptor, and 1 μg of cDNA of the CB_1, $CB_1^{A467-A468}$, or the $CB^{1A321-A322}$ receptors). Cells were treated for 5 min with 200 nM CGS 21680 (*CGS*), 1 μM quinpirole (*Quinp*), or both (*CGS+Quinp*) and ERK1/2 phosphorylation was determined as indicated under "Experimental Procedures." The immunoreactive bands from four experiments performed in duplicate were quantified, and the values represent the mean ± S.E. of % of phosphorylation relative to the basal levels found in untreated cells. *c*, assays were performed in striatal slices from wild-type (*WT*) or CB_1 knock-out mice (*CB_1-KO*). The slices were treated for 10 min with 1 μM CGS 21680 (*CGS*), 1 μM quinpirole (*quinpirole*) or both, and ERK1/2 phosphorylation was determined as indicated under "Experimental Procedures." The immunoreactive bands from four to eight slices obtained from five to nine animals were quantified, and values represent the mean ± S.E. of the % of phosphorylation relative to basal levels found in untreated slices. Significant differences respect to the wild-type mice were calculated by bifactorial ANOVA followed by post hoc Bonferroni's tests (**, $p < 0.01$; ***, $p < 0.001$).

receptor knock-out mice, we found the same qualitative differences as those observed in co-transfected cells with and without CB_1 receptors (compare Fig. 8, *a* and *c*). Thus, in striatal slices from CB_1 receptor knock-out mice, there was a significantly lower ERK1/2 phosphorylation upon co-activation of A_{2A} and D_2 receptors compared with that obtained from striatal slices from wild-type animals. A bifactorial ANOVA demonstrated a significant genotype effect ($p < 0.05$) and significant treatment/genotype interaction ($p < 0.05$), and post hoc Bonferroni tests only showed a significant difference between both groups when the striatal slices were co-treated with CGS 21680 (1 μM) and quinpirole (1 μM) (Fig. 9*c*).

DISCUSSION

This study shows, for the first time, that GPCR heteromers display emerging properties that depend on their folding into a certain quaternary structure, determined not only by interactions between TM domains but also involving interactions between hydrophilic intracellular domains. Significantly, we have found that each receptor, A_{2A}, CB_1, and D_2, contains two key intracellular domains to interact in a selective manner with intracellular domains of the other two receptors by means of electrostatic interactions in the formation of the quaternary structure of the A_{2A}-D_2, A_{2A}-CB_1, CB_1-D_2, and A_1-CB_1-D_2 receptor heteromers. Thus, the D_2 receptor contains two Arg-rich epitopes, ^{215}VL**RRRR**-**KR**VN^{224} and ^{266}N**RRR**VEAA**RR**^{275}, that interact with potential CK1/2-dependent phosphorylatable Ser/Thr residues in CT (Ser^{374}) of the A_{2A} receptor and in IL3 (Thr^{321}–Ser^{322}) of the CB_1 receptor, respectively; CB_1 receptor contains adjacent phosphorylatable Ser and Thr residues in IL3 (Thr^{321} and Ser^{322}) and the CT (Thr^{467} and Ser^{468}) that interact with Arg residues in IL3 (^{266}N**RRR**VEAA**RR**^{275}) of the D_2 receptor and Arg^{205}–Arg^{206} of the A_{2A} receptor, respectively; and the A_{2A} receptor contains Arg residues at the end of TM5 in the cytoplasm at Arg^{205}–Arg^{206} and a phosphorylatable Ser residue in the CT (Ser^{374}), which interact with phosphorylatable Ser/Thr residues in the CB_1 receptor CT (Thr^{467} and Ser^{468}) and an Arg-rich epitope of the D_2 receptor located in the cytoplasm at the end of TM5 (^{215}VL**RRRRKR**VN^{224}), respectively. The fact that each of these three receptors forms electrostatic interactions involving evolutionarily conserved adjacent Arg residues and CK1/2-dependent phosphorylatable Ser and Thr residues with the other two receptors suggests that these particular electrostatic interactions constitute a general mechanism for receptor heteromerization. In studies using synthetic peptides, it has been shown that these electrostatic interactions are particularly stable. Thus, the Arg-phosphate interaction is so stable that when using collision-induced dissociation, the noncovalent interactions between the Arg guanidinium groups and the phosphate group remain intact even though the covalent bond between the serine and phosphate breaks (16, 31–33).

Using bioluminescence resonance energy transfer techniques with mutant receptors, we propose for the first time the quaternary structure for three interacting GPCRs. Characterization of protomer organization within the A_1-CB_1-D_2 receptor heteromer requires, in addition to our findings, integration of information from a variety of different approaches. Most compelling are studies that apply disulfide cross-linking to map TM interfaces between protomers (10, 12, 13). Modeling of the CB_1-D_2, A_{2A}-CB_1, and A_{2A}-D_2 receptor heterodimers was performed through the entire set of proposed TM interfaces (*i.e.* TM1, TM4, or TM5). Our results are compatible with models proposed for other family A GPCRs, where oligomerization involves primarily TM4 and TM5 interfaces (Fig. 8). Thus, our study supports a triangular rather than a linear arrangement of receptors in the A_{2A}-CB_1-D_2 heteromer. This arrangement allows the possibility of simultaneous homodimerization of

each receptor unit using the TM1 interface, which is a well established phenomenon in the GPCR field. Thus, this study opens up a new conceptual challenge in the field of receptor heteromerization, which is the idea that GPCRs can form not only heteromultimers of three different receptor units but also higher order heteromultimers or "receptor nets."

The interactions of the intracellular domains of the CB_1 receptor with A_{2A} and D_2 receptors were found to be fundamental for the correct formation of the quaternary structure needed for the function of the A_{2A}-CB_1-D_2 receptor heteromers. Thus, mutant receptors lacking the interacting amino acids significantly disrupted RET and a specific qualitative pattern of ERK1/2 phosphorylation induced by co-activation of A_{2A} and D_2 receptors. The fact that such a disruption of the quaternary structure of the A_{2A}-CB_1-D_2 receptor heteromer (as demonstrated by SRET experiments) was associated with a significant qualitative change in signaling indicates that electrostatic interactions between intracellular domains are also key determinants for the specific biochemical properties of the A_{2A}-CB_1-D_2 receptor heteromer. These biochemical characteristics and the specific qualitative pattern of MAPK activation could be used as a biochemical fingerprint of the A_{2A}-CB_1-D_2 receptor heteromer presence in the brain. CB_1 receptor KO mice experiments provided strong support for the existence of A_{2A}-CB_1-D_2 receptor heteromer in the striatum. It has been hypothesized that A_{2A}-CB_1-D_2 receptor heteromers are mostly located in one subtype of striatal neuron, the GABAergic enkephalinergic neuron, where the three receptors are highly co-expressed and exert a significant control of basal ganglia function (34). Most probably, the results obtained with MAPK signaling are just a minor but the first described example of many of the potential properties of the A_{2A}-CB_1-D_2 receptor heteromers.

Acknowledgments—We thank Prof. Olga Valverde and Prof. Catherine Ledent (Department of Experimental and Health Sciences, Biomedical Research Park, Barcelona University Pompeu Fabra, Barcelona, Spain) for generously supplying wild-type and CB_1 receptor KO mice. We thank the Office of National Drug Control Policy and Jodie Franklin (The Johns Hopkins Synthesis and Sequencing Facility) for the peptide synthesis. We acknowledge the technical help obtained from Jasmina Jiménez (Molecular Neurobiology Laboratory, Barcelona University).

REFERENCES

1. Ferré, S., Ciruela, F., Woods, A. S., Lluis, C., and Franco, R. (2007) *Trends Neurosci.* **30,** 440–446
2. Pin, J. P., Neubig, R., Bouvier, M., Devi, L., Filizola, M., Javitch, J. A., Lohse, M. J., Milligan, G., Palczewski, K., Parmentier, M., and Spedding, M. (2007) *Pharmacol. Rev.* **59,** 5–13
3. Ferré, S., Baler, R., Bouvier, M., Caron, M. G., Devi, L. A., Durroux, T., Fuxe, K., George, S. R., Javitch, J. A., Lohse, M. J., Mackie, K., Milligan, G., Pfleger, K. D., Pin, J. P., Volkow, N. D., Waldhoer, M., Woods, A. S., and Franco, R. (2009) *Nat. Chem. Biol.* **5,** 131–134
4. Dalrymple, M. B., Pfleger, K. D., and Eidne, K. A. (2008) *Pharmacol. Ther.* **118,** 359–371
5. Carriba, P., Navarro, G., Ciruela, F., Ferré, S., Casadó, V., Agnati, L., Cortés, A., Mallol, J., Fuxe, K., Canela, E. I., Lluís, C., and Franco, R. (2008) *Nat. Methods* **5,** 727–733
6. Gandia, J., Galino, J., Amaral, O. B., Soriano, A., Lluís, C., Franco, R., and Ciruela, F. (2008) *FEBS Lett.* **582,** 2979–2984
7. Davies, A., Gowen, B. E., Krebs, A. M., Schertler, G. F., and Saibil, H. R. (2001) *J. Mol. Biol.* **314,** 455–463
8. Maurel, D., Comps-Agrar, L., Brock, C., Rives, M. L., Bourrier, E., Ayoub, M. A., Bazin, H., Tinel, N., Durroux, T., Prézeau, L., Trinquet, E., and Pin, J. P. (2008) *Nat. Methods* **5,** 561–567
9. Fotiadis, D., Liang, Y., Filipek, S., Saperstein, D. A., Engel, A., and Palczewski, K. (2003) *Nature* **421,** 127–128
10. Klco, J. M., Lassere, T. B., and Baranski, T. J. (2003) *J. Biol. Chem.* **278,** 35345–35353
11. Liang, Y., Fotiadis, D., Filipek, S., Saperstein, D. A., Palczewski, K., and Engel, A. (2003) *J. Biol. Chem.* **278,** 21655–21662
12. Guo, W., Shi, L., Filizola, M., Weinstein, H., and Javitch, J. A. (2005) *Proc. Natl. Acad. Sci. U.S.A.* **102,** 17495–17500
13. Guo, W., Urizar, E., Kralikova, M., Mobarec, J. C., Shi, L., Filizola, M., and Javitch, J. A. (2008) *EMBO J.* **27,** 2293–2304
14. González-Maeso, J., Ang, R. L., Yuen, T., Chan, P., Weisstaub, N. V., López-Giménez, J. F., Zhou, M., Okawa, Y., Callado, L. F., Milligan, G., Gingrich, J. A., Filizola, M., Meana, J. J., and Sealfon, S. C. (2008) *Nature* **452,** 93–97
15. Han, Y., Moreira, I. S., Urizar, E., Weinstein, H., and Javitch, J. A. (2009) *Nat. Chem. Biol.* **5,** 688–695
16. Woods, A. S., and Ferré, S. (2005) *J. Proteome Res.* **4,** 1397–1402
17. Zimmermann, T., Rietdorf, J., Girod, A., Georget, V., and Pepperkok, R. (2002) *FEBS Lett.* **531,** 245–249
18. Ledent, C., Valverde, O., Cossu, G., Petitet, F., Aubert, J. F., Beslot, F., Böhme, G. A., Imperato, A., Pedrazzini, T., Roques, B. P., Vassart, G., Fratta, W., and Parmentier, M. (1999) *Science* **283,** 401–404
19. Aso, E., Ozaita, A., Valdizán, E. M., Ledent, C., Pazos, A., Maldonado, R., and Valverde, O. (2008) *J. Neurochem.* **105,** 565–572
20. Jaakola, V. P., Griffith, M. T., Hanson, M. A., Cherezov, V., Chien, E. Y., Lane, J. R., Ijzerman, A. P., and Stevens, R. C. (2008) *Science* **322,** 1211–1217
21. Cherezov, V., Rosenbaum, D. M., Hanson, M. A., Rasmussen, S. G., Thian, F. S., Kobilka, T. S., Choi, H. J., Kuhn, P., Weis, W. I., Kobilka, B. K., and Stevens, R. C. (2007) *Science* **318,** 1258–1265
22. Rasmussen, S. G., Choi, H. J., Rosenbaum, D. M., Kobilka, T. S., Thian, F. S., Edwards, P. C., Burghammer, M., Ratnala, V. R., Sanishvili, R., Fischetti, R. F., Schertler, G. F., Weis, W. I., and Kobilka, B. K. (2007) *Nature* **450,** 383–387
23. Ballesteros, J. A., and Weinstein, H. (1995) in *Methods in Neurosciences*, Vol. 25, pp. 366–428, Elsevier, San Diego, CA
24. Park, J. H., Scheerer, P., Hofmann, K. P., Choe, H. W., and Ernst, O. P. (2008) *Nature* **454,** 183–187
25. Murakami, M., and Kouyama, T. (2008) *Nature* **453,** 363–367
26. Li, J., Edwards, P. C., Burghammer, M., Villa, C., and Schertler, G. F. (2004) *J. Mol. Biol.* **343,** 1409–1438
27. Blom, N., Gammeltoft, S., and Brunak, S. (1999) *J. Mol. Biol.* **294,** 1351–1362
28. Ciruela, F., Burgueño, J., Casadó, V., Canals, M., Marcellino, D., Goldberg, S. R., Bader, M., Fuxe, K., Agnati, L. F., Lluis, C., Franco, R., Ferré, S., and Woods, A. S. (2004) *Anal. Chem.* **76,** 5354–5363
29. Azdad, K., Gall, D., Woods, A. S., Ledent, C., Ferré, S., and Schiffmann, S. N. (2009) *Neuropsychopharmacology* **34,** 972–986
30. Missale, C., Nash, S. R., Robinson, S. W., Jaber, M., and Caron, M. G. (1998) *Physiol. Rev.* **78,** 189–225
31. Jackson, S. N., Wang, H. Y., and Woods, A. S. (2005) *J. Proteome Res.* **4,** 2360–2363
32. Jackson, S. N., Moyer, S. C., and Woods, A. S. (2008) *J. Am. Soc. Mass Spectrom.* **19,** 1535–1541
33. Jackson, S. N., Wang, H. Y., Yergey, A., and Woods, A. S. (2006) *J. Proteome Res.* **5,** 122–126
34. Ferré, S., Goldberg, S. R., Lluis, C., and Franco, R. (2009) *Neuropharmacology* **56,** Suppl. 1, 226–234

Suppl. Figure 1

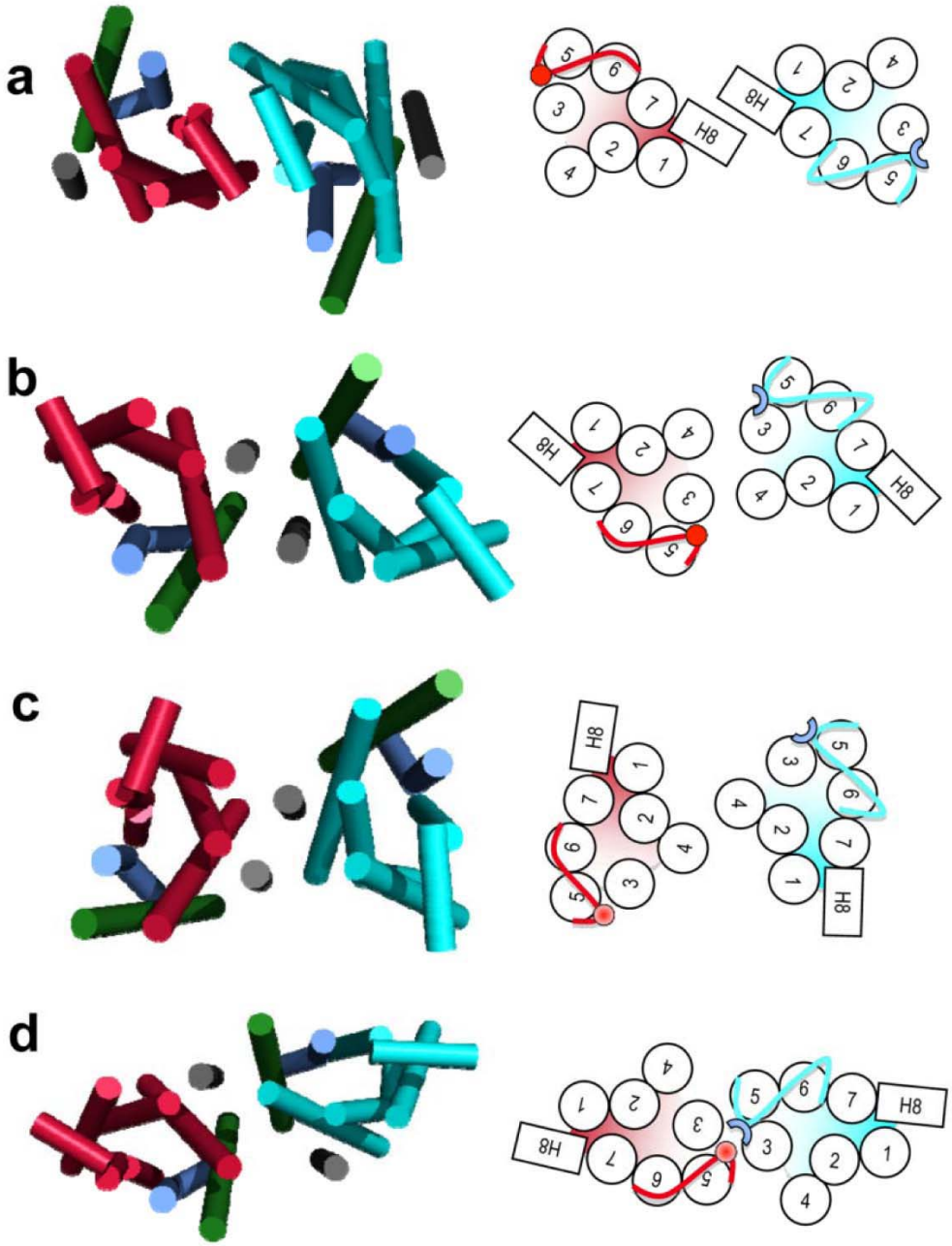

Cytoplasmic view (left) and cartoon of this footprint (right) of the CB_1 (in red) and D_2 (in cyan) receptor heterodimer involving the TM1-TM1 (a), TM4-TM4^{invago} (b), TM4-TM4^{ago} (c), or TM5-TM5 (d) interfaces (see Methods). Red and cyan solid lines symbolize IL3 of CB_1 (29 amino acids long) or D_2 (142 amino acids long) receptors, respectively, which were not modeled. The red sphere represents Thr_{321}-Ser_{322} of CB_1; and the blue half circle represents $_{266}NRRRVEAARR_{275}$ of the D_2 receptor. Please note that the direction of the sphere and half circle within IL3 is totally arbitrary. Helices are shown as cylinders with the following color codes: TM4 in gray, TM5 in green, TM6 in blue, and the other helices in red for CB_1 and cyan for D_2 receptors.

Suppl. Figure 2

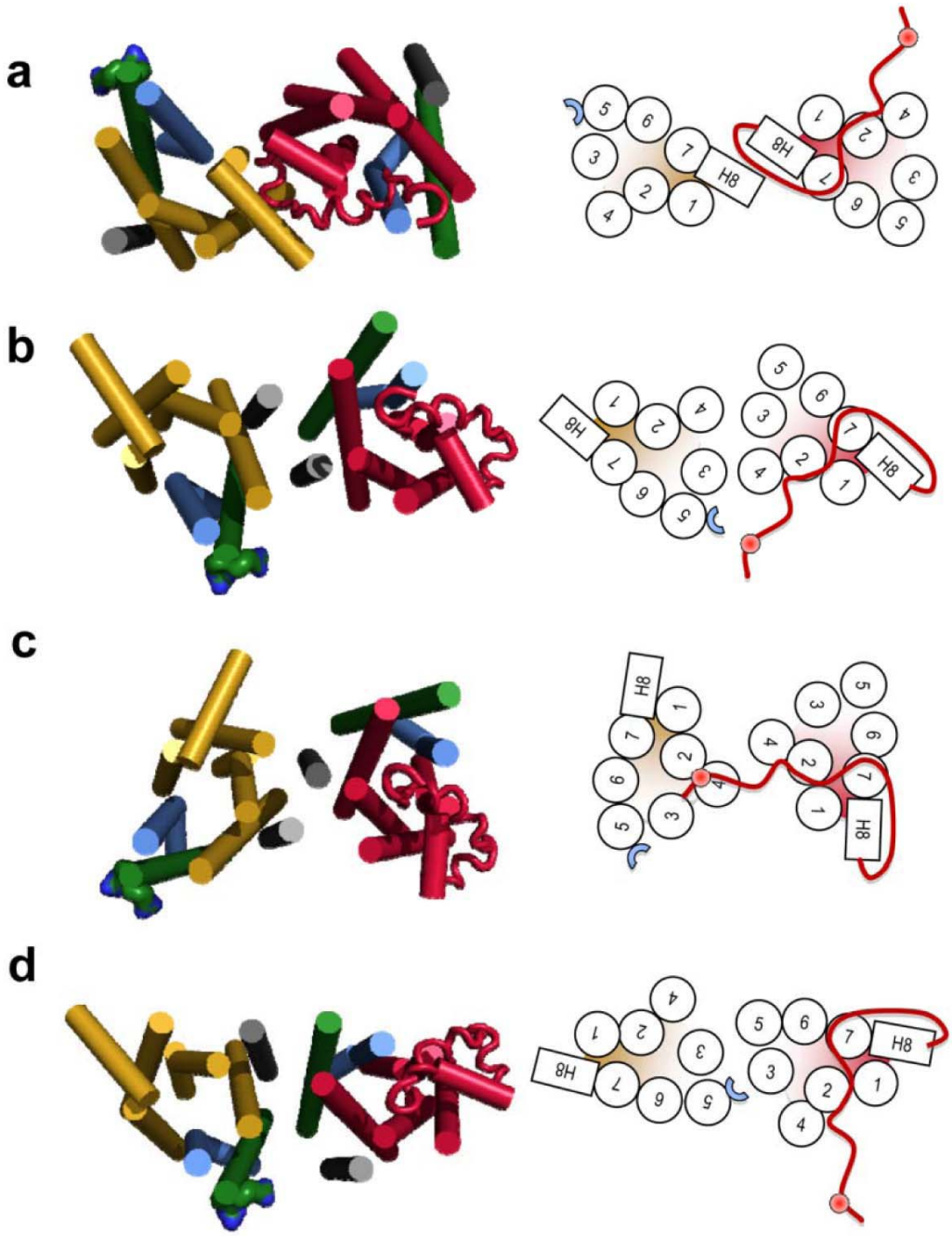

Cytoplasmic view (left) and cartoon of this footprint (right) of the CB_1 (in red) and A_{2A} (in gold) receptor heterodimer involving the TM1-TM1 (a), TM4-TM4^{invago} (b), TM4-TM4^{ago} (c), or TM5-TM5 (d) interfaces (see Methods). Red solid line represents CT of the CB_1 receptor, which was arbitrarily modeled as in squid rhodopsin, red sphere represents Thr_{467}(CT)-Ser_{468}(CT) of CB_1; and blue half circle represents Arg_{206}(5.67) of the A_{2A} receptor. Helices are shown as cylinders with the following color codes: TM4 in gray, TM5 in green, TM6 in blue, and the other helices in red for CB_1 and gold for A_{2A} receptors.

Supplementary Table I. Interspecies comparison of the A_{2A}, D_2 and CB_1 receptor epitopes

A_{2A} receptor 5TM			
Species	**Sequence**	**Residues**	**Accession #**
Human	LRIFLAARR	198-206	P29274
Dog	LRIFLAARR	198-206	P11617
Horse	LRIFLAARR	198-206	Q6TLI7
Bovine	LRIFLAARR	195-203	IPI00716182
Guinea pig	LRIFLAARR	195-203	P46616
Rat	LRIFLAARR	193-201	P30543
Mouse	LRIFLAARR	193-201	Q60613
A_{2A} receptor CT			
Species	**Sequence**	**Residues**	**Accession #**
Human	SAQEpSQGNT	370-378	P29274
Dog	IAPEpSHGDM	370-378	P11617
Horse	SAREpSPGDT	370-378	Q6TLI7
Bovine	GARGpSQRDA	366-374	IPI00716182
Guinea pig	SAQRpSHGDA	367-375	P46616
Rat	SAQGpSPRDV	365-373	P30543
Mouse	STQGpSPGDV	365-373	Q60613
D_2 receptor 5TM			
Species	**Sequence**	**Residues**	**Accession #**
Human	VLRRRRKRVN	215-224	P14416
Monkey	VLRRRRKRVN	215-224	P52702
Bovine	VLRRRRKRVN	215-224	P20288
Dog	VLRRRRKRVN	215-224	Q9GJU1
Mouse	VLRKRRKRVN	215-224	P61168
Rat	VLRKRRKRVN	215-224	P61169
Ferret	VLRKRRKRVN	215-224	Q6TLI9
D_2 receptor IL3			
Species	**Sequence**	**Residues**	**Accession #**
Human	NRRRVEAARR	266-275	P14416
Monkey	NRRRVEAARR	266-275	P52702
Bovine	NRRRVEAARR	266-275	P20288
Dog	NRRRVEAARR	266-275	Q9GJU1
Mouse	NRRRMDAARR	266-275	P61168
Rat	NRRRMDAARR	266-275	P61169
Ferret	NRRRVEAARR	266-275	Q6TLI9
CB_1 receptor IL3			
Species	**Sequence**	**Residues**	**Accession #**
Human	pTpSEDGKVQVT	321-330	P21554
Chimpanzee	pTpSEDGKVQVT	321-330	Q5IS73
Mouse	pTpSEDGKVQVT	322-331	P47746
Rat	pTpSEDGKVQVT	322-331	P20272
Cat	pTpSEDGKVQVT	321-330	O02777
Frog	pTpSEDGKVHIT	321-330	Q801M1
Fish	pSpTEDGKVQIT	323-332	P56971

CB_1 receptor CT			
Species	**Sequence**	**Residues**	**Accession #**
Human	SVSTDpTpSAE	462-470	P21554
Chimpanzee	SVSTDpTpSAE	462-470	Q5IS73
Mouse	SVSTDpTpSAE	463-471	P47746
Rat	SVSTDpTpSAE	463-471	P20272
Cat	SVSTNpTpSAK	462-470	O02777
Frog	SVSTDpTpSAE	460-468	Q801M1
Fish	SVSTDpTpTAE	463-471	P56971

6.3 La adenosina desaminasa modula alostéricamente la unión y la señalización de ligandos del receptor A_{2A} de adenosina

Eduard Gracia, Kamil Pérez-Capote, Estefanía Moreno, Jana Bakešová, Josefa Mallol, Carme Lluís, Rafael Franco[*], Antoni Cortés, Vicent Casadó and Enric I. Canela

Institut d'Investigacions Biomèdiques August Pi i Sunyer, Centro de Investigación Biomédica en Red sobre Enfermedades Neurodegenerativas (CIBERNED), y Departamento de Bioquímica y Biología Molecular, Facultad de Biología, Universidad de Barcelona, España,
[*]Centro de Investigación Médica Aplicada (CIMA). Universidad de Navarra. Avda. Pio XII, 55. 31008 Pamplona.

Manuscrito publicado en Biochemical Journal (2011 May); ***435(3)****: 701-709.*

Los receptores A_{2A} de adenosina se expresan de forma abundante en el estriado, zona principal del control motor en el sistema nervioso central. Mediante técnicas de transferencia de energía de resonancia bioluminiscente (BRET) se ha demostrado que los homómeros de los receptores A_{2A} pueden actuar como proteínas de anclaje del enzima adenosina desaminasa (ADA; EC 3.5.4.4) en la superficie celular. De hecho, se observó que la unión de la ADA modifica la estructura cuaternaria de los homómeros A_{2A}-A_{2A} presentes en la superficie celular, e incrementa tanto la afinidad del receptor por agonistas como por antagonistas en experimentos de unión de radioligandos a membranas estriatales. La ADA también incrementó la fosforilación de ERK 1/2 mediada por los agonistas del receptor. En conjunto, todos estos resultados muestran que la ADA, además de regular la concentración extracelular de adenosina, puede actuar como modulador alostérico incrementando de forma considerable la afinidad del receptor por sus ligandos y su funcionalidad. Esta regulación puede tener implicaciones en la fisiología y farmacología de los receptores A_{2A} de adenosina neuronales.

BJ www.biochemj.org

BJ Signal

A_{2A} adenosine receptor ligand binding and signalling is allosterically modulated by adenosine deaminase

Eduard GRACIA, Kamil PÉREZ-CAPOTE, Estefanía MORENO, Jana BARKEŠOVÁ, Josefa MALLOL, Carme LLUÍS, Rafael FRANCO[1], Antoni CORTÉS, Vicent CASADÓ and Enric I. CANELA[2]

Centro de Investigacón Biomédica en Red sobre Enfermedades Neurodegenerativas (CIBERNED), and Department of Biochemistry and Molecular Biology, Faculty of Biology, University of Barcelona, Avda. Diagonal 645, 08028 Barcelona, Spain

A_{2A}Rs (adenosine A_{2A} receptors) are highly enriched in the striatum, which is the main motor control CNS (central nervous system) area. BRET (bioluminescence resonance energy transfer) assays showed that A_{2A}R homomers may act as cell-surface ADA (adenosine deaminase; EC 3.5.4.4)-binding proteins. ADA binding affected the quaternary structure of A_{2A}Rs present on the cell surface. ADA binding to adenosine A_{2A}Rs increased both agonist and antagonist affinity on ligand binding to striatal membranes where these proteins are co-expressed. ADA also increased receptor-mediated ERK1/2 (extracellular-signal-regulated kinase 1/2) phosphorylation. Collectively, the results of the present study show that ADA, apart from regulating the concentration of extracellular adenosine, may behave as an allosteric modulator that markedly enhances ligand affinity and receptor function. This powerful regulation may have implications for the physiology and pharmacology of neuronal A_{2A}Rs.

Key words: adenosine deaminase, adenosine receptor, allosteric interaction, G-protein-coupled receptor, protein–protein interaction, receptor binding parameter.

INTRODUCTION

Self-association of proteins to form dimers and higher-order oligomers and/or interaction with other proteins are key factors in cell signalling [1–3]. A paradigmatic example are adenosine receptors. The nucleoside adenosine exerts a modulatory action in many areas of the CNS (central nervous system) via its four GPCR (G-protein-coupled receptor) subtypes: A_1Rs (adenosine A_1 receptors) and A_3Rs (adenosine A_3 receptors) that are negatively coupled to the adenylate cyclase, and A_{2A}Rs (adenosine A_{2A} receptors) and A_{2B}Rs (adenosine A_{2B} receptors) that mediate the stimulation of adenylate cyclase activity [4]. Along the plasma membrane (horizontal plane), A_1Rs and A_{2A}Rs may form homo-oligomers [5–7] and heteromers with other receptors [8–11], and the oligomerization generates new and unique biochemical and functional characteristics by modulating the binding properties, G-protein coupling and receptor trafficking [3,12,13]. Across the membrane (vertical to the plane of the membrane), A_1Rs interact with intracellular proteins that are not directly involved in the signalling cascade, such as the Hsc73 (heat-shock cognate 73 stress protein), and this direct interaction is relevant for receptor function [14]. Also across the membrane, both A_1Rs and A_{2B}Rs interact with a protein that has an extracellular topology, ADA (adenosine deaminase) [15–18].

ADA is an enzyme involved in purine metabolism which catalyses the hydrolytic deamination of adenosine and 2′-deoxyadenosine to inosine or 2′-deoxyinosine and ammonia. Congenital defects of ADA lead to SCID (severe combined immunodeficiency), which is characterized by the absence of functional T- and B-lymphocytes in affected individuals [19,20]. Neurological abnormalities, which are less life threatening than immunological abnormalities, have also been described in a portion of patients [21]. Neurological alterations may be secondary to infections, or may be due to the accumulation of adenosine and derivatives in brain. Although the location of ADA is mainly cytosolic, it has been found on the cell surface of many cell types, including neurons [22]; therefore it can be considered as an ecto-enzyme [19]. Since ADA is a peripheral membrane protein it needs integral membrane proteins to be anchored to the membrane. Apart from A_1Rs and A_{2B}Rs, another class of ecto-ADA-binding protein is CD26, a multifunctional transmembrane glycoprotein, acting as a receptor and a proteolytic enzyme [23]. It has been shown that ADA anchored to the dendritic cell surface, probably by the A_{2B}R, binds to CD26 expressed on the surface of T-cells, triggering co-stimulation and enabling an enhanced immune response [24–26].

We have also demonstrated that binding of enzymatically active or inactive ADA to A_{2B}R increases its affinity and signalling by a protein–protein interaction [17]. In the case of A_1Rs, the ADA–A_1R interaction is very relevant since the enzyme potentiates signal transduction and modulates the desensitization of A_1Rs [15,18,27]. Despite the well-established positive modulation exerted by ADA on A_1Rs and A_{2B}Rs, it is not known whether the enzyme is able to modulate the A_{2A}R subtype. There is currently a major interest in the ability of central A_{2A}Rs to control synaptic plasticity at glutamatergic synapses due to a combined ability of these receptors to facilitate the release of glutamate and the activation of NMDA; furthermore, A_{2A}Rs also control glial function and brain metabolic adaptation, and are important in controlling the demise of neurodegeneration [28]. In

Abbreviations used: A_{2A}R, adenosine A_{2A} receptor; A_{2B}R, adenosine A_{2B} receptor; ADA, adenosine deaminase; BCA, bicinchoninic acid; BRET, bioluminescence resonance energy transfer; CHO, Chinese-hamster ovary; ERK, extracellular-signal-regulated kinase; FBS, fetal bovine serum; GABA, γ-aminobutyric acid; GFP, green fluorescent protein; GPCR, G-protein-coupled receptor; HEK-293T, HEK-293 cells expressing the large T-antigen of SV40 (simian virus 40); PEI, polyethylenimine; Rluc, *Renilla* luciferase; SCID, severe combined immunodeficiency; TM, transmembrane domain; YFP, yellow fluorescent protein.

[1] Present address: Centro de Investigación Médica Aplicada (CIMA), University of Navarra, Avda. Pio XII, 55, 31008 Pamplona, Spain.
[2] To whom correspondence should be addressed (email ecanela@ub.edu).

the present paper we report the molecular interaction between ADA and $A_{2A}R$ that results in ADA-induced conformational changes in the quaternary structure of $A_{2A}Rs$ homodimers and in the pharmacological and functional characteristics of brain striatal $A_{2A}Rs$. A fine-tune regulation exerted by ADA probably has important implications for the physiology and pharmacology of neuronal $A_{2A}Rs$.

EXPERIMENTAL

Fusion proteins and expression vectors

The human cDNA for the $A_{2A}Rs$ or $GABA_{B2}$ (γ-aminobutyric acid B2) receptors cloned into pcDNA3.1 were amplified (removing stop codons) using sense and antisense primers harbouring either unique EcoRI or KpnI sites. The fragments were then subcloned to be in-frame with Rluc (*Renilla* luciferase) into the EcoRI and KpnI restriction site of an Rluc-expressing vector (pRluc-N1; PerkinElmer), or into the EcoRI and KpnI or BamHI restriction site of the variant of GFP (green fluorescent protein) (EYFP-N3; enhanced yellow variant of GFP; Clontech), to give the plasmids that express $A_{2A}Rs$ or $GABA_{B2}$ receptors fused to Rluc or YFP (yellow fluorescent protein) on the C-terminal end of the receptor ($A_{2A}R$–Rluc, $A_{2A}R$–YFP or $GABA_{B2}R$–Rluc). As previously reported [9,11], when analysed by confocal microscopy, it was observed that all fusion proteins showed a similar membrane distribution as naïve receptors, and fusion of Rluc and YFP to $A_{2A}Rs$ did not modify receptor function, as determined by cAMP assays.

Transient transfection

HEK-293T [HEK-293 cells expressing the large T-antigen of SV40 (simian virus 40)] cells were grown in DMEM (Dulbecco's modified Eagle's medium; Gibco) supplemented with 2 mM L-glutamine, 100 units/ml penicillin/streptomycin and 5 % (v/v) heat-inactivated FBS (fetal bovine serum) (all supplements were from Invitrogen). HEK-293T cells growing in six-well dishes were transiently transfected with the corresponding fusion protein cDNA using the PEI (polyethylenimine; Sigma) method. Cells were incubated (for 4 h) with the corresponding cDNA together with PEI (5.47 mM nitrogen residues) and 150 mM NaCl in a serum-starved medium. After 4 h, the medium was changed to a fresh complete culture medium. At 48 h after transfection, cells were washed twice in quick succession in HBSS (Hanks balanced salt solution) with 10 mM glucose, detached and resuspended in the same buffer containing 1 mM EDTA. To control the cell number, the protein concentration of the sample was determined using the BCA (bicinchoninic acid) method (Pierce) using BSA dilutions as standards.

Generation of a CHO (Chinese-hamster ovary) cell clone expressing $A_{2A}Rs$

CHO cells were maintained at 37 °C in an atmosphere of 5 % CO_2 in αMEM (α-minimal essential medium) without nucleosides (Invitrogen), containing 10 % FBS, 50 μg/ml penicillin, 50 μg/ml streptomycin and 2 mM L-glutamine (300 μg/ml). CHO cells were transfected with the cDNA corresponding to human $A_{2A}R$ and cloned into a pcDNA3.1/Hygro vector with a hygromycin-resistance gene using the Lipofectamine™ (Invitrogen) method following the manufacturer's instructions. At 1 day after transfection, the selection antibiotic was added at a concentration that was previously determined using a selection antibiotic test. The antibiotic-resistant clones were isolated and cultured in six-well plates in the presence of the selection antibiotic. After an appropriate number of days/passages, a stable line expressing 6 ± 1 pmol/mg of protein, with an affinity constant for the $A_{2A}R$ antagonist ZM 241385 of 1 ± 0.3 nM, was selected and cultured in the presence of hygromycin (300 μg/ml).

BRET (bioluminescence resonance energy tranfer)

HEK-293T cells were co-transfected with 0.15 μg of cDNA corresponding to $A_{2A}R$–Rluc acting as a BRET donor, and increasing amounts of cDNA corresponding to $A_{2A}R$–YFP (0.8–3 μg of cDNA) acting as a BRET acceptor. As a negative control, HEK-293T cells were co-transfected with 0.15 μg of $A_{2A}R$–Rluc and increasing amounts of cDNAs corresponding to the $GABA_{B2}$–YFP receptor (0.3–3 μg of cDNA). After 48 h of transfection, the cell suspension (20 μg of protein) was dispensed in duplicate into 96-well black microplates with a transparent bottom (Porvair), and the fluorescence was measured using a Mithras LB940 fluorescence-luminescence detector (Berthold) with an excitation filter of 485 nm and an emission filter of 535 nm. For BRET measurement, 20 μg of cell suspension was distributed in duplicate into 96-well white opaque microplates (Porvair), and coelenterazine H (Molecular Probes) was added at a final concentration of 5 μmol/l. After 1 min the readings were collected in a Mithras LB 940 instrument which allows the integration of the signals detected in the short-wavelength filter at 485 nm (440–500 nm) and the long-wavelength filter at 530 nm (510–590 nm). The same samples were incubated for 10 min, and the luminescence was measured to quantify the donor. The BRET ratio is defined as:

$$[(\text{emission at } 510-590)/(\text{emission at } 440-500)] - \text{Cf}$$

where Cf corresponds to (emission at 510–590)/(emission 440–500) for the A_{2A}–Rluc construct expressed alone in the same experiment. Curves were fitted to a non-linear regression equation, assuming a single phase with GraphPad Prism software (San Diego, CA, U.S.A.).

Immunostaining

Wild-type CHO cells and $A_{2A}R$-expressing CHO cells, grown on glass coverslips, were washed with PBS and fixed with 2 % paraformaldehyde and 60 mM sucrose (pH 7.4) for 15 min at room temperature (25 °C). Cells were washed twice with PBS containing 15 mM glycine, and treated with 1 % BSA, 20 mM glycine and 0.05 % sodium azide for 20 min before the addition of the antibodies. Then, cells were labelled for 45 min either with 100 μg/ml of the anti-$A_{2A}R$ antibody [14,29] or 50 μg/ml of the anti-ADA antibody [30], both conjugated with FITC as described previously [14]. Cells were washed with PBS containing 1 % BSA, 20 mM glycine and 0.05 % sodium azide, and placed on coverslips for the subsequent fluorescence microscopy analysis in a Leica TCS 4D confocal laser-scanning microscope (Leica Lasertechnik).

Brain striatal membrane preparation and protein determination

Sheep brains were obtained from the local slaughterhouse. Membrane suspensions from sheep brain striatum were prepared as described previously [31]. Tissue was disrupted with a Polytron homogenizer (PTA 20 TS rotor, setting 3; Kinematica) for three 5 s periods in 10 vol. of 50 mM Tris/HCl buffer (pH 7.4), containing a protease inhibitor cocktail (Sigma, 1:1000). After eliminating cell debris by centrifugation at 1000 ***g*** for 10 min, membranes were obtained by centrifugation at 35 000 rev./min (40 min at

4 °C; rotor type 90 Ti, Beckman) and the pellet was resuspended and recentrifuged under the same conditions. The pellet was stored at − 80 °C and was washed once more as described above and resuspended in 50 mM Tris/HCl buffer for immediate use. Protein was quantified using the BCA method (Pierce) using BSA dilutions as the standard.

Enzyme activity of ADA and ADA inhibition by Hg^{2+}

Bovine ADA (Roche) enzyme activity was determined at 25 °C with 0.1 mM adenosine as the substrate in 50 mM Tris/HCl buffer (pH 7.4). The decrease in the absorbance at 265 nm ($\Delta\varepsilon = 7800\ M^{-1} \cdot cm^{-1}$) was monitored in an Ultrospec 3300 pro spectrophotometer (Biochrom); 1 ml cuvettes with a 1 cm light pathlength were used. Hg^{2+}-inactivation of bovine ADA was performed by a pre-incubation (2 h), of 15 units/ml desalted ADA with 100 μM $HgCl_2$, and removal of free Hg^{2+} by gel filtration as described previously [16]. No residual activity was found after a 4 h incubation with 0.1 mM adenosine and a high excess (10 μg/ml) of inhibited enzyme in the conditions described above.

Radioligand-binding experiments

ADA dose-dependent curves were obtained by incubating (2 h) sheep brain striatal membrane suspensions (0.3 mg of protein/ml) with the indicated concentration of $A_{2A}R$ agonist [^{3}H]CGS 21680 (42.7 Ci/mmol; PerkinElmer) or $A_{2A}R$ antagonist [^{3}H]ZM 241385 (27 Ci/mmol; American Radiolabelled Chemicals) in the presence or the absence of the indicated amounts of desalted bovine ADA at 25 °C in 50 mM Tris/HCl buffer (pH 7.4), containing 10 mM $MgCl_2$.

Saturation experiments were performed by incubating striatal membrane suspensions (0.3 mg of protein/ml) with increasing concentrations of the $A_{2A}R$ antagonist [^{3}H]ZM 241385 (triplicates of ten different concentrations, from 0.1 to 27 nM), at 25 °C in 50 mM Tris/HCl buffer (pH 7.4), containing 10 mM $MgCl_2$, in the absence or the presence of 0.2 i.u./ml (1 μg/ml) ADA.

Competition experiments were performed by incubating striatal membrane suspensions (0.3 mg of protein/ml) with a constant amount of [^{3}H]CGS 21680 or [^{3}H]ZM 241385 and it was increasing concentrations of CGS 21680 (triplicates of ten different concentrations from 1 nM to 10 μM; Tocris) or ZM 241385 (triplicates of 11 different concentrations, from 0.01 nM to 10 μM; Tocris) in the absence or presence of 0.2 i.u./ml (1 μg/ml) desalted ADA at 25 °C in 50 mM Tris/HCl buffer (pH 7.4), containing 10 mM $MgCl_2$, providing sufficient time to achieve equilibrium for the lowest radioligand concentration (5 h). In all experiments, non-specific binding was determined in the presence of 10 μM CGS 21680 or 10 μM ZM 241385 and it was confirmed that the value was the same as calculated by extrapolation of the competition curves. Free and membrane-bound ligand were separated by rapid filtration of 500 μl aliquots in a cell harvester (Brandel) through Whatman GF/C filters embedded in 0.3 % PEI, which were subsequently washed for 5 s with 5 ml of ice-cold Tris/HCl buffer (pH 7.4). The filters were incubated with 10 ml of Ecoscint H scintillation cocktail (National Diagnostics) overnight at room temperature, and radioactivity counts were determined using a Tri-Carb 1600 scintillation counter (PerkinElmer) with an efficiency of 62 % [14].

Binding-data analysis

Since $A_{2A}Rs$ are expressed as dimers or higher-order oligomers [6,13], radioligand competition curves were analysed by non-linear regression using the commercial Grafit curve-fitting software (Erithacus Software), by fitting the specific binding data to the mechanistic two-state dimer receptor model [32,33]. This model considers a homodimer as the minimal structural unit of the receptor. To calculate the macroscopic equilibrium dissociation constants from saturation binding experiments the following equation previously deduced [34] was considered (eqn 1):

$$A_{bound} = (K_{DA2} \times A + 2A^2) \times R_T / (K_{DA1} \times K_{DA2} + K_{DA2} \times A + A^2) \quad (1)$$

where A represents the free radioligand (the $A_{2A}R$ antagonist [^{3}H]ZM 241385) concentration, R_T is the total amount of receptor dimers, and K_{DA1} and K_{DA2} are the macroscopic dissociation constants describing the binding of the first and the second radioligand molecule to the dimeric receptor.

When binding of A to the dimer is non-co-operative, $K_{DA2}/K_{DA1} = 4$ (see [32,33] for details) and, therefore, K_{DA1} is enough to characterize the binding. In this case, the above equation can be reduced to (eqn 2):

$$A_{bound} = 2A \times R_T / (2K_{DA1} + A) \quad (2)$$

To calculate the macroscopic equilibrium dissociation constants from competition binding experiments the following equation previously deduced [34,35] was considered (eqn 3):

$$A_{total\,bound} = (K_{DA2} \times A + 2A^2 + K_{DA2} \times A \times B / K_{DAB}) \times R_T / [K_{DA1} \times K_{DA2} + K_{DA2} \times A + A^2 + K_{DA2} \times A \times B / K_{DAB} + K_{DA1} \times K_{DA2} \times B / K_{DB1} + K_{DA1} \times K_{DA2} \times B^2 / (K_{DB1} \times K_{DB2})] + A_{non-specific\,bound} \quad (3)$$

Here A represents free radioligand (the $A_{2A}R$ agonist [^{3}H]CGS 21680 or the $A_{2A}R$ antagonist [^{3}H]ZM 241385) concentration, B represents the assayed competing compound (CGS 21680 or ZM 241385) concentration, and K_{DB1} and K_{DB2} are, respectively, the macroscopic equilibrium dissociation constants of the first and second binding of B; K_{DAB} is the hybrid equilibrium radioligand/competitor dissociation constant, which is the dissociation constant of B binding to a receptor dimer semi-occupied by A.

Binding to GPCRs can display negative co-operativity and in these circumstances $K_{D2}/K_{D1} > 4$. On the other hand, for positive co-operativity, $K_{D2}/K_{D1} < 4$ [34]. To measure the degree of co-operativity, the two-state dimer receptor model also introduces a co-operativity index (D_C). The dimer co-operativity index for the radioligand A ([^{3}H]ZM 241385) or the competing ligand B (CGS 21680 or ZM 241385) was calculated as [13,34,35] (eqn 4):

$$D_{CA} = \log(4K_{DA1}/K_{DA2}); \; D_{CB} = \log(4K_{DB1}/K_{DB2}) \quad (4)$$

D_C measures the affinity modifications occurring when a protomer senses the binding of the same ligand molecule to the partner protomer in a dimer. The way the index is defined is such that its value is '0' for non-co-operative binding, positive values of D_C indicate positive co-operativity, whereas negative values imply negative co-operativity [13,34,35].

In the experimental conditions when both the radioligand A ([^{3}H]CGS 21680 or [^{3}H]ZM 241385) and the competitor B (CGS 21680 or ZM 241385) show non-co-operativity ($D_C = 0$), it results that $K_{DA2} = 4K_{DA1}$ and $K_{DB2} = 4K_{DB1}$, and eqn (3) was simplified

to (eqn 5):

$$A_{\text{total bound}} = (4K_{DA1} \times A + 2A^2 + 4K_{DA1} \times A \times B/K_{DAB}) \times R_T/\left(4K_{DA1}^2 + 4K_{DA1} \times A + A^2 + 4K_{DA1} \times A \times B/K_{DAB} + 4K_{DA1}^2 \times B/K_{DB1} + K_{DA1}^2 \times B^2/K_{DB1}^2\right) + A_{\text{non-specific bound}} \quad (5)$$

When both the radioligand A ([^{3}H]CGS 21680 or [^{3}H]ZM 241385) and the competitor B are the same compound and the binding is non-co-operative, eqn (5) simplifies to (eqn 6):

$$A_{\text{total bound}} = (4K_{DA1} \times A + 2A^2 + A \times B) \times R_T/\left(4K_{DA1}^2 + 4K_{DA1} \times A + A^2 + A \times B + 4K_{DA1} \times B + B^2\right) + A_{\text{non-specific bound}} \quad (6)$$

Goodness of fit was tested according to a reduced χ^2 value given by the non-linear regression program. The test of significance for two different population variances was based upon the F-distribution (see [32] for details). Using this F test, a probability greater than 95 % ($P < 0.05$) was considered the criterion to select a more complex equation to fit binding data over the simplest one. In all cases, a probability of less than 70 % ($P > 0.30$) resulted when one equation to fit binding data was not significantly better than the other. Results are given as parameter values ± S.E.M. of three to four independent experiments.

ERK (extracellular-signal-regulated kinase) phosphorylation assay

A_{2A}R-expressing CHO cells were cultured in serum-free medium for 16 h before the addition of any agent. Cells were treated (for 1 h at 37 °C) with medium or the indicated concentration of ADA before the addition of the A_{2A}R agonist CGS 21680 for a further incubation of 5 min. Cell were washed with ice-cold PBS and lysed by the addition of 500 μl of ice-cold lysis buffer [50 mM Tris/HCl (pH 7.4), 50 mM NaF, 150 mM NaCl, 45 mM 2-glycerophosphate, 1 % Triton X-100, 20 μM phenyl-arsine oxide, 0.4 mM sodium orthovanadate and protease inhibitor cocktail]. Cell debris was removed by centrifugation at 13 000 ***g*** for 5 min at 4 °C and the protein was quantified using the BCA method using BSA dilutions as standards. To determine the level of ERK1/2 phosphorylation, equivalent amounts of protein (15 μg) were separated by electrophoresis on denaturing SDS/PAGE (10 % gels) and transferred on to PVDF-FL membranes. Odyssey blocking buffer (LI-COR Biosciences) was then added, and membranes were rocked for 90 min. Membranes were then probed with a mixture of a mouse anti-(phospho-ERK 1/2) antibody (1:2500 dilution; Sigma) and rabbit anti-ERK 1/2 antibody (1:40 000 dilution; Sigma) for 2–3 h. Bands were visualized by the addition of a mixture of IRDye 800 (anti-mouse) antibody (1:10 000 dilution; Sigma) and IRDye 680 (anti-rabbit) antibody (1:10 000 dilution; Sigma) for 1 h and scanned by the Odyssey IR scanner (LI-COR Biosciences). Bands densities were quantified using the scanner software and exported to Excel (Microsoft). The level of phosphorylated ERK1/2 isoforms was normalized for differences in loading using the total ERK protein band intensities.

RESULTS

ADA was anchored to the cell surface of A_{2A}R-expressing cells

To investigate a potential direct interaction of ADA and A_{2A}Rs, wild-type CHO cells and a CHO–A_{2A}R clone were selected, since CHO cells do not constitutively express adenosine receptors and since rodent CD26 endogenously expressed in CHO cells does not interact with ADA [36]. Parental CHO cells did not express A_{2A}Rs since they could not be labelled using a specific anti-A_{2A}R antibody (Figure 1b). The CHO–A_{2A}R clone showed a marked staining for A_{2A}R (Figure 1a). ADA, which was detected in the cytoplasm using permeabilized CHO cells (results not shown), did not appear at the cell surface of parental CHO cells (Figure 1d). However, cell-surface ADA was detected in CHO–A_{2A}R cells (Figure 1c), indicating that the ADA released to the cell culture may bind to the cell surface only in cells expressing A_{2A}Rs. These results indicate that the cell-surface A_{2A}R behaved as an ADA-anchoring protein.

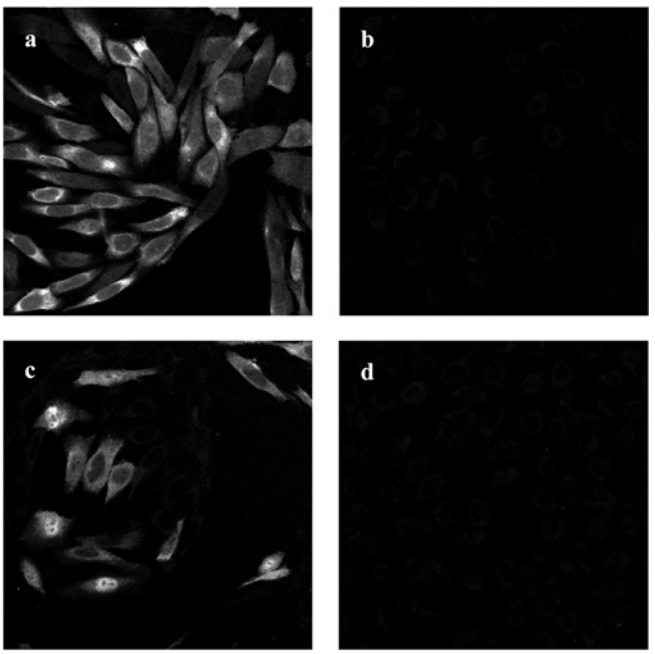

Figure 1 Expression of ADA on the cell surface of wild-type and A_{2A}R-expressing CHO cells

Non-permeabilized wild-type CHO cells (**b** and **d**) or CHO–A_{2A}R cell clone (**a** and **c**) were labelled with FITC-conjugated anti-A_{2A}R antibody (**a** and **b**) or with FITC-conjugated anti-ADA antibody (**c** and **d**). Cells were processed for confocal microscopy analysis as described in the Experimental section.

ADA binding affected the quaternary structure of A_{2A}Rs

To investigate the consequences of the ADA–A_{2A}R interaction, and taking into consideration that A_{2A}Rs are expressed as dimers or higher-order oligomers [6], the effect of ADA on the quaternary structure of A_{2A}R–A_{2A}R homomers was analysed by BRET experiments. Cells were co-transfected with 0.15 μg of the cDNA encoding A_{2A}R–Rluc and increasing amounts of the cDNA corresponding to A_{2A}R–YFP. At 48 h post-transfection, cells were treated (20 min at 37 °C) with medium or with 1 μg/ml ADA in medium, and BRET was measured. In the absence of ADA, the hyperbola obtained upon increasing the acceptor expression indicated a specific interaction between the two fusion proteins (Figure 2). The $BRET_{max}$ was 43 ± 3 mBU and the $BRET_{50}$ was 9 ± 2. The specificity of the A_{2A}R homomerization was confirmed by the unspecific (linear) BRET signal obtained in cells co-transfected with the cDNA corresponding to A_{2A}R–Rluc and increasing amounts of the cDNA corresponding to $GABA_{B2}$–YFP receptor (Figure 2). Interestingly, in the presence of ADA, a significant ($P < 0.01$) increase in the $BRET_{max}$ was observed

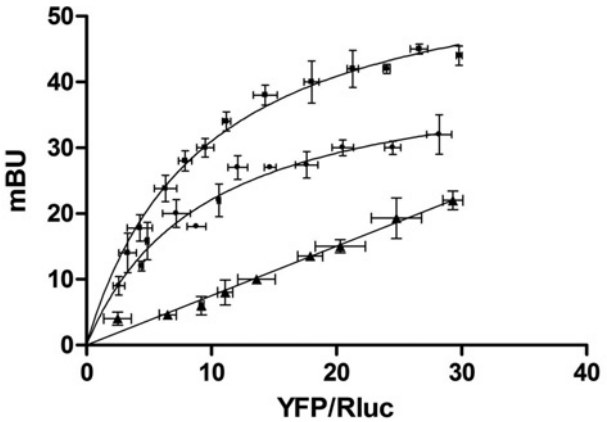

Figure 2 Effect of ADA on A_{2A}R homomerization detected by BRET experiments

BRET saturation experiments were performed as described in the Experimental section using cells transfected with 0.15 μg of cDNA corresponding to A_{2A}R–Rluc and increasing amounts of cDNA corresponding to A_{2A}R–YFP (0.8–3 μg of cDNA) (■ and ●) or to $GABA_{B2}$–YFP receptor (0.3–3 μg of cDNA) as a negative control (▲). After 48 h of transfection, cells were treated for 20 min with medium (● and ▲) or with 1 μg/ml ADA (■) before BRET determination. Both fluorescence and luminescence for each sample were measured before every experiment to confirm similar donor expressions (approximately 120 000 bioluminescence units) while monitoring the increase in acceptor expression (10 000–50 000 fluorescence units). The relative amount of BRET is given as the ratio between the fluorescence of the acceptor (YFP) and the luciferase activity of the donor (Rluc). BRET data are expressed as means ± S.E.M. of three to four different experiments grouped as a function of the amount of BRET acceptor.

(60 ± 2 mBU) without significant alterations in $BRET_{50}$ (9 ± 1). These results can be interpreted in two ways. In one, ADA led to conformational changes in A_{2A}R homomers that reduces the distance between Rluc and YFP fused to the C-terminal domain of the two A_{2A}R-containing fusion proteins. In the other, ADA increases the receptor homomerization by increasing the affinity between protomers. In this last case, a decrease in the $BRET_{50}$ values could be expected as there is binding between monomers to give homomers; $BRET_{50}$ might represent the affinity between protomers. Since the $BRET_{50}$ values were not changed in the presence of ADA we favour the first interpretation, that of ADA causing conformational changes.

ADA modulated the agonist and antagonist binding to A_{2A}Rs

The effect of ADA on ligand binding to A_{2A}Rs was first determined using A_{2A}Rs expressed in a more physiological context. For this purpose striatal membranes, which express a high amount of A_{2A}R, were selected. Isolated membranes were incubated with increasing concentrations of ADA and 17 nM of the radiolabelled A_{2A}R agonist ([^{3}H]CGS 21680, see the Experimental section). ADA enhanced in a dose-dependent manner the agonist binding to A_{2A}Rs (Figure 3a) with an EC_{50} value of 0.26 ± 0.03 ng/ml, which approximately corresponds to 6 pM. To test whether the effect of ADA was independent of its enzymatic activity, a preparation containing an irreversible-inhibited enzyme was used. ADA was inactivated using a preparation containing 100 μM Hg^{2+}; non-bound Hg^{2+} was removed by gel filtration prior to the assays (see the Experimental section). Membrane suspensions were incubated with 17 nM [^{3}H]CGS 21680 in the absence or in the presence of 1 μg/ml of active or Hg^{2+}-inactivated ADA. Both, active or Hg^{2+}-inactivated ADA enhanced to a similar extent agonist binding to striatal A_{2A}Rs (Figure 3a, inset), thus demonstrating that the effect was independent of the enzyme activity and suggesting that, in our exhaustively washed membrane preparation, there is not enough endogenous adenosine to interfere with the ligand binding

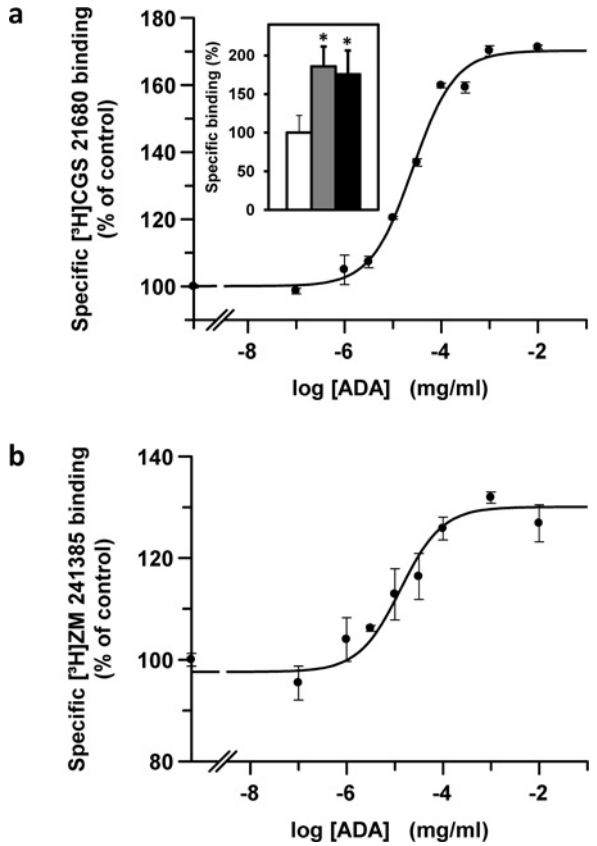

Figure 3. Effect of ADA on A_{2A}R agonist and antagonist binding to brain striatal membranes

Binding of 17 nM [^{3}H]CGS 21680 (**a**) or 1.6 nM [^{3}H]ZM 241385 (**b**) to striatal membranes (0.3 mg of protein/ml) was performed as described in the Experimental section, in the presence of increasing concentrations of ADA. Data points on the *y* axis correspond to the binding in the absence of ADA. Inset in (**a**): 17 nM [^{3}H]CGS 21680 binding in the absence (white bar) or in the presence of 1 μg/ml of active (grey bar) or Hg^{2+}-inactivated (black bar) ADA was performed as described above. Data are means ± S.E.M. ($n = 3$). Significant differences with respect to the samples in the absence of ADA were calculated by an unpaired Student's *t* test (*$P < 0.05$).

to receptors. ADA also enhanced the A_{2A}R antagonist [^{3}H]ZM 241385 binding to striatal membranes in a dose-dependent manner (Figure 3b) with an EC_{50} value of 0.13 ± 0.06 ng/ml, which is approximately equivalent to 3 pM ADA. Purified BSA (1–10 nM) did not modify agonist or antagonist binding to striatal A_{2A}Rs, showing that the ADA effect was specific (results not shown). All of these results suggest that ADA is an allosteric modulator of A_{2A}Rs.

To further investigate the modulating effect of ADA on agonist and antagonist binding, the pharmacological parameters for ligand binding to A_{2A}Rs were calculated by means of saturation and competition experiments. To investigate the modulating effect of ADA on the A_{2A}R antagonist equilibrium dissociation constants, brain striatal membranes were incubated with increasing concentrations of [^{3}H]ZM 241385 in the absence or in the presence of 1 μg/ml ADA, and saturation experiments were performed as indicated in the Experimental section. Since A_{2A}Rs are expressed as dimers or higher-order oligomers [6], radioligand saturation curves were analysed by fitting the specific binding data to the mechanistic two-state dimer receptor model [32,33], which considers a homodimer as the minimal structural unit of the receptor. In the absence or in the presence of ADA, the saturation curves (Figure 4a) were monophasic ($D_C = 0$)

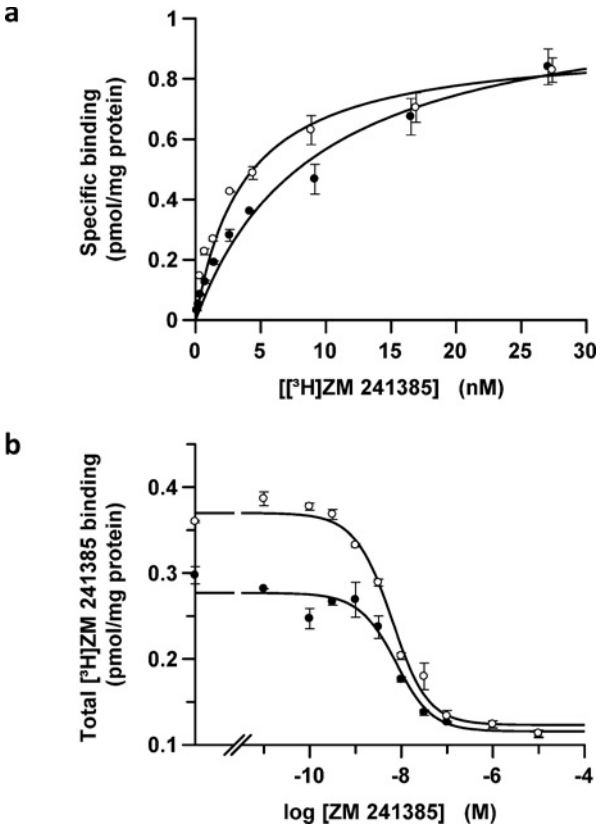

Figure 4 Effect of ADA on $A_{2A}R$ antagonist affinity constants

(**a**) Saturation binding experiments of increasing concentrations of the radiolabelled antagonist [^{3}H]ZM 241385 (0.1–27 nM) or (**b**) competition experiments of the antagonist [^{3}H]ZM 241385 (1.6 nM) binding against increasing concentrations of ZM 241385, in the absence (●) or in the presence (○) of 1 μg/ml ADA. Data are means ± S.E.M. from a representative experiment ($n = 3$) performed in triplicate.

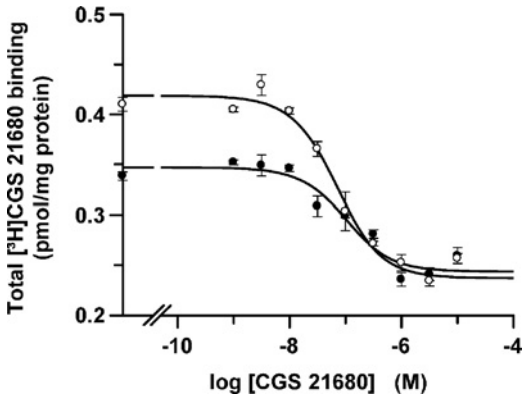

Figure 5 Effect of ADA on $A_{2A}R$ agonist affinity constants

Competition experiments of the agonist [^{3}H]CGS 21680 (17 nM) binding against increasing concentrations of CGS 21680, in the absence (●) or in the presence (○) of 1 μg/ml ADA. Data are means ± S.E.M. from a representative experiment ($n = 3$) performed in triplicate.

according to the non-co-operative behaviour of ZM 241385 binding to A_{2A}Rs [35]. The resulting equilibrium constants from fitting data to eqn (2) were 4.6 ± 0.8 nM and 1.9 ± 0.4 nM in the absence or in the presence of ADA respectively (mean ± S.E.M. of three different assays). This effect of ADA on antagonist affinity was also analysed by competition-binding experiments with 1.6 nM [^{3}H]ZM 241385 and increasing concentrations of ZM 241385 in the absence or in the presence of 1 μg/ml ADA. In the absence or in the presence of ADA, the competition curves (Figure 4b) were also monophasic ($D_C = 0$). The resulting equilibrium constants from fitting data to eqn (6) were 5.1 ± 0.7 nM and 3.3 ± 0.8 nM in the absence or in the presence of ADA respectively (mean ± S.E.M. of three different assays), not significantly different from saturation parameters. Thus ADA significantly ($P < 0.05$) increased the affinity of A_{2A}Rs for the antagonist.

To determine the modulating effect of ADA on the $A_{2A}R$ agonist CGS 21680 equilibrium dissociation constants, we only carried out competition-binding experiments since saturation experiments with a low-affinity ligand are not reliable. Radioligand binding was therefore determined in brain striatal membranes incubated with a constant amount of [^{3}H]CGS 21680 (17 nM) and increasing concentrations of CGS 21680, in the absence or presence of 1 μg/ml ADA. As shown in Figure 5, competition curves of [^{3}H]CGS 21680 against CGS 21680 were monophasic ($D_C = 0$) according to the non-co-operative behaviour expected for CGS 21680 binding [37]. The resulting equilibrium constant from fitting data to eqn (6) were 90 ± 20 nM and 41 ± 4 nM in the absence or in the presence of ADA respectively (mean ± S.E.M. of three different assays). Thus ADA also significantly ($P < 0.05$) increased the affinity of A_{2A}Rs for the agonist.

Signalling consequences of the ADA–$A_{2A}R$ interaction

To investigate the functional consequences of the interaction of ADA with A_{2A}Rs, the $A_{2A}R$-mediated signal transduction was determined in cells expressing the receptors. Accordingly, CHO–$A_{2A}R$ cells were treated for 5 min at 37 °C with increasing amounts of the $A_{2A}R$ agonist CGS 21680 in the absence or presence of 1 μg/ml ADA, and ERK1/2 phosphorylation was determined as indicated in the Experimental section. In the absence of ADA, CGS 21680 up to 200 nM dose-dependently increased ERK1/2 phosphorylation followed by a decrease of signalling at high CGS 21680 concentrations (Figure 6). The phenomenon in which previous or continued exposure of receptor to agonist results in a diminished functional response of the receptor upon subsequent or sustained agonist treatment has been defined as desensitization [38]. It has been described that $A_{2A}R$-mediated adenylate cyclase stimulation desensitizes rapidly in cultured cells (see [38] for a review). The results of the present study suggest that in $A_{2A}R$-expressing CHO cells there is also a CGS 21680-promoted desensitization of ERK1/2 phosphorylation. In the presence of ADA, a significant increase in the CGS 21680-induced ERK1/2 phosphorylation was observed, resulting in a bell-shaped concentration–response curve (Figure 6). According to an ADA-induced increase in ligand affinity for A_{2A}Rs, ADA also increased the $A_{2A}R$ signalling, determined as ERK1/2 phosphorylation. These results show that ADA not only increased ligand affinity for A_{2A}Rs, but also was able to modulate, in a positive manner, signal transduction. ADA may then be considered an enhancer of ligand binding and of $A_{2A}R$-mediated signalling events.

DISCUSSION

Cell-surface ADA needs to be anchored to the plasma membrane by means of specific receptors. In the present paper we describe that ADA may bind to A_{2A}Rs on the surface of living cells. By FRET or BRET it has previously been demonstrated that A_{2A}Rs form homomers and that homomers, but not monomers, appear to be the functional species at the cell surface of transfected cells [6]. Thus the quaternary structure of A_{2A}Rs is constituted by,

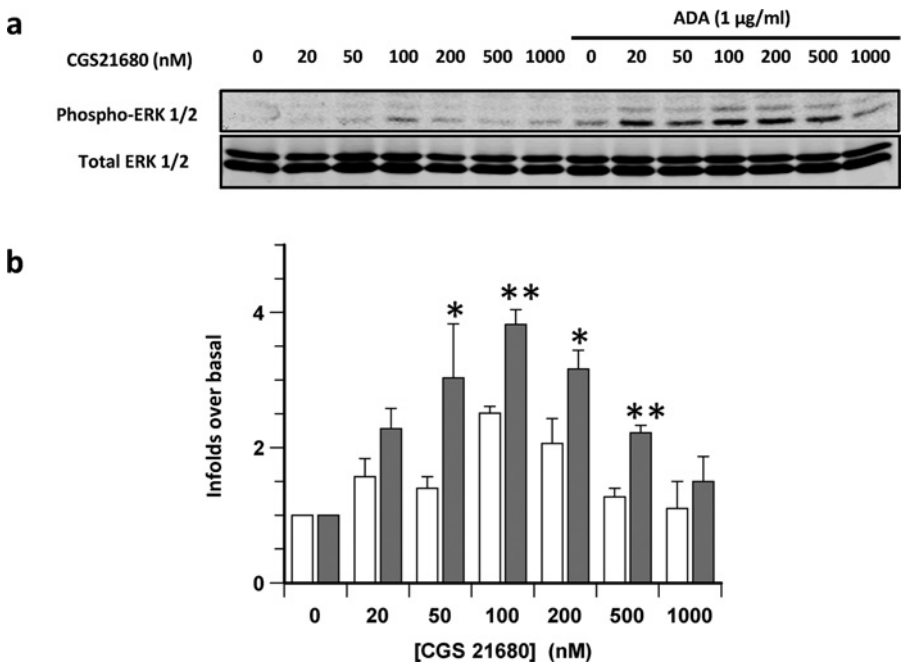

Figure 6 Effect of ADA on A_{2A}R-mediated ERK1/2 phosphorylation

A_{2A}R-expressing CHO cells were stimulated with increasing concentrations of the A_{2A}R agonist CGS 21680 in the presence or in the absence of 1 μg/ml ADA. In (**a**) a representative Western blot is shown. In (**b**) values are means ± S.E.M. of three independent experiments. Grey columns are in the presence of 1 μg/ml ADA, white columns are in the absence of 1 μg/ml ADA. Significant differences with respect to the samples in the absence of ADA were calculated by an unpaired Student's *t* test ($^*P < 0.05$ and $^{**}P < 0.01$).

at least, two protomers that form a dimer. Probably resulting from a decrease in the distance between the C-termini of the A_{2A}R protomers fused to Rluc and YFP, ADA binding led to modifications in the quaternary structure of A_{2A}R homomers that could be detected by BRET experiments. Using a similar set up Canals et al. [6] showed that A_{2A}R agonists are not able to modify the BRET signal. Therefore the ability of BRET to detect ADA-triggered conformational changes within the A_{2A}R homomers suggests that ADA exerts a control of the function of A_{2A}R homomers by a strong modification of their quaternary structure. In fact, the ADA-induced structural changes in the A_{2A}R molecule correlated with marked affinity modifications in the binding of both agonist and antagonist. Irrespective of its enzymatic activity, ADA was able to significantly decrease agonist and antagonist equilibrium dissociation constants. The ADA-induced increase in the ligand affinities indicates that ADA behaved as a positive modulator of A_{2A}Rs.

In addition to orthosteric sites, many GPCRs have been found to possess structurally distinct allosteric domains. One characteristic feature of the allosteric interaction is that the receptor is able to simultaneously bind an orthosteric and an allosteric ligand, introducing complexity into pharmacological responses by modifying the affinity or the signal imparted by the orthosteric ligand [39]. An allosteric effect results in a positive modulation if the modulator facilitates the interaction, or in a negative modulation if it inhibits the interaction of the ligand with the orthosteric-binding site [39,40]. According to these concepts, ADA is an allosteric ligand of A_{2A}Rs that positively modulates the agonist and antagonist binding to the orthosteric site of the receptor. Kreth et al. [41] have shown that an endogenous allosteric modulator leads to a reduced ligand affinity and to an impaired function of the A_{2A}R of human granulocytes in sepsis. Furthermore, some compounds have been synthesized and evaluated as positive enhancers of agonist and antagonist radioligands for the neuronal A_{2A}R [42,43]. A_{2A}Rs are allosterically modulated by sodium ions binding to an allosteric site linked to Glu^{13} in TM1 (TM is transmembrane domain) and His^{278} in TM7, and by the potassium-sparing diuretic amiloride [43–45]. The ability of allosteric modulators to fine-tune pharmacological responses has sparked interest in their potential applications in both clinical and basic science settings [40]. This interest is more relevant in the case of neurotransmitter receptor targets due to the fact that synaptic neurotransmission occurs in extremely complex circuits implicated in many neurological functions. Owing to the implication of A_{2A}Rs in many neurodegenerative diseases, such as Parkinson's and Huntington's disease, obsessive-compulsive disorders and drug addiction [46], different approaches have been tested to find allosteric modulators, i.e. a structure-based ligand-discovery methodology provided new routes for modulation of this neuronal key target [47–49]. Conceptually the allosteric interaction described in the present study is different from the one exerted by small molecules since it comes from the interaction across the membrane with a protein that has an extracellular topology. By means of the interaction with an extracellular domain of A_{2A}Rs, ADA exerts a fine-tune modulation of adenosine neuroregulation that may have important implications for the function of neuronal A_{2A}Rs, which are enriched in and play a key role in the brain striatum. The presence of ADA bound to the cell surface of neurons has been demonstrated [22], reinforcing the concept that this allosteric effect of ADA is likely to occur *in vivo*. With this in mind one may hypothesize that ADA SCID patients with ADA mutations affecting the binding of ADA to A_{2A}R may manifest neurological alterations that are predicted to be different from those resulting from mutations not affecting the ADA–A_{2A}R interface. Probably, mutations affecting the interaction would be less deleterious for striatal function since it would attenuate overactivation of A_{2A}R exerted by the elevated

adenosine levels. Irrespective of this, the results described in the present study show that ADA, apart from reducing the adenosine concentration, binds to $A_{2A}R$ behaving as an allosteric effector that markedly enhances agonist-induced signalling thought to be the MAPK (mitogen-activated protein kinase) pathway, increasing ERK1/2 phosphorylation. Thus the physiological role of the ADA–adenosine receptor interaction is to make those receptors more functional.

AUTHOR CONTRIBUTION

Eduard Gracia, Carme Lluís, Antoni Cortés, Vicent Casadó, Rafael Franco and Enric Canela conceived and designed the experiments; Eduard Gracia, Kamil Perez-Capote, Estefanía Moreno, Jana Barkesová, Josefa Mallol, Antoni Cortés and Vicent Casadó performed the experiments; Eduard Gracia, Kamil Pérez-Capote, Estefanía Moreno, Jana Barkešová, Josefa Mallol, Carme Lluís, Enric Canela, Antoni Cortés and Vicent Casadó discussed and analysed data; Carme Lluís, Rafael Franco, Antoni Cortés, Vicent Casadó and Enric Canela wrote the paper.

ACKNOWLEDGEMENTS

We thank Jasmina Jiménez for technical help (Molecular Neurobiology Laboratory, Barcelona University, Barcelona, Spain).

FUNDING

This work was supported by the Spanish Ministerio de Ciencia y Tecnología [grant numbers SAF2008-00146, SAF2008-03229-E, SAF2009-07276]; and the Fundació La Marató de TV3 [grant number 060110].

REFERENCES

1 Marianayagam, N. J., Sunde, M. and Matthews, J. M. (2004) The power of two: protein dimerization in biology. Trends Biochem. Sci. **29**, 618–625
2 Franco, R., Canals, M., Marcellino, D., Ferré, S., Agnati, L., Mallol, J., Casadó, V., Ciruela, F., Fuxe, K., Lluís, C. and Canela, E. I. (2003) Regulation of heptaspanning-membrane-receptor function by dimerization and clustering. Trends Biochem. Sci. **28**, 238–243
3 Ferré, S., Baler, R., Bouvier, M., Caron, M. G., Devi, L. A., Durroux, T., Fuxe, K., George, S. R., Javitch, J. A., Lohse, M. J. et al. (2009) Building a new conceptual framework for receptor heteromers. Nat. Chem. Bio. **5**, 131–134
4 Trincavelli, M. L., Daniele, S. and Martini, C. (2010) Adenosine receptors: what we know and what we are learning. Curr. Top. Med. Chem. **10**, 860–877
5 Ciruela, F., Casadó, V., Mallol, J., Canela, E. I., Lluis, C. and Franco, R. (1995) Immunological identification of A1 adenosine receptors in brain cortex. J. Neurosci. Res. **42**, 818–828
6 Canals, M., Burgueño, J., Marcellino, D., Cabello, N., Canela, E. I., Mallol, J., Agnati, L., Ferré, S., Bouvier, M., Fuxe, K. et al. (2004) Homodimerization of adenosine A2A receptors: qualitative and quantitative assessment by fluorescence and bioluminescence energy transfer. J. Neurochem. **88**, 726–734
7 Gandia, J., Galino, J., Amaral, O. B., Soriano, A., Lluís, C., Franco, R. and Ciruela, F. (2008) Detection of higher-order G protein-coupled receptor oligomers by a combined BRET-BiFC technique. FEBS Lett. **582**, 2979–2984
8 Ciruela, F., Casadó, V., Rodrigues, R. J., Luján, R., Burgueño, J., Canals, M., Borycz, J., Rebola, N., Goldberg, S. R., Mallol, J. et al. (2006) Presynaptic control of striatal glutamatergic neurotransmission by adenosine A1-A2A receptor heteromers. J. Neurosci. **26**, 2080–2087
9 Canals, M., Marcellino, D., Fanelli, F., Ciruela, F., de Benedetti, P., Goldberg, S. R., Neve, K., Fuxe, K., Agnati, L. F., Woods, A. S. et al. (2003) Adenosine A_{2A}-dopamine D_2 receptor-receptor heteromerization. Qualitative and quantitative assessment by fluorescence and bioluminescence resonance energy transfer. J. Biol. Chem. **278**, 46741–46749
10 Franco, R., Ciruela, F., Casadó, V., Cortes, A., Canela, E. I., Mallol, J., Agnati, L. F., Ferré, S., Fuxe, K. and Lluís, C. (2005) Partners for adenosine A1 receptors. J. Mol. Neurosci. **26**, 221–232
11 Carriba, P., Navarro, G., Ciruela, F., Ferré, S., Casadó, V., Agnati, L., Cortés, A., Mallol, J., Fuxe, K., Canela, E. I. et al. (2008) Detection of heteromerization of more than two proteins by sequential BRET-FRET. Nat. Methods **5**, 727–733
12 Ferré, S., Ciruela, F., Quiroz, C., Luján, R., Popoli, P., Cunha, R. A., Agnati, L. F., Fuxe, K., Woods, A. S., Lluis, C. and Franco, R. (2007) Adenosine receptor heteromers and their integrative role in striatal function. ScientificWorldJournal **7**, 74–85
13 Casadó, V., Cortés, A., Mallol, J., Pérez-Capote, K., Ferré, S., Lluís, C., Franco, R. and Canela, E. I. (2009) GPCR homomers and heteromers: a better choice as targets for drug development than GPCR monomers? Pharmacol. Ther. **124**, 248–257
14 Sarrió, S., Casadó, V., Escriche, M., Ciruela, F., Mallol, J., Canela, E. I., Lluís, C. and Franco, R. (2000) The heat shock cognate protein hsc73 assembles with A_1 adenosine receptors to form functional modules in the cell membrane. Mol. Cell. Biol. **20**, 5164–5174
15 Ciruela, F., Saura, C., Canela, E. I., Mallol, J., Lluís, C. and Franco, R. (1996) Adenosine deaminase affects ligand-induced signaling by interacting with cell surface adenosine receptors. FEBS Lett. **380**, 219–223
16 Saura, C., Ciruela, F., Casadó, V., Canela, E. I., Mallol, J., Lluís, C. and Franco, R. (1996) Adenosine deaminase interacts with A_1 adenosine receptors in pig brain cortical membranes. J. Neurochem. **66**, 1675–1682
17 Herrera, C., Casadó, V., Ciruela, F., Schofield, P., Mallol, J., Iluís, C. and Franco, R. (2001) Adenosine A_{2B} receptors behave as an alternative anchoring protein for cell surface adenosine deaminase in lymphocytes and cultured cells. Mol. Pharmacol. **59**, 127–134
18 Gracia, E., Cortés, A., Meana, J. J., García-Sevilla, J., Hershfield, M. S., Canela, E. I., Mallol, J., Lluís, C., Franco, R. and Casadó, V. (2008) Human adenosine deaminase as an allosteric modulator of human A_1 adenosine receptor: abolishment of negative cooperativity for [^{3}H](R)-PIA binding to the caudate nucleus. J. Neurochem. **107**, 161–170
19 Franco, R., Valenzuela, A., Lluís, C. and Blanco, J. (1998) Enzymatic and extraenzymatic role of ecto-adenosine deaminase in lymphocytes. Immunol. Rev. **161**, 27–42
20 Hershfield, M. S. (2003) Genotype is an important determinant of phenotype in adenosine deaminase deficiency. Curr. Opin. Immunol. **15**, 571–577
21 Hirschhorn, R. (1985) Complete and partial adenosine deaminase deficiency. Ann. NY Acad. Sci. **451**, 20–26
22 Ruiz, M. A., Escriche, M., Lluís, C., Franco, R., Martín, M., Andrés, A. and Ros, M. (2000) Adenosine A_1 receptor in cultured neurons from rat cerebral cortex: colocalization with adenosine deaminase. J. Neurochem. **75**, 656–664
23 Engel, M., Hoffmann, T., Wagner, L., Wermann, M., Heiser, U., Kiefersauer, R., Huber, R., Bode, W., Demuth, H. U. and Brandstetter, H. (2003) The crystal structure of dipeptidyl peptidase IV (CD26) reveals its functional regulation and enzymatic mechanism. Proc. Natl. Acad. Sci. U.S.A. **100**, 5063–5068
24 Pacheco, R., Martínez-Navío, J. M., Lejeune, M., Climent, N., Oliva, H., Gatell, J. M., Gallart, T., Mallol, J., Lluís, C. and Franco, R. (2005) CD26, adenosine deaminase, and adenosine receptors mediate costimulatory signals in the immunological synapse. Proc. Natl. Acad. Sci. U.S.A. **102**, 9583–9588
25 Martinez-Navio, J. M., Climent, N., Pacheco, R., Garcia, F., Plana, M., Nomdedeu, M., Oliva, H., Rovira, C., Miralles, L., Gatell, J. M. et al. (2009) Immunological dysfunction in HIV-1-infected individuals caused by impairment of adenosine deaminase-induced costimulation of T-cell activation. Immunology **128**, 393–404
26 Climent, N., Martinez-Navio, J. M., Gil, C., Garcia, F., Rovira, C., Hurtado, C., Miralles, L., Gatell, J. M., Gallart, T., Mallol, J. et al. (2009) Adenosine deaminase enhances T-cell response elicited by dendritic cells loaded with inactivated HIV. Immunol. Cell. Biol. **87**, 634–639
27 Saura, C., Mallol, J., Canela, E. I., Lluís, C. and Franco, R. (1998) Adenosine deaminase and A_1 adenosine receptors internalize together following agonist-induced receptor desensitization. J. Biol. Chem. **273**, 17610–17617
28 Cunha, R. A., Ferré, S., Vaugeois, J. M. and Chen, J. F. (2008) Potential therapeutic interest of A_{2A} receptors in psychiatric disorders. Curr. Pharm. Des. **14**, 1512–1524
29 Hillion, J., Canals, M., Torvinen, M., Casadó, V., Scott, R., Terasmaa, A., Hansson, A., Watson, S., Olah, M. E., Mallol, J. et al. (2002) Coaggregation, cointernalization, and codesensitization of adenosine A2A receptors and dopamine D2 receptors. J. Biol. Chem. **277**, 18091–18097
30 Ginés, S., Ciruela, F., Burgueño, J., Casadó, V., Canela, E. I., Mallol, J., Lluís, C. and Franco, R. (2001) Involvement of caveolin in ligand-induced recruitment and internalization of A_1 adenosine receptor and adenosine deaminase in an epithelial cell line. Mol. Pharmacol. **59**, 1314–23
31 Casadó, V., Cantí, C., Mallol, J., Canela, E. I., Lluís, C. and Franco, R. (1990) Solubilization of A1 adenosine receptor from pig brain: characterization and evidence of the role of the cell membrane on the coexistence of high- and low-affinity states. J. Neurosci. Res. **26**, 461–473
32 Franco, R., Casadó, V., Mallol, J., Ferré, S., Fuxe, K., Cortés, A., Ciruela, F., Lluís, C. and Canela, E. I. (2005) Dimer-based model for heptaspanning membrane receptors. Trends Biochem. Sci. **30**, 360–366
33 Franco, R., Casadó, V., Mallol, J., Ferrada, C., Ferré, S., Fuxe, K., Cortés, A., Ciruela, F., Lluís, C. and Canela, E. I. (2006) The two-state dimer receptor model: a general model for receptor dimers. Mol. Pharmacol. **69**, 1905–1912

34 Casadó, V., Cortés, A., Ciruela, F., Mallol, J., Ferré, S., Lluís, C., Canela, E. I. and Franco, R. (2007) Old and new ways to calculate the affinity of agonists and antagonists interacting with G-protein coupled monomeric and dimeric receptors: the receptor-dimer cooperativity index. Pharmacol. Ther. **116**, 343–354
35 Casadó, V., Ferrada, C., Bonaventura, J., Gracia, E., Mallol, J., Canela, E. I., Lluís, C., Cortés, A. and Franco, R. (2009) Useful pharmacological parameters for G-protein-coupled receptor homodimers obtained from competition experiments. Agonist-antagonist binding modulation. Biochem. Pharmacol. **78**, 1456–1463
36 Dong, R.-P., Tachibana, K., Hegen, M., Munakata, Y., Cho, D., Schlossman, S. F. and Morimoto, C. (1997) Determination of adenosine deaminase binding domain on CD26 and its immunoregulatory effect on T cell activation. J. Immunol. **159**, 6070–6076
37 Gao, Z. G., Mamedova, L. K., Chen, P. and Jacobson, K. A. (2004) 2-Substituted adenosine derivatives: affinity and efficacy at four subtypes of human adenosine receptors. Biochem. Pharmacol. **68**, 1985–1993
38 Olah, M. E. and Stiles, G. L. (2000) The role of receptor structure in determining adenosine receptor activity. Pharmacol. Ther. **85**, 55–75
39 May, L. T., Leach, K., Sexton, P. M. and Christopoulos, A. (2007) Allosteric modulation of G protein-coupled receptors. Annu. Rev. Pharmacol. Toxicol. **47**, 1–51
40 Conn, P. J., Christopoulos, A. and Lindsley, C. W. (2009) Allosteric modulators of GPCRs: a novel approach for the treatment of CNS disorders. Nat. Rev. Drug Discovery **8**, 41–54
41 Kreth, S., Kaufmann, I., Ledderose, C., Luchting, B. and Thiel, M. (2009) Reduced ligand affinity leads to an impaired function of the adenosine A2A receptor of human granulocytes in sepsis. J. Cell. Mol. Med. **13**, 985–994

Received 25 October 2010/24 January 2011; accepted 9 February 2011
Published as BJ Immediate Publication 9 February 2011, doi:10.1042/BJ20101749

42 van den Nieuwendijk, A. M., Pietra, D., Heitman, L., Göblyös, A. and Ijzerman, A. P. (2004) Synthesis and biological evaluation of 2,3,5-substituted [1,2,4]thiadiazoles as allosteric modulators of adenosine receptors. J. Med. Chem. **47**, 663–672
43 Gao, Z. G., Kim, S. K., Ijzerman, A. P. and Jacobson, K. A. (2005) Allosteric modulation of the adenosine family of receptors. Mini Rev. Med. Chem. **5**, 545–553
44 Gao, Z.-G., Jiang, Q., Jacobson, K. A. and Ijzerman, A. P. (2000) Site-directed mutagenesis studies of human A2A adenosine receptors: involvement of Glu^{13} and His^{278} in ligand binding and sodium modulation. Biochem. Pharmacol. **60**, 661–668
45 Göblyös, A. and Ijzerman, A. P. (2010) Allosteric modulation of adenosine receptors. Biochim. Biophys. Acta, doi:10.1016/j. bbamem.2010.06.013
46 Stone, T. W., Ceruti, S. and Abbracchio, M. P. (2009) Adenosine receptors and neurological disease: neuroprotection and neurodegeneration. Handb. Exp. Pharmacol. **193**, 535–587
47 Cristalli, G., Lambertucci, C., Marucci, G., Volpini, R. and Dal Ben, D. (2008) A2A adenosine receptor and its modulators: overview on a druggable GPCR and on structure-activity relationship analysis and binding requirements of agonists and antagonists. Curr. Pharm. Des. **14**, 1525–1552
48 Carlsson, J., Yoo, L., Gao, Z. G., Irwin, J. J., Shoichet, B. K. and Jacobson, K. A. (2010) Structure-based discovery of A2A adenosine receptor ligands. J. Med. Chem. **53**, 3748–3755
49 Katritch, V., Jaakola, V. P., Lane, J. R., Lin, J., Ijzerman, A. P., Yeager, M., Kufareva, I., Stevens, R. C. and Abagyan, R. (2010) Structure-based discovery of novel chemotypes for adenosine A(2A) receptor antagonists. J. Med. Chem. **53**, 1799–1809

6.4 La homodimerización de receptores de adenosina A_1 en el cortex cerebral explica el comportamiento bifásico de la cafeína

Eduard Gracia*, Estefanía Moreno*, Carme Lluís, Josefa Mallol, Peter McCormick, Enric I. Canela**, Antoni Cortés, Vicent Casadó**

*Coautores del manuscrito,
**Codirectores del manuscrito

Centro de Investigación Biomédica en Red sobre Enfermedades Neurodegenerativas (CIBERNED), y Departamento de Bioquímica y Biología Molecular, Facultad de Biología, Universidad de Barcelona, Avda Diagonal 645, 08028 Barcelona, España.

Manuscrito enviado para su publicación Biochemical Pharmacology

Mediante técnicas de transferencia de energía de resonancia bioluminiscente y de ligación por proximidad (PLA) hemos demostrado, por primera vez, que los receptores A_1 de adenosina forman homómeros tanto en cultivos celulares como en córtex cerebral. Mediante experimentos de unión de radioligandos, en ausencia o en presencia de la adenosina desaminasa, modulador alostérico del receptor A_1, y mediante el uso del modelo de receptores diméricos para ajustar los datos de los experimentos de unión de radioligandos, hemos demostrado que las interacciones protómero-protómero existentes en los homómeros del receptor A_1 de adenosina justifican algunas de las características farmacológicas de la unión de agonistas y de antagonistas a dichos receptores. Estas propiedades farmacológicas incluyen: la existencia de un comportamiento cooperativo en la unión del agonista R-PIA, la obtención de curvas de saturación monofásicas cuando se utiliza una única concentración baja o elevada del radioligando, y la detección de una interacción molecular en ensayos de competición cuando dos moléculas específicas distintas se unen al receptor. En este último caso, se ha puesto de manifiesto que la unión del antagonista cafeína a un protómero incrementa la afinidad del agonista R-PIA por el segundo protómero del homómero, lo que podría explicar los efectos bifásicos observados sobre la actividad locomotora, al utilizar concentraciones bajas o elevadas de cafeína.

Homodimerization of adenosine A_1 receptors in brain cortex explains the biphasic effects of caffeine

Eduard Gracia[&], Estefania Moreno[&], Carme Lluís, Josefa Mallol, Antoni Cortés, Peter J. McCormick, Enric I.Canela[&], Vicent Casadó[&]*

Centro de Investigación Biomédica en Red sobre Enfermedades Neurodegenerativas (CIBERNED), and Department of Biochemistry and Molecular Biology, Faculty of Biology, University of Barcelona, Av. Diagonal 643, 08028 Barcelona, Spain

[&]Both authors contributed equally to this work

*** Corresponding author:** Vicent Casadó. Department of Biochemistry and Molecular Biology, Faculty of Biology, University of Barcelona, Av. Diagonal 643, 08028 Barcelona, Spain. Tel.: (34) 934039279; fax: (34) 934021559; vcasado@ub.edu

E-mail addresses: edugss@gmail.com (E. Gracia), fifa877@hotmail.com (E. Moreno), clluis@ub.edu (C. Lluís), jmallol@ub.edu (J. Mallol), antonicortes@ub.edu (A. Cortés), peter.mccormick@ub.edu (P.J. McCormick), ecanela@ub.edu (E.I. Canela), vcasado@ub.edu (V. Casadó).

Type of paper: Full-length Research Paper

Category: Neuropharmacology

ABSTRACT
Using bioluminescence resonance energy tranfer and proximity ligation assays, we obtained the first direct evidence that adenosine A_1 receptors (A_1Rs) form homomers not only in cell cultures but also in brain cortex. By radioligand binding experiments in the absence or in the presence of the A_1Rs allosteric modulator, adenosine deaminase, and by using the two-state dimer receptor model to fit our binding data, we demonstrated that the protomer-protomer interactions in the A_1R homomers account for some of the pharmacological characteristics of agonist and antagonist binding to A_1Rs. These pharmacological properties include the appearance of cooperativity in agonist binding, the change from a biphasic saturation curve to a monophasic curve in self-competition experiments when a constant low and high concentration of the radioligand were used and the molecular cross-talk detected when two different specific molecules bind to the receptor. In this last case, we discovered that caffeine binding to one protomer increases the agonist affinity for the other protomer in the A_1R homomer, a pharmacological property that can explain the biphasic effects obtained at low and high concentration of caffeine on locomotor activity.

Keywords
G protein-coupled receptor, binding parameter, cooperativity, allosteric interaction, two-state dimer receptor model.

Abbreviations
GPCRs, G protein-coupled receptors; A_1R, adenosine A_1 receptor; A_{2A}R adenosine A_{2A} receptor; A_{2B}R, adenosine A_{2B} receptor; A_3R, adenosine A_3 receptor; BRET, Bioluminiscence Resonance Energy Transfer; PLA, Proximity Ligation Assay; DPCPX, dipropyl-8-cyclopentyl-1-,3-dipropylxanthine; R-PIA, R-phenyl-isopropyl-adenosine; ADA, adenosine deaminase

1. Introduction

More than 90% of known guanine nucleotide-binding protein coupled receptors (GPCRs) are expressed in the brain [1] and are involved in virtually all functions controlled by the nervous system. Until recently, GPCRs were believed to exist and to function as monomeric entities; however, a specialized type of protein-protein interaction, now known to occur for many GPCRs, is receptor oligomerization [2]. Oligomerization appears essential for receptor folding and for further processing as well as for transport to the plasma membrane [3,4]. Although highly controversial up to a few years ago, the idea that most GPCRs may form dimers or potentially higher order oligomers is now largely accepted [5-12]. Oligomeric structures are essential for the function and regulation of the receptors, once they are brought to the cell surface [3,4,11]. One example are the adenosine receptors. It has been suggested by western blot experiments that A_1 adenosine receptors (A_1Rs) can form homomers [13] and it was demonstrated that they can form functional heteromers with other GPCRs [14-16].

A_1Rs are one of the four subtypes of adenosine receptors (A_1R, A_{2A}R, A_{2B}R and A_3R) that couples with Gi protein, decreases cAMP by inhibiting adenylate cyclase, and modulates the activity of several K^+ and Ca^{2+}-channels [17]. A_1Rs are distributed in brain areas which are important for integrating brain functions such as the hippocampus, cerebral cortex, some thalamic nuclei, basal ganglia, cerebellar cortex and dorsal horn of spinal cord in human and experimental animals [18-20]. They play a role in important functions, such as in the modulation of neurotransmitter release, sleep regulation, and cognition enhancement [21,22] and selective A_1R agonists and antagonists have many potential therapeutic applications [23-25]. Caffeine, the most consumed psychoactive drug in the world, is a non-selective adenosine receptor antagonist with reported similar in vitro affinities for A_1R and A_{2A}R, the preferential targets for caffeine in the brain [26]. Both receptors are involved in the motor-activating, reinforcing and arousal effects of this drug [27]. Apart from the classical agonist and antagonist that bind to the receptor's orthosteric site, other ligands modulate receptor function by binding to an allosteric site, which is distinct from the primary ligand binding site [28]. Small molecules and ions have been described as allosteric modulators of A_1Rs [29-31] as well as proteins such as adenosine deaminase (ADA), which binds to A_1R behaving as an allosteric effector that markedly enhances agonist affinity and increases receptor functionality [32].

The understanding of the correlation between the pharmacological properties of agonist, antagonist and allosteric modulators and the structural properties of receptor homomers has been hampered by the lack of appropiate models to fit binding data that take into account the homomeric nature of the receptors. Recently, models that consider dimers as the minimal structure of a receptor have been developed [33-35] and from the two-state dimer receptor model [34,36] easily handy equations have been deduced [35,37]. In this paper we obtain direct evidence that A_1Rs can form homomers not only in cell cultures but also in brain cortex and using the two-state dimer receptor model, we correlated the protomer-protomer interactions in the A_1R homomers with the appearance of cooperativity in the agonist binding and with the molecular cross-talk detected when two different specific molecules bind to the receptor. In this last case we discovered that caffeine binding to one protomer increases the agonist affinity for the other protomer in the A_1R homomer, a pharmacological property that can explain the biphasic effects obtained at low and high concentration of caffeine on locomotor activity.

2. Material and methods

2.1. Fusion proteins and expression vector

The cDNA for the hA_1R cloned in pcDNA3.1 was amplified without its stop codon using sense and antisense primers harboring either unique *EcoRI* and *KpnI* sites. The fragment was then subcloned to be in-frame with Rluc into the *EcoRI* and *KpnI* restriction site of an Rluc-expressing vector (pRluc-N1; PerkinElmer, Wellesley, MA) or into the *EcoRI* and *KpnI* restriction site of the variant of GFP vector (EYFP-N3; enhanced yellow variant of GFP; Clontech, Heidelberg, Germany) to give the plasmids that express A_1R fused to Rluc or YFP on the C-terminal end of the receptor (A_1R-Rluc, A_1R-YFP). The cDNA of the human serotonin $5HT_{2B}$-YFP fusion protein was kindly provided by Dr. Irma Nardi (University of Pisa, Italy).

2.2. Cell culture, transient transfection and receptor expression

Human embryonic kidney (HEK-293T) cells were grown in Dulbecco's modified Eagle's medium (DMEM; Gibco Paisley, Scotland, UK) supplemented with 2 mM L-glutamine, 100 µg/ml sodium pyruvate, 100 U/ml penicillin/streptomycin, and 5% (v/v) heat inactivated Fetal Bovine Serum (FBS) (all supplements were from Invitrogen, Paisley, Scotland, UK).

HEK-293T growing in 6-well plates were transiently transfected with the corresponding fusion protein cDNA by the PEI (PolyEthylenImine, Sigma, St. Louis, MO, USA) method. Cells were incubated (4 h) with the corresponding cDNA together with ramified PEI (5 ml of 10 mM PEI for each mg cDNA) and 150 mM NaCl in a serum-starved medium. After 4 hours, the medium was changed to a fresh complete culture medium. Forty-eight hours after transfection, cells were washed twice in quick succession in Hanks' balanced salt solution HBSS (137 mM NaCl, 5 mM KCl, 0.34 mM $Na_2HPO_4x12H_2O$, 0.44 mM KH_2PO_4, 1.26 mM $CaCl_2x2H_2O$, 0.4 mM $MgSO_4x7H_2O$, 0.5 mM $MgCl_2$, 10 mM HEPES, pH 7.4) supplemented with 0.1% glucose (w/v), detached, and resuspended in the same buffer. To control the cell number, sample protein concentration was determined using the Bradford assay kit (Bio-Rad, Munich, Germany) using bovine serum albumin dilutions as standards.

The membrane expression of the fusion proteins was detected by immunocytochemistry in HEK-293T cells transfected with 1 µg of cDNA corresponding to A_1R-RLuc or A_1R-YFP. After 48h of transfection cells were fixed in 4% paraformaldehyde and permeabilized with PBS-glycine containing 0.05% Triton X-100 before labeling with the primary mouse monoclonal anti-Rluc antibody (1/100, Chemicon, Billerica, MA) and the secondary antibody Cy3 Donkey anti-mouse (1/200, Jackson Immunoresearch Laboratories, West Grove, PA, USA). The A_1R-YFP construct was detected by monitoring fluorescence emission at 530 nm. Samples were observed using a Leica SP2 confocal microscope (Leica Microsystems, Mannheim, Germany).

The functionality of fusion proteins was checked in HEK-293T cells transfected with 1 µg of cDNA corresponding to A_1R-RLuc, A_1R-YFP or A_1R. After 48h of transfection cells were cultured in serum-free medium for 16 h before the addition of the indicated concentration of agonist for the indicated time and were lysed in ice-cold lysis buffer (50 mM Tris-HCl pH 7.4, 50 mM NaF, 150 mM NaCl, 45 mM β-glycerophosphate, 1% Triton X-100, 20 µM phenyl-arsine oxide, 0.4 mM $NaVO_4$ and protease inhibitor cocktail). The ERK 1/2 phosphorylation was determined as indicated elsewhere [38].

2.3. Bioluminiscence Resonance Energy Transfer (BRET) experiments

HEK-293T cells were co-transfected with 0.5 µg of cDNA corresponding to A_1R-Rluc, acting as a BRET donor and increasing amounts of cDNA corresponding to A_1R-YFP (1 to 4.8 µg cDNA) or to $5HT_{2B}R$-YFP as negative control (0.5 to 5 µg cDNA), acting as a BRET acceptor and used after 48 h of transfection. With aliquots of transfected cells (20 µg of protein), three different determinations were performed in parallel: i) To quantify fluorescence proteins expression, cells were distributed in 96-well microplates (black plates with a transparent bottom, Porvair, King´s Lynn, UK),) and fluorescence was read in a Fluostar Optima Fluorimeter (BMG Labtechnologies, Offenburg, Germany) equipped with a high-energy xenon flash lamp, using a 10 nm bandwidth excitation filter at 400 nm reading.. Receptor-fluorescence expression was determined as fluorescence of the sample minus the fluorescence of cells expressing receptor-Rluc alone. ii) For BRET measurements, the equivalent of 20 µg of cell suspension were distributed in 96-well microplates (Corning 3600, white plates with white bottom, Sigma) and 5 µM coelenterazine H (Molecular Probes, Eugene, OR) was added. After 1 minute of adding coelenterazine H, the readings were collected using a Mithras LB 940 that allows the integration of the signals detected in the short-wavelength filter at 485 nm and the long-wavelength filter at 530 nm. iii) To quantify receptor-Rluc expression luminescence readings were performed after 10 minutes of adding 5 µM coelenterazine H. The net BRET is defined as [(long-wavelength emission)/(short-wavelength emission)]-Cf where Cf corresponds to [(long-wavelength emission)/(short-wavelength emission)] for the Rluc construct expressed alone in the same experiment. Curves were fitted to a non-linear regression equation, assuming a single phase with GraphPad Prism software (San Diego, CA, USA).

2.4. Immunohistochemistry

Bovine brain cortex and pontine sections from brains obtained at the local slaughterhouse were fixed with 4% paraformaldehyde solution for 48 h at 4ºC. Sections were then washed in PBS, cryo-

preserved in a 30% sucrose solution for 48 h at 4ºC and stored at -20ºC until sectioning. 15 µm thick slices were cut on a freezing cryostat (Leica Jung CM-3000) and mounted on slide glass. Slices were thawed at 4ºC, washed in Tris-HCl 50 mM, NaCl 0.9% pH 7.8 buffer (TBS), treated 5 min with 1% Na_2BH_4 dissolved in TBS, followed by successive TBS washes until all Na_2BH_4 was eliminated and rocked in Blocking reagent 1% (Roche, Sant Cugat del Vallés, Spain) for 1 h at 37ºC in a humidified atmosphere. The slices were then incubated overnight at 4ºC in a humidified atmosphere with the primary antibody anti A_1R peptide antibody (1:100, AB1587P, Millipore, Billerica, MA, USA, previously characterized in our laboratory [13]) in a solution with 0.1 % TBS-Tween, 0.1% BSA-Acetylated (Aurion, Wageningen, The Netherlands), 7% SND. Then, the slices were washed in TBS-Tween 0.05% and left for 2 h at room temperature in a humidified atmosphere with goat anti-rabbit-POD (1:200, Thermo Scientific, Fremont, CA, USA) as secondary antibody in 0.1% TBS-Tween, 0.1% BSA, 7% SND. The amplification system TSA-Cyanine 3 (1:100, Tyramide Signal Amplification, Perkin Elmer, Wellesley, MA, USA) was used as described in the TSA Plus Fluorescence amplification Kit. Then, the slices were washed in TBS-Tween 0.05%, followed by a single wash in TBS before mounting in Mowiol medium (Calbiochem, Merck, Darmstadt, Germany), covered with a glass and left to dry at 4ºC for 24 h. The sections were observed and imaged in a Leica SP2 confocal microscope.

2.5. Homomer detection by in situ Proximity Ligation Assay (PLA) in brain slices

Cortical and pontine slices, obtained as described above, were mounted on slide glass. A_1R homomers were detected using the Duolink II in situ PLA detection Kit (OLink; Bioscience, Uppsala, Sweden). After 1 h incubation at 37°C with the blocking solution in a pre-heated humidity chamber, slices were incubated overnight in the antibody dilution medium with a mixture of equal amounts of anti A_1R peptide antibody (1:100 AB1587P, Millipore) directly coupled to a DNA chain minus and the same antibody directly coupled to a DNA chain plus, obtained following the instructions of the supplier. The slices were washed with wash buffer A at room temperature and were incubated in a pre-heated humidity chamber for 30 min at 37°C, with the ligation solution (Duolink II Ligation stock 1:5 and Duolink II Ligase 1:40). Amplification was done with the Duolink II Detection Reagents Red Kit. After exhaustively washing at room temperature with wash buffer B, the slices were mounted using the mounting medium with DAPI. The samples were observed in a Leica SP2 confocal microscope. Images were opened and processed with Image J confocal. For quantification red punctuated staining-presenting cells were counted from 400-500 cells detected by the stained nucleus from four different slices.

2.6. Brain cortical membranes preparation and protein determination

Membrane suspensions from bovine brain cortex were processed as described previously [39,40]. Tissue was disrupted with a Polytron homogenizer (PTA 20 TS rotor, setting 3; Kinematica, Basel, Switzerland) for three 5 s-periods in 10 volumes of 50 mM Tris–HCl buffer, pH 7.4 containing a proteinase inhibitor cocktail (Sigma). Cell debris was eliminated by centrifugation at 10,000 g (10 min, 4ºC) and membranes were obtained by centrifugation at 105,000 g (40 min, 4ºC). The pellet was resuspended and recentrifuged under the same conditions and was stored at -80ºC. Membranes were washed once more as described above and resuspended in 50 mM Tris–HCl buffer, pH 7.4, for immediate use. Protein was quantified by the bicinchoninic acid method (Pierce Chemical Co., Rockford, IL, USA) using bovine serum albumin dilutions as standard.

2.7. Radioligand binding experiments

Binding experiments were performed with bovine brain cortical membrane suspensions at 25ºC in 50 mM Tris-HCl buffer, pH 7.4, containing 10 mM $MgCl_2$. For saturation experiments, membranes (0.1 mg of protein/ml) were incubated with increasing free concentrations (1 pM to 20 nM) of the A_1R agonist [^{3}H](R)-PIA (30 Ci/mmol; Moravek Biochemicals Inc., Brea, CA, USA) or with increasing free concentrations (1 pM to 10 nM) of the A_1R antagonist [^{3}H]DPCPX (93.0 Ci/mmol; GE Healthcare UK Limited, Buchinghamshire, UK) in the absence or in the presence of 0.2 I.U./ml (1 µg/ml) of active or Hg^{2+}-inactivated ADA (EC 3.5.4.4; Roche, Basel, Switzerland). Enzyme inactivation was performed by a pre-incubation (2 h) of 15 I.U./ml ADA with 100 µM $HgCl_2$ and removal of free Hg^{2+} by gel filtration as described previously [41]. For competition experiments, we incubated membrane suspensions (0.1 mg of protein/ml) with a constant free [^{3}H](R)-PIA concentration (0.3 nM or 3.8 nM) in the absence or in the

presence of free increasing concentrations of (R)-PIA (0.1 pM to 10 µM, Sigma), DPCPX (1 pM to 10 µM, Tocris, Bristol, UK) or caffeine (1 µM to 30 mM, Sigma), in the absence or in the presence of 0.2 I.U./ml of ADA. When indicated, competition experiments were also performed using a constant free [^{3}H]DPCPX concentration (0.3 nM), in the absence or in the presence of increasing free concentrations of caffeine (1 µM to 30 mM). In all cases, membranes were incubated with ligands providing enough time (8 h) to achieve stable equilibrium for the lower ligand concentrations. This is an important condition since low incubation time for the lower ligand concentrations implies to obtain an equilibrium dissociation constant value 5 fold higher than the correct value (data not shown). The amount of A_{2A}Rs expressed in bovine brain cortex was determined incubating membrane suspensions (0.1 mg of protein/ml) with a constant free [^{3}H]ZM241385 concentration (10 nM; 50.0 Ci/mmol, American Radiolabeled Chemicals Inc., St. Louis, MO, USA) at 25ºC, 2 h, in 50 mM Tris-HCl buffer, pH 7.4, containing 10 mM $MgCl_2$. Nonspecific binding was determined in the presence of 10 µM (R)-PIA, 10 µM DPCPX or 10 µM ZM241385 (Tocris) and confirmed that the value was the same as calculated by extrapolation of the competition curves. In all cases, free and membrane bound ligand were separated by rapid filtration of 500 µl aliquots in a cell harvester (Brandel, Gaithersburg, MD, USA) through Whatman GF/C filters embedded in 0.3% polyethylenimine that were subsequently washed for 5 s with 5 ml of ice-cold Tris–HCl buffer. The filters were incubated with 10 ml of Ecoscint H scintillation cocktail (National Diagnostics, Atlanta, GA, USA) overnight at room temperature and radioactivity counts were determined using a Tri-Carb 1600 scintillation counter (PerkinElmer, Boston, MO, USA) with an efficiency of 62% [40].

2.8. Binding data analysis

[^{3}H](R)-PIA or [^{3}H]DPCPX saturation curves were analyzed by non-linear regression, using the commercial Grafit software (Erithacus Software), by fitting the binding data to the two-state dimer receptor model [35,37]. To calculate the macroscopic equilibrium dissociation constants to the A_1R dimer as a whole, equation (1) deduced by Casadó et al. [36] was used.

$A_{bound} = (K_{DA2}A + 2\ A^2)\ R_T / (K_{DA1}\ K_{DA2} + K_{DA2}\ A + A^2)$ eq. 1

where A represents the radioligand concentration, R_T is the total amount of receptor dimers, and K_{DA1} and K_{DA2} are the macroscopic dissociation constants describing the binding of the first and the second ligand molecule to the dimeric receptor. The dimer cooperativity index for the radioligand A is defined by Casadó et al. [36] as:

$D_{CA} = \log (4K_{DA1} / K_{DA2})$ eq. 2

In non-cooperative conditions ($D_{CA} = 0$), $K_{DA2}/K_{DA1} = 4$ (see [35,37] for details) and, therefore, K_{DA1} is enough to characterize the binding. In this case, the equation (1) can be reduced to:

$A_{bound} = 2\ A\ R_T / (2\ K_{DA1} + A)$ eq. 3

A direct calculation of the concentration of the radioligand A providing half saturation in the binding of the radioligand, is possible [36]:

$A_{50} = (K_{DA1}K_{DA2})^{1/2}$ eq. 4

In non-cooperative conditions, A_{50} coincides with the intrinsic equilibrium dissociation constant describing the binding of A to the two orthosteric centers of the dimer.

To calculate the macroscopic equilibrium dissociation constants from competition experiments, the following general equation deduced by Casadó et al. [36] was considered:

$A_{bound} = (K_{DA2}\ A + 2A^2 + K_{DA2}\ A\ B / K_{DAB})\ R_T / (K_{DA1}\ K_{DA2} + K_{DA2}\ A + A^2 + K_{DA2}\ A\ B/ K_{DAB} + K_{DA1}\ K_{DA2}\ B / K_{DB1} + K_{DA1}\ K_{DA2}\ B^2 / (K_{DB1}\ K_{DB2}))$ eq. 5

where A represents the radioligand concentration ([^{3}H](R)-PIA or [^{3}H]DPCPX), R_T is the total amount of receptor dimers and K_{DA1} and K_{DA2} are the macroscopic dissociation constants describing the binding of the first and the second radioligand molecule (A) to the dimeric receptor; B represents the assayed competing compound concentration ((R)-PIA, DPCPX or caffeine), and K_{DB1} and K_{DB2} are, respectively, the equilibrium dissociation constants of the first and second binding of B; K_{DAB} can be described as a hybrid equilibrium radioligand/competitor dissociation constant, which is the dissociation constant of B binding to a receptor dimer semi-occupied by A. In a similar way a K_{DBA} constant can be described, that is related with the K_{DAB} by the following relationship [36]:

$K_{DBA} = K_{DAB}\ K_{DA1}/K_{DB1}$ eq. 6

To quantify cooperativity, the dimer cooperativity index for the competing ligand B is defined by Casadó et al. [36] as:

$D_{CB} = \log (4K_{DB1} / K_{DB2})$ eq. 7

A direct calculation of the concentration of competitor (B) providing half saturation, i.e. a 50% decrease in the binding of the radioligand, is possible (see [36]):

$B_{50} = (K_{DB1} K_{DB2})^{1/2}$ eq. 8

The "dimer radioligand / competitor modulation index" (D_{AB} or D_{BA}) was defined as Casadó et al. [38]:

$D_{AB} = \log (2K_{DB1} / K_{DAB})$ eq. 9

$D_{BA} = \log (2K_{DA1} / K_{DBA})$ eq. 10

This index is defined in such a way that its value is "0" when the presence of radioligand does not affect the competitor binding to the empty protomer in the dimer. Positive or negative values of D_{AB} indicate that the presence of radioligand increases or decreases, respectively, the competitor affinity for binding to the empty protomer in the dimer.

Depending on the characteristics of the ligands (the radioligand A and the competitor B) the following simplifications of the equation (5) were considered:

For A cooperative and B non-cooperative:

Equation (5) was simplified to equation (11) due to the fact that $K_{DB2} = 4K_{DB1}$:

$A_{bound} = (K_{DA2} A + 2A^2 + K_{DA2} A B / K_{DAB}) R_T / (K_{DA1} K_{DA2} + K_{DA2} A + A^2 + K_{DA2} A B/ K_{DAB} + K_{DA1} K_{DA2} B / K_{DB1} + K_{DA1} K_{DA2} B^2 / 4K_{DB1}^2)$ eq. 11

For A and B cooperative being A and B the same compound:

Equation (5) was simplified to equation (12) due to the fact that $K_{DA1} = K_{DB1}$, $K_{DA2} = K_{DB2}$ and $K_{DAB} = K_{DA2}$:

$A_{bound} = (K_{DA2} A + 2A^2 + A B) R_T / (K_{DA1} K_{DA2} + K_{DA2} A + A^2 + A B + K_{DA2} B + B^2)$ eq. 12

For A and B non-cooperative:

Equation (5) was simplified to equation (13) due to the fact that $K_{DA2} = 4K_{DA1}$ and $K_{DB2} = 4K_{DB1}$:

$A_{bound} = (4K_{DA1} A + 2A^2 + 4K_{DA1} A B / K_{DAB}) R_T / (4K_{DA1}^2 + 4K_{DA1} A + A^2 + 4K_{DA1} A B / K_{DAB} + 4K_{DA1}^2 B / K_{DB1} + K_{DA1}^2 B^2 / K_{DB1}^2)$ eq. 13

For A and B non-cooperative being the A and B the same compound:

Equation (5) was simplified to equation (14) due to the fact that $K_{DA2} = 4K_{DA1}$, $K_{DB2} = 4K_{DB1}$, $K_{DA1} = K_{DB1}$, $K_{DA2} = K_{DB2}$ and $K_{DAB} = 4K_{DA1}$ (see [42]):

$A_{bound} = (4K_{DA1} A + 2A^2 + A B) R_T / (4K_{DA1}^2 + 4K_{DA1} A + A^2 + A B + 4K_{DA1} B + B^2)$ eq. 14

2.9. Statistical analysis

Goodness of fit was tested according to reduced chi-squared value given by the non-linear regression program. The test of significance for two different model population variances was based upon the F-distribution (see [39] for details). Using this F-test, a probability greater than 95% ($p < 0.05$) was considered the criterion to select a more complex model (cooperativity) over the simplest one (non-cooperativity). In all cases, a probability of less than 70% ($p > 0.30$) resulted when one model was not significantly better than the other. Results are given as parameter values ± S.E.M. of three independent experiments, and differences respect to controls have been tested for significance ($p < 0.05$) using Student's t-test for unpaired samples.

3. Results

3.1. A_1Rs are expressed as homomers in tranfected cells and in brain cortex.

The ability of A_1Rs to form homomers was previously suggested by western-blot assays [13]. However, detergents used in cell lysis often mask the true identities of higher order complexes and only provide indirect evidence of association. In addition, there was no direct evidence for A_1R homomerization in brain tissues, and thus no indication of physiological relevance. Here, to provide insight on A_1R-A_1R homomer formation, we explored the interactions between A_1R receptors in

transfected cells using a more direct biophysical approach via Bioluminescence Resonance Energy Transfer (BRET). First, we checked that the fusion proteins were correctly expressed at the membrane level (Fig. 1a) and that are functional as determined by ERK 1/2 phosphorylation assays (Fig. 1b). BRET experiments were performed in HEK-293 cells co-transfected with 0.5 µg of cDNA corresponding to A_1R-Rluc and increasing amounts of cDNA corresponding to A_1R-YFP. After 48 h of transfection, cells express moderate amounts of both A_1R-YFP, (ranging from 0.04 to 1.25 pmol/mg protein) and A_1R-Rluc (0.05 pmol/mg of protein), as determined by radioligand binding. The BRET saturation curve was hyperbolic indicating a specific interaction between both fusion proteins (Fig. 1c). The $BRET_{max}$ was 49 ± 6 mBU and the $BRET_{50}$ was 4 ± 2. The specificity of the A_1Rs to form homomers was confirmed by the non-specific (low and linear) BRET signal obtained when cells were co-transfected with the cDNA corresponding to A_1R-Rluc and increasing amounts of the cDNA corresponding to $5HT_{2B}$R-YFP as negative control (Fig. 1c).

Biophysical techniques to detect homomers cannot be easily applied in native tissue, but other direct and indirect methods can be used. We looked for evidence of expression of A_1R homomers in bovine brain cortex by the Proximity Ligation Assay (PLA) using an anti-A_1R antibody. The specificity of the anti-A_1R antibody used was tested by immunohistochemistry comparing slices from bovine cortex and pontine area, since high expression of A_1R in cortex and very low expression in pontine area have been reported [43]. According to this, A_1Rs staining was observed in cortical slices and no significant staining was observed in pontine slices (Fig. 2a) showing that the antibody is specific. The PLA technology requires that the two interacting receptors be close enough to allow the antibody-probes to be able to ligate. If the receptors are within proximity, a punctate fluorescent signal can be detected by confocal microscopy. Punctate fluorescence was observed for the endogenously expressed A_1Rs in bovine brain cortical slices (Fig. 2b, 45% of cells presented punctate pattern of fluorescence) but not for the negative controls, in bovine pontine slices (less than 5% of cells were stained) showing the specificity of the interaction. It must be noted that the punctate pattern detected in cortical slices most likely reflects less than the total number of existing homomers expressed since no PLA detection can be seen for homomers bound to both antibodies linked to plus or both linked to minus DNA probes. Results shown in Figure 1e indicated that A_1Rs are indeed expressed as homomers in the brain cortex and the minimal structural unit would thus be homodimers.

3.2. Cooperative interactions between protomers in A_1R homomers.

Having established that A_1R homomers exist in the brain, the next question was to establish their physiological role. To this end, we investigated the effect of ligand binding to one protomer on the same ligand binding affinity for the other protomer in the A_1R homodimers. Agonist saturation binding experiments using bovine brain cortical membranes were performed. Cortical membranes were used because its high levels of A_1Rs (1.06 ± 0.02 pmol/mg of protein) and negligible levels (<0.02 pmol/mg of protein) of the other adenosine receptor, the A_{2A}R, that can bind (R)-PIA and DPCPX with very low affinity [44-46]. Membranes were incubated with increasing [^{3}H](R)-PIA concentrations (1 pM to 20 nM) enough time to reach the equilibrium for the lower radioligand concentrations used (8h) and binding was performed as described in Material and methods. Fitting the binding data to equation (1) (saturation in cooperative conditions) was significantly better than fitting the data to equation (3) (saturation in non-cooperative conditions) ($p < 0.05$) and a biphasic saturation curve for [^{3}H](R)-PIA binding to A_1Rs was obtained (Fig. 3). The parameter values are summarized in Table 1 (control values). The biphasic saturation curve reflected a negative cooperativity for (R)-PIA binding to A_1Rs with a negative D_{CA} value (see Material and methods) of – 0.62. Considering homodimers and our mechanistic two-state dimer receptor model for A_1Rs, negative cooperativity is naturally explained by assuming that the binding of the first agonist molecule (with a K_{DA1} value) diminishes the affinity of the second agonist molecule for the semi-occupied dimer (with a $K_{DA2} > 4K_{DA1}$ value) [36].

In order to test this assumption, we hypothetized that at low radioligand agonist concentrations (when the radioligand binds to one protomer preferentially over the empty homodimer) or at high radioligand agonist concentrations (when the radioligand binds to one protomer preferentially over the semi-occupied homodimer), the agonist binding behavior, in self-competition experiments, would be apparently non-cooperative. To corroborate this hypothesis we have performed self-competition experiments, incubating cortical membranes with low (0.3 nM) or high (3.8 nM) [^{3}H](R)-PIA

concentrations in the absence or in the presence of increasing non-tritiated (R)-PIA concentrations (0.1 pM -10 μM) as described in Material and methods. Fitting the binding data to equation (12) (cooperative self competition) was not better than fitting the data to equation (14) (non-cooperative self competition) and, as shown in Fig. 4a and b, a monophasic competition curve was obtained in both cases. Fitting the binding data to equation (14), the affinity constants determined were 0.23 ± 0.04 nM and 3.9 ± 0.8 nM for the low and high radioligand concentrations respectively, that were very similar to the K_{DA1} and K_{DA2} values for R-PIA determined by saturation experiments (see Table 1).

Simulation techniques are another experimental approach that can be employed to study if it is possible to obtain monophasic curves in self-competition experiments when a constant (low or high) concentration of this radioligand is used considering the parameters obtained from saturation experiments in which a cooperative behavior was observed. Simulated competition curves were generated using either equation (12) (cooperative self competition) or equation (14) (non-cooperative self competition), the [^{3}H](R)-PIA concentration of 0.3 nM (Fig. 4c) or 3.8 nM (Fig. 4d) and the experimental parameter values obtained from saturation curves (see Table 1) and described in the Fig. 4 legend. Both cases yielded monophasic and superimposed curves irrespective of the equation used (Fig. 4c and d). Thus, considering the parameters stated in Table 1, obtained from a cooperative saturation curve, simulated competition experiments give rise to monophasic curves in these particular experimental conditions.

If cooperativity in agonist binding is a consequence of the protomer-protomer interactions in the homodimer, changes in the quaternary structure of the homodimer would impact cooperativity. Changes in the quaternary structure of A_1Rs upon ligand binding have not been detected by BRET assays (Figure 5a) but binding of the A_1R allosteric modulator ADA (33) induced a strong modification of their quaternary structure. In fact, when BRET saturation curves were determined as described above but in the presence of 0.2 I.U./ml of ADA a significant ($p < 0.01$) increase in the $BRET_{max}$ was observed ($BRET_{max}$ was 66 ± 5) without significant modification of $BRET_{50}$ ($BRET_{50}$ was 5 ± 1) (Fig. 5b). These results can be interpreted in two ways. In one, ADA led to conformational changes in A_1Rs homomers that reduces the distance between Rluc and YFP fused to the C-terminal domain of the two A_1R-containing fusion proteins. In the other, ADA increases the receptor homomerization by increasing the affinity between protomers. In the latter, as monomers and homomers must be in equilibrium and $BRET_{50}$ should represent the affinity between protomers, a decrease in the $BRET_{50}$ values could be expected, reflecting an increase in affinity between protomers. Since the $BRET_{50}$ values were not changed in the presence of ADA we favor the first interpretation, that of ADA causing conformational changes (Figure 5 top images).

Next, we tested if the ADA-induced changes in the A_1R quaternary structure are able to modify the cooperativity in the agonist binding by performing the saturation curves with increasing [^{3}H](R)-PIA concentrations described above but in the presence of 0.2 I.U./ml of ADA. In the presence of the enzyme, fitting the binding data to equation (1) (saturation in cooperative conditions) was not better than how the data fit to equation (3) (saturation in non-cooperative conditions) and a monophasic saturation curve was detected (Fig. 6a). As shown in Table 1, ADA induced a 4.7 fold decrease of K_{DA1}, a ~ 10 fold decrease of the $[R\text{-}PIA]_{50}$ and abolished the negative cooperativity for (R)-PIA binding ($D_{CA} = 0$). Thus, the ADA binding to A_1Rs homomers blocks the protomer-protomer interactions stabilizing the high affinity receptor conformation. Similar results were obtained using ADA inactivated with Hg^{2+} (Table 1) indicating that ADA interacts with A_1Rs in an activity-independent form and suggesting that, in our exhaustively washed membrane preparation, there is not enough endogenous adenosine to interfere with the exogenous ligand binding to receptors.

Receptor homomers not only can bind agonist but also antagonist. Since antagonists are not able to induce signaling, the antagonist-induced structural changes on receptor homomers might be less notorious than the agonist-induced ones. To test the effect of antagonist binding to one protomer on the same antagonist affinity for the other protomer in the A_1Rs homodimers, we performed saturation experiments incubating cortical membranes with increasing [^{3}H]DPCPX concentrations (1 pM to 10 nM) as described in Material and methods. Fitting the binding data to equation (1) (saturation in cooperative conditions) was not better than the data fit to equation (3) (saturation in non-cooperative conditions) and a monophasic saturation curve was obtained (Fig. 6b). The parameter values are summarized in Table 1. A non-cooperative behavior for antagonist binding was usually observed for G-protein coupled receptors

[37,47-51] and means that an antagonist cannot induce the protomer-protomer interactions in the homodimer. Moreover, if the ADA binding to A_1Rs homomers blocks the protomer-protomer interactions stabilizing the high affinity receptor conformation, we can predict that ADA should have minimal consequences on antagonist binding. From [^{3}H]DPCPX saturation curves performed as indicated above but in the presence of 0.2 I.U./ml of ADA (Fig. 6b), similar pharmacological parameters to those obtained in the absence of ADA have been deduced (Table 1). In both cases, $K_{DA2} = 4\ K_{DA1}$ (see Material and methods), $D_{CA} = 0$ and there is a slight increase (~ 2 fold) in the affinity of the receptor for the DPCPX in the presence of ADA.

3.3. The caffeine binding to one protomer increases the agonist affinity for the other protomer in the A_1R homomer.

Since the protomer-protomer interactions in a homodimer can account for the cooperativity in agonist binding, we investigated if through protomer-protomer interactions there is a molecular cross-talk when two different compounds, i.e. a radiolabelled agonist and a competing antagonist, bind to a receptor in a competition experiment. To test this, we have performed competition experiments using the agonist [^{3}H](R)-PIA (0.3 nM) and increasing concentrations (1 µM to 30 mM) of a drug widely consumed by humans, the natural antagonist caffeine, as described in Material and methods. Fitting the binding data to equation (5) (competition with two different cooperative ligands) was not better than data fit to equation (11) (cooperative radioligand *vs.* non-cooperative competitor) indicating that the caffeine binding was not cooperative ($D_{CB} = 0$), as usually corresponds to an antagonist. The equilibrium constants are summarized in Table 2. Interestingly, the competition curve of [^{3}H](R)-PIA *vs*. caffeine was biphasic (Fig. 7a). According to the two-state dimer receptor model [36] this biphasic behavior in the absence of cooperativity is justified by the existence of an agonist-antagonist cross-talk that it is explained by the hybrid equilibrium dissociation constant (K_{DAB}, see equations in Material and methods). This parameter corresponds to the equilibrium dissociation constant of the antagonist caffeine binding to a receptor dimer semi-occupied by the agonist [^{3}H](R)-PIA. Accordingly, a "dimer radioligand/competitor modulation index" (D_{AB}) can be calculated as indicated in Material and methods (equation 9). D_{AB} is a measure of competitor (caffeine) affinity modifications occurring when a protomer senses the binding of [^{3}H](R)-PIA to the partner protomer in a dimer. As it is shown in Table 2, the agonist [^{3}H](R)-PIA binding to an empty receptor dimer positively modulates the antagonist caffeine binding to the other subunit in the dimer ($K_{DAB} = 26$ µM; $D_{AB} = + 0.33$). According to the two-state dimer receptor model, an inverse cross-talk can be deduced from equations (6) and (10), where K_{DBA} corresponds to the equilibrium dissociation constant of the agonist (R)-PIA binding to a receptor dimer semi-occupied by a molecule of the antagonist caffeine. The $K_{DBA} = 0.17 \pm 0.02$ nM and $D_{BA} = + 0.33$ values indicate that caffeine binding to an empty receptor dimer enhances the agonist (R)-PIA binding to the other subunit in the dimer.

To test if the detected caffeine-(R)-PIA cross-talk is a consequence of protomer-protomer interactions in the A_1R homomers, we analyzed the effect of ADA in this cross-talk taking into account that ADA induced a strong change in the quaternary structure of A_1R homomers (see Figure 5b) that blocks the protomer-protomer interactions stabilizing the high affinity receptor conformation. We have performed competition experiments using the agonist [^{3}H](R)-PIA (0.3 nM) and increasing concentrations of caffeine (1 µM to 30 mM) in the presence of 0.2 I.U./ml of ADA. Fitting the binding data to equation (5) (competition with two different cooperative ligands) was not better than data fitting to equation (13) (non-cooperative radioligand *vs.* non-cooperative competitor) indicating that caffeine binding was not cooperative also in these conditions. The equilibrium constants are summarized in Table 2 showing a slight increase in caffeine affinity induced by ADA. Interestingly, in the presence of ADA, the competition curve of [^{3}H](R)-PIA *vs.* caffeine was monophasic (Fig. 7a) and, as expected in this case (see Material and methods), $K_{DAB} = 2\ K_{DB1}$ and $D_{AB} = 0$. The complete loss of agonist-antagonist cross-talk agrees with the ADA-induced blockade of the protomer-protomer interactions in the A_1R homomers and indicates that caffeine-(R)-PIA cross-talk is a consequence of the protomer-protomer interactions in the A_1R homomers.

When in the absence of ADA the agonist [^{3}H](R)-PIA is substituted by the antagonist [^{3}H]DPCPX (0.3 nM) and competition experiments are carried out using increasing caffeine concentrations (1 mM to 30 mM) in the same experimental conditions described above, monophasic

curves were obtained (K_{DAB} = 2 K_{DB1} and D_{AB} = 0). Therefore, the antagonist DPCPX binding to one protomer in the dimer does not change the affinity of caffeine for the other protomer in the dimer. Affinity constant values for caffeine in these conditions (K_{DB1} = 29 μM; K_{DB2} = 116 μM) were analogous to that obtained for this compound from competition experiments between [^{3}H] (R)-PIA and caffeine (see Table 2).

Caffeine is not the only antagonist that can modulate the agonist binding to A_1R homomers. In fact we have obtained qualitatively similar results using DPCPX, a selective non-physiological antagonist of this adenosine receptor. Competition experiments using the agonist [^{3}H](R)-PIA (0.3 nM) as radioligand and the antagonist DPCPX as a competitor (1 pM to 10 μM), in the absence or in the presence of 0.2 I.U./ml of ADA, were performed and analyzed as indicated above. The equilibrium constants are summarized in Table 2. As expected, the DPCPX binding was non-cooperative (K_{DB2} = 4 K_{DB1}, see Material and methods). According to the two-state dimer receptor model, an inverse cross-talk can be deduced from equations (6) and (10), where K_{DBA} corresponds to the equilibrium dissociation constant of the agonist (R)-PIA binding to a receptor dimer semi-occupied by a molecule of the antagonist DPCPX. In the absence of ADA, the K_{DBA} (0.06 ± 0.01 nM) and D_{BA} (+ 0.79) values indicate that DPCPX binding to an empty receptor dimer enhances the agonist (R)-PIA binding to the other subunit in the dimer giving a biphasic competition curve (Fig. 7b). In the presence of ADA (Fig. 7b) insignificant changes in the dissociation equilibrium constants were observed but, also in this case, the K_{DBA} = 0.047 ± 0.005 nM and D_{BA} = + 0.25 values indicate a considerable loss (~ 3 fold) of the molecular cross-talk between agonist and antagonist in the presence of ADA.

4. Discussion

GPCRs are membrane bound proteins that translate extracellular signals delivered as neurotransmitters or hormones into intracellular cascades and events of signaling [52]. GPCR-mediated communication can be obtained in several ways in which three major properties seem particularly important: specific interactions between the ligand (agonist) and the receptor, interactions between the receptor and the intracellular components of the signaling cascade or intracellular or extracellular modulators [53] and interactions between receptor (protomers) in a receptor oligomer [36,38]. In this paper we focused in this last property for A_1Rs. We first demonstrated by BRET and PLA experiments that A_1Rs form homomers in transfected cells and in bovine brain cortex. This is the first direct demonstration that A_1Rs are expressed as homomers in a native tissue, implying that the minimal structural unit of A_1R homomers is a homodimer formed by two protomers. From this point, we demonstrated that molecular interactions between protomers in a homodimer can account for some pharmacological characteristics of agonist and antagonist binding to A_1Rs.

The phenomenon of GPCR homo and heteromerization is now accepted [3-10,12,54]. Some recent studies support the existence of receptor homomers at the membrane level [55-58] and, under the pharmacological point of view, there are some receptor behaviors that cannot be explained without considering receptor homomers expression [36,38,42]. Although the ability of A_1Rs to form homomers was previously suggested by western-blot assays [13], there was no direct evidence for A_1R homomerization. Here, we first demonstrated by BRET experiments that A_1Rs form homomers in transfected cells expressing similar levels of A_1Rs to that those found in native tissues. These results indicate that dimerization is not merely an artifact derived from the high levels of expression that are often achieved in heterologous cell systems and that A_1R are expressed as homomers in cell cultures. Biophysical techniques cannot be easily applied in native tissues, so we here applied the Proximity Ligation Assay (PLA) to demonstrate, for the first time, that A_1R homomers are expressed in the brain cortex. PLA is an antibody-based method in which either a single or two proteins (or antigens) are immunolabeled with two primary antibodies conjugated to complementary oligonucleotides. When two antibody molecules are in close proximity, the complementary DNA strands can be ligated, amplified in the presence of fluorescence-labeled nucleotides, and visualized as fluorescent puncta [59,60]. Using this last approach, we detected by confocal microscopy a punctate fluorescent signal which reveals that receptors are within close proximity (<16 nm) [59,60], only slightly larger than that for resonance energy transfer between fluorophores (<10 nm), the most common approach used to infer GPCR

oligomerization. Our results show, for the first time, the existence of A_1Rs homomers in the brain cortex ex vivo constituted, at least, by two protomers that form a dimer.

Having established that A_1R homomers are expressed in the bovine brain cortex, we took advantage of the mechanistic two-state dimer receptor model that considers receptors as dimers, to fit data of agonist and antagonist binding to cortical membranes. The actual stoichiometry of A_1R homomers is not known. It should be, however, noted that models based on trimers, tetramers, etc., would be more complex, but also they would be of little added value in terms of fitting radioligand binding data. In fact the experimental error, inherent in this type of ligand binding experiments, and the limited number of data points that can be achieved in an experimental session, would not give sufficient improvement and the F test would refuse a model with higher number of parameters [36]. Thus, two-state dimer receptor model is the optimal one for receptor homomers. Using this model we found that negative cooperativity in agonist binding can be explained as a consequence of the protomer-protomer interactions in the homodimer in which the binding of the first agonist molecule diminishes the affinity of the second agonist molecule for the semi-occupied dimer. To check this, the role of ADA as an allosteric modulator of A_1Rs was considered. ADA is able to bind to adenosine receptors [33,41,61-63] and the ADA molecular determinants interacting with A_1R have been determined (manuscript in preparation). Independent of its enzymatic activity, ADA behaves as an allosteric effector that markedly enhances agonist affinity and increases receptor functionality [33,63]. Likely resulting from a decrease in the distance between the C-termini of the A_1R protomers fused to Rluc and YFP, ADA binding led to modifications in the quaternary structure of A_1R homomers that could be detected by BRET experiments. Using a similar set up it was shown that A_1R agonists and antagonist are not able to modify the BRET signal. Therefore, the ability of BRET to detect ADA-triggered conformational changes within the A_1R homomers suggests that ADA exerts a strong modification of their quaternary structure. If cooperativity in agonist binding is a consequence of the protomer-protomer interactions in the homodimer, changes in the quaternary structure of the homodimer can be very relevant for cooperativity. Here we demonstrate that ADA-induced changes in the quaternary structure of the homodimer are, in fact, very relevant for cooperativity since ADA binding to A_1Rs homomers blocks the protomer-protomer interactions, stabilizing the high affinity receptor conformation, indicating that cooperativity in agonist binding is a consequence of the protomer-protomer interactions in the homodimer. One important aspect of our results is that the protomer-protomer interactions in the receptor homodimer provide an explanation for previous pharmacological observations that have no other explanation without considering receptor dimers as a minimal quaternary structure. Analyzing agonist binding, we observed a cooperative behavior in saturation experiments using variable concentrations of a radioligand, but, in contrast, we obtain monophasic curves in self-competition experiments when a constant low or high concentration of this radioligand was used. This can only be explained considering that radioligand agonist at low concentrations binds to one protomer preferentially over the empty homodimer and at high concentrations radioligand binds to one protomer preferentially over the semi-occupied homodimer. By simulation experiments, considering a receptor dimer model and cooperativity for the agonist binding, it was demonstrated that, in both cases, the agonist binding behavior in self-competition experiments might be apparently non-cooperative.

Finally, we have also demonstrated that protomer-protomer interactions in A_1R homomers can account for the molecular cross-talk that appears when two different specific molecules, such as an agonist and an antagonist, bind to the A_1R homomers. This is of particular relevance for caffeine binding to A_1Rs. We observed that caffeine binding was not cooperative, an expected result for an antagonist [37, 47-51], but, surprisingly, the competition curve of [^{3}H](R)-PIA *vs.* caffeine was biphasic. Although A_1Rs and A_{2A}Rs are the preferential targets for caffeine in the brain [17,28], the amount of A_{2A}R that we have determined in bovine brain cortex is negligible in comparison with the levels of A_1R and the biphasic behavior for caffeine binding only can be justified by the existence of an agonist-antagonist cross-talk. This corresponds to the agonist [^{3}H](R)-PIA-induced changes in the antagonist caffeine binding affinity to a receptor dimer semi-occupied by [^{3}H](R)-PIA. This cross-talk must be bidirectional and implies that at low caffeine concentrations (when caffeine only binds to one protomer of the empty homodimer), caffeine binding increased the agonist affinity for the other protomer in the A_1R homomer. Obviously, at high caffeine concentrations (when caffeine highly saturates both protomers of the homodimer) caffeine acts as an A_1R antagonist diminishing the agonist binding to the receptors. This means that low caffeine

concentrations might increase low endogenous adenosine binding to A_1R homomers. This is another pharmacological behavior that has no explanation without considering receptor dimers as a minimal quaternary structure. This pharmacological property can explain some biphasic effects reported at low and high concentration of caffeine on locomotor activity. Although caffeine is among the most widely used behavioral stimulant substance [64], molecular mechanisms for its effects are in some aspects unclear. It is now accepted that the stimulant behavior of caffeine is due to the blockade of adenosine receptors [17]. Both striatal A_1R and $A_{2A}R$ are involved in the motor-activating and probably reinforcing effects of caffeine, although they play a different role under conditions of acute or chronic caffeine administration (see [28] for a review). Nevertheless, caffeine when administered alone, elicits biphasic effects, with locomotor depression at lower doses and stimulation at higher doses in mice [65,66]. Our results can account for this behavior since low doses of caffeine can increase the endogenous adenosine binding to A_1Rs increasing locomotor depression whilst high doses of caffeine obviously act as A_1Rs antagonist blocking the effect of endogenous adenosine and inducing locomotor activation. These results open new perspectives on the behavior of this A_1Rs antagonist.

Conflicts of interest statement

The authors have no conflict of interests.

Acknowledgements

We acknowledge the technical help obtained from Jasmina Jiménez (Molecular Neurobiology laboratory, Barcelona University). This study was supported by Grants from Spanish Ministerio de Ciencia y Tecnología (SAF2008-00146 and SAF2010-18472). PJM is a Ramón y Cajal Fellow

References

[1] Vassilatis DK, Hohmann JG, Zeng H, Li F, Ranchalis JE, Mortud MT, et al. The G protein-coupled receptor repertoires of human and mouse. Proc Natl Acad Sci USA 2003;100:4903-8.
[2] Park PS, Filipek S, Wells JW, Palczewski K. Oligomerization of G protein-coupled receptors: past, present and future. Biochemistry 2004;43:15643-56.
[3] Bulenger S, Marullo S, Bouvier M. Emerging role of homo- and heterodimerization in G-protein-coupled receptor biosynthesis and maturation. Trends Pharmacol Sci 2005;26:131-7.
[4] Maggio R, Innamorati G, Parenti M. G protein-coupled receptor oligomerization provides the framework for signal discrimination. J Neurochem 2007;103:1741-52.
[5] George SR, O'Dowd BF, Lee SP. G-protein-coupled receptor oligomerization and its potential for drug discovery. Nat Rev Drug Discov 2002;1:808-20.
[6] Franco R, Canals M, Marcellino D, Ferré S, Agnati L, Mallol J, et al. Regulation of heptaspanning-membrane-receptor function by dimerization and clustering. Trends Biochem Sci 2003;28:238-43.
[7] Franco R, Casadó V, Cortés A, Mallol J, Ciruela F, Ferré S, et al. G-protein-coupled receptor heteromers: function and ligand pharmacology. Br J Pharmacol 2008;153:S90-8.
[8] Javitch JA. The ants go marching two by two: oligomeric structure of G-protein-coupled receptors. Mol Pharmacol 2004;66:1077-82.
[9] Terrillon S, Bouvier M. Roles of G-protein-coupled receptor dimerization. EMBO Rep 2004;5:30-4.
[10] Waldhoer M, Fong J, Jones RM, Lunzer MM, Sharma SK, Kostenis E, et al. A heterodimer-selective agonist shows in vivo relevance of G protein-coupled receptor dimers. Proc Natl Acad Sci USA 2005;102:9050-5.
[11] Milligan G. G-protein-coupled receptor heterodimers: pharmacology, function and relevance to drug discovery. Drug Discov Today 2006;11:541-9.
[12] Ferré S, Baler R, Bouvier M, Caron MG, Devi LA, Durroux T, et al. Building a new conceptual framework for receptor heteromers. Nature Chem Biol 2009;5:131-4.
[13] Ciruela F, Casadó V, Mallol J, Canela EI, Lluís C, Franco R Immunological identification of A_1 adenosine receptors in brain cortex. J Neurosci Res 1995;42:818-28.

[14] Ginés S, Hillion J, Torvinen M, Le Crom S, Casadó V, Canela EI, et al. Dopamine D_1 and adenosine A_1 receptors form functionally interacting heteromeric complexes. Proc Natl Acad Sci USA 2000;97:8606-11.
[15] Ciruela F, Escriche M, Burgueño J, Angulo E, Casadó V, Soloviev MM, et al. Metabotropic glutamate 1 alpha and adenosine A_1 receptors assemble into functionally interacting complexes. J Biol Chem 2001;276:18345-51.
[16] Ciruela F, Casadó V, Rodrigues RJ, Luján R, Burgueño J, Canals M, et al. Presynaptic control of striatal glutamatergic neurotransmission by adenosine A_1-A_{2A} receptor heteromers. J Neurosci 2006;26:2080-7.
[17] Fredholm BB, Ijzerman AP, Jacobson KA, Klotz KN, Linden J. International Union of Pharmacology. XXV. Nomenclature and classification of adenosine receptors. Pharmacol Rev 2001;53:527-52.
[18] Dixon AK, Guvitz AK, Sirinathsinghji DJS, Richardson PJ, Freeman TC. Tissue distribution of adenosine receptor mRNAs in the rat. Br J Pharmacol 1996;118:1461-8.
[19] Fukumitsu N, Ishii K, Kimura Y, Oda K, Sasaki T, Mori Y, et al. Imaging of adenosine A_1 receptors in the human brain by positron emission tomography with [^{11}C]MPDX. Ann Nucl Med 2003;17:511-5.
[20] Ribeiro JA, Sebastiao AM, de Mendonça A. Adenosine receptors in the nervous system: pathophysiological implications. Prog Neurobiol 2002;68:377-92.
[21] Porkka-Heiskanen T, Strecker RE, Thakkar M, Bjorkum AA, Greene RW, McCarley RW. Adenosine: A mediator of the sleep-inducing effects of prolonged wakefulness. Science 1997;276:1265-8.
[22] Dunwiddle TV, Masino SA. The role and regulation of adenosine in the central nervous system. Annu Rev Neurosci 2001;24:31-55.
[23] Heurteaux C, Lauritzen I, Widmann C, Lazdunski M. Essential role of adenosine, adenosine A_1 receptor, and ATP-sensitive K^+ channels in cerebral ischemic preconditioning. Proc Natl Acad Sci USA 1995;92:4666-70.
[24] Gottlieb SS. Renal effects of adenosine A_1-receptor antagonists in congestive heart failure. Drugs 2001;61:1387-93.
[25] Dhalla AK, Shryock JC, Shreeniwas R, Belardinelli L. Pharmacology and therapeutic applications of A_1 adenosine receptor ligands. Curr Top Med Chem 2003;3:369-85.
[26] Solinas M, Ferré S, Antoniou K, Quarta D, Justinova Z, Hockemeyer J, et al. Involvement of adenosine A_1 receptors in the discriminative-stimulus effects of caffeine in rats. Psychopharmacology 2005;179:576-86.
[27] Ferré S. An update on the mechanisms of the psychostimulant effects of caffeine. J Neurochem 2008;105:1067-79.
[28] Christopoulos A, Kenakin T. G protein-coupled receptor allosterism and complexing. Pharmacol Rev 2002;54:323-74.
[29] Bruns RF, Fergus JH. Allosteric enhancement of adenosine A_1 receptor binding and function by 2-amino-3-benzoylthiophenes. Mol Pharmacol 1990;38:939-49.
[30] Gao ZG, Melman N, Erdmann A, Kim SG, Müller CE, Ijzerman AP, et al. Differential allosteric modulation by amiloride analogues of agonist and antagonist binding at A_1 and A_3 adenosine receptors. Biochem Pharmacol 2003;65:525-34.
[31] De Ligt RAF, Rivkees SA, Lorenzen A, Leurs R, Ijzerman, AP. A ¨locked-on¨, constitutively active mutant of the adenosine A_1 receptor. Eur J Pharmacol 2005;510:1-8.
[32] Gracia E, Cortés A, Meana JJ, García-Sevilla J, Hershfield MS, Canela EI, et al. Human adenosine deaminase as an allosteric modulator of human A_1 adenosine receptor: abolishment of negative cooperativity for [^{3}H](R)-PIA binding to the caudate nucleus. J Neurochem 2008;107:161-70.
[33] Durroux T. Principles: a model for the allosteric interactions between ligand binding sites within a dimeric GPCR. Trends Pharmacol Sci 2005;26:376-84.
[34] Franco R, Casadó V, Mallol J, Ferré S, Fuxe K, Cortés A, et al. Dimer-based model for heptaspanning membrane receptors. Trends Biochem Sci 2005;30:360–6.

[35] Casadó V, Cortés A, Ciruela F, Mallol J, Ferré S, Lluís C, et al. Old and new ways to calculate the affinity of agonists and antagonists interacting with G-protein coupled monomeric and dimeric receptors: the receptor-dimer cooperativity index. Pharmacol Ther 2007;116:343–54.
[36] Franco R, Casadó V, Mallol J, Ferrada C, Ferré S, Fuxe K, et al. The two-state dimer receptor model: a general model for receptor dimers. Mol Pharmacol 2006;69:1905–12.
[37] Casadó V, Ferrada C, Bonaventura J, Gracia E, Mallol J, Canela EI, et al. Useful pharmacological parameters for G-protein-coupled receptor homodimers obtained from competition experiments. Agonist-antagonist binding modulation. Biochem Pharmacol 2009;78:1456-63.
[38] Moreno E, Hoffmann H, González-Sepúlveda M, Navarro G, Casadó V, Cortés A, et al. Dopamine D1-histamine H3 receptor heteromers provide a selective link to MAPK signaling in GABAergic neurons of the direct striatal pathway. J. Biol. Chem 2011;286:5846-54.
[39] Casadó V, Cantí C, Mallol J, Canela EI, Lluís C, Franco R Solubilization of A_1 adenosine receptor from pig brain: characterization and evidence of the role of the cell membrane on the coexistence of high- and low-affinity states. J Neurosci Res 1990;26:461–73.
[40] Sarrió S, Casadó V, Escriche M, Ciruela F, Mallol J, Canela EI, et al. The heat shock cognate protein hsc73 assembles with A(1) adenosine receptors to form functional modules in the cell membrane. Mol Cell Biol 2000;20:5164–74.
[41] Saura C, Ciruela F, Casadó V, Canela EI, Mallol J, Lluís C, et al. Adenosine deaminase interacts with A_1 adenosine receptors in pig brain cortical membranes. J Neurochem 1996;66:1675-82.
[42] Casadó V, Cortés A, Mallol J, Pérez-Capote K, Ferré S, Lluís C, et al. GPCR homomers and heteromers: a better choice as targets for drug development than GPCR monomers? Pharmacol Ther 2009;124:248-57.
[43] Goodman RR, Snyder SH. Autoradiographic localization of adenosine receptors in rat brain using [3H]cyclohexyladenosine. J Neurosci 1982;2:1230-41.
[44] Halldner L, Lopes LV, Daré E, Lindström K, Johansson B, Ledent C, et al. Binding of adenosine receptor ligands to brain of adenosine receptor knock-out mice: evidence that CGS 21680 binds to A_1 receptors in hippocampus. Naunyn-Schmiedeberg's Arch Pharmacol 2004;370:270-8.
[45] Franchetti P, Cappellacci L, Marchetti S, Trincavelli L, Martini C, Mazzoni MR, et al. 2'C-methyl analogues of selective adenosine receptor agonists: synthesis and binding studies. J Med Chem 1998;41:1708-15.
[46] Maemoto T, Finlayson K, Overman HJ, Akahane A, Horton RW, Butcher SP. Species differences in brain A_1 adenosine receptor pharmacology revealed by use of xanthine and pyrazolpyridine based antagonists. Br J Pharmacol 1997;122:1202-8.
[47] Burris KD, Filtz TM, Chumpradit S, Kung MP, Foulon C, Hensler JG, et al. Characterization of [^{125}I](R)-trans-7-Hydroxy-2-[N-propyl-N-(3'-iodo-2'-propenyl)amino]tetralin binding to dopamine D_3 receptors in rat olfactory tubercle. J Pharmacol Exp Ther 1994;268:935-42.
[48] Aloyo VJ, Harvey JA. Antagonist binding of 5-HT_{2A} and 5-HT_{2C} receptors in the rabbit: High correlation with the profile for the human receptors. Eur J Pharmacol 2000;406:163-9.
[49] Jansen FP, Mochizuki T, Maeyama K, Leurs R, Timmerman H. Characterization of histamine H_3 receptors in mouse brain using the H_3 antagonist [^{125}I]iodophenpropit. Naunyn-Schmiedeberg's Arch Pharmacol 2000;362:60-7.
[50] Kuriyama T, Schmidt TJ, Okuyama E, Ozoe Y. Structure-activity relationships of seco-Pretizaane terpenoids in γ-aminobutyric acid receptors of houseflies and rats. Bioorg Med Chem 2002;10:1873-81.
[51] Gullapalli S, Amrutkar D, Gupta S, Kandadi MR, Kumar H, Gandhi M, et al. Characterization of active and inactive states of CB1 receptor and the differential binding state modulation by cannabinoid agonists, antagonists and inverse agonists. Neuropharmacology 2010;58:1215-9.
[52] Luttrell LM. Reviews in molecular biology and biotechnology: transmembrane signaling by G protein-coupled receptors. Mol Biotechnol 2008;39:239-64.
[53] Lagerström MC, Schiöth HB. Structural diversity of G protein-coupled receptors and significance for drug discovery. Nat Rev Drug Discov 2008;7:339-57.
[54] Milligan G. G protein-coupled receptor dimerisation: molecular basis and relevance to function. Biochim Biophys Acta 2007;1768:825-35.

[55] Guo W, Urizar E, Kralikova M, Mobarec JC, Shi L, Filizola M, et al. Dopamine D2 receptors form higher order oligomers at physiological expression levels. EMBO J 2008;27:2293-304.
[56] Han Y, Moreira IS, Urizar E, Weinstein H, Javitch JA. Allosteric communication between protomers of dopamine class A GPCR dimers modulates activation. Nat Chem Biol 2009;5:688-95.
[57] Rivero-Müller A, Chou YY, Ji I, Lajic S, Hanyaloglu AC, Jonas K, et al. Rescue of defective G protein–coupled receptor function in vivo by intermolecular cooperation. Proc Natl Acad Sci USA 2010;107:2319–24.
[58] Vassart G. An in vivo demonstration of functional G protein–coupled receptor dimers. Proc Natl Acad Sci USA 2010;107:1819–20.
[59] Söderberg O, Gullberg M, Jarvius M, Ridderstrale, K, Leuchowius K-J, Jarvius J, et al. Direct observation of individual endogenous protein complexes in situ by proximity ligation. Nat Methods 2006;3:995-1000.
[60] Trifilieff P, Rives M-L, Urizar E, Piskorowski RA, Vishwasrao HD, Castrillon J, et al. Detection of antigen interactions ex vivo by proximity ligation assay: endogenous dopamine D2-adenosine A2A receptor complexes in the striatum. BioTechniques 2011;50:111-8.
[61] Ciruela F, Saura C, Canela EI, Mallol J, Lluís C, Franco R. Adenosine deaminase affects ligand-induced signalling by interacting with cell surface adenosine receptors. FEBS Lett 1996;380:219-23.
[62] Herrera C, Casadó V, Ciruela F, Schofield P, Mallol J, Lluís C, et al. Adenosine A_{2B} receptors behave as an alternative anchoring protein for cell surface adenosine deaminase in lymphocytes and cultured cells. Mol. Pharmacol 2001;59:127-34.
[63] Gracia E, Pérez-Capote K, Moreno E, Bakesova J, Mallol J, Lluís C, et al. A_{2A} adenosine receptor ligand binding and signalling is allosterically modulated by adenosine deaminase. Biochem J 2011;435:701-9.
[64] Frary CD, Johnson RK, Wang MQ. Food sources and intakes of caffeine in the diets of persons in the United States. J Am Diet Assoc 2005;105:110-3.
[65] Snyder SH, Katims JJ, Annau Z, Bruns RF, Daly JW. Adenosine receptors and behavioral actions of methylxanthines. Proc Natl Acad Sci USA 1981;78:3260-4.
[66] Katims JJ, Annau Z, Snyder SH. Interactions in the behavioral effects of methylxanthines and adenosine derivatives. J Pharmacol Exp Ther 1983;227:167-73.

Table 1. *Pharmacological parameters of A_1R agonist and antagonist obtained from saturation experiments.*

Saturation experiment	Parameters			
	K_{DA1} (nM)	K_{DA2} (nM)	A_{50} (nM)	D_{CA}
[^{3}H]R-PIA binding				
control	0.18 ± 0.01	3.0 ± 0.6	0.7 ± 0.1	-0.62
+ADA	0.038 ± 0.002***	0.15 ± 0.01**	0.075 ± 0.005**	0
+Hg^{2+}-inactivated ADA	0.035 ± 0.003***	0.14 ± 0.02**	0.071 ± 0.008**	0
[^{3}H]DPCPX binding				
control	0.038 ± 0.002	0.15 ± 0.01	0.076 ± 0.004	0
+ADA	0.021 ± 0.003**	0.08 ± 0.01**	0.042 ± 0.006**	0

Saturation curves were carried out in the absence (control) or in the presence of 0.2 I.U./ml of active or Hg^{2+}-inactivated ADA using bovine cortical brain membranes. K_{DA1} and K_{DA2} are, respectively, the equilibrium dissociation constants of the first and the second binding of A ([^{3}H]R-PIA or [^{3}H]DPCPX) to the receptor dimer. A_{50} is the concentration providing half saturation for A. D_{CA} is the dimer cooperativity index for the binding of the ligand A. Data are mean ± S.E.M. values of three independent experiments performed in triplicate. $^{**}p < 0.01$, $^{***}p < 0.001$ against control. Note that when $D_{CA} = 0$, $K_{DA2} = 4\ K_{DA1}$, thus, for non-cooperative conditions K_{DA1} is enough to characterize the binding.

Table 2. *Pharmacological parameters of A_1R antagonists obtained from competition experiments.*

Competition experiment	Parameters				
	K_{DB1} (μM)	K_{DB2} (μM)	K_{DAB} (μM)	B_{50} (μM)	D_{AB}
[^{3}H]R-PIA *vs*. caffeine					
control	28 ± 4	112 ± 16	26 ± 3	56 ± 8	+0.33
+ADA	18 ± 1*	72 ± 4*	36 ± 2*	36 ± 2*	0
	K_{DB1} (nM)	K_{DB2} (nM)	K_{DAB} (nM)	B_{50} (nM)	D_{AB}
[^{3}H]R-PIA *vs*. DPCPX					
control	0.040 ± 0.002	0.16 ± 0.01	0.013 ± 0.001	0.080 ± 0.005	+0.79
+ADA	0.022 ± 0.002**	0.09 ± 0.01**	0.025 ± 0.003*	0.044 ±0.004**	+0.25

Competition curves were carried out in the absence (control) or the presence of 0.2 I.U./ml of ADA using bovine cortical brain membranes. K_{DB1} and K_{DB2} are, respectively, the equilibrium dissociation constants of the first and the second binding of competing ligand B (caffeine or DPCPX) to the receptor dimer. K_{DAB} is the hybrid equilibrium dissociation constant of B binding to a receptor dimer semi-occupied by the radioligand A ([^{3}H]R-PIA). B_{50} is the concentration providing half saturation for B. D_{AB} is the dimer radioligand/competition modulation index. Data are mean ± S.E.M. values of three independent experiments performed in triplicate. $^*p < 0.05$, $^{**}p < 0.01$ against control. Note that when $D_{AB} = 0$, when the presence of radioligand does not affect the affinity of the competitor, $K_{DAB} = 2\ K_{DA1}$.

FIGURES AND FIGURE CAPTIONS

Figure 1

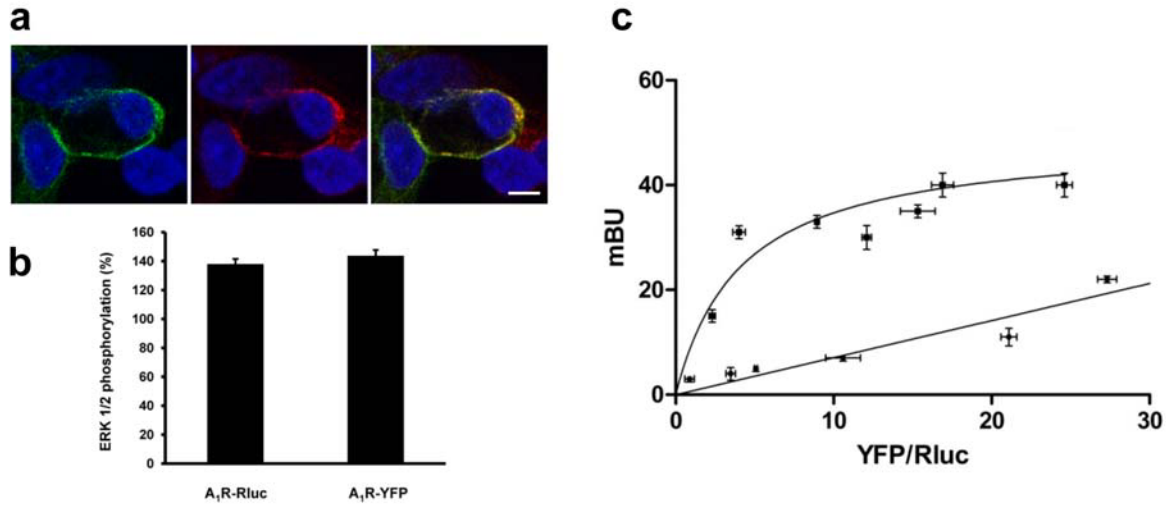

Fig. 1. A_1Rs homomer expression in cell culture. In (a) confocal microscopy images of HEK-293 cells transfected with 1 µg of cDNA corresponding to A_1R-Rluc and 1 µg of cDNA corresponding to to A_1R-YFP are shown. Proteins were identified by fluorescence or by immunocytochemistry. A_1R-Rluc is shown in red, A_1R-YFP is shown in green and co-localization is shown in yellow. Cell nuclei were stained with DAPI (blue). Scale bar: 5 µm. In (b) functionality of the fusion proteins in cells transfected with 1 µg of cDNA corresponding to A_1R, A_1R-Rluc or A_1R-YFP is shown. 48 h post-transfection, cells were treated for 5 min with 0.5 nM R-PIA and ERK1/2 phosphorylation was determined. Results (means ± S.E.M. of 3 different experiments) are represented as percentage of ERK 1/2 phosphorylation detected in cells expressing the corresponding receptors not fused to Rluc or YFP. In (c) BRET saturation experiments were performed as described in Material and methods using HEK-293 cells 48 h post-transfection with 0.5 µg of cDNA corresponding to A_1R-Rluc and increasing amounts of cDNA corresponding to A_1R-YFP (1 to 4.8 µg cDNA) (squares) or to $5HT_{2B}$R-YFP (0.5 to 5 µg cDNA) as negative controls (circles). Both fluorescence and luminescence of each sample were measured before every experiment to confirm similar donor expression (approximately 110,000 bioluminescence units) while monitoring the increase in acceptor expression (1,000 to 27,000 fluorescence units). The relative amount of BRET is given as a function of 100 x the ratio between the fluorescence of the acceptor (YFP) and the luciferase activity of the donor (Rluc). BRET is expressed as mili BRET units (mBU = net BRET x 1,000) and is means ± S.E.M. of three to four different experiments grouped according to the amount of BRET acceptor.

Figure 2

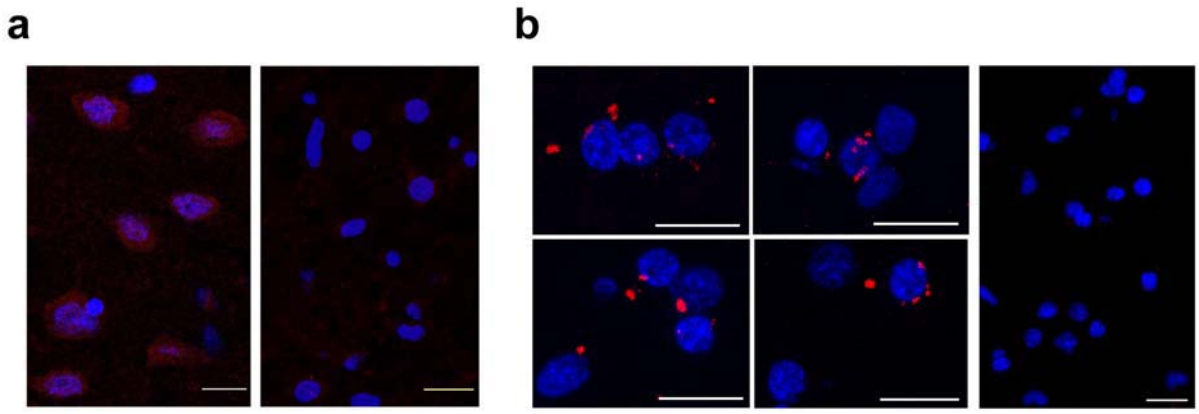

Fig. 2. A_1Rs homomer expression in bovine brain cortex. In (a) confocal microscopy images (superimposed sections) of bovine brain cortex (left image) or pontine (right image, negative control) slices stained for immunohistochemistry with the anti-A1Rs antibody as indicated in Material and methods. In (b) in situ Proximity Ligation Assays (PLA) were performed as indicated in Material and methods. Confocal microscopy images (superimposed sections) of bovine brain cortex (left images from four representative slices) or pontine (right image, negative control) slices are shown. Homomers are detected as red clusters. Scale bars = 15 µm. In all cases, cell nuclei were stained with DAPI (blue).

Figure 3

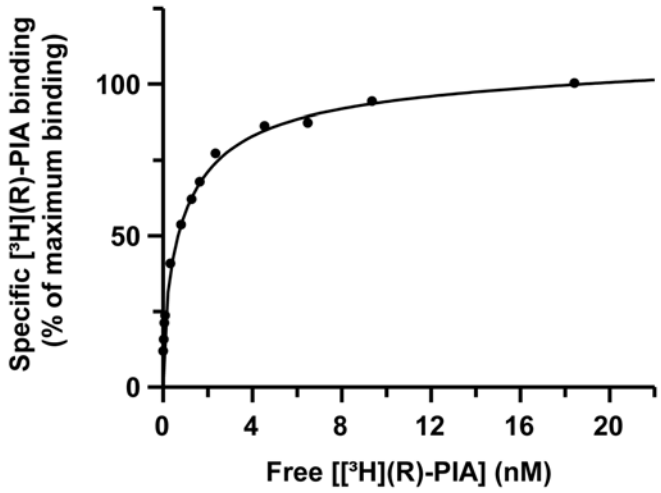

Fig. 3. Saturation curves of agonist binding to A_1Rs. [^{3}H](R)-PIA binding to bovine cortical brain membranes was performed as indicated in Material and methods. Experimental data were fitted to the two-state dimer receptor model equation (1). Values are mean ± S.E.M. from a representative experiment (n = 3) performed in triplicate. 100% corresponds to 1.04 ± 0.06 pmol/mg of protein.

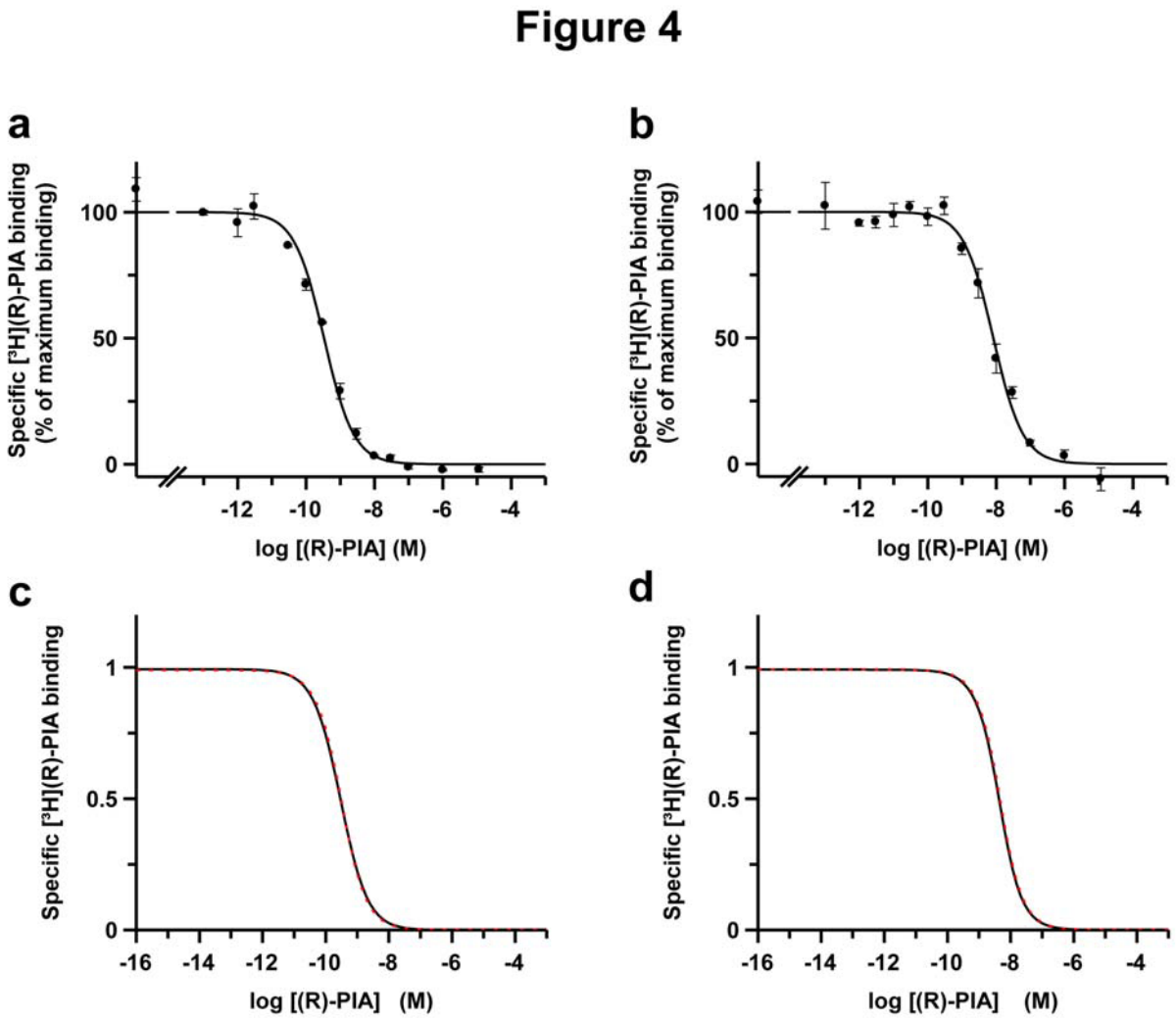

Fig. 4. Competition curves of A_1R agonist [^{3}H](R)-PIA binding versus increasing concentrations of free (R)-PIA. In (a) and (b) competition experiments were performed as indicated in Material and methods using bovine cortical brain membranes with 0.3 nM (a) or 3.8 nM (b) [^{3}H](R)-PIA versus increasing concentrations of (R)-PIA (0.1 pM to 10 µM). Experimental data were fitted to the two-state dimer receptor model equation (14). Values are mean ± S.E.M. from a representative experiment (n = 3) performed in triplicate. 100% corresponds to 0.38 ± 0.02 (a) or 0.87 ± 0.03 (b) pmol/mg of protein. In (c) and (d) simulation curves were obtained using equation (14) (black solid curves) or equation (12) (red dotted curves) considering the following parameters values: [A] = 0.3 nM (c) or 3.8 nM (d), K_{DA1} = 0.18 nM, K_{DA2} = 3.0 nM and increasing concentrations of the non-labelled agonist.

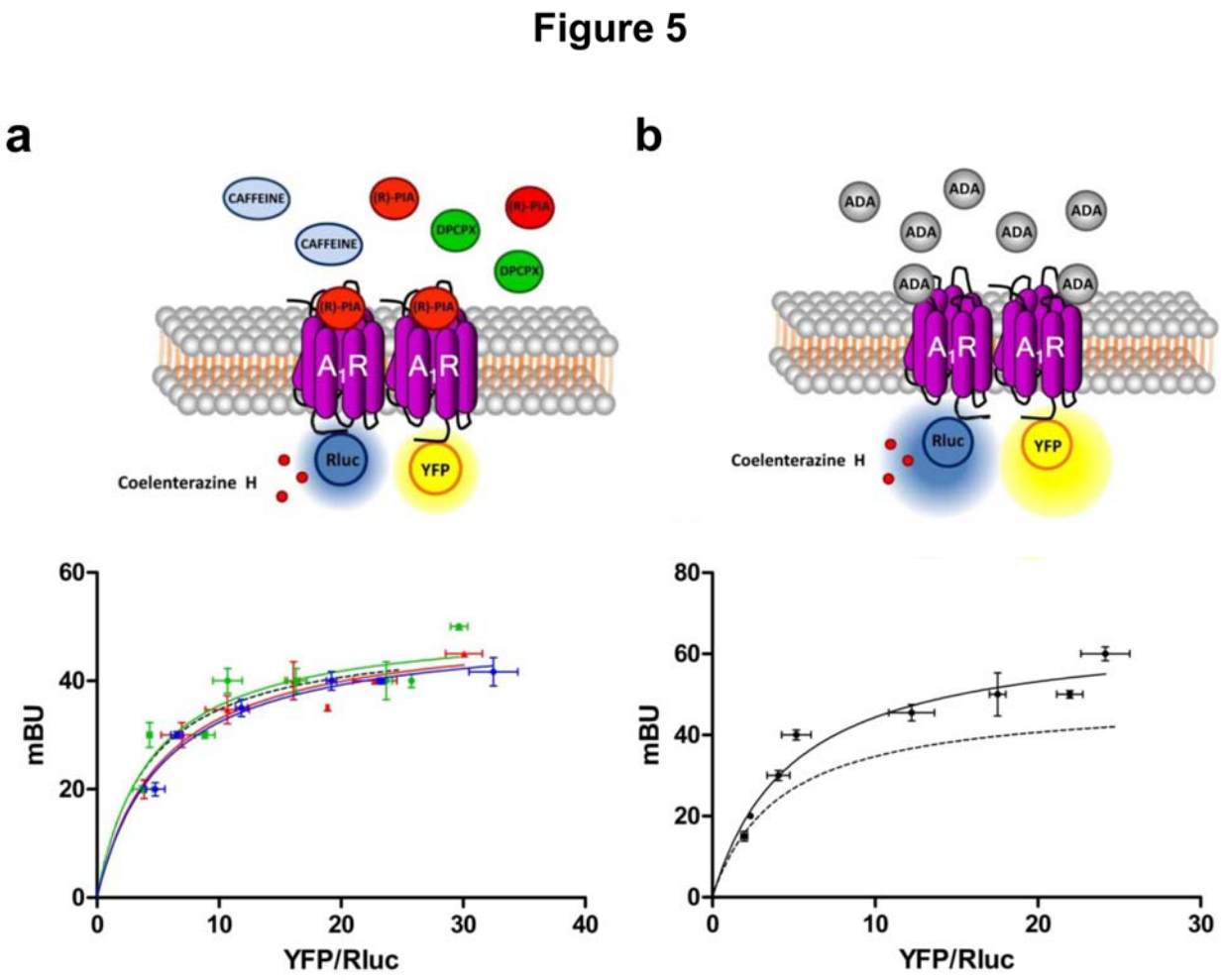

Fig. 5. Effect of ligand binding to A_1Rs on the quaternary structure of the receptor homomers. BRET saturation experiments were performed as described in Material and methods using cells 48 h post-transfection with 0.5 µg of cDNA corresponding to A_1R-Rluc and increasing amounts of cDNA corresponding to A_1R-YFP receptor (1 to 4.8 µg cDNA) treated for 10 min with: (a) medium (dotted line, see Fig. 1c), 30 nM (R)-PIA (red triangles), 3 nM DPCPX (green circles) or 100 mM caffeine (blue rhombus) or (b) for 30 min with 0.2 I.U./ml of ADA compared with non-treated cells (dotted line, see Fig. 1c). Both fluorescence and luminescence of each sample were measured before every experiment to confirm similar donor expressions (approximately 110,000 bioluminescence units) while monitoring the increase in acceptor expression (10,000 to 40,000 fluorescence units). The relative amount of BRET is given as a function of 100 x the ratio between the fluorescence of the acceptor (YFP) and the luciferase activity of the donor (Rluc). BRET is expressed as mili BRET units (mBU = net BRET x 1,000) and is means ± S.E.M. of three to four different experiments grouped as a function of the amount of BRET acceptor. At top is a schematic representation of the BRET energy transfer in control cells or in cells treated with agonist or antagonist (a) and in cells treated with ADA (b).

Figure 6

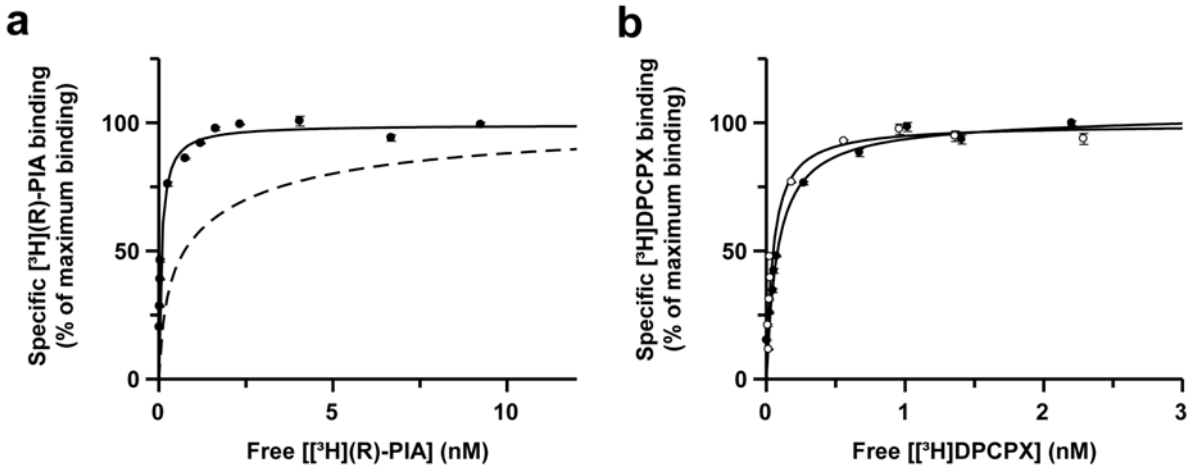

Fig. 6. Effect of ADA on agonist and antagonist binding to A_1Rs. Saturation experiments were performed as indicated in Material and methods using bovine cortical brain membranes. (a) [^{3}H](R)-PIA binding was performed in the presence of 0.2 I.U./ml of ADA (solid line) and compared with the saturation curve obtained in the absence of ADA (dotted line, see Fig 3). (b) [^{3}H]-DPCPX binding in the absence (●) or in the presence (○) of 0.2 I.U./ml of ADA. Experimental data were fitted to the two-state dimer receptor model equation (3). Values are mean ± S.E.M. from a representative experiment (n = 3) performed in triplicate. 100% corresponds to 1.00 ± 0.04 pmol/mg of protein.

Figure 7

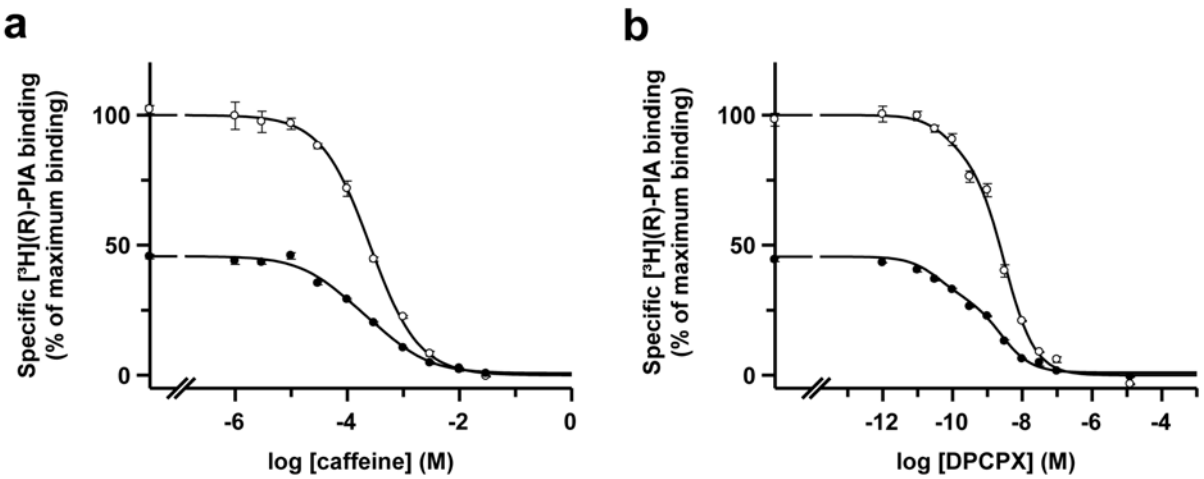

Fig. 7. Competition curves of A_1R agonist [^{3}H](R)-PIA binding versus increasing free concentrations of A_1R antagonists. Competition experiments of the agonist 0.3 nM [^{3}H](R)-PIA binding versus increasing concentrations of the antagonist caffeine (a) or DPCPX (b), in the absence (●) or in the presence (○) of 0.2 I.U./ml of ADA, were performed as indicated in Material and methods using bovine cortical brain membranes. Experimental data were fitted to the two-state dimer receptor model equation (11) and (13). Values are mean ± S.E.M. from a representative experiment (n = 3) performed in triplicate. 100% corresponds to 0.85 ± 0.03 pmol/mg of protein.

BIBLIOGRAFÍA

Abbas, A., J. Raju, J. Milles and S. Ramachandran (2010) A circadian rhythm sleep disorder: melatonin resets the biological clock. *J R Coll Physicians Edinb*. **40**, 311-3.

AbdAlla, S., H. Lother and U. Quitterer (2000) AT1-receptor heterodimers show enhanced G-protein activation and altered receptor sequestration. *Nature*. **407**, 94-8.

Abi-Dargham, A. (2004) Do we still believe in the dopamine hypothesis? New data bring new evidence. *Int J Neuropsychopharmacol*. **7 Suppl 1**, S1-5.

Acquas, E. and H. C. Fibiger (1998) Dopaminergic regulation of striatal acetylcholine release: the critical role of acetylcholinesterase inhibition. *J Neurochem*. **70**, 1088-93.

Acquas, E., A. Pisanu, S. Spiga, A. Plumitallo, G. Zernig and G. Di Chiara (2007) Differential effects of intravenous R,S-(+/-)-3,4-methylenedioxymethamphetamine (MDMA, Ecstasy) and its S(+)- and R(-)-enantiomers on dopamine transmission and extracellular signal regulated kinase phosphorylation (pERK) in the rat nucleus accumbens shell and core. *J Neurochem*. **102**, 121-32.

Adams, M. R., E. P. Brandon, E. H. Chartoff, R. L. Idzerda, D. M. Dorsa and G. S. McKnight (1997) Loss of haloperidol induced gene expression and catalepsy in protein kinase A-deficient mice. *Proc Natl Acad Sci U S A*. **94**, 12157-61.

Adell, A. and F. Artigas (2004) The somatodendritic release of dopamine in the ventral tegmental area and its regulation by afferent transmitter systems. *Neurosci Biobehav Rev*. **28**, 415-31.

Adler, L. A. and H. C. Chua (2002) Management of ADHD in adults. *J Clin Psychiatry*. **63 Suppl 12**, 29-35.

Agnati, L. F., S. Ferré, C. Lluis, R. Franco and K. Fuxe (2003) Molecular mechanisms and therapeutical implications of intramembrane receptor/receptor interactions among heptahelical receptors with examples from the striatopallidal GABA neurons. *Pharmacol Rev*. **55**, 509-50.

Agnati, L. F., K. Fuxe and S. Ferré (2005) How receptor mosaics decode transmitter signals. Possible relevance of cooperativity. *Trends Biochem Sci*. **30**, 188-93.

Akimoto, Y., T. Horinouchi, M. Shibano, M. Matsushita, Y. Yamashita, T. Okamoto, F. Yamaki, Y. Tanaka and K. Koike (2002) Nitric oxide (NO) primarily accounts for endothelium-dependent component of beta-adrenoceptor-activated smooth muscle relaxation of mouse aorta in response to isoprenaline. *J Smooth Muscle Res*. **38**, 87-99.

Akunne, H. C., S. Z. Whetzel, J. N. Wiley, A. E. Corbin, F. W. Ninteman, H. Tecle, Y. Pei, T. A. Pugsley and T. G. Heffner (1997) The pharmacology of the novel and selective sigma ligand, PD 144418. *Neuropharmacology*. **36**, 51-62.

Albizu, L., M. N. Balestre, C. Breton, J. P. Pin, M. Manning, B. Mouillac, C. Barberis and T. Durroux (2006) Probing the existence of G protein-coupled receptor dimers by positive and negative ligand-dependent cooperative binding. *Mol Pharmacol*. **70**, 1783-91.

Alexander, G. E. and M. D. Crutcher (1990) Functional architecture of basal ganglia circuits: neural substrates of parallel processing. *Trends Neurosci*. **13**, 266-71.

Almeida, J. and G. Mengod (2010) D2 and D4 dopamine receptor mRNA distribution in pyramidal neurons and GABAergic subpopulations in monkey prefrontal cortex: implications for schizophrenia treatment. *Neuroscience*. **170**, 1133-9.

Alonso, G., V. Phan, I. Guillemain, M. Saunier, A. Legrand, M. Anoal and T. Maurice (2000) Immunocytochemical localization of the sigma(1) receptor in the adult rat central nervous system. *Neuroscience*. **97**, 155-70.

American Academy of Pediatrics (2001) Clinical Practice Guideline: Treatment of the School-Aged Child With Attention-Deficit/Hyperactivity Disorder. *Pediatrics*. **108, No. 4**

Anderson, S. M. and R. C. Pierce (2005) Cocaine-induced alterations in dopamine receptor signaling: implications for reinforcement and reinstatement. *Pharmacol Ther*. **106**, 389-403.

Angers, S., A. Salahpour, E. Joly, S. Hilairet, D. Chelsky, M. Dennis and M. Bouvier (2000) Detection of beta 2-adrenergic receptor dimerization in living cells using bioluminescence resonance energy transfer (BRET). *Proc Natl Acad Sci U S A*. **97**, 3684-9.

Anichtchik, O. V., M. Huotari, N. Peitsaro, J. W. Haycock, P. T. Mannisto and P. Panula (2000a) Modulation of histamine H3 receptors in the brain of 6-hydroxydopamine-lesioned rats. *Eur J Neurosci*. **12**, 3823-32.

Anichtchik, O. V., N. Peitsaro, J. O. Rinne, H. Kalimo and P. Panula (2001) Distribution and modulation of histamine H(3) receptors in basal ganglia and frontal cortex of healthy controls and patients with Parkinson's disease. *Neurobiol Dis*. **8**, 707-16.

Anichtchik, O. V., J. O. Rinne, H. Kalimo and P. Panula (2000b) An altered histaminergic innervation of the substantia nigra in Parkinson's disease. *Exp Neurol*. **163**, 20-30.

Antshel, K. M., T. M. Hargrave, M. Simonescu, P. Kaul, K. Hendricks and S. V. Faraone (2011) Advances in understanding and treating ADHD. *BMC Med*. **9**, 72.

Arias-Montano, J. A., B. Floran, M. Garcia, J. Aceves and J. M. Young (2001) Histamine H(3) receptor-mediated inhibition of depolarization-induced, dopamine D(1) receptor-dependent release of [(3)H]-gamma-aminobutryic acid from rat striatal slices. *Br J Pharmacol*. **133**, 165-71.

Arrang, J. M., S. Morisset and F. Gbahou (2007) Constitutive activity of the histamine H3 receptor. *Trends Pharmacol Sci*. **28**, 350-7.

Asghari, V., S. Sanyal, S. Buchwaldt, A. Paterson, V. Jovanovic and H. H. Van Tol (1995) Modulation of intracellular cyclic AMP levels by different human dopamine D4 receptor variants. *J Neurochem*. **65**, 1157-65.

Aston-Jones, G. (2005) Brain structures and receptors involved in alertness. *Sleep Med*. **6 Suppl 1**, S3-7.

Aston-Jones, G. and J. D. Cohen (2005) Adaptive gain and the role of the locus coeruleus-norepinephrine system in optimal performance. *J Comp Neurol*. **493**, 99-110.

Attwood, T. K. and J. B. Findlay (1994) Fingerprinting G-protein-coupled receptors. *Protein Eng*. **7**, 195-203.

Axelrod, J. (1970) The pineal gland. *Endeavour*. **29**, 144-8.

Axelrod, J. (1972) Dopamine- -hydroxylase: regulation of its synthesis and release from nerve terminals. *Pharmacol Rev*. **24**, 233-43.

Axelrod, J. and R. Weinshilboum (1972) Catecholamines. *N Engl J Med*. **287**, 237-42.

Baan, B., E. Pardali, P. ten Dijke and H. van Dam (2010) In situ proximity ligation detection of c-Jun/AP-1 dimers reveals increased levels of c-Jun/Fra1 complexes in aggressive breast cancer cell lines in vitro and in vivo. *Mol Cell Proteomics*. **9**, 1982-90.

Badie-Mahdavi, H., X. Lu, M. M. Behrens and T. Bartfai (2005) Role of galanin receptor 1 and galanin receptor 2 activation in synaptic plasticity associated with 3',5'-cyclic AMP response element-binding protein phosphorylation in the dentate gyrus: studies with a galanin receptor 2 agonist and galanin receptor 1 knockout mice. *Neuroscience*. **133**, 591-604.

Bai, M., S. Trivedi and E. M. Brown (1998) Dimerization of the extracellular calcium-sensing receptor (CaR) on the cell surface of CaR-transfected HEK293 cells. *J Biol Chem*. **273**, 23605-10.

Bailey, M. J., S. L. Coon, D. A. Carter, A. Humphries, J. S. Kim, Q. Shi, P. Gaildrat, F. Morin, S. Ganguly, J. B. Hogenesch, J. L. Weller, M. F. Rath, M. Moller, R. Baler, D. Sugden, Z. G. Rangel, P. J. Munson and D. C. Klein (2009) Night/day changes in pineal expression of >600 genes: central role of adrenergic/cAMP signaling. *J Biol Chem*. **284**, 7606-22.

Bakker, R. A. (2004) Histamine H3-receptor isoforms. *Inflamm Res*. **53**, 509-16.

Bakker, R. A., A. F. Lozada, A. van Marle, F. C. Shenton, G. Drutel, K. Karlstedt, M. Hoffmann, M. Lintunen, Y. Yamamoto, R. M. van Rijn, P. L. Chazot, P. Panula and R. Leurs (2006) Discovery of naturally occurring splice variants of the rat histamine H3 receptor that act as dominant-negative isoforms. *Mol Pharmacol*. **69**, 1194-206.

Baneres, J. L. and J. Parello (2003) Structure-based analysis of GPCR function: evidence for a novel pentameric assembly between the dimeric leukotriene B4 receptor BLT1 and the G-protein. *J Mol Biol*. **329**, 815-29.

Banihashemi, B. and P. R. Albert (2002) Dopamine-D2S receptor inhibition of calcium influx, adenylyl cyclase, and mitogen-activated protein kinase in pituitary cells: distinct Galpha and Gbetagamma requirements. *Mol Endocrinol*. **16**, 2393-404.

Bardo, M. T. (1998) Neuropharmacological mechanisms of drug reward: beyond dopamine in the nucleus accumbens. *Crit Rev Neurobiol*. **12**, 37-67.

Barishpolets, V. V., O. Fedotova Iu and N. S. Sapronov (2009) [Structural and functional organization of the cerebral dopaminergic system]. *Eksp Klin Farmakol*. **72**, 44-9.

Bartfai, T., T. Hokfelt and U. Langel (1993) Galanin--a neuroendocrine peptide. *Crit Rev Neurobiol*. **7**, 229-74.

Basile, M., R. Lin, N. Kabbani, K. Karpa, M. Kilimann, I. Simpson and M. Kester (2006) Paralemmin interacts with D3 dopamine receptors: implications for membrane localization and cAMP signaling. *Arch Biochem Biophys*. **446**, 60-8.

Bateup, H. S., E. Santini, W. Shen, S. Birnbaum, E. Valjent, D. J. Surmeier, G. Fisone, E. J. Nestler and P. Greengard (2010) Distinct subclasses of medium spiny neurons differentially regulate striatal motor behaviors. *Proc Natl Acad Sci U S A*. **107**, 14845-50.

Beaudry, P., R. Fontaine, G. Chouinard and L. Annable (1986) Clonazepam in the treatment of patients with recurrent panic attacks. *J Clin Psychiatry*. **47**, 83-5.

Beaulieu, J. M. and R. R. Gainetdinov (2011) The physiology, signaling, and pharmacology of dopamine receptors. *Pharmacol Rev*. **63**, 182-217.

Bedecs, K., M. Berthold and T. Bartfai (1995) Galanin--10 years with a neuroendocrine peptide. *Int J Biochem Cell Biol*. **27**, 337-49.

Ben-Shahar, O., P. Keeley, M. Cook, W. Brake, M. Joyce, M. Nyffeler, R. Heston and A. Ettenberg (2007) Changes in levels of D1, D2, or NMDA receptors during withdrawal from brief or extended daily access to IV cocaine. *Brain Res*. **1131**, 220-8.

Benkirane, M., D. Y. Jin, R. F. Chun, R. A. Koup and K. T. Jeang (1997) Mechanism of transdominant inhibition of CCR5-mediated HIV-1 infection by ccr5delta32. *J Biol Chem*. **272**, 30603-6.

Bertolino, A., L. Fazio, A. Di Giorgio, G. Blasi, R. Romano, P. Taurisano, G. Caforio, L. Sinibaldi, G. Ursini, T. Popolizio, E. Tirotta, A. Papp, B. Dallapiccola, E. Borrelli and W. Sadee (2009) Genetically determined interaction between the dopamine transporter and the D2 receptor on prefronto-striatal activity and volume in humans. *J Neurosci*. **29**, 1224-34.

Bertran-Gonzalez, J., C. Bosch, M. Maroteaux, M. Matamales, D. Herve, E. Valjent and J. A. Girault (2008) Opposing patterns of signaling activation in dopamine D1 and D2 receptor-expressing striatal neurons in response to cocaine and haloperidol. *J Neurosci*. **28**, 5671-85.

Beuming, T., J. Kniazeff, M. L. Bergmann, L. Shi, L. Gracia, K. Raniszewska, A. H. Newman, J. A. Javitch, H. Weinstein, U. Gether and C. J. Loland (2008) The binding sites for cocaine and dopamine in the dopamine transporter overlap. *Nat Neurosci*. **11**, 780-9.

Binda, A. V., N. Kabbani, R. Lin and R. Levenson (2002) D2 and D3 dopamine receptor cell surface localization mediated by interaction with protein 4.1N. *Mol Pharmacol*. **62**, 507-13.

Bloomquist, B. T., M. R. Beauchamp, L. Zhelnin, S. E. Brown, A. R. Gore-Willse, P. Gregor and L. J. Cornfield (1998) Cloning and expression of the human galanin receptor GalR2. *Biochem Biophys Res Commun*. **243**, 474-9.

Bofill-Cardona, E., O. Kudlacek, Q. Yang, H. Ahorn, M. Freissmuth and C. Nanoff (2000) Binding of calmodulin to the D2-dopamine receptor reduces receptor signaling by arresting the G protein activation switch. *J Biol Chem*. **275**, 32672-80.

Bohm, S. K., E. F. Grady and N. W. Bunnett (1997) Regulatory mechanisms that modulate signalling by G-protein-coupled receptors. *Biochem J*. **322 (Pt 1)**, 1-18.

Bongers, G., R. A. Bakker and R. Leurs (2007a) Molecular aspects of the histamine H3 receptor. *Biochem Pharmacol*. **73**, 1195-204.

Bongers, G., K. M. Krueger, T. R. Miller, J. L. Baranowski, B. R. Estvander, D. G. Witte, M. I. Strakhova, P. van Meer, R. A. Bakker, M. D. Cowart, A. A. Hancock, T. A. Esbenshade and R. Leurs (2007b) An 80-amino acid deletion in the third intracellular loop of a naturally occurring human histamine H3 isoform confers pharmacological differences and constitutive activity. *J Pharmacol Exp Ther*. **323**, 888-98.

Bongers, G., T. Sallmen, M. B. Passani, C. Mariottini, D. Wendelin, A. Lozada, A. Marle, M. Navis, P. Blandina, R. A. Bakker, P. Panula and R. Leurs (2007c) The Akt/GSK-3beta axis as a new signaling pathway of the histamine H(3) receptor. *J Neurochem*. **103**, 248-58.

Borjigin, J. and J. Deng (2000) Madame Curie Bioscience Database. *Ed. Landes Bioscience, Austin Texas, EEUU*.

Borjigin, J., X. Li and S. H. Snyder (1999) The pineal gland and melatonin: molecular and pharmacologic regulation. *Annu Rev Pharmacol Toxicol*. **39**, 53-65.

Borowsky, B., M. W. Walker, L. Y. Huang, K. A. Jones, K. E. Smith, J. Bard, T. A. Branchek and C. Gerald (1998) Cloning and characterization of the human galanin GALR2 receptor. *Peptides*. **19**, 1771-81.

Boulay, F. and M. J. Rabiet (2005) The chemoattractant receptors FPR and C5aR: same functions--different fates. *Traffic*. **6**, 83-6.

Bouvier, M. (2001) Oligomerization of G-protein-coupled transmitter receptors. *Nat Rev Neurosci*. **2**, 274-86.

Bouvier, M., N. Heveker, R. Jockers, S. Marullo and G. Milligan (2007) BRET analysis of GPCR oligomerization: newer does not mean better. *Nat Methods*. **4**, 3-4; author reply 4.

Bradberry, C. W. (2000) Acute and chronic dopamine dynamics in a nonhuman primate model of recreational cocaine use. *J Neurosci*. **20**, 7109-15.

Brady, A. E. and L. E. Limbird (2002) G protein-coupled receptor interacting proteins: emerging roles in localization and signal transduction. *Cell Signal*. **14**, 297-309.

Brami-Cherrier, K., E. Valjent, M. Garcia, C. Pages, R. A. Hipskind and J. Caboche (2002) Dopamine induces a PI3-kinase-independent activation of Akt in striatal neurons: a new route to cAMP response element-binding protein phosphorylation. *J Neurosci*. **22**, 8911-21.

Branchek, T., K. E. Smith and M. W. Walker (1998) Molecular biology and pharmacology of galanin receptors. *Ann N Y Acad Sci*. **863**, 94-107.

Branchek, T. A., K. E. Smith, C. Gerald and M. W. Walker (2000) Galanin receptor subtypes. *Trends Pharmacol Sci*. **21**, 109-17.

Bridges, T. M. and C. W. Lindsley (2008) G-protein-coupled receptors: from classical modes of modulation to allosteric mechanisms. *ACS Chem Biol*. **3**, 530-41.

Brock, C., N. Oueslati, S. Soler, L. Boudier, P. Rondard and J. P. Pin (2007) Activation of a dimeric metabotropic glutamate receptor by intersubunit rearrangement. *J Biol Chem*. **282**, 33000-8.

Brown, R. E. and H. L. Haas (1999) On the mechanism of histaminergic inhibition of glutamate release in the rat dentate gyrus. *J Physiol*. **515 (Pt 3)**, 777-86.

Brown, R. E., D. R. Stevens and H. L. Haas (2001) The physiology of brain histamine. *Prog Neurobiol*. **63**, 637-72.

Brzostowski, J. A. and A. R. Kimmel (2001) Signaling at zero G: G-protein-independent functions for 7-TM receptors. *Trends Biochem Sci*. **26**, 291-7.

Bulenger, S., S. Marullo and M. Bouvier (2005) Emerging role of homo- and heterodimerization in G-protein-coupled receptor biosynthesis and maturation. *Trends Pharmacol Sci*. **26**, 131-7.

Bunzow, J. R., H. H. Van Tol, D. K. Grandy, P. Albert, J. Salon, M. Christie, C. A. Machida, K. A. Neve and O. Civelli (1988) Cloning and expression of a rat D2 dopamine receptor cDNA. *Nature*. **336**, 783-7.

Burgevin, M. C., I. Loquet, D. Quarteronet and E. Habert-Ortoli (1995) Cloning, pharmacological characterization, and anatomical distribution of a rat cDNA encoding for a galanin receptor. *J Mol Neurosci*. **6**, 33-41.

Burgueño, J., C. Enrich, E. I. Canela, J. Mallol, C. Lluis, R. Franco and F. Ciruela (2003) Metabotropic glutamate type 1alpha receptor localizes in low-density caveolin-rich plasma membrane fractions. *J Neurochem*. **86**, 785-91.

Burgueño, J., R. Franco and F. Ciruela (2007) Antidepressants, Antipsychotics and Anxiolytics. Neurobiological Aspects of Attention Deficit and Hyperactivity Disorders. *H. Buschmann, J.L. Díaz, J. Holenz, A. Párraga, A. Torrens and J.M. Vela. Wiley-VCF*. **2**.

Bylund, D. B., D. C. Eikenberg, J. P. Hieble, S. Z. Langer, R. J. Lefkowitz, K. P. Minneman, P. B. Molinoff, R. R. Ruffolo, Jr. and U. Trendelenburg (1994) International Union of Pharmacology nomenclature of adrenoceptors. *Pharmacol Rev*. **46**, 121-36.

Caine, S. B., S. S. Negus, N. K. Mello and J. Bergman (1999) Effects of dopamine D(1-like) and D(2-like) agonists in rats that self-administer cocaine. *J Pharmacol Exp Ther*. **291**, 353-60.

Caine, S. B., S. S. Negus, N. K. Mello, S. Patel, L. Bristow, J. Kulagowski, D. Vallone, A. Saiardi and E. Borrelli (2002) Role of dopamine D2-like receptors in cocaine self-administration: studies with D2 receptor mutant mice and novel D2 receptor antagonists. *J Neurosci*. **22**, 2977-88.

Canals, M., J. Burgueño, D. Marcellino, N. Cabello, E. I. Canela, J. Mallol, L. Agnati, S. Ferré, M. Bouvier, K. Fuxe, F. Ciruela, C. Lluis and R. Franco (2004) Homodimerization of adenosine A2A receptors: qualitative and quantitative assessment by fluorescence and bioluminescence energy transfer. *J Neurochem*. **88**, 726-34.

Canals, M., D. Marcellino, F. Fanelli, F. Ciruela, P. de Benedetti, S. R. Goldberg, K. Neve, K. Fuxe, L. F. Agnati, A. S. Woods, S. Ferré, C. Lluis, M. Bouvier and R. Franco (2003) Adenosine A2A-dopamine D2 receptor-receptor heteromerization: qualitative and quantitative assessment by fluorescence and bioluminescence energy transfer. *J Biol Chem*. **278**, 46741-9.

Carlsson, A., N. Waters, S. Holm-Waters, J. Tedroff, M. Nilsson and M. L. Carlsson (2001) Interactions between monoamines, glutamate, and GABA in schizophrenia: new evidence. *Annu Rev Pharmacol Toxicol*. **41**, 237-60.

Carriba, P., G. Navarro, F. Ciruela, S. Ferré, V. Casadó, L. Agnati, A. Cortés, J. Mallol, K. Fuxe, E. I. Canela, C. Lluis and R. Franco (2008) Detection of heteromerization of more than two proteins by sequential BRET-FRET. *Nat Methods*. **5**, 727-33.

Carriba, P., O. Ortiz, K. Patkar, Z. Justinova, J. Stroik, A. Themann, C. Muller, A. S. Woods, B. T. Hope, F. Ciruela, V. Casadó, E. I. Canela, C. Lluis, S. R. Goldberg, R. Moratalla, R. Franco and S. Ferré (2007) Striatal adenosine A2A and cannabinoid CB1 receptors form functional heteromeric complexes that mediate the motor effects of cannabinoids. *Neuropsychopharmacology*. **32**, 2249-59.

Carte, E. T., J. T. Nigg and S. P. Hinshaw (1996) Neuropsychological functioning, motor speed, and language processing in boys with and without ADHD. *J Abnorm Child Psychol*. **24**, 481-98.

Casadó, V., A. Cortés, F. Ciruela, J. Mallol, S. Ferré, C. Lluis, E. I. Canela and R. Franco (2007) Old and new ways to calculate the affinity of agonists and antagonists interacting with G-protein-coupled monomeric and dimeric receptors: the receptor-dimer cooperativity index. *Pharmacol Ther*. **116**, 343-54.

Casadó, V., A. Cortés, J. Mallol, K. Perez-Capote, S. Ferré, C. Lluis, R. Franco and E. I. Canela (2009a) GPCR homomers and heteromers: a better choice as targets for drug development than GPCR monomers? *Pharmacol Ther*. **124**, 248-57.

Casadó, V., C. Ferrada, J. Bonaventura, E. Gracia, J. Mallol, E. I. Canela, C. Lluis, A. Cortés and R. Franco (2009b) Useful pharmacological parameters for G-protein-coupled receptor homodimers obtained from competition experiments. Agonist-antagonist binding modulation. *Biochem Pharmacol*. **78**, 1456-63.

Casadó, V., J. Mallol, E. I. Canela, C. Lluis and R. Franco (1991) The binding of [3H]R-PIA to A1 adenosine receptors produces a conversion of the high- to the low-affinity state. *FEBS Lett*. **286**, 221-4.

Castelletti, L., M. Memo, C. Missale, P. F. Spano and A. Valerio (1989) Potassium channels involved in the transduction mechanism of dopamine D2 receptors in rat lactotrophs. *J Physiol*. **410**, 251-65.

Cazaubon, S. M., F. Ramos-Morales, S. Fischer, F. Schweighoffer, A. D. Strosberg and P. O. Couraud (1994) Endothelin induces tyrosine phosphorylation and GRB2 association of Shc in astrocytes. *J Biol Chem*. **269**, 24805-9.

Centonze, D., B. Picconi, C. Baunez, E. Borrelli, A. Pisani, G. Bernardi and P. Calabresi (2002) Cocaine and amphetamine depress striatal GABAergic synaptic transmission through D2 dopamine receptors. *Neuropsychopharmacology*. **26**, 164-75.

Chausmer, A. L., G. I. Elmer, M. Rubinstein, M. J. Low, D. K. Grandy and J. L. Katz (2002) Cocaine-induced locomotor activity and cocaine discrimination in dopamine D2 receptor mutant mice. *Psychopharmacology (Berl)*. **163**, 54-61.

Chen, J. C., P. C. Chen and Y. C. Chiang (2009) Molecular mechanisms of psychostimulant addiction. *Chang Gung Med J*. **32**, 148-54.

Chen, L., C. Klass and A. Woods (2004) Syndecan-2 regulates transforming growth factor-beta signaling. *J Biol Chem*. **279**, 15715-8.

Chen, Y., D. Grall, A. E. Salcini, P. G. Pelicci, J. Pouyssegur and E. Van Obberghen-Schilling (1996) Shc adaptor proteins are key transducers of mitogenic signaling mediated by the G protein-coupled thrombin receptor. *EMBO J*. **15**, 1037-44.

Cheon, K. A., B. N. Kim and S. C. Cho (2007) Association of 4-repeat allele of the dopamine D4 receptor gene exon III polymorphism and response to methylphenidate treatment in Korean ADHD children. *Neuropsychopharmacology*. **32**, 1377-83.

Chiavegatto, S., A. G. Nasello and M. M. Bernardi (1998) Histamine and spontaneous motor activity: biphasic changes, receptors involved and participation of the striatal dopamine system. *Life Sci*. **62**, 1875-88.

Chien, E. Y., W. Liu, Q. Zhao, V. Katritch, G. W. Han, M. A. Hanson, L. Shi, A. H. Newman, J. A. Javitch, V. Cherezov and R. C. Stevens (2010) Structure of the human dopamine D3 receptor in complex with a D2/D3 selective antagonist. *Science*. **330**, 1091-5.

Chio, C. L., R. F. Drong, D. T. Riley, G. S. Gill, J. L. Slightom and R. M. Huff (1994) D4 dopamine receptor-mediated signaling events determined in transfected Chinese hamster ovary cells. *J Biol Chem*. **269**, 11813-9.

Christopoulos, A. (2002) Allosteric binding sites on cell-surface receptors: novel targets for drug discovery. *Nat Rev Drug Discov*. **1**, 198-210.

Chun, M., U. K. Liyanage, M. P. Lisanti and H. F. Lodish (1994) Signal transduction of a G protein-coupled receptor in caveolae: colocalization of endothelin and its receptor with caveolin. *Proc Natl Acad Sci U S A*. **91**, 11728-32.

Ciliax, B. J., N. Nash, C. Heilman, R. Sunahara, A. Hartney, M. Tiberi, D. B. Rye, M. G. Caron, H. B. Niznik and A. I. Levey (2000) Dopamine D(5) receptor immunolocalization in rat and monkey brain. *Synapse*. **37**, 125-45.

Ciruela, F., C. Albergaria, A. Soriano, L. Cuffi, L. Carbonell, S. Sanchez, J. Gandía and V. Fernandez-Duenas (2010) Adenosine receptors interacting proteins (ARIPs): Behind the biology of adenosine signaling. *Biochim Biophys Acta*. **1798**, 9-20.

Ciruela, F., J. Burgueno, V. Casadó, M. Canals, D. Marcellino, S. R. Goldberg, M. Bader, K. Fuxe, L. F. Agnati, C. Lluis, R. Franco, S. Ferré and A. S. Woods (2004) Combining mass spectrometry and pull-down techniques for the study of receptor heteromerization. Direct epitope-epitope electrostatic interactions between adenosine A2A and dopamine D2 receptors. *Anal Chem*. **76**, 5354-63.

Ciruela, F., L. Canela, J. Burgueno, A. Soriguera, N. Cabello, E. I. Canela, V. Casadó, A. Cortés, J. Mallol, A. S. Woods, S. Ferré, C. Lluis and R. Franco (2005) Heptaspanning membrane receptors and cytoskeletal/scaffolding proteins: focus on adenosine, dopamine, and metabotropic glutamate receptor function. *J Mol Neurosci*. **26**, 277-92.

Ciruela, F., V. Casadó, R. J. Rodrigues, R. Lujan, J. Burgueno, M. Canals, J. Borycz, N. Rebola, S. R. Goldberg, J. Mallol, A. Cortés, E. I. Canela, J. F. Lopez-Gimenez, G. Milligan, C. Lluis, R. A. Cunha, S. Ferré and R. Franco (2006) Presynaptic control of striatal glutamatergic neurotransmission by adenosine A1-A2A receptor heteromers. *J Neurosci*. **26**, 2080-7.

Civelli, O., J. R. Bunzow and D. K. Grandy (1993) Molecular diversity of the dopamine receptors. *Annu Rev Pharmacol Toxicol*. **33**, 281-307.

Claing, A., S. J. Perry, M. Achiriloaie, J. K. Walker, J. P. Albanesi, R. J. Lefkowitz and R. T. Premont (2000) Multiple endocytic pathways of G protein-coupled receptors delineated by GIT1 sensitivity. *Proc Natl Acad Sci U S A*. **97**, 1119-24.

Clifford, J. J. and J. L. Waddington (2000) Topographically based search for an "Ethogram" among a series of novel D(4) dopamine receptor agonists and antagonists. *Neuropsychopharmacology*. **22**, 538-44.

Cobos, E. J., J. M. Entrena, F. R. Nieto, C. M. Cendan and E. Del Pozo (2008) Pharmacology and therapeutic potential of sigma(1) receptor ligands. *Curr Neuropharmacol*. **6**, 344-66.

Cogé, F., S. P. Guenin, V. Audinot, A. Renouard-Try, P. Beauverger, C. Macia, C. Ouvry, N. Nagel, H. Rique, J. A. Boutin and J. P. Galizzi (2001) Genomic organization and characterization of splice variants of the human histamine H3 receptor. *Biochem J*. **355**, 279-88.

Colpaert, F. C., C. J. Niemegeers and P. A. Janssen (1978) Discriminative stimulus properties of cocaine and d-amphetamine, and antagonism by haloperidol: a comparative study. *Neuropharmacology*. **17**, 937-42.

Cooper, J. R., F. E. Bloom and R. H. Roth (1996) The biochemical basis of neuropharmacology. *7th Ed. New York/Oxford, Oxford University Press*, 293-351.

Corrigall, W. A. and K. M. Coen (1991) Cocaine self-administration is increased by both D1 and D2 dopamine antagonists. *Pharmacol Biochem Behav*. **39**, 799-802.

Costa, T. and A. Herz (1989) Antagonists with negative intrinsic activity at delta opioid receptors coupled to GTP-binding proteins. *Proc Natl Acad Sci U S A*. **86**, 7321-5.

Cotecchia, S. (2010) The alpha1-adrenergic receptors: diversity of signaling networks and regulation. *J Recept Signal Transduct Res*. **30**, 410-9.

Counts, S. E., S. E. Perez and E. J. Mufson (2008) Galanin in Alzheimer's disease: neuroinhibitory or neuroprotective? *Cell Mol Life Sci*. **65**, 1842-53.

Crawley, J. N. (1996) Minireview. Galanin-acetylcholine interactions: relevance to memory and Alzheimer's disease. *Life Sci*. **58**, 2185-99.

Crawley, J. N. (1999) The role of galanin in feeding behavior. *Neuropeptides*. **33**, 369-75.

Crespo, P., T. G. Cachero, N. Xu and J. S. Gutkind (1995) Dual effect of beta-adrenergic receptors on mitogen-activated protein kinase. Evidence for a beta gamma-dependent activation and a G alpha s-cAMP-mediated inhibition. *J Biol Chem*. **270**, 25259-65.

Cristóvão-Ferreira, S., G. Navarro, M. Brugarolas, K. Pérez-Capote, S. H. Vaz, G. Fattorini, F. Conti, C. Lluis, J. A. Ribeiro, P. J. McCormick, V. Casadó, R. Franco and A. M. Sebastião (2011) Modulation of GABA transport by adenosine A1R-A2AR heteromers, which are coupled to both Gs- and G(i/o)-proteins. *J Neurosci*. **31**, 15629-39.

Curran, S., J. Mill, E. Tahir, L. Kent, S. Richards, A. Gould, L. Huckett, J. Sharp, C. Batten, S. Fernando, F. Ozbay, Y. Yazgan, E. Simonoff, M. Thompson, E. Taylor and P. Asherson (2001) Association study of a dopamine transporter polymorphism and attention deficit hyperactivity disorder in UK and Turkish samples. *Mol Psychiatry*. **6**, 425-8.

Cvejic, S. and L. A. Devi (1997) Dimerization of the delta opioid receptor: implication for a role in receptor internalization. *J Biol Chem*. **272**, 26959-64.

Daaka, Y., L. M. Luttrell, S. Ahn, G. J. Della Rocca, S. S. Ferguson, M. G. Caron and R. J. Lefkowitz (1998) Essential role for G protein-coupled receptor endocytosis in the activation of mitogen-activated protein kinase. *J Biol Chem*. **273**, 685-8.

Dai, H., Q. Fu, Y. Shen, W. Hu, Z. Zhang, H. Timmerman, R. Leurs and Z. Chen (2007) The histamine H3 receptor antagonist clobenpropit enhances GABA release to protect against NMDA-induced excitotoxicity through the cAMP/protein kinase A pathway in cultured cortical neurons. *Eur J Pharmacol*. **563**, 117-23.

Dal Toso, R., B. Sommer, M. Ewert, A. Herb, D. B. Pritchett, A. Bach, B. D. Shivers and P. H. Seeburg (1989) The dopamine D2 receptor: two molecular forms generated by alternative splicing. *EMBO J*. **8**, 4025-34.

Dale, M. (2000) Sistema nervioso central: Otros neurotransmisores y neuromoduladores: Dopamina. *Farmacología Ed Harcourt, 4ª edición, Barcelona*, 517-535.

Dalley, J. W. and B. J. Everitt (2009) Dopamine receptors in the learning, memory and drug reward circuitry. *Semin Cell Dev Biol*. **20**, 403-10.

Damian, M., A. Martin, D. Mesnier, J. P. Pin and J. L. Baneres (2006) Asymmetric conformational changes in a GPCR dimer controlled by G-proteins. *EMBO J*. **25**, 5693-702.

Daubner, S. C., T. Le and S. Wang (2011) Tyrosine hydroxylase and regulation of dopamine synthesis. *Arch Biochem Biophys*. **508**, 1-12.

Davis, R. J. (1995) Transcriptional regulation by MAP kinases. *Mol Reprod Dev*. **42**, 459-67.

De, A. (2011) The new era of bioluminescence resonance energy transfer technology. *Curr Pharm Biotechnol*. **12**, 558-68.

de Boer, S. F., M. Lesourd, E. Mocaer and J. M. Koolhaas (1999) Selective antiaggressive effects of alnespirone in resident-intruder test are mediated via 5-hydroxytryptamine1A receptors: A comparative pharmacological study with 8-hydroxy-2-dipropylaminotetralin, ipsapirone, buspirone, eltoprazine, and WAY-100635. *J Pharmacol Exp Ther*. **288**, 1125-33.

de Esch, I. J., R. L. Thurmond, A. Jongejan and R. Leurs (2005) The histamine H4 receptor as a new therapeutic target for inflammation. *Trends Pharmacol Sci*. **26**, 462-9.

De Keyser, J., H. Walraevens, J. P. De Backer, G. Ebinger and G. Vauquelin (1989) D2 dopamine receptors in the human brain: heterogeneity based on differences in guanine nucleotide effect on agonist binding, and their presence on corticostriatal nerve terminals. *Brain Res*. **484**, 36-42.

De Mei, C., M. Ramos, C. Iitaka and E. Borrelli (2009) Getting specialized: presynaptic and postsynaptic dopamine D2 receptors. *Curr Opin Pharmacol*. **9**, 53-8.

De Wit, H. and R. A. Wise (1977) Blockade of cocaine reinforcement in rats with the dopamine receptor blocker pimozide, but not with the noradrenergic blockers phentolamine or phenoxybenzamine. *Can J Psychol*. **31**, 195-203.

Dearry, A., J. A. Gingrich, P. Falardeau, R. T. Fremeau, Jr., M. D. Bates and M. G. Caron (1990) Molecular cloning and expression of the gene for a human D1 dopamine receptor. *Nature*. **347**, 72-6.

DeBoer, P. and E. D. Abercrombie (1996) Physiological release of striatal acetylcholine in vivo: modulation by D1 and D2 dopamine receptor subtypes. *J Pharmacol Exp Ther*. **277**, 775-83.

DeFea, K. A., Z. D. Vaughn, E. M. O'Bryan, D. Nishijima, O. Dery and N. W. Bunnett (2000a) The proliferative and antiapoptotic effects of substance P are facilitated by formation of a beta - arrestin-dependent scaffolding complex. *Proc Natl Acad Sci U S A*. **97**, 11086-91.

DeFea, K. A., J. Zalevsky, M. S. Thoma, O. Dery, R. D. Mullins and N. W. Bunnett (2000b) beta-arrestin-dependent endocytosis of proteinase-activated receptor 2 is required for intracellular targeting of activated ERK1/2. *J Cell Biol*. **148**, 1267-81.

Degroot, A. and D. Treit (2004) Anxiety is functionally segregated within the septo-hippocampal system. *Brain Res*. **1001**, 60-71.

Del Valle, J. and I. Gantz (1997) Novel insights into histamine H2 receptor biology. *Am J Physiol*. **273**, G987-96.

Delgado, P. L. and F. A. Moreno (2000) Role of norepinephrine in depression. *J Clin Psychiatry*. **61 Suppl 1**, 5-12.

Demchyshyn, L. L., K. S. Sugamori, F. J. Lee, S. A. Hamadanizadeh and H. B. Niznik (1995) The dopamine D1D receptor. Cloning and characterization of three pharmacologically distinct D1-like receptors from Gallus domesticus. *J Biol Chem*. **270**, 4005-12.

Devi, L. A. (2001) Heterodimerization of G-protein-coupled receptors: pharmacology, signaling and trafficking. *Trends Pharmacol Sci*. **22**, 532-7.

Dickinson, S. D., J. Sabeti, G. A. Larson, K. Giardina, M. Rubinstein, M. A. Kelly, D. K. Grandy, M. J. Low, G. A. Gerhardt and N. R. Zahniser (1999) Dopamine D2 receptor-deficient mice exhibit decreased dopamine transporter function but no changes in dopamine release in dorsal striatum. *J Neurochem*. **72**, 148-56.

Ding, W., H. Zou, J. Dai and Z. Duan (2005) Combining restriction digestion and touchdown PCR permits detection of trace isoforms of histamine H3 receptor. *Biotechniques*. **39**, 841-5.

Ding, X., D. MacTavish, S. Kar and J. H. Jhamandas (2006) Galanin attenuates beta-amyloid (Abeta) toxicity in rat cholinergic basal forebrain neurons. *Neurobiol Dis*. **21**, 413-20.

Ding, Y. C., H. C. Chi, D. L. Grady, A. Morishima, J. R. Kidd, K. K. Kidd, P. Flodman, M. A. Spence, S. Schuck, J. M. Swanson, Y. P. Zhang and R. K. Moyzis (2002) Evidence of positive selection acting at the human dopamine receptor D4 gene locus. *Proc Natl Acad Sci U S A*. **99**, 309-14.

Dohlman, H. G., M. G. Caron and R. J. Lefkowitz (1987) A family of receptors coupled to guanine nucleotide regulatory proteins. *Biochemistry*. **26**, 2657-64.

Dolmetsch, R. E., U. Pajvani, K. Fife, J. M. Spotts and M. E. Greenberg (2001) Signaling to the nucleus by an L-type calcium channel-calmodulin complex through the MAP kinase pathway. *Science*. **294**, 333-9.

Doreulee, N., Y. Yanovsky, I. Flagmeyer, D. R. Stevens, H. L. Haas and R. E. Brown (2001) Histamine H(3) receptors depress synaptic transmission in the corticostriatal pathway. *Neuropharmacology*. **40**, 106-13.

Drutel, G., N. Peitsaro, K. Karlstedt, K. Wieland, M. J. Smit, H. Timmerman, P. Panula and R. Leurs (2001) Identification of rat H3 receptor isoforms with different brain expression and signaling properties. *Mol Pharmacol*. **59**, 1-8.

Durroux, T. (2005) Principles: a model for the allosteric interactions between ligand binding sites within a dimeric GPCR. *Trends Pharmacol Sci*. **26**, 376-84.

Eisenberg, J., A. Zohar, G. Mei-Tal, A. Steinberg, E. Tartakovsky, I. Gritsenko, L. Nemanov and R. P. Ebstein (2000) A haplotype relative risk study of the dopamine D4 receptor (DRD4) exon III repeat polymorphism and attention deficit hyperactivity disorder (ADHD). *Am J Med Genet*. **96**, 258-61.

Elliott-Hunt, C. R., R. J. Pope, P. Vanderplank and D. Wynick (2007) Activation of the galanin receptor 2 (GalR2) protects the hippocampus from neuronal damage. *J Neurochem*. **100**, 780-9.

Elliott, M. E., T. L. Goodfriend, D. L. Ball and C. R. Jefcoate (1997) Angiotensin-responsive adrenal glomerulosa cell proteins: characterization by protease mapping, species comparison, and specific angiotensin receptor antagonists. *Endocrinology*. **138**, 2530-6.

Ellis, J., J. D. Pediani, M. Canals, S. Milasta and G. Milligan (2006) Orexin-1 receptor-cannabinoid CB1 receptor heterodimerization results in both ligand-dependent and -independent coordinated alterations of receptor localization and function. *J Biol Chem*. **281**, 38812-24.

Elmer, G. I., J. O. Pieper, J. Levy, M. Rubinstein, M. J. Low, D. K. Grandy and R. A. Wise (2005) Brain stimulation and morphine reward deficits in dopamine D2 receptor-deficient mice. *Psychopharmacology (Berl)*. **182**, 33-44.

Elsworth, J. D. and R. H. Roth (1997) Dopamine synthesis, uptake, metabolism, and receptors: relevance to gene therapy of Parkinson's disease. *Exp Neurol*. **144**, 4-9.

Enjalbert, A., F. Sladeczek, G. Guillon, P. Bertrand, C. Shu, J. Epelbaum, A. Garcia-Sainz, S. Jard, C. Lombard, C. Kordon and et al. (1986) Angiotensin II and dopamine modulate both cAMP and inositol phosphate productions in anterior pituitary cells. Involvement in prolactin secretion. *J Biol Chem*. **261**, 4071-5.

Escriche, M., J. Burgueno, F. Ciruela, E. I. Canela, J. Mallol, C. Enrich, C. Lluis and R. Franco (2003) Ligand-induced caveolae-mediated internalization of A1 adenosine receptors: morphological evidence of endosomal sorting and receptor recycling. *Exp Cell Res*. **285**, 72-90.

Esler, M., G. Lambert, H. P. Brunner-La Rocca, G. Vaddadi and D. Kaye (2003) Sympathetic nerve activity and neurotransmitter release in humans: translation from pathophysiology into clinical practice. *Acta Physiol Scand*. **177**, 275-84.

Evans, H. F. and J. Shine (1991) Human galanin: molecular cloning reveals a unique structure. *Endocrinology*. **129**, 1682-4.

Everitt, B. J. and T. W. Robbins (2005) Neural systems of reinforcement for drug addiction: from actions to habits to compulsion. *Nat Neurosci*. **8**, 1481-9.

Fan, T., G. Varghese, T. Nguyen, R. Tse, B. F. O'Dowd and S. R. George (2005) A role for the distal carboxyl tails in generating the novel pharmacology and G protein activation profile of mu and delta opioid receptor hetero-oligomers. *J Biol Chem*. **280**, 38478-88.

Faraone, S. V. and A. E. Doyle (2001) The nature and heritability of attention-deficit/hyperactivity disorder. *Child Adolesc Psychiatr Clin N Am*. **10**, 299-316, VIII-IX.

Faraone, S. V., R. H. Perlis, A. E. Doyle, J. W. Smoller, J. J. Goralnick, M. A. Holmgren and P. Sklar (2005) Molecular genetics of attention-deficit/hyperactivity disorder. *Biol Psychiatry*. **57**, 1313-23.

Fathi, Z., P. M. Battaglino, L. G. Iben, H. Li, E. Baker, D. Zhang, R. McGovern, C. D. Mahle, G. R. Sutherland, T. P. Iismaa, K. E. Dickinson and I. A. Zimanyi (1998) Molecular characterization, pharmacological properties and chromosomal localization of the human GALR2 galanin receptor. *Brain Res Mol Brain Res*. **58**, 156-69.

Fathi, Z., A. M. Cunningham, L. G. Iben, P. B. Battaglino, S. A. Ward, K. A. Nichol, K. A. Pine, J. Wang, M. E. Goldstein, T. P. Iismaa and I. A. Zimanyi (1997) Cloning, pharmacological characterization and distribution of a novel galanin receptor. *Brain Res Mol Brain Res*. **51**, 49-59.

Faure, M., T. A. Voyno-Yasenetskaya and H. R. Bourne (1994) cAMP and beta gamma subunits of heterotrimeric G proteins stimulate the mitogen-activated protein kinase pathway in COS-7 cells. *J Biol Chem*. **269**, 7851-4.

Felder, C. C., P. A. Jose and J. Axelrod (1989) The dopamine-1 agonist, SKF 82526, stimulates phospholipase-C activity independent of adenylate cyclase. *J Pharmacol Exp Ther*. **248**, 171-5.

Ferguson, S. S. (2001) Evolving concepts in G protein-coupled receptor endocytosis: the role in receptor desensitization and signaling. *Pharmacol Rev*. **53**, 1-24.

Fernandez-Novoa, L. and R. Cacabelos (2001) Histamine function in brain disorders. *Behav Brain Res*. **124**, 213-33.

Ferrada, C., S. Ferré, V. Casadó, A. Cortés, Z. Justinova, C. Barnes, E. I. Canela, S. R. Goldberg, R. Leurs, C. Lluis and R. Franco (2008) Interactions between histamine H3 and dopamine D2 receptors and the implications for striatal function. *Neuropharmacology*. **55**, 190-7.

Ferré, S., R. Baler, M. Bouvier, M. G. Caron, L. A. Devi, T. Durroux, K. Fuxe, S. R. George, J. A. Javitch, M. J. Lohse, K. Mackie, G. Milligan, K. D. Pfleger, J. P. Pin, N. D. Volkow, M. Waldhoer, A. S. Woods and R. Franco (2009) Building a new conceptual framework for receptor heteromers. *Nat Chem Biol*. **5**, 131-4.

Ferré, S., F. Ciruela, A. S. Woods, C. Lluis and R. Franco (2007) Functional relevance of neurotransmitter receptor heteromers in the central nervous system. *Trends Neurosci*. **30**, 440-6.

Ferré, S., L. Gimenez-Llort, F. Artigas and E. Martinez (1994) Motor activation in short- and long-term reserpinized mice: role of N-methyl-D-aspartate, dopamine D1 and dopamine D2 receptors. *Eur J Pharmacol*. **255**, 203-13.

Ferré, S., M. Herrera-Marschitz, M. Grabowska-Anden, U. Ungerstedt, M. Casas and N. E. Anden (1991a) Postsynaptic dopamine/adenosine interaction: I. Adenosine analogues inhibit dopamine D2-mediated behaviour in short-term reserpinized mice. *Eur J Pharmacol*. **192**, 25-30.

Ferré, S., M. Karcz-Kubicha, B. T. Hope, P. Popoli, J. Burgueno, M. A. Gutierrez, V. Casadó, K. Fuxe, S. R. Goldberg, C. Lluis, R. Franco and F. Ciruela (2002) Synergistic interaction between adenosine A2A and glutamate mGlu5 receptors: implications for striatal neuronal function. *Proc Natl Acad Sci U S A*. **99**, 11940-5.

Ferré, S., G. Navarro, V. Casadó, A. Cortés, J. Mallol, E. I. Canela, C. Lluis and R. Franco (2010) G protein-coupled receptor heteromers as new targets for drug development. *Prog Mol Biol Transl Sci*. **91**, 41-52.

Ferré, S., G. von Euler, B. Johansson, B. B. Fredholm and K. Fuxe (1991b) Stimulation of high-affinity adenosine A2 receptors decreases the affinity of dopamine D2 receptors in rat striatal membranes. *Proc Natl Acad Sci U S A*. **88**, 7238-41.

Filbey, F. M., L. Ray, A. Smolen, E. D. Claus, A. Audette and K. E. Hutchison (2008) Differential neural response to alcohol priming and alcohol taste cues is associated with DRD4 VNTR and OPRM1 genotypes. *Alcohol Clin Exp Res*. **32**, 1113-23.

Filipek, S., K. A. Krzysko, D. Fotiadis, Y. Liang, D. A. Saperstein, A. Engel and K. Palczewski (2004) A concept for G protein activation by G protein-coupled receptor dimers: the transducin/rhodopsin interface. *Photochem Photobiol Sci*. **3**, 628-38.

Fillenz, M. (1990) Regulation of catecholamine synthesis: Multiple mechanisms and their significance. *Neurochem Int*. **17**, 303-20.

Filteau, F., F. Veilleux and D. Levesque (1999) Effects of reciprocal chimeras between the C-terminal portion of third intracellular loops of the human dopamine D2 and D3 receptors. *FEBS Lett*. **447**, 251-6.

Filtz, T. M., R. P. Artymyshyn, W. Guan and P. B. Molinoff (1993) Paradoxical regulation of dopamine receptors in transfected 293 cells. *Mol Pharmacol*. **44**, 371-9.

Fisone, G., C. F. Wu, S. Consolo, O. Nordstrom, N. Brynne, T. Bartfai, T. Melander and T. Hokfelt (1987) Galanin inhibits acetylcholine release in the ventral hippocampus of the rat: histochemical, autoradiographic, in vivo, and in vitro studies. *Proc Natl Acad Sci U S A*. **84**, 7339-43.

Fitzgerald, L. W., J. P. Patterson, D. S. Conklin, R. Horlick and B. L. Largent (1998) Pharmacological and biochemical characterization of a recombinant human galanin GALR1 receptor: agonist character of chimeric galanin peptides. *J Pharmacol Exp Ther*. **287**, 448-56.

Floet, A. M., C. Scheiner and L. Grossman (2010) Attention-deficit/hyperactivity disorder. *Pediatr Rev*. **31**, 56-69.

Flórez, J. and A. Pazos (2003) Neurotransmisión en el sistema nervioso central. *Farmacología Humana, Flórez J, Armijo JA, Mediavilla A. Ed Masson 4ª edición, Barcelona*, 435-460.

Fontanilla, D., M. Johannessen, A. R. Hajipour, N. V. Cozzi, M. B. Jackson and A. E. Ruoho (2009) The hallucinogen N,N-dimethyltryptamine (DMT) is an endogenous sigma-1 receptor regulator. *Science*. **323**, 934-7.

Förster, T. (1948) Intermolecular energy migration and fluorescence. *Ann. Phys.* **2**, 55-75.

Fotiadis, D., Y. Liang, S. Filipek, D. A. Saperstein, A. Engel and K. Palczewski (2003) Atomic-force microscopy: Rhodopsin dimers in native disc membranes. *Nature*. **421**, 127-8.

Fotiadis, D., Y. Liang, S. Filipek, D. A. Saperstein, A. Engel and K. Palczewski (2004) The G protein-coupled receptor rhodopsin in the native membrane. *FEBS Lett*. **564**, 281-8.

Franco, R. (2009) G-protein-coupled receptor heteromers or how neurons can display differently flavoured patterns in response to the same neurotransmitter. *Br J Pharmacol*. **158**, 23-31.

Franco, R., M. Canals, D. Marcellino, S. Ferré, L. Agnati, J. Mallol, V. Casadó, F. Ciruela, K. Fuxe, C. Lluis and E. I. Canela (2003) Regulation of heptaspanning-membrane-receptor function by dimerization and clustering. *Trends Biochem Sci*. **28**, 238-43.

Franco, R., V. Casadó, F. Ciruela, J. Mallol, C. Lluis and E. I. Canela (1996) The cluster-arranged cooperative model: a model that accounts for the kinetics of binding to A1 adenosine receptors. *Biochemistry*. **35**, 3007-15.

Franco, R., V. Casadó, A. Cortés, C. Ferrada, J. Mallol, A. Woods, C. Lluis, E. I. Canela and S. Ferré (2007a) Basic concepts in G-protein-coupled receptor homo- and heterodimerization. *ScientificWorldJournal*. **7**, 48-57.

Franco, R., V. Casadó, A. Cortés, J. Mallol, F. Ciruela, S. Ferré, C. Lluis and E. I. Canela (2008a) G-protein-coupled receptor heteromers: function and ligand pharmacology. *Br J Pharmacol*. **153 Suppl 1**, S90-8.

Franco, R., V. Casadó, A. Cortés, K. Perez-Capote, J. Mallol, E. Canela, S. Ferré and C. Lluis (2008b) Novel pharmacological targets based on receptor heteromers. *Brain Res Rev*. **58**, 475-82.

Franco, R., V. Casadó, J. Mallol, C. Ferrada, S. Ferré, K. Fuxe, A. Cortés, F. Ciruela, C. Lluis and E. I. Canela (2006) The two-state dimer receptor model: a general model for receptor dimers. *Mol Pharmacol*. **69**, 1905-12.

Franco, R., V. Casadó, J. Mallol, S. Ferré, K. Fuxe, A. Cortés, F. Ciruela, C. Lluis and E. I. Canela (2005a) Dimer-based model for heptaspanning membrane receptors. *Trends Biochem Sci*. **30**, 360-6.

Franco, R., F. Ciruela, V. Casadó, A. Cortés, E. I. Canela, J. Mallol, L. F. Agnati, S. Ferré, K. Fuxe and C. Lluis (2005b) Partners for adenosine A1 receptors. *J Mol Neurosci*. **26**, 221-32.

Franco, R., C. Lluis, E. I. Canela, J. Mallol, L. Agnati, V. Casadó, F. Ciruela, S. Ferré and K. Fuxe (2007b) Receptor-receptor interactions involving adenosine A1 or dopamine D1 receptors and accessory proteins. *J Neural Transm*. **114**, 93-104.

Fredholm, B. B., T. Hokfelt and G. Milligan (2007) G-protein-coupled receptors: an update. *Acta Physiol (Oxf)*. **190**, 3-7.

Fredriksson, R., M. C. Lagerstrom, L. G. Lundin and H. B. Schioth (2003) The G-protein-coupled receptors in the human genome form five main families. Phylogenetic analysis, paralogon groups, and fingerprints. *Mol Pharmacol*. **63**, 1256-72.

Friedman, E., L. Q. Jin, G. P. Cai, T. R. Hollon, J. Drago, D. R. Sibley and H. Y. Wang (1997) D1-like dopaminergic activation of phosphoinositide hydrolysis is independent of D1A dopamine receptors: evidence from D1A knockout mice. *Mol Pharmacol*. **51**, 6-11.

Fuentes, R., P. Petersson and M. A. Nicolelis (2010) Restoration of locomotive function in Parkinson's disease by spinal cord stimulation: mechanistic approach. *Eur J Neurosci*. **32**, 1100-8.

Fuller, R. W. and D. T. Wong (1977) Inhibition of serotonin reuptake. *Fed Proc*. **36**, 2154-8.

Fung, J. J., X. Deupi, L. Pardo, X. J. Yao, G. A. Velez-Ruiz, B. T. Devree, R. K. Sunahara and B. K. Kobilka (2009) Ligand-regulated oligomerization of beta(2)-adrenoceptors in a model lipid bilayer. *EMBO J*. **28**, 3315-28.

Fung, S. I., J. Y. Chan, D. Manzoni, S. R. White, Y. Y. Lai, H. K. Strahlendorf, H. Zhuo, R. H. Liu, V. K. Reddy and C. D. Barnes (1994) Cotransmitter-mediated locus coeruleus action on motoneurons. *Brain Res Bull*. **35**, 423-32.

Gandía, J., C. Lluis, S. Ferré, R. Franco and F. Ciruela (2008) Light resonance energy transfer-based methods in the study of G protein-coupled receptor oligomerization. *Bioessays*. **30**, 82-9.

Garcia, M., B. Floran, J. A. Arias-Montano, J. M. Young and J. Aceves (1997) Histamine H3 receptor activation selectively inhibits dopamine D1 receptor-dependent [3H]GABA release from depolarization-stimulated slices of rat substantia nigra pars reticulata. *Neuroscience*. **80**, 241-9.

Gargaglioni, L. H., L. K. Hartzler and R. W. Putnam (2010) The locus coeruleus and central chemosensitivity. *Respir Physiol Neurobiol*. **173**, 264-73.

Garland, E. M. and I. Biaggioni (2001) Genetic polymorphisms of adrenergic receptors. *Clin Auton Res*. **11**, 67-78.

Garland, E. M., M. K. Hahn, T. P. Ketch, N. R. Keller, C. H. Kim, K. S. Kim, I. Biaggioni, J. R. Shannon, R. D. Blakely and D. Robertson (2002) Genetic basis of clinical catecholamine disorders. *Ann N Y Acad Sci*. **971**, 506-14.

Garrett, R. H. and C. M. Grisham (1999) Biochemistry. *Ed. Holt Rinehart and Winston, 2ª Ed.*

Gasca-Martinez, D., A. Hernandez, A. Sierra, R. Valdiosera, V. Anaya-Martinez, B. Floran, D. Erlij and J. Aceves (2010) Dopamine inhibits GABA transmission from the globus pallidus to the thalamic reticular nucleus via presynaptic D4 receptors. *Neuroscience*. **169**, 1672-81.

Gbahou, F., A. Rouleau, S. Morisset, R. Parmentier, S. Crochet, J. S. Lin, X. Ligneau, J. Tardivel-Lacombe, H. Stark, W. Schunack, C. R. Ganellin, J. C. Schwartz and J. M. Arrang (2003) Protean agonism at histamine H3 receptors in vitro and in vivo. *Proc Natl Acad Sci U S A*. **100**, 11086-91.

Gehl, C., R. Waadt, J. Kudla, R. R. Mendel and R. Hansch (2009) New GATEWAY vectors for High Throughput Analyses of Protein-Protein Interactions by Bimolecular Fluorescence Complementation. *Mol Plant*. **2**, 1051-8.

George, S. R., T. Fan, Z. Xie, R. Tse, V. Tam, G. Varghese and B. F. O'Dowd (2000) Oligomerization of mu- and delta-opioid receptors. Generation of novel functional properties. *J Biol Chem*. **275**, 26128-35.

George, S. R., B. F. O'Dowd and S. P. Lee (2002) G-protein-coupled receptor oligomerization and its potential for drug discovery. *Nat Rev Drug Discov*. **1**, 808-20.

Gerfen, C. R. (2000) Molecular effects of dopamine on striatal-projection pathways. *Trends Neurosci*. **23**, S64-70.

Gerfen, C. R. (2004) The Rat Nervous System. *(Paxinos G ed), Elseiver Academis Press, Amsterdam*, 445-508.

Gerfen, C. R., T. M. Engber, L. C. Mahan, Z. Susel, T. N. Chase, F. J. Monsma, Jr. and D. R. Sibley (1990) D1 and D2 dopamine receptor-regulated gene expression of striatonigral and striatopallidal neurons. *Science*. **250**, 1429-32.

Gerfen, C. R., S. Miyachi, R. Paletzki and P. Brown (2002) D1 dopamine receptor supersensitivity in the dopamine-depleted striatum results from a switch in the regulation of ERK1/2/MAP kinase. *J Neurosci*. **22**, 5042-54.

Gershon, A. A., T. Vishne and L. Grunhaus (2007) Dopamine D2-like receptors and the antidepressant response. *Biol Psychiatry*. **61**, 145-53.

Gether, U. (2000) Uncovering molecular mechanisms involved in activation of G protein-coupled receptors. *Endocr Rev*. **21**, 90-113.

Ghahremani, M. H., P. Cheng, P. M. Lembo and P. R. Albert (1999) Distinct roles for Galphai2, Galphai3, and Gbeta gamma in modulation of forskolin- or Gs-mediated cAMP accumulation and calcium mobilization by dopamine D2S receptors. *J Biol Chem*. **274**, 9238-45.

Ghasemzadeh, M. B., L. C. Nelson, X. Y. Lu and P. W. Kalivas (1999) Neuroadaptations in ionotropic and metabotropic glutamate receptor mRNA produced by cocaine treatment. *J Neurochem*. **72**, 157-65.

Gilchrist, A. (2007) Modulating G-protein-coupled receptors: from traditional pharmacology to allosterics. *Trends Pharmacol Sci*. **28**, 431-7.

Gines, S., F. Ciruela, J. Burgueno, V. Casadó, E. I. Canela, J. Mallol, C. Lluis and R. Franco (2001) Involvement of caveolin in ligand-induced recruitment and internalization of A(1) adenosine receptor and adenosine deaminase in an epithelial cell line. *Mol Pharmacol*. **59**, 1314-23.

Gines, S., J. Hillion, M. Torvinen, S. Le Crom, V. Casadó, E. I. Canela, S. Rondin, J. Y. Lew, S. Watson, M. Zoli, L. F. Agnati, P. Verniera, C. Lluis, S. Ferré, K. Fuxe and R. Franco (2000) Dopamine D1 and adenosine A1 receptors form functionally interacting heteromeric complexes. *Proc Natl Acad Sci U S A*. **97**, 8606-11.

Gingrich, J. A. and M. G. Caron (1993) Recent advances in the molecular biology of dopamine receptors. *Annu Rev Neurosci*. **16**, 299-321.

Giovannini, M. G., M. Efoudebe, M. B. Passani, E. Baldi, C. Bucherelli, F. Giachi, R. Corradetti and P. Blandina (2003) Improvement in fear memory by histamine-elicited ERK2 activation in hippocampal CA3 cells. *J Neurosci*. **23**, 9016-23.

Giros, B., M. Jaber, S. R. Jones, R. M. Wightman and M. G. Caron (1996) Hyperlocomotion and indifference to cocaine and amphetamine in mice lacking the dopamine transporter. *Nature*. **379**, 606-12.

Giros, B., P. Sokoloff, M. P. Martres, J. F. Riou, L. J. Emorine and J. C. Schwartz (1989) Alternative splicing directs the expression of two D2 dopamine receptor isoforms. *Nature*. **342**, 923-6.

Goeders, N. E. and J. E. Smith (1983) Cortical dopaminergic involvement in cocaine reinforcement. *Science*. **221**, 773-5.

Golan, M., G. Schreiber and S. Avissar (2009) Antidepressants, beta-arrestins and GRKs: from regulation of signal desensitization to intracellular multifunctional adaptor functions. *Curr Pharm Des*. **15**, 1699-708.

Gomes, I., B. A. Jordan, A. Gupta, N. Trapaidze, V. Nagy and L. A. Devi (2000) Heterodimerization of mu and delta opioid receptors: A role in opiate synergy. *J Neurosci*. **20**, RC110.

Gomez-Ramirez, J., T. H. Johnston, N. P. Visanji, S. H. Fox and J. M. Brotchie (2006) Histamine H3 receptor agonists reduce L-dopa-induced chorea, but not dystonia, in the MPTP-lesioned nonhuman primate model of Parkinson's disease. *Mov Disord*. **21**, 839-46.

Gomez-Ramirez, J., J. Ortiz and I. Blanco (2002) Presynaptic H3 autoreceptors modulate histamine synthesis through cAMP pathway. *Mol Pharmacol*. **61**, 239-45.

Gonzalez-Brito, A., M. E. Troiani, A. Menendez-Pelaez, M. J. Delgado and R. J. Reiter (1990) mRNA transcription determines the lag period for the induction of pineal melatonin synthesis in the Syrian hamster pineal gland. *J Cell Biochem*. **44**, 55-60.

Gonzalez-Maeso, J., R. L. Ang, T. Yuen, P. Chan, N. V. Weisstaub, J. F. Lopez-Gimenez, M. Zhou, Y. Okawa, L. F. Callado, G. Milligan, J. A. Gingrich, M. Filizola, J. J. Meana and S. C. Sealfon (2008) Identification of a serotonin/glutamate receptor complex implicated in psychosis. *Nature*. **452**, 93-7.

Goodchild, R. E., J. A. Court, I. Hobson, M. A. Piggott, R. H. Perry, P. Ince, E. Jaros and E. K. Perry (1999) Distribution of histamine H3-receptor binding in the normal human basal ganglia: comparison with Huntington's and Parkinson's disease cases. *Eur J Neurosci*. **11**, 449-56.

Goudet, C., J. Kniazeff, V. Hlavackova, F. Malhaire, D. Maurel, F. Acher, J. Blahos, L. Prezeau and J. P. Pin (2005) Asymmetric functioning of dimeric metabotropic glutamate receptors disclosed by positive allosteric modulators. *J Biol Chem*. **280**, 24380-5.

Gouldson, P. R., C. Higgs, R. E. Smith, M. K. Dean, G. V. Gkoutos and C. A. Reynolds (2000) Dimerization and domain swapping in G-protein-coupled receptors: a computational study. *Neuropsychopharmacology*. **23**, S60-77.

Gracia, E., A. Cortés, J. J. Meana, J. Garcia-Sevilla, M. S. Herhsfield, E. I. Canela, J. Mallol, C. Lluis, R. Franco and V. Casadó (2008) Human adenosine deaminase as an allosteric modulator of human A(1) adenosine receptor: abolishment of negative cooperativity for [H](R)-pia binding to the caudate nucleus. *J Neurochem*. **107**, 161-70.

Grady, D. L., H. C. Chi, Y. C. Ding, M. Smith, E. Wang, S. Schuck, P. Flodman, M. A. Spence, J. M. Swanson and R. K. Moyzis (2003) High prevalence of rare dopamine receptor D4 alleles in children diagnosed with attention-deficit hyperactivity disorder. *Mol Psychiatry*. **8**, 536-45.

Grandy, D. K., Y. A. Zhang, C. Bouvier, Q. Y. Zhou, R. A. Johnson, L. Allen, K. Buck, J. R. Bunzow, J. Salon and O. Civelli (1991) Multiple human D5 dopamine receptor genes: a functional receptor and two pseudogenes. *Proc Natl Acad Sci U S A*. **88**, 9175-9.

Greengard, P., P. B. Allen and A. C. Nairn (1999) Beyond the dopamine receptor: the DARPP-32/protein phosphatase-1 cascade. *Neuron*. **23**, 435-47.

Grimm, M. and J. H. Brown (2010) Beta-adrenergic receptor signaling in the heart: role of CaMKII. *J Mol Cell Cardiol*. **48**, 322-30.

Gu, Q. (2002) Neuromodulatory transmitter systems in the cortex and their role in cortical plasticity. *Neuroscience*. **111**, 815-35.

Gudermann, T., T. Schoneberg and G. Schultz (1997) Functional and structural complexity of signal transduction via G-protein-coupled receptors. *Annu Rev Neurosci*. **20**, 399-427.

Guiramand, J., J. P. Montmayeur, J. Ceraline, M. Bhatia and E. Borrelli (1995) Alternative splicing of the dopamine D2 receptor directs specificity of coupling to G-proteins. *J Biol Chem*. **270**, 7354-8.

Guitart, X., X. Codony and X. Monroy (2004) Sigma receptors: biology and therapeutic potential. *Psychopharmacology (Berl)*. **174**, 301-19.

Gundlach, A. L. (2002) Galanin/GALP and galanin receptors: role in central control of feeding, body weight/obesity and reproduction? *Eur J Pharmacol*. **440**, 255-68.

Guo, W., L. Shi, M. Filizola, H. Weinstein and J. A. Javitch (2005) Crosstalk in G protein-coupled receptors: changes at the transmembrane homodimer interface determine activation. *Proc Natl Acad Sci U S A*. **102**, 17495-500.

Guo, W., E. Urizar, M. Kralikova, J. C. Mobarec, L. Shi, M. Filizola and J. A. Javitch (2008) Dopamine D2 receptors form higher order oligomers at physiological expression levels. *EMBO J*. **27**, 2293-304.

Gustafsdottir, S. M., E. Schallmeiner, S. Fredriksson, M. Gullberg, O. Soderberg, M. Jarvius, J. Jarvius, M. Howell and U. Landegren (2005) Proximity ligation assays for sensitive and specific protein analyses. *Anal Biochem*. **345**, 2-9.

Gustafson, E. L., K. E. Smith, M. M. Durkin, C. Gerald and T. A. Branchek (1996) Distribution of a rat galanin receptor mRNA in rat brain. *Neuroreport*. **7**, 953-7.

Haas, H. and P. Panula (2003) The role of histamine and the tuberomamillary nucleus in the nervous system. *Nat Rev Neurosci*. **4**, 121-30.

Haas, H. L., O. A. Sergeeva and O. Selbach (2008) Histamine in the nervous system. *Physiol Rev*. **88**, 1183-241.

Habert-Ortoli, E., B. Amiranoff, I. Loquet, M. Laburthe and J. F. Mayaux (1994) Molecular cloning of a functional human galanin receptor. *Proc Natl Acad Sci U S A*. **91**, 9780-3.

Hamarman, S., J. Fossella, C. Ulger, M. Brimacombe and J. Dermody (2004) Dopamine receptor 4 (DRD4) 7-repeat allele predicts methylphenidate dose response in children with attention deficit hyperactivity disorder: a pharmacogenetic study. *J Child Adolesc Psychopharmacol*. **14**, 564-74.

Han, Y., I. S. Moreira, E. Urizar, H. Weinstein and J. A. Javitch (2009) Allosteric communication between protomers of dopamine class A GPCR dimers modulates activation. *Nat Chem Biol*. **5**, 688-95.

Hancock, A. A. (2006) The challenge of drug discovery of a GPCR target: analysis of preclinical pharmacology of histamine H3 antagonists/inverse agonists. *Biochem Pharmacol*. **71**, 1103-13.

Hancock, A. A., T. A. Esbenshade, K. M. Krueger and B. B. Yao (2003) Genetic and pharmacological aspects of histamine H3 receptor heterogeneity. *Life Sci*. **73**, 3043-72.

Hardeland, R., J. A. Madrid, D. X. Tan and R. J. Reiter (2011) Melatonin, the circadian multioscillator system and health: the need for detailed analyses of peripheral melatonin signaling. *J Pineal Res*.

Hasbi, A., B. F. O'Dowd and S. R. George (2010) Heteromerization of dopamine D2 receptors with dopamine D1 or D5 receptors generates intracellular calcium signaling by different mechanisms. *Curr Opin Pharmacol*. **10**, 93-9.

Hausdorff, W. P., M. Bouvier, B. F. O'Dowd, G. P. Irons, M. G. Caron and R. J. Lefkowitz (1989) Phosphorylation sites on two domains of the beta 2-adrenergic receptor are involved in distinct pathways of receptor desensitization. *J Biol Chem*. **264**, 12657-65.

Hawes, J. J., R. Narasimhaiah and M. R. Picciotto (2006) Galanin and galanin-like peptide modulate neurite outgrowth via protein kinase C-mediated activation of extracellular signal-related kinase. *Eur J Neurosci*. **23**, 2937-46.

Hawes, J. J. and M. R. Picciotto (2004) Characterization of GalR1, GalR2, and GalR3 immunoreactivity in catecholaminergic nuclei of the mouse brain. *J Comp Neurol*. **479**, 410-23.

Hayashi, T. and T. Su (2005) The sigma receptor: evolution of the concept in neuropsychopharmacology. *Curr Neuropharmacol*. **3**, 267-80.

Hayashi, T. and T. P. Su (2001) Regulating ankyrin dynamics: Roles of sigma-1 receptors. *Proc Natl Acad Sci U S A*. **98**, 491-6.

Hayashi, T. and T. P. Su (2003) Intracellular dynamics of sigma-1 receptors (sigma(1) binding sites) in NG108-15 cells. *J Pharmacol Exp Ther*. **306**, 726-33.

Hebert, T. E., S. Moffett, J. P. Morello, T. P. Loisel, D. G. Bichet, C. Barret and M. Bouvier (1996) A peptide derived from a beta2-adrenergic receptor transmembrane domain inhibits both receptor dimerization and activation. *J Biol Chem*. **271**, 16384-92.

Heikkila, R. E., F. S. Cabbat and R. C. Duvoisin (1979) Motor activity and rotational behavior after analogs of cocaine: correlation with dopamine uptake blockade. *Commun Psychopharmacol*. **3**, 285-90.

Hepler, J. R. and A. G. Gilman (1992) G proteins. *Trends Biochem Sci*. **17**, 383-7.

Hering, H. and M. Sheng (2001) Dendritic spines: structure, dynamics and regulation. *Nat Rev Neurosci*. **2**, 880-8.

Hermans, E., M. A. Vanisberg, M. Geurts and J. M. Maloteaux (1997) Down-regulation of neurotensin receptors after ligand-induced internalization in rat primary cultured neurons. *Neurochem Int*. **31**, 291-9.

Hernandez-Lopez, S., T. Tkatch, E. Perez-Garci, E. Galarraga, J. Bargas, H. Hamm and D. J. Surmeier (2000) D2 dopamine receptors in striatal medium spiny neurons reduce L-type Ca2+ currents and excitability via a novel PLC[beta]1-IP3-calcineurin-signaling cascade. *J Neurosci*. **20**, 8987-95.

Herrera, C., V. Casadó, F. Ciruela, P. Schofield, J. Mallol, C. Lluis and R. Franco (2001) Adenosine A2B receptors behave as an alternative anchoring protein for cell surface adenosine deaminase in lymphocytes and cultured cells. *Mol Pharmacol*. **59**, 127-34.

Herrick-Davis, K., E. Grinde, T. J. Harrigan and J. E. Mazurkiewicz (2005) Inhibition of serotonin 5-hydroxytryptamine2c receptor function through heterodimerization: receptor dimers bind two molecules of ligand and one G-protein. *J Biol Chem*. **280**, 40144-51.

Herrick-Davis, K., E. Grinde and J. E. Mazurkiewicz (2004) Biochemical and biophysical characterization of serotonin 5-HT2C receptor homodimers on the plasma membrane of living cells. *Biochemistry*. **43**, 13963-71.

Hersi, A. I., K. Kitaichi, L. K. Srivastava, P. Gaudreau and R. Quirion (2000) Dopamine D-5 receptor modulates hippocampal acetylcholine release. *Brain Res Mol Brain Res*. **76**, 336-40.

Hersi, A. I., J. W. Richard, P. Gaudreau and R. Quirion (1995) Local modulation of hippocampal acetylcholine release by dopamine D1 receptors: a combined receptor autoradiography and in vivo dialysis study. *J Neurosci*. **15**, 7150-7.

Hervouet, E., P. Hulin, F. M. Vallette and P. F. Cartron (2011) Proximity ligation in situ assay for monitoring the global DNA methylation in cells. *BMC Biotechnol*. **11**, 31.

Hieble, J. P., W. E. Bondinell and R. R. Ruffolo, Jr. (1995) Alpha- and beta-adrenoceptors: from the gene to the clinic. 1. Molecular biology and adrenoceptor subclassification. *J Med Chem*. **38**, 3415-44.

Hill, S. J., C. R. Ganellin, H. Timmerman, J. C. Schwartz, N. P. Shankley, J. M. Young, W. Schunack, R. Levi and H. L. Haas (1997) International Union of Pharmacology. XIII. Classification of histamine receptors. *Pharmacol Rev*. **49**, 253-78.

Hillion, J., M. Canals, M. Torvinen, V. Casadó, R. Scott, A. Terasmaa, A. Hansson, S. Watson, M. E. Olah, J. Mallol, E. I. Canela, M. Zoli, L. F. Agnati, C. F. Ibanez, C. Lluis, R. Franco, S. Ferré and K. Fuxe (2002) Coaggregation, cointernalization, and codesensitization of adenosine A2A receptors and dopamine D2 receptors. *J Biol Chem*. **277**, 18091-7.

Hiranita, T., P. L. Soto, G. Tanda and J. L. Katz (2010) Reinforcing effects of sigma-receptor agonists in rats trained to self-administer cocaine. *J Pharmacol Exp Ther*. **332**, 515-24.

Hirschberg, B. T. and M. I. Schimerlik (1994) A kinetic model for oxotremorine M binding to recombinant porcine m2 muscarinic receptors expressed in Chinese hamster ovary cells. *J Biol Chem*. **269**, 26127-35.

Hlavackova, V., C. Goudet, J. Kniazeff, A. Zikova, D. Maurel, C. Vol, J. Trojanova, L. Prezeau, J. P. Pin and J. Blahos (2005) Evidence for a single heptahelical domain being turned on upon activation of a dimeric GPCR. *EMBO J*. **24**, 499-509.

Hobson, S. A., F. E. Holmes, N. C. Kerr, R. J. Pope and D. Wynick (2006) Mice deficient for galanin receptor 2 have decreased neurite outgrowth from adult sensory neurons and impaired pain-like behaviour. *J Neurochem*. **99**, 1000-10.

Hökfelt, T., Z. Q. Xu, T. J. Shi, K. Holmberg and X. Zhang (1998) Galanin in ascending systems. Focus on coexistence with 5-hydroxytryptamine and noradrenaline. *Ann N Y Acad Sci*. **863**, 252-63.

Holmes, A. and M. R. Picciotto (2006) Galanin: a novel therapeutic target for depression, anxiety disorders and drug addiction? *CNS Neurol Disord Drug Targets*. **5**, 225-32.

Holmes, J., T. Hever, L. Hewitt, C. Ball, E. Taylor, K. Rubia and A. Thapar (2002) A pilot twin study of psychological measures of attention deficit hyperactivity disorder. *Behav Genet*. **32**, 389-95.

Howard, A. D., C. Tan, L. L. Shiao, O. C. Palyha, K. K. McKee, D. H. Weinberg, S. D. Feighner, M. A. Cascieri, R. G. Smith, L. H. Van Der Ploeg and K. A. Sullivan (1997) Molecular cloning and characterization of a new receptor for galanin. *FEBS Lett*. **405**, 285-90.

Hu, C. D., Y. Chinenov and T. K. Kerppola (2002) Visualization of interactions among bZIP and Rel family proteins in living cells using bimolecular fluorescence complementation. *Mol Cell*. **9**, 789-98.

Huang, C., J. R. Hepler, L. T. Chen, A. G. Gilman, R. G. Anderson and S. M. Mumby (1997) Organization of G proteins and adenylyl cyclase at the plasma membrane. *Mol Biol Cell*. **8**, 2365-78.

Huber, A. (2001) Scaffolding proteins organize multimolecular protein complexes for sensory signal transduction. *Eur J Neurosci*. **14**, 769-76.

Humbert-Claude, M., S. Morisset, F. Gbahou and J. M. Arrang (2007) Histamine H3 and dopamine D2 receptor-mediated [35S]GTPgamma[S] binding in rat striatum: evidence for additive effects but lack of interactions. *Biochem Pharmacol*. **73**, 1172-81.

Huotari, M., K. Kukkonen, N. Liikka, T. Potasev, A. Raasmaja and P. T. Mannisto (2000) Effects of histamine H(3)-ligands on the levodopa-induced turning behavior of hemiparkinsonian rats. *Parkinsonism Relat Disord*. **6**, 159-164.

Hussain, N., B. A. Flumerfelt and N. Rajakumar (2002) Muscarinic, adenosine A(2) and histamine H(3) receptor modulation of haloperidol-induced c-fos expression in the striatum and nucleus accumbens. *Neuroscience*. **112**, 427-38.

Hyman, S. E. (2007) The neurobiology of addiction: implications for voluntary control of behavior. *Am J Bioeth*. **7**, 8-11.

Iismaa, T. P., Z. Fathi, Y. J. Hort, L. G. Iben, J. L. Dutton, E. Baker, G. R. Sutherland and J. Shine (1998) Structural organization and chromosomal localization of three human galanin receptor genes. *Ann N Y Acad Sci*. **863**, 56-63.

Ilani, T., C. S. Fishburn, B. Levavi-Sivan, S. Carmon, L. Raveh and S. Fuchs (2002) Coupling of dopamine receptors to G proteins: studies with chimeric D2/D3 dopamine receptors. *Cell Mol Neurobiol*. **22**, 47-56.

Innamorati, G., C. Le Gouill, M. Balamotis and M. Birnbaumer (2001) The long and the short cycle. Alternative intracellular routes for trafficking of G-protein-coupled receptors. *J Biol Chem*. **276**, 13096-103.

Ito, C. (2004) The role of the central histaminergic system on schizophrenia. *Drug News Perspect*. **17**, 383-7.

Ito, C., K. Onodera, E. Sakurai, M. Sato and T. Watanabe (1997) Effect of cocaine on the histaminergic neuron system in the rat brain. *J Neurochem*. **69**, 875-8.

Ito, K., T. Haga, J. Lameh and W. Sadee (1999) Sequestration of dopamine D2 receptors depends on coexpression of G-protein-coupled receptor kinases 2 or 5. *Eur J Biochem*. **260**, 112-9.

Ito, R., T. W. Robbins and B. J. Everitt (2004) Differential control over cocaine-seeking behavior by nucleus accumbens core and shell. *Nat Neurosci*. **7**, 389-97.

Jaber, M., S. W. Robinson, C. Missale and M. G. Caron (1996) Dopamine receptors and brain function. *Neuropharmacology*. **35**, 1503-19.

Jacoby, A. S., G. C. Webb, M. L. Liu, B. Kofler, Y. J. Hort, Z. Fathi, C. D. Bottema, J. Shine and T. P. Iismaa (1997) Structural organization of the mouse and human GALR1 galanin receptor genes (Galnr and GALNR) and chromosomal localization of the mouse gene. *Genomics*. **45**, 496-508.

Jacoby, E., R. Bouhelal, M. Gerspacher and K. Seuwen (2006) The 7 TM G-protein-coupled receptor target family. *ChemMedChem*. **1**, 761-82.

Jeanneteau, F., J. Diaz, P. Sokoloff and N. Griffon (2004) Interactions of GIPC with dopamine D2, D3 but not D4 receptors define a novel mode of regulation of G protein-coupled receptors. *Mol Biol Cell*. **15**, 696-705.

Jockers, R., S. Angers, A. Da Silva, P. Benaroch, A. D. Strosberg, M. Bouvier and S. Marullo (1999) Beta(2)-adrenergic receptor down-regulation. Evidence for a pathway that does not require endocytosis. *J Biol Chem*. **274**, 28900-8.

Johnson, J. A. and S. B. Liggett (2011) Cardiovascular pharmacogenomics of adrenergic receptor signaling: clinical implications and future directions. *Clin Pharmacol Ther*. **89**, 366-78.

Jones, K. A., B. Borowsky, J. A. Tamm, D. A. Craig, M. M. Durkin, M. Dai, W. J. Yao, M. Johnson, C. Gunwaldsen, L. Y. Huang, C. Tang, Q. Shen, J. A. Salon, K. Morse, T. Laz, K. E. Smith, D. Nagarathnam, S. A. Noble, T. A. Branchek and C. Gerald (1998) GABA(B) receptors function as a heteromeric assembly of the subunits GABA(B)R1 and GABA(B)R2. *Nature*. **396**, 674-9.

Jordan, B. A. and L. A. Devi (1999) G-protein-coupled receptor heterodimerization modulates receptor function. *Nature*. **399**, 697-700.

Jordan, B. A., N. Trapaidze, I. Gomes, R. Nivarthi and L. A. Devi (2001) Oligomerization of opioid receptors with beta 2-adrenergic receptors: a role in trafficking and mitogen-activated protein kinase activation. *Proc Natl Acad Sci U S A*. **98**, 343-8.

Jovanovic, V., H. C. Guan and H. H. Van Tol (1999) Comparative pharmacological and functional analysis of the human dopamine D4.2 and D4.10 receptor variants. *Pharmacogenetics*. **9**, 561-8.

Kabbani, N. and R. Levenson (2007) A proteomic approach to receptor signaling: molecular mechanisms and therapeutic implications derived from discovery of the dopamine D2 receptor signalplex. *Eur J Pharmacol*. **572**, 83-93.

Kakuyama, H., A. Kuwahara, T. Mochizuki, M. Hoshino and N. Yanaihara (1997) Role of N-terminal active sites of galanin in neurally evoked circular muscle contractions in the guinea-pig ileum. *Eur J Pharmacol*. **329**, 85-91.

Kalivas, P. W. (2007) Neurobiology of cocaine addiction: implications for new pharmacotherapy. *Am J Addict*. **16**, 71-8.

Kanagy, N. L. (2005) Alpha(2)-adrenergic receptor signalling in hypertension. *Clin Sci (Lond)*. **109**, 431-7.

Kanazawa, T., T. Iwashita, P. Kommareddi, T. Nair, K. Misawa, Y. Misawa, Y. Ueda, T. Tono and T. E. Carey (2007) Galanin and galanin receptor type 1 suppress proliferation in squamous carcinoma cells: activation of the extracellular signal regulated kinase pathway and induction of cyclin-dependent kinase inhibitors. *Oncogene*. **26**, 5762-71.

Kandel, E., J. Schwartz and T. Jessell (2000) Principles of neural science. *McGraw-Hill, 4th Edition, New York*.

Kaplan, L. M., E. R. Spindel, K. J. Isselbacher and W. W. Chin (1988) Tissue-specific expression of the rat galanin gene. *Proc Natl Acad Sci U S A*. **85**, 1065-9.

Kask, K., M. Berthold and T. Bartfai (1997) Galanin receptors: involvement in feeding, pain, depression and Alzheimer's disease. *Life Sci*. **60**, 1523-33.

Kask, K., U. Langel and T. Bartfai (1995) Galanin--a neuropeptide with inhibitory actions. *Cell Mol Neurobiol*. **15**, 653-73.

Kaupmann, K., B. Malitschek, V. Schuler, J. Heid, W. Froestl, P. Beck, J. Mosbacher, S. Bischoff, A. Kulik, R. Shigemoto, A. Karschin and B. Bettler (1998) GABA(B)-receptor subtypes assemble into functional heteromeric complexes. *Nature*. **396**, 683-7.

Kazmi, M. A., L. A. Snyder, A. M. Cypess, S. G. Graber and T. P. Sakmar (2000) Selective reconstitution of human D4 dopamine receptor variants with Gi alpha subtypes. *Biochemistry*. **39**, 3734-44.

Kearn, C. S., K. Blake-Palmer, E. Daniel, K. Mackie and M. Glass (2005) Concurrent stimulation of cannabinoid CB1 and dopamine D2 receptors enhances heterodimer formation: a mechanism for receptor cross-talk? *Mol Pharmacol*. **67**, 1697-704.

Kelly, E., C. P. Bailey and G. Henderson (2008) Agonist-selective mechanisms of GPCR desensitization. *Br J Pharmacol*. **153 Suppl 1**, S379-88.

Keys, J. R. and W. J. Koch (2004) The adrenergic pathway and heart failure. *Recent Prog Horm Res*. **59**, 13-30.

Kim, H. W., D. H. Roh, S. Y. Yoon, H. S. Seo, Y. B. Kwon, H. J. Han, K. W. Kim, A. J. Beitz and J. H. Lee (2008) Activation of the spinal sigma-1 receptor enhances NMDA-induced pain via PKC- and PKA-dependent phosphorylation of the NR1 subunit in mice. *Br J Pharmacol*. **154**, 1125-34.

Kim, J. S., M. J. Bailey, J. L. Weller, D. Sugden, M. F. Rath, M. Moller and D. C. Klein (2010) Thyroid hormone and adrenergic signaling interact to control pineal expression of the dopamine receptor D4 gene (Drd4). *Mol Cell Endocrinol*. **314**, 128-35.

Kim, K. M., K. J. Valenzano, S. R. Robinson, W. D. Yao, L. S. Barak and M. G. Caron (2001) Differential regulation of the dopamine D2 and D3 receptors by G protein-coupled receptor kinases and beta-arrestins. *J Biol Chem*. **276**, 37409-14.

Kim, S. Y., K. C. Choi, M. S. Chang, M. H. Kim, Y. S. Na, J. E. Lee, B. K. Jin, B. H. Lee and J. H. Baik (2006) The dopamine D2 receptor regulates the development of dopaminergic neurons via extracellular signal-regulated kinase and Nurr1 activation. *J Neurosci*. **26**, 4567-76.

Kimura, K., B. H. White and A. Sidhu (1995) Coupling of human D-1 dopamine receptors to different guanine nucleotide binding proteins. Evidence that D-1 dopamine receptors can couple to both Gs and G(o). *J Biol Chem*. **270**, 14672-8.

Kinney, J. W., G. Starosta, A. Holmes, C. C. Wrenn, R. J. Yang, A. P. Harris, K. C. Long and J. N. Crawley (2002) Deficits in trace cued fear conditioning in galanin-treated rats and galanin-overexpressing transgenic mice. *Learn Mem*. **9**, 178-90.

Klco, J. M., T. B. Lassere and T. J. Baranski (2003) C5a receptor oligomerization. I. Disulfide trapping reveals oligomers and potential contact surfaces in a G protein-coupled receptor. *J Biol Chem*. **278**, 35345-53.

Klein, D. C., S. L. Coon, P. H. Roseboom, J. L. Weller, M. Bernard, J. A. Gastel, M. Zatz, P. M. Iuvone, I. R. Rodriguez, V. Begay, J. Falcon, G. M. Cahill, V. M. Cassone and R. Baler (1997) The melatonin rhythm-generating enzyme: molecular regulation of serotonin N-acetyltransferase in the pineal gland. *Recent Prog Horm Res*. **52**, 307-57; discussion 357-8.

Kobilka, B. K. (2011) Structural insights into adrenergic receptor function and pharmacology. *Trends Pharmacol Sci*. **32**, 213-8.

Koch, W. J., B. E. Hawes, L. F. Allen and R. J. Lefkowitz (1994) Direct evidence that Gi-coupled receptor stimulation of mitogen-activated protein kinase is mediated by G beta gamma activation of p21ras. *Proc Natl Acad Sci U S A*. **91**, 12706-10.

Koeltzow, T. E., M. Xu, D. C. Cooper, X. T. Hu, S. Tonegawa, M. E. Wolf and F. J. White (1998) Alterations in dopamine release but not dopamine autoreceptor function in dopamine D3 receptor mutant mice. *J Neurosci*. **18**, 2231-8.

Kofler, B., M. L. Liu, A. S. Jacoby, J. Shine and T. P. Iismaa (1996) Molecular cloning and characterisation of the mouse preprogalanin gene. *Gene*. **182**, 71-5.

Kolakowski, L. F., Jr. (1994) GCRDb: a G-protein-coupled receptor database. *Receptors Channels*. **2**, 1-7.

Kolakowski, L. F., Jr., G. P. O'Neill, A. D. Howard, S. R. Broussard, K. A. Sullivan, S. D. Feighner, M. Sawzdargo, T. Nguyen, S. Kargman, L. L. Shiao, D. L. Hreniuk, C. P. Tan, J. Evans, M. Abramovitz, A. Chateauneuf, N. Coulombe, G. Ng, M. P. Johnson, A. Tharian, H. Khoshbouei, S. R. George, R. G. Smith and B. F. O'Dowd (1998) Molecular characterization and expression of cloned human galanin receptors GALR2 and GALR3. *J Neurochem*. **71**, 2239-51.

Kong, M. M., T. Fan, G. Varghese, F. O'Dowd B and S. R. George (2006) Agonist-induced cell surface trafficking of an intracellularly sequestered D1 dopamine receptor homo-oligomer. *Mol Pharmacol*. **70**, 78-89.

Kong, M. M., A. Hasbi, M. Mattocks, T. Fan, B. F. O'Dowd and S. R. George (2007) Regulation of D1 dopamine receptor trafficking and signaling by caveolin-1. *Mol Pharmacol*. **72**, 1157-70.

Konradi, C. (1998) The molecular basis of dopamine and glutamate interactions in the striatum. *Adv Pharmacol*. **42**, 729-33.

Krueger, K. M., Y. Daaka, J. A. Pitcher and R. J. Lefkowitz (1997) The role of sequestration in G protein-coupled receptor resensitization. Regulation of beta2-adrenergic receptor dephosphorylation by vesicular acidification. *J Biol Chem*. **272**, 5-8.

Krupnick, J. G. and J. L. Benovic (1998) The role of receptor kinases and arrestins in G protein-coupled receptor regulation. *Annu Rev Pharmacol Toxicol*. **38**, 289-319.

Lachowicz, J. E. and D. R. Sibley (1997) Chimeric D2/D3 dopamine receptor coupling to adenylyl cyclase. *Biochem Biophys Res Commun*. **237**, 394-9.

Landry, M., D. Roche, E. Vila-Porcile and A. Calas (2000) Effects of centrally administered galanin (1-16) on galanin expression in the rat hypothalamus. *Peptides*. **21**, 1725-33.

Lang, R., A. L. Gundlach and B. Kofler (2007) The galanin peptide family: receptor pharmacology, pleiotropic biological actions, and implications in health and disease. *Pharmacol Ther*. **115**, 177-207.

Langer, S. Z. (1997) 25 years since the discovery of presynaptic receptors: present knowledge and future perspectives. *Trends Pharmacol Sci*. **18**, 95-9.

Laplante, F., J. N. Crawley and R. Quirion (2004a) Selective reduction in ventral hippocampal acetylcholine release in awake galanin-treated rats and galanin-overexpressing transgenic mice. *Regul Pept*. **122**, 91-8.

Laplante, F., D. R. Sibley and R. Quirion (2004b) Reduction in acetylcholine release in the hippocampus of dopamine D5 receptor-deficient mice. *Neuropsychopharmacology*. **29**, 1620-7.

Laurier, L. G., W. A. Corrigall and S. R. George (1994) Dopamine receptor density, sensitivity and mRNA levels are altered following self-administration of cocaine in the rat. *Brain Res*. **634**, 31-40.

Lauzon, N. M. and S. R. Laviolette (2010) Dopamine D4-receptor modulation of cortical neuronal network activity and emotional processing: Implications for neuropsychiatric disorders. *Behav Brain Res*. **208**, 12-22.

Lee, K. W., J. H. Hong, I. Y. Choi, Y. Che, J. K. Lee, S. D. Yang, C. W. Song, H. S. Kang, J. H. Lee, J. S. Noh, H. S. Shin and P. L. Han (2002) Impaired D2 dopamine receptor function in mice lacking type 5 adenylyl cyclase. *J Neurosci*. **22**, 7931-40.

Lee, S. P., C. H. So, A. J. Rashid, G. Varghese, R. Cheng, A. J. Lanca, B. F. O'Dowd and S. R. George (2004) Dopamine D1 and D2 receptor Co-activation generates a novel phospholipase C-mediated calcium signal. *J Biol Chem*. **279**, 35671-8.

Lee, S. P., Z. Xie, G. Varghese, T. Nguyen, B. F. O'Dowd and S. R. George (2000) Oligomerization of dopamine and serotonin receptors. *Neuropsychopharmacology*. **23**, S32-40.

Lefkowitz, R. J. (1998) G protein-coupled receptors. III. New roles for receptor kinases and beta-arrestins in receptor signaling and desensitization. *J Biol Chem*. **273**, 18677-80.

Lefkowitz, R. J. (2007) Seven transmembrane receptors: something old, something new. *Acta Physiol (Oxf)*. **190**, 9-19.

Lefkowitz, R. J., S. Cotecchia, P. Samama and T. Costa (1993) Constitutive activity of receptors coupled to guanine nucleotide regulatory proteins. *Trends Pharmacol Sci*. **14**, 303-7.

Leurs, R., R. A. Bakker, H. Timmerman and I. J. de Esch (2005) The histamine H3 receptor: from gene cloning to H3 receptor drugs. *Nat Rev Drug Discov*. **4**, 107-20.

Leurs, R., M. J. Smit and H. Timmerman (1995) Molecular pharmacological aspects of histamine receptors. *Pharmacol Ther*. **66**, 413-63.

Levi, R., N. Seyedi, U. Schaefer, R. Estephan, C. J. Mackins, E. Tyler and R. B. Silver (2007) Histamine H3-receptor signaling in cardiac sympathetic nerves: Identification of a novel MAPK-PLA2-COX-PGE2-EP3R pathway. *Biochem Pharmacol*. **73**, 1146-56.

Levi, R. and N. C. Smith (2000) Histamine H(3)-receptors: a new frontier in myocardial ischemia. *J Pharmacol Exp Ther*. **292**, 825-30.

Liebmann, C. (2004) G protein-coupled receptors and their signaling pathways: classical therapeutical targets susceptible to novel therapeutic concepts. *Curr Pharm Des*. **10**, 1937-58.

Liggett, S. B. (2003) Polymorphisms of adrenergic receptors: variations on a theme. *Assay Drug Dev Technol*. **1**, 317-26.

Limbird, L. E., P. D. Meyts and R. J. Lefkowitz (1975) Beta-adrenergic receptors: evidence for negative cooperativity. *Biochem Biophys Res Commun*. **64**, 1160-8.

Lin, R., K. Karpa, N. Kabbani, P. Goldman-Rakic and R. Levenson (2001) Dopamine D2 and D3 receptors are linked to the actin cytoskeleton via interaction with filamin A. *Proc Natl Acad Sci U S A*. **98**, 5258-63.

Little, K. Y., J. A. Kirkman, F. I. Carroll, G. R. Breese and G. E. Duncan (1993) [125I]RTI-55 binding to cocaine-sensitive dopaminergic and serotonergic uptake sites in the human brain. *J Neurochem*. **61**, 1996-2006.

Liu, C., X. Ma, X. Jiang, S. J. Wilson, C. L. Hofstra, J. Blevitt, J. Pyati, X. Li, W. Chai, N. Carruthers and T. W. Lovenberg (2001) Cloning and pharmacological characterization of a fourth histamine receptor (H(4)) expressed in bone marrow. *Mol Pharmacol*. **59**, 420-6.

Liu, F., Q. Wan, Z. B. Pristupa, X. M. Yu, Y. T. Wang and H. B. Niznik (2000) Direct protein-protein coupling enables cross-talk between dopamine D5 and gamma-aminobutyric acid A receptors. *Nature*. **403**, 274-80.

Liu, H. X. and T. Hokfelt (2002) The participation of galanin in pain processing at the spinal level. *Trends Pharmacol Sci*. **23**, 468-74.

Liu, X. Y., X. P. Chu, L. M. Mao, M. Wang, H. X. Lan, M. H. Li, G. C. Zhang, N. K. Parelkar, E. E. Fibuch, M. Haines, K. A. Neve, F. Liu, Z. G. Xiong and J. Q. Wang (2006) Modulation of D2R-NR2B interactions in response to cocaine. *Neuron*. **52**, 897-909.

Liu, Y. and R. H. Edwards (1997) Differential localization of vesicular acetylcholine and monoamine transporters in PC12 cells but not CHO cells. *J Cell Biol*. **139**, 907-16.

Liu, Y. F., O. Civelli, D. K. Grandy and P. R. Albert (1992a) Differential sensitivity of the short and long human dopamine D2 receptor subtypes to protein kinase C. *J Neurochem*. **59**, 2311-7.

Liu, Y. F., O. Civelli, Q. Y. Zhou and P. R. Albert (1992b) Cholera toxin-sensitive 3',5'-cyclic adenosine monophosphate and calcium signals of the human dopamine-D1 receptor: selective potentiation by protein kinase A. *Mol Endocrinol*. **6**, 1815-24.

Lohse, M. J., J. L. Benovic, M. G. Caron and R. J. Lefkowitz (1990) Multiple pathways of rapid beta 2-adrenergic receptor desensitization. Delineation with specific inhibitors. *J Biol Chem*. **265**, 3202-11.

Lovenberg, T. W., J. Pyati, H. Chang, S. J. Wilson and M. G. Erlander (2000) Cloning of rat histamine H(3) receptor reveals distinct species pharmacological profiles. *J Pharmacol Exp Ther*. **293**, 771-8.

Lovenberg, T. W., B. L. Roland, S. J. Wilson, X. Jiang, J. Pyati, A. Huvar, M. R. Jackson and M. G. Erlander (1999) Cloning and functional expression of the human histamine H3 receptor. *Mol Pharmacol*. **55**, 1101-7.

Lundberg, J. M. (1996) Pharmacology of cotransmission in the autonomic nervous system: integrative aspects on amines, neuropeptides, adenosine triphosphate, amino acids and nitric oxide. *Pharmacol Rev*. **48**, 113-78.

Lundkvist, J., T. Land, U. Kahl, K. Bedecs and T. Bartfai (1995) cDNA sequence, ligand biding, and regulation of galanin/GMAP in mouse brain. *Neurosci Lett*. **200**, 121-4.

Lundstrom, K. (2006) Latest development in drug discovery on G protein-coupled receptors. *Curr Protein Pept Sci*. **7**, 465-70.

Luo, Z., N. D. Volkow, N. Heintz, Y. Pan and C. Du (2011) Acute cocaine induces fast activation of D1 receptor and progressive deactivation of D2 receptor striatal neurons: in vivo optical microprobe [Ca2+]i imaging. *J Neurosci*. **31**, 13180-90.

Luttrell, L. M., S. S. Ferguson, Y. Daaka, W. E. Miller, S. Maudsley, G. J. Della Rocca, F. Lin, H. Kawakatsu, K. Owada, D. K. Luttrell, M. G. Caron and R. J. Lefkowitz (1999) Beta-arrestin-dependent formation of beta2 adrenergic receptor-Src protein kinase complexes. *Science*. **283**, 655-61.

Luttrell, L. M. and R. J. Lefkowitz (2002) The role of beta-arrestins in the termination and transduction of G-protein-coupled receptor signals. *J Cell Sci*. **115**, 455-65.

Ma, Y. C. and X. Y. Huang (2002) Novel signaling pathway through the beta-adrenergic receptor. *Trends Cardiovasc Med*. **12**, 46-9.

Madras, B. K., G. M. Miller and A. J. Fischman (2005) The dopamine transporter and attention-deficit/hyperactivity disorder. *Biol Psychiatry*. **57**, 1397-409.

Maggio, R., Z. Vogel and J. Wess (1993) Coexpression studies with mutant muscarinic/adrenergic receptors provide evidence for intermolecular "cross-talk" between G-protein-linked receptors. *Proc Natl Acad Sci U S A*. **90**, 3103-7.

Mahan, L. C., R. M. Burch, F. J. Monsma, Jr. and D. R. Sibley (1990) Expression of striatal D1 dopamine receptors coupled to inositol phosphate production and Ca2+ mobilization in Xenopus oocytes. *Proc Natl Acad Sci U S A*. **87**, 2196-200.

Malek, D., G. Munch and D. Palm (1993) Two sites in the third inner loop of the dopamine D2 receptor are involved in functional G protein-mediated coupling to adenylate cyclase. *FEBS Lett*. **325**, 215-9.

Mandela, P. and G. A. Ordway (2006) The norepinephrine transporter and its regulation. *J Neurochem*. **97**, 310-33.

Marcellino, D., S. Ferré, V. Casadó, A. Cortés, B. Le Foll, C. Mazzola, F. Drago, O. Saur, H. Stark, A. Soriano, C. Barnes, S. R. Goldberg, C. Lluis, K. Fuxe and R. Franco (2008) Identification of dopamine D1-D3 receptor heteromers. Indications for a role of synergistic D1-D3 receptor interactions in the striatum. *J Biol Chem*. **283**, 26016-25.

Marcellino, D., D. C. Roberts, G. Navarro, M. Filip, L. Agnati, C. Lluis, R. Franco and K. Fuxe (2007) Increase in A2A receptors in the nucleus accumbens after extended cocaine self-administration and its disappearance after cocaine withdrawal. *Brain Res*. **1143**, 208-20.

Margeta-Mitrovic, M., Y. N. Jan and L. Y. Jan (2000) A trafficking checkpoint controls GABA(B) receptor heterodimerization. *Neuron*. **27**, 97-106.

Marinissen, M. J. and J. S. Gutkind (2001) G-protein-coupled receptors and signaling networks: emerging paradigms. *Trends Pharmacol Sci*. **22**, 368-76.

Maronde, E. and J. H. Stehle (2007) The mammalian pineal gland: known facts, unknown facets. *Trends Endocrinol Metab*. **18**, 142-9.

Marshall, F. H. (2001) Heterodimerization of G-protein-coupled receptors in the CNS. *Curr Opin Pharmacol*. **1**, 40-4.

Marshall, K. C., M. J. Christie, P. G. Finlayson and J. T. Williams (1991) Developmental aspects of the locus coeruleus-noradrenaline system. *Prog Brain Res*. **88**, 173-85.

Martemyanov, K. A. and V. Y. Arshavsky (2009) Biology and functions of the RGS9 isoforms. *Prog Mol Biol Transl Sci*. **86**, 205-27.

Martin, W. R., C. G. Eades, J. A. Thompson, R. E. Huppler and P. E. Gilbert (1976) The effects of morphine- and nalorphine- like drugs in the nondependent and morphine-dependent chronic spinal dog. *J Pharmacol Exp Ther*. **197**, 517-32.

Martinez, D., A. Broft, R. W. Foltin, M. Slifstein, D. R. Hwang, Y. Huang, A. Perez, W. G. Frankle, T. Cooper, H. D. Kleber, M. W. Fischman and M. Laruelle (2004) Cocaine dependence and d2 receptor availability in the functional subdivisions of the striatum: relationship with cocaine-seeking behavior. *Neuropsychopharmacology*. **29**, 1190-202.

Martinez, D., M. Slifstein, R. Narendran, R. W. Foltin, A. Broft, D. R. Hwang, A. Perez, A. Abi-Dargham, M. W. Fischman, H. D. Kleber and M. Laruelle (2009) Dopamine D1 receptors in cocaine dependence measured with PET and the choice to self-administer cocaine. *Neuropsychopharmacology*. **34**, 1774-82.

Massinen, S., K. Tammimies, I. Tapia-Paez, H. Matsson, M. E. Hokkanen, O. Soderberg, U. Landegren, E. Castren, J. A. Gustafsson, E. Treuter and J. Kere (2009) Functional interaction of DYX1C1 with estrogen receptors suggests involvement of hormonal pathways in dyslexia. *Hum Mol Genet*. **18**, 2802-12.

Matozaki, T., H. Nakanishi and Y. Takai (2000) Small G-protein networks: their crosstalk and signal cascades. *Cell Signal*. **12**, 515-24.

Matsukawa, N., M. Maki, T. Yasuhara, K. Hara, G. Yu, L. Xu, K. M. Kim, J. C. Morgan, K. D. Sethi and C. V. Borlongan (2007) Overexpression of D2/D3 receptors increases efficacy of ropinirole in chronically 6-OHDA-lesioned Parkinsonian rats. *Brain Res*. **1160**, 113-23.

Matsumoto, R. R., D. L. Gilmore, B. Pouw, W. D. Bowen, W. Williams, A. Kausar and A. Coop (2004) Novel analogs of the sigma receptor ligand BD1008 attenuate cocaine-induced toxicity in mice. *Eur J Pharmacol*. **492**, 21-6.

Matsumoto, R. R., K. L. Hewett, B. Pouw, W. D. Bowen, S. M. Husbands, J. J. Cao and A. Hauck Newman (2001a) Rimcazole analogs attenuate the convulsive effects of cocaine: correlation with binding to sigma receptors rather than dopamine transporters. *Neuropharmacology*. **41**, 878-86.

Matsumoto, R. R., Y. Liu, M. Lerner, E. W. Howard and D. J. Brackett (2003) Sigma receptors: potential medications development target for anti-cocaine agents. *Eur J Pharmacol*. **469**, 1-12.

Matsumoto, R. R., K. A. McCracken, M. J. Friedman, B. Pouw, B. R. De Costa and W. D. Bowen (2001b) Conformationally restricted analogs of BD1008 and an antisense oligodeoxynucleotide targeting sigma1 receptors produce anti-cocaine effects in mice. *Eur J Pharmacol*. **419**, 163-74.

Matsumoto, R. R., K. A. McCracken, B. Pouw, Y. Zhang and W. D. Bowen (2002) Involvement of sigma receptors in the behavioral effects of cocaine: evidence from novel ligands and antisense oligodeoxynucleotides. *Neuropharmacology*. **42**, 1043-55.

Matsumoto, R. R., B. Pouw, A. L. Mack, A. Daniels and A. Coop (2007) Effects of UMB24 and (+/-)-SM 21, putative sigma2-preferring antagonists, on behavioral toxic and stimulant effects of cocaine in mice. *Pharmacol Biochem Behav*. **86**, 86-91.

Mattera, R., B. J. Pitts, M. L. Entman and L. Birnbaumer (1985) Guanine nucleotide regulation of a mammalian myocardial muscarinic receptor system. Evidence for homo- and heterotropic

cooperativity in ligand binding analyzed by computer-assisted curve fitting. *J Biol Chem*. **260**, 7410-21.

May, L. T., K. Leach, P. M. Sexton and A. Christopoulos (2007) Allosteric modulation of G protein-coupled receptors. *Annu Rev Pharmacol Toxicol*. **47**, 1-51.

Mazarati, A. M., J. G. Hohmann, A. Bacon, H. Liu, R. Sankar, R. A. Steiner, D. Wynick and C. G. Wasterlain (2000) Modulation of hippocampal excitability and seizures by galanin. *J Neurosci*. **20**, 6276-81.

McDonald, M. P., T. C. Gleason, J. K. Robinson and J. N. Crawley (1998) Galanin inhibits performance on rodent memory tasks. *Ann N Y Acad Sci*. **863**, 305-22.

McVey, M., D. Ramsay, E. Kellett, S. Rees, S. Wilson, A. J. Pope and G. Milligan (2001) Monitoring receptor oligomerization using time-resolved fluorescence resonance energy transfer and bioluminescence resonance energy transfer. The human delta -opioid receptor displays constitutive oligomerization at the cell surface, which is not regulated by receptor occupancy. *J Biol Chem*. **276**, 14092-9.

Mediavilla-Garcia, C. (2003) [Neurobiology of hyperactivity disorder]. *Rev Neurol*. **36**, 555-65.

Meiergerd, S. M., T. A. Patterson and J. O. Schenk (1993) D2 receptors may modulate the function of the striatal transporter for dopamine: kinetic evidence from studies in vitro and in vivo. *J Neurochem*. **61**, 764-7.

Meitzen, J., J. I. Luoma, C. M. Stern and P. G. Mermelstein (2011) beta1-Adrenergic receptors activate two distinct signaling pathways in striatal neurons. *J Neurochem*. **116**, 984-95.

Melander, T., T. Hokfelt, A. Rokaeus, A. C. Cuello, W. H. Oertel, A. Verhofstad and M. Goldstein (1986a) Coexistence of galanin-like immunoreactivity with catecholamines, 5-hydroxytryptamine, GABA and neuropeptides in the rat CNS. *J Neurosci*. **6**, 3640-54.

Melander, T., C. Kohler, S. Nilsson, T. Hokfelt, E. Brodin, E. Theodorsson and T. Bartfai (1988) Autoradiographic quantitation and anatomical mapping of 125I-galanin binding sites in the rat central nervous system. *J Chem Neuroanat*. **1**, 213-33.

Melander, T., W. A. Staines, T. Hokfelt, A. Rokaeus, F. Eckenstein, P. M. Salvaterra and B. H. Wainer (1985) Galanin-like immunoreactivity in cholinergic neurons of the septum-basal forebrain complex projecting to the hippocampus of the rat. *Brain Res*. **360**, 130-8.

Melander, T., W. A. Staines and A. Rokaeus (1986b) Galanin-like immunoreactivity in hippocampal afferents in the rat, with special reference to cholinergic and noradrenergic inputs. *Neuroscience*. **19**, 223-40.

Menkel, M., P. Terry, M. Pontecorvo, J. L. Katz and J. M. Witkin (1991) Selective sigma ligands block stimulant effects of cocaine. *Eur J Pharmacol*. **201**, 251-2.

Mercuri, N. B., A. Saiardi, A. Bonci, R. Picetti, P. Calabresi, G. Bernardi and E. Borrelli (1997) Loss of autoreceptor function in dopaminergic neurons from dopamine D2 receptor deficient mice. *Neuroscience*. **79**, 323-7.

Mesangeau, C., S. Narayanan, A. M. Green, J. Shaikh, N. Kaushal, E. Viard, Y. T. Xu, J. A. Fishback, J. H. Poupaert, R. R. Matsumoto and C. R. McCurdy (2008) Conversion of a highly selective sigma-1 receptor-ligand to sigma-2 receptor preferring ligands with anticocaine activity. *J Med Chem*. **51**, 1482-6.

Miczek, K. A. and H. Yoshimura (1982) Disruption of primate social behavior by d-amphetamine and cocaine: differential antagonism by antipsychotics. *Psychopharmacology (Berl)*. **76**, 163-71.

Miguez, J. M., V. Simonneaux and P. Pevet (1997) The role of the intracellular and extracellular serotonin in the regulation of melatonin production in rat pinealocytes. *J Pineal Res*. **23**, 63-71.

Miller, M. A., P. E. Kolb and M. A. Raskind (1997) GALR1 galanin receptor mRNA is co-expressed by galanin neurons but not cholinergic neurons in the rat basal forebrain. *Brain Res Mol Brain Res*. **52**, 121-9.

Milligan, G. (2006) G-protein-coupled receptor heterodimers: pharmacology, function and relevance to drug discovery. *Drug Discov Today*. **11**, 541-9.

Milligan, G. and M. Bouvier (2005) Methods to monitor the quaternary structure of G protein-coupled receptors. *FEBS J*. **272**, 2914-25.

Milligan, G. and E. Kostenis (2006) Heterotrimeric G-proteins: a short history. *Br J Pharmacol*. **147 Suppl 1**, S46-55.

Milligan, G., H. Murdoch, E. Kellett, J. H. White and G. J. Feng (2004) Interactions between G-protein-coupled receptors and periplakin: a selective means to regulate G-protein activation. *Biochem Soc Trans*. **32**, 878-80.

Minneman, K. P., T. L. Theroux, S. Hollinger, C. Han and T. A. Esbenshade (1994) Selectivity of agonists for cloned alpha 1-adrenergic receptor subtypes. *Mol Pharmacol*. **46**, 929-36.

Missale, C., S. R. Nash, S. W. Robinson, M. Jaber and M. G. Caron (1998) Dopamine receptors: from structure to function. *Physiol Rev*. **78**, 189-225.

Mitchell, H. A. and D. Weinshenker (2010) Good night and good luck: norepinephrine in sleep pharmacology. *Biochem Pharmacol*. **79**, 801-9.

Mitsukawa, K., X. Lu and T. Bartfai (2008) Galanin, galanin receptors and drug targets. *Cell Mol Life Sci*. **65**, 1796-805.

Miyazono, K., Y. Kamiya and M. Morikawa (2009) Bone morphogenetic protein receptors and signal transduction. *J Biochem*. **147**, 35-51.

Molina-Hernandez, A., A. Nunez and J. A. Arias-Montano (2000) Histamine H3-receptor activation inhibits dopamine synthesis in rat striatum. *Neuroreport*. **11**, 163-6.

Molina-Hernandez, A., A. Nunez, J. J. Sierra and J. A. Arias-Montano (2001) Histamine H3 receptor activation inhibits glutamate release from rat striatal synaptosomes. *Neuropharmacology*. **41**, 928-34.

Monassier, L. and P. Bousquet (2002) Sigma receptors: from discovery to highlights of their implications in the cardiovascular system. *Fundam Clin Pharmacol*. **16**, 1-8.

Mons, N., A. Harry, P. Dubourg, R. T. Premont, R. Iyengar and D. M. Cooper (1995) Immunohistochemical localization of adenylyl cyclase in rat brain indicates a highly selective concentration at synapses. *Proc Natl Acad Sci U S A*. **92**, 8473-7.

Monsma, F. J., Jr., L. D. McVittie, C. R. Gerfen, L. C. Mahan and D. R. Sibley (1989) Multiple D2 dopamine receptors produced by alternative RNA splicing. *Nature*. **342**, 926-9.

Moore, J. D., D. A. Mason, S. A. Green, J. Hsu and S. B. Liggett (1999) Racial differences in the frequencies of cardiac beta(1)-adrenergic receptor polymorphisms: analysis of c145A>G and c1165G>C. *Hum Mutat*. **14**, 271.

Moore, K. E. and G. A. Gudelsky (1977) Drug actions on dopamine turnover in the median eminence. *Adv Biochem Psychopharmacol*. **16**, 227-35.

Moore, R. J., S. L. Vinsant, M. A. Nader, L. J. Porrino and D. P. Friedman (1998) Effect of cocaine self-administration on dopamine D2 receptors in rhesus monkeys. *Synapse*. **30**, 88-96.

Morgan, D., K. Brebner, W. J. Lynch and D. C. Roberts (2002a) Increases in the reinforcing efficacy of cocaine after particular histories of reinforcement. *Behav Pharmacol*. **13**, 389-96.

Morgan, D., K. A. Grant, H. D. Gage, R. H. Mach, J. R. Kaplan, O. Prioleau, S. H. Nader, N. Buchheimer, R. L. Ehrenkaufer and M. A. Nader (2002b) Social dominance in monkeys: dopamine D2 receptors and cocaine self-administration. *Nat Neurosci*. **5**, 169-74.

Morisset, S., A. Rouleau, X. Ligneau, F. Gbahou, J. Tardivel-Lacombe, H. Stark, W. Schunack, C. R. Ganellin, J. C. Schwartz and J. M. Arrang (2000) High constitutive activity of native H3 receptors regulates histamine neurons in brain. *Nature*. **408**, 860-4.

Morisset, S., A. Sasse, F. Gbahou, A. Heron, X. Ligneau, J. Tardivel-Lacombe, J. C. Schwartz and J. M. Arrang (2001) The rat H3 receptor: gene organization and multiple isoforms. *Biochem Biophys Res Commun*. **280**, 75-80.

Mortensen, O. V. and S. G. Amara (2003) Dynamic regulation of the dopamine transporter. *Eur J Pharmacol*. **479**, 159-70.

Morton, J. S., C. J. Daly, V. M. Jackson and J. C. McGrath (2007) Alpha(1A)-adrenoceptors mediate contractions to phenylephrine in rabbit penile arteries. *Br J Pharmacol*. **150**, 112-20.

Moser, E., J. Kargl, J. L. Whistler, M. Waldhoer and P. Tschische (2010) G protein-coupled receptor-associated sorting protein 1 regulates the postendocytic sorting of seven-transmembrane-spanning G protein-coupled receptors. *Pharmacology*. **86**, 22-9.

Munzar, P., G. Tanda, Z. Justinova and S. R. Goldberg (2004) Histamine h3 receptor antagonists potentiate methamphetamine self-administration and methamphetamine-induced accumbal dopamine release. *Neuropsychopharmacology*. **29**, 705-17.

Naber, P. A. and M. P. Witter (1998) Subicular efferents are organized mostly as parallel projections: a double-labeling, retrograde-tracing study in the rat. *J Comp Neurol*. **393**, 284-97.

Nader, M. A., J. B. Daunais, T. Moore, S. H. Nader, R. J. Moore, H. R. Smith, D. P. Friedman and L. J. Porrino (2002) Effects of cocaine self-administration on striatal dopamine systems in rhesus monkeys: initial and chronic exposure. *Neuropsychopharmacology*. **27**, 35-46.

Nader, M. A., D. Morgan, H. D. Gage, S. H. Nader, T. L. Calhoun, N. Buchheimer, R. Ehrenkaufer and R. H. Mach (2006) PET imaging of dopamine D2 receptors during chronic cocaine self-administration in monkeys. *Nat Neurosci*. **9**, 1050-6.

Nakamura, S., K. Ohnishi, M. Nishimura, T. Suenaga, I. Akiguchi, J. Kimura and T. Kimura (1996) Large neurons in the tuberomammillary nucleus in patients with Parkinson's disease and multiple system atrophy. *Neurology*. **46**, 1693-6.

Nakamura, T., H. Itadani, Y. Hidaka, M. Ohta and K. Tanaka (2000) Molecular cloning and characterization of a new human histamine receptor, HH4R. *Biochem Biophys Res Commun*. **279**, 615-20.

Nath, C. and M. B. Gupta (2001) Role of central histaminergic system in lorazepam withdrawal syndrome in rats. *Pharmacol Biochem Behav*. **68**, 777-82.

Navarro, G., M. S. Aymerich, D. Marcellino, A. Cortés, V. Casadó, J. Mallol, E. I. Canela, L. Agnati, A. S. Woods, K. Fuxe, C. Lluis, J. L. Lanciego, S. Ferré and R. Franco (2009) Interactions between calmodulin, adenosine A2A, and dopamine D2 receptors. *J Biol Chem*. **284**, 28058-68.

Navarro, G., P. Carriba, J. Gandía, F. Ciruela, V. Casadó, A. Cortés, J. Mallol, E. I. Canela, C. Lluis and R. Franco (2008) Detection of heteromers formed by cannabinoid CB1, dopamine D2, and

adenosine A2A G-protein-coupled receptors by combining bimolecular fluorescence complementation and bioluminescence energy transfer. *ScientificWorldJournal*. **8**, 1088-97.

Nayak, P. K., A. L. Misra and S. J. Mule (1976) Physiological disposition and biotransformation of (3H) cocaine in acutely and chronically treated rats. *J Pharmacol Exp Ther*. **196**, 556-69.

Neubig, R. R., M. Spedding, T. Kenakin and A. Christopoulos (2003) International Union of Pharmacology Committee on Receptor Nomenclature and Drug Classification. XXXVIII. Update on terms and symbols in quantitative pharmacology. *Pharmacol Rev*. **55**, 597-606.

Neve, K. A., J. K. Seamans and H. Trantham-Davidson (2004) Dopamine receptor signaling. *J Recept Signal Transduct Res*. **24**, 165-205.

Newman-Tancredi, A., D. Cussac and R. Depoortere (2007) Neuropharmacological profile of bifeprunox: merits and limitations in comparison with other third-generation antipsychotics. *Curr Opin Investig Drugs*. **8**, 539-54.

Ng, G. Y., B. F. O'Dowd, S. P. Lee, H. T. Chung, M. R. Brann, P. Seeman and S. R. George (1996) Dopamine D2 receptor dimers and receptor-blocking peptides. *Biochem Biophys Res Commun*. **227**, 200-4.

Ng, G. Y., G. Varghese, H. T. Chung, J. Trogadis, P. Seeman, B. F. O'Dowd and S. R. George (1997) Resistance of the dopamine D2L receptor to desensitization accompanies the up-regulation of receptors on to the surface of Sf9 cells. *Endocrinology*. **138**, 4199-206.

Nguyen, T., D. A. Shapiro, S. R. George, V. Setola, D. K. Lee, R. Cheng, L. Rauser, S. P. Lee, K. R. Lynch, B. L. Roth and B. F. O'Dowd (2001) Discovery of a novel member of the histamine receptor family. *Mol Pharmacol*. **59**, 427-33.

Nicholl, J., B. Kofler, G. R. Sutherland, J. Shine and T. P. Iismaa (1995) Assignment of the gene encoding human galanin receptor (GALNR) to 18q23 by in situ hybridization. *Genomics*. **30**, 629-30.

Nicola, S. M., J. Surmeier and R. C. Malenka (2000) Dopaminergic modulation of neuronal excitability in the striatum and nucleus accumbens. *Annu Rev Neurosci*. **23**, 185-215.

Nieoullon, A. and M. Amalric (2002) [Dopaminergic receptors: structural features and functional implications]. *Rev Neurol (Paris)*. **158 Spec no 1**, S59-68.

Nishi, A., G. L. Snyder and P. Greengard (1997) Bidirectional regulation of DARPP-32 phosphorylation by dopamine. *J Neurosci*. **17**, 8147-55.

Nowak, P., J. Dabrowska, A. Bortel, I. Biedka, G. Szczerbak, G. Slomian, R. M. Kostrzewa and R. Brus (2006) Histamine H3 receptor agonist- and antagonist-evoked vacuous chewing movements in 6-OHDA-lesioned rats occurs in an absence of change in microdialysate dopamine levels. *Eur J Pharmacol*. **552**, 46-54.

Nutt, J. G. (1990) Levodopa-induced dyskinesia: review, observations, and speculations. *Neurology*. **40**, 340-5.

O'Donnell, D., S. Ahmad, C. Wahlestedt and P. Walker (1999) Expression of the novel galanin receptor subtype GALR2 in the adult rat CNS: distinct distribution from GALR1. *J Comp Neurol*. **409**, 469-81.

O'Hara, C. M., L. Tang, R. Taussig, R. D. Todd and K. L. O'Malley (1996) Dopamine D2L receptor couples to G alpha i2 and G alpha i3 but not G alpha i1, leading to the inhibition of adenylate cyclase in transfected cell lines. *J Pharmacol Exp Ther*. **278**, 354-60.

Oak, J. N., N. Lavine and H. H. Van Tol (2001) Dopamine D(4) and D(2L) Receptor Stimulation of the Mitogen-Activated Protein Kinase Pathway Is Dependent on trans-Activation of the Platelet-Derived Growth Factor Receptor. *Mol Pharmacol*. **60**, 92-103.

Oak, J. N., J. Oldenhof and H. H. Van Tol (2000) The dopamine D(4) receptor: one decade of research. *Eur J Pharmacol*. **405**, 303-27.

Obeso, J. A., M. C. Rodriguez-Oroz, B. Benitez-Temino, F. J. Blesa, J. Guridi, C. Marin and M. Rodriguez (2008) Functional organization of the basal ganglia: therapeutic implications for Parkinson's disease. *Mov Disord*. **23 Suppl 3**, S548-59.

Oda, T., N. Morikawa, Y. Saito, Y. Masuho and S. Matsumoto (2000) Molecular cloning and characterization of a novel type of histamine receptor preferentially expressed in leukocytes. *J Biol Chem*. **275**, 36781-6.

Ogawa, N. (1995) Molecular and chemical neuropharmacology of dopamine receptor subtypes. *Acta Med Okayama*. **49**, 1-11.

Ögren, S. O., E. Kuteeva, E. Elvander-Tottie and T. Hokfelt (2010) Neuropeptides in learning and memory processes with focus on galanin. *Eur J Pharmacol*. **626**, 9-17.

Ögren, S. O., P. A. Schott, J. Kehr, T. Yoshitake, I. Misane, P. Mannstrom and J. Sandin (1998) Modulation of acetylcholine and serotonin transmission by galanin. Relationship to spatial and aversive learning. *Ann N Y Acad Sci*. **863**, 342-63.

Ohara, K., K. Haga, G. Berstein, T. Haga and A. Ichiyama (1988) The interaction between D2 dopamine receptors and GTP-binding proteins. *Mol Pharmacol*. **33**, 290-6.

Oldenhof, J., R. Vickery, M. Anafi, J. Oak, A. Ray, O. Schoots, T. Pawson, M. von Zastrow and H. H. Van Tol (1998) SH3 binding domains in the dopamine D4 receptor. *Biochemistry*. **37**, 15726-36.

Orru, M., J. Bakesova, M. Brugarolas, C. Quiroz, V. Beaumont, S. R. Goldberg, C. Lluis, A. Cortés, R. Franco, V. Casadó, E. I. Canela and S. Ferré (2011) Striatal pre- and postsynaptic profile of adenosine A(2A) receptor antagonists. *PLoS One*. **6**, e16088.

Ostrom, R. S. and P. A. Insel (2004) The evolving role of lipid rafts and caveolae in G protein-coupled receptor signaling: implications for molecular pharmacology. *Br J Pharmacol*. **143**, 235-45.

Pak, Y., B. F. O'Dowd, J. B. Wang and S. R. George (1999) Agonist-induced, G protein-dependent and -independent down-regulation of the mu opioid receptor. The receptor is a direct substrate for protein-tyrosine kinase. *J Biol Chem*. **274**, 27610-6.

Palczewski, K., T. Kumasaka, T. Hori, C. A. Behnke, H. Motoshima, B. A. Fox, I. Le Trong, D. C. Teller, T. Okada, R. E. Stenkamp, M. Yamamoto and M. Miyano (2000) Crystal structure of rhodopsin: A G protein-coupled receptor. *Science*. **289**, 739-45.

Pang, L., T. Hashemi, H. J. Lee, M. Maguire, M. P. Graziano, M. Bayne, B. Hawes, G. Wong and S. Wang (1998) The mouse GalR2 galanin receptor: genomic organization, cDNA cloning, and functional characterization. *J Neurochem*. **71**, 2252-9.

Pani, L. (2002) Clinical implications of dopamine research in schizophrenia. *Curr Med Res Opin*. **18 Suppl 3**, s3-7.

Panula, P., J. Rinne, K. Kuokkanen, K. S. Eriksson, T. Sallmen, H. Kalimo and M. Relja (1998) Neuronal histamine deficit in Alzheimer's disease. *Neuroscience*. **82**, 993-7.

Parker, E. M., D. G. Izzarelli, H. P. Nowak, C. D. Mahle, L. G. Iben, J. Wang and M. E. Goldstein (1995) Cloning and characterization of the rat GALR1 galanin receptor from Rin14B insulinoma cells. *Brain Res Mol Brain Res*. **34**, 179-89.

Passani, M. B., L. Bacciottini, P. F. Mannaioni and P. Blandina (2000) Central histaminergic system and cognition. *Neurosci Biobehav Rev*. **24**, 107-13.

Paulmurugan, R. and S. S. Gambhir (2003) Monitoring protein-protein interactions using split synthetic renilla luciferase protein-fragment-assisted complementation. *Anal Chem*. **75**, 1584-9.

Paxinos, G. and Watson. (2005) The rat brain in stereotaxic coordinates. *Elsevier, 5th Ed. Amsterdam.*

Pedersen, U. B., B. Norby, A. A. Jensen, M. Schiodt, A. Hansen, P. Suhr-Jessen, M. Scheideler, O. Thastrup and P. H. Andersen (1994) Characteristics of stably expressed human dopamine D1a and D1b receptors: atypical behavior of the dopamine D1b receptor. *Eur J Pharmacol*. **267**, 85-93.

Pelech, S. L. and J. S. Sanghera (1992) Mitogen-activated protein kinases: versatile transducers for cell signaling. *Trends Biochem Sci*. **17**, 233-8.

Perry, S. J. and R. J. Lefkowitz (2002) Arresting developments in heptahelical receptor signaling and regulation. *Trends Cell Biol*. **12**, 130-8.

Pfeffer, M. A. and L. W. Stevenson (1996) Beta-adrenergic blockers and survival in heart failure. *N Engl J Med*. **334**, 1396-7.

Pfleger, K. D., J. R. Dromey, M. B. Dalrymple, E. M. Lim, W. G. Thomas and K. A. Eidne (2006) Extended bioluminescence resonance energy transfer (eBRET) for monitoring prolonged protein-protein interactions in live cells. *Cell Signal*. **18**, 1664-70.

Pfleger, K. D. and K. A. Eidne (2005) Monitoring the formation of dynamic G-protein-coupled receptor-protein complexes in living cells. *Biochem J*. **385**, 625-37.

Pfleger, K. D. and K. A. Eidne (2006) Illuminating insights into protein-protein interactions using bioluminescence resonance energy transfer (BRET). *Nat Methods*. **3**, 165-74.

Picciotto, M. R. (2008) Galanin and addiction. *Cell Mol Life Sci*. **65**, 1872-9.

Picciotto, M. R., C. Brabant, E. B. Einstein, H. M. Kamens and N. M. Neugebauer (2009) Effects of galanin on monoaminergic systems and HPA axis: Potential mechanisms underlying the effects of galanin on addiction- and stress-related behaviors. *Brain Res*. **1314**, 206-18.

Pierce, K. L. and R. J. Lefkowitz (2001) Classical and new roles of beta-arrestins in the regulation of G-protein-coupled receptors. *Nat Rev Neurosci*. **2**, 727-33.

Pierce, K. L., L. M. Luttrell and R. J. Lefkowitz (2001) New mechanisms in heptahelical receptor signaling to mitogen activated protein kinase cascades. *Oncogene*. **20**, 1532-9.

Pillai, G., N. A. Brown, G. McAllister, G. Milligan and G. R. Seabrook (1998) Human D2 and D4 dopamine receptors couple through betagamma G-protein subunits to inwardly rectifying K+ channels (GIRK1) in a Xenopus oocyte expression system: selective antagonism by L-741,626 and L-745,870 respectively. *Neuropharmacology*. **37**, 983-7.

Pillot, C., A. Heron, V. Cochois, J. Tardivel-Lacombe, X. Ligneau, J. C. Schwartz and J. M. Arrang (2002) A detailed mapping of the histamine H(3) receptor and its gene transcripts in rat brain. *Neuroscience*. **114**, 173-93.

Pin, J. P., T. Galvez and L. Prezeau (2003) Evolution, structure, and activation mechanism of family 3/C G-protein-coupled receptors. *Pharmacol Ther*. **98**, 325-54.

Pin, J. P., R. Neubig, M. Bouvier, L. Devi, M. Filizola, J. A. Javitch, M. J. Lohse, G. Milligan, K. Palczewski, M. Parmentier and M. Spedding (2007) International Union of Basic and Clinical Pharmacology. LXVII. Recommendations for the recognition and nomenclature of G protein-coupled receptor heteromultimers. *Pharmacol Rev*. **59**, 5-13.

Pippig, S., S. Andexinger and M. J. Lohse (1995) Sequestration and recycling of beta 2-adrenergic receptors permit receptor resensitization. *Mol Pharmacol*. **47**, 666-76.

Pontieri, F. E., G. Tanda and G. Di Chiara (1995) Intravenous cocaine, morphine, and amphetamine preferentially increase extracellular dopamine in the "shell" as compared with the "core" of the rat nucleus accumbens. *Proc Natl Acad Sci U S A*. **92**, 12304-8.

Powell, S. B., M. P. Paulus, D. S. Hartman, T. Godel and M. A. Geyer (2003) RO-10-5824 is a selective dopamine D4 receptor agonist that increases novel object exploration in C57 mice. *Neuropharmacology*. **44**, 473-81.

Premont, R. T. and R. R. Gainetdinov (2007) Physiological roles of G protein-coupled receptor kinases and arrestins. *Annu Rev Physiol*. **69**, 511-34.

Prinster, S. C., C. Hague and R. A. Hall (2005) Heterodimerization of g protein-coupled receptors: specificity and functional significance. *Pharmacol Rev*. **57**, 289-98.

Probst, W. C., L. A. Snyder, D. I. Schuster, J. Brosius and S. C. Sealfon (1992) Sequence alignment of the G-protein coupled receptor superfamily. *DNA Cell Biol*. **11**, 1-20.

Prossnitz, E. R. (2004) Novel roles for arrestins in the post-endocytic trafficking of G protein-coupled receptors. *Life Sci*. **75**, 893-9.

Ranade, K., E. Jorgenson, W. H. Sheu, D. Pei, C. A. Hsiung, F. T. Chiang, Y. D. Chen, R. Pratt, R. A. Olshen, D. Curb, D. R. Cox, D. Botstein and N. Risch (2002) A polymorphism in the beta1 adrenergic receptor is associated with resting heart rate. *Am J Hum Genet*. **70**, 935-42.

Rang, H. P., M. M. Dale, J. M. Ritter and R. J. Flower (2008) Farmacología. *Elsevier, 6ª edición, Madrid.*

Rankin, M. L., L. A. Hazelwood, R. B. Free, Y. Namkung, E. B. Rex, R. A. Roof and D. R. Sibley (2010) Molecular pharmacology of the dopamine receptors, in Dopamine Handbook (Iversen LL, Dunnett SB, Iversen SD, Bjorklund A ed) Oxford University, New York. 63-87.

Rashid, A. J., C. H. So, M. M. Kong, T. Furtak, M. El-Ghundi, R. Cheng, B. F. O'Dowd and S. R. George (2007) D1-D2 dopamine receptor heterooligomers with unique pharmacology are coupled to rapid activation of Gq/11 in the striatum. *Proc Natl Acad Sci U S A*. **104**, 654-9.

Ravna, A. W., I. Sylte and S. G. Dahl (2009) Structure and localisation of drug binding sites on neurotransmitter transporters. *J Mol Model*. **15**, 1155-64.

Ray, K. and B. C. Hauschild (2000) Cys-140 is critical for metabotropic glutamate receptor-1 dimerization. *J Biol Chem*. **275**, 34245-51.

Reeves, S., R. Brown, R. Howard and P. Grasby (2009) Increased striatal dopamine (D2/D3) receptor availability and delusions in Alzheimer disease. *Neurology*. **72**, 528-34.

Renfrow, J. J., A. C. Scheck, N. S. Dhawan, P. J. Lukac, H. Vogel, J. P. Chandler, J. J. Raizer, G. R. Harsh, A. Chakravarti and M. Bredel (2011) Gene-protein correlation in single cells. *Neuro Oncol*. **13**, 880-5.

Rinne, J. O., O. V. Anichtchik, K. S. Eriksson, J. Kaslin, L. Tuomisto, H. Kalimo, M. Roytta and P. Panula (2002) Increased brain histamine levels in Parkinson's disease but not in multiple system atrophy. *J Neurochem*. **81**, 954-60.

Rios, C. D., B. A. Jordan, I. Gomes and L. A. Devi (2001) G-protein-coupled receptor dimerization: modulation of receptor function. *Pharmacol Ther*. **92**, 71-87.

Rios, E. R., E. T. Venancio, N. F. Rocha, D. J. Woods, S. Vasconcelos, D. Macedo, F. C. Sousa and M. M. Fonteles (2010) Melatonin: pharmacological aspects and clinical trends. *Int J Neurosci*. **120**, 583-90.

Risinger, F. O., P. A. Freeman, M. Rubinstein, M. J. Low and D. K. Grandy (2000) Lack of operant ethanol self-administration in dopamine D2 receptor knockout mice. *Psychopharmacology (Berl)*. **152**, 343-50.

Ritter, S. L. and R. A. Hall (2009) Fine-tuning of GPCR activity by receptor-interacting proteins. *Nat Rev Mol Cell Biol*. **10**, 819-30.

Ritz, M. C., R. J. Lamb, S. R. Goldberg and M. J. Kuhar (1987) Cocaine receptors on dopamine transporters are related to self-administration of cocaine. *Science*. **237**, 1219-23.

Rivero-Müller, A., Y. Y. Chou, I. Ji, S. Lajic, A. C. Hanyaloglu, K. Jonas, N. Rahman, T. H. Ji and I. Huhtaniemi (2010) Rescue of defective G protein-coupled receptor function in vivo by intermolecular cooperation. *Proc Natl Acad Sci U S A*. **107**, 2319-24.

Robbins, M. J., F. Ciruela, A. Rhodes and R. A. McIlhinney (1999) Characterization of the dimerization of metabotropic glutamate receptors using an N-terminal truncation of mGluR1alpha. *J Neurochem*. **72**, 2539-47.

Roberts, D. C., M. E. Corcoran and H. C. Fibiger (1977) On the role of ascending catecholaminergic systems in intravenous self-administration of cocaine. *Pharmacol Biochem Behav*. **6**, 615-20.

Robinson, T. E., G. Gorny, E. Mitton and B. Kolb (2001) Cocaine self-administration alters the morphology of dendrites and dendritic spines in the nucleus accumbens and neocortex. *Synapse*. **39**, 257-66.

Robinson, T. E. and B. Kolb (1999) Alterations in the morphology of dendrites and dendritic spines in the nucleus accumbens and prefrontal cortex following repeated treatment with amphetamine or cocaine. *Eur J Neurosci*. **11**, 1598-604.

Rocheville, M., D. C. Lange, U. Kumar, S. C. Patel, R. C. Patel and Y. C. Patel (2000a) Receptors for dopamine and somatostatin: formation of hetero-oligomers with enhanced functional activity. *Science*. **288**, 154-7.

Rocheville, M., D. C. Lange, U. Kumar, R. Sasi, R. C. Patel and Y. C. Patel (2000b) Subtypes of the somatostatin receptor assemble as functional homo- and heterodimers. *J Biol Chem*. **275**, 7862-9.

Rokaeus, A. and M. J. Brownstein (1986) Construction of a porcine adrenal medullary cDNA library and nucleotide sequence analysis of two clones encoding a galanin precursor. *Proc Natl Acad Sci U S A*. **83**, 6287-91.

Roman, T., M. Schmitz, G. Polanczyk, M. Eizirik, L. A. Rohde and M. H. Hutz (2001) Attention-deficit hyperactivity disorder: a study of association with both the dopamine transporter gene and the dopamine D4 receptor gene. *Am J Med Genet*. **105**, 471-8.

Romano, C., J. K. Miller, K. Hyrc, S. Dikranian, S. Mennerick, Y. Takeuchi, M. P. Goldberg and K. L. O'Malley (2001) Covalent and noncovalent interactions mediate metabotropic glutamate receptor mGlu5 dimerization. *Mol Pharmacol*. **59**, 46-53.

Romano, C., W. L. Yang and K. L. O'Malley (1996) Metabotropic glutamate receptor 5 is a disulfide-linked dimer. *J Biol Chem*. **271**, 28612-6.

Romieu, P., R. Martin-Fardon and T. Maurice (2000) Involvement of the sigma1 receptor in the cocaine-induced conditioned place preference. *Neuroreport*. **11**, 2885-8.

Romieu, P., V. L. Phan, R. Martin-Fardon and T. Maurice (2002) Involvement of the sigma(1) receptor in cocaine-induced conditioned place preference: possible dependence on dopamine uptake blockade. *Neuropsychopharmacology*. **26**, 444-55.

Rondou, P., G. Haegeman and K. Van Craenenbroeck (2010) The dopamine D4 receptor: biochemical and signalling properties. *Cell Mol Life Sci*. **67**, 1971-86.

Ross, S. B. and A. L. Renyi (1967) Inhibition of the uptake of tritiated catecholamines by antidepressant and related agents. *Eur J Pharmacol*. **2**, 181-6.

Rossmanith, W. G., D. K. Clifton and R. A. Steiner (1996) Galanin gene expression in hypothalamic GnRH-containing neurons of the rat: a model for autocrine regulation. *Horm Metab Res*. **28**, 257-66.

Rouge-Pont, F., A. Usiello, M. Benoit-Marand, F. Gonon, P. V. Piazza and E. Borrelli (2002) Changes in extracellular dopamine induced by morphine and cocaine: crucial control by D2 receptors. *J Neurosci*. **22**, 3293-301.

Rouleau, A., A. Heron, V. Cochois, C. Pillot, J. C. Schwartz and J. M. Arrang (2004) Cloning and expression of the mouse histamine H3 receptor: evidence for multiple isoforms. *J Neurochem*. **90**, 1331-8.L

Rozenfeld, R., F. M. Décaillot, A. P. IJzerman and L. A. Devi (2006) Heterodimers of G protein-coupled receptors as novel and distinct drug targets. *Drug Discovery Today: Therapeutic Strategies*. **3**, 437-43.

Rozenfeld, R. and L. A. Devi (2011) Exploring a role for heteromerization in GPCR signalling specificity. *Biochem J*. **433**, 11-8.

Rozengurt, E. (2007) Mitogenic signaling pathways induced by G protein-coupled receptors. *J Cell Physiol*. **213**, 589-602.

Rubinstein, M., O. Gershanik and F. J. Stefano (1988) Different roles of D-1 and D-2 dopamine receptors involved in locomotor activity of supersensitive mice. *Eur J Pharmacol*. **148**, 419-26.

Ryu, J. H., K. Yanai, R. Iwata, T. Ido and T. Watanabe (1994a) Heterogeneous distributions of histamine H3, dopamine D1 and D2 receptors in rat brain. *Neuroreport*. **5**, 621-4.

Ryu, J. H., K. Yanai and T. Watanabe (1994b) Marked increase in histamine H3 receptors in the striatum and substantia nigra after 6-hydroxydopamine-induced denervation of dopaminergic neurons: an autoradiographic study. *Neurosci Lett*. **178**, 19-22.

Ryu, J. H., K. Yanai, X. L. Zhao and T. Watanabe (1996) The effect of dopamine D1 receptor stimulation on the up-regulation of histamine H3-receptors following destruction of the ascending dopaminergic neurones. *Br J Pharmacol*. **118**, 585-92.

Sadoshima, J. and S. Izumo (1996) The heterotrimeric G q protein-coupled angiotensin II receptor activates p21 ras via the tyrosine kinase-Shc-Grb2-Sos pathway in cardiac myocytes. *EMBO J*. **15**, 775-87.

Sahlholm, K., J. Nilsson, D. Marcellino, K. Fuxe and P. Arhem (2007) The human histamine H3 receptor couples to GIRK channels in Xenopus oocytes. *Eur J Pharmacol*. **567**, 206-10.

Sahu, A., K. R. Tyeryar, H. O. Vongtau, D. R. Sibley and A. S. Undieh (2009) D5 dopamine receptors are required for dopaminergic activation of phospholipase C. *Mol Pharmacol*. **75**, 447-53.

Sahu, N. and A. August (2009) ITK inhibitors in inflammation and immune-mediated disorders. *Curr Top Med Chem*. **9**, 690-703.

Sakmar, T. P. (1998) Rhodopsin: a prototypical G protein-coupled receptor. *Prog Nucleic Acid Res Mol Biol*. **59**, 1-34.

Salazar, M., C. Peralta and J. Pastor (2006) Manual de Psicofarmacología. *Ed Medica Panamericana, Madrid*.

Sanchez-Lemus, E. and J. A. Arias-Montano (2004) Histamine H3 receptor activation inhibits dopamine D1 receptor-induced cAMP accumulation in rat striatal slices. *Neurosci Lett*. **364**, 179-84.

Santanavanich, C., M. Ebadi and P. Govitrapong (2005) Dopamine receptor activation in bovine pinealocyte via a cAMP-dependent transcription pathway. *J Pineal Res*. **38**, 170-5.

Santini, E., E. Valjent and G. Fisone (2008) Parkinson's disease: levodopa-induced dyskinesia and signal transduction. *FEBS J*. **275**, 1392-9.

Sara, S. J. (2009) The locus coeruleus and noradrenergic modulation of cognition. *Nat Rev Neurosci*. **10**, 211-23.

Sasa, M. and N. Yoshimura (1994) Locus coeruleus noradrenergic neurons as a micturition center. *Microsc Res Tech*. **29**, 226-30.

Saura, C., F. Ciruela, V. Casadó, E. I. Canela, J. Mallol, C. Lluis and R. Franco (1996) Adenosine deaminase interacts with A1 adenosine receptors in pig brain cortical membranes. *J Neurochem*. **66**, 1675-82.

Scahill, L. and M. Schwab-Stone (2000) Epidemiology of ADHD in school-age children. *Child Adolesc Psychiatr Clin N Am*. **9**, 541-55, VII.

Scarselli, M., M. Armogida, S. Chiacchio, M. G. DeMontis, A. Colzi, G. U. Corsini and R. Maggio (2000) Reconstitution of functional dopamine D(2s) receptor by co-expression of amino- and carboxyl-terminal receptor fragments. *Eur J Pharmacol*. **397**, 291-6.

Schaferling, M. and S. Nagl (2011) Forster resonance energy transfer methods for quantification of protein-protein interactions on microarrays. *Methods Mol Biol*. **723**, 303-20.

Schapira, A. H., E. Bezard, J. Brotchie, F. Calon, G. L. Collingridge, B. Ferger, B. Hengerer, E. Hirsch, P. Jenner, N. Le Novere, J. A. Obeso, M. A. Schwarzschild, U. Spampinato and G. Davidai (2006) Novel pharmacological targets for the treatment of Parkinson's disease. *Nat Rev Drug Discov*. **5**, 845-54.

Schiattarella, G. G., C. Perrino, G. Gargiulo, S. Sorrentino, A. Franzone, G. Capretti, G. Esposito and M. Chiariello (2010) [Novel concepts in beta-adrenergic receptor signaling: therapeutic options for heart failure]. *G Ital Cardiol (Rome)*. **11**, 221-8.

Schiffmann, S. N., G. Fisone, R. Moresco, R. A. Cunha and S. Ferré (2007) Adenosine A2A receptors and basal ganglia physiology. *Prog Neurobiol*. **83**, 277-92.

Schilström, B., R. Yaka, E. Argilli, N. Suvarna, J. Schumann, B. T. Chen, M. Carman, V. Singh, W. S. Mailliard, D. Ron and A. Bonci (2006) Cocaine enhances NMDA receptor-mediated currents in ventral tegmental area cells via dopamine D5 receptor-dependent redistribution of NMDA receptors. *J Neurosci*. **26**, 8549-58.

Schlicker, E., K. Fink, M. Detzner and M. Gothert (1993) Histamine inhibits dopamine release in the mouse striatum via presynaptic H3 receptors. *J Neural Transm Gen Sect*. **93**, 1-10.

Schmitt, J. M. and P. J. Stork (2000) beta 2-adrenergic receptor activates extracellular signal-regulated kinases (ERKs) via the small G protein rap1 and the serine/threonine kinase B-Raf. *J Biol Chem*. **275**, 25342-50.

Schmitz, J. M., R. M. Graham, A. Sagalowsky and W. A. Pettinger (1981) Renal alpha-1 and alpha-2 adrenergic receptors: biochemical and pharmacological correlations. *J Pharmacol Exp Ther*. **219**, 400-6.

Schneider, C., D. Risser, L. Kirchner, E. Kitzmuller, N. Cairns, H. Prast, N. Singewald and G. Lubec (1997) Similar deficits of central histaminergic system in patients with Down syndrome and Alzheimer disease. *Neurosci Lett*. **222**, 183-6.

Schulte, G. and B. B. Fredholm (2003) Signalling from adenosine receptors to mitogen-activated protein kinases. *Cell Signal*. **15**, 813-27.

Schulz, A., R. Grosse, G. Schultz, T. Gudermann and T. Schoneberg (2000) Structural implication for receptor oligomerization from functional reconstitution studies of mutant V2 vasopressin receptors. *J Biol Chem*. **275**, 2381-9.

Segal, M., G. Richter-Levin and N. Maggio (2010) Stress-induced dynamic routing of hippocampal connectivity: a hypothesis. *Hippocampus*. **20**, 1332-8.

Segawa, M. (2003) Neurophysiology of Tourette's syndrome: pathophysiological considerations. *Brain Dev*. **25 Suppl 1**, S62-9.

Seifert, R. and K. Wenzel-Seifert (2002) Constitutive activity of G-protein-coupled receptors: cause of disease and common property of wild-type receptors. *Naunyn Schmiedebergs Arch Pharmacol*. **366**, 381-416.

Senogles, S. E. (1994) The D2 dopamine receptor isoforms signal through distinct Gi alpha proteins to inhibit adenylyl cyclase. A study with site-directed mutant Gi alpha proteins. *J Biol Chem*. **269**, 23120-7.

Senogles, S. E., J. L. Benovic, N. Amlaiky, C. Unson, G. Milligan, R. Vinitsky, A. M. Spiegel and M. G. Caron (1987) The D2-dopamine receptor of anterior pituitary is functionally associated with a pertussis toxin-sensitive guanine nucleotide binding protein. *J Biol Chem*. **262**, 4860-7.

Seyedi, N., C. J. Mackins, T. Machida, A. C. Reid, R. B. Silver and R. Levi (2005) Histamine H3-receptor-induced attenuation of norepinephrine exocytosis: a decreased protein kinase a activity mediates a reduction in intracellular calcium. *J Pharmacol Exp Ther*. **312**, 272-80.

Sharkey, J., K. A. Glen, S. Wolfe and M. J. Kuhar (1988) Cocaine binding at sigma receptors. *Eur J Pharmacol*. **149**, 171-4.

Sheng, M. and C. C. Hoogenraad (2007) The postsynaptic architecture of excitatory synapses: a more quantitative view. *Annu Rev Biochem*. **76**, 823-47.

Shenton, F. C., V. Hann and P. L. Chazot (2005) Evidence for native and cloned H3 histamine receptor higher oligomers. *Inflamm Res*. **54 Suppl 1**, S48-9.

Sherin, J. E., J. K. Elmquist, F. Torrealba and C. B. Saper (1998) Innervation of histaminergic tuberomammillary neurons by GABAergic and galaninergic neurons in the ventrolateral preoptic nucleus of the rat. *J Neurosci*. **18**, 4705-21.

Shimohama, S., H. Sawada, Y. Kitamura and T. Taniguchi (2003) Disease model: Parkinson's disease. *Trends Mol Med*. **9**, 360-5.

Sibley, D. R. (1999) New insights into dopaminergic receptor function using antisense and genetically altered animals. *Annu Rev Pharmacol Toxicol*. **39**, 313-41.

Sidhu, A., M. Sullivan, T. Kohout, P. Balen and P. H. Fishman (1991) D1 dopamine receptors can interact with both stimulatory and inhibitory guanine nucleotide binding proteins. *J Neurochem*. **57**, 1445-51.

Silver, R. B., C. J. Mackins, N. C. Smith, I. L. Koritchneva, K. Lefkowitz, T. W. Lovenberg and R. Levi (2001) Coupling of histamine H3 receptors to neuronal Na+/H+ exchange: a novel protective mechanism in myocardial ischemia. *Proc Natl Acad Sci U S A*. **98**, 2855-9.

Silver, R. B., K. S. Poonwasi, N. Seyedi, S. J. Wilson, T. W. Lovenberg and R. Levi (2002) Decreased intracellular calcium mediates the histamine H3-receptor-induced attenuation of norepinephrine exocytosis from cardiac sympathetic nerve endings. *Proc Natl Acad Sci U S A*. **99**, 501-6.

Simonneaux, V., L. C. Murrin and M. Ebadi (1990) Characterization of D1 dopamine receptors in the bovine pineal gland with [3H]SCH 23390. *J Pharmacol Exp Ther*. **253**, 214-20.

Simonneaux, V. and C. Ribelayga (2003) Generation of the melatonin endocrine message in mammals: a review of the complex regulation of melatonin synthesis by norepinephrine, peptides, and other pineal transmitters. *Pharmacol Rev*. **55**, 325-95.

Small, K. M., M. R. Schwarb, C. Glinka, C. T. Theiss, K. M. Brown, C. A. Seman and S. B. Liggett (2006) Alpha2A- and alpha2C-adrenergic receptors form homo- and heterodimers: the heterodimeric state impairs agonist-promoted GRK phosphorylation and beta-arrestin recruitment. *Biochemistry*. **45**, 4760-7.

Smit, M. J., M. Hoffmann, H. Timmerman and R. Leurs (1999) Molecular properties and signalling pathways of the histamine H1 receptor. *Clin Exp Allergy*. **29 Suppl 3**, 19-28.

Smith, K. E., C. Forray, M. W. Walker, K. A. Jones, J. A. Tamm, J. Bard, T. A. Branchek, D. L. Linemeyer and C. Gerald (1997) Expression cloning of a rat hypothalamic galanin receptor coupled to phosphoinositide turnover. *J Biol Chem*. **272**, 24612-6.

Smith, K. E., M. W. Walker, R. Artymyshyn, J. Bard, B. Borowsky, J. A. Tamm, W. J. Yao, P. J. Vaysse, T. A. Branchek, C. Gerald and K. A. Jones (1998) Cloned human and rat galanin GALR3 receptors. Pharmacology and activation of G-protein inwardly rectifying K+ channels. *J Biol Chem*. **273**, 23321-6.

Sneader, W. (2001) The discovery and synthesis of epinephrine. *Drug News Perspect*. **14**, 491-4.

So, C. H., V. Verma, M. Alijaniaram, R. Cheng, A. J. Rashid, B. F. O'Dowd and S. R. George (2009) Calcium signaling by dopamine D5 receptor and D5-D2 receptor hetero-oligomers occurs by a mechanism distinct from that for dopamine D1-D2 receptor hetero-oligomers. *Mol Pharmacol*. **75**, 843-54.

Soderberg, O., M. Gullberg, M. Jarvius, K. Ridderstrale, K. J. Leuchowius, J. Jarvius, K. Wester, P. Hydbring, F. Bahram, L. G. Larsson and U. Landegren (2006) Direct observation of individual endogenous protein complexes in situ by proximity ligation. *Nat Methods*. **3**, 995-1000.

Soderberg, O., K. J. Leuchowius, M. Gullberg, M. Jarvius, I. Weibrecht, L. G. Larsson and U. Landegren (2008) Characterizing proteins and their interactions in cells and tissues using the in situ proximity ligation assay. *Methods*. **45**, 227-32.

Sokoloff, P., J. Diaz, B. Le Foll, O. Guillin, L. Leriche, E. Bezard and C. Gross (2006) The dopamine D3 receptor: a therapeutic target for the treatment of neuropsychiatric disorders. *CNS Neurol Disord Drug Targets*. **5**, 25-43.

Soriano, A., R. Ventura, A. Molero, R. Hoen, V. Casadó, A. Cortés, F. Fanelli, F. Albericio, C. Lluis, R. Franco and M. Royo (2009) Adenosine A2A receptor-antagonist/dopamine D2 receptor-agonist bivalent ligands as pharmacological tools to detect A2A-D2 receptor heteromers. *J Med Chem*. **52**, 5590-602.

Sotnikova, T. D., J. M. Beaulieu, R. R. Gainetdinov and M. G. Caron (2006) Molecular biology, pharmacology and functional role of the plasma membrane dopamine transporter. *CNS Neurol Disord Drug Targets*. **5**, 45-56.

Spano, P. F., S. Govoni and M. Trabucchi (1978) Studies on the pharmacological properties of dopamine receptors in various areas of the central nervous system. *Adv Biochem Psychopharmacol*. **19**, 155-65.

Starke, K., M. Gothert and H. Kilbinger (1989) Modulation of neurotransmitter release by presynaptic autoreceptors. *Physiol Rev*. **69**, 864-989.

Starr, B. S., M. S. Starr and I. C. Kilpatrick (1987) Behavioural role of dopamine D1 receptors in the reserpine-treated mouse. *Neuroscience*. **22**, 179-88.

Starr, S., L. B. Kozell and K. A. Neve (1995) Drug-induced up-regulation of dopamine D2 receptors on cultured cells. *J Neurochem*. **65**, 569-77.

Steininger, T. L., H. Gong, D. McGinty and R. Szymusiak (2001) Subregional organization of preoptic area/anterior hypothalamic projections to arousal-related monoaminergic cell groups. *J Comp Neurol*. **429**, 638-53.

Sten Shi, T. J., X. Zhang, K. Holmberg, Z. Q. Xu and T. Hokfelt (1997) Expression and regulation of galanin-R2 receptors in rat primary sensory neurons: effect of axotomy and inflammation. *Neurosci Lett*. **237**, 57-60.

Stiles, G. L., B. B. Hoffman, M. Hubbard, M. G. Caron and R. J. Lefkowitz (1983a) Guanine nucleotides and alpha 1 adrenergic receptors in the heart. *Biochem Pharmacol*. **32**, 69-71.

Stiles, G. L., S. Taylor and R. J. Lefkowitz (1983b) Human cardiac beta-adrenergic receptors: subtype heterogeneity delineated by direct radioligand binding. *Life Sci*. **33**, 467-73.

Stryer, L. (1978) Fluorescence energy transfer as a spectroscopic ruler. *Annu Rev Biochem*. **47**, 819-46.

Su, T. P. and T. Hayashi (2001) Cocaine affects the dynamics of cytoskeletal proteins via sigma(1) receptors. *Trends Pharmacol Sci*. **22**, 456-8.

Su, T. P. and T. Hayashi (2003) Understanding the molecular mechanism of sigma-1 receptors: towards a hypothesis that sigma-1 receptors are intracellular amplifiers for signal transduction. *Curr Med Chem*. **10**, 2073-80.

Sugamori, K. S., L. L. Demchyshyn, M. Chung and H. B. Niznik (1994) D1A, D1B, and D1C dopamine receptors from Xenopus laevis. *Proc Natl Acad Sci U S A*. **91**, 10536-40.

Sugden, D. (1990) 5-Hydroxytryptamine amplifies beta-adrenergic stimulation of N-acetyltransferase activity in rat pinealocytes. *J Neurochem*. **55**, 1655-8.

Sugita, S. (2008) Mechanisms of exocytosis. *Acta Physiol (Oxf)*. **192**, 185-93.

Sun, X., J. Deng, T. Liu and J. Borjigin (2002) Circadian 5-HT production regulated by adrenergic signaling. *Proc Natl Acad Sci U S A*. **99**, 4686-91.

Surmeier, D. J., J. Bargas, H. C. Hemmings, Jr., A. C. Nairn and P. Greengard (1995) Modulation of calcium currents by a D1 dopaminergic protein kinase/phosphatase cascade in rat neostriatal neurons. *Neuron*. **14**, 385-97.

Suzuki, Y., E. Moriyoshi, D. Tsuchiya and H. Jingami (2004) Negative cooperativity of glutamate binding in the dimeric metabotropic glutamate receptor subtype 1. *J Biol Chem*. **279**, 35526-34.

Svingos, A. L., S. Periasamy and V. M. Pickel (2000) Presynaptic dopamine D(4) receptor localization in the rat nucleus accumbens shell. *Synapse*. **36**, 222-32.

Swanson, J., M. Posner, J. Fusella, M. Wasdell, T. Sommer and J. Fan (2001) Genes and attention deficit hyperactivity disorder. *Curr Psychiatry Rep*. **3**, 92-100.

hi and N. Akaike (1998) Histamine modulates high-voltage-activated calcium channels in neurons dissociated from the rat tuberomammillary nucleus. *Neuroscience*. **87**, 797-805.

Tan, M., W. M. Walwyn, C. J. Evans and C. W. Xie (2009) p38 MAPK and beta-arrestin 2 mediate functional interactions between endogenous micro-opioid and alpha2A-adrenergic receptors in neurons. *J Biol Chem*. **284**, 6270-81.

Tanaka, S. and A. Ichikawa (2006) Recent advances in molecular pharmacology of the histamine systems: immune regulatory roles of histamine produced by leukocytes. *J Pharmacol Sci*. **101**, 19-23.

Tapp, E. and M. Huxley (1972) The histological appearance of the human pineal gland from puberty to old age. *J Pathol*. **108**, 137-44.

Taraskevich, P. S. and W. W. Douglas (1978) Catecholamines of supposed inhibitory hypophysiotrophic function suppress action potentials in prolactin cells. *Nature*. **276**, 832-4.

Tarazi, F. I., E. C. Tomasini and R. J. Baldessarini (1998) Postnatal development of dopamine D4-like receptors in rat forebrain regions: comparison with D2-like receptors. *Brain Res Dev Brain Res*. **110**, 227-33.

Tardivel-Lacombe, J., S. Morisset, F. Gbahou, J. C. Schwartz and J. M. Arrang (2001) Chromosomal mapping and organization of the human histamine H3 receptor gene. *Neuroreport*. **12**, 321-4.

Tardivel-Lacombe, J., A. Rouleau, A. Heron, S. Morisset, C. Pillot, V. Cochois, J. C. Schwartz and J. M. Arrang (2000) Cloning and cerebral expression of the guinea pig histamine H3 receptor: evidence for two isoforms. *Neuroreport*. **11**, 755-9.

Tatemoto, K., A. Rokaeus, H. Jornvall, T. J. McDonald and V. Mutt (1983) Galanin - a novel biologically active peptide from porcine intestine. *FEBS Lett*. **164**, 124-8.

Terrillon, S. and M. Bouvier (2004) Roles of G-protein-coupled receptor dimerization. *EMBO Rep*. **5**, 30-4.

Thapar, A., M. O'Donovan and M. J. Owen (2005) The genetics of attention deficit hyperactivity disorder. *Hum Mol Genet*. **14 Spec No. 2**, R275-82.

Thibault, D., P. R. Albert, G. Pineyro and L. E. Trudeau (2011) Neurotensin triggers dopamine D2 receptor desensitization through a protein kinase C and beta-arrestin1-dependent mechanism. *J Biol Chem*. **286**, 9174-84.

Thymiakou, E., V. I. Zannis and D. Kardassis (2007) Physical and functional interactions between liver X receptor/retinoid X receptor and Sp1 modulate the transcriptional induction of the human ATP binding cassette transporter A1 gene by oxysterols and retinoids. *Biochemistry*. **46**, 11473-83.

Tiberi, M., K. R. Jarvie, C. Silvia, P. Falardeau, J. A. Gingrich, N. Godinot, L. Bertrand, T. L. Yang-Feng, R. T. Fremeau, Jr. and M. G. Caron (1991) Cloning, molecular characterization, and chromosomal assignment of a gene encoding a second D1 dopamine receptor subtype: differential expression pattern in rat brain compared with the D1A receptor. *Proc Natl Acad Sci U S A*. **88**, 7491-5.

Togias, A. (2003) H1-receptors: localization and role in airway physiology and in immune functions. *J Allergy Clin Immunol*. **112**, S60-8.

Torrent, A., D. Moreno-Delgado, J. Gomez-Ramirez, D. Rodriguez-Agudo, C. Rodriguez-Caso, F. Sanchez-Jimenez, I. Blanco and J. Ortiz (2005) H3 autoreceptors modulate histamine synthesis through calcium/calmodulin- and cAMP-dependent protein kinase pathways. *Mol Pharmacol*. **67**, 195-203.

Toyota, H., C. Dugovic, M. Koehl, A. D. Laposky, C. Weber, K. Ngo, Y. Wu, D. H. Lee, K. Yanai, E. Sakurai, T. Watanabe, C. Liu, J. Chen, A. J. Barbier, F. W. Turek, W. P. Fung-Leung and T. W. Lovenberg (2002) Behavioral characterization of mice lacking histamine H(3) receptors. *Mol Pharmacol*. **62**, 389-97.

Treisman, R. (1996) Regulation of transcription by MAP kinase cascades. *Curr Opin Cell Biol*. **8**, 205-15.

Trejo, J., S. R. Hammes and S. R. Coughlin (1998) Termination of signaling by protease-activated receptor-1 is linked to lysosomal sorting. *Proc Natl Acad Sci U S A*. **95**, 13698-702.

Tsao, P., T. Cao and M. von Zastrow (2001) Role of endocytosis in mediating downregulation of G-protein-coupled receptors. *Trends Pharmacol Sci*. **22**, 91-6.

Tsao, P. and M. von Zastrow (2000) Downregulation of G protein-coupled receptors. *Curr Opin Neurobiol*. **10**, 365-9.

Tsuji, Y., Y. Shimada, T. Takeshita, N. Kajimura, S. Nomura, N. Sekiyama, J. Otomo, J. Usukura, S. Nakanishi and H. Jingami (2000) Cryptic dimer interface and domain organization of the extracellular region of metabotropic glutamate receptor subtype 1. *J Biol Chem*. **275**, 28144-51.

Ujike, H., S. Kuroda and S. Otsuki (1996) sigma Receptor antagonists block the development of sensitization to cocaine. *Eur J Pharmacol*. **296**, 123-8.

Ulrich, C. D., 2nd, M. Holtmann and L. J. Miller (1998) Secretin and vasoactive intestinal peptide receptors: members of a unique family of G protein-coupled receptors. *Gastroenterology*. **114**, 382-97.

Undie, A. S. and E. Friedman (1990) Stimulation of a dopamine D1 receptor enhances inositol phosphates formation in rat brain. *J Pharmacol Exp Ther*. **253**, 987-92.

Usiello, A., J. H. Baik, F. Rouge-Pont, R. Picetti, A. Dierich, M. LeMeur, P. V. Piazza and E. Borrelli (2000) Distinct functions of the two isoforms of dopamine D2 receptors. *Nature*. **408**, 199-203.

Uveges, A. J., D. Kowal, Y. Zhang, T. B. Spangler, J. Dunlop, S. Semus and P. G. Jones (2002) The role of transmembrane helix 5 in agonist binding to the human H3 receptor. *J Pharmacol Exp Ther*. **301**, 451-8.

Valjent, E., J. C. Corvol, C. Pages, M. J. Besson, R. Maldonado and J. Caboche (2000) Involvement of the extracellular signal-regulated kinase cascade for cocaine-rewarding properties. *J Neurosci*. **20**, 8701-9.

Valjent, E., C. Pages, D. Herve, J. A. Girault and J. Caboche (2004) Addictive and non-addictive drugs induce distinct and specific patterns of ERK activation in mouse brain. *Eur J Neurosci*. **19**, 1826-36.

Valjent, E., C. Pages, M. Rogard, M. J. Besson, R. Maldonado and J. Caboche (2001) Delta 9-tetrahydrocannabinol-induced MAPK/ERK and Elk-1 activation in vivo depends on dopaminergic transmission. *Eur J Neurosci*. **14**, 342-52.

Valjent, E., V. Pascoli, P. Svenningsson, S. Paul, H. Enslen, J. C. Corvol, A. Stipanovich, J. Caboche, P. J. Lombroso, A. C. Nairn, P. Greengard, D. Herve and J. A. Girault (2005) Regulation of a protein phosphatase cascade allows convergent dopamine and glutamate signals to activate ERK in the striatum. *Proc Natl Acad Sci U S A*. **102**, 491-6.

Vallone, D., R. Picetti and E. Borrelli (2000) Structure and function of dopamine receptors. *Neurosci Biobehav Rev*. **24**, 125-32.

van Corven, E. J., P. L. Hordijk, R. H. Medema, J. L. Bos and W. H. Moolenaar (1993) Pertussis toxin-sensitive activation of p21ras by G protein-coupled receptor agonists in fibroblasts. *Proc Natl Acad Sci U S A*. **90**, 1257-61.

Vassart, G. (2010) An in vivo demonstration of functional G protein-coupled receptor dimers. *Proc Natl Acad Sci U S A*. **107**, 1819-20.

Vilardaga, J. P., V. O. Nikolaev, K. Lorenz, S. Ferrandon, Z. Zhuang and M. J. Lohse (2008) Conformational cross-talk between alpha2A-adrenergic and mu-opioid receptors controls cell signaling. *Nat Chem Biol*. **4**, 126-31.

Volkow, N. D., J. S. Fowler, G. J. Wang, R. Hitzemann, J. Logan, D. J. Schlyer, S. L. Dewey and A. P. Wolf (1993) Decreased dopamine D2 receptor availability is associated with reduced frontal metabolism in cocaine abusers. *Synapse*. **14**, 169-77.

Volkow, N. D. and J. M. Swanson (2003) Variables that affect the clinical use and abuse of methylphenidate in the treatment of ADHD. *Am J Psychiatry*. **160**, 1909-18.

Volkow, N. D., G. J. Wang, J. S. Fowler, M. Fischman, R. Foltin, N. N. Abumrad, S. J. Gatley, J. Logan, C. Wong, A. Gifford, Y. S. Ding, R. Hitzemann and N. Pappas (1999) Methylphenidate and cocaine have a similar in vivo potency to block dopamine transporters in the human brain. *Life Sci*. **65**, PL7-12.

Volovyk, Z. M., M. J. Wolf, S. V. Prasad and H. A. Rockman (2006) Agonist-stimulated beta-adrenergic receptor internalization requires dynamic cytoskeletal actin turnover. *J Biol Chem*. **281**, 9773-80.

Vrontakis, M. E., L. M. Peden, M. L. Duckworth and H. G. Friesen (1987) Isolation and characterization of a complementary DNA (galanin) clone from estrogen-induced pituitary tumor messenger RNA. *J Biol Chem*. **262**, 16755-8.

Vuoriluoto, M., L. J. Laine, P. Saviranta, J. Pouwels and M. J. Kallio (2010) Spatio-temporal composition of the mitotic Chromosomal Passenger Complex detected using in situ proximity ligation assay. *Mol Oncol*. **5**, 105-11.

Waldhoer, M., J. Fong, R. M. Jones, M. M. Lunzer, S. K. Sharma, E. Kostenis, P. S. Portoghese and J. L. Whistler (2005) A heterodimer-selective agonist shows in vivo relevance of G protein-coupled receptor dimers. *Proc Natl Acad Sci U S A*. **102**, 9050-5.

Wang, E., Y. C. Ding, P. Flodman, J. R. Kidd, K. K. Kidd, D. L. Grady, O. A. Ryder, M. A. Spence, J. M. Swanson and R. K. Moyzis (2004) The genetic architecture of selection at the human dopamine receptor D4 (DRD4) gene locus. *Am J Hum Genet*. **74**, 931-44.

Wang, S., A. Clemmons, C. Strader and M. Bayne (1998a) Evidence for hydrophobic interaction between galanin and the GalR1 galanin receptor and GalR1-mediated ligand internalization: fluorescent probing with a fluorescein-galanin. *Biochemistry*. **37**, 9528-35.

Wang, S., T. Hashemi, S. Fried, A. L. Clemmons and B. E. Hawes (1998b) Differential intracellular signaling of the GalR1 and GalR2 galanin receptor subtypes. *Biochemistry*. **37**, 6711-7.

Wang, S., T. Hashemi, C. He, C. Strader and M. Bayne (1997a) Molecular cloning and pharmacological characterization of a new galanin receptor subtype. *Mol Pharmacol*. **52**, 337-43.

Wang, S., C. He, T. Hashemi and M. Bayne (1997b) Cloning and expressional characterization of a novel galanin receptor. Identification of different pharmacophores within galanin for the three galanin receptor subtypes. *J Biol Chem*. **272**, 31949-52.

Wang, S., C. He, M. T. Maguire, A. L. Clemmons, R. E. Burrier, M. F. Guzzi, C. D. Strader, E. M. Parker and M. L. Bayne (1997c) Genomic organization and functional characterization of the mouse GalR1 galanin receptor. *FEBS Lett*. **411**, 225-30.

Wang, Y., R. Xu, T. Sasaoka, S. Tonegawa, M. P. Kung and E. B. Sankoorikal (2000) Dopamine D2 long receptor-deficient mice display alterations in striatum-dependent functions. *J Neurosci*. **20**, 8305-14.

Watts, V. J., M. N. Vu, B. L. Wiens, V. Jovanovic, H. H. Van Tol and K. A. Neve (1999) Short- and long-term heterologous sensitization of adenylate cyclase by D4 dopamine receptors. *Psychopharmacology (Berl)*. **141**, 83-92.

Weibrecht, I., K. J. Leuchowius, C. M. Clausson, T. Conze, M. Jarvius, W. M. Howell, M. Kamali-Moghaddam and O. Soderberg (2010) Proximity ligation assays: a recent addition to the proteomics toolbox. *Expert Rev Proteomics*. **7**, 401-9.

Weiner, N., S. Z. Langer and U. Trendelenburg (1967) Demonstration by the histochemical fluorescence method of the prolonged disappearance of catecholamines from the denervated nictitating membrane of the cat. *J Pharmacol Exp Ther*. **157**, 284-9.

Wellendorph, P., M. W. Goodman, E. S. Burstein, N. R. Nash, M. R. Brann and D. M. Weiner (2002) Molecular cloning and pharmacology of functionally distinct isoforms of the human histamine H(3) receptor. *Neuropharmacology*. **42**, 929-40.

Welter, M., D. Vallone, T. A. Samad, H. Meziane, A. Usiello and E. Borrelli (2007) Absence of dopamine D2 receptors unmasks an inhibitory control over the brain circuitries activated by cocaine. *Proc Natl Acad Sci U S A*. **104**, 6840-5.

Werner, P., N. Hussy, G. Buell, K. A. Jones and R. A. North (1996) D2, D3, and D4 dopamine receptors couple to G protein-regulated potassium channels in Xenopus oocytes. *Mol Pharmacol*. **49**, 656-61.

West, R. E., Jr., A. Zweig, R. T. Granzow, M. I. Siegel and R. W. Egan (1990) Biexponential kinetics of (R)-alpha-[3H]methylhistamine binding to the rat brain H3 histamine receptor. *J Neurochem*. **55**, 1612-6.

White, J. H., A. Wise, M. J. Main, A. Green, N. J. Fraser, G. H. Disney, A. A. Barnes, P. Emson, S. M. Foord and F. H. Marshall (1998) Heterodimerization is required for the formation of a functional GABA(B) receptor. *Nature*. **396**, 679-82.

Wiedemann, P., H. Bonisch, F. Oerters and M. Bruss (2002) Structure of the human histamine H3 receptor gene (HRH3) and identification of naturally occurring variations. *J Neural Transm*. **109**, 443-53.

Wieland, K., G. Bongers, Y. Yamamoto, T. Hashimoto, A. Yamatodani, W. M. Menge, H. Timmerman, T. W. Lovenberg and R. Leurs (2001) Constitutive activity of histamine h(3) receptors stably expressed in SK-N-MC cells: display of agonism and inverse agonism by H(3) antagonists. *J Pharmacol Exp Ther*. **299**, 908-14.

Wise, R. A. (1996) Neurobiology of addiction. *Curr Opin Neurobiol*. **6**, 243-51.

Wittau, N., R. Grosse, F. Kalkbrenner, A. Gohla, G. Schultz and T. Gudermann (2000) The galanin receptor type 2 initiates multiple signaling pathways in small cell lung cancer cells by coupling to G(q), G(i) and G(12) proteins. *Oncogene*. **19**, 4199-209.

Witte, D. G., B. B. Yao, T. R. Miller, T. L. Carr, S. Cassar, R. Sharma, R. Faghih, B. W. Surber, T. A. Esbenshade, A. A. Hancock and K. M. Krueger (2006) Detection of multiple H3 receptor affinity states utilizing [3H]A-349821, a novel, selective, non-imidazole histamine H3 receptor inverse agonist radioligand. *Br J Pharmacol*. **148**, 657-70.

Wong, H. M., M. J. Sole and J. W. Wells (1986) Assessment of mechanistic proposals for the binding of agonists to cardiac muscarinic receptors. *Biochemistry*. **25**, 6995-7008.

Woods, A. S. (2004) The mighty arginine, the stable quaternary amines, the powerful aromatics, and the aggressive phosphate: their role in the noncovalent minuet. *J Proteome Res*. **3**, 478-84.

Woods, A. S. and M. A. Huestis (2001) A study of peptide--peptide interaction by matrix-assisted laser desorption/ionization. *J Am Soc Mass Spectrom*. **12**, 88-96.

Woods, A. S., J. M. Koomen, B. T. Ruotolo, K. J. Gillig, D. H. Russel, K. Fuhrer, M. Gonin, T. F. Egan and J. A. Schultz (2002) A study of peptide-peptide interactions using MALDI ion mobility o-TOF and ESI mass spectrometry. *J Am Soc Mass Spectrom*. **13**, 166-9.

Wreggett, K. A. and J. W. Wells (1995) Cooperativity manifest in the binding properties of purified cardiac muscarinic receptors. *J Biol Chem*. **270**, 22488-99.

Wu, D. F., L. Q. Yang, A. Goschke, R. Stumm, L. O. Brandenburg, Y. J. Liang, V. Hollt and T. Koch (2008) Role of receptor internalization in the agonist-induced desensitization of cannabinoid type 1 receptors. *J Neurochem*. **104**, 1132-43.

Wulff, B. S., S. Hastrup and K. Rimvall (2002) Characteristics of recombinantly expressed rat and human histamine H3 receptors. *Eur J Pharmacol*. **453**, 33-41.

Wurtman, R. J. (2002) Stress and the adrenocortical control of epinephrine synthesis. *Metabolism*. **51**, 11-4.

Xu, M., X. T. Hu, D. C. Cooper, R. Moratalla, A. M. Graybiel, F. J. White and S. Tonegawa (1994) Elimination of cocaine-induced hyperactivity and dopamine-mediated neurophysiological effects in dopamine D1 receptor mutant mice. *Cell*. **79**, 945-55.

Xu, X. J., T. Hokfelt and Z. Wiesenfeld-Hallin (2008) Galanin and spinal pain mechanisms: where do we stand in 2008? *Cell Mol Life Sci*. **65**, 1813-9.

Yamaguchi, I., S. K. Harmon, R. D. Todd and K. L. O'Malley (1997) The rat D4 dopamine receptor couples to cone transducin (Galphat2) to inhibit forskolin-stimulated cAMP accumulation. *J Biol Chem*. **272**, 16599-602.

Yamauchi, J., M. Nagao, Y. Kaziro and H. Itoh (1997) Activation of p38 mitogen-activated protein kinase by signaling through G protein-coupled receptors. Involvement of Gbetagamma and Galphaq/11 subunits. *J Biol Chem*. **272**, 27771-7.

Yan, Z., J. Feng, A. A. Fienberg and P. Greengard (1999) D(2) dopamine receptors induce mitogen-activated protein kinase and cAMP response element-binding protein phosphorylation in neurons. *Proc Natl Acad Sci U S A*. **96**, 11607-12.

Yang, J. W., W. S. Jang, S. D. Hong, Y. I. Ji, D. H. Kim, J. Park, S. W. Kim and Y. S. Joung (2008) A case-control association study of the polymorphism at the promoter region of the DRD4 gene in Korean boys with attention deficit-hyperactivity disorder: evidence of association with the -521 C/T SNP. *Prog Neuropsychopharmacol Biol Psychiatry*. **32**, 243-8.

Yao, W. D., R. D. Spealman and J. Zhang (2008) Dopaminergic signaling in dendritic spines. *Biochem Pharmacol*. **75**, 2055-69.

Yin, H. H. and D. M. Lovinger (2006) Frequency-specific and D2 receptor-mediated inhibition of glutamate release by retrograde endocannabinoid signaling. *Proc Natl Acad Sci U S A*. **103**, 8251-6.

Yoon, S., M. H. Choi, M. S. Chang and J. H. Baik (2011) Wnt5a-dopamine D2 receptor interactions regulate dopamine neuron development via extracellular signal-regulated kinase (ERK) activation. *J Biol Chem*. **286**, 15641-51.

Yu, P. B., C. C. Hong, C. Sachidanandan, J. L. Babitt, D. Y. Deng, S. A. Hoyng, H. Y. Lin, K. D. Bloch and R. T. Peterson (2008) Dorsomorphin inhibits BMP signals required for embryogenesis and iron metabolism. *Nat Chem Biol*. **4**, 33-41.

Yuferov, V., Y. Zhou, R. Spangler, C. E. Maggos, A. Ho and M. J. Kreek (1999) Acute "binge" cocaine increases mu-opioid receptor mRNA levels in areas of the rat mesolimbic mesocortical dopamine system. *Brain Res Bull*. **48**, 109-12.

Zack, M. and C. X. Poulos (2009) Parallel roles for dopamine in pathological gambling and psychostimulant addiction. *Curr Drug Abuse Rev*. **2**, 11-25.

Zawilska, J. B., M. Berezinska, J. Rosiak, D. J. Skene, B. Vivien-Roels and J. Z. Nowak (2004) Suppression of melatonin biosynthesis in the chicken pineal gland by retinally perceived light - involvement of D1-dopamine receptors. *J Pineal Res*. **36**, 80-6.

Zhang, D., L. Zhang, Y. Tang, Q. Zhang, D. Lou, F. R. Sharp, J. Zhang and M. Xu (2005) Repeated cocaine administration induces gene expression changes through the dopamine D1 receptors. *Neuropsychopharmacology*. **30**, 1443-54.

Zhang, L., D. Lou, H. Jiao, D. Zhang, X. Wang, Y. Xia, J. Zhang and M. Xu (2004) Cocaine-induced intracellular signaling and gene expression are oppositely regulated by the dopamine D1 and D3 receptors. *J Neurosci*. **24**, 3344-54.

Zhang, L. J., J. E. Lachowicz and D. R. Sibley (1994) The D2S and D2L dopamine receptor isoforms are differentially regulated in Chinese hamster ovary cells. *Mol Pharmacol*. **45**, 878-89.

Zhang, M., R. L. Thurmond and P. J. Dunford (2007) The histamine H(4) receptor: a novel modulator of inflammatory and immune disorders. *Pharmacol Ther*. **113**, 594-606.

Zhen, X., K. Uryu, H. Y. Wang and E. Friedman (1998) D1 dopamine receptor agonists mediate activation of p38 mitogen-activated protein kinase and c-Jun amino-terminal kinase by a protein kinase A-dependent mechanism in SK-N-MC human neuroblastoma cells. *Mol Pharmacol*. **54**, 453-8.

Zheng, W. and P. A. Cole (2002) Serotonin N-acetyltransferase: mechanism and inhibition. *Curr Med Chem*. **9**, 1187-99.

Zhu, X. and J. Wess (1998) Truncated V2 vasopressin receptors as negative regulators of wild-type V2 receptor function. *Biochemistry*. **37**, 15773-84.

Zhu, Y., D. Michalovich, H. Wu, K. B. Tan, G. M. Dytko, I. J. Mannan, R. Boyce, J. Alston, L. A. Tierney, X. Li, N. C. Herrity, L. Vawter, H. M. Sarau, R. S. Ames, C. M. Davenport, J. P. Hieble, S. Wilson, D. J. Bergsma and L. R. Fitzgerald (2001) Cloning, expression, and pharmacological characterization of a novel human histamine receptor. *Mol Pharmacol*. **59**, 434-41.

Zimmermann, T., J. Rietdorf, A. Girod, V. Georget and R. Pepperkok (2002) Spectral imaging and linear un-mixing enables improved FRET efficiency with a novel GFP2-YFP FRET pair. *FEBS Lett*. **531**, 245-9.

Zini, S., M. P. Roisin, U. Langel, T. Bartfai and Y. Ben-Ari (1993) Galanin reduces release of endogenous excitatory amino acids in the rat hippocampus. *Eur J Pharmacol*. **245**, 1-7.

Zink, C. F., G. Pagnoni, M. E. Martin, M. Dhamala and G. S. Berns (2003) Human striatal response to salient nonrewarding stimuli. *J Neurosci*. **23**, 8092-7.

El misterio es la cosa más bonita que podemos experimentar. Es la fuente de todo arte y ciencia verdaderos. Albert Einstein.

En el fondo, los científicos somos gente con suerte: podemos jugar a lo que queramos durante toda la vida. Lee Smolin.

El experimentador que no sabe lo que está buscando no comprenderá lo que encuentra. Claude Bernard.

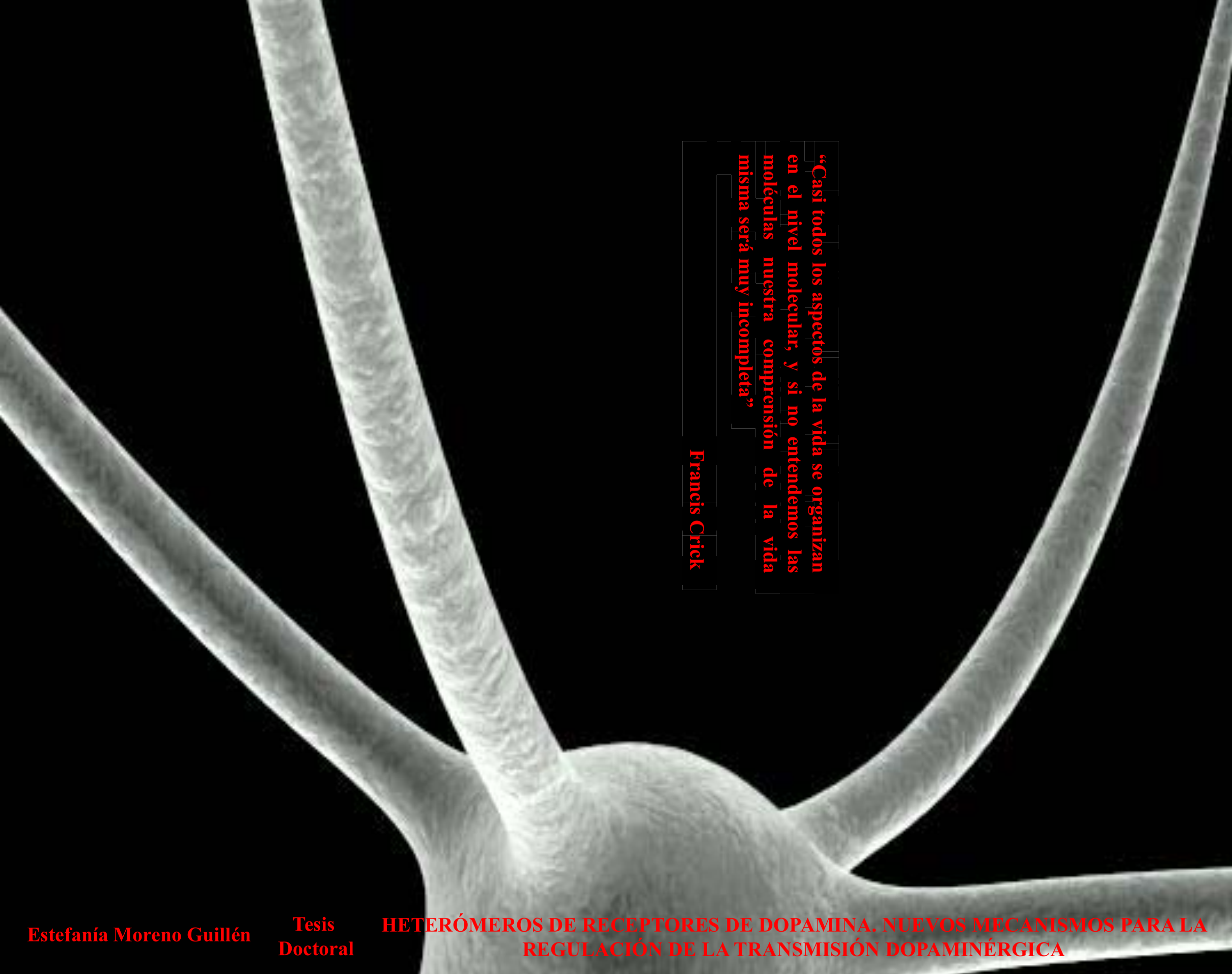

"Casi todos los aspectos de la vida se organizan en el nivel molecular, y si no entendemos las moléculas nuestra comprensión de la vida misma será muy incompleta"

Francis Crick

Estefanía Moreno Guillén

Tesis Doctoral

HETERÓMEROS DE RECEPTORES DE DOPAMINA. NUEVOS MECANISMOS PARA LA REGULACIÓN DE LA TRANSMISIÓN DOPAMINÉRGICA